Arthritis & Rheumatology

An Official Journal of the American College of Rheumatology
www.arthritisrheum.org and wileyonlinelibrary.com

GENERAL INFORMATION

TO SUBSCRIBE

Institutions and Non-Members

Email: wileyonlinelibrary.com
Phone: (201) 748-6645
Write: Wiley Periodicals LLC
Attn: Journals Admin Dept UK
111 River Street
Hoboken, NJ 07030

Volumes 74, 2022:
Institutional Print Only: **Arthritis & Rheumatology and Arthritis Care & Research:** $2,603 in US, Canada, and Mexico; $2,603 outside North America
Institutional Online Only: $2,495 in US, Canada, Mexico, and outside North America
Institutional Print and Online Only: $2,802 in US, Canada, and Mexico; $2,802 outside North America

For submission instructions, subscription, and all other information visit: wileyonlinelibrary.com.

Arthritis & Rheumatology accepts articles for Open Access publication. Please visit https://authorservices.wiley.com/author-resources/Journal-Authors/open-access/hybrid-open-access.html for further information about OnlineOpen.

Wiley's Corporate Citizenship initiative seeks to address the environmental, social, economic, and ethical challenges faced in our business and which are important to our diverse stakeholder groups. Since launching the initiative, we have focused on sharing our content with those in need, enhancing community philanthropy, reducing our carbon impact, creating global guidelines and best practices for paper use, establishing a vendor code of ethics, and engaging our colleagues and other stakeholders in our efforts.
Follow our progress at www.wiley.com/go/citizenship.

Access to this journal is available free online within institutions in the developing world through the HINARI initiative with the WHO. For information, visit www.healthinternetwork.org.

Disclaimer

The Publisher, the American College of Rheumatology, and Editors cannot be held responsible for errors or any consequences arising from the use of information contained in this journal; the views and opinions expressed do not necessarily reflect those of the Publisher, the American College of Rheumatology and Editors, neither does the publication of advertisements constitute any endorsement by the Publisher, the American College of Rheumatology and Editors of the products advertised.

Members:

American College of Rheumatology/Association of Rheumatology Professionals

For membership rates, journal subscription information, and change of address, please write:
American College of Rheumatology
2200 Lake Boulevard
Atlanta, GA 30319-5312
(404) 633-3777

ADVERTISING SALES AND COMMERCIAL REPRINTS

Sales: Kathleen Malseed, National Account Manager
E-mail: kmalseed@pminy.com
Phone: (215) 852-9824
Pharmaceutical Media, Inc.
30 East 33rd Street, New York, NY 10016

Production: Patti McCormack
E-mail: pmccormack@pminy.com
Phone: (212) 904-0376
Pharmaceutical Media, Inc.
30 East 33rd Street, New York, NY 10016

Publisher: Arthritis & Rheumatology is published by Wiley Periodicals LLC, 101 Station Landing, Suite 300, Medford, MA 02155
Production Editor: Ramona Talantor, artprod@wiley.com

ARTHRITIS & RHEUMATOLOGY (Print ISSN 2326-5191; Online ISSN 2326-5205 at Wiley Online Library, wileyonlinelibrary.com) is published monthly on behalf of the American College of Rheumatology by Wiley Periodicals LLC, a Wiley Company, 111 River Street, Hoboken, NJ 07030-5774. Periodicals postage paid at Hoboken, NJ and additional offices. POSTMASTER: Send all address changes to Arthritis & Rheumatology, Wiley Periodicals LLC, c/o The Sheridan Press, PO Box 465, Hanover, PA 17331. **Send subscription inquiries care of** Wiley Periodicals LLC, Attn: Journals Admin Dept UK, 111 River Street, Hoboken, NJ 07030, (201) 748-6645 (nonmember subscribers only; American College of Rheumatology/Association of Rheumatology Health Professionals members should contact the American College of Rheumatology). **Subscription Price:** (Volumes 74, 2022: Arthritis & Rheumatology and Arthritis Care & Research) Print only: $2,603.00 in U.S., Canada and Mexico, $2,603.00 rest of world. For all other prices please consult the journal's website at wileyonlinelibrary.com. All subscriptions containing a print element, shipped outside U.S., will be sent by air. Payment must be made in U.S. dollars drawn on U.S. bank. Prices are exclusive of tax. Asia-Pacific GST, Canadian GST and European VAT will be applied at the appropriate rates. For more information on current tax rates, please go to www.wileyonlinelibrary.com/tax-vat. The price includes online access to the current and all online backfiles to January 1st 2018, where available. For other pricing options including access information and terms and conditions, please visit https://onlinelibrary.wiley.com/library-info/products/price-lists. Terms of use can be found here: https://onlinelibrary.wiley.com/terms-and-conditions. **Delivery Terms and Legal Title:** Where the subscription price includes print issues and delivery is to the recipient's address, delivery terms are Delivered at Place (DAP); the recipient is responsible for paying any import duty or taxes. Title to all issues transfers Free of Board (FOB) our shipping point, freight prepaid. We will endeavor to fulfill claims for missing or damaged copies within six months of publication, within our reasonable discretion and subject to availability. **Change of Address:** Please forward to the subscriptions address listed above 6 weeks prior to move; enclose present mailing label with change of address. **Claims** for undelivered copies will be accepted only after the following issue has been received. Please enclose a copy of the mailing label or cite your subscriber reference number in order to expedite handling. Missing copies will be supplied when losses have been sustained intransit and where reserve stock permits. Send claims care of Wiley Periodicals LLC, Attn: Journals Admin Dept UK, 111 River Street, Hoboken, NJ 07030. If claims are not resolved satisfactorily, please write to Subscription Distribution c/o Wiley Periodicals LLC, 111 River Street, Hoboken, NJ 07030. **Cancellations:** Subscription cancellations will not be accepted after the first issue has been mailed. **Journal Customer Services:** For ordering information, claims and any enquiry concerning your journal subscription please go to https://wolsupport.wiley.com/s/contactsupport?tabset-a7d10=2 or contact your nearest office. **Americas:** Email: cs-journals@wiley.com; Tel: +1 877 762 2974. **Europe, Middle East and Africa:** Email: cs-journals@wiley.com; Tel: +44 (0) 1865 778315; 0800 1800 536 (Germany). **Asia Pacific:** Email: cs-journals@wiley.com; Tel: +65 6511 8000. **Japan:** For Japanese speaking support, Email: cs-japan@wiley.com. **Visit our Online Customer Help** at https://wolsupport.wiley.com/s/contactsupport?tabset-a7d10=2. **Back Issues:** Single issues from current and prior year volumes are available at the current single issue price from csjournals@wiley.com. Earlier issues may be obtained from Periodicals Service Company, 351 Fairview Avenue-Ste 300, Hudson, NY 12534, USA. Tel: + 1 518 822-9300, Fax: +1 518 822-9305, Email: psc@periodicals.com. Printed in the USA by The Sheridan Group.

Arthritis & Rheumatology

An Official Journal of the American College of Rheumatology
www.arthritisrheum.org and wileyonlinelibrary.com

Cover design: Todd Machen

This journal is printed on acid-free paper.

Arthritis & Rheumatology

An Official Journal of the American College of Rheumatology
www.arthritisrheum.org and wileyonlinelibrary.com

VOLUME 74 • March 2022 • NO. 3

Cover image: The figure on the cover (from Suzuki et al, https://onlinelibrary.wiley.com/doi/10.1002/art.42069) shows elastic–Masson staining of a temporal artery from a patient with giant cell arteritis who had no halo sign on ultrasound, demonstrating typical histopathologic findings of giant cell arteritis. Multinucleated giant cells and lymphocytic infiltration were observed, forming a granuloma. Partial tearing of the internal elastic lamina was also seen.

In this Issue

Highlights from this issue of *A&R* | By Lara C. Pullen, PhD

Inhibition of Pyroptosis Leads to Attenuation of Arthritis

Programmed cell death can take place via apoptosis or necrosis, although these 2 pathways affect inflammation and the immune response in very different ways. p. 427 Apoptosis is noninflammatory, necrosis is inflammatory, and pyroptosis, a specific form of programmed necrosis, is highly proinflammatory in nature. Intracellular levels of gasdermin E (GSDME) help to determine whether caspase 3–activated cells undergo apoptosis (low levels of GDSME) or pyroptosis (high levels of GSDME).

Persistent synovitis is a hallmark of rheumatoid arthritis (RA), and studies have shown that GSDME-mediated pyroptosis plays an essential role in the pathogenesis and progression of RA. In this issue, Zhai et al (p. 427) describe results of their efforts to identify the initial trigger for pyroptosis in patients with RA. Their findings support a pathogenic role of GSDME in RA and suggest that tumor necrosis factor (TNF) activation of GSDME-mediated pyroptosis of monocytes and macrophages may contribute to RA pathogenesis. Specifically, the authors propose a feedback loop wherein monocytes and macrophages produce TNF and then respond to the cytokine by undergoing pyroptosis.

The investigators compared monocytes and synovial macrophages from healthy patients to those in patients with RA and found that the cells from the latter had increased expression of activated caspase 3, GSDME, and the N-terminal of GSDME (GSDME-N) relative to controls. Moreover, the expression of GSDME-N in monocytes from patients with RA correlated positively with disease activity as measured by the Disease Activity Score in 28 joints and C-reactive protein level.

Having established the high expression of GSDME in the peripheral blood monocytes of patients with RA, investigators sought to explore the role of pyroptosis in purified peripheral blood monocytes from healthy controls compared to patients with RA. They found that monocytes from RA patients with higher GSDME levels were more susceptible to pyroptosis. After noting high TNF expression in synovial tissue samples from patients with RA, the team sought to determine whether TNF triggers caspase 3/GSDME-mediated pyroptosis in macrophages. Thus, they incubated THP-1 cells with phorbol 12-myristate 13-acetate to induce differentiation into macrophages and found that when these THP-1 cell–derived macrophages were cultured in the presence of different concentrations of TNF for 36 hours, TNF increased the expression of activated caspase 3, GSDME, and GSDME-N in a concentration-dependent manner. When they used TNF to induce pyroptosis in monocytes and macrophages, they found that TNF activated the caspase 3/GSDME pathway.

To verify the role of caspase 3 in TNF-induced macrophage pyroptosis, the researchers pretreated THP-1 cell–derived macrophages with a caspase 3–specific inhibitor for 1 hour, followed by treatment with TNF for 36 hours. An examination of TNF-induced pyroptosis in these cells showed that the caspase 3 inhibitor, as well as small interfering RNA designed to silence GSDME, were able to significantly block TNF-induced pyroptosis.

Given that RA synovial macrophages and circulating monocytes showed high expression of activated caspase 3 and GSDME, and that TNF activated caspase 3/GSDME-mediated pyroptosis, the researchers hypothesized that inhibition of pyroptosis by Gsdme knockout might protect mice against arthritis. While *Gsdme*$^{-/-}$ B6 and wild-type (WT) B6 mice did not differ in the absence of collagen exposure, induction of collagen-induced arthritis (CIA) in *Gsdme*-deficient mice yielded less arthritis than that seen in control B6 mice. The study authors concluded that targeting GSDME might be a potential therapeutic approach for RA.

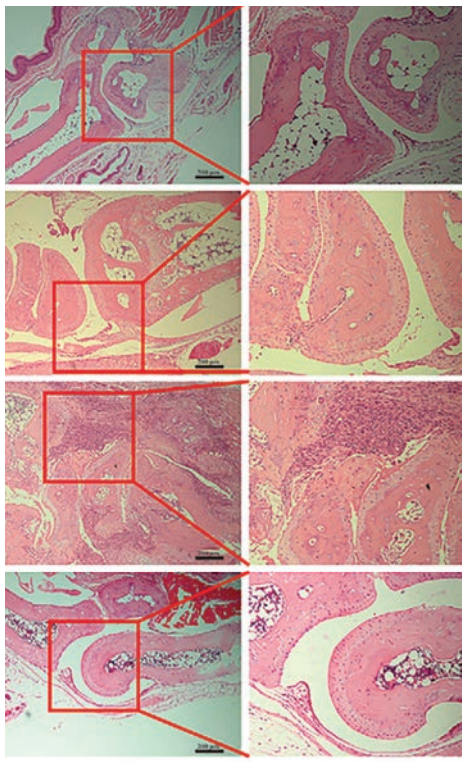

Figure 1. Decreased arthritis incidence, clinical scores, and synovial inflammation in *Gsdme*-deficient mice with collagen-induced arthritis (CIA) compared to wild-type (WT) mice with CIA. Male WT C57BL/6 mice (n = 10) and Gsdme / mice (n = 8) were immunized with chicken type II collagen emulsified in Freund's complete Q42 adjuvant on days 0 and 21 for CIA induction. Mice of the same background without CIA were used as controls (n = 6 WT and 6 Gsdme / mice). Above: Hematoxylin and eosin–stained joint sections from WT and *Gsdme*$^{-/-}$ mice. Right panels show higher-magnification views (bars = 100 μm) of the boxed areas in the left panels (bars = 200 μm).

Up-regulated Interleukin-10 Contributes to Autoantibody Production in Lupus

In this issue, Xu et al (p. 496) report that IL-10 promotes extrafollicular autoimmune responses in patients with active systemic lupus erythematosus (SLE). Their findings demonstrate a prominent role for IL-10+ double-negative 2 (DN2; IgD–CD27–CD21–CD11c+) B cells in the generation of SLE autoantibodies.

p. 496

The study included 2 independent cohorts of patients with different ethnic backgrounds and from 2 different continents. The investigators found that SLE patients exhibited increased proportions of IL-10+ DN2 cells relative to age-, sex-, and ancestry-matched controls. Additionally, in vitro coculture studies revealed that there was a critical role for IL-10 in the function of Th10 cells from SLE patients.

Noting that *E2F2* is one of the top 10 highly expressed genes in IL-10+ enriched $CD24^{high}CD38^{high}$ transitional B cells compared to naive B cells, the researchers discovered that elevated levels of the transcription factor *E2F2* up-regulated IL-10 in B cells. Since microRNAs (miRNAs) are well-known for fine-tuning cellular gene expression, the investigators then identified miRNAs that could down-regulate IL-10 levels in SLE B cells. They conclude by suggesting that the extrafollicular autoimmune responses may be dampened by targeting the *E2F2*–miRNA-17-5p circuitry. This study provides new insights into the mechanisms and regulatory networks of IL10 expression, which could allow for development of strategies to modulate expansion of the extrafollicular pathway in SLE.

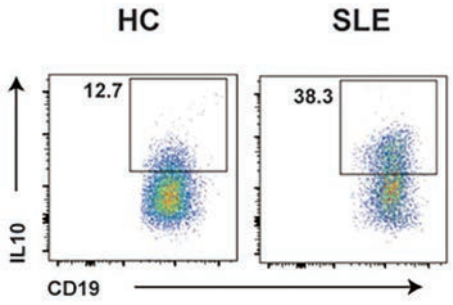

Figure 1. Representative flow cytometry plots show increased total $IL10^+$ B cells in SLE patients in multiple cohorts.

Journal Club

A monthly feature designed to facilitate discussion on research methods in rheumatology.

Association Between Race and Radiographic, Symptomatic, and Clinical Hand OA: A Propensity Score–Matched Study Using OAI Data

Pishgar et al, *Arthritis Rheumatol* 2022;74:453–461

Mounting evidence points to the potential heterogeneity of the pathologies that are sometimes grouped under the osteoarthritis (OA) umbrella term. The association between race and OA in different joints supports the hypothesis that different risk factor profiles play a role in the pathogenesis of OA in the knee and hip versus the hand. Knee and hip OA are more prevalent among Black subjects, while few observational studies have suggested that hand OA may be less common among Black subjects. Pishgar et al sought to determine whether differences exist in the prevalence and severity of hand OA among Black and non-Black subjects.

In the study, a propensity score (PS)–matching procedure was used to balance the potential effects of known (and available) risk factors of hand OA between the 2 groups of Black subjects and non-Black subjects in the OA initiative (OAI) cohort (n = 4,699). Hand radiographs and clinical examinations of subjects at baseline were assessed and used to diagnose phenotypes of hand OA (e.g., radiographic, symptomatic, and erosive). The presence and severity of these hand OA phenotypes were compared among the PS-matched groups of Black and non-Black subjects using regression analyses. By selecting Black and non-Black subjects with a similar profile of hand OA risk factors, the PS-matching method provided a quasi-experimental design to study the potential association between race and hand OA, after accounting for effects of other risk factors. The findings suggest lower prevalence and less severe phenotypes of hand OA among the Black subjects in the study.

Questions

1. **What is currently known about the association between race and OA in knee and hip joints versus hand joints?**
2. **How did the authors evaluate the presence and severity of hand OA among the participants in this study?**
3. **What are the advantages and disadvantages of using the PS-matching procedure compared to adjustment for hand OA risk factors in the regression models?**
4. **Are there any potential and relevant risk factors of hand OA not included in the PS-matching method?**
5. **What are the clinical implications of the findings in this study?**

In this Issue

Highlights from this issue of *A&R* | By Lara C. Pullen, PhD

Inhibition of Pyroptosis Leads to Attenuation of Arthritis

Programmed cell death can take place via apoptosis or necrosis, although these 2 pathways affect inflammation and the immune response in very different ways. p. 427 Apoptosis is noninflammatory, necrosis is inflammatory, and pyroptosis, a specific form of programmed necrosis, is highly proinflammatory in nature. Intracellular levels of gasdermin E (GSDME) help to determine whether caspase 3–activated cells undergo apoptosis (low levels of GDSME) or pyroptosis (high levels of GSDME).

Persistent synovitis is a hallmark of rheumatoid arthritis (RA), and studies have shown that GSDME-mediated pyroptosis plays an essential role in the pathogenesis and progression of RA. In this issue, Zhai et al (p. 427) describe results of their efforts to identify the initial trigger for pyroptosis in patients with RA. Their findings support a pathogenic role of GSDME in RA and suggest that tumor necrosis factor (TNF) activation of GSDME-mediated pyroptosis of monocytes and macrophages may contribute to RA pathogenesis. Specifically, the authors propose a feedback loop wherein monocytes and macrophages produce TNF and then respond to the cytokine by undergoing pyroptosis.

The investigators compared monocytes and synovial macrophages from healthy patients to those in patients with RA and found that the cells from the latter had increased expression of activated caspase 3, GSDME, and the N-terminal of GSDME (GSDME-N) relative to controls. Moreover, the expression of GSDME-N in monocytes from patients with RA correlated positively with disease activity as measured by the Disease Activity Score in 28 joints and C-reactive protein level.

Having established the high expression of GSDME in the peripheral blood monocytes of patients with RA, investigators sought to explore the role of pyroptosis in purified peripheral blood monocytes from healthy controls compared to patients with RA. They found that monocytes from RA patients with higher GSDME levels were more susceptible to pyroptosis. After noting high TNF expression in synovial tissue samples from patients with RA, the team sought to determine whether TNF triggers caspase 3/GSDME-mediated pyroptosis in macrophages. Thus, they incubated THP-1 cells with phorbol 12-myristate 13-acetate to induce differentiation into macrophages and found that when these THP-1 cell–derived macrophages were cultured in the presence of different concentrations of TNF for 36 hours, TNF increased the expression of activated caspase 3, GSDME, and GSDME-N in a concentration-dependent manner. When they used TNF to induce pyroptosis in monocytes and macrophages, they found that TNF activated the caspase 3/GSDME pathway.

To verify the role of caspase 3 in TNF-induced macrophage pyroptosis, the researchers pretreated THP-1 cell–derived macrophages with a caspase 3–specific inhibitor for 1 hour, followed by treatment with TNF for 36 hours. An examination of TNF-induced pyroptosis in these cells showed that the caspase 3 inhibitor, as well as small interfering RNA designed to silence GSDME, were able to significantly block TNF-induced pyroptosis.

Given that RA synovial macrophages and circulating monocytes showed high expression of activated caspase 3 and GSDME, and that TNF activated caspase 3/GSDME-mediated pyroptosis, the researchers hypothesized that inhibition of pyroptosis by Gsdme knockout might protect mice against arthritis. While *Gsdme*$^{-/-}$ B6 and wild-type (WT) B6 mice did not differ in the absence of collagen exposure, induction of collagen-induced arthritis (CIA) in *Gsdme*-deficient mice yielded less arthritis than that seen in control B6 mice. The study authors concluded that targeting GSDME might be a potential therapeutic approach for RA.

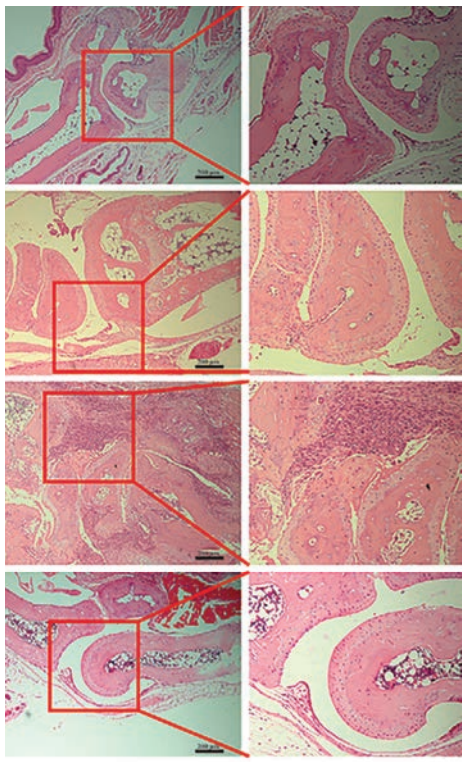

Figure 1. Decreased arthritis incidence, clinical scores, and synovial inflammation in *Gsdme*-deficient mice with collagen-induced arthritis (CIA) compared to wild-type (WT) mice with CIA. Male WT C57BL/6 mice (n = 10) and Gsdme / mice (n = 8) were immunized with chicken type II collagen emulsified in Freund's complete Q42 adjuvant on days 0 and 21 for CIA induction. Mice of the same background without CIA were used as controls (n = 6 WT and 6 Gsdme / mice). Above: Hematoxylin and eosin–stained joint sections from WT and *Gsdme*$^{-/-}$ mice. Right panels show higher-magnification views (bars = 100 μm) of the boxed areas in the left panels (bars = 200 μm).

Up-regulated Interleukin-10 Contributes to Autoantibody Production in Lupus

In this issue, Xu et al (p. 496) report that IL-10 promotes extrafollicular autoimmune responses in patients with active systemic lupus erythematosus (SLE). Their findings demonstrate a prominent role for IL-10+ double-negative 2 (DN2; IgD–CD27–CD21–CD11c+) B cells in the generation of SLE autoantibodies.

p. 496

The study included 2 independent cohorts of patients with different ethnic backgrounds and from 2 different continents. The investigators found that SLE patients exhibited increased proportions of IL-10+ DN2 cells relative to age-, sex-, and ancestry-matched controls. Additionally, in vitro coculture studies revealed that there was a critical role for IL-10 in the function of Th10 cells from SLE patients.

Noting that *E2F2* is one of the top 10 highly expressed genes in IL-10+ enriched $CD24^{high}CD38^{high}$ transitional B cells compared to naive B cells, the researchers discovered that elevated levels of the transcription factor *E2F2* up-regulated IL-10 in B cells. Since microRNAs (miRNAs) are well-known for fine-tuning cellular gene expression, the investigators then identified miRNAs that could down-regulate IL-10 levels in SLE B cells. They conclude by suggesting that the extrafollicular autoimmune responses may be dampened by targeting the *E2F2*–miRNA-17-5p circuitry. This study provides new insights into the mechanisms and regulatory networks of IL10 expression, which could allow for development of strategies to modulate expansion of the extrafollicular pathway in SLE.

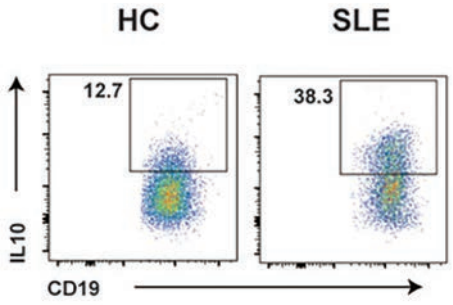

Figure 1. Representative flow cytometry plots show increased total $IL10^+$ B cells in SLE patients in multiple cohorts.

Journal Club

A monthly feature designed to facilitate discussion on research methods in rheumatology.

Association Between Race and Radiographic, Symptomatic, and Clinical Hand OA: A Propensity Score–Matched Study Using OAI Data

Pishgar et al, *Arthritis Rheumatol* 2022;74:453–461

Mounting evidence points to the potential heterogeneity of the pathologies that are sometimes grouped under the osteoarthritis (OA) umbrella term. The association between race and OA in different joints supports the hypothesis that different risk factor profiles play a role in the pathogenesis of OA in the knee and hip versus the hand. Knee and hip OA are more prevalent among Black subjects, while few observational studies have suggested that hand OA may be less common among Black subjects. Pishgar et al sought to determine whether differences exist in the prevalence and severity of hand OA among Black and non-Black subjects.

In the study, a propensity score (PS)–matching procedure was used to balance the potential effects of known (and available) risk factors of hand OA between the 2 groups of Black subjects and non-Black subjects in the OA initiative (OAI) cohort (n = 4,699). Hand radiographs and clinical examinations of subjects at baseline were assessed and used to diagnose phenotypes of hand OA (e.g., radiographic, symptomatic, and erosive). The presence and severity of these hand OA phenotypes were compared among the PS-matched groups of Black and non-Black subjects using regression analyses. By selecting Black and non-Black subjects with a similar profile of hand OA risk factors, the PS-matching method provided a quasi-experimental design to study the potential association between race and hand OA, after accounting for effects of other risk factors. The findings suggest lower prevalence and less severe phenotypes of hand OA among the Black subjects in the study.

Questions

1. **What is currently known about the association between race and OA in knee and hip joints versus hand joints?**
2. **How did the authors evaluate the presence and severity of hand OA among the participants in this study?**
3. **What are the advantages and disadvantages of using the PS-matching procedure compared to adjustment for hand OA risk factors in the regression models?**
4. **Are there any potential and relevant risk factors of hand OA not included in the PS-matching method?**
5. **What are the clinical implications of the findings in this study?**

Clinical Connections

SHP-2 Inhibition Attenuates OA by Maintaining Homeostasis of Cartilage Metabolism via the DOK1/UPP1/Uridine Cascade

Liu et al, *Arthritis Rheumatol* 2022;74:462–473

CORRESPONDENCE
Qiang Xu, PhD: quangxu@nju.edu.cn
Minjia Tan, PhD: mjtan@simm.ac.cn
Yang Sun, PhD: yangsun@nju.edu.cn

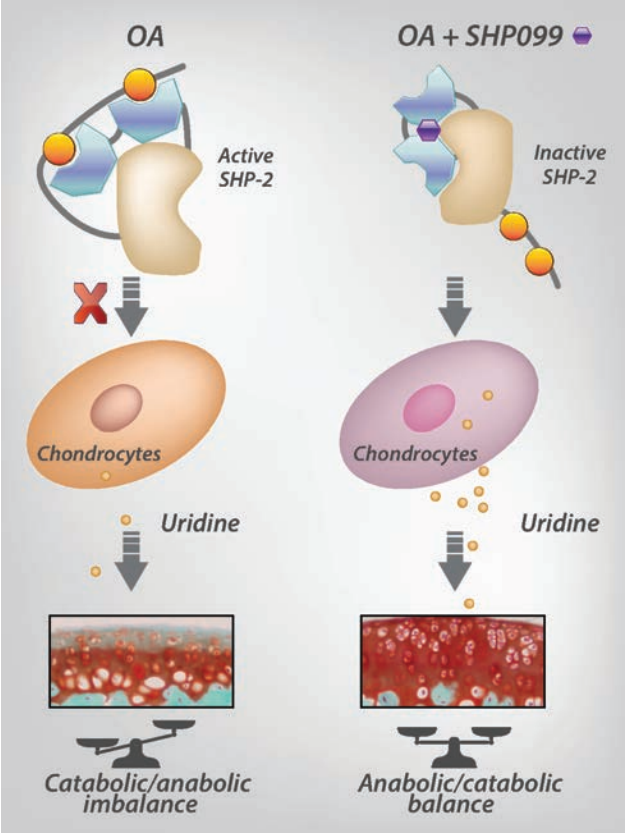

KEY POINTS

- SHP-2 enzyme activity is significantly increased in OA.
- SHP-2 inhibitors exert a dual effect of inhibiting cartilage degradation and promoting cartilage synthesis.
- SHP-2/DOK1/uridine axis is a novel pathway for the prevention and treatment of OA.

SUMMARY

One of the key features of osteoarthritis (OA) is articular cartilage damage. In recent years, an increasing number of novel chondroprotective strategies have been proposed and tested, but so far, none have been approved. SHP-2 is an SH2 domain–containing tyrosine phosphatase encoded by *PTPN11*. Liu et al demonstrated that SHP-2 enzyme activity significantly increased in samples from human OA patients with serious articular cartilage injury and in interleukin-1β (IL-1β)–stimulated chondrocytes. In mice, SHP-2 inhibitor SHP099 dramatically reduced the expression of cartilage degradation–related genes (e.g., *Mmp13* and *Mmp3*) and simultaneously promoted the expression of cartilage synthesis–related genes (e.g., *Sox9*, *Col2a1*, and *Acan*). The 10-plex TMT labeling–based global proteomic analysis and stable isotope labeling with amino acids in cell culture (SILAC)/SH-2 domain superbinder–based tyrosine phosphoproteomic analysis revealed that SHP-2 inhibition suppressed the dephosphorylation of docking protein 1 (DOK1) and subsequently reduced the expression of uridine phosphorylase 1 (UPP1) and increased the uridine level, thereby contributing to the homeostasis of cartilage metabolism.

These findings suggest that SHP-2 is a novel accelerator of the imbalance in the cartilage homeostasis. SHP-2 inhibition exhibits chondroprotective effects through the DOK1/UPP1/uridine cascade, and targeting SHP-2 may serve as a promising therapeutic approach for OA.

Predictors of Rheumatic Immune-Related Adverse Events and De Novo Inflammatory Arthritis After ICI Treatment for Cancer

Cunningham-Bussel et al, *Arthritis Rheumatol* 2022;74:527–540

CORRESPONDENCE
Jeffrey A. Sparks, MD, MMSc: jsparks@bwh.harvard.edu
Amy Cunningham-Bussel, MD, PhD: acunningham-bussel@bwh.harvard.edu

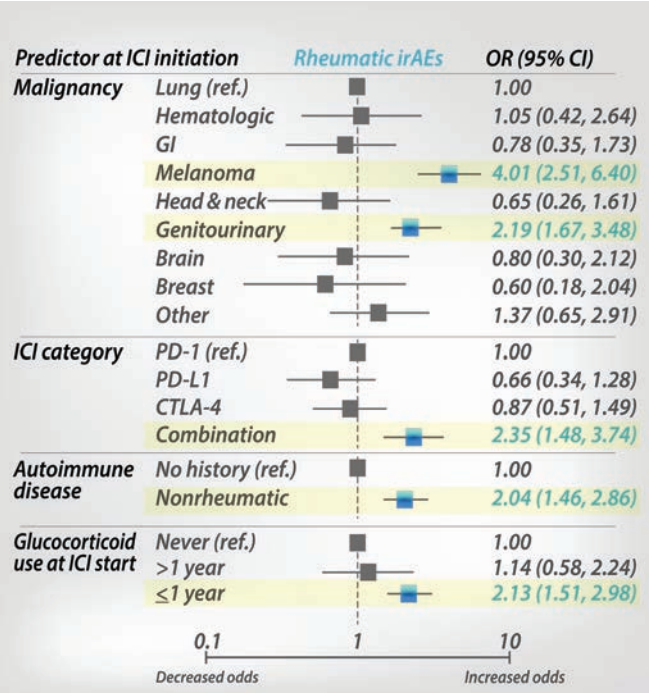

KEY POINTS

- ICIs to treat cancer may lead to irAEs that sometimes resemble primary rheumatic diseases.
- irAEs often require treatment with glucocorticoids or immunomodulators such as disease-modifying antirheumatic drugs.
- Melanoma and genitourinary cancer are associated with higher odds of developing rheumatic irAEs.
- Preexisting autoimmune disease, recent glucocorticoid use, and combination ICI use are also associated with developing rheumatic irAEs.

SUMMARY

Immune-related adverse events (irAEs) are common toxicities resulting from immune checkpoint inhibitors (ICIs) used to treat cancer. ICIs target programmed death 1 (PD-1), programmed death ligand 1 (PD-L1), or CTLA-4. Some irAEs resemble primary rheumatic diseases such as de novo inflammatory arthritis, sicca syndrome, myositis, or polymyalgia rheumatica–like syndrome. Glucocorticoids and immunomodulators such as disease-modifying antirheumatic drugs are commonly used to treat irAEs.

Cunningham-Bussel et al identified all cancer patients initiating ICIs at a large health care system and cancer center (n = 8,028), including those evaluated by rheumatologists and those prescribed nonglucocorticoid immunomodulators to treat irAEs after initiation of ICIs. About half of the patients evaluated by rheumatologists were diagnosed as having a rheumatic irAE. The authors systematically identified all incident rheumatic irAE cases occurring after ICI initiation (n = 226) that met criteria. Hydroxychloroquine, infliximab, methotrexate, and sulfasalazine were the most frequent immunomodulators used to treat de novo inflammatory arthritis as an irAE. In a case–control study to identify patient characteristics associated with rheumatic irAEs at time of ICI initiation, the following factors were found to be significant: a diagnosis of melanoma, a diagnosis of genitourinary cancer, combination ICI use (compared to PD-1 monotherapy), preexisting autoimmune (AI) disease, and glucocorticoid use within 1 year before ICI treatment (compared to never receiving glucocorticoids). The associations of melanoma and genitourinary cancer may be due to inflammatory potential of tumors caused by neoantigen production. These findings may help clinicians identify patients at risk of rheumatic irAEs.

Arthritis & Rheumatology
Vol. 74, No. 3, March 2022, pp 373–374
DOI 10.1002/art.42014

American College of Rheumatology
Empowering Rheumatology Professionals

SPECIAL ARTICLE

Winner of the 2021 American College of Rheumatology Annual Image Competition

American College of Rheumatology Image Library Diversity Task Force

The mission of the American College of Rheumatology Image Library is to provide ACR members, as well as the entire medical community, access to a wide variety of clinical images to help educators effectively present the manifestations of rheumatic diseases. Additionally, the images have been widely used in peer-reviewed publications and textbooks. Since its inception, the ACR's Rheumatology Image Library has become the preeminent collection devoted to rheumatic diseases. The collection is a dynamic one, changing yearly because of submissions from the medical community. Additionally, many nonwinning images are introduced into the Image Library, greatly enhancing the collection. Winners, as well as those images selected for inclusion in the Image Library, are chosen based on image quality and educational value.

As part of the ACR's pledge to be a leader for inclusion and change for members, trainees, staff, and rheumatology patients, the ACR held a special image competition in conjunction with ACR Convergence 2021, dedicated exclusively to images of rheumatic disease in skin of color. For the 2021 competition, 205 entries were received, and the reviewers carefully evaluated each entry.

The 2021 grand prize winner was a series of images showing classic cutaneous manifestations of dermatomyositis in

Figure 1. Cutaneous manifestations of dermatomyositis. Classic cutaneous manifestations of dermatomyositis, including heliotrope rash, periorbital edema with complete closure of the eyes, erythema nodosum on the lower extremity overlying the tibia, hyperkeratosis of the hands (mechanic's hands), postinflammatory hypopigmentation on the metacarpophalangeal, proximal interphalangeal (PIP), and distal interphalangeal joints, Gottron's sign over the PIP joints and elbow, and periungual infarcts and hyperkeratosis of the feet (hiker's feet), are shown in this 32-year-old Black female patient. Submitted by Santhanam Lakshminarayanan, MD, Farmington, CT.

Members of the Image Library Diversity Task Force of the American College of Rheumatology Committee on Education: Noelle Rolle, MBBS: Columbus, Georgia (Chair); Reem Alkilany, MD: Cleveland, Ohio; Senada Arabelovic, DO: Boston, Massachusetts; Ashira Blazer, MD: New York, New York; Sonam Kiwalkar, MD: Portland, Oregon; Ronald Laxer, MD: Toronto, Ontario, Canada; Rebecca Manno, MD: St. Thomas, US Virgin Islands; Mohammad Ursani, MD: Kingwood, Texas.
Submitted for publication October 7, 2021; accepted October 26, 2021.

a 32-year-old Black woman (Figure 1). The winning submission, as well as several other outstanding images, will be added to the Image Library.

The Rheumatology Image Library provides the medical community with 24/7 online access to the world's foremost collection of rheumatology images. It features contributions from all over the world and is an invaluable resource for countless physicians and other health care professionals, researchers, and journalists. Since the launch of the online edition of the Rheumatology Image Library in 2009, it has received more than 2.5 million unique visitors worldwide. To view the winning images and many others, visit the Rheumatology Image Library at http://images.rheumatology.org.

The ACR encourages the continued submission of images to its annual Image Competition. Submissions of high-quality images that illustrate rheumatic conditions or are relevant to the practice of rheumatology are welcomed. Visit https://www.rheumatology.org/Annual-Meeting/Program/Image-Competition for competition rules and entry/deadline dates. Details about the 2022 Image Competition will be available in spring 2022. If you have any questions regarding the Image Competition, please contact education@rheumatology.org.

Arthritis & Rheumatology
Vol. 74, No. 3, March 2022, pp 375–382
DOI 10.1002/art.42039

American College of Rheumatology
Empowering Rheumatology Professionals

ACR PRESIDENTIAL ADDRESS

Rheumatology Is Amazing

David R. Karp

Good afternoon, and welcome to ACR Convergence 2021, the annual meeting of the American College of Rheumatology. This is our second all-virtual Convergence, and the first thing I'd like to say is, "We have to stop meeting like this."

One year ago, when we were only 6 months into the COVID-19 pandemic, I, along with all of the staff and volunteers at the ACR as well as all of the ACR members I have spoken with, hoped that we would be in San Francisco—hearing outstanding talks in person instead of on our computers, enjoying the great food of that world-class city, and having the wonderful conversations with our friends and colleagues from around the world that make ACR Convergence a special event in the lives of rheumatologists and rheumatology professionals.

However, when the pandemic did not seem to be going away after 12 months, we realized that to protect the health and safety of our attendees and to acknowledge travel restrictions still in place last spring, we needed to have a virtual meeting again. This was before the rise of the more contagious delta variant of SARS–CoV-2 over the summer, so our decision looks very wise in retrospect. Nonetheless, I, and all of us at the ACR, remain optimistic that we will be able to welcome you to a live meeting in Philadelphia in the fall of 2022.

In the spring and summer of 2020, when societies around the world went into lockdown; when we closed our laboratories and started teaching our students online; when we suddenly had to care for our patients using telehealth; when travel, leisure, and entertainment ceased to exist for a time, one of the questions on everyone's mind was, "When is life going to return to *normal*? When can I do all the *normal* things I used to do? What will the '*new normal*' look like?" I'd like to be able to tell you I have answers to all these questions, but as the eminently quotable New York Yankees catcher Yogi Berra once said, "It's tough to make predictions, especially about the future" (1).

It's important to consider, though, what we mean by "*normal*." For many of us, the first sign of return to *normality* will be feeling safe enough to work together, learn together, and socialize without worrying about contracting COVID-19 and without wearing personal protective equipment at work, at school, or in the community. The time frame for this to happen is uncertain and depends a great deal on reaching "herd immunity" to prevent community transmission of SARS–CoV-2. When this happens will be a function of many variables including the emergence of viral variants, adherence to physical distancing and mask use, and of course, the vaccination of populations around the world.

My first thought here is that despite the pandemic, life for the ACR has been pretty "*normal*" all along. Many of the activities we associate with the College have not slowed or stopped at all. All our committees devoted to improving the ability of our members to excel in their specialty have continued to meet and deliver their work virtually. The Board of Directors has met on schedule virtually to conduct the typical business of the College as well as address some new challenges. Importantly, at the start of the pandemic, our Executive Vice President, Steve Echard, moved all the operations of the over 100 ACR staffers out of our headquarters in Atlanta and created work-from-home capabilities that have supported our providers, our trainees, our researchers, and our patients without skipping a beat. There is remarkable nimbleness and resilience in our professional staff. We have not seen burnout and we have even hired 15 new staffers who have never been inside the ACR offices and some who have never even been to Atlanta.

However, I think that being *normal* doesn't really describe what the ACR wants to be. The great American author, poet, and civil rights activist, Maya Angelou has said, "If you are always trying to be *normal*, you will never know how *amazing* you can be" (Figure 1). Through her 7 autobiographical novels, beginning with the critically acclaimed *I Know Why the Caged Bird Sings*, she chronicles her experiences as a Black woman growing up during the Great Depression, her life in Ghana, and then becoming the confidant of Martin Luther King, Jr. and several US Presidents.

Presented at Convergence 2021, the 85th Annual Meeting of the American College of Rheumatology, November 5, 2021.

David R. Karp, MD, PhD: University of Texas Southwestern Medical Center, Dallas; President, American College of Rheumatology, 2020–2021.

Address correspondence to David R. Karp, MD, PhD, Rheumatic Diseases Division, University of Texas Southwestern Medical Center, 5323 Harry Hines Boulevard, Dallas, TX 75390-8884. Email: David.Karp@UTSouthwestern.edu.

Submitted for publication November 28, 2021; accepted November 28, 2021.

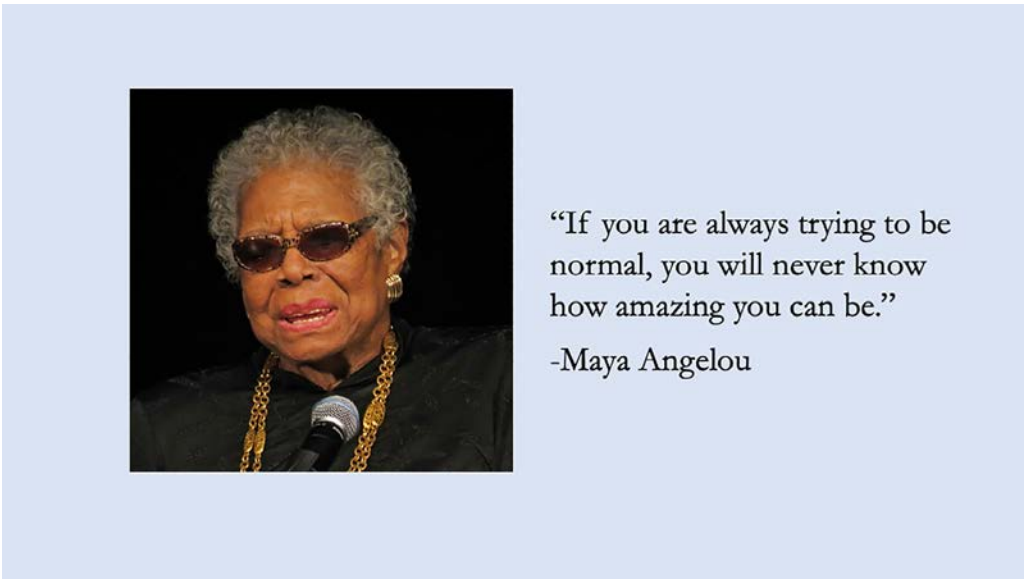

Figure 1. The poet and author Maya Angelou felt that trying to be normal prevented you from being amazing. In the last 20 months, the ACR has maintained normal operations while accomplishing truly amazing things.

I think that for her, being normal meant doing the things people expected her to do and being amazing meant achieving greatness that was never anticipated. In this regard, I think that the ACR and the providers it represents are beyond normal; they exceed all expectations.

In truth, I cannot imagine anything more amazing than the ACR's response to the COVID pandemic and its effect on rheumatology providers, rheumatology patients, and rheumatology trainees. Most of these activities were started by Dr. Ellen Gravallese, ACR President last year, and we are in debt to her for her foresight and ability to issue several simultaneous "calls to action." Task forces charged with providing members with guidance for the management of adult and pediatric patients with rheumatic diseases who were exposed to, or infected with, SARS–CoV-2 (2,3) as well as the multisystem inflammatory syndrome in children (4) continue to be updated and published on the ACR website well before they appear in our journals. Just as amazing, a task force headed by Dr. Jeff Curtis from the University of Alabama at Birmingham and consisting of rheumatologists, infectious disease specialists, and vaccine experts met as soon as the Pfizer mRNA vaccine was approved last December, and in a little over a 1-month period produced the first of 4 versions of guidance for the administration of COVID-19 vaccines in our patients (5). This guidance has been instrumental in answering questions about whether COVID vaccines were safe in patients with autoimmune conditions, how we might optimize responses to vaccines by temporarily stopping some of the medications that could affect an immune response, and whether our patients should get additional immunizations due to the possibility of poor initial responses. In this process of generating multiple versions of these COVID-19 guidance documents, we learned that rapid-cycle revision is possible when new data are available, and this suggests that we can offer real-time updates to the advice we give our providers and patients on other topics in the future.

While the College was outstanding in its communication to providers about the use of COVID-19 vaccines through town halls and several *ACR on Air* podcasts, we know that concerns in our patients were quickly apparent and frustrated what we hoped would be the key to a quick end of the pandemic. We were thrilled to have Dr. Kimberly Manning, Professor of Medicine and the associate vice-chair of diversity, equity and inclusion at Emory University in Atlanta, provide her insight and wisdom on overcoming vaccine hesitancy and concerns. Dr. Manning is one of America's foremost medical educators, whose writing is full of passion and deep understanding of the human condition. She is acclaimed for her stories of how the patients at Grady Hospital are often the real teachers of the medical staff. She led a masterful discussion of how to overcome individual patient concerns by asking "What is your Why?" Ask and then listen. Remember the patient is a person with their own lived experience. Don't judge their concerns. Keep talking and don't give up (Figure 2). If you did not have an opportunity to view this amazing talk, it is still available on the ACR website along with all the other recorded material on COVID-19 clinical topics and patient education.

One of the most incredible things that has happened in the last 20 months has been the creation of the COVID-19 Global Rheumatology Alliance, or GRA (6). This effort came about one evening on Twitter when several rheumatologists wondered whether a registry would help answer questions about the effects of SARS–CoV-2 on patients with rheumatic and autoimmune musculoskeletal diseases. I watched as this idea circled the globe and took hold with people volunteering to create the infrastructure

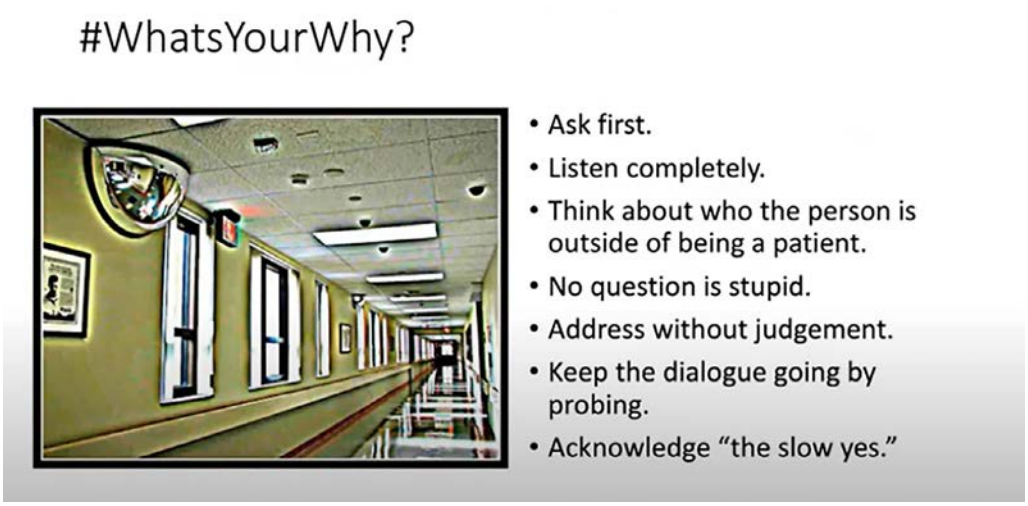

Figure 2. Dr. Kimberly Manning spoke to ACR members about COVID vaccine concerns in patients. This is her approach to helping providers understand their patients' reasons for not getting vaccinated and how to maintain an open dialog.

needed online and beginning to formulate the questions to be answered. I think the result has been spectacular. The ACR assisted the GRA by making it a section of the College, providing administrative support and structure needed to manage this grassroots global project. The GRA has an absolutely stellar steering committee led by Phillip Robinson from Australia and Jinoos Yazdany from San Francisco. The full team is shown in Figure 3.

To date, the GRA has collected data on almost 20,000 individuals with rheumatic and musculoskeletal diseases who have contracted COVID-19, including 9,000 from the European Alliance of Associations for Rheumatology/European registry. In addition, they collected data directly from patients about their experience during the COVID-19 pandemic. Over 14,000 responses were received from all 50 US states and over 100 countries around the globe. They are currently collecting

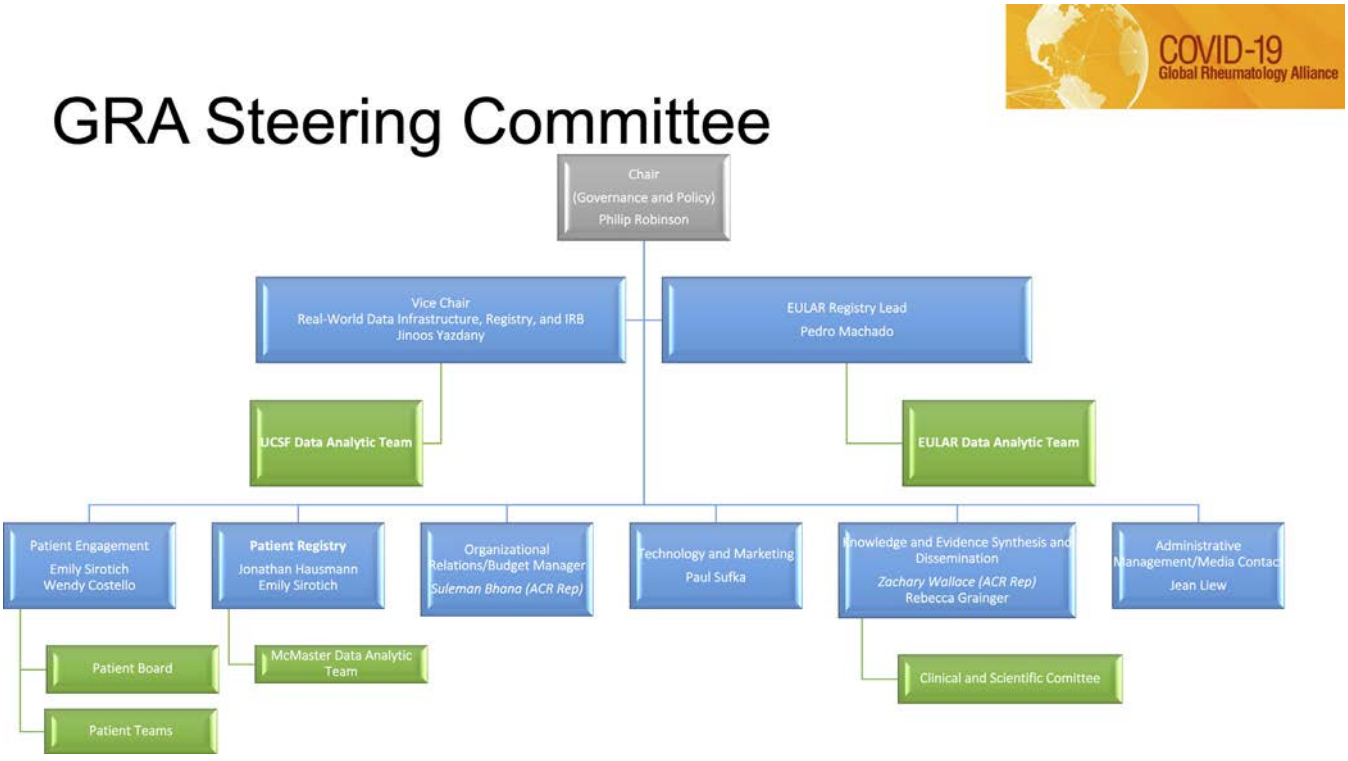

Figure 3. The organizational structure of the COVID-19 Global Rheumatology Alliance.

Figure 4. With many academic teaching conferences cancelled and fellows-in-training assigned to other clinical duties, the Virtual Rheumatology Program was developed. It provided an opportunity for trainees across the globe to access learning provided by experts in the field on their own schedule.

data from patients on their experience with COVID-19 vaccination.

Beginning with ACR Convergence 2020 and continuing over the past year, the GRA has presented and published nearly 30 manuscripts related to COVID-19 and issues important to rheumatology. They have shown the association of both poor disease control as well as certain drugs, such as high-dose corticosteroids, Janus kinase inhibitors, and rituximab, with COVID-19 severity and death. Their patient surveys revealed the extent to which COVID-19 changed the lives of people with rheumatic diseases. For example, 27% had a change in employment status and nearly 20% discontinued at least one of their antirheumatic medications because of unavailability or fears of immunosuppression. At Convergence 2021 beginning tomorrow, the GRA continues to present important insights into the effect of COVID-19 on specific patient populations including people with lupus and vasculitis, as well as the effect of the pandemic on rheumatology trainees and patients' perceptions of telehealth.

It is clear that this has been an amazing effort—linking hundreds of individuals around the globe, including patients and trainees in research. Will this be the way of the future? I think so, and the lessons learned from the GRA will be refined and applied to many more questions even when the pandemic is behind us.

I would be remiss if I did not mention the efforts of the Rheumatology Research Foundation in addressing COVID-19. Mere months into the pandemic, the Foundation issued a notice of special interest for research related to COVID-19. Early last winter, they funded 4 high-quality studies, including a prospective analysis of the effects of immunomodulatory therapy on the susceptibility to and outcomes of COVID-19 in patients with inflammatory arthritis, a study of the role of antiphospholipid antibodies in COVID-19, and 2 studies on the optimization of telehealth in rheumatology, including 1 study done exclusively in community rheumatology practices.

While I am speaking about the Rheumatology Research Foundation, it is important to note that this is their 35th anniversary. Since 1982, the Foundation has committed 192 million dollars directly to the mission priorities of increasing patient access to rheumatology and accelerating discoveries affecting patient care. They have funded over 4,000 awards for recruitment, education and training, career development research, and innovation. In this fiscal year, the Foundation has committed nearly 13 million dollars to awards across their portfolio—a 12% increase over last year. You will be hearing more about the Rheumatology Research Foundation from its President, Dr. Lou Bridges, throughout Convergence, and I urge you to visit the Foundation exhibits on the Convergence platform. The Rheumatology Research Foundation is the largest nongovernmental funder of research and training in rheumatology and is a model organization for other specialty societies. In addition to this being a special anniversary year for the Foundation, I am pleased to announce that they have a new executive director. After a national search, Ms. Rachel Myslinski, the ACR Vice-President of Practice, Advocacy, and Quality, was selected to lead the Foundation. Rachel brings years of experience at the ACR, overseeing our guidelines process, our interactions with elected officials, and most importantly, the development of our hugely successful RISE registry. We are all thrilled that she brings these skills to her new position promoting research and training to enhance the lives of patients with rheumatic and musculoskeletal diseases. Please join me in congratulating Ms. Myslinski on her new role, and the Rheumatology Research Foundation for a fantastic 35 years with many more to come.

In February of 2020, the ACR Board of Directors held their last in person meeting. At that meeting they approved a strategic

plan for the ACR's educational activities. One of the goals of that plan was to investigate the possibility of having virtual meetings sometime in the next several years. Obviously, we achieved that goal early as all our conferences were transitioned to online events last year. Despite the drawbacks of virtual lectures and gatherings, I have to say this is another area where rheumatology has excelled. In 2020, our first all-virtual ACR Convergence had over 14,000 scientific attendees from 111 countries, setting a new record. There were nearly 300 more US attendees and more than 3,000 additional international registrants compared to 2019. While the necessity of the pandemic forced a virtual meeting upon us, it seems clear that there are many individuals for whom travel or time away from the office or family is a barrier to attending, and we now have the opportunity to reach a wider audience.

The ubiquitous virtual conferencing technology thrust upon us by the pandemic also spurred innovation in education. Led by Dr. Anisha Dua and Dr. Marcy Bolster, a group of rheumatology fellowship training directors and the ACR Committee on Training and Workforce realized that this was an opportunity to provide novel educational experiences to rheumatology fellows whose weekly in-person conferences had been cancelled due to COVID-19 closings and schedule changes. They developed 3 highly successful programs (7). Virtual Rheumatology Learning, or ViRL, consisted of 24 lectures on topics typically encountered in fellowship curriculum. Nearly 2,000 adult and pediatric fellows from 55 countries participated in these lectures (Figure 4). Typically, 500 learners were in the audience when the lecture was presented live, and each recorded lecture was viewed nearly 900 times. The Virtual Rheumatology Practicum, or ViP, consisted of 32 lectures aimed at first year fellows who started their training in the summer of 2020. These virtual sessions were designed for US and Canadian adult fellows, although some of them, such as those on the topics of the approach to rheumatologic emergencies, methods of joint aspiration, lupus, and vasculitis, were viewed over 1,500 times by people around the globe. Finally, the Virtual Rheumatology Teaching Lessons, or ViTLs, took place earlier this year, using a sophisticated, interactive learning method to discuss more advanced topics, including inflammatory eye disease, interstitial lung disease, health disparities in lupus, and, of course, COVID-19 in rheumatology. Nearly 800 learners, including 174 from 27 countries outside the US, took part in these sessions.

Each of these educational activities is remarkable not only because they were created in the middle of the COVID-19 pandemic, but also in that they are outstanding examples of how education can be delivered globally and asynchronously, linking the most interesting educators with the most interested learners—when and where it is most convenient for them.

I would now like to turn to an area where the ACR has had incredible success, but without much fanfare or publicity. This is an area where I have a special interest. As a lupus researcher

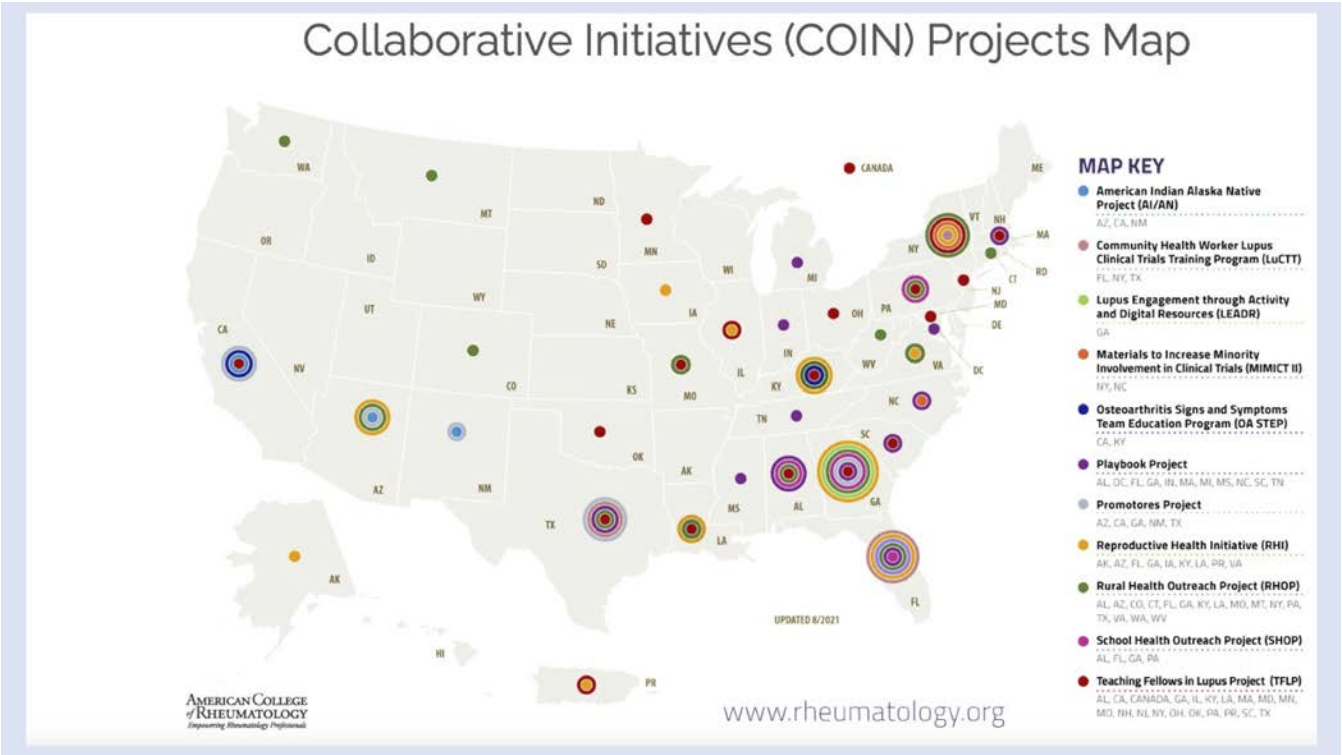

Figure 5. The Collaborative Initiatives (COIN) department of the ACR has activities spanning the entire US designed to address health care disparities and assist providers and patients. This map shows the places and activities of COIN.

Figure 6. I was lucky to have many great mentors, 2 of whom are shown here—Dr. Irving Kushner and Dr. John Atkinson. The CARMA and AMIGO programs of the ACR illustrate the deliberate commitment to mentoring that the College has taken to ensure the success of the next generation of adult and pediatric academic rheumatologists.

and lupus physician in Dallas, Texas, I see health disparities firsthand. I spend much of my time seeing patients in a safety-net hospital serving an underinsured, largely Black and Hispanic population. Our literature in rheumatology, as well as that of other specialties, has clearly documented inequities in health outcomes borne by people of color as well as those with low socioeconomic status (8–11). While ancestry is certain to have some effect, it is clear there are other, more significant, drivers of this health care disparity, including poverty, lack of health insurance, poor access to medical care, environmental exposure, and other structural social barriers to health.

The ACR has pledged to be a leader in the effort to eliminate bias and reduce health disparities (12). One way it is doing this is through the Collaborative Initiatives, or COIN, department within the College. COIN began as a project simply called The Lupus Initiative in 2009 (13). Since that time, it has received over 21 million dollars in grant funding from the Centers for Disease Control and Prevention, the Department of Health and Human Services Office of Minority Health, the Office of Women's Health, and other support. These 30 grants and contracts have led to the creation of a phenomenal catalog of programs aimed at educating health care providers about implicit bias and health care disparity, helping community members understand the issues facing people with chronic rheumatic conditions such as lupus, and tackling the tough problem of including more minority participants in clinical research. This has been a team effort, with 7 full-time staff members and over 90 ACR volunteers involved in the creation and dissemination of these programs. In addition to systemic lupus erythematosus, COIN initiatives have addressed osteoarthritis, rheumatoid arthritis, psoriatic arthritis, and lupus nephritis. Figure 5 shows some of the current COIN projects and places where they have been implemented.

COIN projects are designed to educate and inform health care providers, students, patients with rheumatic and musculoskeletal diseases, and the lay public. By doing so, they try to close some of the health care gaps in communities at risk. Their culturally appropriate materials are being used in a number of settings, including rural health, Native American communities, by students in historically Black colleges and universities, by promotoras who provide health care in Hispanic neighborhoods, and in federally funded community health clinics. There are projects that focus on school health care providers, on medical students, and for rheumatology fellows in training—educational materials they can use at their medical centers or in the community, thus both honing their own teaching skills as well as informing them on the health issues facing many of our patients.

COIN is partnering with academic medical centers such as Morehouse School of Medicine, the University of North Carolina, the University of California at San Francisco, and others. They are creating novel programs that use digital health coaching tools to improve physical activity in lupus patients, ones that use digital disease self-management tools to reduce symptoms and improve health-related quality of life, and others that improve the skills and confidence of primary care providers serving the Navajo Nation to care for patients where there is currently *no* access to a rheumatologist or rheumatology professional.

COIN also collaborates with other ACR departments and offers both CME credits and Maintenance of Certification points for rheumatologists and nonrheumatologists alike who take their online courses in lupus diagnosis, lupus and pregnancy, and coming soon, lupus and health disparities. Lastly, COIN has multiple programs in place to help those of us who do clinical research. There are educational materials for researchers and their staff to help them understand the concerns that Black and

Hispanic patients have about research participation, as well as printed materials for those patients and short videos in both English and Spanish describing the clinical research process.

Through its online messaging, COIN has thus far reached over 9 million individuals. Over 7,000 people have attended in-person events prior to the pandemic, and their training materials have been viewed and downloaded almost 300,000 times. I have been privileged to be associated with COIN from its earliest days. I think it is one of the hidden gems of the ACR and a phenomenal resource for rheumatologists, our trainees, and most importantly, our patients.

The last area of rheumatology excellence I will touch on today is mentorship. I have benefited from many excellent mentors throughout my career. Irving Kushner, a Master of the College, allowed me to work in his lab at what was then Cleveland Metropolitan General Hospital while I was a high school and college student. I learned what a physician-scientist did and was exposed to the field of rheumatology. Irv sparked a curiosity about autoimmunity that was fanned by my next mentor, John Atkinson at Washington University, where I was a medical student. As John mentioned in his ACR Presidential Gold Medal address, we spent many Saturday mornings discussing the great cases he had seen as fellow at the NIH, and what my career could look like (Figure 6).

I was extremely lucky to meet these mentors at critical times in my professional and even pre-professional development. This is an area where the ACR and partner organizations have created outstanding efforts that remove some of the luck in mentoring (14). The CARMA and AMIGO programs link our junior faculty in adult and pediatric rheumatology divisions, respectively, with mentors chosen specifically to meet their career goals and aspirations. In 2020, despite the virtual nature of these mentoring activities, 90% of participants felt these programs enhanced their careers, in terms of both their academic productivity as well as a connection to the profession of rheumatology. Through these facilitated mentor–mentee interactions, the ACR is helping to bring people into our incredible profession and ensuring their successful careers.

I hope these few examples have shown that despite all that has happened in the last 20 months, the ACR, its members, and our global rheumatology community have been accomplishing things that are not just normal. They are truly amazing. We have solved problems we never thought we would have faced, using tools we never imagined would have existed. Rheumatologists and rheumatology health professionals continue to be the most creative, collaborative, and constructive group of people I know. Through these awesome accomplishments, the stage is now set for a better future for our members, our profession, and most of all, for our patients.

I want to conclude by thanking the people who have helped me over the past year. I particularly want to acknowledge the highly engaged and supportive Executive Committee consisting of Ken Saag, Doug White, Deborah Desir, Christine Stamatos, Barbara Slusher, Lou Bridges, and Mike Holers, who have been a joy to work with, as well as our ACR Board of Directors, who have given freely of their time, their knowledge, and their creativity as we dealt with the issues of the present and planned for the ACR of the future. In addition to the many enthusiastic ACR volunteers I have worked with, I am indebted to the stellar ACR staff members whose dedication keeps our College running and who help the volunteers realize their goals. In particular, Julie Anderson, our Senior Director of Governance and Steve Echard, our Executive Vice-President were there by phone, video, or text message to listen to my ideas over the past year.

We all stand on the shoulders of the giants in our field. For me, those have included the 2 UT Southwestern division chiefs who preceded me, the late Morris Ziff—a President of the College—and Peter Lipsky. Both of them taught me important lessons that have held me in good stead for the past 30 years. I also must thank the 9 Presidents of the ACR who have been my friends and my guides while I have served on their Executive Committees and Boards.

I also want to acknowledge my colleagues in the Rheumatic Diseases Division at UT Southwestern who have supported me this year. In particular, our clinical chief, Dr. Bonnie Bermas and the ACR Government Affairs Chair, Dr. Blair Solow were always there to give me perspective. Most importantly, I am eternally grateful for the constant love and support of my wife Corinne and my son Alex. I could not be here today without their tremendous encouragement and equanimity during times when the ACR intruded on our family life.

It has been my honor to serve you as President of the ACR this year. And now, let us begin Convergence 2021.

REFERENCES

1. Berra Y. Yogi Berra quotes. URL: https://www.goodreads.com/quotes/261863-it-s-tough-to-make-predictions-especially-about-the-future.
2. American College of Rheumatology COVID-19 Pediatric Rheumatology Clinical Guidance Task Force. Clinical guidance for pediatric patients with rheumatic disease – version 2. URL: https://www.rheumatology.org/Portals/0/Files/COVID-19-Clinical-Guidance-Summary-for-Pediatric-Patients-with-Rheumatic-Disease.pdf.
3. American College of Rheumatology COVID-19 Clinical Guidance Task Force. COVID-19 clincal guidance for adult patients with rheumatic diseases. URL: https://www.rheumatology.org/Portals/0/Files/ACR-COVID-19-Clinical-Guidance-Summary-Patients-with-Rheumatic-Diseases.pdf.
4. American College of Rheumatology MIS-C and COVID-19 Related Hyperinflammation Task Force. Clinical guidance for pediatric patients with multisystem inflammatory sndrome in children (MIS-C) associated with SARS-CoV-2 and hyperinflammation in COVID-19. URL: https://www.rheumatology.org/Portals/0/Files/ACR-COVID-19-Clinical-Guidance-Summary-MIS-C-Hyperinflammation.pdf.
5. American College of Rheumatology COVID-19 Vaccine Clinical Guidance Task Force. COVID-19 vaccine clinical guidance summary for patients with rheumatic and musculoskeletal diseases. URL: https://www.rheumatology.org/Portals/0/Files/COVID-19-Vaccine-Clinical-Guidance-Rheumatic-Diseases-Summary.pdf.
6. COVID-19 Global Rheumatology Alliance. The global rheumatiology community's response to the worldwide COVID-19 pandemic. URL: https://rheum-covid.org.

7. American College of Rheumatology Committee on Training and Workforce. Virtual rheumatology program: fellows in training. URL: https://www.rheumatology.org/I-Am-A/Fellow-in-Training/Virtual-Rheumatology-Program.
8. Yip K, Navarro-Millan I. Racial, ethnic, and healthcare disparities in rheumatoid arthritis. Curr Opin Rheumatol 2021;33:117–21.
9. Pryor KP, Barbhaiya M, Costenbader KH, Feldman CH. Disparities in lupus and lupus nephritis care and outcomes among US Medicaid beneficiaries. Rheum Dis Clin North Am 2021;47:41–53.
10. Izadi Z, Li J, Evans M, Hammam N, Katz P, Ogdie A, et al. Socioeconomic disparities in functional status in a national sample of patients with rheumatoid arthritis. JAMA Netw Open 2021;4:e2119400.
11. Drenkard C, Lim SS. Update on lupus epidemiology: advancing health disparities research through the study of minority populations. Curr Opin Rheumatol 2019;31:689–96.
12. American College of Rheumatology Board of Directors. ACR statement on racial disparities. URL: https://www.rheumatology.org/Portals/0/Files/ACR-Statement-on-Racial-Disparities.pdf.
13. American College of Rheumatology Collaborative Initiatives. The lupus initiative. URL: https://thelupusinitiative.org.
14. American College of Rheumatology Committee on Training and Workforce. Mentoring. https://www.rheumatology.org/Get-Involved/Mentoring.

Arthritis & Rheumatology
Vol. 74, No. 3, March 2022, pp 383–385
DOI 10.1002/art.41984

American College of Rheumatology
Empowering Rheumatology Professionals

EDITORIAL

New Classification Criteria for Small-Vessel Vasculitis: Is Antineutrophil Cytoplasmic Antibody Inclusion Their Major Advance?

Christian Dejaco[1] and Loïc Guillevin[2]

Vasculitis is the generic term characterizing an inflammatory disease of the blood vessels that affects arteries and veins of different types, sizes, and histologies. Clinical manifestations can be relatively specific for a single vasculitic entity (e.g., anterior ischemic optic neuropathy for giant cell arteritis) or common to several vasculitides (e.g., pauci-immune glomerulonephritis). Most vasculitides are primary, but some develop secondary to viral infections, malignancies, genetic abnormalities, other autoimmune diseases, or drugs. Therefore, classifications, nomenclatures, and diagnostic criteria are needed to facilitate their description and distinction, and foster academic studies among clinicians and researchers all over the world (1–3).

In this issue of *Arthritis & Rheumatology*, the 2022 American College of Rheumatology (ACR)/European Alliance of Associations for Rheumatology (EULAR) classification criteria for granulomatosis with polyangiitis (GPA) (4), microscopic polyangiitis (MPA) (5), and eosinophilic granulomatosis with polyangiitis (EGPA) (6) are presented. They are based on the analysis of the most ambitious prospective cohort study ever on vasculitis, the Diagnostic and Classification Criteria in Vasculitis (DCVAS) project, involving almost 7,000 patients from 136 sites worldwide. The methodology for the development of criteria was robust, including a mixture of a data-driven approach to derive and weight the individual items of the criteria, expert opinion, and final validation.

According to the new criteria, a patient can only be classified as having a specific entity if 2 requirements are fulfilled: 1) an established diagnosis of small- or medium-vessel vasculitis and 2) the exclusion of vasculitis mimics. Weighted parameters are then combined to obtain a final score, with cutoffs of 5 points for GPA and MPA, and 6 points for EGPA. The new criteria outperformed the 1990 ACR classification criteria for GPA and EGPA (2,3) with regard to sensitivity and specificity using the DCVAS data set, whereas for MPA, no previous criteria had been available. Unlike the version preceding the 1990 ACR vasculitis criteria and the Chapel Hill Consensus Conference nomenclature (1), these new classification criteria focus predominantly on vasculitides characterized by their belonging to the antineutrophil cytoplasmic antibody (ANCA)–associated small-vessel vasculitis group.

A major question is how the 2022 ACR/EULAR classification criteria will be used in real life. The purpose of classification is to distinguish GPA, MPA, and EGPA from one another and from other forms of vasculitis and mimics of vasculitis. Classification criteria are designed for drug trials and other academic studies. However, it is highly likely that clinicians will also use them to guide their clinical and therapeutic decisions, and probably also misuse them for diagnostic purposes, like earlier classification criteria. It is clear that diagnoses of patients included in the DCVAS cohort were largely based on the detection of ANCAs and, more specifically, antimyeloperoxidase (anti-MPO) and anti–proteinase 3 (anti-PR3). As a consequence, the criteria of ANCA detection and type outweighed the other (diagnostically relevant) typical characteristics of small-vessel vasculitis, such as certain clinical manifestations (e.g., constitutional symptoms or skin lesions) or histologically confirmed pauci-immune glomerulonephritis, which are either not included among the new classification criteria or were accorded relatively low weights. Patients with ANCA-negative limited GPA, for example, would hardly fulfill the new classification criteria and therefore be missed if the criteria were (mis)used for diagnostic purposes (4).

The main objective of the experts developing the 2022 ACR/EULAR classification criteria seemed to be distinguishing among GPA, MPA, and EGPA, given the high number of cases selected as comparators, in order to derive the individual parameters and their weights by statistical means. Regarding the

[1]Christian Dejaco, MD, PhD, MBA: Medical University of Graz, Graz, Austria, and Hospital of Brunico (SABES-ASDAA), Brunico, Italy; [2]Loïc Guillevin, MD: French Vasculitis Study Group and University Paris Descartes, Paris, France.

Dr. Dejaco has received consulting fees, speaking fees, and/or honoraria from AbbVie, Roche, Pfizer, Lilly, Sanofi, Janssen, and Novartis (less than $10,000 each). Dr. Guillevin has received research support from Roche.

Address correspondence to Christian Dejaco, MD, PhD, MBA, Hospital of Brunico (SABES-ASDAA), Department of Rheumatology, Spitalstraße 11, 39031 Brunico, Italy. Email: christian.dejaco@gmx.net.

Submitted for publication March 4, 2021; accepted in revised form September 21, 2021.

classification criteria for GPA, for example, 64% of comparator cases had either MPA or EGPA. It remains debatable whether the distinction between GPA and MPA is central, or whether greater attention should have been placed on distinguishing them from other types of vasculitides and vasculitis mimics, given that several therapeutic trials, even the most recent, considered GPA and MPA as a single group. This may certainly have practical reasons, fostering recruitment of patients with rare diseases into a drug trial; however, randomization was stratified according to ANCA status rather than clinical diagnosis (7,8).

Among the vasculitides, EGPA has a special place because, in addition to its characteristics, specific phenotypes have been described, supported by the presence or absence of anti–MPO-ANCA (9) and specific genomic variants associated with ANCA positivity (10). Classification—separating EGPA from other vasculitides and mimics—is a major task, especially for patients with asthma with eosinophilia. A patient with obstructive airway disease and nasal polyps can now be classified as having EGPA if a diagnosis of small-vessel vasculitis has been determined. Another challenge is to distinguish EGPA from hypereosinophilic syndrome; however, the 2022 ACR/EULAR classification criteria are not intended to differentiate EGPA from other related hypereosinophilic syndromes or eosinophilic-associated malignancies (6).

The detection of cytoplasmic ANCA or anti–PR3-ANCA is sufficient to categorize a patient with small-vessel vasculitis as having GPA, and perinuclear ANCA or anti–MPO-ANCA positivity classifies a patient as having MPA. All other clinical characteristics are relevant in those relatively uncommon ANCA-negative, ANCA double-positive, anti–MPO-ANCA–positive GPA, or anti–PR3-ANCA–positive MPA patients. Similarly, elevated eosinophilic counts are a much stronger predictor of EGPA than any other parameter. Indeed, blood eosinophil counts $\geq 1 \times 10^9$/liter alone would result in classification of a patient as having EGPA, if a slightly lower specificity of the criteria (with a threshold of 97.5% for 5 points, instead of 99.1% for 6 points) were to be accepted.

The main point of the discussion here is whether the clinical distinction between GPA and MPA is still relevant, or whether classification based on ANCA test results would be more appropriate. PR3-ANCA and MPO-ANCA normally go hand in hand with the clinical diagnoses of GPA and MPA, respectively, as also reflected by the new classification criteria. However, observational study results indicated that clinical course (PR3-ANCA– or MPO-ANCA–associated vasculitis predicting a relapsing course or higher mortality, respectively) (11,12), genetic susceptibility (13), inflammatory cytokine profiles (14), or response to rituximab (15) are more closely associated with serologic ANCA detection than with clinical classification.

What is the way forward from these new classification criteria? Undoubtedly, they will be applied in research and will help reduce some uncertainties concerning the classification of patients included in clinical trials. The concern is that clinicians will misuse the criteria for diagnostic purposes, as is commonly but inappropriately done in clinical practice with other classification criteria (16).

Because the DCVAS cohort is large and well-documented, we suggest that the authors also consider diagnostic criteria, especially for EGPA, for which it is not easy to establish a diagnosis and classify patients. The development of diagnostic criteria is certainly challenging given the absence of a gold standard and the fact that such criteria must reflect the different features of the disease (17). The ACR has decided, in part because of these issues but also due to legal and financial implications, to no longer consider funding or endorsement of diagnostic criteria (17).

The yardstick by which small- or medium-vessel vasculitides are diagnosed still needs to be specified; otherwise, it will remain a source of heterogeneity, given that not all investigators enrolling patients in clinical trials have the same level of mastery as the experts who formulated the classification criteria. The debate about whether patients would be more appropriately classified according to clinical phenotype or ANCA type will continue, and, perhaps in the future, revised classification and/or diagnostic criteria will be based on serology, genetics, and other parameters rather than on clinical phenotypes alone.

AUTHOR CONTRIBUTIONS

Drs. Dejaco and Guillevin drafted the article, revised it critically for important intellectual content, and approved the final version to be published.

REFERENCES

1. Jennette JC, Falk RJ, Bacon PA, Basu N, Cid MC, Ferrario F, et al. 2012 revised International Chapel Hill Consensus Conference nomenclature of vasculitides. Arthritis Rheum 2013;65:1–11.
2. Leavitt RY, Fauci AS, Bloch DA, Michel BA, Hunder GG, Arend WP, et al. The American College of Rheumatology 1990 criteria for the classification of Wegener's granulomatosis. Arthritis Rheum 1990; 33:1101–7.
3. Masi AT, Hunder GG, Lie JT, Michel BA, Bloch DA, Arend WP, et al. The American College of Rheumatology 1990 criteria for the classification of Churg-Strauss syndrome (allergic granulomatosis and angiitis). Arthritis Rheum 1990;33:1094–100.
4. Robson JC, Grayson PC, Ponte C, Suppiah R, Craven A, Judge A, et al. 2022 American College of Rheumatology/European Alliance of Associations for Rheumatology classification criteria for granulomatosis with polyangiitis. Arthritis Rheumatol 2022;74:393–9.
5. Suppiah R, Robson JC, Grayson PC, Ponte C, Craven A, Khalid S, et al. 2022 American College of Rheumatology/European Alliance of Associations for Rheumatology classification criteria for microscopic polyangiitis. Arthritis Rheumatol 2022;74:400–6.
6. Grayson PC, Ponte C, Suppiah R, Robson JC, Craven A, Judge A, et al. 2022 American College of Rheumatology/European Alliance of Associations for Rheumatology classification criteria for eosinophilic granulomatosis with polyangiitis. Arthritis Rheumatol 2022;74:386–92.

7. Jayne DR, Merkel PA, Schall TJ, Bekker P, ADVOCATE Study Group. Avacopan for the treatment of ANCA-associated vasculitis. N Engl J Med 2021;384:599–609.
8. Walsh M, Merkel PA, Peh CA, Szpirt WM, Puéchal X, Fujimoto S, et al. Plasma exchange and glucocorticoids in severe ANCA-associated vasculitis. N Engl J Med 2020;382:622–31.
9. Sablé-Fourtassou R, Cohen P, Mahr A, Pagnoux C, Mouthon L, Jayne D, et al. Antineutrophil cytoplasmic antibodies and the Churg-Strauss syndrome. Ann Intern Med 2005;143:632–8.
10. Lyons PA, Peters JE, Alberici F, Liley J, Coulson RM, Astle W, et al. Genome-wide association study of eosinophilic granulomatosis with polyangiitis reveals genomic loci stratified by ANCA status. Nat Commun 2019;10:5120.
11. Lionaki S, Blyth ER, Hogan SL, Hu Y, Senior BA, Jennette CE, et al. Classification of antineutrophil cytoplasmic autoantibody vasculitides: the role of antineutrophil cytoplasmic autoantibody specificity for myeloperoxidase or proteinase 3 in disease recognition and prognosis. Arthritis Rheum 2012;64:3452–62.
12. Schirmer JH, Wright MN, Herrmann K, Laudien M, Nölle B, Reinhold-Keller E, et al. Myeloperoxidase–antineutrophil cytoplasmic antibody (ANCA)–positive granulomatosis with polyangiitis (Wegener's) is a clinically distinct subset of ANCA-associated vasculitis: a retrospective analysis of 315 patients from a German vasculitis referral center. Arthritis Rheumatol 2016;68:2953–63.
13. Lyons PA, Rayner TF, Trivedi S, Holle JU, Watts RA, Jayne DR, et al. Genetically distinct subsets within ANCA-associated vasculitis. N Engl J Med 2012;367:214–23.
14. Berti A, Warner R, Johnson K, Cornec D, Schroeder D, Kabat B, et al. Circulating cytokine profiles and antineutrophil cytoplasmic antibody specificity in patients with antineutrophil cytoplasmic antibody–associated vasculitis. Arthritis Rheumatol 2018;70:1114–21.
15. Unizony S, Villarreal M, Miloslavsky EM, Lu N, Merkel PA, Spiera R, et al. Clinical outcomes of treatment of anti-neutrophil cytoplasmic antibody (ANCA)-associated vasculitis based on ANCA type. Ann Rheum Dis 2016;75:1166–9.
16. June RR, Aggarwal R. The use and abuse of diagnostic/classification criteria. Best Pract Res Clin Rheumatol 2014;28:921–34.
17. Aggarwal R, Ringold S, Khanna D, Neogi T, Johnson SR, Miller A, et al. Distinctions between diagnostic and classification criteria? [review]. Arthritis Care Res (Hoboken) 2015;67:891–7.

American College of Rheumatology
Empowering Rheumatology Professionals

Arthritis & Rheumatology
Vol. 74, No. 3, March 2022, pp 386–392
DOI 10.1002/art.41982

2022 American College of Rheumatology/European Alliance of Associations for Rheumatology Classification Criteria for Eosinophilic Granulomatosis With Polyangiitis

Peter C. Grayson,[1] Cristina Ponte,[2] Ravi Suppiah,[3] Joanna C. Robson,[4] Anthea Craven,[5] Andrew Judge,[6] Sara Khalid,[5] Andrew Hutchings,[7] Raashid A. Luqmani,[5] Richard A. Watts,[8] and Peter A. Merkel[9]

This criteria set has been approved by the American College of Rheumatology (ACR) Board of Directors and the European Alliance of Associations for Rheumatology (EULAR) Executive Committee. This signifies that the criteria set has been quantitatively validated using patient data, and it has undergone validation based on an independent data set. All ACR/EULAR-approved criteria sets are expected to undergo intermittent updates.

The ACR is an independent, professional, medical and scientific society that does not guarantee, warrant, or endorse any commercial product or service.

Objective. To develop and validate revised classification criteria for eosinophilic granulomatosis with polyangiitis (EGPA).

Methods. Patients with vasculitis or comparator diseases were recruited into an international cohort. The study proceeded in 5 phases: 1) identification of candidate criteria items using consensus methodology, 2) prospective collection of candidate items present at the time of diagnosis, 3) data-driven reduction of the number of candidate items, 4) expert panel review of cases to define the reference diagnosis, and 5) derivation of a points-based risk score for disease classification in a development set using least absolute shrinkage and selection operator logistic regression, with subsequent validation of performance characteristics in an independent set of cases and comparators.

Results. The development set for EGPA consisted of 107 cases of EGPA and 450 comparators. The validation set consisted of an additional 119 cases of EGPA and 437 comparators. From 91 candidate items, regression analysis identified 11 items for EPGA, 7 of which were retained. The final criteria and their weights were as follows: maximum eosinophil count ≥1 × 10^9/liter (+5), obstructive airway disease (+3), nasal polyps (+3), cytoplasmic antineutrophil cytoplasmic antibody (ANCA) or anti–proteinase 3 ANCA positivity (−3), extravascular eosinophilic predominant inflammation (+2), mononeuritis multiplex/motor neuropathy not due to radiculopathy (+1), and hematuria (−1). After excluding mimics of vasculitis, a patient with a diagnosis of small- or medium-vessel vasculitis could be classified as having EGPA if the cumulative score was ≥6 points. When these criteria were tested in the validation data set, the sensitivity was 85% (95% confidence interval [95% CI] 77–91%) and the specificity was 99% (95% CI 98–100%).

Conclusion. The 2022 American College of Rheumatology/European Alliance of Associations for Rheumatology classification criteria for EGPA demonstrate strong performance characteristics and are validated for use in research.

This article is published simultaneously in the March 2022 issue of *Annals of the Rheumatic Diseases*.

The Diagnostic and Classification Criteria in Vasculitis (DCVAS) study, of which the development of these classification criteria was a part, was funded by grants from the American College of Rheumatology (ACR), the European Alliance of Associations for Rheumatology (EULAR), the Vasculitis Foundation, and the University of Pennsylvania Vasculitis Center.

[1]Peter C. Grayson, MD, MSc: National Institute of Arthritis and Musculoskeletal and Skin Diseases, NIH, Bethesda, Maryland; [2]Cristina Ponte, MD, PhD: Hospital de Santa Maria, Centro Hospitalar Universitário Lisboa Norte, Universidade de Lisboa, and Centro Académico de Medicina de Lisboa, Lisbon, Portugal; [3]Ravi Suppiah, MD: Auckland District Health Board, Auckland, New Zealand; [4]Joanna C. Robson, MBBS, PhD: Centre for Health and Clinical Research, University of the West of England, and University Hospitals and Weston NHS Foundation Trust, Bristol, UK; [5]Anthea Craven, BSc, Sara Khalid, DPhil, Raashid A Luqmani, DM, FRCP: Oxford NIHR Biomedical Research Centre and University of Oxford, Oxford, UK; [6]Andrew Judge, PhD: Oxford NIHR Biomedical Research Centre and University of Oxford, Oxford, UK, and Bristol NIHR Biomedical Research Centre and University of Bristol, Bristol, UK; [7]Andrew Hutchings, MSc: London School of Hygiene and Tropical Medicine, London, UK;

INTRODUCTION

Eosinophilic granulomatosis with polyangiitis (EGPA), formerly known as Churg-Strauss syndrome, is a form of vasculitis that is histologically defined by eosinophil-rich, necrotizing granulomatous inflammation primarily involving the respiratory tract, along with necrotizing vasculitis of small- to medium-sized arteries (1). EGPA is considered a form of antineutrophil cytoplasmic antibody (ANCA)–associated vasculitis (AAV), along with granulomatosis with polyangiitis (GPA) and microscopic polyangiitis (MPA). ANCAs are detected in ~40–60% of patients with EGPA and are typically directed against myeloperoxidase (MPO) (2,3).

In 1990, the American College of Rheumatology (ACR) published classification criteria for EGPA (4). By current standards, these criteria have never been validated because they were developed using data from only 20 patients with EGPA without independent test and validation sets. Furthermore, the criteria were derived by comparing clinical data from patients with EGPA to data from 787 patients with other forms of vasculitis. Many of these comparators were patients with giant cell arteritis, a form of large-vessel vasculitis that is typically not difficult to readily distinguish from EGPA based on obvious clinical differences. Despite these methodologic weaknesses, the 1990 ACR criteria for EGPA have existed unchanged for several decades and have been useful to advance clinical research in these diseases. This article outlines the development and validation of the new ACR/European Alliance of Associations for Rheumatology (EULAR)–endorsed classification criteria for EGPA.

METHODS

A detailed and complete description of the methods involved in the development and validation of the classification criteria for EGPA is provided in Supplementary Appendix 1, available on the *Arthritis & Rheumatology* website at http://onlinelibrary.wiley.com/doi/10.1002/art.41982/abstract. Briefly, an international Steering Committee comprising clinician investigators with expertise in vasculitis, statisticians, and data managers was established to oversee the overall Diagnostic and Classification Criteria in Vasculitis (DCVAS) project (5). The Steering Committee established a 5-stage plan using data-driven and consensus methodology to develop the criteria for each of 6 forms of vasculitis.

Stage 1: generation of candidate classification items for the systemic vasculitides. Candidate classification items were generated by expert opinion and reviewed by a group of vasculitis experts across a range of specialties using a nominal group technique.

Stage 2: DCVAS prospective observational study. A prospective, international, multisite observational study was conducted (see Appendix A for study investigators and sites). Ethical approval was obtained from national and local ethics committees. Consecutive patients representing the full spectrum of disease were recruited from academic and community practices. Patients were included if they were 18 years or older and had a diagnosis of vasculitis or a condition that mimics vasculitis. Patients with AAV could only be enrolled within 2 years of diagnosis. Only data present at diagnosis were recorded.

Stage 3: refinement of candidate items specifically for AAV. The Steering Committee conducted a data-driven process to reduce the number of candidate items of relevance to cases and comparators for AAV. Items were selected for exclusion if they had a prevalence of <5% within the data set and/or they were not clinically relevant for classification criteria (e.g., related to infection, malignancy, or demographic characteristics). Low-frequency items of clinical importance could be combined, when appropriate.

Stage 4: expert review to derive a gold standard–defined final set of cases of AAV. Experts in vasculitis from a wide range of geographic locations and specialties reviewed all submitted cases of vasculitis and a random subset of mimics of vasculitis. Each reviewer was asked to review ~50 submitted cases to confirm the diagnosis and to specify the certainty of their diagnosis as follows: very certain, moderately certain, uncertain, or very uncertain. Only cases agreed upon with at least moderate certainty were retained for further analysis.

Stage 5: derivation and validation of the final classification criteria for EGPA. The DCVAS AAV data set was randomly split into development (50%) and validation (50%) sets. Comparisons were performed between cases of EGPA and a comparator group randomly selected from the DCVAS cohort in the following proportions: another type of AAV (including GPA and MPA), 60%; another form of small-vessel vasculitis (e.g., cryoglobulinemic vasculitis) or medium-vessel

[8]Richard A. Watts, MD: Oxford NIHR Biomedical Research Centre and University of Oxford, Oxford, UK, and University of East Anglia, Norwich, UK; [9]Peter A. Merkel, MD, MPH: University of Pennsylvania, Philadelphia.

[Correction added on 20 June 2022, after first online publication: Appendices A and S1 have been replaced and Appendix S2 has been added online.]

Author disclosures are available at https://onlinelibrary.wiley.com/action/downloadSupplement?doi=10.1002%2Fart.41982&file=art41982-sup-0001-Disclosureform.pdf.

Address correspondence to Peter A. Merkel, MD, MPH, Chief, Division of Rheumatology, University of Pennsylvania, White Building, Fifth Floor, 3400 Spruce Street, Philadelphia, PA 19104 (email: pmerkel@upenn.edu); or to Raashid A. Luqmani, DM, FRCP, Rheumatology Department, Nuffield Orthopaedic Centre, University of Oxford, Windmill Road, Oxford OX3 7LD, UK (email: raashid.luqmani@ndorms.ox.ac.uk).

Submitted for publication February 28, 2020; accepted in revised form September 21, 2021.

vasculitis (e.g., polyarteritis nodosa), 40%. Least absolute shrinkage and selection operator (lasso) logistic regression was used to identify items from the data set and create a parsimonious model including only the most important items. The final items in the model were formulated into a clinical risk-scoring tool with each factor assigned a weight based on its respective regression coefficient. A threshold that best balanced sensitivity and specificity was identified for classification.

In sensitivity analyses, the final classification criteria were applied to an unselected population of cases and comparators from the DCVAS data set based on the submitting physician diagnosis. Comparison was also made between the measurement properties of the new classification criteria for EGPA and the 1990 ACR classification criteria for EGPA using pooled data from the development and validation sets.

RESULTS

Generation of candidate classification items for the systemic vasculitides. The Steering Committee identified >1,000 candidate items for the DCVAS case report form (see Supplementary Appendix 2, available on the *Arthritis & Rheumatology* website at http://onlinelibrary.wiley.com/doi/10.1002/art.41982/abstract).

DCVAS prospective observational study. Between January 2011 and December 2017, the DCVAS study recruited 6,991 participants from 136 sites in 32 countries. Information on the DCVAS sites, investigators, and participants is listed in Supplementary Appendices 3, 4, and 5, available on the *Arthritis & Rheumatology* website at http://onlinelibrary.wiley.com/doi/10.1002/art.41982/abstract.

Refinement of candidate items specifically for AAV. Following a data-driven and expert consensus process, 91 items from the DCVAS case report form were retained for regression analysis, including 45 clinical (14 composite), 18 laboratory (2 composite), 12 imaging (all composite), and 16 biopsy (1 composite) items. Some clinical items were removed in favor of similar but more specific pathophysiologic descriptors. For example, "Hearing loss or reduction" was removed, and the composite item "Conductive hearing loss/sensorineural hearing loss" was retained. See Supplementary Appendix 6, available on the *Arthritis & Rheumatology* website at http://onlinelibrary.wiley.com/doi/10.1002/art.41982/abstract, for the final candidate items used in the derivation of the classification criteria for GPA, MPA, and EGPA.

Expert review to derive a gold standard–defined final set of cases of AAV. Fifty-five independent experts reviewed vignettes derived from the case report forms for 2,871 cases submitted with a diagnosis of either small-vessel vasculitis (90% of case report forms) or another type of vasculitis or a mimic of vasculitis (10% of case report forms). The characteristics of the expert reviewers are shown in Supplementary Appendix 7, available on the *Arthritis & Rheumatology* website at http://onlinelibrary.wiley.com/doi/10.1002/art.41982/abstract. A flow chart showing the results of the expert review process is shown in Supplementary Appendix 8, available on the *Arthritis & Rheumatology* website at http://onlinelibrary.wiley.com/doi/10.1002/art.41982/abstract. A total of 2,072 cases (72%) passed the process and were designated as cases of vasculitis; these cases were used for the stage 5 analyses.

After expert panel review, 226 of 315 cases of EGPA were retained for subsequent analysis. Compared to patients who were retained, patients who were excluded from further analysis

Table 1. Demographic and disease features of cases of EGPA and comparators*

	EGPA (n = 226)	Comparators (n = 887)†	*P*
Age, mean ± SD years	52.9 ± 14.4	56.2 ± 17.6	0.009
Sex, no. (%) female	113 (50.0)	445 (50.2)	1.000
Maximum serum creatinine, mean ± SD			<0.001
μmoles/liter	85.0 ± 53.6	205.90 ± 237.0	
mg/dl	0.96 ± 0.6	2.33 ± 2.7	
cANCA positive, no. (%)	17 (7.5)	251 (28.3)	<0.001
pANCA positive, no. (%)	83 (36.7)	289 (32.6)	0.271
Anti–PR3-ANCA positive, no. (%)	7 (3.1)	264 (29.8)	<0.001
Anti–MPO-ANCA positive, no. (%)	98 (43.4)	323 (36.4)	0.065
Maximum eosinophil count ≥1 × 10^9/liter, no. (%)	208 (92.0)	53 (6.0)	<0.001

* cANCA = cytoplasmic antineutrophil cytoplasmic antibody; pANCA = perinuclear ANCA; anti–PR3-ANCA = anti–proteinase 3–ANCA; anti–MPO-ANCA = anti–myeloperoxidase-ANCA.
† Diagnoses of comparators for the classification criteria for eosinophilic granulomatosis with polyangiitis (EGPA) included granulomatosis with polyangiitis (n = 300), microscopic polyangiitis (n = 291), polyarteritis nodosa (n = 51), non–ANCA-associated small-vessel vasculitis that could not be subtyped (n = 51), Behçet's disease (n = 50), IgA vasculitis (n = 50), cryoglobulinemic vasculitis (n = 34), ANCA-associated vasculitis that could not be subtyped (n = 25), primary central nervous system vasculitis (n = 19), and anti–glomerular basement membrane disease (n = 16).

had significantly higher serum creatinine levels (mean ± SD 102.8 ± 88.7 versus 85.0 ± 53.6 μmoles/liter; $P = 0.03$), lower rates of MPO-ANCA positivity (22% versus 43%; $P < 0.01$), and were less likely to have maximum eosinophil counts ≥1 × 10^9/liter (62% versus 92%; $P < 0.01$). There were 887 comparators randomly selected for analysis. Table 1 shows the demographic and disease features of the 1,113 cases included in this analysis (226 patients with EGPA and 887 comparators), of which 557 (50%;107 patients with EGPA and 450 comparators) were in the development set, and 556 (50%; 119 patients with EGPA and 437 comparators) were in the validation set.

Derivation and validation of the final classification criteria for EGPA. Lasso regression of the previously selected 91 items yielded 11 independent items for EGPA (Supplementary Appendix 9A, available on the *Arthritis & Rheumatology* website at http://onlinelibrary.wiley.com/doi/10.1002/art.41982/abstract). Each item was then adjudicated by the DCVAS Steering Committee for inclusion based on clinical relevance and specificity to EGPA, resulting in 7 final items. Weighting of an individual criterion was based on logistic regression fitted to the 7 selected items (see Supplementary Appendix 10A, available on the *Arthritis & Rheumatology* website at http://onlinelibrary.wiley.com/doi/10.1002/art.41982/abstract).

Model performance. Use of a cutoff of ≥6 for total risk score (see Supplementary Appendix 11A, available on the *Arthritis & Rheumatology* website at http://onlinelibrary.wiley.com/doi/10.1002/art.41982/abstract, for different cut points) yielded a sensitivity of 84.9% (95% confidence interval [95% CI] 77.2–90.8%) and a specificity of 99.1% (95% CI 98.3–99.8%) in the validation set. The area under the curve (AUC) for the model was 0.98 (95% CI 0.97–1.00) in the development set and 0.99 (95% CI 0.97–1.00) in the validation set for the final EGPA classification criteria (Supplementary Appendix 12A, available on the *Arthritis & Rheumatology* website at http://onlinelibrary.wiley.com/doi/10.1002/art.41982/abstract).

2022 AMERICAN COLLEGE OF RHEUMATOLOGY / EUROPEAN ALLIANCE OF ASSOCIATIONS FOR RHEUMATOLOGY

CLASSIFICATION CRITERIA FOR EOSINOPHILIC GRANULOMATOSIS WITH POLYANGIITIS

CONSIDERATIONS WHEN APPLYING THESE CRITERIA

- **These classification criteria should be applied to classify a patient as having eosinophilic granulomatosis with polyangiitis when a diagnosis of small- or medium-vessel vasculitis has been made**
- **Alternate diagnoses mimicking vasculitis should be excluded prior to applying the criteria**

CLINICAL CRITERIA

Obstructive airway disease	+3
Nasal polyps	+3
Mononeuritis multiplex	+1

LABORATORY AND BIOPSY CRITERIA

Blood eosinophil count ≥ 1 x10^9/liter	+5
Extravascular eosinophilic-predominant inflammation on biopsy	+2
Positive test for cytoplasmic antineutrophil cytoplasmic antibodies (cANCA) or antiproteinase 3 (anti-PR3) antibodies	-3
Hematuria	-1

Sum the scores for 7 items, if present. A score of ≥ 6 is needed for classification of EOSINOPHILIC GRANULOMATOSIS WITH POLYANGIITIS.

Figure 1. 2022 American College of Rheumatology/European Alliance of Associations for Rheumatology classification criteria for eosinophilic granulomatosis with polyangiitis.

The final classification criteria for EGPA are presented in Figure 1 (for the slide presentation version, see Supplementary Figure 1, available on the *Arthritis & Rheumatology* website at http://onlinelibrary.wiley.com/doi/10.1002/art.41982/abstract).

Sensitivity analyses. The classification criteria for EGPA were applied to 2,871 patients in the DCVAS database using the original physician-submitted diagnosis (n = 315 EGPA and 2,556 randomly selected comparators). Use of the same cut point of ≥6 points for the classification of EGPA yielded a similar specificity of 99% but a lower sensitivity of 75%. This upheld the a priori hypothesis that specificity would remain unchanged but sensitivity would be reduced in a population of patients that included fewer clearcut diagnoses of EGPA (i.e., cases that did not pass expert panel review).

When the 1990 ACR classification criteria for EGPA were applied to the DCVAS data set, the criteria performed poorly due to low sensitivity (44%) but retained excellent specificity (99%), with an AUC of 0.72 (95% CI 0.68–0.75).

DISCUSSION

Presented here are the final 2022 ACR/EULAR EGPA classification criteria. A 5-stage approach has been used, underpinned by data from the multinational prospective DCVAS study and informed by expert review and consensus at each stage. The comparator group for developing and validating the criteria were patients with other forms of AAV and other small- and medium-vessel vasculitides, which are the clinical entities where discrimination from EGPA is difficult, but important. The new criteria for EGPA have excellent sensitivity and specificity and incorporate ANCA testing. The criteria were designed to have face and content validity for use in clinical trials and other research studies.

These criteria are validated and intended for the purpose of *classification* of vasculitis and are not appropriate for use in establishing a *diagnosis* of vasculitis. The aim of the classification criteria is to differentiate cases of EGPA from similar types of vasculitis in research settings. Therefore, the criteria should only be applied when a diagnosis of small- or medium-vessel vasculitis has been made and all potential "vasculitis mimics" have been excluded. The exclusion of mimics is a key aspect of many classification criteria, including those for Sjögren's syndrome (6) and rheumatoid arthritis (7). The 1990 ACR classification criteria for vasculitis perform poorly when used for diagnosis (i.e., when used to differentiate between cases of vasculitis versus mimics without vasculitis) (8), and it is expected that the 2022 criteria would also perform poorly if used inappropriately as diagnostic criteria in people in whom alternative diagnoses, such as infection or other non-vasculitis inflammatory diseases, are still being considered. Specifically, the criteria were not developed to differentiate patients with EGPA from those with other related hypereosinophilic syndromes or eosinophilic malignancies (9).

The 2022 ACR/EULAR EGPA classification criteria reflect the collaborative effort of the international vasculitis community to delineate the salient clinical features that differentiate EGPA from other forms of vasculitis. The final criteria include 7 clinical items that are easily assessed during routine clinical evaluation of patients with EGPA. The criteria highlight the importance of blood eosinophilia, asthma, and eosinophilic inflammation to classify EGPA among other forms of vasculitis and specify additional features (e.g., nasal polyps, mononeuritis multiplex) that function as important disease classifiers. Classification criteria are intended to define a homogeneous group of patients with a particular disease for inclusion into clinical research studies. By maximizing specificity, the revised criteria for EGPA ensure that few cases will inappropriately meet the criteria threshold of ≥6 points; thus, these criteria will function to facilitate the conduct of future clinical trials and other studies in EGPA.

The negative items included in the final criteria underscore that these criteria are intended for use as classification, not diagnostic, criteria to differentiate EGPA from other forms of vasculitis in research settings. Both hematuria and anti–proteinase 3 ANCA (anti–PR3-ANCA) function as negative items in the new EGPA classification criteria, yet glomerulonephritis and ANCA are features of disease that, when present, can be useful to diagnose EGPA. When compared to other forms of AAV, however, biopsy-proven glomerulonephritis was significantly less common in the DCVAS cohort in patients with EGPA (4.9%) compared to those with GPA (27.8%) or MPA (48.5%). Similarly, anti–PR3-ANCAs have been reported in few patients with EGPA but are much more prevalent in GPA (10). For these reasons, hematuria and anti–PR3-ANCAs work against a patient with small-vessel vasculitis being classified as having EGPA. Although anti–MPO-ANCAs can be detected in 40–60% of patients with EGPA, anti–MPO-ANCA positivity was not included in the final criteria because these antibodies are significantly more prevalent in diseases like MPA and thus are not discriminant classifiers for EGPA (11).

There are some study limitations to consider. Although this was the largest international study ever conducted in vasculitis, most patients were recruited from Europe, Asia, and North America. The performance characteristics of the criteria should be further tested in African and South American populations, which may have different clinical presentations of vasculitis. These criteria were developed using data collected from adult patients with vasculitis. Although the clinical characteristics of EGPA and the other vasculitides which these criteria were tested against are not known to differ substantially between adults and children, these criteria should be applied to children with some caution. The scope of the criteria is intentionally narrow and applies only to patients who have been diagnosed as having vasculitis. Diagnostic criteria are not specified. The criteria are intended to identify homogeneous populations of disease and, therefore, may not be appropriate for studies focused on the full spectrum of clinical heterogeneity in these conditions. To maximize relevance and face

validity of the new criteria, study sites and expert reviewers were recruited from a broad range of countries and different medical specialties. Nonetheless, the majority of patients were recruited from academic rheumatology or nephrology units, which could have introduced referral bias.

There are several strengths to the new 2022 ACR/EULAR EGPA classification criteria. The criteria were developed within a large cohort reflecting international expertise in systemic vasculitis according to ACR guidance for classification criteria development (11). The criteria represent several important methodologic advancements compared to the original 1990 ACR classification criteria for EGPA. Expert review rather than submitting physician diagnosis was used as the diagnostic reference standard to minimize investigator bias. Second, while the 1990 ACR criteria were entirely derived in 20 patients with EGPA and not validated, the new criteria were developed in 107 patients with EGPA and validated in an independent test set that contained an additional 119 patients with EGPA. Third, unlike the 1990 ACR criteria, the new ACR/EULAR EGPA criteria are weighted to reflect the relative importance of specific items (e.g., eosinophil counts). Finally, when both criteria sets were tested within the DCVAS cohort, the performance characteristics of the 1990 ACR criteria were suboptimal when compared to the 2022 revised ACR/EULAR EGPA criteria.

The 2022 ACR/EULAR classification criteria for EGPA are the product of a rigorous methodologic process that utilized an extensive data set generated by the work of a remarkable international group of collaborators. These criteria have been endorsed by the ACR and EULAR and are now ready for use to differentiate one type of vasculitis from another to define populations in research studies.

ACKNOWLEDGMENTS

We acknowledge the patients and clinicians who provided data to the DCVAS project.

AUTHOR CONTRIBUTIONS

All authors were involved in drafting the article or revising it critically for important intellectual content, and all authors approved the final version to be published. Dr. Merkel had full access to all of the data in the study and takes responsibility for the integrity of the data and the accuracy of the data analysis.

Study conception and design. Grayson, Ponte, Suppiah, Robson, Craven, Judge, Hutchings, Luqmani, Watts, Merkel.

Acquisition of data. Grayson, Ponte, Suppiah, Robson, Craven, Luqmani, Watts, Merkel.

Analysis and interpretation of data. Grayson, Ponte, Suppiah, Robson, Craven, Judge, Khalid, Hutchings, Luqmani, Watts, Merkel.

REFERENCES

1. Jennette JC, Falk RJ, Bacon PA, Basu N, Cid MC, Ferrario F, et al. 2012 revised International Chapel Hill Consensus Conference nomenclature of vasculitides. Arthritis Rheum 2013;65:1–11.
2. Sable-Fourtassou R, Cohen P, Mahr A, Pagnoux C, Mouthon L, Jayne D, et al. Antineutrophil cytoplasmic antibodies and the Churg-Strauss syndrome. Ann Intern Med 2005;143:632–8.
3. Sinico RA, Di Toma L, Maggiore U, Bottero P, Radice A, Tosoni C, et al. Prevalence and clinical significance of antineutrophil cytoplasmic antibodies in Churg-Strauss syndrome. Arthritis Rheum 2005;52:2926–35.
4. Masi AT, Hunder GG, Lie JT, Michel BA, Bloch DA, Arend WP, et al. The American College of Rheumatology 1990 criteria for the classification of Churg-Strauss syndrome (allergic granulomatosis and angiitis). Arthritis Rheum 1990;33:1094–100.
5. Craven A, Robson J, Ponte C, Grayson PC, Suppiah R, Judge A, et al. ACR/EULAR-endorsed study to develop Diagnostic and Classification Criteria for Vasculitis (DCVAS). Clin Exp Nephrol 2013;17:619–21.
6. Shiboski SC, Shiboski CH, Criswell L, Baer A, Challacombe S, Lanfranchi H, et al. American College of Rheumatology classification criteria for Sjögren's syndrome: a data-driven, expert consensus approach in the Sjögren's International Collaborative Clinical Alliance cohort. Arthritis Care Res (Hoboken) 2012;64:475–87.
7. Aletaha D, Neogi T, Silman AJ, Funovits J, Felson DT, Bingham CO III, et al. 2010 rheumatoid arthritis classification criteria: an American College of Rheumatology/European League Against Rheumatism collaborative initiative. Arthritis Rheum 2010;62:2569–81.
8. Rao JK, Allen NB, Pincus T. Limitations of the 1990 American College of Rheumatology classification criteria in the diagnosis of vasculitis. Ann Intern Med 1998;129:345–52.
9. Rosenberg HF, Dyer KD, Foster PS. Eosinophils: changing perspectives in health and disease. Nat Rev Immunol 2013;13:9–22.
10. Comarmond C, Pagnoux C, Khellaf M, Cordier JF, Hamidou M, Viallard JF, et al. Eosinophilic granulomatosis with polyangiitis (Churg-Strauss): clinical characteristics and long-term followup of the 383 patients enrolled in the French Vasculitis Study Group cohort. Arthritis Rheum 2013;65:270–81.
11. Singh JA, Solomon DH, Dougados M, Felson D, Hawker G, Katz P, et al. Development of classification and response criteria for rheumatic diseases. Arthritis Rheum 2006;55:348–52.

APPENDIX A: THE DCVAS INVESTIGATORS

The DCVAS study investigators are as follows: Paul Gatenby (ANU Medical Centre, Canberra, Australia); Catherine Hill (Central Adelaide Local Health Network: The Queen Elizabeth Hospital, Australia); Dwarakanathan Ranganathan (Royal Brisbane and Women's Hospital, Australia); Andreas Kronbichler (Medical University Innsbruck, Austria); Daniel Blockmans (University Hospitals Leuven, Belgium); Lillian Barra (Lawson Health Research Institute, London, Ontario, Canada); Simon Carette, Christian Pagnoux (Mount Sinai Hospital, Toronto, Canada); Navjot Dhindsa (University of Manitoba, Winnipeg, Canada); Aurore Fifi-Mah (University of Calgary, Alberta, Canada); Nader Khalidi (St Joseph's Healthcare, Hamilton, Ontario, Canada); Patrick Liang (Sherbrooke University Hospital Centre, Canada); Nataliya Milman (University of Ottawa, Canada); Christian Pineau (McGill University, Canada); Xinping Tian (Peking Union Medical College Hospital, Beijing, China); Guochun Wang (China-Japan Friendship Hospital, Beijing, China); Tian Wang (Anzhen Hospital, Capital Medical University, China); Ming-hui Zhao (Peking University First Hospital, China); Vladimir Tesar (General University Hospital, Prague, Czech Republic); Bo Baslund (University Hospital, Copenhagen [Rigshospitalet], Denmark); Nevin Hammam (Assiut University, Egypt); Amira Shahin (Cairo University, Egypt); Laura Pirila (Turku University Hospital, Finland); Jukka Putaala (Helsinki University Central Hospital, Finland); Bernhard Hellmich (Kreisklinken Esslingen, Germany); Jörg Henes (Universitätsklinikum Tübingen, Germany); Julia Holle (Klinikum Bad Bramstedt, Germany); Peter

Lamprecht (Klinikum Bad Bramstedt, Germany); Frank Moosig (Klinikum Bad Bramstedt, Germany); Thomas Neumann (Universitätsklinikum Jena, Germany); Wolfgang Schmidt (Immanuel Krankenhaus Berlin, Germany); Cord Sunderkoetter (Universitätsklinikum Müenster, Germany); Zoltan Szekanecz (University of Debrecen Medical and Health Science Center, Hungary); Debashish Danda (Christian Medical College & Hospital, Vellore, India); Siddharth Das (Chatrapathi Shahuji Maharaj Medical Center, Lucknow [IP], India); Rajiva Gupta (Medanta, Delhi, India); Liza Rajasekhar (NIMS, Hyderabad, India); Aman Sharma (Postgraduate Institute of Medical Education and Research, Chandigarh, India); Shrikant Wagh (Jehangir Clinical Development Centre, Pune [IP], India); Michael Clarkson (Cork University Hospital, Ireland); Eamonn Molloy (St. Vincent's University Hospital, Dublin, Ireland); Carlo Salvarani (Santa Maria Nuova Hospital, Reggio Emilia, Italy); Franco Schiavon (L'Azienda Ospedaliera of University of Padua, Italy); Enrico Tombetti (Università Vita-Salute San Raffaele Milano, Italy); Augusto Vaglio (University of Parma, Italy); Koichi Amano (Saitama Medical University, Japan); Yoshihiro Arimura (Kyorin University Hospital, Japan); Hiroaki Dobashi (Kagawa University Hospital, Japan); Shouichi Fujimoto (Miyazaki University Hospital [HUB], Japan); Masayoshi Harigai, Fumio Hirano (Tokyo Medical and Dental University Hospital, Japan); Junichi Hirahashi (University Tokyo Hospital, Japan); Sakae Honma (Toho University Hospital, Japan); Tamihiro Kawakami (St. Marianna University Hospital Dermatology, Japan); Shigeto Kobayashi (Juntendo University Koshigaya Hospital, Japan); Hajime Kono (Teikyo University, Japan); Hirofumi Makino (Okayama University Hospital, Japan); Kazuo Matsui (Kameda Medical Centre, Kamogawa, Japan); Eri Muso (Kitano Hospital, Japan); Kazuo Suzuki, Kei Ikeda (Chiba University Hospital, Japan); Tsutomu Takeuchi (Keio University Hospital, Japan); Tatsuo Tsukamoto (Kyoto University Hospital, Japan); Shunya Uchida (Teikyo University Hospital, Japan); Takashi Wada (Kanazawa University Hospital, Japan); Hidehiro Yamada (St. Marianna University Hospital Internal Medicine, Japan); Kunihiro Yamagata (Tsukuba University Hospital, Japan); Wako Yumura (IUHW Hospital [Jichi Medical University Hospital], Japan); Kan Sow Lai (Penang General Hospital, Malaysia); Luis Felipe Flores-Suarez (Instituto Nacional de Enfermedades Respiratorias, Mexico City, Mexico); Andrea Hinojosa-Azaola (Instituto Nacional de Ciencias Médicas y Nutrición Salvador Zubirán, Mexico City, Mexico); Bram Rutgers (University Hospital Groningen, Netherlands); Paul-Peter Tak (Academic Medical Centre, University of Amsterdam, Netherlands); Rebecca Grainger (Wellington, Otago, New Zealand); Vicki Quincey (Waikato District Health Board, New Zealand); Lisa Stamp (University of Otago, Christchurch, New Zealand); Ravi Suppiah (Auckland District Health Board, New Zealand); Emilio Besada (Tromsø, Northern Norway, Norway); Andreas Diamantopoulos (Hospital of Southern Norway, Kristiansand, Norway); Jan Sznajd (University of Jagiellonian, Poland); Elsa Azevedo (Centro Hospitalar de São João, Porto, Portugal); Ruth Geraldes (Hospital de Santa Maria, Lisbon, Portugal); Miguel Rodrigues (Hospital Garcia de Orta, Almada, Portugal); Ernestina Santos (Hospital Santo Antonio, Porto, Portugal); Yeong-Wook Song (Seoul National University Hospital, Republic of Korea); Sergey Moiseev (First Moscow State Medical University, Russia); Alojzija Hočevar (University Medical Centre Ljubljana, Slovenia); Maria Cinta Cid (Hospital Clinic de Barcelona, Spain); Xavier Solanich Moreno (Hospital de Bellvitge-Idibell, Spain); Inoshi Atukorala (University of Colombo, Sri Lanka); Ewa Berglin (Umeå University Hospital, Sweden); Aladdin Mohammed (Lund-Malmo University, Sweden); Mårten Segelmark (Linköping University, Sweden); Thomas Daikeler (University Hospital Basel, Switzerland); Haner Direskeneli (Marmara University Medical School, Turkey); Gulen Hatemi (Istanbul University, Cerrahpasa Medical School, Turkey); Sevil Kamali (Istanbul University, Istanbul Medical School, Turkey); Ömer Karadağ (Hacettepe University, Turkey); Seval Pehlevan (Fatih University Medical Faculty, Turkey); Matthew Adler (Frimley Health NHS Foundation Trust, Wexham Park Hospital, UK); Neil Basu (NHS Grampian, Aberdeen Royal Infirmary, UK); Iain Bruce (Manchester University Hospitals NHS Foundation Trust, UK); Kuntal Chakravarty (Barking, Havering and Redbridge University Hospitals NHS Trust, UK); Bhaskar Dasgupta (Southend University Hospital NHS Foundation Trust, UK); Oliver Flossmann (Royal Berkshire NHS Foundation Trust, UK); Nagui Gendi (Basildon and Thurrock University Hospitals NHS Foundation Trust, UK); Alaa Hassan (North Cumbria University Hospitals, UK); Rachel Hoyles (Oxford University Hospitals NHS Foundation Trust, UK); David Jayne (Cambridge University Hospitals NHS Foundation Trust, UK); Colin Jones (York Teaching Hospitals NHS Foundation Trust, UK); Rainer Klocke (The Dudley Group NHS Foundation Trust, UK); Peter Lanyon (Nottingham University Hospitals NHS Trust, UK); Cathy Laversuch (Taunton & Somerset NHS Foundation Trust, Musgrove Park Hospital, UK); Raashid Luqmani, Joanna Robson (Nuffield Orthopaedic Centre, Oxford, UK); Malgorzata Magliano (Buckinghamshire Healthcare NHS Trust, UK); Justin Mason (Imperial College Healthcare NHS Trust, UK); Win Win Maw (Mid Essex Hospital Services NHS Trust, UK); Iain McInnes (NHS Greater Glasgow & Clyde, Gartnavel Hospital & GRI, UK); John Mclaren (NHS Fife, Whyteman's Brae Hospital, UK); Matthew Morgan (University Hospitals Birmingham NHS Foundation Trust, Queen Elizabeth Hospital, UK); Ann Morgan (Leeds Teaching Hospitals NHS Trust, UK); Chetan Mukhtyar (Norfolk and Norwich University Hospitals NHS Foundation Trust, UK); Edmond O'Riordan (Salford Royal NHS Foundation Trust, UK); Sanjeev Patel (Epsom and St Helier University Hospitals NHS Trust, UK); Adrian Peall (Wye Valley NHS Trust, Hereford County Hospital, UK); Joanna Robson (University Hospitals Bristol NHS Foundation Trust, UK); Srinivasan Venkatachalam (The Royal Wolverhampton NHS Trust, UK); Erin Vermaak, Ajit Menon (Staffordshire & Stoke on Trent Partnership NHS Trust, Haywood Hospital, UK); Richard Watts (East Suffolk and North Essex NHS Foundation Trust, UK); Chee-Seng Yee (Doncaster and Bassetlaw Hospitals NHS Foundation Trust, UK); Daniel Albert (Dartmouth-Hitchcock Medical Center, US); Leonard Calabrese (Cleveland Clinic Foundation, US); Sharon Chung (University of California, San Francisco, US); Lindsy Forbess (Cedars-Sinai Medical Center, US); Angelo Gaffo (University of Alabama at Birmingham, US); Ora Gewurz-Singer (University of Michigan, US); Peter Grayson (Boston University School of Medicine, US); Kimberly Liang (University of Pittsburgh, US); Eric Matteson (Mayo Clinic, US); Peter A. Merkel (University of Pennsylvania, US); Rennie Rhee (University of Pennsylvania, US); Jason Springer (University of Kansas Medical Center Research Institute, US); and Antoine Sreih (Rush University Medical Center, US).

Arthritis & Rheumatology
Vol. 74, No. 3, March 2022, pp 393–399
DOI 10.1002/art.41986

American College of Rheumatology
Empowering Rheumatology Professionals

2022 American College of Rheumatology/European Alliance of Associations for Rheumatology Classification Criteria for Granulomatosis With Polyangiitis

Joanna C. Robson,[1] Peter C. Grayson,[2] Cristina Ponte,[3] Ravi Suppiah,[4] Anthea Craven,[5] Andrew Judge,[6] Sara Khalid,[5] Andrew Hutchings,[7] Richard A. Watts,[8] Peter A. Merkel,[9] and Raashid A. Luqmani[5]

This criteria set has been approved by the American College of Rheumatology (ACR) Board of Directors and the European Alliance of Associations for Rheumatology (EULAR) Executive Committee. This signifies that the criteria set has been quantitatively validated using patient data, and it has undergone validation based on an independent data set. All ACR/EULAR-approved criteria sets are expected to undergo intermittent updates.

The ACR is an independent, professional, medical and scientific society that does not guarantee, warrant, or endorse any commercial product or service.

Objective. To develop and validate revised classification criteria for granulomatosis with polyangiitis (GPA).

Methods. Patients with vasculitis or comparator diseases were recruited into an international cohort. The study proceeded in 5 phases: 1) identification of candidate criteria items using consensus methodology, 2) prospective collection of candidate items present at the time of diagnosis, 3) data-driven reduction of the number of candidate items, 4) expert panel review of cases to define the reference diagnosis, and 5) derivation of a points-based risk score for disease classification in a development set using least absolute shrinkage and selection operator logistic regression, with subsequent validation of performance characteristics in an independent set of cases and comparators.

Results. The development set for GPA consisted of 578 cases of GPA and 652 comparators. The validation set consisted of an additional 146 cases of GPA and 161 comparators. From 91 candidate items, regression analysis identified 26 items for GPA, 10 of which were retained. The final criteria and their weights were as follows: bloody nasal discharge, nasal crusting, or sino-nasal congestion (+3); cartilaginous involvement (+2); conductive or sensorineural hearing loss (+1); cytoplasmic antineutrophil cytoplasmic antibody (ANCA) or anti–proteinase 3 ANCA positivity (+5); pulmonary nodules, mass, or cavitation on chest imaging (+2); granuloma or giant cells on biopsy (+2); inflammation or consolidation of the nasal/paranasal sinuses on imaging (+1); pauci-immune glomerulonephritis (+1); perinuclear ANCA or antimyeloperoxidase ANCA positivity (−1); and eosinophil count ≥1 × 10^9/liter (−4). After excluding mimics of vasculitis, a patient with a diagnosis of small- or medium-vessel vasculitis could be classified as having GPA if the cumulative score was ≥5 points. When these criteria were tested in the validation data set, the sensitivity was 93% (95% confidence interval [95% CI] 87–96%) and the specificity was 94% (95% CI 89–97%).

Conclusion. The 2022 American College of Rheumatology/European Alliance of Associations for Rheumatology classification criteria for GPA demonstrate strong performance characteristics and are validated for use in research.

This article is published simultaneously in the March 2022 issue of *Annals of the Rheumatic Diseases*.

The Diagnostic and Classification Criteria in Vasculitis (DCVAS) study, of which the development of these classification criteria was a part, was funded by grants from the American College of Rheumatology (ACR), the European Alliance of Associations for Rheumatology (EULAR), the Vasculitis Foundation, and the University of Pennsylvania Vasculitis Center.

[1]Joanna C. Robson, MBBS, PhD: Centre for Health and Clinical Research, University of the West of England, and University Hospitals and Weston NHS Foundation Trust, Bristol, UK; [2]Peter C. Grayson, MD, MSc: National Institute of Arthritis and Musculoskeletal and Skin Diseases, NIH, Bethesda, Maryland; [3]Cristina Ponte, MD, PhD: Hospital de Santa Maria, Centro Hospitalar Universitário Lisboa Norte, Universidade de Lisboa, and Centro Académico de Medicina de Lisboa, Lisbon, Portugal; [4]Ravi Suppiah, MD: Auckland District Health Board, Auckland, New Zealand; [5]Anthea Craven, BSc, Sara Khalid, DPhil, Raashid A. Luqmani, DM, FRCP: Oxford NIHR Biomedical Research Centre and University of Oxford, Oxford, UK; [6]Andrew Judge, PhD: Oxford NIHR Biomedical Research Centre and University of Oxford, Oxford, UK, and Bristol NIHR Biomedical Research Centre and University of Bristol, Bristol, UK; [7]Andrew Hutchings, MSc: London School of Hygiene and Tropical Medicine, London, UK;

INTRODUCTION

The antineutrophil cytoplasmic antibody (ANCA)–associated vasculitides (AAV) are multisystem disorders involving inflammation of the small blood vessels and include granulomatosis with polyangiitis (GPA), microscopic polyangiitis (MPA), and eosinophilic granulomatosis with polyangiitis (EGPA) (1). GPA is characterized by necrotizing granulomatous inflammation involving the ears, nose, and upper and lower respiratory tracts, and necrotizing vasculitis affecting predominantly small- to medium-sized vessels, often including necrotizing glomerulonephritis (1).

Unlike diagnostic criteria, the purpose of classification criteria is to ensure that a homogeneous population is selected for inclusion in clinical trials and other research studies of GPA. In 1990, the American College of Rheumatology (ACR) published criteria for the classification of GPA (then named Wegener's granulomatosis) (2–4). The 1990 criteria were effective and widely accepted, facilitating coordinated approaches to international randomized controlled trials (5,6). In 2011 it was proposed to change the name "Wegener's granulomatosis" to "granulomatosis with polyangiitis" with subsequent wide adoption of the new terminology (7–9). The 1994 and 2012 publications of the international Chapel Hill Consensus Conference (CHCC) nomenclature for vasculitis clarified and standardized the nomenclature of the systemic vasculitides (1,10). The CHCC is a nomenclature system based on expert consensus rather than a classification system (1).

There are several important reasons for the development of revised classification criteria for the vasculitides, including a decline in the sensitivity of the 1990 ACR classification criteria, particularly for AAV (11); a consensus that any such criteria must now incorporate testing for ANCA; increased and widespread use, since 1990, of cross-sectional diagnostic imaging tools, including magnetic resonance imaging and computed tomography (12,13); and the introduction and adoption of the classification of patients with MPA, a term not in use in the 1990 ACR classification criteria.

There have been methodologic advances in the derivation of classification criteria, moving from the "number of criteria" rule, as used in the ACR 1990 criteria (3), toward weighted criteria with threshold scores, as demonstrated in the 2010 classification criteria for rheumatoid arthritis (14). Weighted criteria improve measurement properties of classification criteria because certain items within a criteria list may be more discriminative. The previous 1990 criteria for vasculitis collected retrospective data from patient files, without specification of which items were relevant at the time of diagnosis compared to those that were important later in the disease process. Criteria based on prospectively collected data sets from newly diagnosed patients should have higher face validity as inclusion criteria for future clinical trials of early-stage disease. This article outlines the development and validation of the revised ACR/European Alliance of Associations for Rheumatology (EULAR)–endorsed classification criteria for GPA.

METHODS

A detailed and complete description of the methods involved in the development and validation of the classification criteria for GPA is provided in Supplementary Appendix 1, available on the *Arthritis & Rheumatology* website at http://onlinelibrary.wiley.com/doi/10.1002/art.41986/abstract. Briefly, an international Steering Committee comprising clinician investigators with expertise in vasculitis, statisticians, and data managers was established to oversee the overall Diagnostic and Classification Criteria in Vasculitis (DCVAS) project (15). The Steering Committee established a 5-stage plan using data-driven and consensus methodology to develop the criteria for each of 6 forms of vasculitis.

Stage 1: generation of candidate classification items for the systemic vasculitides. Candidate classification items were generated by expert opinion and reviewed by a group of vasculitis experts across a range of specialties using a nominal group technique.

Stage 2: DCVAS prospective observational study. A prospective, international, multisite observational study was conducted (see Appendix A for study investigators and sites). Ethical approval was obtained from national and local ethics committees. Consecutive patients representing the full spectrum of disease were recruited from academic and community practices. Patients were included if they were 18 years or older and had a diagnosis of vasculitis or a condition that mimics vasculitis. Patients with AAV could only be enrolled within 2 years of diagnosis. Only data present at diagnosis were recorded.

Stage 3: refinement of candidate items specifically for AAV. The Steering Committee conducted a data-driven process to reduce the number of candidate items of relevance to cases and comparators for AAV. Items were selected for exclusion if they had a prevalence of <5% within the data set and/or they were not clinically relevant for classification criteria (e.g., related to infection, malignancy, or demographic characteristics). Low-frequency items of clinical importance could be combined, when appropriate.

[8]Richard A. Watts, MD: Oxford NIHR Biomedical Research Centre and University of Oxford, Oxford, UK, and University of East Anglia, Norwich, UK; [9]Peter A. Merkel, MD, MPH: University of Pennsylvania, Philadelphia.

[Correction added on 20 June 2022, after first online publication: Appendices A and S1 have been replaced and Appendix S2 has been added online.]

Author disclosures are available at https://onlinelibrary.wiley.com/action/downloadSupplement?doi=10.1002%2Fart.41986&file=art41986-sup-0001-Disclosureform.pdf.

Address correspondence to Peter A. Merkel, MD, MPH, Chief, Division of Rheumatology, University of Pennsylvania, White Building, Fifth Floor, 3400 Spruce Street, Philadelphia, PA 19104 (email: pmerkel@upenn.edu); or to Raashid A. Luqmani, DM, FRCP, Rheumatology Department, Nuffield Orthopaedic Centre, University of Oxford, Windmill Road, Oxford OX3 7LD, UK (email: raashid.luqmani@ndorms.ox.ac.uk).

Submitted for publication February 28, 2020; accepted in revised form September 21, 2021.

Stage 4: expert review to derive a gold standard–defined set of cases of AAV. Experts in vasculitis from a wide range of geographic locations and specialties reviewed all submitted cases of vasculitis and a random selection of mimics of vasculitis. Each reviewer was asked to review ~50 submitted cases to confirm the diagnosis and to specify the certainty of their diagnosis as follows: very certain, moderately certain, uncertain, or very uncertain. Only cases agreed upon with at least moderate certainty were retained for further analysis.

Stage 5: derivation and validation of the final classification criteria for GPA. The DCVAS AAV data set was randomly split into development (80%) and validation (20%) sets. Comparisons were performed between cases of GPA confirmed by expert review and a comparator group randomly selected from the DCVAS cohort in the following proportions: another type of AAV (including MPA and EGPA), 64%; another form of small-vessel vasculitis (e.g., cryoglobulinemic vasculitis) or medium-vessel vasculitis (e.g., polyarteritis nodosa), 36%. Least absolute shrinkage and selection operator (lasso) logistic regression was used to identify items from the data set and create a parsimonious model including only the most important items. The final items in the model were formulated into a clinical risk-scoring tool with each factor assigned a weight based on its respective regression coefficient. A threshold that best balanced sensitivity and specificity was identified for classification.

In sensitivity analyses, the final classification criteria were applied to an unselected population of cases and comparators from the DCVAS data set based on the submitting physician diagnosis. Comparison was also made between the measurement properties of the new classification criteria for GPA and the 1990 ACR classification criteria for GPA using pooled data from the development and validation sets.

RESULTS

Generation of candidate classification items for the systemic vasculitides. The Steering Committee identified >1,000 candidate items for the DCVAS case report form (see Supplementary Appendix 2, available on the *Arthritis & Rheumatology* website at http://onlinelibrary.wiley.com/doi/10.1002/art.41986/abstract).

DCVAS prospective observational study. Between January 2011 and December 2017, the DCVAS study recruited 6,991 participants from 136 sites in 32 countries. Information on the DCVAS sites, investigators, and study participants is listed in Supplementary Appendices 3, 4, and 5, available on the *Arthritis & Rheumatology* website at http://onlinelibrary.wiley.com/doi/10.1002/art.41986/abstract.

Refinement of candidate items specifically for AAV. Following a data-driven and expert consensus process, 91 items from the DCVAS case report form were retained for regression analysis, including 45 clinical (14 composite), 18 laboratory (2 composite), 12 imaging (all composite), and 16 biopsy (1 composite) items. Some clinical items were removed in favor of similar but more specific pathophysiologic descriptors. Supplementary Appendix 6, available on the *Arthritis & Rheumatology* website at http://onlinelibrary.wiley.com/doi/10.1002/art.41986/abstract, lists the final candidate items used in the derivation of the classification criteria for GPA, MPA, and EGPA.

Expert review to derive a gold standard–defined final set of cases of AAV. Fifty-five independent experts reviewed vignettes derived from the case report forms for 2,871 cases submitted with a diagnosis of either small-vessel vasculitis

Table 1. Demographic and disease features of cases of GPA and comparators*

	GPA (n = 724)	Comparators (n = 813)†	*P*
Age, mean ± SD years	53.6 ± 16.2	56.4 ± 17.1	0.001
Sex, no. (%) female	340 (47.0)	424 (52.2)	0.048
Maximum serum creatinine, mean			0.077
μmoles/liter	168.3	185.2	
mg/dl	1.9	2.1	
cANCA positive, no. (%)	531 (73.3)	40 (4.9)	<0.001
pANCA positive, no. (%)	71 (9.8)	342 (42.1)	<0.001
Anti–PR3-ANCA positive, no. (%)	595 (82.2)	21 (2.6)	<0.001
Anti–MPO-ANCA positive, no. (%)	59 (8.1)	399 (49.1)	<0.001
Maximum eosinophil count ≥1 × 10^9/liter, no. (%)	196 (27)	366 (45)	<0.001

* cANCA = cytoplasmic antineutrophil cytoplasmic antibody; pANCA = perinuclear ANCA; anti–PR3-ANCA = anti–proteinase 3–ANCA; anti–MPO-ANCA = anti–myeloperoxidase-ANCA.
† Diagnoses of comparators for the classification criteria for granulomatosis with polyangiitis (GPA) included microscopic polyangiitis (n = 291), eosinophilic granulomatosis with polyangiitis (n = 226), polyarteritis nodosa (n = 51), non–ANCA-associated small-vessel vasculitis that could not be subtyped (n = 51), Behçet's disease (n = 50), IgA vasculitis (n = 50), cryoglobulinemic vasculitis (n = 34), ANCA-associated vasculitis that could not be subtyped (n = 25), primary central nervous system vasculitis (n = 19), and anti–glomerular basement membrane disease (n = 16).

(90% of case report forms) or another type of vasculitis or a mimic of vasculitis (10% of case report forms). The characteristics of the expert reviewers are shown in Supplementary Appendix 7, available on the *Arthritis & Rheumatology* website at http://onlinelibrary.wiley.com/doi/10.1002/art.41986/abstract. A flow chart showing the results of the expert review process is shown in Supplementary Appendix 8, available on the *Arthritis & Rheumatology* website at http://onlinelibrary.wiley.com/doi/10.1002/art.41986/abstract. A total of 2,072 cases (72%) passed the process and were designated as cases of vasculitis; these cases were used for the stage 5 analyses.

After expert review, 724 of 843 cases retained a reference diagnosis of GPA. There were 813 comparators randomly selected for analysis. Table 1 shows the demographic and disease features of the 1,537 cases included in this analysis (724 patients with GPA and 813 comparators), of which 1,230 (80%, 578 patients with GPA and 652 comparators) were in the development set, and 307 (20%, 146 patients with GPA and 161 comparators) were in the validation set.

Derivation and validation of the final classification criteria for GPA. Lasso logistic regression analysis using all 91 items resulted in a model of 26 independent items (see Supplementary Appendix 9B, available on the *Arthritis & Rheumatology* website at http://onlinelibrary.wiley.com/doi/10.1002/art.41986/abstract). The variables "positive test for cytoplasmic ANCA (cANCA)" and "positive test for anti–proteinase 3 (anti-PR3)

2022 AMERICAN COLLEGE OF RHEUMATOLOGY / EUROPEAN ALLIANCE OF ASSOCIATIONS FOR RHEUMATOLOGY

CLASSIFICATION CRITERIA FOR **GRANULOMATOSIS WITH POLYANGIITIS**

CONSIDERATIONS WHEN APPLYING THESE CRITERIA

- **These classification criteria should be applied to classify a patient as having granulomatosis with polyangiitis when a diagnosis of small- or medium-vessel vasculitis has been made**
- **Alternate diagnoses mimicking vasculitis should be excluded prior to applying the criteria**

CLINICAL CRITERIA

Nasal involvement: bloody discharge, ulcers, crusting, congestion, blockage, or septal defect / perforation	+3
Cartilaginous involvement (inflammation of ear or nose cartilage, hoarse voice or stridor, endobronchial involvement, or saddle nose deformity)	+2
Conductive or sensorineural hearing loss	+1

LABORATORY, IMAGING, AND BIOPSY CRITERIA

Positive test for cytoplasmic antineutrophil cytoplasmic antibodies (cANCA) or antiproteinase 3 (anti-PR3) antibodies	+5
Pulmonary nodules, mass, or cavitation on chest imaging	+2
Granuloma, extravascular granulomatous inflammation, or giant cells on biopsy	+2
Inflammation, consolidation, or effusion of the nasal/paranasal sinuses, or mastoiditis on imaging	+1
Pauci-immune glomerulonephritis on biopsy	+1
Positive test for perinuclear antineutrophil cytoplasmic antibodies (pANCA) or antimyeloperoxidase (anti-MPO) antibodies	-1
Blood eosinophil count ≥ 1 x10^9/liter	-4

Sum the scores for 10 items, if present. A score of ≥ 5 is needed for classification of GRANULOMATOSIS WITH POLYANGIITIS.

Figure 1. 2022 American College of Rheumatology/European Alliance of Associations for Rheumatology classification criteria for granulomatosis with polyangiitis.

antibody" and the variables "positive test for perinuclear ANCA (pANCA)" and "positive test for antimyeloperoxidase (anti-MPO) antibody" were strongly colinear and were combined within the model as "positive test for cANCA or positive test for anti-PR3 antibody" and "positive test for pANCA or positive test for anti-MPO antibody," respectively. Each item was scrutinized for inclusion based on statistical significance, clinical relevance, and specificity to GPA, resulting in 10 final items. Weighting of an individual criterion was based on logistic regression fitted to the 10 selected items (see Supplementary Appendix 10B, available on the *Arthritis & Rheumatology* website at http://onlinelibrary.wiley.com/doi/10.1002/art.41986/abstract).

Model performance. Use of a cutoff of ≥5 for total risk score (see Supplementary Appendix 11B, available on the *Arthritis & Rheumatology* website at http://onlinelibrary.wiley.com/doi/10.1002/art.41986/abstract, for different cut points) yielded a sensitivity of 92.5% (95% confidence interval [95% CI] 86.9–96.2%) and a specificity of 93.8% (95% CI 88.9–97.0%) in the validation set. The area under the curve (AUC) for the model was 0.98 (95% CI 0.98–0.99) in the development set and 0.99 (95% CI 0.98–1.00) in the validation set (Supplementary Appendix 12B, available on the *Arthritis & Rheumatology* website at http://onlinelibrary.wiley.com/doi/10.1002/art.41986/abstract). The final classification criteria for GPA are shown in Figure 1 (for the slide presentation version, see Supplementary Figure 1, available on the *Arthritis & Rheumatology* website at http://onlinelibrary.wiley.com/doi/10.1002/art.41986/abstract).

Sensitivity analyses. The classification criteria for GPA were applied to 2,511 patients randomly selected from the DCVAS database using the original physician-submitted diagnosis (n = 483 GPA and 2,028 comparators). Use of the same cut point of ≥5 points for the classification of GPA yielded a similar specificity of 94.6% but a lower sensitivity of 83.8%. This upheld the a priori hypothesis that specificity would remain unchanged but sensitivity would be reduced in a population with fewer clear-cut diagnoses of GPA (i.e., cases that did not pass expert review).

When the 1990 ACR classification criteria for GPA were applied to the DCVAS data set, the criteria performed poorly due to low sensitivity (69.3%) and moderate specificity (75.8%), with an AUC of 0.73 (95% CI 0.70–0.75).

DISCUSSION

Presented here are the final 2022 ACR/EULAR GPA classification criteria. A 5-stage approach has been used, underpinned by data from the multinational prospective DCVAS study and informed by expert review and consensus at each stage. The comparator group for developing and validating the criteria were other forms of AAV and other small- and medium-vessel vasculitides, the clinical entities where discrimination from GPA is difficult, but important. The new criteria for GPA have excellent sensitivity and specificity and incorporate ANCA testing and modern imaging techniques. The criteria were designed to have face and content validity for use in clinical trials and other research studies.

These criteria are validated and intended for the purpose of *classification* of vasculitis and are not appropriate for use in establishing a *diagnosis* of vasculitis. The aim of the classification criteria is to differentiate cases of GPA from similar types of vasculitis in research settings. Therefore, the criteria should only be applied when a diagnosis of small- or medium-vessel vasculitis has been made and all potential "vasculitis mimics" have been excluded. The exclusion of mimics is a key aspect of many classification criteria, including those for Sjögren's syndrome (16) and rheumatoid arthritis (14). The 1990 ACR classification criteria for vasculitis perform poorly when used for diagnosis (i.e., when used to differentiate between cases of vasculitis versus mimics without vasculitis) (17), and it is expected that the 2022 criteria would also perform poorly if used inappropriately as diagnostic criteria in people in whom alternative diagnoses, such as infection or other non-vasculitis inflammatory diseases, are still being considered. The relatively low weight assigned to glomerulonephritis in these classification criteria highlights the distinction between classification and diagnostic criteria. While detection of kidney disease is important to diagnose GPA, glomerulonephritis is common among patients with either GPA or MPA and thus does not function as a strong classifier between these conditions.

These criteria differ from the previous 1990 ACR criteria in that they have been developed using cases presenting prospectively at the start of their disease process. This approach is different from the methods used to generate the 1990 ACR criteria, in which prevalent case records were utilized, potentially including items related to irreversible damage accrued over time. Inclusion of newly diagnosed cases in these criteria should improve their accuracy within the context of early intervention trials as well as refractory disease. The comparators used for these new criteria are also more appropriate and are closer mimics of GPA; for example, comparators with predominantly small-vessel vasculitis rather than predominantly giant cell arteritis were included. The new criteria perform better than previous criteria within this data set (11). ANCA is a major discriminator within these criteria, although patients can be classified as having GPA without having a positive test result for ANCA if they have a sufficient number of other features. These new criteria were validated in an independent data set and are weighted with threshold scores (14,16) to maximize predictive ability.

There are some study limitations to consider. Although this was the largest international study ever conducted in vasculitis, most patients were recruited from Europe, Asia, and North America. The performance characteristics of the criteria should be further tested in African and South American populations, which may have different clinical presentations of vasculitis. These

criteria were developed using data collected from adult patients with vasculitis. Although the clinical characteristics of GPA and the other vasculitides which these criteria were tested against are not known to differ substantially between adults and children, these criteria should be applied to children with some caution. The scope of the criteria is intentionally narrow and applies only to patients who have been diagnosed as having vasculitis. Diagnostic criteria are not specified. The criteria are intended to identify homogeneous populations of disease and, therefore, may not be appropriate for studies focused on the full spectrum of clinical heterogeneity in these conditions. To maximize relevance and face validity of the new criteria, study sites and expert reviewers were recruited from a broad range of countries and different medical specialties. Nonetheless, the majority of patients were recruited from academic rheumatology or nephrology units, which could have introduced referral bias.

A key strength of this study is the use of an independent expert review process to confirm cases of GPA and comparators to avoid the circularity of using predefined criteria to define the gold standard. Approximately one-quarter of cases were excluded via this process, due to either a lack of consensus on exact diagnosis or insufficient data available to make the diagnosis. A limitation of this approach, however, could be the exclusion of true, but less clearcut, cases submitted by the original physicians. It is important that cases are classified accurately for inclusion in clinical trials; therefore, some loss of sensitivity may be appropriate. Importantly, this study also demonstrated that applying the new criteria for GPA to the whole unselected DCVAS data set resulted in a reduction in sensitivity while maintaining specificity. Thus, the criteria should also be useful in a more generalized, "real-world" population.

The 2022 ACR/EULAR classification criteria for GPA are the product of a rigorous methodologic process that utilized an extensive data set generated by the work of a remarkable international group of collaborators. These criteria have been endorsed by the ACR and EULAR and are now ready for use to differentiate one type of vasculitis from another to define populations in research studies.

ACKNOWLEDGMENTS

We acknowledge the patients and clinicians who provided data to the DCVAS project.

AUTHOR CONTRIBUTIONS

All authors were involved in drafting the article or revising it critically for important intellectual content, and all authors approved the final version to be published. Dr. Merkel had full access to all of the data in the study and takes responsibility for the integrity of the data and the accuracy of the data analysis.

Study conception and design. Robson, Grayson, Ponte, Suppiah, Craven, Judge, Hutchings, Watts, Merkel, Luqmani.

Acquisition of data. Robson, Grayson, Ponte, Suppiah, Craven, Watts, Merkel, Luqmani.

Analysis and interpretation of data. Robson, Grayson, Ponte, Suppiah, Craven, Judge, Khalid, Hutchings, Watts, Merkel, Luqmani.

REFERENCES

1. Jennette JC, Falk RJ, Bacon PA, Basu N, Cid MC, Ferrario F, et al. 2012 revised International Chapel Hill Consensus Conference nomenclature of vasculitides. Arthritis Rheum 2013;65:1–11.
2. Fries JF, Hunder GG, Bloch DA, Michel BA, Arend WP, Calabrese LH, et al. The American College of Rheumatology 1990 criteria for the classification of vasculitis. Arthritis Rheum 1990;33:1135–6.
3. Bloch DA, Michel BA, Hunder GG, McShane DJ, Arend WP, Calabrese LH, et al. The American College of Rheumatology 1990 criteria for the classification of vasculitis: patients and methods. Arthritis Rheum 1990;33:1068–73.
4. Leavitt RY, Fauci AS, Bloch DA, Michel BA, Hunder GG, Arend WP, et al. The American College of Rheumatology 1990 criteria for the classification of Wegener's granulomatosis. Arthritis Rheum 1990; 33:1101–7.
5. Jones RB, Tervaert JW, Hauser T, Luqmani R, Morgan MD, Peh CA, et al. Rituximab versus cyclophosphamide in ANCA-associated renal vasculitis. N Engl J Med 2010;363:211–20.
6. Stone JH, Merkel PA, Spiera R, Seo P, Langford CA, Hoffman GS, et al. Rituximab versus cyclophosphamide for ANCA-associated vasculitis. N Engl J Med 2010;363:221–32.
7. Falk RJ, Gross WL, Guillevin L, Hoffman GS, Jayne DR, Jennette JC, et al. Granulomatosis with polyangiitis (Wegener's): an alternative name for Wegener's granulomatosis. Arthritis Rheum 2011;63:863–4.
8. Falk RJ, Gross WL, Guillevin L, Hoffman G, Jayne DR, Jennette JC, et al. Granulomatosis with polyangiitis (Wegener's): an alternative name for Wegener's granulomatosis. Ann Rheum Dis 2011;70:704.
9. Falk RJ, Gross WL, Guillevin L, Hoffman G, Jayne DR, Jennette JC, et al. Granulomatosis with polyangiitis (Wegener's): an alternative name for Wegener's granulomatosis. J Am Soc Nephrol 2011;22: 587–8.
10. Jennette JC, Falk RJ, Andrassy K, Bacon PA, Churg J, Gross WL, et al. Nomenclature of systemic vasculitides: proposal of an international consensus conference. Arthritis Rheum 1994;37:187–92.
11. Seeliger B, Sznajd J, Robson JC, Judge A, Craven A, Grayson PC, et al. Are the 1990 American College of Rheumatology vasculitis classification criteria still valid? Rheumatology (Oxford) 2017;56:1154–61.
12. Watts RA, Suppiah R, Merkel PA, Luqmani R. Systemic vasculitis—is it time to reclassify? Rheumatology (Oxford) 2011;50:643–5.
13. Basu N, Watts R, Bajema I, Baslund B, Bley T, Boers M, et al. EULAR points to consider in the development of classification and diagnostic criteria in systemic vasculitis. Ann Rheum Dis 2010;69: 1744–50.
14. Aletaha D, Neogi T, Silman AJ, Funovits J, Felson DT, Bingham CO III, et al. 2010 rheumatoid arthritis classification criteria: an American College of Rheumatology/European League Against Rheumatism collaborative initiative. Arthritis Rheum 2010;62:2569–81.
15. Craven A, Robson J, Ponte C, Grayson PC, Suppiah R, Judge A, et al. ACR/EULAR-endorsed study to develop Diagnostic and Classification Criteria for Vasculitis (DCVAS). Clin Exp Nephrol 2013;17: 619–21.
16. Shiboski SC, Shiboski CH, Criswell L, Baer A, Challacombe S, Lanfranchi H, et al. American College of Rheumatology classification criteria for Sjögren's syndrome: a data-driven, expert consensus approach in the Sjögren's International Collaborative Clinical Alliance cohort. Arthritis Care Res (Hoboken) 2012;64:475–87.
17. Rao JK, Allen NB, Pincus T. Limitations of the 1990 American College of Rheumatology classification criteria in the diagnosis of vasculitis. Ann Intern Med 1998;129:345–52.

APPENDIX A: THE DCVAS INVESTIGATORS

The DCVAS study investigators are as follows: Paul Gatenby (ANU Medical Centre, Canberra, Australia); Catherine Hill (Central Adelaide Local Health Network: The Queen Elizabeth Hospital, Australia); Dwarakanathan Ranganathan (Royal Brisbane and Women's Hospital, Australia); Andreas Kronbichler (Medical University Innsbruck, Austria); Daniel Blockmans (University Hospitals Leuven, Belgium); Lillian Barra (Lawson Health Research Institute, London, Ontario, Canada); Simon Carette, Christian Pagnoux (Mount Sinai Hospital, Toronto, Canada); Navjot Dhindsa (University of Manitoba, Winnipeg, Canada); Aurore Fifi-Mah (University of Calgary, Alberta, Canada); Nader Khalidi (St Joseph's Healthcare, Hamilton, Ontario, Canada); Patrick Liang (Sherbrooke University Hospital Centre, Canada); Nataliya Milman (University of Ottawa, Canada); Christian Pineau (McGill University, Canada); Xinping Tian (Peking Union Medical College Hospital, Beijing, China); Guochun Wang (China-Japan Friendship Hospital, Beijing, China); Tian Wang (Anzhen Hospital, Capital Medical University, China); Ming-hui Zhao (Peking University First Hospital, China); Vladimir Tesar (General University Hospital, Prague, Czech Republic); Bo Baslund (University Hospital, Copenhagen [Rigshospitalet], Denmark); Nevin Hammam (Assiut University, Egypt); Amira Shahin (Cairo University, Egypt); Laura Pirila (Turku University Hospital, Finland); Jukka Putaala (Helsinki University Central Hospital, Finland); Bernhard Hellmich (Kreisklinken Esslingen, Germany); Jörg Henes (Universitätsklinikum Tübingen, Germany); Julia Holle (Klinikum Bad Bramstedt, Germany); Peter Lamprecht (Klinikum Bad Bramstedt, Germany); Frank Moosig (Klinikum Bad Bramstedt, Germany); Thomas Neumann (Universitätsklinikum Jena, Germany); Wolfgang Schmidt (Immanuel Krankenhaus Berlin, Germany); Cord Sunderkoetter (Universitätsklinikum Müenster, Germany); Zoltan Szekanecz (University of Debrecen Medical and Health Science Center, Hungary); Debashish Danda (Christian Medical College & Hospital, Vellore, India); Siddharth Das (Chatrapathi Shahuji Maharaj Medical Center, Lucknow [IP], India); Rajiva Gupta (Medanta, Delhi, India); Liza Rajasekhar (NIMS, Hyderabad, India); Aman Sharma (Postgraduate Institute of Medical Education and Research, Chandigarh, India); Shrikant Wagh (Jehangir Clinical Development Centre, Pune [IP], India); Michael Clarkson (Cork University Hospital, Ireland); Eamonn Molloy (St. Vincent's University Hospital, Dublin, Ireland); Carlo Salvarani (Santa Maria Nuova Hospital, Reggio Emilia, Italy); Franco Schiavon (L'Azienda Ospedaliera of University of Padua, Italy); Enrico Tombetti (Università Vita-Salute San Raffaele Milano, Italy); Augusto Vaglio (University of Parma, Italy); Koichi Amano (Saitama Medical University, Japan); Yoshihiro Arimura (Kyorin University Hospital, Japan); Hiroaki Dobashi (Kagawa University Hospital, Japan); Shouichi Fujimoto (Miyazaki University Hospital [HUB], Japan); Masayoshi Harigai, Fumio Hirano (Tokyo Medical and Dental University Hospital, Japan); Junichi Hirahashi (University Tokyo Hospital, Japan); Sakae Honma (Toho University Hospital, Japan); Tamihiro Kawakami (St. Marianna University Hospital Dermatology, Japan); Shigeto Kobayashi (Juntendo University Koshigaya Hospital, Japan); Hajime Kono (Teikyo University, Japan); Hirofumi Makino (Okayama University Hospital, Japan); Kazuo Matsui (Kameda Medical Centre, Kamogawa, Japan); Eri Muso (Kitano Hospital, Japan); Kazuo Suzuki, Kei Ikeda (Chiba University Hospital, Japan); Tsutomu Takeuchi (Keio University Hospital, Japan); Tatsuo Tsukamoto (Kyoto University Hospital, Japan); Shunya Uchida (Teikyo University Hospital, Japan); Takashi Wada (Kanazawa University Hospital, Japan); Hidehiro Yamada (St. Marianna University Hospital Internal Medicine, Japan); Kunihiro Yamagata (Tsukuba University Hospital, Japan); Wako Yumura (IUHW Hospital [Jichi Medical University Hospital], Japan); Kan Sow Lai (Penang General Hospital, Malaysia); Luis Felipe Flores-Suarez (Instituto Nacional de Enfermedades Respiratorias, Mexico City, Mexico); Andrea Hinojosa-Azaola (Instituto Nacional de Ciencias Médicas y Nutrición Salvador Zubirán, Mexico City, Mexico); Bram Rutgers (University Hospital Groningen, Netherlands); Paul-Peter Tak (Academic Medical Centre, University of Amsterdam, Netherlands); Rebecca Grainger (Wellington, Otago, New Zealand); Vicki Quincey (Waikato District Health Board, New Zealand); Lisa Stamp (University of Otago, Christchurch, New Zealand); Ravi Suppiah (Auckland District Health Board, New Zealand); Emilio Besada (Tromsø, Northern Norway, Norway); Andreas Diamantopoulos (Hospital of Southern Norway, Kristiansand, Norway); Jan Sznajd (University of Jagiellonian, Poland); Elsa Azevedo (Centro Hospitalar de São João, Porto, Portugal); Ruth Geraldes (Hospital de Santa Maria, Lisbon, Portugal); Miguel Rodrigues (Hospital Garcia de Orta, Almada, Portugal); Ernestina Santos (Hospital Santo Antonio, Porto, Portugal); Yeong-Wook Song (Seoul National University Hospital, Republic of Korea); Sergey Moiseev (First Moscow State Medical University, Russia); Alojzija Hočevar (University Medical Centre Ljubljana, Slovenia); Maria Cinta Cid (Hospital Clinic de Barcelona, Spain); Xavier Solanich Moreno (Hospital de Bellvitge-Idibell, Spain); Inoshi Atukorala (University of Colombo, Sri Lanka); Ewa Berglin (Umeå University Hospital, Sweden); Aladdin Mohammed (Lund-Malmo University, Sweden); Mårten Segelmark (Linköping University, Sweden); Thomas Daikeler (University Hospital Basel, Switzerland); Haner Direskeneli (Marmara University Medical School, Turkey); Gulen Hatemi (Istanbul University, Cerrahpasa Medical School, Turkey); Sevil Kamali (Istanbul University, Istanbul Medical School, Turkey); Ömer Karadağ (Hacettepe University, Turkey); Seval Pehlevan (Fatih University Medical Faculty, Turkey); Matthew Adler (Frimley Health NHS Foundation Trust, Wexham Park Hospital, UK); Neil Basu (NHS Grampian, Aberdeen Royal Infirmary, UK); Iain Bruce (Manchester University Hospitals NHS Foundation Trust, UK); Kuntal Chakravarty (Barking, Havering and Redbridge University Hospitals NHS Trust, UK); Bhaskar Dasgupta (Southend University Hospital NHS Foundation Trust, UK); Oliver Flossmann (Royal Berkshire NHS Foundation Trust, UK); Nagui Gendi (Basildon and Thurrock University Hospitals NHS Foundation Trust, UK); Alaa Hassan (North Cumbria University Hospitals, UK); Rachel Hoyles (Oxford University Hospitals NHS Foundation Trust, UK); David Jayne (Cambridge University Hospitals NHS Foundation Trust, UK); Colin Jones (York Teaching Hospitals NHS Foundation Trust, UK); Rainer Klocke (The Dudley Group NHS Foundation Trust, UK); Peter Lanyon (Nottingham University Hospitals NHS Trust, UK); Cathy Laversuch (Taunton & Somerset NHS Foundation Trust, Musgrove Park Hospital, UK); Raashid Luqmani, Joanna Robson (Nuffield Orthopaedic Centre, Oxford, UK); Malgorzata Magliano (Buckinghamshire Healthcare NHS Trust, UK); Justin Mason (Imperial College Healthcare NHS Trust, UK); Win Win Maw (Mid Essex Hospital Services NHS Trust, UK); Iain McInnes (NHS Greater Glasgow & Clyde, Gartnavel Hospital & GRI, UK); John Mclaren (NHS Fife, Whyteman's Brae Hospital, UK); Matthew Morgan (University Hospitals Birmingham NHS Foundation Trust, Queen Elizabeth Hospital, UK); Ann Morgan (Leeds Teaching Hospitals NHS Trust, UK); Chetan Mukhtyar (Norfolk and Norwich University Hospitals NHS Foundation Trust, UK); Edmond O'Riordan (Salford Royal NHS Foundation Trust, UK); Sanjeev Patel (Epsom and St Helier University Hospitals NHS Trust, UK); Adrian Peall (Wye Valley NHS Trust, Hereford County Hospital, UK); Joanna Robson (University Hospitals Bristol NHS Foundation Trust, UK); Srinivasan Venkatachalam (The Royal Wolverhampton NHS Trust, UK); Erin Vermaak, Ajit Menon (Staffordshire & Stoke on Trent Partnership NHS Trust, Haywood Hospital, UK); Richard Watts (East Suffolk and North Essex NHS Foundation Trust, UK); Chee-Seng Yee (Doncaster and Bassetlaw Hospitals NHS Foundation Trust, UK); Daniel Albert (Dartmouth-Hitchcock Medical Center, US); Leonard Calabrese (Cleveland Clinic Foundation, US); Sharon Chung (University of California, San Francisco, US); Lindsy Forbess (Cedars-Sinai Medical Center, US); Angelo Gaffo (University of Alabama at Birmingham, US); Ora Gewurz-Singer (University of Michigan, US); Peter Grayson (Boston University School of Medicine, US); Kimberly Liang (University of Pittsburgh, US); Eric Matteson (Mayo Clinic, US); Peter A. Merkel (University of Pennsylvania, US); Rennie Rhee (University of Pennsylvania, US); Jason Springer (University of Kansas Medical Center Research Institute, US); and Antoine Sreih (Rush University Medical Center, US).

American College of Rheumatology
Empowering Rheumatology Professionals

Arthritis & Rheumatology
Vol. 74, No. 3, March 2022, pp 400–406
DOI 10.1002/art.41983

2022 American College of Rheumatology/European Alliance of Associations for Rheumatology Classification Criteria for Microscopic Polyangiitis

Ravi Suppiah,[1] Joanna C. Robson,[2] Peter C. Grayson,[3] Cristina Ponte,[4] Anthea Craven,[5] Sara Khalid,[5] Andrew Judge,[6] Andrew Hutchings,[7] Peter A. Merkel,[8] Raashid A. Luqmani,[5] and Richard A. Watts[9]

This criteria set has been approved by the American College of Rheumatology (ACR) Board of Directors and the European Alliance of Associations for Rheumatology (EULAR) Executive Committee. This signifies that the criteria set has been quantitatively validated using patient data, and it has undergone validation based on an independent data set. All ACR/EULAR-approved criteria sets are expected to undergo intermittent updates.

The ACR is an independent, professional, medical and scientific society that does not guarantee, warrant, or endorse any commercial product or service.

Objective. To develop and validate classification criteria for microscopic polyangiitis (MPA).

Methods. Patients with vasculitis or comparator diseases were recruited into an international cohort. The study proceeded in 5 phases: 1) identification of candidate items using consensus methodology, 2) prospective collection of candidate items present at the time of diagnosis, 3) data-driven reduction of the number of candidate items, 4) expert panel review of cases to define the reference diagnosis, and 5) derivation of a points-based risk score for disease classification in a development set using least absolute shrinkage and selection operator logistic regression, with subsequent validation of performance characteristics in an independent set of cases and comparators.

Results. The development set for MPA consisted of 149 cases of MPA and 408 comparators. The validation set consisted of an additional 142 cases of MPA and 414 comparators. From 91 candidate items, regression analysis identified 10 items for MPA, 6 of which were retained. The final criteria and their weights were as follows: perinuclear antineutrophil cytoplasmic antibody (ANCA) or anti–myeloperoxidase-ANCA positivity (+6), pauci-immune glomerulonephritis (+3), lung fibrosis or interstitial lung disease (+3), sino-nasal symptoms or signs (−3), cytoplasmic ANCA or anti–proteinase 3 ANCA positivity (−1), and eosinophil count ≥1 × 10^9/liter (−4). After excluding mimics of vasculitis, a patient with a diagnosis of small- or medium-vessel vasculitis could be classified as having MPA with a cumulative score of ≥5 points. When these criteria were tested in the validation data set, the sensitivity was 91% (95% confidence interval [95% CI] 85–95%) and the specificity was 94% (95% CI 92–96%).

Conclusion. The 2022 American College of Rheumatology/European Alliance of Associations for Rheumatology classification criteria for MPA are now validated for use in clinical research.

This article is published simultaneously in the March 2022 issue of *Annals of the Rheumatic Diseases*.

The Diagnostic and Classification Criteria in Vasculitis (DCVAS) study, of which the development of these classification criteria was a part, was funded by grants from the American College of Rheumatology (ACR), the European Alliance of Associations for Rheumatology (EULAR), the Vasculitis Foundation, and the University of Pennsylvania Vasculitis Center.

[1]Ravi Suppiah, MD: Auckland District Health Board, Auckland, New Zealand; [2]Joanna C. Robson, MBBS, PhD: Centre for Health and Clinical Research, University of the West of England, and University Hospitals and Weston NHS Foundation Trust, Bristol, UK; [3]Peter C. Grayson, MD, MSc: National Institute of Arthritis and Musculoskeletal and Skin Diseases, NIH, Bethesda, Maryland; [4]Cristina Ponte, MD, PhD: Hospital de Santa Maria, Centro Hospitalar Universitário Lisboa Norte, Universidade de Lisboa, and Centro Académico de Medicina de Lisboa, Lisbon, Portugal; [5]Anthea Craven, BSc, Sara Khalid, DPhil, Raashid A. Luqmani, DM, FRCP: Oxford NIHR Biomedical Research Centre and University of Oxford, Oxford, UK; [6]Andrew Judge, PhD: Oxford NIHR Biomedical Research Centre and University of Oxford, Oxford, UK, and Bristol NIHR Biomedical Research Centre and University of Bristol, Bristol, UK; [7]Andrew Hutchings, MSc: London School of Hygiene and Tropical Medicine, London, UK; [8]Peter A. Merkel, MD, MPH: University of

INTRODUCTION

The first description of "periarteritis nodosa" was made by Kussmaul and Maier in 1866 (1). In 1948, Davson et al described 14 cases at autopsy that fitted the clinical description of periarteritis nodosa (2). They divided the cases into 2 groups based on the histologic findings in the kidneys. The clinical presentations of both groups were similar, but their pathologic features differed: 9 patients showed a distinctive pattern of necrotizing glomerulonephritis with no arterial aneurysms, whereas the other 5 patients showed no glomerular lesions in the kidney but had widespread renal arterial aneurysms and renal infarcts. This is the first time that a clear distinction was made between the microscopic form of polyarteritis nodosa (now called microscopic polyangiitis [MPA]) and classic polyarteritis nodosa (PAN). The 1990 American College of Rheumatology (ACR) criteria for the classification of vasculitis did not make this distinction; instead both entities were included under the term "polyarteritis nodosa" (3) or possibly "granulomatosis with polyangiitis" (then called Wegener's granulomatosis).

The publication that resulted from the 1994 Chapel Hill Consensus Conference (CHCC) aimed to standardize the nomenclature and commented that "different names are being used for the same disease and the same name is being used for different diseases" (4). The distinction between MPA and PAN is recognized in the CHCC definitions. The main discriminating feature between MPA and PAN is the presence in MPA of pauci-immune vasculitis in arterioles, venules, or capillaries. PAN is restricted to a medium-vessel disease, and MPA is a predominantly small-vessel vasculitis that can also involve medium-sized vessels.

The resulting inconsistency between disease definitions and existing classification criteria highlights an important need to update the classification criteria and to include MPA as its own entity. Additionally, over time there have been improvements in our understanding of the different forms of vasculitis, which have been informed in part by routine testing for antineutrophil cytoplasmic antibody (ANCA) in patients with vasculitis and increased utilization of cross-sectional imaging, both of which have occurred since the 1990 ACR criteria were published. Indeed, most investigators regard MPA as part of the group of small-vessel vasculitides related to the presence of ANCA. This article outlines the development and validation of the new ACR/European Alliance of Associations for Rheumatology (EULAR)–endorsed classification criteria for MPA.

METHODS

A detailed and complete description of the methods involved in the development and validation of the classification criteria for MPA is provided in Supplementary Appendix 1, available on the *Arthritis & Rheumatology* website at http://onlinelibrary.wiley.com/doi/10.1002/art.41983/abstract. Briefly, an international Steering Committee comprising clinician investigators with expertise in vasculitis, statisticians, and data managers was established to oversee the overall Diagnostic and Classification Criteria in Vasculitis (DCVAS) project. The Steering Committee established a 5-stage plan using data-driven and consensus methodology to develop the criteria for each of 6 forms of vasculitis.

Stage 1: generation of candidate classification items for the systemic vasculitides. Candidate classification items were generated by expert opinion and reviewed by a group of vasculitis experts across a range of specialties using a nominal group technique.

Stage 2: DCVAS prospective observational study. A prospective, international multisite observational study was conducted (see Appendix A for study investigators and sites). Ethical approval was obtained from national and local ethics committees. Consecutive patients representing the full spectrum of disease were recruited from academic and community practices. Patients were included if they were 18 years or older and had a diagnosis of vasculitis or a condition that mimics vasculitis. Patients with ANCA-associated vasculitis (AAV) could only be enrolled within 2 years of diagnosis. Only data present at diagnosis were recorded.

Stage 3: refinement of candidate items specifically for AAV. The Steering Committee conducted a data-driven process to reduce the number of candidate items of relevance to cases and comparators for AAV. Items were selected for exclusion if they had a prevalence of <5% within the data set and/or they were not clinically relevant for classification criteria (e.g., related to infection, malignancy, or demographic characteristics). Low-frequency items of clinical importance could be combined, when appropriate.

Stage 4: expert review to derive a gold standard–defined set of cases of AAV. Experts in vasculitis from a wide range of geographic locations and specialties reviewed all submitted cases of vasculitis and a random selection of mimics of

Pennsylvania, Philadelphia; [9]Richard A. Watts, MD: Oxford NIHR Biomedical Research Centre and University of Oxford, Oxford, UK, and University of East Anglia, Norwich, UK.

[Correction added on 20 June 2022, after first online publication: Appendices A and 1 have been replaced and Appendix S2 has been added online.]

Author disclosures are available at https://onlinelibrary.wiley.com/action/downloadSupplement?doi=10.1002%2Fart.41983&file=art41983-sup-0001-Disclosureform.pdf.

Address correspondence to Peter A. Merkel, MD, MPH, Chief, Division of Rheumatology, University of Pennsylvania, White Building, Fifth Floor, 3400 Spruce Street, Philadelphia, PA 19104 (email: pmerkel@upenn.edu); or to Raashid A. Luqmani, DM, FRCP, Rheumatology Department, Nuffield Orthopaedic Centre, University of Oxford, Windmill Road, Oxford OX3 7LD, UK (email: raashid.luqmani@ndorms.ox.ac.uk).

Submitted for publication February 28, 2020; accepted in revised form September 21, 2021.

vasculitis. Each reviewer was asked to review ~50 submitted cases to confirm the diagnosis and to specify the certainty of their diagnosis as follows: very certain, moderately certain, uncertain, or very uncertain. Only cases agreed upon with at least moderate certainty were retained for further analysis.

Stage 5: derivation and validation of the final classification criteria for MPA. The DCVAS AAV data set was randomly split into development (50%) and validation (50%) sets. Comparisons were performed between cases of MPA and a comparator group randomly selected from the DCVAS cohort in the following proportions: another type of AAV (including granulomatosis with polyangiitis [GPA] and eosinophilic granulomatosis with polyangiitis [EGPA]), 60%; another form of small-vessel vasculitis (e.g., cryoglobulinemic vasculitis) or medium-vessel vasculitis (e.g., PAN), 40%. Least absolute shrinkage and selection operator (lasso) logistic regression was used to identify items from the data set and create a parsimonious model including only the most important items. The final items in the model were formulated into a clinical risk-scoring tool with each factor assigned a weight based on its respective regression coefficient. A threshold that best balanced sensitivity and specificity was identified for classification.

In sensitivity analyses, the final classification criteria were applied to an unselected population of cases and comparators from the DCVAS data set based on the submitting physician diagnosis.

RESULTS

Generation of candidate classification items for the systemic vasculitides. The Steering Committee identified >1,000 candidate items for the DCVAS case report form (see Supplementary Appendix 2, available on the *Arthritis & Rheumatology* website at http://onlinelibrary.wiley.com/doi/10.1002/art.41983/abstract).

DCVAS prospective observational study. Between January 2011 and December 2017, the DCVAS study recruited 6,991 participants from 136 sites in 32 countries. Information on the DCVAS sites, investigators, and participants is listed in Supplementary Appendices 3, 4, and 5, available on the *Arthritis & Rheumatology* website at http://onlinelibrary.wiley.com/doi/10.1002/art.41983/abstract.

Refinement of candidate items specifically for AAV. Following a data-driven and expert consensus process, 91 items from the DCVAS case report form were retained for regression analysis, including 45 clinical (14 composite), 18 laboratory (2 composite), 12 imaging (all composite), and 16 biopsy (1 composite) items. Some clinical items were removed in favor of similar but more specific pathophysiologic descriptors. For example, "Hearing loss or reduction" was removed, and the composite item "Conductive hearing loss/sensorineural hearing loss" was retained. See Supplementary Appendix 6, available on the *Arthritis & Rheumatology* website at http://onlinelibrary.wiley.com/doi/10.1002/art.41983/abstract, for the final candidate items used in the derivation of the classification criteria for GPA, MPA, and EGPA.

Expert review to derive a gold standard–defined final set of cases of AAV. Fifty-five independent experts reviewed vignettes derived from the case report forms for 2,871 cases submitted with a diagnosis of either small-vessel vasculitis (90% of case report forms) or another type of vasculitis or a mimic of vasculitis (10% of case report forms). The characteristics of the expert reviewers are shown in Supplementary Appendix 7, available on the *Arthritis & Rheumatology* website at http://onlinelibrary.wiley.com/doi/10.1002/art.41983/abstract. A flow chart showing the results of the expert review process is shown in Supplementary Appendix 8, available on the *Arthritis &*

Table 1. Demographic and disease features of cases of MPA and comparators*

	MPA (n = 291)	Comparators (n = 822)†	*P*
Age, mean ± SD years	65.5 ± 13.2	52.0 ± 16.9	<0.001
Sex, no. (%) female	164 (56.4)	394 (47.9)	0.016
Maximum serum creatinine, mean			<0.001
μmoles/liter	126.4	185.2	
mg/dl	1.4	2.1	
cANCA positive, no. (%)	11 (3.8)	257 (31.3)	<0.001
pANCA positive, no. (%)	236 (81.1)	136 (16.5)	<0.001
Anti–PR3-ANCA positive, no. (%)	6 (2.1)	265 (32.2)	<0.001
Anti–MPO-ANCA positive, no. (%)	279 (95.9)	142 (17.3)	<0.001
Maximum eosinophil count ≥1 × 10^9/liter, no. (%)	15 (5.2)	244 (29.7)	<0.001

* cANCA = cytoplasmic antineutrophil cytoplasmic antibody; pANCA = perinuclear ANCA; anti–PR3-ANCA = anti–proteinase 3–ANCA; anti–MPO-ANCA = anti–myeloperoxidase-ANCA.
† Diagnoses of comparators for the classification criteria for microscopic polyangiitis (MPA) included granulomatosis with polyangiitis (n = 300), eosinophilic granulomatosis with polyangiitis (n = 226), polyarteritis nodosa (n = 51), non–ANCA-associated small-vessel vasculitis that could not be subtyped (n = 51), Behçet's disease (n = 50), IgA vasculitis (n = 50), cryoglobulinemic vasculitis (n = 34), ANCA-associated vasculitis that could not be subtyped (n = 25), primary central nervous system vasculitis (n = 19), and anti–glomerular basement membrane disease (n = 16).

Rheumatology website at http://onlinelibrary.wiley.com/doi/10.1002/art.41983/abstract. A total of 2,072 cases (72%) passed the process and were designated as cases of vasculitis; these cases were used for the stage 5 analyses.

After expert panel review by 55 investigators, 269 of 404 of the cases retained the submitting physician diagnosis of MPA, and 22 additional cases were reclassified as having MPA by consensus of 2 expert reviewers. Compared to the 291 patients with a reference diagnosis of MPA, the 135 cases that were excluded had lower rates of perinuclear ANCA (pANCA) or anti–myeloperoxidase-ANCA (anti–MPO-ANCA) positivity (76% versus 98%; $P < 0.01$), were less likely to have pauci-immune glomerulonephritis (16% versus 49%; $P < 0.01$), were more likely to have maximum eosinophil counts $\geq 1 \times 10^9$/liter (12% versus 6%; $P = 0.02$), and were more likely to be cytoplasmic ANCA– or proteinase 3–ANCA–positive (20% versus 4%; $P < 0.01$). There were 822 comparators randomly selected for analysis. Table 1 shows the demographic and disease features of the 1,113 cases included in this analysis (291 patients with MPA and 822 comparators), of which 557 (50%; 149 patients with MPA and 408 comparators) were in the development set, and 556 (50%; 142 patients with MPA and 414 comparators) were in the validation set.

Derivation and validation of the final classification criteria for MPA. Lasso regression of the previously selected 91 items yielded 10 independent items for MPA (see Supplementary Appendix 9C, available on the *Arthritis & Rheumatology* website at http://onlinelibrary.wiley.com/doi/10.1002/art.41983/abstract). Each item was then adjudicated by the DCVAS Steering Committee for inclusion based on clinical relevance and specificity to MPA, resulting in 6 final items. Weighting of an individual criterion was based on logistic regression fitted to the 6 selected items (see Supplementary Appendix 10C, available on the *Arthritis & Rheumatology* website at http://onlinelibrary.wiley.com/doi/10.1002/art.41983/abstract).

2022 AMERICAN COLLEGE OF RHEUMATOLOGY / EUROPEAN ALLIANCE OF ASSOCIATIONS FOR RHEUMATOLOGY

CLASSIFICATION CRITERIA FOR **MICROSCOPIC POLYANGIITIS**

CONSIDERATIONS WHEN APPLYING THESE CRITERIA

- **These classification criteria should be applied to classify a patient as having microscopic polyangiitis when a diagnosis of small- or medium-vessel vasculitis has been made**
- **Alternate diagnoses mimicking vasculitis should be excluded prior to applying the criteria**

CLINICAL CRITERIA

Nasal involvement: bloody discharge, ulcers, crusting, congestion, blockage or septal defect / perforation	-3

LABORATORY, IMAGING, AND BIOPSY CRITERIA

Positive test for perinuclear antineutrophil cytoplasmic antibodies (pANCA) or antimyeloperoxidase (anti-MPO) antibodies ANCA positive	+6
Fibrosis or interstitial lung disease on chest imaging	+3
Pauci-immune glomerulonephritis on biopsy	+3
Positive test for cytoplasmic antineutrophil cytoplasmic antibodies (cANCA) or antiproteinase 3 (anti-PR3) antibodies	-1
Blood eosinophil count ≥ 1 x10^9/liter	-4

Sum the scores for 6 items, if present. A score of ≥ 5 is needed for classification of MICROSCOPIC POLYANGIITIS.

Figure 1. 2022 American College of Rheumatology/European Alliance of Associations for Rheumatology classification criteria for microscopic polyangiitis.

Model performance. Use of a cutoff of ≥5 in total risk score (see Supplementary Appendix 11C, available on the *Arthritis & Rheumatology* website at http://onlinelibrary.wiley.com/doi/10.1002/art.41983/abstract, for different cut points) yielded a sensitivity of 90.8% (95% confidence interval [95% CI] 84.9–95.0%) and a specificity of 94.2% (95% CI 91.5–96.3%) in the validation set. The area under the curve for the model was 0.98 (95% CI 0.97–0.99) in the development set and 0.97 (95% CI 0.95–0.98) in the validation set for the final MPA classification criteria (Supplementary Appendix 12C, available on the *Arthritis & Rheumatology* website at http://onlinelibrary.wiley.com/doi/10.1002/art.41983/abstract). The final classification criteria for MPA are shown in Figure 1 (for the slide presentation version, see Supplementary Figure 1, available on the *Arthritis & Rheumatology* website at http://onlinelibrary.wiley.com/doi/10.1002/art.41983/abstract).

Sensitivity analysis. The classification criteria for MPA were applied to 2,871 patients in the DCVAS database using the original physician-submitted diagnosis (n = 404 cases of MPA and 2,467 randomly selected comparators). Use of the same cut point of ≥5 points for the classification for MPA yielded a similar specificity of 92.5% but a lower sensitivity of 82.4%. This is consistent with the a priori hypothesis that specificity would remain unchanged but sensitivity would be reduced in a population with fewer clearcut diagnoses of MPA (i.e., cases that did not pass expert panel review).

DISCUSSION

Presented here are the 2022 ACR/EULAR MPA classification criteria. These are the first formal criteria for MPA. A 5-stage approach has been used, underpinned by data from the multinational prospective DCVAS study and informed by expert review and consensus at each stage. The comparator group for developing and validating the criteria were predominantly patients with other forms of AAV and other small- and medium-vessel vasculitides, the clinical entities where discrimination from MPA is difficult, but important. The new criteria for MPA have excellent sensitivity and specificity and incorporate ANCA testing and modern imaging techniques. The criteria were designed to have face and content validity for use in clinical trials and other research studies.

These criteria are validated and intended for the purpose of *classification* of vasculitis and are not appropriate for use in establishing a *diagnosis* of vasculitis. The aim of the classification criteria is to differentiate cases of MPA from similar types of vasculitis in research settings. Therefore, the criteria should only be applied when a diagnosis of small- or medium-vessel vasculitis has been made and all potential "vasculitis mimics" have been excluded. The exclusion of mimics is a key aspect of many classification criteria, including those for Sjögren's syndrome (5) and rheumatoid arthritis (6). The 1990 ACR classification criteria for vasculitis perform poorly when used for diagnosis (i.e., when used to differentiate between cases of vasculitis versus mimics without vasculitis) (7), and it is expected that the 2022 criteria would also perform poorly if used inappropriately as diagnostic criteria in people in whom alternative diagnoses, such as infection or other non-vasculitis inflammatory diseases, are still being considered. The relatively low weight assigned to glomerulonephritis in these classification criteria highlights the distinction between classification and diagnostic criteria. While detection of kidney disease is important to diagnose MPA, glomerulonephritis is common among patients with either GPA or MPA and thus does not function as a strong classifier between these conditions.

MPA was not recognized as a separate entity in the 1990 ACR classification criteria for vasculitis, although the disease was recognized as pathologically distinct from PAN over 40 years earlier. This omission of MPA caused difficulties in defining clear homogeneous populations for research; thus, over the last 2 decades, investigators have often relied on the disease definitions of the CHCC nomenclature for eligibility criteria when enrolling patients with MPA into clinical trials (4,8–11). This approach resulted in heterogeneity between patients enrolled in therapeutic trials and epidemiologic studies (12). Due to inconsistent methods employed by researchers when applying the 1990 ACR criteria and the CHCC definitions in parallel, the European Medicines Agency (EMA) convened meetings to develop a consensus on how to utilize the 2 systems, leading to the publication of the EMA algorithm in 2007 (13). The algorithm works by first excluding EGPA and GPA, and then relying on the CHCC histologic descriptions to discriminate between MPA and PAN. The new 2022 ACR/EULAR classification criteria for MPA and other vasculitides provide validated criteria that can replace the EMA interim solution and should harmonize future research studies.

A potential limitation of these new criteria is that, through the expert panel consensus methodology, only the most definite cases were included in the analyses. However, the purpose of these criteria is to enable homogeneous groupings so that individual diseases can be studied. Overall, the use of more definitive cases is consistent with the purpose of classification criteria. Additionally, positive testing for MPO-ANCA is weighted heavily in the criteria, and it is theoretically possible to classify a patient as having MPA on the basis of a positive test for MPO-ANCA only. However, the criteria are intended to only be applied to patients with an established diagnosis of small- or medium-vessel vasculitis; in this setting, the criteria sets should result in a reduction of the score away from a classification of MPA if the patient has features of another form of AAV. When criteria were tested in a much less clearly defined population using the submitting physician diagnosis as the gold standard, the sensitivity of the criteria fell substantially despite 91% of this group being pANCA- or MPO-ANCA positive, which supports the contention that ANCA positivity is not overly dominant for the classification. Nonetheless, ANCA testing is obviously a key discriminator between the different forms of AAV and other small- and medium-vessel vasculitides.

There are some additional study limitations to consider. Although this was the largest international study ever conducted in vasculitis, most patients were recruited from Europe, Asia, and North America. The performance characteristics of the criteria should be further tested in African and South American populations, which may have different clinical presentations of vasculitis. These criteria were developed using data collected from adult patients with vasculitis. Although the clinical characteristics of MPA and the other vasculitides which these criteria were tested against are not known to differ substantially between adults and children, these criteria should be applied to children with some caution. The scope of the criteria is intentionally narrow and applies only to patients who have been diagnosed as having vasculitis. Diagnostic criteria are not specified. The criteria are intended to identify homogeneous populations of disease and, therefore, may not be appropriate for studies focused on the full spectrum of clinical heterogeneity in these conditions. To maximize relevance and face validity of the new criteria, study sites and expert reviewers were recruited from a broad range of countries and different medical specialties. Nonetheless, the majority of patients were recruited from academic rheumatology or nephrology units, which could have introduced referral bias.

The 2022 ACR/EULAR classification criteria for MPA are the product of a rigorous methodologic process that utilized an extensive data set generated by the work of a remarkable international group of collaborators. These are the first classification criteria for this disease. The criteria can now be applied to patients who have been diagnosed as having a small- or medium-vessel vasculitis. These criteria have been endorsed by the ACR and EULAR and are now ready for use to differentiate one type of vasculitis from another to define populations in research studies.

ACKNOWLEDGMENTS

We acknowledge the patients and clinicians who provided data to the DCVAS project.

AUTHOR CONTRIBUTIONS

All authors were involved in drafting the article or revising it critically for important intellectual content, and all authors approved the final version to be published. Dr. Merkel had full access to all of the data in the study and takes responsibility for the integrity of the data and the accuracy of the data analysis.

Study conception and design. Suppiah, Robson, Grayson, Ponte, Craven, Judge, Hutchings, Merkel, Luqmani, Watts.

Acquisition of data. Suppiah, Robson, Grayson, Ponte, Craven, Merkel, Luqmani, Watts.

Analysis and interpretation of data. Suppiah, Robson, Grayson, Ponte, Craven, Khalid, Judge, Hutchings, Merkel, Luqmani, Watts.

REFERENCES

1. Kussmaul A, Maier R. Ueber eine bisher nicht beschriebene eigenthumliche Arterienerkrankung (Periarteritis nodosa), die mit Morbus Brightti und rapid fortschreitender allgemeiner Muskellahmung einhergeht. Dtsch Arch Klin Med 1866;1:484–518.
2. Davson J, Ball J, Platt R. The kidney in periarteritis nodosa. Q J Med 1948;17:175–202.
3. Lightfoot RW Jr, Michel BA, Bloch DA, Hunder GG, Zvaifler NJ, McShane DJ, et al. The American College of Rheumatology 1990 criteria for the classification of polyarteritis nodosa. Arthritis Rheum 1990:33:1088–93.
4. Jennette JC, Falk RJ, Andrassy K, Bacon PA, Churg J, Gross WL, et al. Nomenclature of systemic vasculitides: proposal of an international consensus conference. Arthritis Rheum 1994;37:187–92.
5. Shiboski SC, Shiboski CH, Criswell L, Baer A, Challacombe S, Lanfranchi H, et al. American College of Rheumatology classification criteria for Sjögren's syndrome: a data-driven, expert consensus approach in the Sjögren's International Collaborative Clinical Alliance cohort. Arthritis Care Res (Hoboken) 2012;64:475–87.
6. Aletaha D, Neogi T, Silman AJ, Funovits J, Felson DT, Bingham CO III, et al. 2010 rheumatoid arthritis classification criteria: an American College of Rheumatology/European League Against Rheumatism collaborative initiative. Arthritis Rheum 2010;62:2569–81.
7. Rao JK, Allen NB, Pincus T. Limitations of the 1990 American College of Rheumatology classification criteria in the diagnosis of vasculitis. Ann Intern Med 1998;129:345–52.
8. De Groot K, Harper L, Jayne DR, Flores Suarez LF, Gregorini G, Gross W L, et al. Pulse versus daily oral cyclophosphamide for induction of remission in antineutrophil cytoplasmic antibody-associated vasculitis: a randomized trial. Ann Intern Med 2009;150:670–80.
9. De Groot K, Rasmussen N, Bacon PA, Tervaert JW, Feighery C, Gregorini G, et al. Randomized trial of cyclophosphamide versus methotrexate for induction of remission in early systemic antineutrophil cytoplasmic antibody–associated vasculitis. Arthritis Rheum 2005;52:2461–9.
10. Jayne D, Rasmussen N, Andrassy K, Bacon P, Tervaert JW, Dadoniene J, et al. A randomized trial of maintenance therapy for vasculitis associated with antineutrophil cytoplasmic autoantibodies. N Engl J Med 2003;349:36–44.
11. Jayne DR, Gaskin G, Rasmussen N, Abramowicz D, Ferrario F, Guillevin L, et al. Randomized trial of plasma exchange or high-dosage methylprednisolone as adjunctive therapy for severe renal vasculitis. J Am Soc Nephrol 2007;18:2180–8.
12. Watts RA, Lane SE, Scott DG, Koldingsnes W, Nossent H, Gonzalez-Gay MA, et al. Epidemiology of vasculitis in Europe. Ann Rheum Dis 2001;60:1156–7.
13. Watts R, Lane S, Hanslik T, Hauser T, Hellmich B, Koldingsnes W, et al. Development and validation of a consensus methodology for the classification of the ANCA-associated vasculitides and polyarteritis nodosa for epidemiological studies. Ann Rheum Dis 2007;66: 222–7.

APPENDIX A: THE DCVAS INVESTIGATORS

The DCVAS study investigators are as follows: Paul Gatenby (ANU Medical Centre, Canberra, Australia); Catherine Hill (Central Adelaide Local Health Network: The Queen Elizabeth Hospital, Australia); Dwarakanathan Ranganathan (Royal Brisbane and Women's Hospital, Australia); Andreas Kronbichler (Medical University Innsbruck, Austria); Daniel Blockmans (University Hospitals Leuven, Belgium); Lillian Barra (Lawson Health Research Institute, London, Ontario, Canada); Simon Carette, Christian Pagnoux (Mount Sinai Hospital, Toronto, Canada); Navjot Dhindsa (University of Manitoba, Winnipeg, Canada); Aurore Fifi-Mah (University of Calgary, Alberta, Canada); Nader Khalidi (St Joseph's Healthcare, Hamilton, Ontario, Canada); Patrick Liang (Sherbrooke University Hospital Centre, Canada); Nataliya Milman (University of Ottawa, Canada); Christian Pineau

(McGill University, Canada); Xinping Tian (Peking Union Medical College Hospital, Beijing, China); Guochun Wang (China-Japan Friendship Hospital, Beijing, China); Tian Wang (Anzhen Hospital, Capital Medical University, China); Ming-hui Zhao (Peking University First Hospital, China); Vladimir Tesar (General University Hospital, Prague, Czech Republic); Bo Baslund (University Hospital, Copenhagen [Rigshospitalet], Denmark); Nevin Hammam (Assiut University, Egypt); Amira Shahin (Cairo University, Egypt); Laura Pirila (Turku University Hospital, Finland); Jukka Putaala (Helsinki University Central Hospital, Finland); Bernhard Hellmich (Kreiskliniken Esslingen, Germany); Jörg Henes (Universitätsklinikum Tübingen, Germany); Julia Holle (Klinikum Bad Bramstedt, Germany); Peter Lamprecht (Klinikum Bad Bramstedt, Germany); Frank Moosig (Klinikum Bad Bramstedt, Germany); Thomas Neumann (Universitätsklinikum Jena, Germany); Wolfgang Schmidt (Immanuel Krankenhaus Berlin, Germany); Cord Sunderkoetter (Universitätsklinikum Müenster, Germany); Zoltan Szekanecz (University of Debrecen Medical and Health Science Center, Hungary); Debashish Danda (Christian Medical College & Hospital, Vellore, India); Siddharth Das (Chatrapathi Shahuji Maharaj Medical Center, Lucknow [IP], India); Rajiva Gupta (Medanta, Delhi, India); Liza Rajasekhar (NIMS, Hyderabad, India); Aman Sharma (Postgraduate Institute of Medical Education and Research, Chandigarh, India); Shrikant Wagh (Jehangir Clinical Development Centre, Pune [IP], India); Michael Clarkson (Cork University Hospital, Ireland); Eamonn Molloy (St. Vincent's University Hospital, Dublin, Ireland); Carlo Salvarani (Santa Maria Nuova Hospital, Reggio Emilia, Italy); Franco Schiavon (L'Azienda Ospedaliera of University of Padua, Italy); Enrico Tombetti (Università Vita-Salute San Raffaele Milano, Italy); Augusto Vaglio (University of Parma, Italy); Koichi Amano (Saitama Medical University, Japan); Yoshihiro Arimura (Kyorin University Hospital, Japan); Hiroaki Dobashi (Kagawa University Hospital, Japan); Shouichi Fujimoto (Miyazaki University Hospital [HUB], Japan); Masayoshi Harigai, Fumio Hirano (Tokyo Medical and Dental University Hospital, Japan); Junichi Hirahashi (University Tokyo Hospital, Japan); Sakae Honma (Toho University Hospital, Japan); Tamihiro Kawakami (St. Marianna University Hospital Dermatology, Japan); Shigeto Kobayashi (Juntendo University Koshigaya Hospital, Japan); Hajime Kono (Teikyo University, Japan); Hirofumi Makino (Okayama University Hospital, Japan); Kazuo Matsui (Kameda Medical Centre, Kamogawa, Japan); Eri Muso (Kitano Hospital, Japan); Kazuo Suzuki, Kei Ikeda (Chiba University Hospital, Japan); Tsutomu Takeuchi (Keio University Hospital, Japan); Tatsuo Tsukamoto (Kyoto University Hospital, Japan); Shunya Uchida (Teikyo University Hospital, Japan); Takashi Wada (Kanazawa University Hospital, Japan); Hidehiro Yamada (St. Marianna University Hospital Internal Medicine, Japan); Kunihiro Yamagata (Tsukuba University Hospital, Japan); Wako Yumura (IUHW Hospital [Jichi Medical University Hospital], Japan); Kan Sow Lai (Penang General Hospital, Malaysia); Luis Felipe Flores-Suarez (Instituto Nacional de Enfermedades Respiratorias, Mexico City, Mexico); Andrea Hinojosa-Azaola (Instituto Nacional de Ciencias Médicas y Nutrición Salvador Zubirán, Mexico City, Mexico); Bram Rutgers (University Hospital Groningen, Netherlands); Paul-Peter Tak (Academic Medical Centre, University of Amsterdam, Netherlands); Rebecca Grainger (Wellington, Otago, New Zealand); Vicki Quincey (Waikato District Health Board, New Zealand); Lisa Stamp (University of Otago, Christchurch, New Zealand); Ravi Suppiah (Auckland District Health Board, New Zealand); Emilio Besada (Tromsø, Northern Norway, Norway); Andreas Diamantopoulos (Hospital of Southern Norway, Kristiansand, Norway); Jan Sznajd (University of Jagiellonian, Poland); Elsa Azevedo (Centro Hospitalar de São João, Porto, Portugal); Ruth Geraldes (Hospital de Santa Maria, Lisbon, Portugal); Miguel Rodrigues (Hospital Garcia de Orta, Almada, Portugal); Ernestina Santos (Hospital Santo Antonio, Porto, Portugal); Yeong-Wook Song (Seoul National University Hospital, Republic of Korea); Sergey Moiseev (First Moscow State Medical University, Russia); Alojzija Hočevar (University Medical Centre Ljubljana, Slovenia); Maria Cinta Cid (Hospital Clinic de Barcelona, Spain); Xavier Solanich Moreno (Hospital de Bellvitge-Idibell, Spain); Inoshi Atukorala (University of Colombo, Sri Lanka); Ewa Berglin (Umeå University Hospital, Sweden); Aladdin Mohammed (Lund-Malmo University, Sweden); Mårten Segelmark (Linköping University, Sweden); Thomas Daikeler (University Hospital Basel, Switzerland); Haner Direskeneli (Marmara University Medical School, Turkey); Gulen Hatemi (Istanbul University, Cerrahpasa Medical School, Turkey); Sevil Kamali (Istanbul University, Istanbul Medical School, Turkey); Ömer Karadağ (Hacettepe University, Turkey); Seval Pehlevan (Fatih University Medical Faculty, Turkey); Matthew Adler (Frimley Health NHS Foundation Trust, Wexham Park Hospital, UK); Neil Basu (NHS Grampian, Aberdeen Royal Infirmary, UK); Iain Bruce (Manchester University Hospitals NHS Foundation Trust, UK); Kuntal Chakravarty (Barking, Havering and Redbridge University Hospitals NHS Trust, UK); Bhaskar Dasgupta (Southend University Hospital NHS Foundation Trust, UK); Oliver Flossmann (Royal Berkshire NHS Foundation Trust, UK); Nagui Gendi (Basildon and Thurrock University Hospitals NHS Foundation Trust, UK); Alaa Hassan (North Cumbria University Hospitals, UK); Rachel Hoyles (Oxford University Hospitals NHS Foundation Trust, UK); David Jayne (Cambridge University Hospitals NHS Foundation Trust, UK); Colin Jones (York Teaching Hospitals NHS Foundation Trust, UK); Rainer Klocke (The Dudley Group NHS Foundation Trust, UK); Peter Lanyon (Nottingham University Hospitals NHS Trust, UK); Cathy Laversuch (Taunton & Somerset NHS Foundation Trust, Musgrove Park Hospital, UK); Raashid Luqmani, Joanna Robson (Nuffield Orthopaedic Centre, Oxford, UK); Malgorzata Magliano (Buckinghamshire Healthcare NHS Trust, UK); Justin Mason (Imperial College Healthcare NHS Trust, UK); Win Win Maw (Mid Essex Hospital Services NHS Trust, UK); Iain McInnes (NHS Greater Glasgow & Clyde, Gartnavel Hospital & GRI, UK); John Mclaren (NHS Fife, Whyteman's Brae Hospital, UK); Matthew Morgan (University Hospitals Birmingham NHS Foundation Trust, Queen Elizabeth Hospital, UK); Ann Morgan (Leeds Teaching Hospitals NHS Trust, UK); Chetan Mukhtyar (Norfolk and Norwich University Hospitals NHS Foundation Trust, UK); Edmond O'Riordan (Salford Royal NHS Foundation Trust, UK); Sanjeev Patel (Epsom and St Helier University Hospitals NHS Trust, UK); Adrian Peall (Wye Valley NHS Trust, Hereford County Hospital, UK); Joanna Robson (University Hospitals Bristol NHS Foundation Trust, UK); Srinivasan Venkatachalam (The Royal Wolverhampton NHS Trust, UK); Erin Vermaak, Ajit Menon (Staffordshire & Stoke on Trent Partnership NHS Trust, Haywood Hospital, UK); Richard Watts (East Suffolk and North Essex NHS Foundation Trust, UK); Chee-Seng Yee (Doncaster and Bassetlaw Hospitals NHS Foundation Trust, UK); Daniel Albert (Dartmouth-Hitchcock Medical Center, US); Leonard Calabrese (Cleveland Clinic Foundation, US); Sharon Chung (University of California, San Francisco, US); Lindsy Forbess (Cedars-Sinai Medical Center, US); Angelo Gaffo (University of Alabama at Birmingham, US); Ora Gewurz-Singer (University of Michigan, US); Peter Grayson (Boston University School of Medicine, US); Kimberly Liang (University of Pittsburgh, US); Eric Matteson (Mayo Clinic, US); Peter A. Merkel (University of Pennsylvania, US); Rennie Rhee (University of Pennsylvania, US); Jason Springer (University of Kansas Medical Center Research Institute, US); and Antoine Sreih (Rush University Medical Center, US).

Arthritis & Rheumatology
Vol. 74, No. 3, March 2022, pp 407–417
DOI 10.1002/art.41961

American College of Rheumatology
Empowering Rheumatology Professionals

Association of Bone Erosions and Osteophytes With Systemic Bone Involvement on High-Resolution Peripheral Quantitative Computed Tomography in Premenopausal Women With Longstanding Rheumatoid Arthritis

Mariana O. Perez, Camille P. Figueiredo, Lucas P. Sales, Ana Cristina Medeiros-Ribeiro, Liliam Takayama, Diogo S. Domiciano, Karina Bonfiglioli, Valeria F. Caparbo, and Rosa M. R. Pereira

Objective. To evaluate premenopausal women with longstanding rheumatoid arthritis (RA) for potential associations between parameters of localized bone involvement and parameters of systemic bone involvement in the affected joints.

Methods. Eighty consecutively evaluated premenopausal women with RA were included in the study, along with 160 healthy female control subjects who were matched to the patients by age and body mass index. Volumetric bone mineral density (vBMD), bone microarchitecture, and finite elements of biomechanical bone strength (bone stiffness and estimated failure load) at the distal radius and distal tibia were analyzed by high-resolution peripheral quantitative computed tomography (HR-pQCT) in patients with RA compared to healthy controls. In addition, in patients with RA, localized bone involvement in the metacarpophalangeal and proximal interphalangeal joints was analyzed by HR-pQCT, to identify bone erosions and osteophytes.

Results. Among the 80 premenopausal women with longstanding RA, the mean ± SD age was 39.4 ± 6.7 years and mean ± SD disease duration was 9.8 ± 5.3 years. Trabecular and cortical bone parameters and bone strength at the distal radius and distal tibia were all impaired in patients with RA compared to healthy controls (each $P < 0.05$). In total, 75% of RA patients had evidence of bone erosions, and 41.3% of RA patients had detectable osteophytes on HR-pQCT. RA patients with bone erosions, as compared to RA patients without bone erosions, had lower cortical vBMD (at the distal radius, mean ± SD 980 ± 72 mg HA/cm^3 versus 1,021 ± 47 mg HA/cm^3 [$P = 0.03$]; at the distal tibia, 979 ± 47 mg HA/cm^3 versus 1,003 ± 34 mg HA/cm^3 [$P = 0.04$]) and higher cortical bone porosity (at the distal radius, mean ± SD 2.8 ± 2.5% versus 1.8 ± 1.6% [$P = 0.04$]; at the distal tibia, 3.7 ± 1.6% versus 2.7 ± 1.6% [$P = 0.01$]). In patients with RA, osteophyte volume at the distal radius was positively correlated with trabecular vBMD ($r = 0.392$, $P = 0.02$), trabecular number ($r = 0.381$, $P = 0.03$), and trabecular stiffness ($r = 0.411$, $P = 0.02$), and negatively correlated with trabecular separation ($r = -0.364$, $P = 0.04$), as determined by Pearson's or Spearman's correlation test.

Conclusion. The findings show that premenopausal women with longstanding RA have systemic bone fragility at peripheral joint sites. Moreover, the presence of bone erosions is mainly associated with cortical bone fragility at the distal radius and tibia, and presence of osteophytes is associated with repair of trabecular bone at the distal radius.

Supported by Fundação de Amparo a Pesquisa do Estado de Sao Paulo (grants 2018/05596-2 to Dr. Perez, 2018/01315-9 to Dr. Figueiredo, and FAPESP 2016/00006-7 to Dr. Pereira), and Conselho Nacional de Desenvolvimento Cientifico e Tecnologico (grant CNPQ 305556/2017-7 to Dr. Pereira).

Mariana O. Perez, MD, PhD, Camille P. Figueiredo, MD, PhD, Lucas P. Sales, MSc, Ana Cristina Medeiros-Ribeiro, MD, PhD, Liliam Takayama, BSc, Diogo S. Domiciano, MD, PhD, Karina Bonfiglioli, MD, PhD, Valeria F. Caparbo, PhD, Rosa M. R. Pereira, MD, PhD: Hospital das Clinicas da Universidade de São Paulo, São Paulo, Brazil.

Author disclosures are available at https://onlinelibrary.wiley.com/action/downloadSupplement?doi=10.1002%2Fart.41961&file=art41961-sup-0001-Disclosureform.pdf.

Address correspondence to Rosa M. R. Pereira, MD, PhD, Division of Rheumatology, Faculdade de Medicina da Universidade de São Paulo, Avenida Dr. Arnaldo, 455, 3rd floor, Room 3193, São Paulo, 01246-903, Brazil. Email: rosamariarp@yahoo.com.

Submitted for publication March 2, 2021; accepted in revised form August 26, 2021.

INTRODUCTION

In patients with rheumatoid arthritis (RA), there are 2 observable patterns of bone involvement, localized bone involvement and systemic (generalized) bone involvement. Both patterns share common pathologic pathways of inflammation and disease activity (1,2). Results of previous studies have suggested that local bone erosion may be correlated with poor bone mineral density (BMD) in RA patients, and osteoporosis might be an important and independent determinant of bone erosions in RA. Osteoporosis is linked to localized bone loss, which, in patients with RA, can be attributable to activation of an osteoclastogenic process that is driven by proinflammatory cytokines (3,4).

In RA, there is an imbalance between bone formation and bone resorption, with the bone resorption process predominating. A profile that is characterized by the presence of key proinflammatory cytokines, chemokines, and pro-osteoclastogenic mediators, including RANK and its ligand, RANKL, plays a decisive role in the bone loss that occurs in RA patients (3,4). In addition, there seems to be resistance to the repair of bone erosions in RA. Repair failure occurs when there is inhibition of bone formation, which is accompanied by impairment of osteoblast differentiation (5). Dkk-1 protein, frizzled-related protein 1, and sclerostin, all of which represent classic inhibitors of the Wnt pathway of bone formation, are up-regulated in the synovial membrane of RA patients, and this is attributable to the presence of proinflammatory cytokines such as tumor necrosis factor (TNF) (6,7).

Importantly, patients with RA can develop bone fractures even when BMD is normal, as fractures can occur in the setting of impaired bone microarchitecture (8). In this sense, some imaging methods, such as high-resolution peripheral quantitative computed tomography (HR-pQCT) at the distal radius and distal tibia, may be promising for the assessment of bone microarchitecture and fracture risk in patients with RA, since these techniques could provide more detailed information independent of the patient's BMD. In addition, HR-pQCT has been demonstrated to be an interesting method for the detection of catabolic bone lesions (erosions) and anabolic bone lesions (osteophytes) in the metacarpophalangeal (MCP) and proximal interphalangeal (PIP) joints (9–13), with an accuracy superior to that of conventional methods (14–17).

Of note, in premenopausal women with longstanding RA, data on bone microarchitecture are scarce. To our knowledge, systemic bone involvement and localized bone involvement have not previously been evaluated simultaneously using HR-pQCT in patients with RA. Therefore, this study was undertaken to 1) evaluate the bone microarchitecture and bone strength at the distal radius and distal tibia, as well as bone erosions and osteophytes in the MCP and PIP joints, using HR-pQCT in premenopausal women with longstanding RA, and 2) explore the relationship between systemic bone involvement and localized bone involvement in patients with RA.

PATIENTS AND METHODS

Study population. For this study, we selected 294 women with RA, ages 18–50 years, who were being consecutively evaluated at the RA outpatient clinic of our tertiary center. All patients fulfilled the American College of Rheumatology/European Alliance of Associations for Rheumatology 2010 classification criteria for RA (18). Of these 294 women, 214 were excluded due to the presence of a confounding factor in the evaluation of bone impairment, including the following factors: postmenopausal (n = 72), prednisone dose >7.5 mg/day (n = 24), other autoimmune diseases associated with bone impairment (n = 32), use of antiresorptive or anabolic agents for osteoporosis (n = 18), decompensated diabetes mellitus (n = 9), condition leading to immobility (such as stroke, neuromuscular disease, permanent use of wheelchair) (n = 9), bariatric surgery (n = 8), malabsorptive disease syndrome (n = 8), neoplasm (n = 7), decompensated thyroid diseases (n = 6), chronic kidney disease (n = 5), cirrhosis (n = 3), pregnant or lactating (n = 3), hepatitis B virus (n = 2), hepatitis C virus (n = 2), HIV infection (n = 1), and refusal to participate (n = 5).

Thus, 80 patients were eligible for the study. Prior to subject enrollment and data collection, the study was approved by the local ethics committee (research protocol no. 51178115.1.0000.0068). All participants gave written informed consent, in accordance with the principles of the Declaration of Helsinki (19).

Clinical and laboratory assessments. Demographic and clinical data were obtained through interviews with the patients and medical chart review, including race, age, disease duration, comorbidities, RA treatment data, and fracture history. Clinical laboratory assays (for C-reactive protein [CRP] levels, presence of rheumatoid factor [RF], and presence of anti–cyclic citrullinated peptide [anti-CCP] antibodies) were performed using standard automated methods. Disease activity was measured in a standard manner, using the Disease Activity Score in 28 joints with CRP level (DAS28-CRP) (low disease activity ≥2.6 and ≤3.2, moderate disease activity >3.2 and ≤5.1, high disease activity >5.1), the Clinical Disease Activity Index (CDAI) (low disease activity >2.8 and ≤10, moderate disease activity >10 and ≤22, high disease activity CDAI >22), and the Simplified Disease Activity Index (SDAI) (low disease activity >3.3 and ≤11, moderate disease activity >11 and ≤26, high disease activity >26) (20–22).

Assessment of BMD. BMD at the spine and hip was determined by dual x-ray absorptiometry (DXA) using a GE Lunar iDXA device. All DXA measurements were performed according to the International Society for Clinical Densitometry criteria (23), and a Z-score less than or equal to −2.0 was defined as low BMD in accordance with the age of the patients, since all patients were premenopausal women. The least significant change in BMD was defined as 0.034 gm/cm^2 at the spine, 0.046 gm/cm^2 at the femoral neck, and 0.044 gm/cm^2 at the total hip.

Assessment of vertebral fractures. A vertebral fracture assessment (VFA) scan of the thoracolumbar spine was performed using the same DXA device (GE Lunar iDXA), with subjects placed in the lateral position. Vertebral fractures were identified by 2 experienced readers (MOP and LT), who evaluated each T4–L4 vertebra image to decide, in agreement, whether it demonstrated a fracture of the vertebrae. Only adequately visualized vertebrae were analyzed for deformity, with the extent of deformity scored using the Genant semiquantitative scale (24), where mild (grade 1) = a reduction of 20–25% in the anterior, middle, and/or posterior height relative to the adjacent vertebral bodies, moderate (grade 2) = a reduction of 26–40% in any height, and severe (grade 3) = a reduction of >40% in any height. All vertebral fractures assessed using VFA were confirmed with standard lateral thoracic and lumbar spine radiographs.

Evaluation of systemic bone involvement using HR-pQCT. *Volumetric BMD (vBMD) and microarchitecture measurements.* Volumetric BMD and bone microarchitecture were evaluated at the distal radius and distal tibia using an HR-pQCT device (Xtreme CT version I; Scanco Medical) with the standard scanning protocol (60 kVp, 1.0 mA). The region of interest was defined using a scout view. Employed measurements included 110 slices spanning 9.02 mm in length (voxel size 82 μm) from the distal end, with positioning at 9.5 mm and 22.5 mm proximal to the reference line for the nondominant distal radius and distal tibia, respectively (25). The entire volume of interest was separated automatically into cortical and trabecular regions, using a threshold-based algorithm. The threshold used to discriminate cortical bone from trabecular bone was set to one-third of the apparent cortical bone density (26,27).

The HR-pQCT outcome variables used in the analysis were as follows: 1) vBMD parameters (mg HA/cm^3), including trabecular vBMD (Tb.vBMD) and cortical vBMD (Ct.vBMD); 2) bone structure parameters, including bone volume/tissue volume (BV/TV; %), trabecular number (Tb.N; 1/mm), trabecular thickness (Tb.Th; mm), and trabecular separation (Tb.Sp; mm); and 3) cortical bone parameters, including cortical thickness (Ct.Th; mm) and cortical porosity (Ct.Po; %) (25,28,29). In terms of evaluation of the precision of HR-pQCT, we calculated coefficients of variation of 0.93–1.41% at the distal radius, and 0.25–1.16% at the distal tibia for density measurements, and coefficients of variation of 1.49–7.59% at the distal radius and 0.78–6.35% at the distal tibia for morphometric measurements.

Finite element analysis (FEA). Linear FE models of the distal radius and distal tibia were created directly from the HR-pQCT images using software-specific finite elements (Finite Element software version 1.13; Scanco Medical). These models were used to assess biomechanical bone strength. The 2 biomechanical properties analyzed using FEA were bone stiffness (kN/mm) and estimated failure load (F.Load; N) (29).

Healthy control group for evaluating systemic bone involvement. The parameters obtained using HR-pQCT at the distal radius and distal tibia sites were compared with the parameters obtained from healthy female subjects (25) who were matched to the patients by age and body mass index (BMI), with matching in a 1:2 ratio of 80 RA patients to 160 healthy controls.

Evaluation of localized bone involvement using HR-pQCT. An HR-pQCT scan (Xtreme CT version I; Scanco Medical) was performed in the second and third MCP and PIP joints of the dominant hand to identify erosions and osteophyte lesions in patients with RA. Images were analyzed using an open-source Digital Imaging and Communication in Medicine viewer (OsiriX Lite, version 11.0.2; 32-bit for MacOS) and were evaluated independently in a blinded manner by an experienced reader (CPF). Erosions were defined as cortical breaks visible in 2 planes and in at least 2 consecutive slices (30). Osteophytes were defined as bony protrusions emerging from the cortical bone shell (30).

For exact localization of the bone lesions, the metacarpal heads and phalangeal surfaces of the second and third MCP and PIP joints were divided into 4 quadrants (quadrant I = palmar, quadrant II = ulnar, quadrant III = dorsal, and quadrant IV = radial). The number of bone lesions in each quadrant was counted. For bone surfaces with >1 erosion or osteophyte, only the size of the largest lesion was measured (largest target erosion and largest target osteophyte) (31). Erosions and osteophyte volume were analyzed using an OsiriX rendering tool. Briefly, the operator contours the erosion in some slices, although all slices can be contoured as well, especially if it is a very irregular erosion. The OsiriX tool then circumscribes the full erosion. After all corrections are made manually by the operator (if necessary), the total volume is automatically calculated; results are expressesd in cubic millimeters (32).

Osteophytes were evaluated following the same method of analysis as used for assessment of erosion volume. For this analysis, the osteophytes were contoured in all slices using the drawing line tool, which makes the method a very accurate one. If necessary, the repulsor tool was used for manual corrections by the operator. Thereafter, calculation of the osteophyte volume was automatically performed; results are expressed in cubic millimeters (32).

Statistical analysis. Statistical analyses were performed using SPSS for Windows (version 22.0; SPSS). Results are presented as the mean ± SD for continuous variables and as percentages for categorical variables. Quantitative variables were analyzed using Student's *t*-test (for normally distributed data) or Mann–Whitney test (for non–normally distributed data), as appropriate. Associations between categorical variables were assessed using the chi-square or Fisher's exact test. Multiple logistic regression analyses were performed using presence of erosions

Table 1. Characteristics and HR-pQCT findings among premenopausal women with longstanding RA compared to healthy controls*

	Patients with RA (n = 80)	Healthy controls (n = 160)†	*P*
Characteristic			
Age, years	39.4 ± 6.7	39.3 ± 7.4	0.58
BMI, kg/m^2	28.0 ± 5.2	28.1 ± 5.0	0.90
HR-pQCT finding			
Distal radius			
Density			
Tb.vBMD, mg HA/cm^3	150 ± 41	174 ± 31	0.001
Ct.vBMD, mg HA/cm^3	989 ± 69	1,023 ± 43	0.002
Microstructure			
BV/TV, %	12.5 ± 3.4	14.5 ± 2.6	0.001
Tb.N, 1/mm	1.9 ± 0.35	2.0 ± 0.26	0.08
Tb.Th, mm	0.06 ± 0.01	0.07 ± 0.01	0.002
Tb.Sp, mm	0.472 ± 0.121	0.427 ± 0.07	0.06
Ct.Th, mm	0.90 ± 0.24	0.85 ± 0.18	0.23
Ct.Po, %	2.6 ± 2.4	1.3 ± 0.72	<0.0001
Bone strength			
Stiffness, KN/mm	72 ± 15	78 ± 14	0.004
F.Load, N	3,444 ± 753	3,778 ± 648	0.001
Distal tibia			
Density			
Tb.vBMD, mg HA/cm^3	143 ± 35	157 ± 34	0.01
Ct.vBMD, mg HA/cm^3	985 ± 45	1,017 ± 34	<0.0001
Microstructure			
BV/TV, %	12.0 ± 2.0	13.0 ± 2.8	0.01
Tb.N, 1/mm	1.6 ± 0.30	1.7 ± 0.33	0.17
Tb.Th, mm	0.070 ± 0.013	0.076 ± 0.014	0.07
Tb.Sp, mm	0.540 ± 0.112	0.513 ± 0.114	0.21
Ct.Th, mm	1.1 ± 0.18	1.2 ± 0.17	0.004
Ct.Po, %	3.4 ± 1.6	2.6 ± 1.0	0.001
Bone strength			
Stiffness, KN/mm	188 ± 32	204 ± 30	0.001
F.Load, N	8,987 ± 1,515	9,738 ± 1,404	0.001

* Values are the mean ± SD. HR-pQCT = high-resolution peripheral quantitative computed tomography; Tb.vBMD = trabecular volumetric bone mineral density; Ct.vBMD = cortical volumetric bone mineral density; BV/TV = bone volume/tissue volume; Tb.N = trabecular number; Tb.Th = trabecular thickness; Tb.Sp = trabecular separation; Ct.Th = cortical thickness; Ct.Po = cortical porosity; F.Load = failure load.
† Controls were healthy female subjects matched to the female rheumatoid arthritis (RA) patients by age and body mass index (BMI).

or presence of osteophytes as dependent variables and HR-pQCT parameters (at the radius and tibia) as independent variables, with adjustments for clinical and laboratory variables that were presented as descriptive values in the bivariate analysis ($P < 0.10$).

Osteophytes (number and volume) were assessed for correlations with the clinical and HR-pQCT parameters at the radius and tibia using Pearson's correlation coefficients for data that conformed to normal distribution or Spearman's correlation coefficients for non–normally distributed data.

Generalized linear models were generated using a Poisson or gamma distribution, as appropriate, to examine the effects of clinical variables and HR-pQCT parameters at the radius and tibia on the osteophyte volume, with adjustments for clinical variables that were presented as descriptive values ($P < 0.10$) in the unadjusted analysis. *P* values less than 0.05 were considered statistically significant.

RESULTS

Clinical and laboratory features. The mean ± SD age of the RA patients was 39.4 ± 6.6 years, and 60% were White. With regard to the clinical characteristics of the patients, the mean ± SD disease duration was 9.8 ± 5.3 years, 85% of the patients were positive for RF, and 82.5% were positive for anti-CCP. The main comorbidities reported were obesity (68.7%), systemic arterial hypertension (18.7%), and dyslipidemia (11.2%). Ten percent of patients reported a status of current smoker.

None of the patients with RA had a history of previous vertebral or nonvertebral fractures, as determined by self-report at the time of assessment. In all patients, the mean ± SD CRP level was 6.8 ± 10 mg/liter (normal value <5 mg/liter). With regard to disease activity levels, patients with RA had a mean ± SD DAS28-CRP score of 3.0 ± 1.3, CDAI score of 14.7 ± 12.4, and SDAI score of 15.4 ± 12.8, indicating mild disease activity

Table 2. HR-pQCT findings in premenopausal women with longstanding RA according to presence or absence of bone erosions*

HR-pQCT variable	Erosions (n = 60)	No erosions (n = 20)	*P*
Distal radius			
Tb.vBMD, mg HA/cm^3	154 ± 45	138 ± 25	0.12
Ct.vBMD, mg HA/cm^3	980 ± 72	1,021 ± 47	0.03
BV/TV, %	13.0 ± 4.0	11.0 ± 2.0	0.13
Tb.N, 1/mm	1.9 ± 0.38	1.9 ± 0.28	0.97
Tb.Th, mm	0.067 ± 0.011	0.060 ± 0.011	0.03
Tb.Sp, mm	0.47 ± 0.13	0.47 ± 0.07	0.96
Ct.Th, mm	0.89 ± 0.22	0.95 ± 0.28	0.31
Ct.Po, %	2.8 ± 2.5	1.8 ± 1.6	0.04
Stiffness, kN/mm	73 ± 17	70 ± 8	0.29
F.Load, N	3,479 ± 834	3,333 ± 383	0.30
Distal tibia			
Tb.vBMD, mg HA/cm^3	143 ± 38	150 ± 32	0.48
Ct.vBMD, mg HA/cm^3	979 ± 47	1,003 ± 34	0.04
BV/TV, %	12.0 ± 3.0	13.0 ± 3.0	0.39
Tb.N, 1/mm	1.7 ± 0.31	1.7 ± 0.28	0.82
Tb.Th, mm	0.071 ± 0.013	0.076 ± 0.019	0.23
Tb.Sp, mm	0.54 ± 0.12	0.53 ± 0.08	0.74
Ct.Th, mm	1.2 ± 0.18	1.2 ± 0.2	0.84
Ct.Po, %	3.7 ± 1.7	2.7 ± 1.5	0.01
Stiffness, kN/mm	188 ± 34	191 ± 30	0.75
F.Load, N	8,987 ± 1,570	9,141 ± 1,371	0.70

* Values are the mean ± SD. See Table 1 for definitions.

(based on the DAS28-CRP) or moderate disease activity (based on the CDAI and SDAI). Approximately one-third of the patients were receiving nonsteroidal antiinflammatory drugs (31.2%), 60% were receiving methotrexate, 60% were receiving prednisone (dose of ≤7.5 mg/day, with a mean ± SD dose of 5.3 ± 1.2 mg/day at the time of assessment), and 35% were receiving biologic therapy (TNF inhibitors in 57% of patients).

DXA measurements. DXA analyses revealed that 9 patients (11.2%) had a Z-score of less than or equal to −2.0 overall, identified specifically at the lumbar spine in 11.2% of patients, at the femoral neck in 3.7% of patients, and at the total hip in 2.5% of patients. The evaluation of vertebral fracture by VFA identified 15 patients (18.7%) with grade I vertebral fracture, most of whom had normal findings on DXA (82.5%). All vertebral fractures were asymptomatic and confirmed with radiography. Most patients had a thoracic fracture (80%), and 60% of patients had a fracture in 2 or more vertebral bodies. No significant differences in clinical, laboratory, BMD, or HR-pQCT parameters were observed between the group with vertebral fracture and the group without vertebral fracture.

HR-pQCT measurements. *Bone parameters analyzed using HR-pQCT in RA patients compared to healthy controls.* In premenopausal women with RA compared to matched healthy female controls, the HR-pQCT scans showed impaired vBMD in both the trabecular and cortical compartments, and impaired bone microstructure and bone biomechanical properties at both peripheral sites (distal radius and distal tibia) (Table 1). Supplementary Table 1 (available on the *Arthritis & Rheumatology* website at https://onlinelibrary.wiley.com/doi/10.1002/art.41961) lists the demographic and clinical characteristics of the RA patients versus healthy controls.

Localized bone involvement evaluated using HR-pQCT in RA patients. Bone erosions were found in 60 RA patients (75%) (total of 201 erosions, mean ± SD 2.5 ± 2.9 erosions per patient). The main site of erosion was the MCP region (75.6% of patients), specifically in the second and third MCP heads. More RA patients with erosions than RA patients without erosions were positive for anti-CCP antibodies (80.3% versus 19.7%; $P = 0.03$). No other clinical features (disease duration, number of swollen joints, number of tender joints, DAS28-CRP score, CDAI score, SDAI score) or laboratory parameters (CRP levels, positivity for RF) were associated with the presence of bone erosions (each $P > 0.05$). Patients with vertebral fracture had a higher volume of erosions compared to RA patients without vertebral fracture (mean ± SD 36.0 ± 125 mm^3 versus 29.3 ± 41.2 mm^3; $P = 0.02$).

Osteophytes were found in 33 RA patients (41.3%) (total of 99 osteophytes, mean ± SD 1.2 ± 1.9 osteophytes per patient). In addition, most of the osteophytes were located in the second and third MCP heads (65.6% of patients). The mean ± SD osteophyte volume was 8.8 ± 19.5 mm^3.

Patients with osteophytes, compared to patients without osteophytes, had a longer disease duration (mean ± SD 11.2 ± 5.6 years versus 8.7 ± 4.9 years; $P = 0.03$), a higher number of swollen joints (mean ± SD 5.8 ± 5.9 versus 2.4 ± 3.0;

Table 3. Multiple logistic regression models assessing the strength of association of presence of bone erosions with HR-pQCT findings in premenopausal women with longstanding RA*

	Presence of erosions			
		95% CI		
HR-pQCT variable	OR	Lower	Upper	*P*
Distal radius				
Ct.vBMD, mg HA/cm^3 (x 100)	0.29	0.09	0.98	0.045
Ct.Po, % (x 0.01)	1.30	0.90	1.86	0.16
Tb.Th, mm (x 0.01)	1.99	1.08	3.68	0.03
Distal tibia				
Ct.vBMD, mg HA/cm^3 (x 100)	0.23	0.05	1.02	0.054
Ct.Po, % (x 0.01)	1.68	1.06	2.66	0.03

* Each HR-pQCT variable was adjusted for the presence of anti–cyclic citrullinated peptide antibodies. Values are the odds ratios (ORs) with 95% confidence intervals (95% CIs). See Table 1 for other definitions.

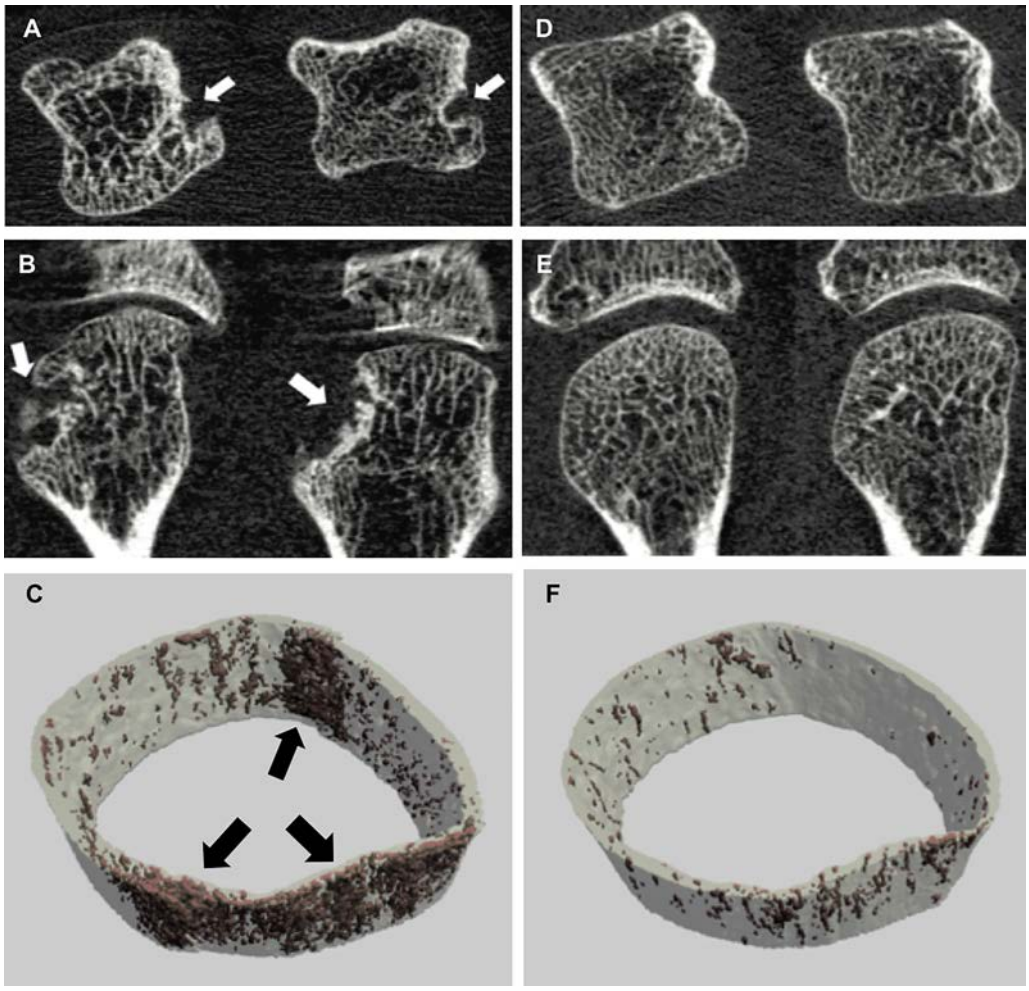

Figure 1. Association between bone erosions in the second and third metacarpophalangeal (MCP) joints and cortical porosity at the distal tibia in rheumatoid arthritis (RA) patients matched by age and disease duration, as visualized by high-resolution peripheral quantitative computed tomography. **A–C**, Representative images of the joints of an RA patient with erosions (patient 1). The patient was age 39 years and had an 8-year history of RA at the time of evaluation. The presence of erosions in the second and third MCP joints is shown (indicated by **arrows** in **A** [axial plane] and **B** [coronal plane]), with evidence of increased cortical porosity (indicated by **arrows** in **C)**. **D–F,** Representative images of the joints of an RA patient without erosions (patient 2). The patient was age 37 years and had an 8-year history of RA at the time of evaluation. No erosions were evident in the second and third MCP joints (axial plane in **D** and coronal plane in **E**), and cortical porosity was within the normal range (**F**). Color figure can be viewed in the online issue, which is available at http://onlinelibrary.wiley.com/doi/10.1002/art.41961/abstract.

$P = 0.001$), and higher disease activity scores (for DAS28-CRP, mean ± SD 3.5 ± 1.5 versus 2.7 ± 1.1 [$P = 0.02$]; for CDAI, 19.2 ± 15.9 versus 11.5 ± 8.0 [$P = 0.03$]; for SDAI, 20.0 ± 16.4 versus 12.1 ± 8.3 [$P = 0.02$]). Supplementary Figures 1A–D and 2A–D (available on the *Arthritis & Rheumatology* website at https://onlinelibrary.wiley.com/doi/10.1002/art.41961) show images of the hand and wrist of a representative RA patient with osteophytes and a representative RA patient with erosions but no joint swelling or osteophytes.

Osteophyte volume was also positively correlated with the number of swollen joints (r = 0.436, $P = 0.001$), number of tender joints (r = 0.383, $P = 0.02$), and disease activity scores, including CDAI scores (r = 0.427, $P = 0.01$) and SDAI scores (r = 0.410, $P = 0.02$). Osteophyte volume was higher in RA patients with erosions than in RA patients without erosions (mean ± SD 11.6 ± 21.8 mm^3 versus 0.17 ± 0.54 mm^3; $P = 0.001$).

Furthermore, we observed an association between the presence of osteophytes and the presence of erosions in RA patients. Osteophytes were found in 52% of patients with erosions (n = 31) compared to 10% of patients without erosions (n = 2) ($P = 0.001$). Supplementary Table 2 (available on the *Arthritis & Rheumatology* website at https://onlinelibrary.wiley.com/doi/10.1002/art.41961) lists the demographic and clinical characteristics of the RA patients with and those without erosions or osteophytes.

Relationship between systemic bone involvement and localized bone involvement in RA patients. At the distal radius, RA patients with erosions, as compared to RA patients without erosions, had lower cortical density (mean ± SD 980 ± 72 mg HA/cm^3 versus 1,021 ± 47 mg HA/cm^3; $P = 0.03$), higher cortical porosity (mean ± SD 2.8 ± 2.5% versus 1.8 ± 1.6%; $P = 0.04$), and higher trabecular thickness (mean ± SD 0.067 ± 0.011 mm versus 0.060 ± 0.011 mm; $P = 0.03$).

At the distal tibia, patients with erosions, as compared to patients without erosions, had lower cortical density (mean ± SD 979 ± 47 mg HA/cm^3 versus 1,003 ± 34 mg HA/cm^3; $P = 0.04$) and higher cortical porosity (mean ± SD 3.7 ± 1.7% versus 2.7 ± 1.5%; $P = 0.01$) (Table 2).

In multiple logistic regression analyses using presence of bone erosions as a dependent variable, with adjustment for the presence of anti-CCP antibodies, the association of bone erosions with lower cortical density ($P = 0.045$) and higher trabecular thickness ($P = 0.03$) at the distal radius remained significant. At the distal tibia, the presence of erosions was significantly associated with higher cortical porosity ($P = 0.03$) and a tendency toward lower cortical density ($P = 0.054$) (Table 3).

Figures 1A–F show images of the distal tibia of 2 RA patients who were matched for age and disease duration, to illustrate the association between presence of erosions and cortical porosity. Patient 1 was age 39 years and had an 8-year duration of RA. In this patient, erosions were present in the second and third MCP joints, and cortical bone porosity was observed to be increased (Ct.Po 5.2%). Patient 2 was age 37 years and also had an 8-year duration of RA. In this patient, no erosions were present in the second and third MCP/PIP joints, and cortical bone porosity was within the normal range (Ct.Po 1.5%).

In all RA patients, osteophyte volume was positively correlated with the trabecular vBMD (r = 0.392, $P = 0.02$), BV/TV (r = 0.392, $P = 0.02$), trabecular number (r = 0.381, $P = 0.03$), cortical thickness (r = 0.302, $P = 0.09$), bone stiffness (r = 0.411, $P = 0.02$), and F.Load (r = 0.419, $P = 0.02$), and was negatively correlated with trabecular separation (r = −0.364, $P = 0.04$) at the distal radius (Table 4).

Multiple logistic regression models assessing the strength of associations of osteophyte volume with clinical characteristics or HR-pQCT parameters showed that all identified associations remained statistically significant after adjustment for the relevant clinical characteristics ($P < 0.05$) (Table 5). The presence of osteophytes was mainly associated with clinical parameters. Multiple logistic regression analyses using the presence of osteophytes as a dependent variable, with adjustments for disease duration, number of swollen joints, number of tender joints, and the CDAI score, showed that none of the HR-pQCT parameters had a statistically significant effect on the presence of osteophytes (each $P > 0.05$). Only disease duration ($P = 0.04$) and the number of swollen joints ($P = 0.04$) remained associated with the presence of osteophytes. With each additional year of disease, there was

Table 4. Correlations between osteophyte volume and HR-pQCT findings in premenopausal women with longstanding RA*

	Osteophyte volume	
HR-pQCT variable	r	*P*
Distal radius		
Tb.vBMD, mg HA/cm^3	0.392	0.02
Ct.vBMD, mg HÁ/cm^3	−0.120	0.52
BV/TV, %	0.392	0.02
Tb.N, 1/mm	0.381	0.03
Tb.Th, mm	0.221	0.22
Tb.Sp, mm	−0.364	0.04
Ct.Th, mm	0.302	0.09
Ct.Po, %	0.188	0.30
Stiffness, kN/mm	0.411	0.02
F.Load, N	0.419	0.02
Distal tibia		
Tb.vBMD, mg HA/cm^3	0.076	0.67
Ct.vBMD, mg HA/cm^3	0.162	0.39
BV/TV, %	0.122	0.51
Tb.N, 1/mm	0.101	0.57
Tb.Th, mm	0.056	0.76
Tb.Sp, mm	−0.048	0.79
Ct.Th, mm	−0.042	0.81
Ct.Po, %	−0.089	0.62
Stiffness, kN/mm	−0.010	0.95
F.Load, N	−0.008	0.96

* Correlations were determined by Pearson's or Spearman's correlation test. See Table 1 for definitions.

Table 5. Multiple logistic regression models assessing the strength of association of osteophyte volume with clinical characteristics and HR-pQCT findings in premenopausal women with longstanding RA*

	Osteophyte volume				
			95% CI		
	β	SE	Lower	Upper	*P*
Clinical characteristic					
Number of tender joints	−1.52	1.62	−4.69	1.65	0.34
Number of swollen joints	−0.21	2.72	−5.54	5.12	0.94
CDAI score	0.75	1.40	−2.00	3.50	0.59
HR-pQCT at distal radius					
Tb.vBMD, mg Hg/cm^3	0.15	0.07	0.00	0.29	0.045
BV/TV, % (x 0.01)	1.75	0.87	0.03	3.46	0.046
Tb.N, 1/mm	14.38	3.53	7.46	21.30	<0.001
Tb.Sp, mm (x 0.01)	−0.25	0.06	−0.37	−0.12	<0.001
Stiffness, kN/mm	0.49	0.21	0.07	0.91	0.02
F.Load, N (x 100)	10.04	4.46	1.31	18.77	0.02

* Values are beta coefficients and the SE and 95% confidence intervals (95% CIs). CDAI = Clinical Disease Activity Index (see Table 1 for other definitions).

a 10.7% increased likelihood of osteophytes being present at the radius, and with each joint that was swollen, there was a 31.6% increased likelihood of osteophytes being present at the radius, regardless of the other characteristics evaluated (see Supplementary Table 3, available on the *Arthritis & Rheumatology* website at https://onlinelibrary.wiley.com/doi/10.1002/art.41961).

Relationship of bone involvement to treatment. There was no association between HR-pQCT parameters and use of glucocorticoid treatment or use of synthetic/biologic disease-modifying antirheumatic drugs (see Supplementary Tables 4 and 5, available on the *Arthritis & Rheumatology* website at https://onlinelibrary.wiley.com/doi/10.1002/art.41961).

DISCUSSION

To our knowledge, this is the first study to simultaneously evaluate systemic and localized bone involvement in premenopausal women with longstanding RA using HR-pQCT. Unlike most RA studies that have assessed patients with early disease, this work evaluated patients with longstanding RA, excluding confounding factors for bone loss, such as menopause. In addition, a high frequency of patients were positive for RF and anti-CCP, both of which are classically associated with a more severe course of RA (33–35). The focus of this study was to evaluate the relationship between systemic and localized bone involvement in this specific population of RA subjects.

These findings provide novel evidence that premenopausal women with longstanding RA had bone impairment in the cortical and trabecular compartments at peripheral joint sites when compared to that in age- and BMI-matched healthy female controls, thereby expanding previous data on postmenopausal women (16). In addition, premenopausal women with RA had higher cortical porosity, which could have resulted in decreased bone strength parameters, in concordance with the observations of Zhu et al, who reported that cortical porosity is the most important variable in bone damage in postmenopausal women with RA (36). Our data support the notion that bone involvement in RA is not restricted to the subchondral bone, but to a systemic involvement of bone tissue, with changes in bone microarchitecture, reduction in bone mass, and bone fragility (37,38).

Remarkably, for the first time in patients with RA, a relationship between bone erosion and cortical systemic bone involvement at peripheral joint sites was demonstrated. Additionally, osteophyte volume was positively correlated with better trabecular parameters at the radius in patients with RA, as evaluated by HR-pQCT.

Regarding erosions, an association between bone erosions with lower cortical density and higher cortical porosity at both peripheral sites was observed. These findings support a close relationship between localized bone involvement and systemic bone involvement. Several studies have demonstrated an association between hand BMD and erosions, but this is expected based on the proximity of the erosions to the region of BMD measurement (39–41). In contrast, in a study by Rossini et al, a relationship between focal bone erosion seen on hand radiographs and lower BMD at the lumbar spine and total hip was observed (42).

Bone damage in RA typically emerges at certain anatomic hotspots corresponding to the so-called "bare area," an intraarticular region between the cartilage and the insertion site of the joint capsule. Interestingly, the "bare area" exhibits cortical microchannels (CoMiCs), a form of structural change in the joints of patients with RA (43,44). CoMiCs are vascular connections between bone marrow and the joint that facilitate migration of inflammatory cells and osteoclast-mediated joint destruction (45). It has been hypothesized that bone damage in RA might start in vascular channels (45). Werner et al, in a study utilizing

HR-pQCT imaging, showed that RA patients had significantly more CoMiCs compared to healthy individuals, and CoMiCs were found early in the course of the disease in RA patients (43). In our study, bone erosions were well characterized and differentiated from CoMiCs: characteristically, the erosions were found in greater numbers, volume, and surface area, accompanied by cortical and trabecular loss, and were seen in several sequential slices.

Furthermore, an association between erosions and osteophytes was found, supporting a possible role of osteophytes in RA bone erosion repair (46). The literature shows that spontaneous repair of bone erosions is rare, due to failure of the Wnt pathway in bone formation (5–7). Histopathologic assessment of synovial tissue in an experimental murine model of RA showed an increase in osteoclasts in bone erosions and a decrease in mature osteoblasts (47). Because our patients had a long disease duration and were using ideal treatment for RA (treat-to-target strategies), the repair could manifest as new bone apposition and osteophyte formation at the base of the erosion (46,48). In our study, the presence of osteophytes was associated with longer disease duration, probably because of the severity of RA in our patients (our hospital is a tertiary care center), even in premenopausal women. In addition, presence of osteophytes and osteophyte volume were also associated with a greater number of swollen joints and worse disease activity scores in the present study, possibly due to a secondary osteoarthritis process or mild persistent disease activity in patients with longstanding RA. In fact, in a case–control study by Zhu et al, it was shown that higher cortical porosity in RA patients was linked to exaggerated periosteal bone apposition, which could mean that a process of secondary osteoarthritis was occurring (36).

In this study, most RA patients had normal BMD, as assessed by DXA. Indeed, the DXA scans were unable to discriminate between RA patients with and those without fractures, which may suggest that deteriorations of bone microstructure are responsible for the level of fracture risk. We observed that 18.7% of RA patients in the present study had evidence of vertebral fracture on DXA, a similar frequency to the prevalence of vertebral fracture reported in the literature, with reported frequencies ranging from 13% to 47% (49,50). Furthermore, our RA patients were premenopausal women who were taking low doses of glucocorticoids, in contrast to the populations in previous studies, in which the prevalence of vertebral fracture was analyzed mainly in older women, postmenopausal women, and women who were taking high doses of glucocorticoids (49,50). Notably, patients with vertebral fracture had a higher volume of bone erosions in the MCP and PIP joints compared to patients without vertebral fracture, linking the severity of RA erosive disease with the risk of vertebral fractures in premenopausal women.

The strengths of this study were the evaluation of localized and systemic bone involvement using HR-pQCT, in contrast to methods used in prior studies, which evaluated localized and systemic bone involvement with DXA and radiographic severity scores (1,39,40). In addition, this study highlights the selection of a population without other potential risk factors for bone loss beyond RA. Limitations of this study were the cross-sectional design and the small sample number, given that we had to apply exclusion criteria to avoid the influence of confounding factors for bone loss.

The results of this study show that premenopausal women with longstanding RA have bone fragility in peripheral joint sites. In addition, a close relationship can be observed between catabolic lesions (erosions) and bone fragility at the cortical compartment, and between anabolic lesions (osteophytes) and trabecular bone repair in premenopausal women with RA.

ACKNOWLEDGMENT

The authors thank Dr. Marcelo Bordalo for his contribution of the magnetic resonance imaging reports and images (as shown in Supplementary Figures 1A and B).

AUTHOR CONTRIBUTIONS

All authors were involved in drafting the article or revising it critically for important intellectual content, and all authors approved the final version to be published. Dr. Pereira had full access to all of the data in the study and takes responsibility for the integrity of the data and the accuracy of the data analysis.

Study conception and design. Perez, Pereira.

Acquisition of data. Perez, Figueiredo, Sales, Medeiros-Ribeiro, Takayama, Caparbo, Pereira.

Analysis and interpretation of data. Perez, Figueiredo, Sales, Medeiros-Ribeiro, Takayama, Domiciano, Bonfiglioli, Caparbo, Pereira.

REFERENCES

1. Gong X, Xu SQ, Tong H, Wang XR, Zong HX, Pan MJ, et al. Correlation between systemic osteoporosis and local bone erosion with rheumatoid arthritis patients in Chinese population. Rheumatology (Oxford) 2019;58:1443–52.
2. Solomon DH, Finkelstein JS, Shadick N, LeBoff MS, Winalski CS, Stedman M, et al. The relationship between focal erosions and generalized osteoporosis in postmenopausal women with rheumatoid arthritis. Arthritis Rheum 2009;60:1624–31.
3. Tanaka Y, Ohira T. Mechanisms and therapeutic targets for bone damage in rheumatoid arthritis, in particular the RANK-RANKL system [review]. Curr Opin Pharmacol 2018;40:110–9.
4. Allard-Chamard H, Carrier N, Dufort P, de Brum-Fernandes AJ, Boire G, Komarova SV, et al. Osteoclasts and their circulating precursors in rheumatoid arthritis: relationships with disease activity and bone erosions. Bone Rep 2020;12:100282.
5. Panagopoulos PK, Lambrou GI. Bone erosions in rheumatoid arthritis: recent developments in pathogenesis and therapeutic implications [review]. J Musculoskelet Neuronal Interact 2018;18:304–19.
6. Delgado-Calle J, Sato AY, Bellido T. Role and mechanism of action of sclerostin in bone [review]. Bone 2017;96:29–37.
7. Cici D, Corrado A, Rotondo C, Cantatore FP. Wnt signaling and biological therapy in rheumatoid arthritis and spondyloarthritis. Int J Mol Sci 2019;20:5552.

8. Xue AL, Wu SY, Jiang L, Feng AM, Guo HF, Zhao P. Bone fracture risk in patients with rheumatoid arthritis: a meta-analysis. Medicine (Baltimore) 2017;96:e6983.
9. Töpfer D, Finzel S, Museyko O, Schett G, Engelke K. Segmentation and quantification of bone erosions in high-resolution peripheral quantitative computed tomography datasets of the metacarpophalangeal joints of patients with rheumatoid arthritis. Rheumatology (Oxford) 2014;53:65–71.
10. Töpfer D, Gerner B, Finzel S, Kraus S, Museyko O, Schett G, et al. Automated three-dimensional registration of high-resolution peripheral quantitative computed tomography data to quantify size and shape changes of arthritic bone erosions. Rheumatology (Oxford) 2015;54:2171–80.
11. Barnabe C, Toepfer D, Marotte H, Hauge EM, Scharmga A, Kocijan R et al. Definition for rheumatoid arthritis erosions imaged with high resolution peripheral quantitative computed tomography and interreader reliability for detection and measurement. J Rheumatol 2016;43: 1935–40.
12. Peters M, van Tubergen A, Scharmga A, Driessen A, van Rietbergen B, Loeffen D et al. Assessment of cortical interruptions in the finger joints of patients with rheumatoid arthritis using HR-pQCT, radiography, and MRI. J Bone Miner Res 2018;33:1676–85.
13. Peters M, de Jong J, Scharmga A, van Tubergen A, Geusens P, Loeffen D et al. An automated algorithm for the detection of cortical interruptions and its underlying loss of trabecular bone: a reproducibility study. BMC Med Imaging 2018;18:13.
14. Finzel S, Ohrndorf S, Englbrecht M, Stach C, Messerschmidt J, Schett G, et al. A detailed comparative study of high-resolution ultrasound and micro–computed tomography for detection of arthritic bone erosions. Arthritis Rheum 2011; 63:1231–6.
15. Albrecht A, Finzel S, Englbrecht M, Rech J, Hueber A, Schlechtweg P, et al. The structural basis of MRI bone erosions: an assessment by microCT. Ann Rheum Dis 2013;72:1351–7.
16. Kocijan R, Finzel S, Englbrecht M, Engelke K, Rech J, Schett G. Decreased quantity and quality of the periarticular and nonperiarticular bone in patients with rheumatoid arthritis: a cross-sectional HR-pQCT study. J Bone Miner Res 2014;29:1005–14.
17. Figueiredo CP, Simon D, Englbrecht M, Haschka J, Kleyer A, Bayat S, et al. Quantification and impact of secondary osteoarthritis in patients with anti–citrullinated protein antibody-positive rheumatoid arthritis. Arthritis Rheumatol 2016;68:2114–21.
18. Aletaha D, Neogi T, Silman AJ, Funovits J, Felson DT, Bingham CO III. 2010 rheumatoid arthritis classification criteria: an American College of Rheumatology/European League Against Rheumatism collaborative initiative. Arthritis Rheum 2010;62:2569–81.
19. World Medical Association. World Medical Association Declaration of Helsinki: ethical principles for medical research involving human subjects. JAMA 2013;310:2191–4.
20. Prevoo ML, van't Hof MA, Kuper HH, van Leeuwen MA, van de Putte LB, van Riel PL. Modified disease activity scores that include twenty-eight–joint counts: development and validation in a prospective longitudinal study of patients with rheumatoid arthritis. Arthritis Rheum 1995;38:44–8.
21. Aletaha D, Nell VP, Stamm T, Uffmann M, Pflugbeil S, Machold K, et al. Acute phase reactants add little to composite disease activity indices for rheumatoid arthritis: validation of a clinical activity score. Arthritis Res Ther 2005;7:R796–806.
22. Smolen JS, Breedveld FC, Schiff MH, Kalden JR, Emery P, Eberl G, et al. A Simplified Disease Activity Index for rheumatoid arthritis for use in clinical practice. Rheumatology (Oxford) 2003;42:244–57.
23. Baim S, Binkley N, Bilezikian JP, Kendler DL, Hans DB, Lewiecki EM, et al. Official Positions of the International Society for Clinical Densitometry and executive summary of the 2007 ISCD Position Development Conference. J Clin Densitom 2008;11:75–91.
24. Genant HK, Wu CY, van Kuijk C, Nevitt MC. Vertebral fracture assessment using a semiquantitative technique. J Bone Miner Res 1993;8: 1137–48.
25. Alvarenga JC, Fuller H, Pasoto SG, Pereira RM. Age-related reference curves of volumetric bone density, structure, and biomechanical parameters adjusted for weight and height in a population of healthy women: an HR-pQCT study. Osteoporos Int 2017;28:1335–46.
26. Boutroy S, Bouxsein ML, Munoz F, Delmas PD. In vivo assessment of trabecular bone microarchitecture by high-resolution peripheral quantitative computed tomography. J Clin Endocrinol Metab 2005;90: 6508–15.
27. Fuller H, Fuller R, Pereira RM. High resolution peripheral quantitative computed tomography for the assessment of morphological and mechanical bone parameters. Rev Bras Reumatol 2015;55:352–62. In Portuguese.
28. Pasoto SG, Augusto KL, Alvarenga JC, Takayama L, Oliveira RM, Bonfa E, et al. Cortical bone density and thickness alterations by high-resolution peripheral quantitative computed tomography: association with vertebral fractures in primary Sjögren's syndrome. Rheumatology (Oxford) 2016;55:2200–11.
29. Paupitz JA, Lima GL, Alvarenga JC, Oliveira RM, Bonfa E, Pereira RM. Bone impairment assessed by HR-pQCT in juvenile-onset systemic lupus erythematosus. Osteoporos Int 2016;27:1839–48.
30. Stach CM, Bäuerle M, Englbrecht M, Kronke G, Engelke K, Manger B, et al. Periarticular bone structure in rheumatoid arthritis patients and healthy individuals assessed by high-resolution computed tomography. Arthritis Rheum 2010;62:330–9.
31. Figueiredo CP, Kleyer A, Simon D, Stemmler F, d'Oliveira I, Weissenfels A, et al. Methods for segmentation of rheumatoid arthritis bone erosions in high-resolution peripheral quantitative computed tomography (HR-pQCT). Semin Arthritis Rheum 2018; 47:611–8.
32. Figueiredo CP, Perez MO, Sales LP, Caparbo VF, Pereira RM. Evaluation of bone erosion in rheumatoid arthritis patients by high resolution peripheral quantitative computed tomography scans: comparison between two semi-automated programs in a 3-dimensional setting. Int J Rheum Dis 2021;24:948–53.
33. Vencovský J, Machácek S, Sedová L, Kafková J, Gatterová J, Pesáková V, et al. Autoantibodies can be prognostic markers of an erosive disease in early rheumatoid arthritis. Ann Rheum Dis 2003; 62:427–30.
34. Smolen JS, Aletaha D, Barton A, Burmester GR, Emery P, Firestein GS, et al. Rheumatoid arthritis [review]. Nat Rev Dis Primers 2018;4:18001.
35. Hecht C, Englbrecht M, Rech J, Schmidt S, Araujo E, Engelke K, et al. Additive effect of anti-citrullinated protein antibodies and rheumatoid factor on bone erosions in patients with RA. Ann Rheum Dis 2015; 74:2151–6.
36. Zhu TY, Griffith JF, Qin L, Hung VW, Fong TN, Au SK, et al. Structure and strength of the distal radius in female patients with rheumatoid arthritis: a case-control study. J Bone Miner Res 2013;28:794–806.
37. Haugeberg G, Uhlig T, Falch JA, Halse JI, Kvien TK. Bone mineral density and frequency of osteoporosis in female patients with rheumatoid arthritis: results from 394 patients in the Oslo County Rheumatoid Arthritis register. Arthritis Rheum 2000;43:522–30.
38. Heinlen L, Humphrey MB. Skeletal complications of rheumatoid arthritis [review]. Osteoporos Int 2017;28:2801–12.
39. Deodhar AA, Brabyn J, Jones PW, Davis MJ, Woolf AD. Measurement of hand bone mineral content by dual energy x-ray absorptiometry: development of the method, and its application in normal volunteers and in patients with rheumatoid arthritis. Ann Rheum Dis 1994;53:685–90.

40. Ardicoglu O, Ozgocmen S, Kamanli A, Pekkutucu I. Relationship between bone mineral density and radiologic scores of hands in rheumatoid arthritis. J Clin Densitom 2001;4:263–9.
41. Hill CL, Schultz CG, Wu R, Chatterton BE, Cleland LG. Measurement of hand bone mineral density in early rheumatoid arthritis using dual energy X-ray absorptiometry. Int J Rheum Dis 2010;13:230–4.
42. Rossini M, Bagnato G, Frediani B, Iagnocco A, La Montagna G, Minisola G, et al. Relationship of focal erosions, bone mineral density, and parathyroid hormone in rheumatoid arthritis. J Rheumatol 2011; 38:997–1002.
43. Werner D, Simon D, Englbrecht M, Stemmler F, Simon C, Berlin A, et al. Early changes of the cortical micro-channel system in the bare area of the joints of patients with rheumatoid arthritis. Arthritis Rheumatol 2017;69:1580–7.
44. Grüneboom A, Hawwari I, Weidner D, Culemann S, Müller S, Henneberg S, et al. A network of trans-cortical capillaries as mainstay for blood circulation in long bones. Nat Metab 2019;1: 236–50.
45. Scharmga A, Keller KK, Peters M, van Tubergen A, van den Bergh JP, van Rietbergen B, et al. Vascular channels in metacarpophalangeal joints: a comparative histologic and high-resolution imaging study. Sci Rep 2017;7:8966.
46. Schett G, Gravallese E. Bone erosion in rheumatoid arthritis: mechanisms, diagnosis and treatment [review]. Nat Rev Rheumatol 2012;8: 656–64.
47. Walsh NC, Reinwald S, Manning CA, Condon KW, Iwata K, Burr DB, et al. Osteoblast function is compromised at sites of focal bone erosion in inflammatory arthritis. J Bone Miner Res 2009;24:1572–85.
48. Finzel S, Rech J, Schmidt S, Engelke K, Englbrecht M, Stach C, et al. Repair of bone erosions in rheumatoid arthritis treated with tumour necrosis factor inhibitors is based on bone apposition at the base of the erosion. Ann Rheum Dis 2011;70:1587–93.
49. Omata Y, Hagiwara F, Nishino J, Matsudaira K, Kadono Y, Juji T, et al. Vertebral fractures affect functional status in postmenopausal rheumatoid arthritis patients. J Bone Miner Metab 2014;32:725–31.
50. Mohammad A, Lohan D, Bergin D, Mooney S, Newell J, O'Donnell M, et al. The prevalence of vertebral fracture on vertebral fracture assessment imaging in a large cohort of patients with rheumatoid arthritis. Rheumatology (Oxford) 2014;53:821–7.

Arthritis & Rheumatology
Vol. 74, No. 3, March 2022, pp 418–426
DOI 10.1002/art.41229

American College of Rheumatology
Empowering Rheumatology Professionals

Microstructural Bone Changes Are Associated With Broad-Spectrum Autoimmunity and Predict the Onset of Rheumatoid Arthritis

David Simon,[1] Arnd Kleyer,[1] Duy Bui Cong,[1] Axel Hueber,[1] Holger Bang,[2] Andreas Ramming,[1] Juergen Rech,[1] and Georg Schett[1]

Objective. To assess if microstructural bone lesions in individuals at risk of developing rheumatoid arthritis (RA) are related to the spectrum of anti–modified protein antibodies (AMPAs) and affect the risk of developing RA.

Methods. Cortical microchannels as well as cortical and trabecular bone mineral density (BMD) volumes (expressed as mg hydroxyapatite/cm^3) were analyzed by high-resolution peripheral quantitative computed tomography of the hand joints of individuals at risk of RA. AMPA response was profiled, including reactivities against citrullinated proteins (vimentin, enolase, and fibrinogen) as well as carbamylated and acetylated vimentin. All subjects were followed up for the development of RA.

Results. Subjects at risk of developing RA (n = 75) who had broad-spectrum AMPAs (6–8 reactivities) had significantly more severe microstructural changes, including a higher mean ± SD number of cortical microchannels per joint (95 ± 3) and lower total volumetric BMD (vBMD; 265 ± 45), trabecular vBMD (176 ± 42), and cortical vBMD (585 ± 138), than those with moderate AMPA reactivity (3–5 reactivities) (number of cortical microchannels, 79 ± 30; total vBMD, 293 ± 33; trabecular vBMD, 195 ± 32; and cortical vBMD, 627 ± 91) and those with narrow AMPA reactivity (1–2 reactivities) (number of cortical microchannels, 47 ± 20; total vBMD, 311 ± 34; trabecular vBMD, 211 ± 30; and cortical vBMD, 674 ± 56). Progressors to RA had significantly higher numbers of cortical microchannels (103 ± 30 versus 71 ± 35) and lower bone volume (258 ± 37 versus 295 ± 34) compared to nonprogressors. Furthermore, rate of progression to RA was high in subjects with broad AMPA reactivity (48%) versus those with medium AMPA reactivity (26%) or narrow AMPA reactivity (0%), as well as in those with a high number of cortical microchannels (44%) versus those with a low number of cortical microchannels (10%).

Conclusion. Microstructural changes in individuals at risk of RA are associated with broad-spectrum autoimmunity and predict the onset of RA. These data support the concept of structural priming of joints by autoimmunity before the onset of the inflammatory phase of the disease.

INTRODUCTION

The development of rheumatoid arthritis (RA) is characterized by a phase of autoimmunity lasting several years, which precedes the onset of the clinical disease (1,2). Usually, this autoimmune phase is clinically silent and characterized by the presence of anti–modified protein antibodies (AMPAs) (3) recognizing citrullinated, carbamylated, or acetylated proteins, as well as rheumatoid factor (RF) (4,5). Individuals who are positive for AMPAs and/or RF but do not show signs of clinical joint swelling are considered "at-risk" of RA due to their higher risk of developing RA (6). Importantly, not all at-risk individuals actually develop RA, suggesting that the at-risk state may represent a heterogeneous condition (7,8). For instance, at-risk individuals who develop pain,

Supported by the DFG (grants SPP1468-IMMUNOBONE and CRC1181), the BMBF (project MASCARA), the Marie Curie project OSTEOIMMUNE, the TEAM project of the European Union, the Innovative Medicines Initiative (project RTCure), the ERC Synergy Grant NanoScope (to Dr. Schett), the Emerging Fields Initiative MIRACLE of the Friedrich–Alexander University Erlangen–Nuremberg, and the Else Kröner Memorial Scholarship (no. 2019_EKMS.27; to Dr. Simon).

[1]David Simon, MD, Arnd Kleyer, MD, Duy Bui Cong, MD, Axel Hueber, MD, PhD, Andreas Ramming, MD, Juergen Rech, MD, Georg Schett, MD: Friedrich–Alexander University Erlangen–Nuremberg and Universitätsklinikum Erlangen, Erlangen, Germany; [2]Holger Bang, PhD: Orgentec Inc., Mainz, Germany.

Dr. Bang owns stock or stock options in Orgentec. No other disclosures relevant to this article were reported.

Address correspondence to Georg Schett, MD, Department of Internal Medicine 3, Friedrich–Alexander University Erlangen–Nuremberg and Universitätsklinikum Erlangen, Erlangen, Ulmenweg 18, 91054 Erlangen, Germany. Email: georg.schett@uk-erlangen.de.

Submitted for publication July 5, 2019; accepted in revised form February 6, 2020.

i.e., clinically suspect arthralgia (9), as well as those with subclinical inflammation (10), are at a higher risk of progressing to RA. Thus, the term "at-risk of RA" can comprise a spectrum of individuals who are either far from developing clinical disease or facing the imminent onset of disease. These differences may likely be explained by the gestalt of autoimmunity in the individual at-risk patient, including autoantibody titer (11), specificity (12,13), and sialylation status (14), which can impact their effector function.

In recent years, the effector function of RA-specific antibodies, especially anti–citrullinated protein antibodies (ACPAs), has attracted increasing attention, leading to the reconsideration of autoimmunity as a pathogenic process that actively influences progression to RA. In this context, it has been suggested that effector functions of ACPAs trigger cytokine release from monocytes (15,16), inflammatory changes in the lungs (17), and differentiation of bone-resorbing osteoclasts (18,19). Such processes may indeed move at-risk individuals closer to the development of RA. With respect to bone, clinical data suggest that ACPA-positive RA patients show more severe bone changes than ACPA-negative patients (20). Furthermore, in a small cohort of ACPA-positive at-risk individuals, microstructural bone changes were detected, indicating that RA-specific autoimmunity could trigger periarticular bone changes (21). Nonetheless, it is currently unknown whether these initial changes in joint structure in at-risk individuals are related to the pattern of RA-specific autoimmunity and whether such changes predict the onset of RA.

In this study we performed a detailed cross-sectional and longitudinal analysis of bone microstructure as well as autoimmunity in a large number of individuals at risk of developing RA, in order to 1) analyze the nature of preclinical microstructural bone changes in light of the newly discovered cortical microchannels (22), 2) determine whether and how such structural changes are related to RA-specific autoimmunity, and 3) most importantly, address whether such microstructural changes are associated with the risk of progression to RA.

PATIENTS AND METHODS

At-risk individuals. Subjects who had a positive test result for antibodies against cyclic citrullinated peptide 2 (anti–CCP-2) or mutated citrullinated vimentin (MCV), as well as no current or previous signs of joint swelling, were included in this cohort of at-risk individuals. Individuals were recruited from 3 sources: 1) public health days that included screening for ACPAs, 2) invitation of healthy relatives of patients with ACPA-positive RA, and 3) referrals from a primary care physician due to a positive test result for ACPAs. Positive anti–CCP-2 or MCV results had to be confirmed by at least 1 additional test before patients were included in the cohort. All patients underwent a detailed examination by experienced rheumatologists (AK and JR) who performed a swollen joint count (66 joints assessed) and tender joint count (68 joints assessed) to exclude the presence of arthritis, as well as an assessment for the presence of clinically suspect arthralgia (9). Age, sex, weight, and height, as well as smoking habits and alcohol intake, were documented at first visit. High-resolution peripheral quantitative computed tomography (QCT) imaging and withdrawal of serum for detailed autoantibody profiling were also performed at the first visit.

By the end of 2018, 75 ACPA-positive at-risk individuals had been recruited. Patients were followed up for the development of RA according to the American College of Rheumatology/European Alliance of Associations for Rheumatology 2010 classification criteria (23) at regularly scheduled visits every 6 months over a total period of 30 months. Written informed consent was obtained from all individuals. The study was performed in accordance with the Declaration of Helsinki and approved by the institutional review board of the University Hospital Erlangen.

Laboratory testing. For screening individuals for inclusion in the study, anti–CCP-2 and MCV were measured by standard enzyme-linked immunosorbent assays (ELISAs) from Phadia/ThermoFisher Scientific and Orgentec, respectively. RF status was assessed by rate nephelometry (Beckman Coulter).

For analysis of AMPA reactivity, ELISAs for detecting antibodies against 4 individual citrullinated peptides (citrullinated vimentin, citrullinated α-enolase, citrullinated fibrinogen α, and citrullinated fibrinogen β) as well as 3 additional vimentin modifications (carbamylated vimentin, ornithine acetylated vimentin, and lysine acetylated vimentin) were performed. With respect to control antigens, the unmodified arginine, ornithine, or lysine versions of the peptide were used to determine the specificity of the reactivities to the modified AMPA peptides. No specific reactivities were detected when sera were tested against unmodified arginine (mean ± SD optical density [OD] 0.094 ± 0.056), ornithine (0.093 ± 0.055), or lysine (0.098 ± 0.087). To further ascertain specificity, cross-inhibition studies were done, in which serum samples were preincubated with 50 μg/ml of citrullinated, carbamylated, or acetylated peptides for 1 hour at room temperature. The antibody–antigen complexes were then added to AMPA peptide–coated plates, and the ELISA readout was performed as described above.

Principles of the assays have been described previously (3). Briefly, streptavidin-coated microtiter plates (Nunc) were coated with 0.5 μg/ml biotinylated peptide in 100 μl of phosphate buffered saline (PBS). Then, serum diluted 1:100 in PBS supplemented with 1% bovine serum albumin was added. After washing, horseradish peroxidase–conjugated affinity-purified goat antibody against the human IgG Fcγ fragment (Dianova) was added, and the reaction was visualized with 3,3′,5,5′-tetramethylbenzidine. Absorbance at 450 nm was determined using an ELISA reader (Rainbow Reader; Tecan). Each serum sample was tested in duplicate. Cutoffs were defined as the mean + 3SD of ELISA OD values obtained from a population of healthy controls (n = 112), showing OD values between 0.24 and 0.34 (3). We therefore used a conservative cutoff of 0.4 for all peptide reactivities.

Measurements of imprecision were taken over 4 and 6 replicates for intraassay variability and interassay variability, respectively. To assess the precision of the AMPA ELISA, a "low value" sample, a "medium value" sample, and a "high value" sample were assayed in 5 independent tests on 1 day (interassay) or in a single run (intraassay). The intraassay coefficient of variation (CV) was 7.7%, 6.9%, and 5.2% for low, medium, and high values, respectively, whereas the interassay CV was 4.2%, 3.5%, and 7.2 % for low, medium, and high values, respectively.

High-resolution peripheral QCT. High-resolution peripheral QCT scanning of the second metacarpal head was performed in each subject by a trained operator (DS) using standard in vivo imaging parameters (voxel size 82 × 82 × 82 μm, effective energy 60 kV, current 900 μA, and integration time 100 msec) according to the recommendations of the Study Group for Extreme Computed Tomography in Rheumatoid Arthritis (SPECTRA) collaboration (24). Strict motion grading was applied, excluding images with a motion grade >3/5. Then, the complete metacarpal head was contoured in the transverse plane. Semiautomatic contouring was performed under the visual inspection of a trained operator (DS) to make minor adjustments in case of inaccurate periosteal surface delineation, followed by evaluation of the created GOBJ. To ensure that only intraarticular surface changes were evaluated, a subregion of the metacarpal head with a dimension of 101 slices was chosen. Transverse slices were generated from this region using the sub dim feature of the manufacturers' 3-dimensional (3-D) viewer. In total, 11 transverse planes with a standardized distance of 10 slices (820 μm), which comprises the area of the metacarpal head, were generated.

Bone structure analysis. Cortical microchannels were quantified in all slices in a blinded manner by 2 independent readers (AK and DBC) as previously described (22). Cortical microchannels were defined as channels ranging from the periosteal to the endosteal region in the bare area of the joint. Total numbers of cortical microchannels per joint were counted as well as numbers in the dorsal, ulnar, palmar, and radial subregions. In addition, the following bone parameters were determined: total volumetric bone mineral density (vBMD), trabecular vBMD, and cortical vBMD (all expressed as mg hydroxyapatite [HA]/cm^3), as well as cortical thickness (expressed in mm).

Statistical analysis. Data were collected, organized, and analyzed using SPSS software for statistics (IBM SPSS 21.0). With respect to demographic and disease-specific characteristics, categorical variables are presented as the number and percentage and continuous variables are presented as the mean ± SD, except where indicated otherwise. Continuous variables assumed to be normally distributed were tested using quantile–quantile plots, the Kolmogorov–Smirnov test, and the Shapiro–Wilk test. The bone parameters described above were compared in 3 predefined groups, with either narrow (1–2), medium (3–5), or broad (6–8) AMPA reactivities, using analysis of variance (ANOVA). For comparison of bone parameters between at-risk individuals progressing to RA and those not progressing to RA, the Mann–Whitney U test was applied. To explore differences in demographic and disease-specific variables between the AMPA groups (narrow, medium, and broad) or the cortical microchannel groups (low [<80/joint] and high [≥80/joint]), ANOVA or the Mann–Whitney U test was applied. For categorical variables, chi-square tests were applied. *P* values less than or equal to 0.05 were considered significant.

RESULTS

Characteristics of the subjects at risk of developing RA. Seventy-five at-risk individuals were included in this cross-sectional, longitudinal study. The mean ± SD age was 50.7 ± 1.5 years, and 50 subjects were women. The mean ± SD body weight was 76.5 ± 2.2 kg and height was 171 ± 1.1 cm. Thirty-two individuals were smokers, and 51 reported regular alcohol consumption. Per the inclusion criteria, no joint swelling was present. Twenty-three subjects reported clinically suspect arthralgia.

Grouping of individuals at risk of RA by narrow, medium, and broad AMPA specificity patterns. We first performed an analysis of AMPA reactivity in individuals at risk of RA. These analyses included RF and anti–CCP-2 reactivity as well as antibodies against 3 additional citrullinated peptides (α-enolase, fibrinogen α, and fibrinogen β) and 3 additional protein modifications (carbamylation, ornithine acetylation, and lysine acetylation). Sixteen individuals had narrow AMPA reactivity (1–2 reactivities), 23 individuals had medium AMPA reactivity (3–5 reactivities), and 36 individuals had broad AMPA reactivity (6–8 reactivities) (Figure 1). The 3 subgroups showed no differences in age, sex, body weight, or height (Table 1). Smoking habits and alcohol intake were also similar among the 3 groups. The prevalence of clinically suspect arthralgia, however, was higher in individuals with broad AMPA reactivity ($P = 0.0028$).

Association of the pattern of AMPA specificity with microstructural bone changes. We next addressed whether broad AMPA reactivity is associated with structural priming of joints. We performed high-resolution peripheral QCT of the metacarpal head in all 75 individuals at risk of RA. We assessed cortical microchannels as well as vBMD of the total, trabecular, and cortical bone. In 58 subjects, image quality was high and without motion artifacts, allowing reliable measurement of all bone parameters. These patients did not differ from those for whom no high quality images could be obtained with respect to age ($P = 0.68$), sex ($P = 1.00$), presence of arthralgia ($P = 0.76$), RF level ($P = 0.71$), anti–CCP-2 antibody level ($P = 0.58$), or AMPA categories ($P = 0.69$).

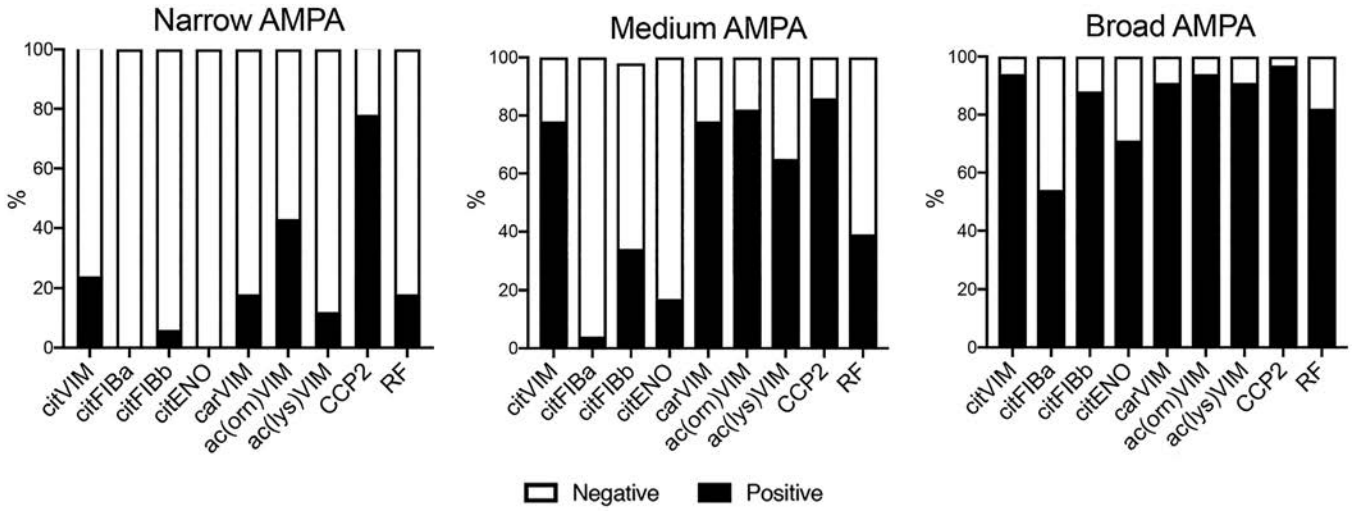

Figure 1. Pattern of autoantigen recognition in subjects at risk of developing rheumatoid arthritis who had narrow, medium, or broad anti–modified protein antibody (AMPA) reactivity. The percentages of subjects whose serum showed reactivity with citrullinated vimentin (citVIIM), citrullinated fibrinogen α (citFIBa), citrullinated fibrinogen β (citFIBb), citrullinated α-enolase (citENO), carbamylated vimentin (carVIM), ornithine acetylated vimentin (ac[orn]VIM), lysine acetylated vimentin (ac[lys]VIM), cyclic citrullinated peptide 2 (CCP-2), and rheumatoid factor (RF) are shown for the groups with narrow AMPA specificity (1–2 specificities), medium AMPA specificity (3–5 specificities), and broad AMPA specificity (6–8 specificities).

The total number of cortical microchannels and the number of radial cortical microchannels, which are specifically altered in the context of RA (22), were significantly increased in individuals with broad AMPA specificity ($P = 0.0009$ and $P = 0.0036$, respectively) (Figure 2). The mean ± SD total numbers of cortical microchannels were 95 ± 3 in those with broad AMPA specificity, 79 ± 30 in those with moderate AMPA specificity, and 47 ± 20 in those with narrow AMPA specificity. Alternatively, when analyzing for specific modifications (citrullinated, carbamylated, and acetylated antibodies), microstructural bone changes were generally more pronounced in subjects with higher autoantibody levels irrespective of the nature of the modification (Supplementary Figure 1, available on the *Arthritis & Rheumatology* website at http://onlinelibrary.wiley.com/doi/10.1002/art.41229/abstract). Additional analyses showed a more widespread bone pathology in individuals with broad AMPA specificity, with significantly lower total vBMD (mean ± SD 265 ± 45 versus 311 ± 34 in those

Table 1. Demographic and clinical characteristics of the subjects at risk of developing RA, according to AMPA profile and bone microstructure*

	Narrow AMPA specificity (n = 16)	Medium AMPA specificity (n = 23)	Broad AMPA specificity (n = 36)	Low number of cortical microchannels (n = 31)†	High number of cortical microchannels (n = 27)†
Age, years	52.0 ± 4.0	53.3 ± 1.5	49.2 ± 2.3	48.8 ± 2.2	52.9 ± 2.1
Sex, no. female	12	14	24	21	18
Weight, kg	74.0 ± 4.7	77.5 ± 3.4	73.3 ± 3.0	73.8 ± 3.0	79.6 ± 3.2
Height, cm	173 ± 2.4	172 ± 2.0	170 ± 1.4	170 ± 1.4	173 ± 1.9
No. with clinically suspect arthralgia	0	6	17‡	6	11
No. of tender joints	0.2 ± 0.2	0.7 ± 0.3	1.1 ± 0.3	0.58 ± 0.23	1.34 ± 0.37§
CRP, mg/liter	3.3 ± 0.6	2.9 ± 0.7	4.8 ± 0.6	3.3 ± 0.4	4.0 ± 0.7
ESR, mm/hour	13.2 ± 2.8	15.4 ± 5.1	18.2 ± 6.9	13.5 ± 3.7	17.3 ± 4.4
Smoker, no.	4	11	17	15	10
Alcohol use, no.	10	15	26	26	20

* Except where indicated otherwise, values are the mean ± SEM. RA = rheumatoid arthritis; CRP = C-reactive protein; ESR = erythrocyte sedimentation rate.
† Cortical microchannel data were available for 58 subjects; for 17 patients, image quality was too poor to score cortical microchannels, because of the occurrence of motion artifacts during imaging. A low number of cortical microchannels was defined as <80 per joint, and a high number of cortical microchannels was defined as ≥80 per joint.
‡ $P = 0.0028$ versus narrow anti–modified protein antibody (AMPA) specificity and medium AMPA specificity.
§ $P = 0.05$ versus subjects with a low number of cortical microchannels.

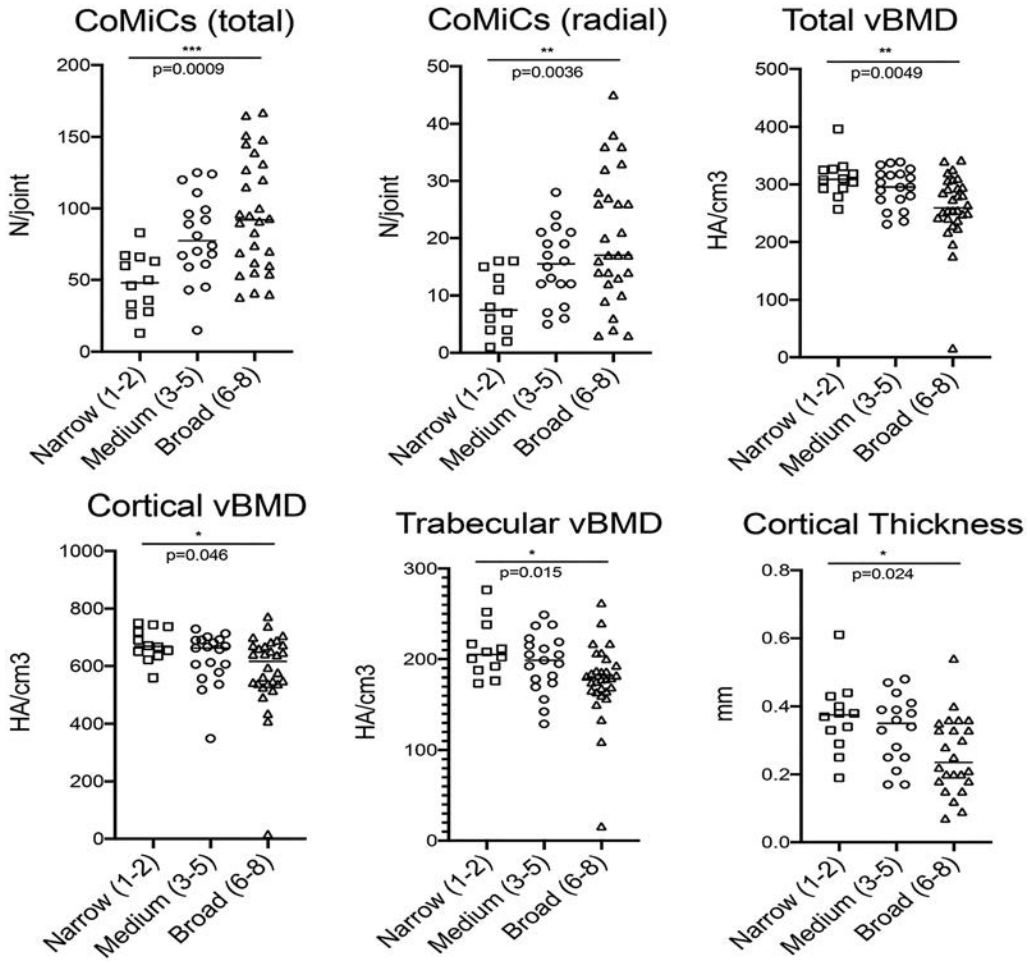

Figure 2. Microstructural bone parameters in subjects at risk of developing rheumatoid arthritis who had different anti–modified protein antibody (AMPA) patterns. The total number of cortical microchannels (CoMiCs) per joint, the number of radial microchannels per joint, total volumetric bone mineral density (vBMD), cortical vBMD, trabecular vBMD, and cortical thickness were compared between subjects with narrow AMPA reactivity, subjects with medium AMPA reactivity, and subjects with broad AMPA reactivity. Symbols represent individual subjects; horizontal lines show the mean. * = $P < 0.05$; ** = $P < 0.01$; *** = $P < 0.001$, by analysis of variance. HA = hydroxyapatite.

with narrow AMPA specificity; $P = 0.0049$), trabecular vBMD (mean ± SD 176 ± 42 versus 211 ± 30 in those with narrow AMPA specificity; $P = 0.015$), and cortical vBMD (mean ± SD 585 ± 138 versus 674 ± 56 in those with narrow AMPA specificity; $P = 0.046$), as well as significant thinning of the cortical bone shell ($P = 0.024$ for cortical thickness), compared to individuals with narrow AMPA reactivity (Figure 2).

Association of the progression to RA with structural priming of the joints. Based on these findings, we next compared bone microstructure between at-risk individuals who progressed to RA and those who did not progress to RA. The total number of cortical microchannels (mean ± SD 103 ± 30 in progressors versus 71 ± 35 in nonprogressors; $P = 0.0009$) and the number of radial microchannels ($P = 0.0014$) were significantly different between progressors and nonprogressors to RA (Figure 3). When vBMD was assessed, progressors had significantly diminished total vBMD (mean ± SD 258 ± 37 versus 295 ± 34 in nonprogressors; $P = 0.0012$), trabecular vBMD ($P = 0.0042$), and cortical vBMD ($P = 0.0240$) compared to nonprogressors. Furthermore, cortical thickness was lower in RA progressors ($P = 0.039$).

Association of broad AMPA specificity and increased cortical microchannels with progression to RA. Considering that broad AMPA specificity was associated with microstructural changes in articular cortical and trabecular bone, we investigated whether AMPA specificity as well as cortical microchannels are associated with the progression of at-risk individuals to RA. Twenty-three of the 75 subjects developed RA during the 1-year follow-up period. Among the 3 aforementioned AMPA subgroups, those with broad AMPA specificity had a high risk of progression to RA (48%), while the progression rate was lower in those with medium AMPA specificity (26%), and no progression

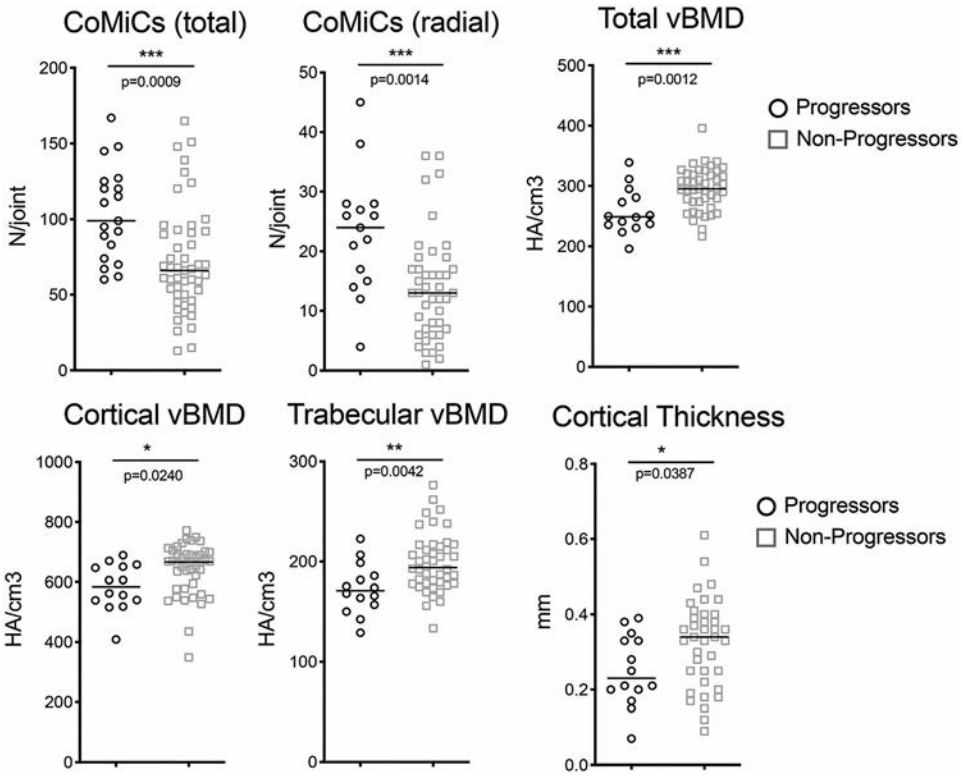

Figure 3. Microstructural bone changes in subjects at risk of developing rheumatoid arthritis (RA) who progressed to RA compared to those who did not progress to RA. Values are the baseline total number of cortical microchannels (CoMiCs), number of radial microchannels, total volumetric bone mineral density (vBMD), cortical vBMD, trabecular vBMD, and cortical thickness. Symbols represent individual subjects; horizontal lines show the mean. * = $P < 0.05$; ** = $P < 0.01$; *** = $P < 0.001$, by Mann–Whitney U test. HA = hydroxyapatite.

to RA was observed in those with narrow AMPA specificity (0%) (Figure 4A). However, no correlation between the number of AMPA categories and the time to onset of RA was observed during the 12-month period.

When the impact of microstructural changes on the progression to RA was assessed, we found that at-risk individuals with a high number of cortical microchannels (≥80 per joint) (Figure 4B) had a higher likelihood of progressing to RA (44%) than those with a low number of cortical microchannels (10%) (Figure 4C). Furthermore, the number of cortical microchannels was significantly correlated with the time to onset of RA during the 12-month period. Subjects with a low number of cortical microchannels and those with a high number of cortical microchannels showed no difference in age, sex, body weight, or height; smoking habits and alcohol intake were also similar (Table 1). Clinically suspect arthralgia was more common in individuals with a high number of cortical microchannels.

DISCUSSION

The data from this study indicate that at-risk individuals who show microstructural changes in their joints are at high risk of developing RA. We also show that such microstructural changes are closely linked to a broader autoantibody repertoire. While RA is considered to be a disease of the synovial membrane, the initial lesions in the joints that precede the onset of RA are still enigmatic. Their characterization, however, is key to better understanding the nature of the joint homing process, which allows systemic autoimmunity to ultimately translate into an inflammatory joint disease (2).

The interphase region between the juxtaarticular bone marrow and the synovial membrane has always been a focus of interest, since magnetic resonance imaging of RA joints shows lesions both in the synovial membrane and in the adjacent bone marrow. These 2 compartments are separated by a very thin lamella of cortical bone, which is traditionally seen as a solid barrier. Due to technical advances, however, this concept has changed. Most importantly, very recent 3-D light sheet microscopy studies as well as X-ray microscopy studies have identified a dense transcortical vascular network in cortical bone, which accounts for >80% of arterial and venous blood flow in bone (25). This vascular system contains numerous osteoclasts, which remodel bone. Furthermore, earlier conventional histologic studies also showed vascular channels in the cortical bone connecting the bone marrow with the synovial space (26). These vessels are usually below the detection limit of high-resolution peripheral QCT. However, if widened by osteoclast-mediated bone resorption, such as in RA or during aging, these channels become detectable and comprise the cortical microchannels described previously in RA (22) and for the first time in this study in individuals at risk of developing RA.

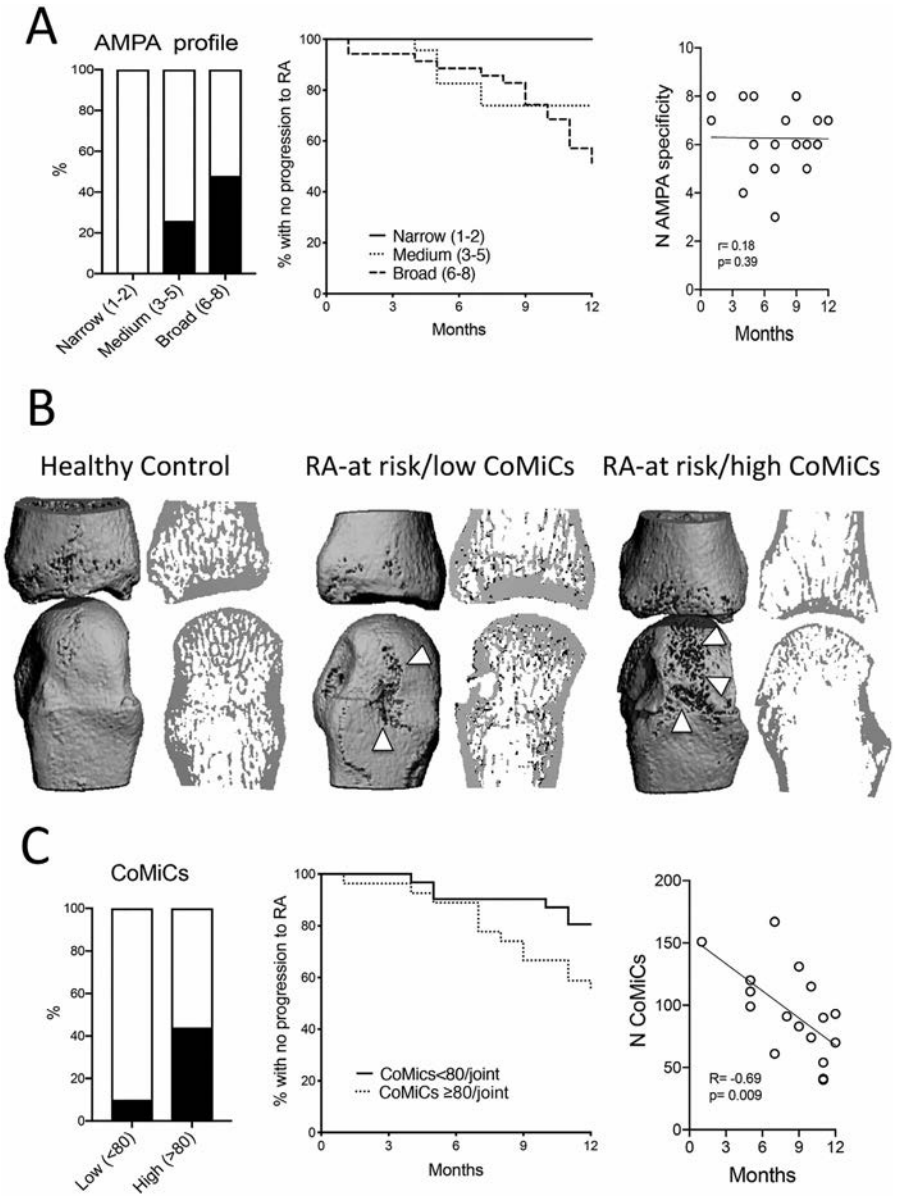

Figure 4. Impact of anti–modified protein antibody (AMPA) pattern and microstructural bone changes on the progression to rheumatoid arthritis (RA). **A**, Percentage of subjects progressing to RA according to AMPA reactivity profile (left), Kaplan-Meier plot showing loss of the RA at-risk state according to AMPA reactivity profile (middle), and correlation between the number of AMPA specificities and the time to onset of RA. Circles represent individual subjects. **B**, High-resolution peripheral quantitative computed tomography scans of the metacarpophalangeal joints of a healthy control, an individual at risk of RA with a low number of cortical microchannels (CoMiCs) (arrowheads), and an individual at risk of RA with a high number of cortical microchannels. **C**, Percentage of subjects showing progression to RA according to number of cortical microchannels (left), Kaplan-Meier plot showing loss of the RA at-risk state according to number of cortical microchannels (middle), and correlation between the number of cortical microchannels and the time to onset of RA. Circles represent individual subjects.

Based on the observation that the increase in cortical microchannels is preferentially seen with broad-spectrum autoimmunity, antibody-mediated osteoclastogenesis, as it has been described previously (27), may be an explanation for the process. This notion is also supported by the significant decrease in cortical and trabecular bone mass in the adjacent periarticular regions, which suggests that a local proresorptive environment is established. Earlier data showing increased bone resorption markers in some individuals at risk of RA are also consistent with these data (28). Notably, both increased cortical microchannels and broad AMPA reactivity were associated with clinically suspect arthralgia. This association may be explained by the fact that forced bone resorption leads to local acidic pH (29), which is a potent mediator for triggering pain responses.

Although these data clearly suggest that microstructural changes in individuals at risk of developing RA are associated with

the pattern of RA-specific autoimmunity, the mechanistic link between autoantibodies and osteoclasts needs further investigation. Antigen-specific binding to citrullinated vimentin on osteoclasts (18,19), but also Fc receptor–mediated effects (30), were shown to trigger enhanced osteoclast differentiation in the context of autoantibodies, both explaining the link between broad-spectrum autoimmunity and bone loss. On the other hand, effects of preparations of monoclonal antibodies against citrullinated proteins have to be interpreted with some caution, since such preparations did not reveal activity against anti–citrullinated proteins (31–33). Notably, Fc-mediated effects on osteoclasts are sufficient to explain autoantibody-triggered bone loss in the predisease phase. Hence, broad-spectrum autoimmunity may favor immune complex formation and more robust Fc receptor engagement. Also, the decrease in autoantibody glycosylation, which happens before the onset of RA, fosters antibody binding to activating Fc receptors (14).

The limitations of this study include the rather small sample size of individuals at risk of developing RA. This is partly due to the limited availability of high-resolution peripheral QCT, which confined this study to a single center. However, this situation ensured an identical scanning protocol and a homogeneous rigorous definition of the subjects, who were all determined to be AMPA positive using the same tests and were all evaluated in the same manner for true absence of joint swelling. Another limitation is the fact that we cannot make definite conclusions about the causality of bone architectural changes and the onset of RA. However, several different pathophysiologic links between bone changes and the onset of RA can be envisioned. First, osteoclasts can be a source of proinflammatory cytokines that support the initiation of local inflammatory responses (18,34). Second, osteoclasts have antigen-presenting function and could thereby present local cartilage-borne molecules to T cells, enhancing local autoimmune reactions (35). Finally, the build-up of connections between the periarticular bone marrow and the synovial space by cortical microchannels could allow neutrophils an easier egress from the bone marrow into the joint by transcortical vessels (25), triggering the first bout of RA.

Taken together, our data suggest that microstructural changes in the periarticular cortical bone represent a link between symptomatic autoimmunity and RA. In this context it will be interesting to see whether inhibitors of bone resorption, such as RANK inhibition, which have been shown to be able to target bone erosive lesions (36), can interfere with the onset of RA.

AUTHOR CONTRIBUTIONS

All authors were involved in drafting the article or revising it critically for important intellectual content, and all authors approved the final version to be published. Dr. Schett had full access to all of the data in the study and takes responsibility for the integrity of the data and the accuracy of the data analysis.

Study conception and design. Simon, Kleyer, Hueber, Ramming, Rech, Schett.

Acquisition of data. Simon, Kleyer, Cong, Bang, Ramming, Rech.

Analysis and interpretation of data. Simon, Kleyer, Ramming, Rech, Schett.

ADDITIONAL DISCLOSURES

Author Bang is an employee of Orgentec Inc.

REFERENCES

1. McInnes IB, Schett G. The pathogenesis of rheumatoid arthritis. N Engl J Med 2011;365:2205–19.
2. Catrina AI, Svensson CI, Malmström V, Schett G, Klareskog L. Mechanisms leading from systemic autoimmunity to joint-specific disease in rheumatoid arthritis. Nat Rev Rheumatol 2017;13:79–86.
3. Figueiredo CP, Bang H, Cobra JF, Englbrecht M, Hueber AJ, Haschka J, et al. Antimodified protein antibody response pattern influences the risk for disease relapse in patients with rheumatoid arthritis tapering disease modifying antirheumatic drugs. Ann Rheum Dis 2017;76:399–407.
4. Rantapää-Dahlqvist S, de Jong BA, Berglin E, Hallmans G, Wadell G, Stenlund H, et al. Antibodies against cyclic citrullinated peptide and IgA rheumatoid factor predict the development of rheumatoid arthritis. Arthritis Rheum 2003;48:2741–9.
5. Shi J, van de Stadt LA, Levarht EW, Huizinga TW, Toes RE, Trouw LA et al. Anti–carbamylated protein antibodies are present in arthralgia patients and predict the development of rheumatoid arthritis. Arthritis Rheum 2013;65:911–5.
6. Gerlag DM, Raza K, van Baarsen LG, Brouwer E, Buckley CD, Burmester GR, et al. EULAR recommendations for terminology and research in individuals at-risk of rheumatoid arthritis: report from the Study Group for Risk Factors for Rheumatoid Arthritis. Ann Rheum Dis 2012;71:638–41.
7. Nam JL, Hunt L, Hensor EM, Emery P. Enriching case selection for imminent RA: the use of anti-CCP antibodies in individuals with new non-specific musculoskeletal symptoms - a cohort study. Ann Rheum Dis 2016;75:1452–6.
8. Van Steenbergen HW, Aletaha D, Beaart-van de Voorde LJ, Brouwer E, Codreanu C, Combe B, et al. EULAR definition of arthralgia suspicious for progression to rheumatoid arthritis. Ann Rheum Dis 2017;76:491–6.
9. Burgers LE, van Steenbergen HW, Ten Brinck RM, Huizinga TW, van der Helm-van Mil AH. Differences in the symptomatic phase preceding ACPA-positive and ACPA-negative RA: a longitudinal study in arthralgia during progression to clinical arthritis. Ann Rheum Dis 2017;76:1751–4.
10. Kleyer A, Krieter M, Oliveira I, Faustini F, Simon D, Kaemmerer N, et al. High prevalence of tenosynovial inflammation before onset of rheumatoid arthritis and its link to progression to RA-A combined MRI/CT study. Semin Arthritis Rheum 2016;46:143–50.
11. Bos WH, van de Stadt LA, Sohrabian A, Rönnelid J, Van Schaardenburg D. Development of anti-citrullinated protein antibody and rheumatoid factor isotypes prior to the onset of rheumatoid arthritis. Arthritis Res Ther 2014;16:405.
12. Ioan-Facsinay A, Willemze A, Robinson DB, Peschken CA, Markland J, van der Woude D, et al. Marked differences in fine specificity and isotype usage of the anti-citrullinated protein antibody in health and disease. Arthritis Rheum 2008;58:3000–8.
13. Sokolove J, Bromberg R, Deane KD, Lahey LJ, Derber LA, Chandra PE, et al. Autoantibody epitope spreading in the pre-clinical phase predicts progression to rheumatoid arthritis. PLoS One 2012;7:e35296.

14. Pfeifle R, Rothe T, Ipseiz N, Scherer HU, Culemann S, Harre U, et al. Regulation of autoantibody activity by the IL-23-T_H17 axis determines the onset of autoimmune disease. Nat Immunol 2017;18:104–113.
15. Clavel C, Ceccato L, Anquetil F, Serre G, Sebbag M. Among human macrophages polarised to different phenotypes, the M-CSF-oriented cells present the highest pro-inflammatory response to the rheumatoid arthritis-specific immune complexes containing ACPA. Ann Rheum Dis 2016;75:2184–91.
16. Laurent L, Anquetil F, Clavel C, Ndongo-Thiam N, Offer G, Miossec P, et al. IgM rheumatoid factor amplifies the inflammatory response of macrophages induced by the rheumatoid arthritis-specific immune complexes containing anticitrullinated protein antibodies. Ann Rheum Dis 2015;74:1425–31.
17. Demoruelle MK, Weisman MH, Simonian PL, Lynch DA, Sachs PB, Pedraza IF, et al. Airways abnormalities and rheumatoid arthritis–related autoantibodies in subjects without arthritis: early injury or initiating site of autoimmunity? Arthritis Rheum 2012;64:1756–61.
18. Harre U, Georgess D, Bang H, Bozec A, Axmann R, Ossipova E et al. Induction of osteoclastogenesis and bone loss by human autoantibodies against citrullinated vimentin. J Clin Invest 2012;122:1791–802.
19. Engdahl C, Bang H, Dietel K, Lang SC, Harre U, Schett G. Periarticular bone loss in arthritis is induced by autoantibodies against citrullinated vimentin. J Bone Miner Res 2017;32:1681–91.
20. Stemmler F, Simon D, Liphardt AM, Englbrecht M, Rech J, Hueber AJ, et al. Biomechanical properties of bone are impaired in patients with ACPA-positive rheumatoid arthritis and associated with the occurrence of fractures. Ann Rheum Dis 2018;77:973–80.
21. Kleyer A, Finzel S, Rech J, Manger B, Krieter M, Faustini F, et al. Bone loss before the clinical onset of rheumatoid arthritis in subjects with anticitrullinated protein antibodies. Ann Rheum Dis 2014;73:854–60.
22. Werner D, Simon D, Englbrecht M, Stemmler F, Simon C, Berlin A, et al. Early changes of the cortical micro-channel system in the bare area of the joints of patients with rheumatoid arthritis. Arthritis Rheumatol 2017;69:1580–7.
23. Aletaha D, Neogi T, Silman AJ, Funovits J, Felson DT, Bingham CO III, et al. 2010 rheumatoid arthritis classification criteria: an American College of Rheumatology/European League Against Rheumatism collaborative initiative. Arthritis Rheum 2010;62:2569–81.
24. Nagaraj S, Finzel S, Stok KS, Barnabe C, on behalf of the SPECTRA Collaboration. High-resolution peripheral quantitative computed tomography imaging in the assessment of periarticular bone of metacarpophalangeal and wrist joints [review]. J Rheumatol 2016;43:1921–34.
25. Grueneboom A, Hawwari I, Weidner D, Culemann S, Müller S, Henneberg S, et al. A network of trans-cortical capillaries forms the mainstay for blood circulation in long bones. Nat Metab 2019;1:236–50.
26. Scharmga A, Keller KK, Peters M, van Tubergen A, van den Bergh JP, van Rietbergen B, et al. Vascular channels in metacarpophalangeal joints: a comparative histologic and high-resolution imaging study. Sci Rep 2017;7:8966.
27. Schett G. Autoimmunity as a trigger for structural bone damage in rheumatoid arthritis. Mod Rheumatol 2017;27:193–7.
28. Van Schaardenburg D, Nielen MM, Lems WF, Twisk JW, Reesink HW, van de Stadt RJ, et al. Bone metabolism is altered in preclinical rheumatoid arthritis. Ann Rheum Dis 2011;70:1173–4.
29. Deval E, Lingueglia E. Acid-sensing ion channels and nociception in the peripheral and central nervous systems. Neuropharmacology 2015;94:49–57.
30. Harre U, Lang SC, Pfeifle R, Rombouts Y, Frühbeißer S, Amara K, et al. Glycosylation of immunoglobulin G determines osteoclast differentiation and bone loss. Nat Commun 2015;6:6651.
31. Wigerblad G, Bas DB, Fernades-Cerqueira C, Krishnamurthy A, Nandakumar KS, Rogoz K, et al. Autoantibodies to citrullinated proteins induce joint pain independent of inflammation via a chemokine-dependent mechanism. Ann Rheum Dis 2016;75:730–8.
32. Krishnamurthy A, Joshua V, Haj Hensvold A, Jin T, Sun M, Vivar N, et al. Identification of a novel chemokine-dependent molecular mechanism underlying rheumatoid arthritis-associated autoantibody-mediated bone loss. Ann Rheum Dis 2016;75:721–9.
33. Holmdahl R. The specificity of monoclonal anti–citrullinated protein antibodies: comment on the article by Steen et al. Arthritis Rheumatol 2019;71:324–5.
34. Kopesky P, Tiedemann K, Alkekhia D, Zechner C, Millard B, Schoeberl B, et al. Autocrine signaling is a key regulatory element during osteoclastogenesis. Biol Open 2014;3:767–76.
35. Li H, Hong S, Qian J, Zheng Y, Yang J, Yi Q. Cross talk between the bone and immune systems: osteoclasts function as antigen-presenting cells and activate CD4+ and CD8+ T cells. Blood 2010;116:210–7.
36. Takeuchi T, Tanaka Y, Ishiguro N, Yamanaka H, Yoneda T, Ohira T, et al. Effect of denosumab on Japanese patients with rheumatoid arthritis: a dose-response study of AMG 162 (Denosumab) in patients with RheumatoId arthritis on methotrexate to Validate inhibitory effect on bone Erosion (DRIVE)-a 12-month, multicentre, randomised, double-blind, placebo-controlled, phase II clinical trial. Ann Rheum Dis 2016;75:983–90

Arthritis & Rheumatology
Vol. 74, No. 3, March 2022, pp 427–440
DOI 10.1002/art.41963

American College of Rheumatology
Empowering Rheumatology Professionals

Attenuation of Rheumatoid Arthritis Through the Inhibition of Tumor Necrosis Factor–Induced Caspase 3/Gasdermin E–Mediated Pyroptosis

Zeqing Zhai, Fangyuan Yang, Wenchao Xu, Jiaochan Han, Guihu Luo, Yehao Li, Jian Zhuang, Hongyu Jie, Xing Li, Xingliang Shi, Xinai Han, Xiaoqing Luo, Rui Song, Yonghong Chen, Jianheng Liang, Shufan Wu, Yi He, and Erwei Sun

Objective. To determine the role of gasdermin E (GSDME)–mediated pyroptosis in the pathogenesis and progression of rheumatoid arthritis (RA), and to explore the potential of GSDME as a therapeutic target in RA.

Methods. The expression and activation of caspase 3 and GSDME in the synovium, macrophages, and monocytes of RA patients were determined by immunohistochemistry, immunofluorescence, and Western blot analysis. The correlation of activated GSDME with RA disease activity was evaluated. The pyroptotic ability of monocytes from RA patients was tested, and the effect of tumor necrosis factor (TNF) on caspase 3/GSDME-mediated pyroptosis of monocytes and macrophages was investigated. In addition, collagen-induced arthritis (CIA) was induced in mice lacking *Gsdme*, and the incidence and severity of arthritis were assessed.

Results. Compared to cells from healthy controls, monocytes and synovial macrophages from RA patients showed increased expression of activated caspase 3, GSDME, and the N-terminal fragment of GSDME (GSDME-N). The expression of GSDME-N in monocytes from RA patients correlated positively with disease activity. Monocytes from RA patients with higher GSDME levels were more susceptible to pyroptosis. Furthermore, TNF induced pyroptosis in monocytes and macrophages by activating the caspase 3/GSDME pathway. The use of a caspase 3 inhibitor and silencing of *GSDME* significantly blocked TNF-induced pyroptosis. *Gsdme* deficiency effectively alleviated arthritis in a mouse model of CIA.

Conclusion. These results support the notion of a pathogenic role of GSDME in RA and provide an alternative mechanism for RA pathogenesis involving TNF, which activates GSDME-mediated pyroptosis of monocytes and macrophages in RA. In addition, targeting GSDME might be a potential therapeutic approach for RA.

INTRODUCTION

Rheumatoid arthritis (RA) is an autoimmune disease characterized by persistent synovitis, systemic inflammation, cartilage loss, and bone erosion, eventually resulting in disability and decreased quality of life (1). A prominent feature of RA is persistent inflammation (2). Identification of specific molecules and their roles in inflammation is important for understanding the pathogenesis of RA and for developing novel therapies.

Pyroptosis is a gasdermin-mediated proinflammatory form of programmed cell death, characterized by cell swelling, large bubble blowing from the membrane, and eventual cell rupture, followed by the release of inflammatory cytokines and danger signals (3). After cleavage of full-length gasdermin proteins, their

Supported by grants from the National Natural Science Foundation of China (81873880 and 81671623), Science and Technology Planning Project of Guangdong Province, China (2014B020212024), Guangdong Natural Science Foundation (2019A1515012113), Guangzhou Science and Technology Program Project (202002030342), and the President's Foundation of The Third Affiliated Hospital of Southern Medical University, Guangzhou, China (QN2020006).

Zeqing Zhai, MD, PhD, Fangyuan Yang, MD, PhD, Wenchao Xu, MD, Jiaochan Han, MD, PhD, Guihu Luo, MD, PhD, Yehao Li, MD, Jian Zhuang, MD, PhD, Hongyu Jie, MD, PhD, Xing Li, MD, PhD, Xingliang Shi, MD, Xinai Han, MD, PhD, Xiaoqing Luo, MD, Rui Song, MD, Yonghong Chen, BS, Jianheng Liang, MD, Shufan Wu, BS, Yi He, MD, PhD, Erwei Sun, MD, PhD: The Third Affiliated Hospital, Southern Medical University, and Guangdong Provincial Key Laboratory of Bone and Joint Degeneration Diseases, Guangzhou, China.

Drs. Zhai, Yang, and Xu contributed equally to this work.

Author disclosures are available at https://onlinelibrary.wiley.com/action/downloadSupplement?doi=10.1002%2Fart.41963&file=art41963-sup-0001-Disclosureform.pdf.

Address correspondence to Yi He, MD, PhD, or Erwei Sun, MD, PhD, Department of Rheumatology and Immunology, The Third Affiliated Hospital, Southern Medical University, Number 183, Zhongshan Avenue West, Tianhe District, Guangzhou 510630, China. Email: heyi1983@smu.edu.cn or sunew@smu.edu.cn.

Submitted for publication January 28, 2021; accepted in revised form August 31, 2021.

N-terminal fragments are released, which oligomerize and insert into the cell membrane, forming pores (4,5). The best understood member of the gasdermin family, gasdermin D (GSDMD), can be cleaved by caspases 1, 4/5, 8, and 11, resulting in the induction of pyroptosis and release of proinflammatory cytokines, such as interleukin-1β (IL-1β) and IL-18 (6–10).

Similar to GSDMD, GSDME is specifically cleaved by caspase 3, which results in the production of pore-forming N-terminal fragments of GSDME (GSDME-N) (11). Caspase 3 generally induces apoptosis in GSDME-negative cells and initiates pyroptosis in cells with high levels of GSDME, converting the non-inflammatory apoptosis-inducing machinery to proinflammatory pyroptosis programming in these cells (12–15). Currently, our understanding of the role of GSDME-mediated pyroptosis is limited to chemotherapy-induced cell death and cancer therapy (11,16–20). Owing to the highly proinflammatory character of pyroptotic cells, we speculated that GSDME-mediated pyroptosis plays a critical role in triggering immunity and in driving the pathogenesis of inflammatory and autoimmune diseases. However, whether GSDME-mediated pyroptosis contributes to the pathogenesis and progression of autoimmune diseases, including RA, remains unknown.

Tumor necrosis factor (TNF) is abundant in the circulation as well as in the synovial fluid and tissues of RA patients (21). It plays a key role in sustained synovial inflammation by enhancing the production of inflammatory cytokines, such as IL-6, and by inducing NF-κB activation and metalloproteinase production (22). Moreover, TNF inhibits bone formation and accelerates bone absorption (23). Excessive production of TNF is associated with the development of RA (24). TNF inhibitors, including monoclonal antibodies and fusion proteins, are the most commonly recommended clinical treatments for RA (25,26). TNF is a strong inducer of apoptosis, owing to its ability to activate caspase 3 (27,28). Activated caspase 3 reportedly cleaves and activates GSDME, which results in pyroptosis in GSDME-expressing cells. In this context, an important question related to RA pathogenesis arises as to whether the abundance of TNF in patients with RA induces pyroptosis in GSDME-expressing cells by activating the caspase 3/GSDME pathway, and thereby, promotes systemic and joint inflammation.

To answer this question, we first tested the expression and activation of caspase 3/GSDME in synovial macrophages and circulating monocytes from RA patients. Second, we investigated whether TNF induced GSDME-mediated pyroptosis in monocyte/macrophages. Finally, we used *Gsdme*$^{-/-}$ mice in a collagen-induced arthritis (CIA) model to further assess the role of GSDME in the pathogenesis of RA. We found that in RA patients, TNF induces the activation of caspase 3/GSDME and initiates pyroptosis in monocytes and macrophages. We also identified a critical role of GSDME-mediated pyroptosis in the pathogenesis and progression of RA.

PATIENTS AND METHODS

Patients and healthy controls. The study was approved by the Ethics Committee of the Third Affiliated Hospital of Southern Medical University (approval number 201608003). Fifty-eight RA patients who met the American College of Rheumatology (ACR) 1987 revised classification criteria for RA (29) or the ACR/European Alliance of Associations for Rheumatology 2010 classification criteria (30) were recruited from the Department of Rheumatology and Immunology at The Third Affiliated Hospital of Southern Medical University between January 2018 and April 2021. All participants provided written informed consent. The clinical characteristics of the RA patients are listed in Supplementary Table 1, available on the *Arthritis & Rheumatology* website at https://onlinelibrary.wiley.com/doi/10.1002/art.41963.

Human synovial tissue samples were obtained from patients with osteoarthritis (OA; n = 7) or RA (n = 7) who had undergone knee replacement surgery. Tissue samples with suspected articular infections were excluded. For in vitro experiments, monocytes were purified from peripheral blood mononuclear cells (PBMCs) from healthy controls (n = 17) and RA patients (n = 58). Patients with RA complicated by severe infection, malignancy, or neurologic disease, and those with other autoimmune diseases, such as myositis, scleroderma, or systemic lupus erythematosus, were excluded. Patients with active RA received combination therapy that included TNF inhibitors. Healthy volunteers and OA patients were recruited as controls.

Cells and reagents. A THP-1 monocyte cell line was purchased from ATCC. In some experiments, macrophages were pretreated with 50 μ*M* Z-DEVD-FMK (a caspase 3 inhibitor) (catalog no. HY-12466; MedChemExpress) and then incubated with a specific medium for further investigation, as indicated below. Cycloheximide (CHX; catalog no. 66-81-9) was purchased from Sigma-Aldrich. All in vitro experiments were repeated at least 3 times.

In vitro isolation of peripheral blood CD14+ monocytes. PBMCs were obtained from fresh whole blood from healthy controls and RA patients and washed twice with phosphate buffered saline (PBS). Peripheral blood monocytes were isolated from PBMCs using an EasySep human monocyte isolation kit (catalog no. 19359; StemCell Technologies) according to the manufacturer's instructions. Purified monocytes were harvested and labeled with PerCP–Cy5.5–conjugated anti-CD14 antibody (BD Biosciences) for flow cytometry (Supplementary Figure 1A, available on the *Arthritis & Rheumatology* website at https://onlinelibrary.wiley.com/doi/10.1002/art.41963). Purified monocytes from healthy controls and RA patients were cultured in RPMI 1640 medium (Gibco) supplemented with 10% fetal bovine serum (FBS; complete 1640 medium) for 4 hours, and then examined by flow cytometric, immunofluorescence, and

Western blot analysis. Lactate dehydrogenase (LDH) release was also measured. In addition, purified monocytes from 8 untreated RA patients and from 7 RA patients after effective treatment were cultured in complete 1640 medium for 4 hours. Finally, Western blot analysis was performed to determine the expression of GSDME-N.

Differentiation of THP-1 cells and bone marrow–derived cells into macrophages. THP-1 monocytes were cultured in RPMI 1640 medium supplemented with 10% FBS (Life Technologies) at 37°C under 5% CO_2. For generation of macrophages, THP-1 cells were incubated with 100 ng/ml phorbol 12-myristate 13-acetate (PMA; Sigma) for 48 hours, which fully induced monocytes to differentiate into adherent macrophages (31) (Supplementary Figure 1B). THP-1 cell–derived macrophages were cultured in complete 1640 medium. The purity of differentiated macrophages was measured by flow cytometry (Supplementary Figure 1C).

Bone marrow cells from the femurs and tibias of C57BL/6 wild-type mice or *Gsdme*$^{-/-}$ mice were induced to differentiate into macrophages. Bone marrow cells were collected in Dulbecco's modified Eagle's medium (DMEM; Gibco) with 10% FBS (complete DMEM) and incubated with 10 ng/ml macrophage colony-stimulating factor (catalog no. 315-02; PeproTech) for 6–7 days to generate bone marrow–derived macrophages (BMMs) (32). Thereafter, murine BMMs were seeded in 24-well plates at 2×10^5 cells/well in 0.5 ml fresh complete DMEM or in 6-well plates at 1.5×10^6 cells/well in 2 ml fresh complete DMEM overnight. For assessment of purity, murine BMMs were labeled with Alexa Fluor 647–conjugated anti-CD11b antibody (BD Biosciences) and phycoerythrin-conjugated anti-F4/80 antibody (BioLegend), and analyzed by flow cytometry (Supplementary Figure 1D).

TNF stimulation of RA monocytes, THP-1 cell–derived macrophages, and murine BMMs. Purified monocytes from each RA patient were divided into 2 parts, seeded in 24-well or 6-well culture plates, and cultured in the presence or absence of human TNF (100 ng/ml) for 24 hours. Immunofluorescence and Western blot analyses were performed to measure cell death and expression of the indicated proteins. THP-1 cell–derived macrophages were seeded in 24-well or 6-well plates and incubated with different concentrations of human TNF (catalog no. 300-01A; PeproTech) for 36 hours. After complete adherence to the walls of the plates, murine BMMs were cultured with different concentrations of murine TNF (catalog no. 315-01A; PeproTech) for 36 hours.

Small interfering RNA (siRNA)–mediated knockdown of *GSDME* in THP-1 cell–derived macrophages. For siRNA-mediated knockdown of *GSDME*, 100 pmoles of 2 specific siRNAs (5′-GCGGTCCTATTTGATGATGAA-3′ and 5′-GATGATGGAGTATCTGATCTT-3′; synthesized by GenePharma) targeting *GSDME* and 1 negative control siRNA (purchased from GenePharma) were used. The siRNAs were transfected into macrophages using Lipofectamine 3000 (Invitrogen). The efficacy of transfection was detected by Western blot analysis and real-time quantitative polymerase chain reaction.

Histologic, immunohistochemical, and immunofluorescence analyses. Human synovial tissue samples were fixed in 4% paraformaldehyde, and serial paraffin sections were stained with hematoxylin and eosin (H&E). Mouse bones were decalcified in 0.5*M* EDTA (pH 7.4) on a shaker for 3 weeks and embedded in paraffin. After deparaffinization and rehydration, serial sections were treated with 200 μg/ml proteinase K (Sigma) for 30 minutes at 37°C or were soaked in citrate buffer (10 m*M* citric acid, pH 6.0) for 16–18 hours at 60°C to unmask the antigen. For immunohistochemical analysis, sections were incubated with 3% hydrogen peroxide for 10 minutes, and then blocked with 1% sheep serum at room temperature for 1 hour. Serial sections were incubated with anti-CD68 (catalog no. 14-0688-82; ThermoFisher), anti-GSDME (catalog no. ab215191; Abcam, and catalog no. PA5-103976; ThermoFisher), anti-cleaved caspase 3 (catalog no. 9661; Cell Signaling Technology), antivimentin (catalog no. sc-373717; Santa Cruz Biotechnology), anti-TNF (catalog no. A11534; ABclonal Technology), anti–IL-1β (catalog no. 12242; Cell Signaling Technology), anti-CD14 (catalog no. 60253-1-Ig; Proteintech, and catalog no. ab181470; Abcam), and anti-F4/80 (catalog no. ab16911; Abcam, and catalog no. sc-377009; Santa Cruz Biotechnology) antibodies overnight at 4°C.

For staining with secondary antibodies, species-matched Alexa Fluor 594–labeled, Alexa Fluor 488–labeled, or horseradish peroxidase (HRP)–labeled antibodies were used (1:400 in 1% bovine serum albumin [BSA] for 1 hour at 37°C). 3,3′-diaminobenzidine was used as a chromogen, and hematoxylin was used as a counterstain in immunohistochemistry. For immunofluorescence staining, DAPI (Thermo) was used to label nuclei.

For immunofluorescence staining, cells were plated on 24-well culture plates with coverslips. After treatment, the medium was aspirated and cells were washed twice with PBS, fixed in 4% paraformaldehyde for 30 minutes, and permeabilized in 0.2% Triton X-100 for 10–20 minutes at room temperature to expose intracellular antigen. Cells were washed with PBS, blocked with 1% BSA for 1 hour, and incubated with primary antibodies, and then treated as described above.

Cell death assays. *Flow cytometry.* Purified monocytes or macrophages were cultured under different conditions. The cells were harvested, washed twice with cold PBS, and stained using an Annexin V–FITC/PI Apoptosis Detection Kit (BD PharMingen), according to the manufacturer's instructions. Cells were then analyzed using a BD FACSAria III flow cytometer. Data were acquired and processed using FlowJo software. Each experiment

was repeated 3 times. Generally, the Annexin V/PI kit is used to detect phosphatidylserine exposed on the external leaflet of the plasma membrane in apoptotic cells. It can also label pyroptotic cells due to membrane rupture, which allows for the recognition of phosphatidylserine on the inner leaflet. Propidium iodide (PI) was used to detect dying cells, according to the manufacturer's instructions.

LDH-based cytotoxicity assay. In vitro, cell death was also detected by an LDH release assay using a CytoTox 96 Non-Radioactive Cytotoxicity Assay kit (catalog no. G1780; Promega), according to the manufacturer's instructions.

Microscopy and PI staining. To morphologically distinguish pyroptotic and apoptotic cells, cells were seeded in 24-well plates, cultured to 40–60% confluency, and then treated as indicated in the figure legends. Lytic cell death was visualized and measured by PI incorporation, as described above. Cells were stained with PI (2 μg/ml; to label necrotic cells) for 10 minutes at room temperature. Nuclei were stained with Hoechst 33342. The cells were then observed and brightfield images were captured using an Olympus microscope. Fluorescent images were captured using a fluorescence microscope and analyzed. All image data displayed are representative of ≥3 randomly selected fields.

Western blot analysis. Western blot analysis was performed to detect protein expression in synovial tissue samples and in in vitro experiments. Synovial tissue samples were frozen and powdered by grinding in liquid nitrogen and then thawed in radioimmunoprecipitation assay buffer supplemented with phenylmethylsulfonyl fluoride. A bicinchoninic acid protein assay kit (Beyotime) was used to quantify the proteins. Samples were separated by sodium dodecyl sulfate–polyacrylamide gel electrophoresis and transferred onto PVDF membranes. Primary antibodies for the following proteins were used for immunodetection: GSDME (catalog no. ab215191; Abcam), activated caspase 3 (catalog no. 9661; Cell Signaling Technology), and β-actin (catalog no. AP071; Bioworld Technology). After washing with Tris buffered saline–Tween, the probed membranes were incubated with HRP-labeled secondary antibodies (HRP-labeled goat anti-rabbit IgG [heavy and light chains] [catalog no. 111-035-003; Jackson ImmunoResearch] and HRP-labeled goat anti-mouse IgG [heavy and light chains] [catalog no. 115-035-003; Jackson ImmunoResearch]) and then visualized with an FDbio-Dura ECL Kit (FD-bio science). Protein expression was analyzed using ImageJ software (National Institutes of Health).

Generation of a mouse model of CIA. Male C57BL/6 wild-type mice were purchased from the Laboratory Animal Center of Southern Medical University. C57BL/6 *Gsdme*-knockout (*Gsdme*$^{-/-}$) mice were generated by CRISPR/Cas-mediated genome engineering (Cyagen Bioscience). CIA was induced in 8-week-old male wild-type and *Gsdme*$^{-/-}$ mice. Chicken type II collagen (catalog no. 20012; Chondrex) was dissolved in 0.05*M* acetic acid (final concentration 2 mg/ml) and then emulsified with Freund's complete adjuvant (CFA) containing heat-killed *Mycobacterium tuberculosis* H37RA (Chondrex). C57BL/6 mice were injected intradermally with a 100-μl emulsion at the base of tail on days 1 and 21 (33). Clinical assessment of CIA was performed daily for each limb as previously described (34).

CIA was generated in DBA/1J mice as previously described (35). Eight-week-old male DBA/1J mice were immunized with 100 mg bovine type II collagen (2 mg/ml; Chondrex) emulsified 1:1 in CFA (containing 1 mg/ml *M tuberculosis*; Chondrex) on day 1 and then injected with Freund's incomplete adjuvant (Chondrex) on day 21.

All animals were maintained under specific pathogen–free conditions in the Laboratory Animal Center of Southern Medical University. The protocols for animal experimentation were approved by the Southern Medical University Experimental Animal Ethics Committee (no. 00171035 and no. 00181785).

Quantitation of inflammatory cytokines. The plasma levels of cytokines in mice were measured with commercially available enzyme-linked immunosorbent assay kits for IL-1β (JM-02323M2), IL-6 (JM-02446M2), and TNF (JM-02415M2).

Statistical analysis. Graphs were prepared and statistical data were analyzed using GraphPad software version 8.4 and IBM SPSS Statistics 25 software. Arthritis scores in mice were compared using the nonparametric Mann–Whitney U test. Data were compared between various groups by one-way analysis of variance, Student's *t*-test, or chi-square test. Spearman's correlation analysis was used to evaluate correlations of the data. *P* values less than 0.05 were considered significant.

RESULTS

Elevated expression and activation of GSDME in synovial macrophages from RA patients. Persistent synovitis is a hallmark of RA. Consistently, we noted infiltration of inflammatory cells into the synovial tissue (Figure 1A). To assess the expression of GSDME, synovial tissue specimens were collected from RA patients and sex-matched OA patients undergoing surgery. By immunohistochemical analysis, we first demonstrated higher expression of GSDME in synovial tissue samples from RA patients than in those from OA patients (Figure 1B and Supplementary Figure 2, available on the *Arthritis & Rheumatology* website at https://onlinelibrary.wiley.com/doi/10.1002/art.41963). We further verified that the expression of GSDME-N was higher in synovial tissue samples from RA patients than in synovial tissue samples from OA patients (Figure 1C). The increased expression of GSDME-N in synovial tissue samples from RA patients led us to presume that caspase 3, which specifically cleaves GSDME,

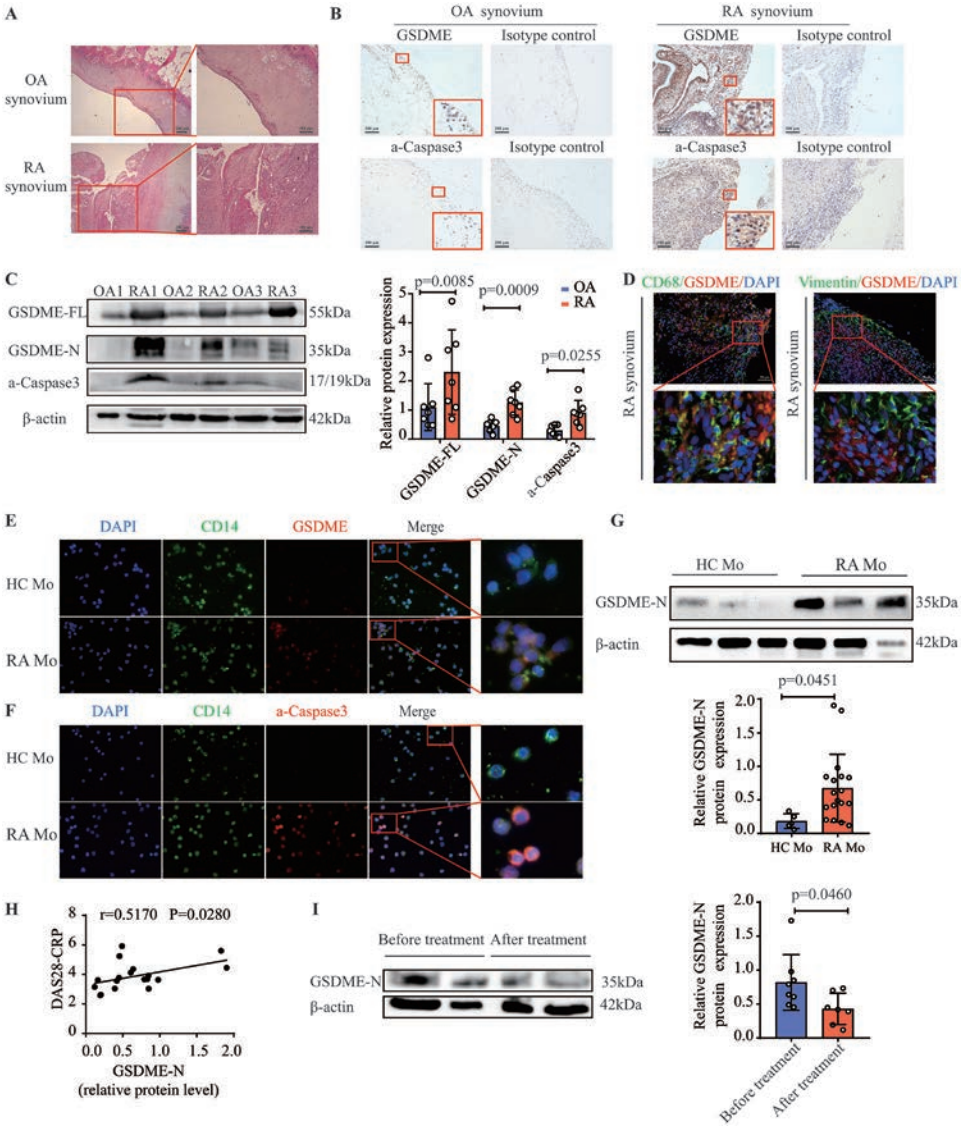

Figure 1. Increased expression and activation of gasdermin E (GSDME) in synovial macrophages and CD14+ monocytes from patients with rheumatoid arthritis (RA), and positive correlation of GSDME level with RA disease activity. **A**, Representative images of hematoxylin and eosin–stained synovial tissue samples from patients with osteoarthritis (OA) and patients with RA. Right panels show higher-magnification views (bars = 100 μm) of the boxed areas in the left panels (bars = 200 μm). **B**, Representative immunohistochemistry images of GSDME and activated caspase 3 (a-caspase 3) expression in synovial tissue samples from OA patients (n = 7) and RA patients (n = 7). Lower boxed areas show higher-magnification views (original magnification × 400) of the upper boxed areas (original magnification × 100). **C**, Western blot (left) and quantification (right) of the expression of full-length GSDME (GSDME-FL), the N-terminal fragment of GSDME (GSDME-N), and activated caspase 3 in synovial tissue samples from OA patients (n = 7) and RA patients (n = 7). **D**, Immunofluorescence images showing the expression of GSDME in CD68-positive synovial macrophages and vimentin-positive fibroblasts in synovial tissue samples from RA patients (n = 7). Bottom panels show higher-magnification views (original magnification × 800) of the boxed areas in the top panels (bars = 50 μm). **E** and **F**, Representative images of immunostaining for DAPI, CD14, GSDME, and activated caspase 3 in peripheral blood monocytes (Mo) from healthy controls (HCs) and RA patients. For the merged images, right panels show higher-magnification views (original magnification × 1600) of the boxed areas in the left panels (original magnification × 400). **G**, Western blot (top) and quantification (bottom) of GSDME-N expression in peripheral blood monocytes from healthy controls and RA patients. **H**, Correlation of GSDME-N expression, measured by Western blot analysis, in peripheral blood monocytes from RA patients (n = 18) with RA disease activity measured by the Disease Activity Score in 28 joints using the C-reactive protein level (DAS28-CRP). **I**, Western blot (left) and quantification (right) of GSDME-N expression in peripheral blood monocytes from patients with active RA before treatment (n = 8) and after treatment with combination therapy that included tumor necrosis factor inhibitors (n = 7). In **C** and **G**, symbols represent individual subjects; bars show the mean ± SD protein level relative to β-actin.

might also be activated. Indeed, the level of activated caspase 3 was significantly increased in the synovial membrane of RA patients compared to OA patients (Figures 1B and C and Supplementary Figure 3, available on the *Arthritis & Rheumatology* website at https://onlinelibrary.wiley.com/doi/10.1002/art.41963).

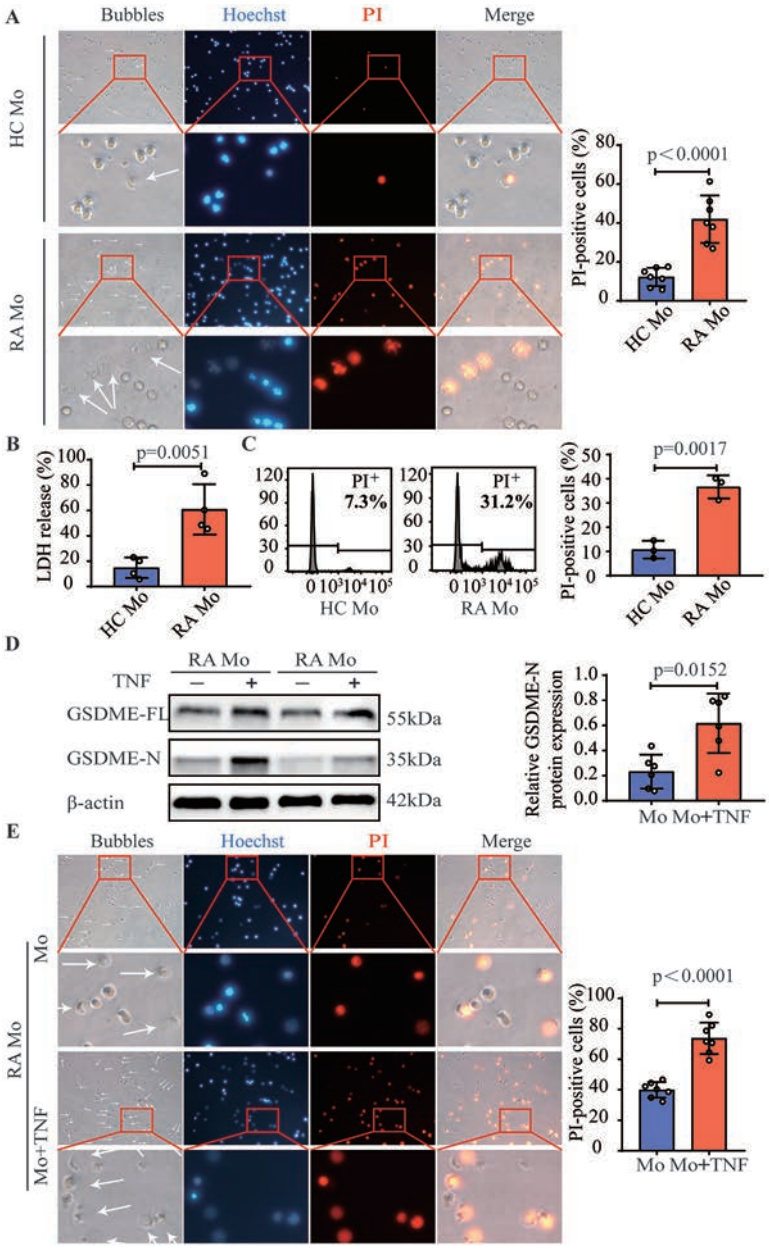

Figure 2. Increased capacity for pyroptosis in GSDME-expressing peripheral blood monocytes from RA patients. CD14+ monocytes were purified from healthy controls and RA patients, and cultured for 4 hours in vitro. **A**, Left, Brightfield and fluorescence microscopy images of peripheral blood monocytes stained with Hoechst and propidium iodide (PI; red) (positive staining indicates lytic cell death). Bottom panels show higher-magnification views (original magnification × 1600) of the boxed areas in the top panels (original magnification × 400). **Arrows** indicate pyroptotic cell bubbles. Right, Percentage of PI-positive cells in 5 randomly chosen fields in peripheral blood monocytes from healthy controls (n = 7) and RA patients (n = 7). **B**, Lactate dehydrogenase (LDH) release from peripheral blood monocytes from healthy controls (n = 4) and RA patients (n = 4). **C**, Flow cytometric analysis (left) and percentage (right) of PI-positive monocytes from healthy controls (n = 3) and RA patients (n = 3). **D**, Western blot of the expression of GSDME-FL and GSDME-N (left) and quantification of the expression of GSDME-N (right) in monocytes from RA patients (n = 6), left untreated or treated with tumor necrosis factor (TNF) for 24 hours. Values are the protein level relative to β-actin. **E**, Left, Phase-contrast and fluorescence microscopy images of RA peripheral blood monocytes stained with Hoechst (blue) and PI (red). Phase-contrast microscopy and PI staining images were merged. Bottom panels show higher-magnification views (original magnification × 1600) of the boxed areas in the top panels (original magnification × 400). **Arrows** indicate pyroptotic cell bubbles. Right, Percentage of PI-positive cells among untreated RA monocytes (n = 7) and RA monocytes treated with TNF (n = 7). Symbols represent individual subjects; bars show the mean ± SD. See Figure 1 for other definitions. Color figure can be viewed in the online issue, which is available at http://onlinelibrary.wiley.com/doi/10.1002/art.41963/abstract.

Next, we determined the expression of GSDME in synovial macrophages and fibroblasts, the 2 major cell populations in the synovium of RA patients, by immunofluorescence. The expression of GSDME was elevated in synovial macrophages but not in synovial fibroblasts (Figure 1D and Supplementary Figures 4 and 5, available on the *Arthritis & Rheumatology* website at https://onlinelibrary.wiley.com/doi/10.1002/art.41963).

Strong correlation between GSDME-N expression in RA peripheral blood monocytes and RA disease activity. Similar to synovial macrophages, we found higher expression of GSDME and GSDME-N in peripheral blood monocytes from RA patients than in those from healthy controls (Figures 1E and G and Supplementary Figure 6, available on the *Arthritis & Rheumatology* website at https://onlinelibrary.wiley.com/doi/10.1002/art.41963). Activated caspase 3 was consistently up-regulated in peripheral blood monocytes from RA patients (Figure 1F and Supplementary Figure 7, available on the *Arthritis & Rheumatology* website at https://onlinelibrary.wiley.com/doi/10.1002/art.41963). Interestingly, the expression of GSDME-N correlated positively with the Disease Activity Score in 28 joints using the C-reactive protein level (36) in RA patients (Figure 1H). Moreover, the expression of GSDME-N was significantly reduced in RA patients after combination therapy that included TNF inhibitors (Figure 1I). These data suggest that GSDME is involved in the pathogenesis and progression of RA.

Propensity for pyroptosis in RA monocytes with higher GSDME expression. Given the high expression of GSDME in peripheral blood monocytes from RA patients, we purified peripheral blood monocytes from healthy controls and RA patients to further investigate pyroptosis in RA peripheral blood monocytes. After incubation in RPMI 1640 medium for 4 hours, peripheral blood monocytes from RA patients exhibited typical cell swelling and large bubble blowing from the plasma membrane (Figure 2A). Using fluorescence microscopy, increased numbers of PI-positive cells were also observed in peripheral blood monocytes from RA patients compared to healthy controls (Figure 2A and Supplementary Figure 8, available on the *Arthritis & Rheumatology* website at https://onlinelibrary.wiley.com/doi/10.1002/art.41963). Moreover, LDH release was notably increased in the RA monocyte supernatant (Figure 2B). Flow cytometry revealed a higher percentage of PI-positive cells among peripheral blood monocytes from RA patients than in those from healthy controls (Figure 2C). These results indicate that peripheral blood monocytes from RA patients are prone to spontaneous GSDME-mediated pyroptosis.

Similar to previous studies, we found high TNF expression in synovial tissue samples from RA patients (21) (Supplementary Figure 9, available on the *Arthritis & Rheumatology* website at https://onlinelibrary.wiley.com/doi/10.1002/art.41963). To determine whether TNF induced GSDME-mediated pyroptosis, we isolated peripheral blood monocytes from RA patients and treated them with TNF. As expected, TNF dramatically increased the expression of GSDME-N in peripheral blood monocytes from RA patients (Figure 2D), and simultaneously increased the induction of pyroptosis, characterized by typical morphologic changes and PI staining (Figure 2E and Supplementary Figure 10, available on the *Arthritis & Rheumatology* website at https://onlinelibrary.wiley.com/doi/10.1002/art.41963). Taken together, these results indicate that TNF alone induces pyroptosis in peripheral blood monocytes from RA patients.

TNF induction of the expression of caspase 3/GSDME and pyroptosis in macrophages. To examine whether TNF triggers caspase 3/GSDME-mediated pyroptosis in macrophages, we incubated THP-1 cells with PMA to induce differentiation into macrophages. We considered TNF + CHX treatment to be a positive control because it induces the activation of GSDME and results in pyroptosis. TNF + CHX dramatically enhanced the expression of activated caspase 3 and GSDME-N, and induced pyroptosis in THP-1 cell–derived macrophages (Figure 3).

Interestingly, when THP-1 cell–derived macrophages were cultured in the presence of different concentrations of TNF for 36 hours, TNF alone also increased the expression of activated caspase 3, GSDME, and GSDME-N in a concentration-dependent manner (Figure 3A and Supplementary Figures 11A and B, available on the *Arthritis & Rheumatology* website at https://onlinelibrary.wiley.com/doi/10.1002/art.41963). In parallel, cell swelling and large bubble blowing were significantly evident after TNF treatment (Figure 3B). The number of PI-positive cells was increased after stimulation with TNF, as demonstrated by fluorescence microscopy and flow cytometry (Figures 3B and D). Moreover, TNF treatment resulted in an increased release of LDH (Figure 3C). To determine whether TNF had the same effect on pyroptosis in mouse macrophages, we generated BMMs from C57BL/6 mice. TNF induced pyroptosis in mouse BMMs, characterized by increased expression of GSDME-FL and GSDME-N and an increased number of PI-positive cells. These results suggest that TNF, a key factor in the pathogenesis of RA, promotes the induction of macrophage pyroptosis by activating the caspase 3/GSDME pathway.

Reduction of TNF-induced macrophage pyroptosis upon inhibition of the caspase 3/GSDME pathway. To further verify the role of caspase 3 in TNF-induced macrophage pyroptosis, THP-1 cell–derived macrophages were pretreated with a caspase 3–specific inhibitor (Z-DEVD-FMK) for 1 hour, followed by treatment with TNF for 36 hours. Z-DEVD-FMK treatment decreased the expression of activated caspase 3, GSDME, and GSDME-N in macrophages treated with TNF (Figures 4A and 4B). Similarly, Z-DEVD-FMK reduced the induction of pyroptosis by TNF in THP-1 cell–derived macrophages (Figures 4C and 4D).

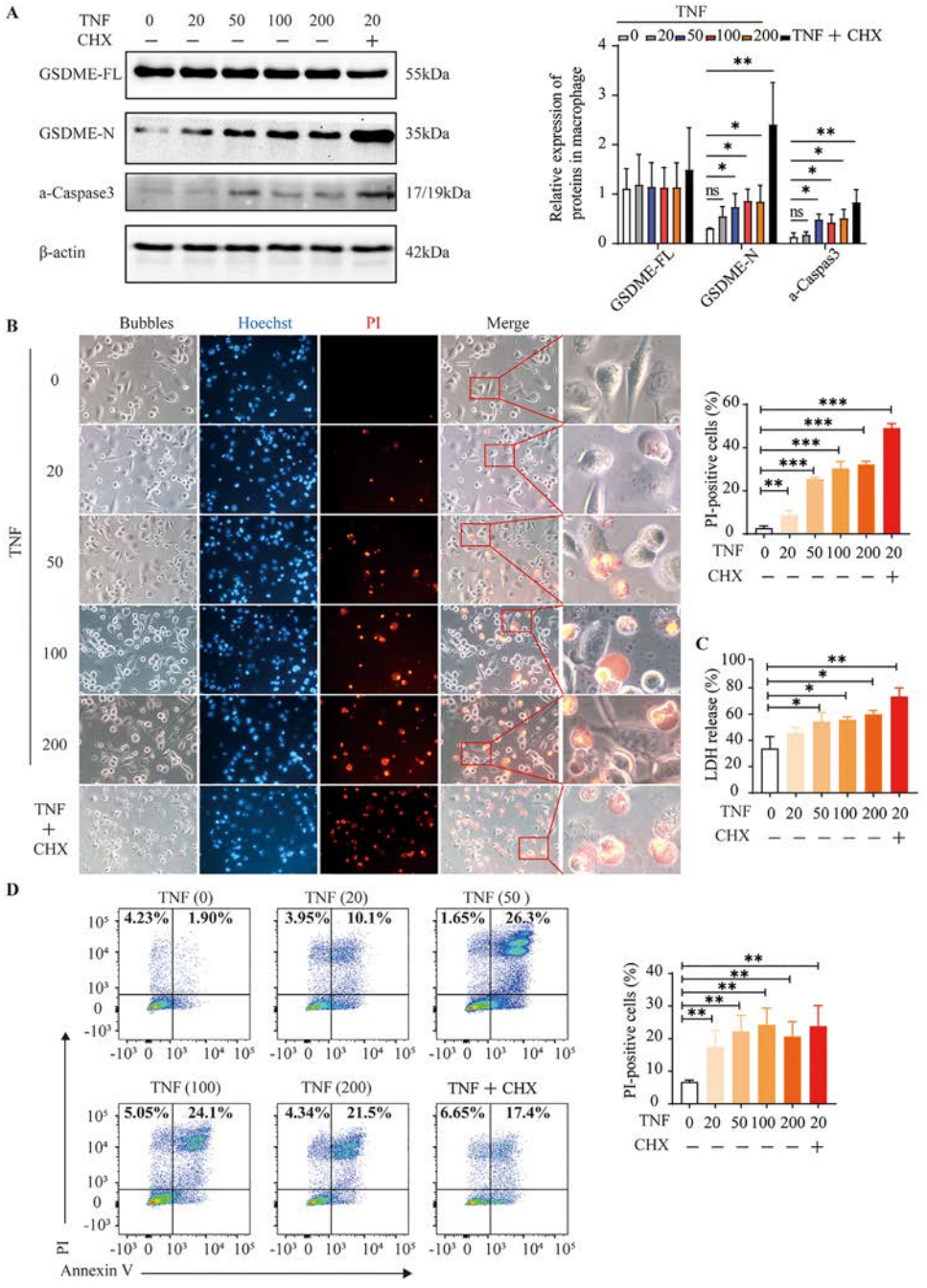

Figure 3. Tumor necrosis factor (TNF) induction of pyroptosis of macrophages through activation of the caspase 3/GSDME pathway in vitro. THP-1 cell–derived macrophages were seeded in 24-well or 6-well plates and incubated with different concentrations of TNF (ng/ml) for 36 hours or TNF and cycloheximide (CHX) (10 μg/ml; positive control) for 24 hours. **A**, Western blot (left) and quantification (right) of GSDME-FL, GSDME-N, and activated caspase 3 expression in macrophage lysates treated as indicated. Values are the protein level relative to β-actin. **B**, Left, Phase-contrast and fluorescence microscopy images of macrophages treated as indicated and stained with Hoechst (blue) and propidium iodide (PI; red). For the merged images, right panels show higher-magnification views (original magnification × 1600) of the boxed areas in the left panels (original magnification × 400). Right, Percentage of PI-positive cells. **C**, Lactate dehydrogenase (LDH) release from macrophages treated as indicated. **D**, Flow cytometric analysis of cells stained with annexin V/PI to determine cell death (left) and percentage of PI-positive cells (right) among macrophages treated as indicated. Data are representative of 3 independent experiments. Bars show the mean ± SD. * = $P < 0.05$; ** = $P < 0.01$; *** = $P < 0.001$. NS = not significant (see Figure 1 for other definitions). Color figure can be viewed in the online issue, which is available at http://onlinelibrary.wiley.com/doi/10.1002/art.41963/abstract.

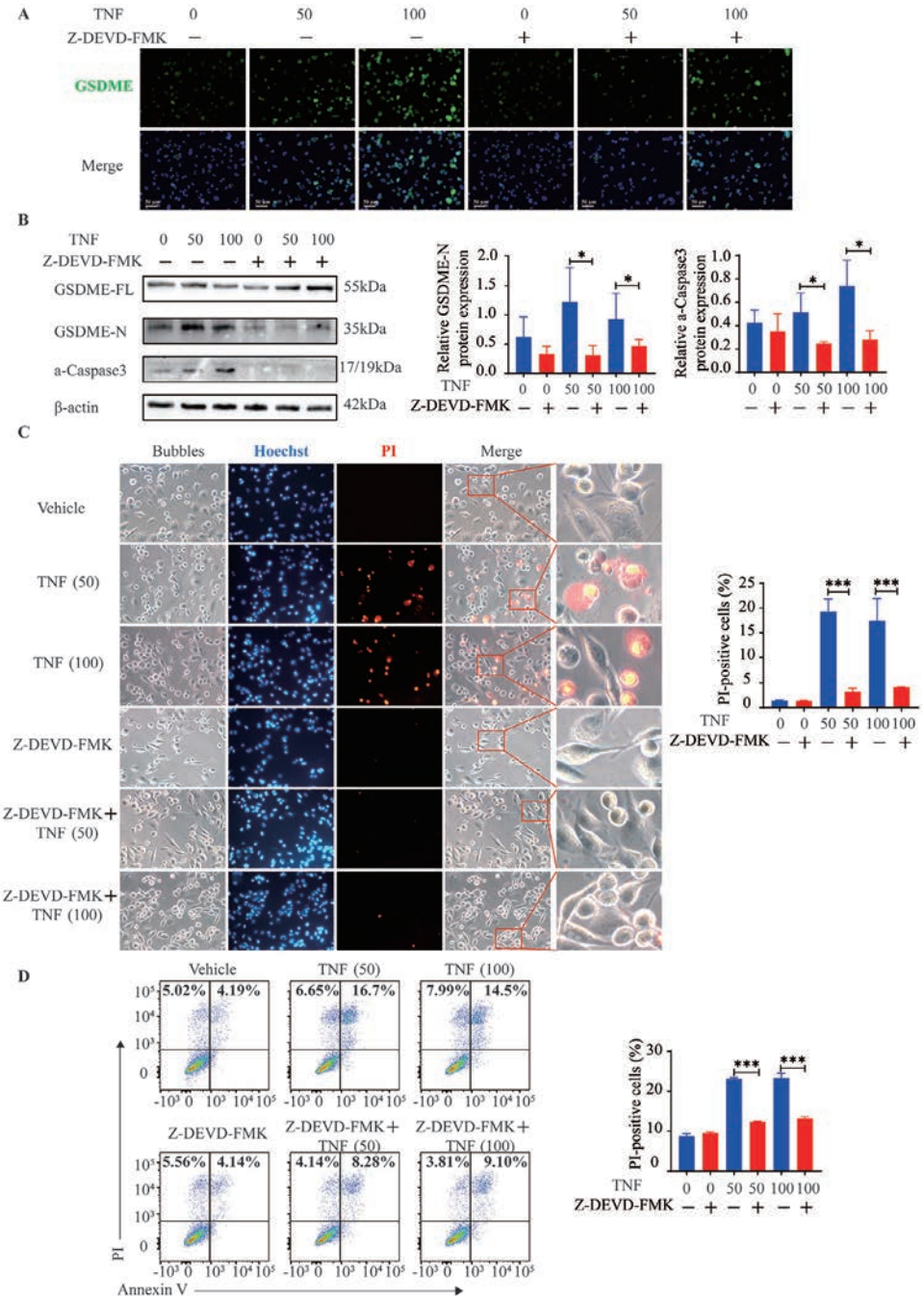

Figure 4. Reduction of tumor necrosis factor (TNF)–induced GSDME-mediated macrophage pyroptosis by the caspase 3–specific inhibitor Z-DEVD-FMK. After treatment with Z-DEVD-FMK for 1 hour, THP-1 cell–derived macrophages were exposed to 50 or 100 ng/ml TNF. **A**, Representative immunofluorescence microscopy images showing the expression of GSDME in macrophages treated as indicated. Bars = 50 μm. **B**, Western blot of GSMDE-FL, GSDME-N, and activated caspase 3 expression (left), quantification of GSDME-N expression (middle), and quantification of activated caspase 3 expression (right) in lysates of macrophages treated as indicated. Values are the protein level relative to β-actin **C**, Left, Representative fluorescence microscopy and brightfield images of macrophages treated as indicated and stained with propidium iodide (PI; red). Nuclei were counterstained with Hoechst (blue). For the merged images, the right panels show higher-magnification views (original magnification × 1600) of the boxed areas in the left panels (original magnification × 400). Right, Percentage of PI-positive cells. **D**, Left, Flow cytometric analysis of cells treated as indicated and stained with annexin V/PI. Data are representative of 3 independent experiments. Right, Percentage of PI-positive cells. In **B**, **C**, and **D**, bars show the mean ± SD. * = $P < 0.05$; *** = $P < 0.001$. See Figure 1 for other definitions. Color figure can be viewed in the online issue, which is available at http://onlinelibrary.wiley.com/doi/10.1002/art.41963/abstract.

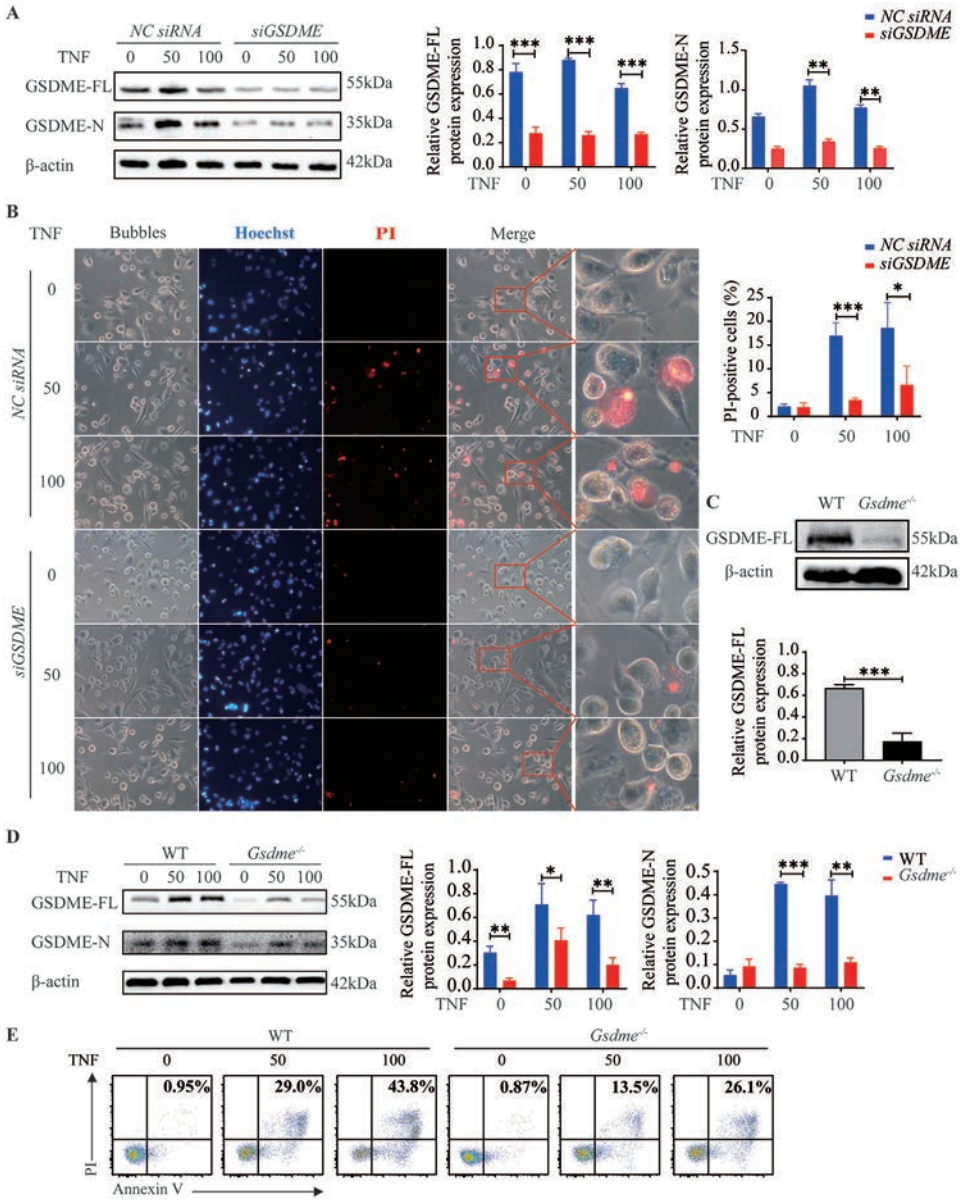

Figure 5. Inhibition of tumor necrosis factor (TNF)–induced pyroptosis in macrophages by *GSDME* silencing. **A** and **B**, After transfection with *GSDME* or negative control (NC) small interfering RNAs (siRNAs) for 48 hours, THP-1 cell–derived macrophages were left untreated or treated with 50 or 100 ng/ml TNF for the indicated times. **A**, Western blot of GSDME-FL and GSDME-N expression (left), quantification of GSDME-FL expression (middle), and quantification of GSDME-N expression (right) in macrophages treated as indicated for 36 hours after the silencing of *GSDME*. Values are the protein level relative to β-actin. **B**, Left, Representative brightfield and fluorescence microscopy images showing the morphology of macrophages treated as indicated after the silencing of *GSDME*. For the merged images, right panels show higher-magnification views (original magnification × 1600) of the boxed areas in the left panels (original magnification × 400). Right, Percentage of propidium iodide (PI)–positive cells. **C**, Western blot (top) and quantification (bottom) of GSDME-FL expression in wild-type (WT) and *Gsdme*$^{-/-}$ mice, showing the efficiency of *Gsdme* knockout. Values are the protein level relative to β-actin. **D**, Western blot of GSDME-FL and GSDME-N expression (left), quantification of GSDME-FL expression (middle), and quantification of GSDME-N expression (right) in lysates of bone marrow–derived macrophages (BMMs) from WT and *Gsdme*$^{-/-}$ mice, cultured with the indicated concentrations of TNF for 36 hours. Values are the protein level relative to β-actin. **E**, Flow cytometric analysis of murine BMMs treated as indicated and stained with annexin V/PI. In **A**, **B**, and **D**, bars show the mean ± SD. * = $P < 0.05$; ** = $P < 0.01$; *** = $P < 0.001$. See Figure 1 for other definitions. Color figure can be viewed in the online issue, which is available at http://onlinelibrary.wiley.com/doi/10.1002/art.41963/abstract.

We successfully silenced *GSDME* with siRNAs in THP-1 cell–derived macrophages and then examined TNF-induced pyroptosis in these cells (Supplementary Figures 12A and B, available on the *Arthritis & Rheumatology* website at https://onlinelibrary.wiley.com/doi/10.1002/art.41963). The silencing resulted in decreased expression of GSDME-N (Figure 5A) and reduction in

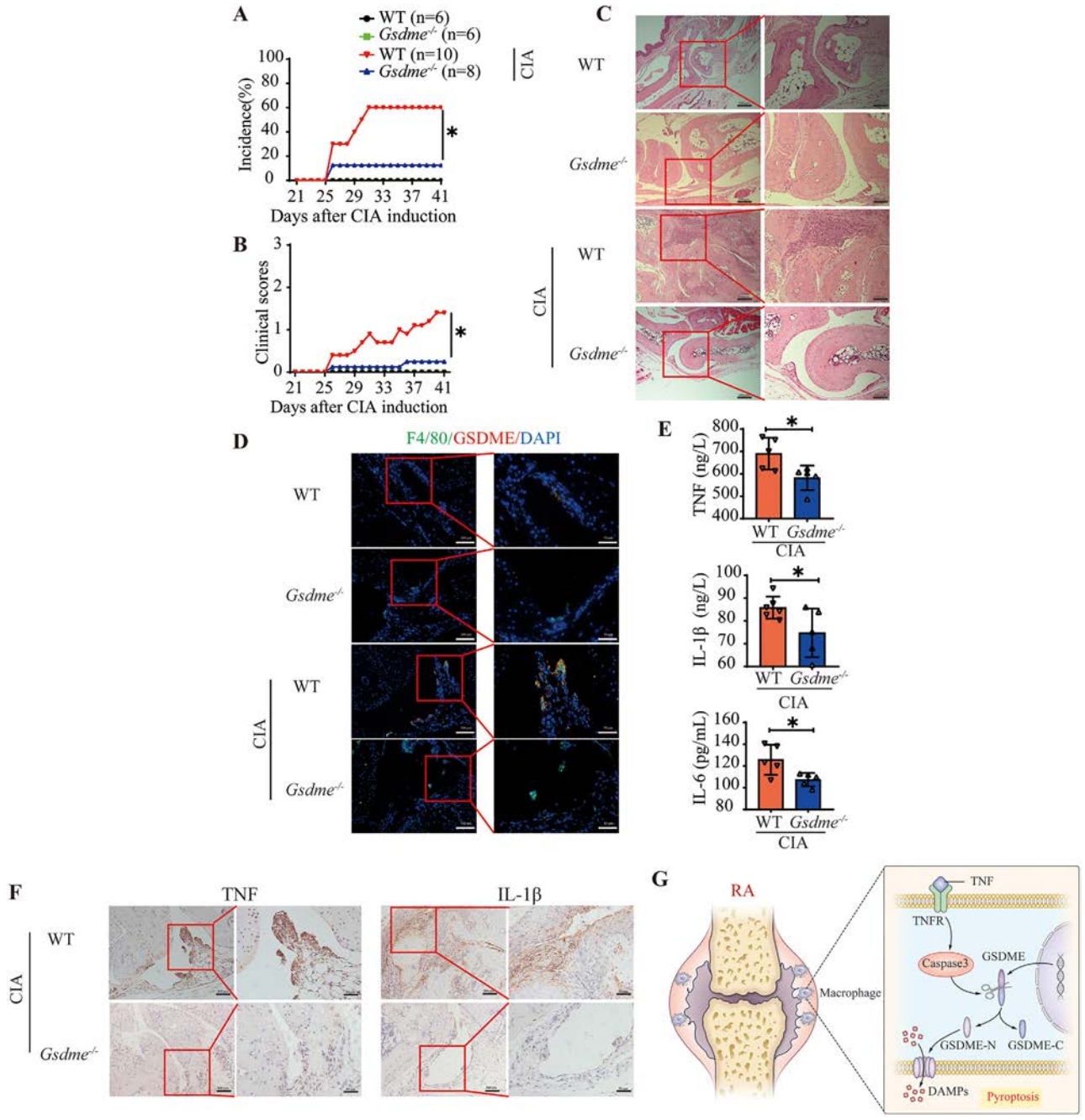

Figure 6. Decreased arthritis incidence, clinical scores, and synovial inflammation in *Gsdme*-deficient mice with collagen-induced arthritis (CIA) compared to wild-type (WT) mice with CIA. Male WT C57BL/6 mice (n = 10) and *Gsdme*$^{-/-}$ mice (n = 8) were immunized with chicken type II collagen emulsified in Freund's complete adjuvant on days 0 and 21 for CIA induction. Mice of the same background without CIA were used as controls (n = 6 WT and 6 *Gsdme*$^{-/-}$ mice). **A** and **B**, Arthritis incidence (**A**) and clinical scores (**B**) in the indicated mouse groups. **C**, Hematoxylin and eosin–stained joint sections from WT and *Gsdme*$^{-/-}$ mice. Right panels show higher-magnification views (bars = 100 μm) of the boxed areas in the left panels (bars = 200 μm). **D**, Immunofluorescence images showing the expression of gasdermin E (GSDME) in F4/80-positive synovial macrophages from WT and *Gsdme*$^{-/-}$ mice. Right panels show higher-magnification views (bars = 50 μm) of the boxed areas in the left panels (bars = 100 μm). **E**, Plasma concentrations of the cytokines tumor necrosis factor (TNF), interleukin-1β (IL-1β), and IL-6 in the joints of WT and *Gsdme*$^{-/-}$ mice after CIA induction. Symbols represent individual mice; bars show the mean ± SD. **F**, Immunohistochemical staining for cytokines in the joints of WT and *Gsdme*$^{-/-}$ mice after CIA induction. Right panels show higher-magnification views (bars = 50 μm) of the boxed areas in the left panels (bars = 100 μm). **G**, Model of the pathogenesis of rheumatoid arthritis (RA). TNF induces pyroptosis by activating the caspase 3/GSDME pathway, promoting an inflammatory response. TNFR = TNF receptor; GSDME-N = N-terminal fragment of GSDME; GSDME-C = C-terminal fragment of GSDME; DAMPs = damage-associated molecular patterns. * = $P < 0.05$. Color figure can be viewed in the online issue, which is available at http://onlinelibrary.wiley.com/doi/10.1002/art.41963/abstract.

TNF-induced pyroptosis (Figure 5B). In addition, BMMs from *Gsdme*$^{-/-}$ mice showed decreased TNF-induced pyroptosis (Figures 5D and E). Overall, these results indicate that inhibition of the caspase 3/GSDME pathway could reduce TNF-induced pyroptosis of macrophages.

Alleviation of experimental arthritis in GSDME-deficient mice. Given that RA synovial macrophages and circulating monocytes showed high expression of activated caspase 3 and GSDME, and that TNF activated caspase 3/GSDME-mediated pyroptosis, we speculated that inhibition of pyroptosis by *Gsdme* knockout could protect mice against arthritis. To test our hypothesis, we immunized *Gsdme*$^{-/-}$ C57BL/6 (*Gsdme*$^{-/-}$ B6) mice and wild-type C57BL/6 (B6) mice with collagen to induce arthritis, and evaluated clinical and immunologic features.

Gsdme$^{-/-}$ B6 and wild-type B6 mice did not show any significant differences in the absence of collagen exposure (Figures 6A–C). However, compared with collagen-treated wild-type B6 mice, *Gsdme*$^{-/-}$ B6 mice had a dramatically decreased incidence of arthritis and decreased clinical arthritis scores following collagen exposure (Figures 6A and B). Moreover, synovitis was alleviated in H&E-stained joint sections from collagen-treated *Gsdme*$^{-/-}$ B6 mice compared to joint sections from collagen-treated wild-type B6 mice (Figure 6C). The expression of GSDME was up-regulated in synovial macrophages from collagen-treated wild-type B6 mice (Figure 6D), as well as in those from collagen-treated DBA/1J mice (Supplementary Figure 13, available on the *Arthritis & Rheumatology* website at https://onlinelibrary.wiley.com/doi/10.1002/art.41963), but was markedly reduced in collagen-treated *Gsdme*$^{-/-}$ B6 mice (Figure 6D). In parallel, the expression of activated caspase 3 was lower in synovial macrophages from collagen-treated *Gsdme*$^{-/-}$ B6 mice than in those from collagen-treated wild-type B6 mice (Supplementary Figure 14, available on the *Arthritis & Rheumatology* website at https://onlinelibrary.wiley.com/doi/10.1002/art.41963). The levels of circulating and synovial proinflammatory cytokines were lower in collagen-treated *Gsdme*$^{-/-}$ B6 mice than in collagen-treated wild-type B6 mice (Figures 6E and F).

DISCUSSION

GSDME shares ~45% sequence homology with other members of the gasdermin family and possesses the most conserved gasdermin-N domain, and forms pores to execute pyroptosis. In tumors, GSDME also functions as a tumor suppressor by activating pyroptosis (16). The key role of GSDME in chemotherapy drug–induced organ toxicity was demonstrated in an animal experiment (12). However, the role of GSDME-mediated pyroptosis in autoimmune diseases remains to be elucidated. We found a significant increase in the expression of GSDME and activated caspase 3 in synovial macrophages and circulating monocytes from RA patients. Activated caspase 3 specifically cleaves GSDME in the linker region, generating GSDME-N. As expected, the expression of GSDME-N was increased in monocytes and synovial macrophages from RA patients, and correlated positively with RA disease activity. Moreover, RA patients in remission exhibited lower expression of GSDME-N. These findings provide the first clinical evidence of the key role of GSDME, identifying the close relationship between GSDME and RA pathogenesis. Interestingly, deletion of *Gsdme* in mice had a protective effect on clinical manifestations and synovitis in mice with CIA, supporting the notion of a pathogenic role of GSDME in RA.

Apoptosis and necrosis are 2 important programmed cell death procedures with different effects on inflammation and immune responses (37,38). In apoptosis, cells shrink and disintegrate into apoptotic bodies that are usually engulfed by surrounding macrophages, leading to the noninflammatory nature of cell death (39). In necrosis, cells disrupt and release endogenous danger signals, resulting in inflammatory and immune responses (40). Unlike apoptosis, pyroptosis is a form of programmed necrosis with a highly proinflammatory nature (41). Although caspase 3 activation has long been regarded as the hallmark of apoptosis, the questions of why and how caspase 3 critically participates in the induction of pyroptosis are very fascinating.

GSDME levels play a role in determining the form of cell death in caspase 3–activated cells. Caspase 3 activation induces apoptosis in cells with low levels of GSDME but pyroptosis in cells with high levels of GSDME. We found that caspase 3 activation and GSDME cleavage led to obvious cell swelling with the formation of large bubbles, enhanced LDH release, and a high percentage of PI-positive RA monocytes. In addition, in *Gsdme*$^{-/-}$ mice, the expression of GSDME was decreased in synovial macrophages and necrotic cell death was reduced in BMMs. Importantly, manifestations of arthritis and inflammatory cytokine release also decreased in *Gsdme*$^{-/-}$ mice after collagen challenge. We also confirmed that other related phenotypes which may lead to arthritis resistance, such as leukopenias or IgG synthesis problems, were not found in *Gsdme*$^{-/-}$ mice (Supplementary Figure 15, available on the *Arthritis & Rheumatology* website at https://onlinelibrary.wiley.com/doi/10.1002/art.41963). Taken together, these results suggest that GSDME-mediated pyroptosis may be strongly associated with the pathogenesis and progression of RA, further verifying the reliability of the "cell death immune recognition model." We previously proposed that apoptosis induces immune tolerance, whereas necrosis initiates immune and inflammation responses (42). A "cell death immune recognition model" can help explain inflammation and autoimmunity in autoimmune diseases, and investigations into the detailed mechanisms of cell death–mediated immune responses may provide novel strategies for the treatment of autoimmune diseases (42,43).

Given that GSDME-mediated pyroptosis plays an essential role in the pathogenesis and progression of RA, we were

curious to identify the initial trigger for pyroptosis in RA patients. In vitro, GSDME-mediated pyroptosis can be triggered by chemotherapeutic drugs (11), metformin (44), apoptotic stimulators, and ATP (45). Consistent with previous clinical and experimental findings, our study indicates that TNF is abundant in synovial tissue samples from RA patients. Since TNF, combined with other stimulators, induces the activation of caspase 3, we wondered whether TNF itself could induce pyroptosis of monocytes and macrophages with high GSDME expression in RA patients. Indeed, TNF alone significantly enhanced the activation of caspase 3 and GSDME, and induced GSDME-mediated pyroptosis of RA monocytes. Moreover, monocytes from RA patients in remission after treatment showed decreased expression of GSDME-N and reduced pyroptosis. TNF also triggered GSDME-mediated pyroptosis of THP-1 cell–derived macrophages and BMMs. Pharmacologic inhibition of caspase 3 or genetic knockout of GSDME significantly blocked TNF-induced pyroptosis. These results indicate that up-regulation of TNF in RA patients might be an essential factor in promoting the activation of caspase 3 and GSDME and in the induction of pyroptosis in vivo.

The fact that TNF is mainly produced and released by monocytes and local macrophages further implies a feedback loop wherein monocytes and macrophages produce TNF and then respond to it by undergoing pyroptosis. Currently, TNF is recognized as a key pathogenic factor in RA and plays important roles in the development of T cells, production of antibodies, and acceleration of arthritis by promotion of the activation and proliferation of synovial fibroblasts (46–48). Therefore, inhibition of TNF is a widely recommended treatment for RA. Our findings provide another possible mechanism for the pathogenesis of RA, wherein TNF induces pyroptosis of monocytes and macrophages through the activation of the caspase 3/GSDME pathway.

In conclusion, our findings indicate that GSDME-mediated pyroptosis is strongly involved in the pathogenesis of RA and that targeting GSDME may be a potential therapeutic approach in RA.

ACKNOWLEDGMENTS

We would like to thank Dr. Hongfen Shen and Dr. Chengzhi Huang for valuable assistance with the fluorescence-activated cell sorting analysis.

AUTHOR CONTRIBUTIONS

All authors were involved in drafting the article or revising it critically for important intellectual content, and all authors approved the final version to be published. Dr. Sun had full access to all of the data in the study and takes responsibility for the integrity of the data and the accuracy of the data analysis.

Study conception and design. He, Sun.

Acquisition of data. Zhai, Yang, Xu, J. Han, G. Luo, Y. Li, X. Li, Shi, X. Han, X. Luo, Song, Chen, Liang, Wu.

Analysis and interpretation of data. Zhai, Xu, Zhuang, Jie.

REFERENCES

1. Smolen JS, Aletaha D, McInnes IB. Rheumatoid arthritis [review]. Lancet 2016;388:2023–38.
2. Mohammed FF, Smookler DS, Khokha R [review]. Metalloproteinases, inflammation, and rheumatoid arthritis. Ann Rheum Dis 2003; 62 Suppl:ii43–7.
3. Shi J, Gao W, Shao F. Pyroptosis: gasdermin-mediated programmed necrotic cell death [review]. Trends Biochem Sci 2017; 42:245–54.
4. Kuang S, Zheng J, Yang H, Li S, Duan S, Shen Y, et al. Structure insight of GSDMD reveals the basis of GSDMD autoinhibition in cell pyroptosis. Proc Natl Acad Sci U S A 2017;114:10642–7.
5. Ding J, Wang K, Liu W, She Y, Sun Q, Shi J, et al. Pore-forming activity and structural autoinhibition of the gasdermin family. Nature 2016; 535:111–6.
6. Shi J, Zhao Y, Wang K, Shi X, Wang Y, Huang H, et al. Cleavage of GSDMD by inflammatory caspases determines pyroptotic cell death. Nature 2015;526:660–5.
7. Aglietti RA, Estevez A, Gupta A, Ramirez MG, Liu PS, Kayagaki N, et al. GsdmD p30 elicited by caspase-11 during pyroptosis forms pores in membranes. Proc Natl Acad Sci U S A 2016;113:7858–63.
8. Sarhan J, Liu BC, Muendlein HI, Li P, Nilson R, Tang AY, et al. Caspase-8 induces cleavage of gasdermin D to elicit pyroptosis during Yersinia infection. Proc Natl Acad Sci U S A 2018;115: E10888–97.
9. Broz P, Dixit VM. Inflammasomes: mechanism of assembly, regulation and signalling [review]. Nat Rev Immunol 2016;16:407–20.
10. He WT, Wan H, Hu L, Chen P, Wang X, Huang Z, et al. Gasdermin D is an executor of pyroptosis and required for interleukin-1β secretion. Cell Res 2015;25:1285–98.
11. Zhang CC, Li CG, Wang YF, Xu LH, He XH, Zeng QZ, et al. Chemotherapeutic paclitaxel and cisplatin differentially induce pyroptosis in A549 lung cancer cells via caspase-3/GSDME activation. Apoptosis 2019;24:312–25.
12. Wang Y, Gao W, Shi X, Ding J, Liu W, He H, et al. Chemotherapy drugs induce pyroptosis through caspase-3 cleavage of a gasdermin. Nature 2017;547:99–103.
13. Rogers C, Fernandes-Alnemri T, Mayes L, Alnemri D, Cingolani G, Alnemri ES. Cleavage of DFNA5 by caspase-3 during apoptosis mediates progression to secondary necrotic/pyroptotic cell death. Nat Commun 2017;8:14128.
14. Li YQ, Peng JJ, Peng J, Luo XJ. The deafness gene GSDME: its involvement in cell apoptosis, secondary necrosis, and cancers [review]. Naunyn Schmiedebergs Arch Pharmacol 2019;392:1043–8.
15. Jiang M, Qi L, Li L, Li Y. The caspase-3/GSDME signal pathway as a switch between apoptosis and pyroptosis in cancer. Cell Death Discov 2020;6:112.
16. Zhang Z, Zhang Y, Xia S, Kong Q, Li S, Liu X, et al. Gasdermin E suppresses tumour growth by activating anti-tumour immunity. Nature 2020;579:415–20.
17. Yu X, He S. GSDME as an executioner of chemotherapy-induced cell death. Sci China Life Sci 2017;60:1291–4.
18. Wang Y, Yin B, Li D, Wang G, Han X, Sun X, et al. GSDME mediates caspase-3-dependent pyroptosis in gastric cancer. Biochem Biophys Res Commun 2018;495:1418–25.
19. Yu J, Li S, Qi J, Chen Z, Wu Y, Guo J, et al. Cleavage of GSDME by caspase-3 determines lobaplatin-induced pyroptosis in colon cancer cells. Cell Death Dis 2019;10:193.
20. Mai FY, He P, Ye JZ, Xu LH, Ouyang DY, Li CG, et al. Caspase-3-mediated GSDME activation contributes to cisplatin- and doxorubicin-induced secondary necrosis in mouse macrophages. Cell Prolif 2019;52:e12663.

21. Tetta C, Camussi G, Modena V, Di Vittorio C, Baglioni C. Tumour necrosis factor in serum and synovial fluid of patients with active and severe rheumatoid arthritis. Ann Rheum Dis 1990;49:665–7.
22. Lee A, Qiao Y, Grigoriev G, Chen J, Park-Min KH, Park SH, et al. Tumor necrosis factor α induces sustained signaling and a prolonged and unremitting inflammatory response in rheumatoid arthritis synovial fibroblasts. Arthritis Rheum 2013;65:928–38.
23. Wu X. Innate lymphocytes in inflammatory arthritis [review]. Front Immunol 2020;11:1–12.
24. Feldmann M, Maini RN. TNF defined as a therapeutic target for rheumatoid arthritis and other autoimmune diseases. Nat Med 2003;9: 1245–50.
25. Cheng Y, Yang F, Huang C, Huang J, Wang Q, Chen Y, et al. Plasmapheresis therapy in combination with TNF-α inhibitor and DMARDs: a multitarget method for the treatment of rheumatoid arthritis. Mod Rheumatol 2017;27:576–81.
26. Radner H, Aletaha D. Anti-TNF in rheumatoid arthritis: an overview. Wien Med Wochenschr 2015;165:3–9.
27. Aggarwal S, Gollapudi S, Gupta S. Increased TNF-α-induced apoptosis in lymphocytes from aged humans: changes in TNF-α receptor expression and activation of caspases. J Immunol 1999;162: 2154–61.
28. Qian Q, Cao X, Wang B, Qu Y, Qian Q, Sun Z, et al. TNF-α–TNFR signal pathway inhibits autophagy and promotes apoptosis of alveolar macrophages in coal worker's pneumoconiosis. J Cell Physiol 2019; 234:5953–63.
29. Arnett FC, Edworthy SM, Bloch DA, McShane DJ, Fries JF, Cooper NS, et al. The American Rheumatism Association 1987 revised criteria for the classification of rheumatoid arthritis. Arthritis Rheum 1988;31:315–24.
30. Aletaha D, Neogi T, Silman AJ, Funovits J, Felson DT, Bingham CO III, et al. 2010 rheumatoid arthritis classification criteria: an American College of Rheumatology/European League Against Rheumatism collaborative initiative. Arthritis Rheum 2010;62:2569–81.
31. Chanput W, Mes JJ, Wichers HJ. THP-1 cell line: an in vitro cell model for immune modulation approach [review]. Int Immunopharmacol 2014; 23:37–45.
32. Kayagaki N, Warming S, Lamkanfi M, Vande WL, Louie S, Dong J, et al. Non-canonical inflammasome activation targets caspase-11. Nature 2011;479:117–21.
33. Inglis JJ, Simelyte E, McCann FE, Criado G, Williams RO. Protocol for the induction of arthritis in C57BL/6 mice. Nat Protoc 2008;3:612–8.
34. Kruglov A, Drutskaya M, Schlienz D, Gorshkova E, Kurz K, Morawietz L, et al. Contrasting contributions of TNF from distinct cellular sources in arthritis. Ann Rheum Dis 2020;79:1453–9.
35. Brand DD, Latham KA, Rosloniec EF. Collagen-induced arthritis. Nat Protoc 2007;2:1269–75.
36. Van Riel PL. Disease Activity Score in rheumatoid arthritis. URL: https://www.das-score.nl.
37. Wallach D, Kang TB, Kovalenko A. Concepts of tissue injury and cell death in inflammation: a historical perspective [review]. Nat Rev Immunol 2014;14:51–9.
38. Calo G, Sabbione F, Vota D, Paparini D, Ramhorst R, Trevanu A, et al. Trophoblast cells inhibit neutrophil extracellular trap formation and enhance apoptosis through vasoactive intestinal peptide-mediated pathways. Hum Reprod 2017;32:55–64.
39. Nowak-Sliwinska P, Griffioen AW. Apoptosis on the move [editorial]. Apoptosis 2018;23:251–4.
40. Wallach D, Kang TB, Dillon CP, Green DR. Programmed necrosis in inflammation: toward identification of the effector molecules [review]. Science 2016;352:aaf2154.
41. Kesavardhana S, Malireddi RK, Kanneganti TD. Caspases in cell death, inflammation, and pyroptosis [review]. Annu Rev Immunol 2020;38:567–95.
42. Yang F, He Y, Zhai Z, Sun E. Programmed cell death pathways in the pathogenesis of systemic lupus erythematosus [review]. J Immunol Res 2019;2019:3638562.
43. He Y, Yang FY, Sun EW. Neutrophil extracellular traps in autoimmune diseases [editorial]. Chin Med J (Engl) 2018;131: 1513–9.
44. Zheng Z, Bian Y, Zhang Y, Ren G, Li G. Metformin activates AMPK/SIRT1/NF-κB pathway and induces mitochondrial dysfunction to drive caspase3/GSDME-mediated cancer cell pyroptosis. Cell Cycle 2020; 19:1089–104.
45. Zeng C, Li C, Shu J, Xu LH, Ouyang DY, Mai FY, et al. ATP induces caspase-3/gasdermin E-mediated pyroptosis in NLRP3 pathway-blocked murine macrophages. Apoptosis 2019;24: 703–17.
46. Kruglov AA, Lampropoulou V, Fillatreau S, Nedospasov SA. Pathogenic and protective functions of TNF in neuroinflammation are defined by its expression in T lymphocytes and myeloid cells. J Immunol 2011;187:5660–70.
47. Tumanov AV, Grivennikov SI, Kruglov AA, Shebzukhov YV, Koroleva EP, Piao Y, et al. Cellular source and molecular form of TNF specify its distinct functions in organization of secondary lymphoid organs. Blood 2010;116:3456–64.
48. Armaka M, Apostolaki M, Jacques P, Kontoyiannis DL, Elewaut D, Kollias G. Mesenchymal cell targeting by TNF as a common pathogenic principle in chronic inflammatory joint and intestinal diseases. J Exp Med 2008;205:331–7.

Arthritis & Rheumatology
Vol. 74, No. 3, March 2022, pp 441–452
DOI 10.1002/art.41958

American College of Rheumatology
Empowering Rheumatology Professionals

Effect of JAK Inhibition on the Induction of Proinflammatory HLA–DR+CD90+ Rheumatoid Arthritis Synovial Fibroblasts by Interferon-γ

Shuyang Zhao,[1] Ricardo Grieshaber-Bouyer,[2] Deepak A. Rao,[3] Philipp Kolb,[4] Haizhang Chen,[4] Ivana Andreeva,[1] Theresa Tretter,[1] Hanns-Martin Lorenz,[1] Carsten Watzl,[5] Guido Wabnitz,[1] Lars-Oliver Tykocinski,[1] and Wolfgang Merkt[6]

Objective. Findings from recent transcriptome analyses of the synovium of patients with rheumatoid arthritis (RA) have revealed that 15-fold expanded HLA–DR+CD90+ synovial fibroblasts potentially act as key mediators of inflammation. The reasons for the expansion of HLA–DR+CD90+ synovial fibroblasts are unclear, but genetic signatures indicate that interferon-γ (IFNγ) plays a central role in the generation of this fibroblast subset. The present study was undertaken to investigate the generation, function and therapeutically intended blockage of HLA–DR+CD90+ synovial fibroblasts.

Methods. We combined functional assays using primary human materials and focused bioinformatic analyses of mass cytometry and transcriptomics patient data sets.

Results. We detected enriched and activated Fcγ receptor type IIIa–positive (CD16+) NK cells in the synovial tissue from patients with active RA. Soluble immune complexes were recognized by CD16 in a newly described reporter cell model, a mechanism that could be contributing to the activation of natural killer (NK) cells in RA. In vitro, NK cell–derived IFNγ induced HLA–DR on CD90+ synovial fibroblasts, leading to an inflammatory, cytokine-secreting HLA–DR+CD90+ phenotype. HLA–DR+CD90+ synovial fibroblasts consecutively activated CD4+ T cells upon receptor crosslinking via superantigens. HLA–DR+CD90+ synovial fibroblasts also activated CD4+ T cells in the absence of superantigens, an effect that was initiated by NK cell–derived IFNγ and that was 4 times stronger in patients with RA compared to patients with osteoarthritis. Finally, JAK inhibition in synovial fibroblasts prevented HLA–DR induction and blocked proinflammatory signals to T cells.

Conclusion. The HLA–DR+CD90+ phenotype represents an activation state of synovial fibroblasts during the process of inflammation in RA that can be induced by IFNγ, likely generated from infiltrating leukocytes such as activated NK cells. The induction of these proinflammatory, interleukin-6–producing, and likely antigen-presenting synovial fibroblasts can be targeted by JAK inhibition.

Supported by the medical faculty of the University of Heidelberg (grant awarded to Dr. Merkt and to Dr. Grieshaber-Bouyer), Eva Luise and Horst Köhler Foundation (grant awarded to Dr. Merkt), German Society for Rheumatology (grant awarded to Dr. Grieshaber-Bouyer), Roche Pharma AG (unrestricted grant awarded to Dr. Merkt), Third Affiliated Hospital of Nantong University (grant awarded to Ms. Zhao), National Institute of Arthritis and Musculoskeletal and Skin Diseases, NIH (grant K08-AR-072791 awarded to Dr. Rao), EQUIP–Funding for Medical Scientists, Faculty of Medicine, University of Freiburg (grant awarded to Dr. Kolb), Deutsche Forschungsgemeinschaft (grant DFG FOR2830 HE 2526/9-1 awarded to Dr. Kolb), NaFoUniMedCovid19 (grant FKZ: 01KX2021–COVIM awarded to Dr. Kolb), and the Joint Biology Consortium, funded by the National Institute of Arthritis and Musculoskeletal and Skin Diseases, NIH (grant P30-AR-070253).

[1]Shuyang Zhao, Ivana Andreeva, Theresa Tretter, PhD, Hanns-Martin Lorenz, MD, Guido Wabnitz, PhD, Lars-Oliver Tykocinski, PhD: University Hospital Heidelberg, Heidelberg, Germany; [2]Ricardo Grieshaber-Bouyer, MD: University Hospital Heidelberg, Heidelberg, Germany, and Brigham and Women's Hospital and Harvard Medical School, Boston, Massachusetts; [3]Deepak A. Rao, MD, PhD: Brigham and Women's Hospital and Harvard Medical School, Boston, Massachusetts; [4]Philipp Kolb, PhD, Haizhang Chen: University Medical Center and Albert Ludwigs University of Freiburg, Freiburg, Germany; [5]Carsten Watzl, PhD: Leibniz Research Center for Working Environment and Human Factors at Technical University Dortmund, Dortmund, Germany; [6]Wolfgang Merkt, MD: University Hospital Heidelberg, Heidelberg, Germany, and Massachusetts General Hospital and Harvard Medical School, Boston, Massachusetts.

Dr. Grieshaber-Bouyer has received research support from Gilead. Dr. Rao has received consulting fees, speaking fees, and/or honoraria from Pfizer, Merck, Scipher Medicine, and Bristol Myers Squibb (less than $10,000 each) and research support from Celgene. Dr. Lorenz has received consulting fees, speaking fees, and/or honoraria from AbbVie, AstraZeneca, Actelion, Alexion, Amgen, Bayer Vital, Baxter, Biogen, Boehringer Ingelheim, Bristol Myers Squibb, Celgene, Fresenius, Genzyme, GlaxoSmithKline, Gilead, Hexal, Janssen-Cilag, Lilly, Medac, MSD, Mundipharma, Mylan, Novartis, Octapharma, Pfizer, Roche/Chugai, Sandoz, Sanofi, Shire, Sobi, ThermoFisher, and UCB (less than $10,000 each), and research support from Pfizer and Novartis. Dr. Tykocinski has received research support from Pfizer. Dr. Merkt has received consulting fees, speaking fees, and/or honoraria from Novartis and Roche (less than $10,000 each) and research support from Roche.

Author disclosures are available at https://onlinelibrary.wiley.com/action/downloadSupplement?doi=10.1002%2Fart.41958&file=art41958-sup-0001-Disclosureform.pdf.

Address correspondence to Wolfgang Merkt, MD, Medizinische Klinik V, Im Neuenheimer Feld 410, 69120 Heidelberg, Germany. Email: wolfgang.merkt@med.uni-heidelberg.de.

Submitted for publication November 1, 2020; accepted in revised form August 24, 2021.

INTRODUCTION

Rheumatoid arthritis (RA) is a systemic inflammatory disease characterized by chronic destructive arthritis (1). Autoantibodies frequently occur in RA and are a risk factor for poor outcome. Genetic risk in RA is based on single-nucleotide polymorphisms in genes involved in immune regulation (1,2), especially in the major histocompatibility complex (MHC) class II region in seropositive RA, including HLA–DRB1 (3).

Synovial fibroblasts are the most abundant cell type in synovial tissue and have been implicated in the pathogenesis of RA (4–6). Synovial fibroblasts are tissue destructive and recruit and activate immune cells in RA (4). Genetic signatures, combined with high-dimensional surface molecule analyses, recently revealed a subset of synovial fibroblasts that is expanded >15-fold in leukocyte-rich RA (5). This Thy-1+ (CD90+) cell subset is characterized by high expression of HLA–DR. The RNA expression profile of HLA–DR+CD90+ synovial fibroblasts identified these cells as pivotal contributors to inflammation in RA based on their production of cytokines and chemokines (5). As such, HLA–DR+CD90+ synovial fibroblasts are a major source of synovial interleukin-6 (IL-6) (4,5). IL-6 is an important proinflammatory cytokine in RA, and blocking it from binding to its receptor is a successful treatment strategy (7).

The functional role of HLA–DR molecules in synovial fibroblasts is not well established (8,9), but the idea that HLA–DR-mediated antigen presentation plays a pathogenic role in RA in general has been intrinsically demonstrated by observations of strong genetic associations with the HLA region and the formation of autoantibodies in patients with RA. It has recently been shown that synovial fibroblasts can internalize, process, and present arthritic antigens via HLA–DR (10–12). Along the same lines, a gene ontology analysis revealed an increased number of genes involved in antigen processing/presentation of peptide antigen via MHC class II, specifically in HLA–DR+CD90+ synovial fibroblasts (5), suggesting that antigen presentation by HLA–DR +CD90+ synovial fibroblasts occurs in vivo in RA.

Importantly, HLA–DR+CD90+ synovial fibroblasts possess a strong interferon-γ (IFNγ) signature (5), indicating that IFNγ may be involved in generation of the distinct phenotype of these synovial fibroblasts. However, functional studies validating a role of IFNγ in the development of the HLA–DR+CD90+ synovial fibroblast phenotype on the protein level have not yet been performed.

Natural killer (NK) cells are immediately acting innate lymphocytes that respond to a variety of stress signals by secreting cytokines, in particular IFNγ (13). NK cells reside in the inflamed synovial fluid of RA patients (14–17), and increased IFNγ production by synovial fluid NK cells is associated with a more erosive disease course (14). Nevertheless, the role of NK cells in RA is not well defined, and data on the presence of NK cells in synovial tissue are limited. Only a few studies with relatively small sample sizes have demonstrated the presence of NK cells in RA synovial tissue (16,18,19). Increasing our understanding of the role of NK cells in RA is of interest, since the presence of polymorphisms in a prominent activating NK cell receptor, low-affinity Fcγ receptor type IIIa (FcγRIIIa) (CD16), is a risk factor for the development of RA (13,20,21). CD16 binds to surface-bound antibodies and immune complexes and triggers cytotoxicity and IFNγ production (22–25). We hypothesized that NK cells may be activated in the proinflammatory environment in RA synovial fluid and tissue and thus represent a source of synovial IFNγ, contributing to the generation of HLA–DR+CD90+ synovial fibroblasts.

The generation of HLA–DR+CD90+ synovial fibroblasts may be a key event in RA pathogenesis, given its expansion, inflammatory profile, and potential to present antigens, along with the strong clinical associations with MHC class II alleles. In the present study, we investigated the generation of HLA–DR+CD90+ synovial fibroblasts and their function in vitro.

MATERIALS AND METHODS

Synovial fluid analysis using flow cytometry. In this study, 100 μl of native synovial fluid (>1 × 10^6 leukocytes) from a total of 5 joints from 3 patients with highly active chronic arthritis (including 1 with juvenile idiopathic arthritis, 1 with seronegative RA, and 1 with seropositive RA) was processed immediately or kept overnight at 4°C. Cells were washed and incubated with antibodies in phosphate buffered saline (PBS) with 2% fetal calf serum (FCS) (see Supplementary Methods, available on the *Arthritis & Rheumatology* website at http://onlinelibrary.wiley.com/doi/10.1002/art.41958). After 30 minutes at 4°C, cells were washed, fixed in 2% paraformaldehyde, and analyzed on a 3-laser flow cytometer (BD LSR II).

Synovial tissue analysis using mass cytometry. Mass cytometry raw data were obtained in the multicenter Accelerating Medicines Partnership resource study AMP-RA (5). In brief, synovial tissue obtained by biopsy or arthroplasty was incorporated in single-cell suspensions, cryopreserved, incubated with a panel of 35 metal ion-linked monoclonal antibodies, and analyzed using mass cytometry. We analyzed normalized Flow Cytometry Standard files from 15 osteoarthritis (OA) patients and 26 RA patients (Supplementary Table 1, available on the *Arthritis & Rheumatology* website at http://onlinelibrary.wiley.com/doi/10.1002/art.41958). FlowJo was used for manual gating. Cytobank was used for unbiased clustering of pre-gated viable cells with the Sequential Pattern Discovery using Equivalence algorithm. The following 20 clustering channels were chosen: CD19, CD64, CD16, CD8a, CD20, CD45RO, CD38, CD279, CD14, CD185, CD4, CD3, CD11c, CD307d, CD138, CD90, CD34, CD66b, CD106, and CD45. The target number of nodes was 300.

RNA-seq data analysis. Transcripts of the IFNγ signaling pathway were individually analyzed, taking advantage of the

online-accessible database from the AMP-RA phase I data set (available at www.immunogenomics.org [5]). Furthermore, we downloaded raw data and obtained transcript expression profiles (with the data expressed as $\log_2$-normalized transcripts per million RNA) from sorted populations of synovial fibroblasts, T cells, B cells, and monocytes (5). The median values for the expression of HLA–DRB1 in each respective cell type in the OA control group was subtracted from individual values in the two RA conditions, with results expressed as the fold change in transcript expression. A Kruskal-Wallis test, followed by unpaired *t*-tests for all pairwise comparisons, was used to assess statistical significance. Values for expression of transcripts for JAK1, JAK2, and JAK3 (expressed as $\log_2$-normalized transcripts per million) were plotted as heatmaps.

Generation of primary human cells. Fibroblasts were isolated from the synovial tissue or skin of all subjects after written informed consent had been provided. Synovial tissue samples were obtained from OA and RA patients who had undergone either arthroscopic synovectomy or joint replacement surgery. Skin samples were collected from healthy volunteers who had undergone mammary reduction surgery, and from patients with morphea who had undergone punch biopsy of the affected skin. Synovial tissue was digested with collagenase and Dispase (CellSystems) at 37°C for 2 hours. The cell suspension was cultured in medium (Dulbecco's modified Eagle's medium [DMEM]/F12; Merck) supplemented with 10% heat-inactivated FCS (ThermoFisher Scientific).

Peripheral blood mononuclear cells (PBMCs) were isolated from heparinized blood from healthy volunteers using density gradient centrifugation with Biocoll separating solution (Biochrom Ltd). NK cells and CD4+ T cells were isolated from PBMCs using MojoSort human NK cell/CD4+ T cell isolation kits (product nos. 480054 and 480010 from BioLegend, respectively). The purity of isolated cells was >90%. Cells were counted manually and checked for viability using trypan blue staining.

Cell culture. All cells were cultured in 5% CO_2 at 37°C. Fibroblasts were cultured in DMEM/Ham's F-12 supplemented with 10% FCS, 1% L-glutamine, and 1% penicillin/streptomycin and were used from passage 4 to passage 10. PBMCs, NK cells, T cells, the NK cell–sensitive myeloid leukemia cell line K562 (ATCCCCL-243), K562 "feeder" cells, and cocultures were maintained in RPMI 1640 supplemented with 10% FCS, 1% L-glutamine, 15 m*M* of HEPES buffer, and 1% penicillin/streptomycin ("R10"). K562 feeder cells were engineered to express green fluorescent protein, 4-1BB ligand, and membrane-bound IL-15 (gifted from Dario Campana at St. Jude Children's Research Hospital) (26).

Coculture of synovial fibroblasts and NK cells. A total of 100,000 synovial fibroblasts were seeded onto each 24-well plate. After attachment, 200 IU/ml of IL-2 (product no. 200-02; PeproTech) with or without 500,000 freshly isolated NK cells was added. After either 3 or 7 days, cells were incubated with fluorochrome-labeled antibodies (Supplementary Methods, available on the *Arthritis & Rheumatology* website at http://onlinelibrary.wiley.com/doi/10.1002/art.41958) and were directly analyzed using flow cytometry. The procedure utilized for intracellular IL-6 staining is also described in the Supplementary Methods.

Generation of conditioned supernatants using freshly isolated NK cells. For the generation of supernatant from NK cell/synovial fibroblast cocultures, NK cells were cultured on 15,000 synovial fibroblasts per 96-well plate for 3 days. For stimulation of NK cells by cytokines, 1×10^6 NK cells/ml were cultured with IL-2 at 200 IU/ml (product no. 200-02; PeproTech) for 3 days. For stimulation of NK cells with FcγRIIIa (CD16), 2×10^6 NK cells/ml were cultured overnight on plates coated with anti-CD16 (1 μg/ml; 3G8) (product no. 302014; BioLegend). For stimulation of NK cells by target cells, 1×10^6 or 2×10^6 NK cells/ml were cultured with log-phase K562 or K562 "feeder" cells in a 1:1 ratio overnight. For the generation of pooled supernatant (NK-SN), NK cells were cultured for 3 days with irradiated (using 30-Gy radiation) K562 feeder cells (1:2 ratio of K562 feeder cells:NK cells) in the presence of 200 units/ml of IL-2 and 100 ng/ml of IL-21 (27). Supernatants were harvested, centrifuged, and stored at –20°C.

Fibroblast culture with recombinant IFNγ and supernatants from activated NK cells. In total, 15,000 synovial fibroblasts were added to each 96-well plate, and the cells were then treated with either 100 ng/ml recombinant IFNγ (product no. 300-02; PeproTech), 20% NK cell supernatant, or control cytokines (100 ng/ml IL-21 [product no. PHC0214; BioSource] and 200 IU/ml IL-2 [product no. 200-02; PeproTech]). In order to neutralize IFNγ, 50 μg/ml of anti-IFNγ antibody (product no. 554698; BD PharMingen) was added to a medium containing recombinant IFNγ or NK cell supernatants 30 minutes before the medium was added to the cultures of synovial fibroblasts. One day prior to the addition of recombinant IFNγ or NK cell supernatant into the synovial fibroblast cultures, upadacitinib or 10 μg/ml of adalimumab was added, and this mixture was maintained throughout the culture period. After 3 days, live synovial fibroblasts were analyzed using flow cytometry (Supplementary Methods, available on the *Arthritis & Rheumatology* website at http://onlinelibrary.wiley.com/doi/10.1002/art.41958).

Coculture of synovial fibroblasts and CD4+ T cells. Treated synovial fibroblasts were washed, incubated with or without 5 μg of *Staphylococcus aureus* enterotoxin B (SEB) (product no. S4881; Sigma-Aldrich) per ml of R10 medium at 37°C for 30 minutes, and washed twice with PBS. A total of 150,000 CD4+ T cells was added overnight and was analyzed using flow cytometry (Supplementary Methods available on the *Arthritis & Rheumatology* website at http://onlinelibrary.wiley.com/doi/10.1002/art.41958).

Enzyme-linked immunosorbent assay (ELISA). For the detection of IFNγ and IL-6 in cell culture supernatants, the following kits were used: a human IFNγ DuoSet ELISA development kit and a human IL-6 DuoSet ELISA development kit (product nos. DY285 and DY206, respectively; R&D Systems).

Western blotting. To measure JAK protein content and phosphorylation, synovial fibroblasts were cultured on 6-well plates for the indicated periods of time and were directly lysed using a standard lysing buffer (radioimmunoprecipitation assay buffer) supplemented with a phosphatase inhibitor cocktail (Sigma). JAK protein content and phosphorylation were determined using the phospho-JAK family antibody sampler kit from Cell Signaling Technology (product no. 97999). Quantification of Western blot bands was performed using densitometric analysis with ImageJ2.

FcγR activation reporter assay. BW5147–FcγRIIIA reporter cells (CD16+ BW5147) and wild-type (parental) BW5147 mouse thymoma cells (obtained from ATCC TIB-47) were maintained at 3×10^5 to 9×10^5 cells/ml in RPMI (RPMI GlutaMAX; Gibco) supplemented with 10% FCS, sodium pyruvate (1X; Gibco), and β-mercaptoethanol (0.1 m*M*; Gibco). FcγRIIIA activation was measured using a cell-based assay that was previously described (23). The assay was adapted to measure FcγRIIIA activation in a solution (25). Briefly, 2×10^5 BW5147–FcγRIIIa reporter cells were incubated with synovial fluid from RA patients at a total volume of 100 μl for 16 hours at 37°C/5% CO_2. Incubation was performed in a 96-well ELISA plate (Nunc MaxiSorp) pretreated with PBS/10% FCS for 1 hour at 4°C. Reporter cell IL-2 secretion was quantified using ELISA. Recombinant human tumor necrosis factor (TNF) (Stem Cell Technologies) and infliximab were mixed in a 1:1 ratio to generate synthetic immune complexes as a positive control (starting dilution 1:100).

Statistical analysis. Exploratory statistical analysis was performed using GraphPad Prism software versions 5 and 8. *P* values less than 0.05 were considered significant and had to be interpreted descriptively. Unless stated otherwise, normal distribution of the data was not assumed, and tests were 2-sided. The specific tests used are indicated in the figure legends. Graphics were in part created with BioRender.com.

Study approval. Written informed consent was obtained from participants prior to inclusion in the study. The local institutional review boards approved this study (ethics committee of the University of Heidelberg). Patient data and samples were treated in a pseudonymized manner.

RESULTS

HLA–DR+CD90+ synovial fibroblasts are greatly expanded in RA and possess a strong IFNγ signature (5), suggesting that IFNγ plays a role in their generation. We hypothesized that activated NK cells may be a source of synovial IFNγ and may play a role in the development of the inflammatory HLA–DR+CD90+ synovial fibroblast phenotype.

HLA–DR induction by NK cell–derived IFNγ in fibroblasts. We first tested whether recombinant IFNγ and soluble factors that are derived from activated NK cells in vitro can induce MHC molecules in human fibroblasts (from both healthy and sclerotic skin and joint samples from OA patients and RA patients). Both recombinant IFNγ and supernatant (NK supernatant) from IFNγ-producing NK cells (Supplementary Figure 1, http://onlinelibrary.wiley.com/doi/10.1002/art.41958) increased surface expression of HLA–ABC and induced HLA–DR (Figure 1 and Supplementary Figure 2). The levels of HLA–DR induced by NK supernatant did not vary between OA and RA (Supplementary Figure 2). Once induced, the presence of HLA–DR on synovial fibroblasts persisted over at least 1 week (Figure 1B). A monoclonal anti-IFNγ antibody inhibited HLA–DR induction by recombinant IFNγ and NK supernatant (Figure 1C). These data confirmed that NK cell–derived IFNγ induces HLA–DR in fibroblasts from different types of samples and diseases, including RASFs.

Activation of CD16-signaling by synovial immune complexes. NK cells secreted IFNγ in response to cytokines, target cells, or triggering FcγRIIIA (CD16) (Supplementary Figure 1, http://onlinelibrary.wiley.com/doi/10.1002/art.41958). We hypothesized that synovial immune complexes may bind to CD16 and thus contribute to NK cell activation. Using a reporter model for CD16 stimulation (25), we found that synovial fluid from seropositive RA patients contained immune complexes that could be recognized by CD16 (Figures 1D–F). In contrast, synovial fluid from seronegative patients did not trigger CD16. Therefore, immune complexes may contribute to CD16+ NK cell activation in seropositive RA.

Activated NK cells in synovial tissue from RA patients. Using flow cytometry, we detected that ~80% of synovial fluid NK cells showed a bright expression of the activation marker CD69 (Figure 2A). To investigate the presence of NK cells in synovial tissue, we analyzed mass cytometry data from 15 OA patients and 26 RA patients (Supplementary Table 1, available on the *Arthritis & Rheumatology* website at http://onlinelibrary.wiley.com/doi/10.1002/art.41958) in the AMP-RA trial (5) (Figures 2B–D). Using the unbiased Sequential Pattern Discovery using Equivalence algorithm, a cell cluster that was CD16+ and negative for all other lineage markers was identified as most likely being CD16+ NK cells (Figures 2B and D and Supplementary Figure 3). The presence of CD16+ NK cells in synovial tissue was confirmed using a manual gating strategy (Figure 2C). The number of NK cells in relation to fibroblasts and expression of CD69 in NK cells was increased in leukocyte-rich synovial samples from patients with RA (Figures 2C and D). These data revealed the

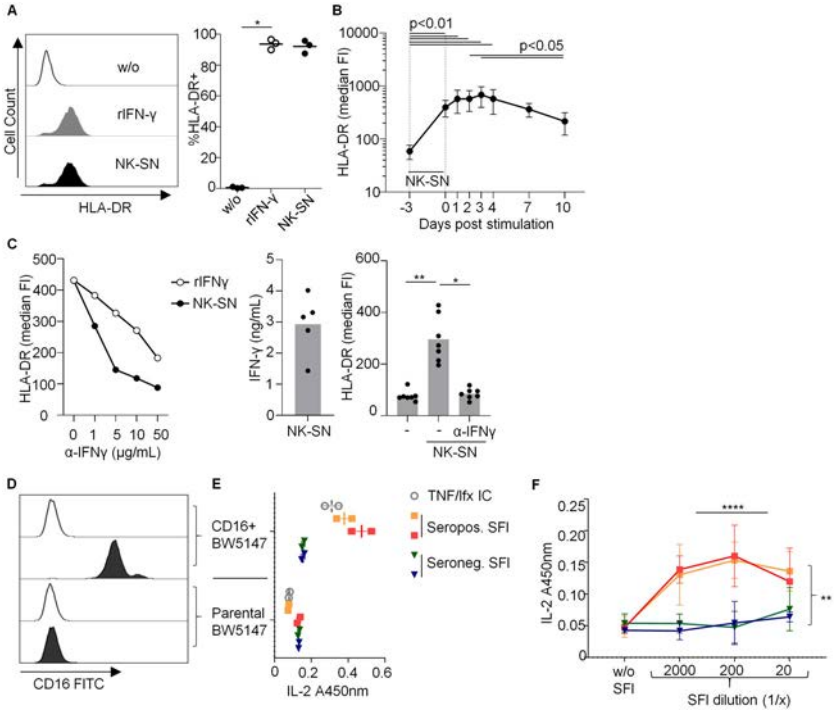

Figure 1. **A–C,** Induction of HLA–DR in synovial fibroblasts in cultures with recombinant interferon-γ (rIFNγ) or pooled natural killer cell–derived supernatant (NK-SN); medium alone without (w/o) stimulants was used as a control. Cells were assessed by flow cytometry. **A,** Example histograms of cell counts and percentages of HLA–DR+ rheumatoid arthritis synovial fibroblasts (RASFs) in each culture condition. Symbols represent individual samples; horizontal lines show the mean. **B,** Kinetics of HLA–DR expression in synovial fibroblasts from 4 RA patients and 3 osteoarthritis (OA) patients at various time points following stimulation with NK-SN. Values are the mean ± SD fluorescence intensity (FI) from 7 experiments ($P <$ 0.001 by Friedman's test; significant post hoc tests are indicated). **C**, Effect of anti-IFNγ (αIFNγ) on HLA–DR induction. Left, HLA–DR expression in RASFs in each culture condition, according to titration of anti-IFNγ (n = 1 experiment). Middle, Concentration of IFNγ in the supernatants pooled to generate NK-SN. Right, HLA–DR expression in RASFs without or with NK-SN and 50 μg/ml anti-IFNγ (n = 7 experiments with 3 different RASFs. $P = 0.003$ by Friedman's test; significant results from post hoc tests are indicated. **D–F**, Activation of CD16 (Fcγ receptor type IIIa) in the presence of synovial fluid from patients with seropositive RA (Seropos. SFI) compared to patients with seronegative joint swelling (seronegative chronic polyarthritis and OA) (Seroneg. SFI). CD16+ mouse BW5147 reporter cells were cultured with synovial fluid from 1 patient with active seropositive RA (2 joints) or 2 patients with seronegative joint swelling (1 joint each; n = 1 with seronegative chronic polyarthritis, n = 1 with OA). **D**, CD16 expression on transfected and parental BW5147 cells. Empty histograms show autofluorescence. FITC = fluorescein isothiocyanate. **E**, CD16 activation in cultures with CD16+ mouse 5147 cells and synovial fluid, at a dilution of 1:1,200. Values are the mean levels of interleukin-2 (IL-2) (absorbance at 450 nm [A450nm]) determined by enzyme-linked immunosorbent assay (n = 1 experiment, in duplicate). Treatment with tumor necrosis factor (TNF) and infliximab (Ifx)–immune complexes (ICs) served as a positive control. **F**, CD16 activation in the presence of titrations of seropositive and seronegative synovial fluid versus cultures without synovial fluid (w/o SFI). Values are the mean ± SD of 3 technical replicates, each performed in triplicate. Three-way analysis of variance was used to confirm the significant effects of synovial fluid dilution ($P < 0.0001$) and seropositivity ($P = 0.002$). * = $P < 0.05$; ** = $P < 0.01$; **** = $P < 0.001$. Color figure can be viewed in the online issue, which is available at http://onlinelibrary.wiley.com/doi/10.1002/art.41958/abstract.

presence of CD16+ NK cells in RA synovial tissue and indicated that NK cells were activated in this environment.

Restriction of increased HLA–DRB1 expression to synovial fibroblasts in leukocyte-rich RA synovial samples. Given the presence of activated NK cells in synovial fluid and synovial tissue and their potential ability to produce IFNγ and induce HLA–DR, we were interested in identifying the general changes in HLA–DR expression in RA. While several cell types intrinsically express HLA–DRB1, the gene with the highest risk association in RA (3), we investigated whether cell type–specific expression patterns of HLA–DRB1 are skewed in RA synovial tissue. We re-analyzed RNA-seq data obtained from sorted T cells, B cells, monocytes, and synovial fibroblasts in synovial tissue (5). Levels of HLA–DRB1 RNA were increased in synovial fibroblasts from leukocyte-rich samples from RA patients, compared to leukocyte-poor samples from RA and OA patients (Figure 3A). In contrast, HLA–DRB1 expression was unaltered in T cells, B cells, and monocytes.

In line with these findings, HLA–DR protein levels were significantly increased in synovial fibroblasts, but not in monocytes, in the mass cytometry data set. Furthermore, HLA–DR protein levels in synovial fibroblasts correlated with the percentage of activated (CD69+) CD16+ synovial NK cells (Figures 3B and C).

These observations linked 2 important pathogenicity factors in RA: MHC class II/HLA–DRB1 (genetic risk) and inflammatory fibroblasts. These findings further emphasized the importance of

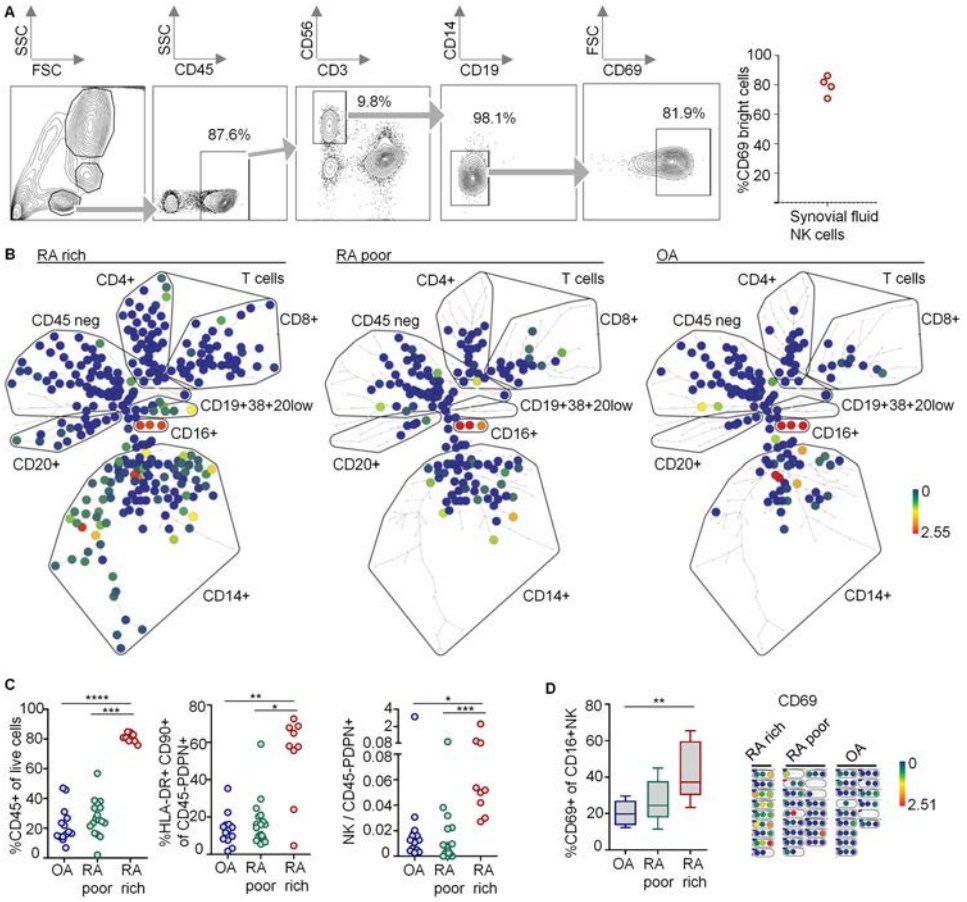

Figure 2. Activated NK cells in synovial tissue. **A**, Flow cytometry analysis of synovial fluid NK cells (CD45+CD3–CD56+CD19–CD14– lymphocytes). Left, Gating strategy. Right, Percentage of CD69^{bright} NK cells. **B**–**D**, Mass cytometry data showing cell distributions in synovial tissue from 26 RA patients and 15 OA patients. **B**, Unbiased clustering using the Sequential Pattern Discovery using Equivalence (SPADE) algorithm. The color code represents CD16 expression in each cell cluster, with red being the highest expression. Clustering channels are shown in Supplementary Figure 3 (https://onlinelibrary.wiley.com/doi/10.1002/art.41958). A representative leukocyte-rich or leukocyte-poor RA and OA synovial tissue sample is shown. **C**, Manual gating strategies were used to define leukocyte-poor RA synovial tissue (defined as having percentages of CD45+ live cells similar to those in OA synovial tissue; n = 17) and leukocyte-rich RA synovial tissue (defined as having percentages of CD45+ live cells higher than the upper range value +1SD in OA synovial tissue; n = 9). Left, Percentages of CD45+ live cells. Middle, Percentages of HLA–DR+CD90+ cells among CD45– podoplanin-positive (PDPN+) fibroblasts. Right, Ratio of NK cell:fibroblasts. **D**, CD69 levels in CD16+ NK cells. Left, Percentages of CD69+ cells among CD16+ NK cells as determined by a manual gating strategy. Samples with <20 CD16+ NK cells were excluded (n = 9 OA samples, n = 8 leukocyte-poor RA samples, n = 9 leukocyte-rich RA samples). Values are shown as box plots, where lines inside the box represent the median, the boxes represent the interquartile range, and whiskers represent the maximum and minimum range. Right, Sections from the clustering trees containing the three CD16+ NK cell clusters shown in **B.** The color code represents CD69 expression in CD16+ NK cells, with red being the highest expression. In **C** and **D,** $P < 0.003$ by Kruskal-Wallis test; significant results from post hoc tests are indicated. * = $P < 0.05$; ** = $P < 0.01$; *** = $P < 0.001$; **** = $P < 0.0001$. See Figure 1 for other definitions.

understanding the mechanism and consequences of HLA–DR induction in synovial fibroblasts, and indicated that synovial fibroblasts interact with IFNγ-producing cells in leukocyte-rich synovial tissue from patients with RA. This prompted us to investigate NK cell/RASF interactions in greater detail.

Induction of inflammatory HLA–DR+CD90+ synovial fibroblasts by activated NK cells. To investigate the direct effect of activated NK cells on synovial fibroblasts, we cocultured NK cells and synovial fibroblasts in vitro. It is known that synovial fibroblasts lose their surface MHC-II (8) and positional identity (28) after only a few passages in vitro. Instead, RASFs in culture tend to converge into a mixed phenotype with homogeneous characteristics (28). Therefore, we determined surface expression of HLA–DR and CD90, the latter being a surrogate measure of positional identity (28), using flow cytometry. Cultured synovial fibroblasts in our study consistently expressed CD90 but not HLA–DR (Figures 4A and B), indicating that CD90 and positional identity may be regulated differently than HLA–DR. In monocultures with the NK cell–activating cytokine IL-2, surface markers on CD90+ synovial fibroblasts were unchanged, including HLA–DR, HLA–ABC, CD54 (intercellular adhesion

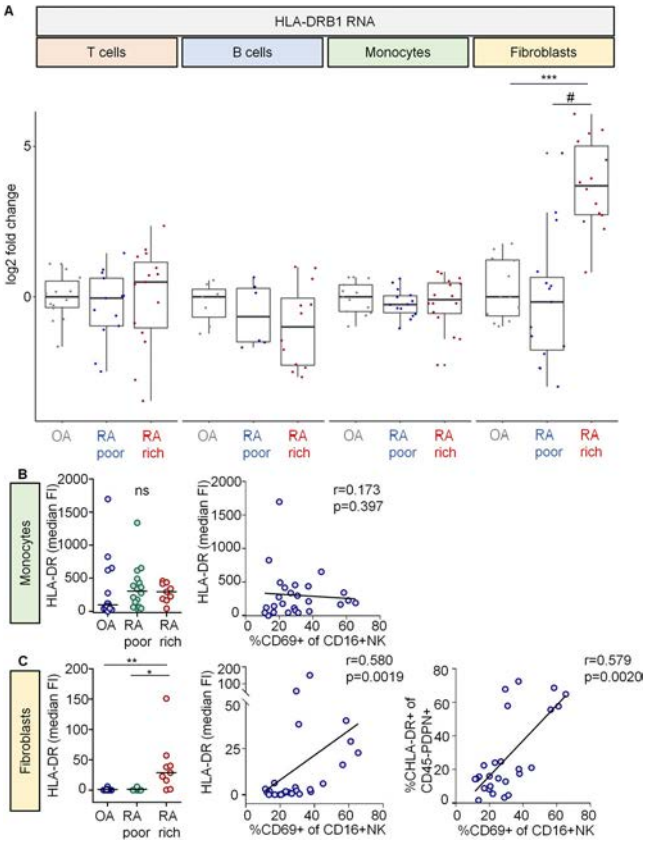

Figure 3. Cell type–specific alterations of HLA–DR expression in leukocyte-rich RA synovial tissue. **A,** HLA–DRB1 RNA expression profiles from sorted populations of T cells, B cells, monocytes, and synovial fibroblasts. Values are the $\log_2$ fold change in expression of HLA–DRB1 RNA in leukocyte-poor and leukocyte-rich RA synovial tissue compared to OA synovial tissue (OA samples, T cells n = 14, B cells n = 7, monocytes n = 13, fibroblasts n = 12; leukocyte-poor RA samples, T cells n = 13, B cells n = 6, monocytes n = 14, fibroblasts n = 15; leukocyte-rich RA samples, T cells n = 15, B cells n = 12, monocytes n = 16, fibroblasts n = 14). Significant differences between OA, leukocyte-poor and leukocyte-rich RA only within the fibroblast group were observed ($P = 2.7 \times 10^{-5}$, by Kruskal-Wallis test). Values are shown as box plots, where lines inside the box represent the median, the boxes represent the interquartile range, and whiskers represent the maximum and minimum range. *** = $P = 2.5 \times 10^{-6}$; # = $P = 5.3 \times 10^{-5}$. **B** and **C**, Protein expression of HLA–DR in manually gated cells from the mass cytometry data set. Left panels show the median FI of HLA–DR expression in CD45+CD14+ monocytes (**B**) and CD45-negative podoplanin-positive (PDPN+) synovial fibroblasts (**C**) from each group of synovial samples. Group comparisons by Kruskal-Wallis test revealed significant differences between OA, leukocyte-poor and leukocyte-rich RA only within synovial fibroblasts in **C**. Significant differences on post hoc tests are indicated. Middle panels show correlations between HLA–DR protein levels in monocytes (**B**) or fibroblasts (**C**) and percentage of activated CD69+CD16+ synovial NK cells. Right panel in **C** shows correlation between percentage of CD45–PDPN+ fibroblasts and percentage of activated CD69+CD16+ synovial NK cells. Percentages of HLA–DR+ monocytes are not shown (all cells were positive). Correlation analyses were performed using Spearman's correlation test. * = $P < 0.05$; ** = $P < 0.01$. NS = not significant (see Figure 1 for other definitions). Color figure can be viewed in the online issue, which is available at http://onlinelibrary.wiley.com/doi/10.1002/art.41958/abstract.

molecule 1 [ICAM-1]), and CD90 (Figures 4A–D and Supplementary Figure 4, http://onlinelibrary.wiley.com/doi/10.1002/art.41958). In contrast, the addition of NK cells was associated with increased levels of CD54 and HLA–ABC and with a de novo induction of HLA–DR (Figures 4A–D). Furthermore, we detected IFNγ in the supernatant of IL-2–treated cocultures, which was most likely produced by NK cells (Supplementary Figure 1).

Moreover, synovial fibroblasts cocultured with IL-2–activated NK cells produced IL-6, as determined using intracellular flow cytometry (Figure 4E). IL-6 secretion was confirmed by treating synovial fibroblasts with NK supernatant (Figure 4F).

In order to further evaluate the inflammatory characteristics of HLA–DR+CD90+ synovial fibroblasts, we established a coculture

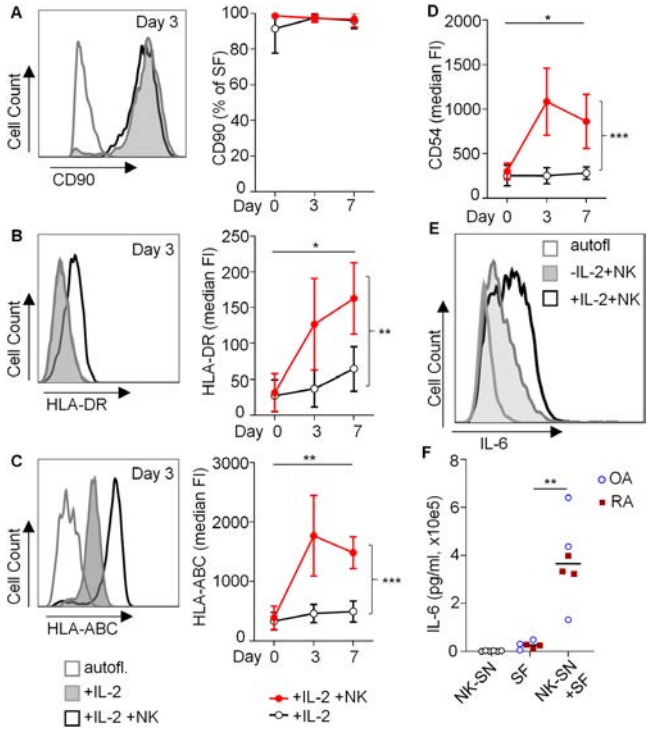

Figure 4. Induction of HLA–DR and IL-6 in CD90+ synovial fibroblasts by activated NK cells in cocultures. **A–D**, Synovial fibroblasts from 3 OA patients were cultured in the absence or presence of IL-2–activated NK cells. Surface expression of CD90 (**A**), HLA–DR (**B**), HLA–ABC (**C**), and CD54 (intercellular adhesion molecule 1) (**D**) was analyzed by flow cytometry. Here, representative histograms (left) and quantification of expression (as percentages or median FI) (right) are shown. Values are the mean ± SD of 3 identical experiments. Day 0 indicates untreated synovial fibroblasts. * = $P < 0.05$; ** = $P < 0.01$; *** = $P < 0.001$, by two-way analysis of variance. **E**, Intracellular staining for IL-6 in OASFs after direct coculture with NK cells over 3 days. One of 2 similar experiments is shown. **F**, For quantification of secreted IL-6, OASFs and RASFs (n = 3 each) were cultured for 3 days with or without 20% pooled NK supernatant. Supernatants were analyzed using enzyme-linked immunosorbent assay (ELISA). Symbols represent individual samples; horizontal lines indicate the mean. ** = $P = 0.0022$, by Mann–Whitney test. In the same ELISA, relevant amounts of IL-6 in NK supernatant were excluded (n = 6). Autofl. = autofluorescence (see Figure 1 for other definitions). Color figure can be viewed in the online issue, which is available at http://onlinelibrary.wiley.com/doi/10.1002/art.41958/abstract.

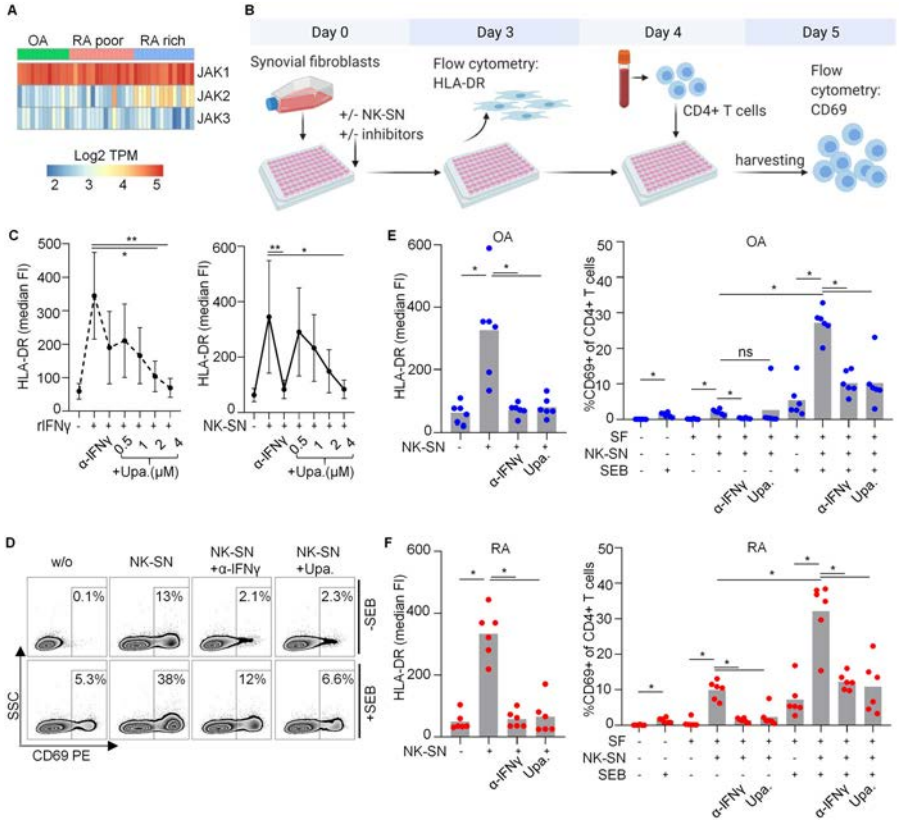

Figure 5. Effect of upadacitinib (Upa.) on the induction of proinflammatory HLA–DR+CD90+ RASFs by NK cell–derived IFNγ. **A**, Shown is the relative mRNA expression of JAK1, JAK2, and JAK3 in synovial fibroblasts in vivo, as displayed on a heatmap with results expressed as log_2-transformed transcripts per million (TPM) in sorted synovial fibroblasts from OA synovial tissue (n = 12), leukocyte-poor RA synovial tissue (n = 15), and leukocyte-rich RA synovial tissue (n = 14). **B–F**, Synovial fibroblasts were cultured with pooled NK cell supernatant with or without anti-IFNγ or JAK1 inhibitor upadacitinib and were subsequently incubated with *Staphylococcus aureus* enterotoxin B (SEB). After washing, freshly isolated CD4+ T cells were added overnight. CD69 expression as a measure of CD4+ T cell activation was analyzed by flow cytometry. **B**, Schematic experimental design. **C**, Expression of HLA–DR on synovial fibroblasts cultured with rIFNγ or NK cell supernatant, and different concentrations of upadacitinib (n = 2 RASFs and n = 3 OASFs receiving 4 μ*M*; n = 3 RASFs and n = 4 OASFs receiving the remaining concentrations). Anti-IFNγ (50 μg/ml) served as a control. Kruskal-Wallis test was used for group comparisons. Significant differences on post hoc tests are indicated. **D–F**, In 6 parallel experiments, synovial fibroblasts from 6 OA patients and 4 RA patients were treated with NK supernatant with or without 4 μ*M* of upadacitinib and with or without SEB. **D**, Representative dot plots show CD4+ T cells and the degree of their CD69 expression under each condition. SSC = sideward scatter; PE = phycoerythrin. **E** and **F,** Expression of HLA–DR in OASFs (**E**) and RASFs (**F**) was assessed in each culture condition (left), and CD69 expression in CD4+ T cells from OA patients and RA patients was also assessed (right). * = $P < 0.05$; ** = $P < 0.01$, by Wilcoxon's test applied to groups of biological interest. NS = not significant (see Figure 1 for other definitions). Color figure can be viewed in the online issue, which is available at http://onlinelibrary.wiley.com/doi/10.1002/art.41958/abstract.

system in which synovial fibroblasts were first treated with NK supernatant and then cocultured overnight with CD4+ T cells that were freshly isolated from healthy donors. Significantly more T cells expressed the activation marker CD69 when cocultured with synovial fibroblasts that were pretreated with NK supernatant (Supplementary Figure 5, available on the *Arthritis & Rheumatology* website at http://onlinelibrary.wiley.com/doi/10.1002/art.41958).

Next, we wanted to know whether surface MHC class II levels in HLA–DR+CD90+ synovial fibroblasts are stable and potentially functionally relevant. We found that crosslinking NK supernatant–induced MHC class II with T cell receptors using superantigen SEB up-regulated the activation marker CD69 in CD4+ T cells (Figure 5 and Supplementary Figure 5, http://onlinelibrary.wiley.com/doi/10.1002/art.41958). We chose this approach to circumvent issues related to the allogenic experimental design. This surrogate measure of CD4+ T cell activation was not observed when synovial fibroblasts were treated with NK supernatant in the presence of a monoclonal anti-IFNγ antibody. In contrast, blocking TNF in NK supernatant with adalimumab had no effect on HLA–DR expression or the surrogate measure of CD4+ T cell activation (Supplementary Figure 5, http://onlinelibrary.wiley.com/doi/10.1002/art.41958). These data indicated that NK cell–derived IFNγ induces MHC class II in synovial fibroblasts in sufficient quantity and with sufficient stability to activate CD4+ T cells by means of superantigens. Consistent with these data, when summarizing the results of all the SEB experiments, MHC class II expression in synovial fibroblasts correlated with the percentage of CD69+CD4+ T cells in the presence of SEB (Figure 6). Taken together, these data

show that, on the protein level, NK cells induce an inflammatory, cytokine-secreting, T cell–activating, HLA–DR+ phenotype in CD90+ synovial fibroblasts.

Dependency of IFNγ-induced HLA–DR in synovial fibroblasts on JAK signaling. IFNγ receptor chains 1 and 2 intracellularly bind to JAK1 and JAK2, which activate STAT1 to dimerize and act as transcription factors (29). We investigated expression levels of these IFNγ pathway transcripts in the AMP-RA database. The receptor chains were unaltered in RA (data not shown). Almost all RASFs expressed JAK1 (~90% in most subsets). Levels of JAK2 were significantly increased in leukocyte-rich RA synovial samples as compared to leukocyte-poor RA and OA synovial samples ($P = 2 \times 10^{-5}$), with the highest percentage of positive cells in the HLA–DR+CD90+ subset (62.9%). The remaining JAK3 and Tyk2 were expressed in <20% of synovial fibroblasts and in 31.2–50.1% of synovial fibroblasts, respectively. Levels of STAT1 were increased in leukocyte-rich RA ($P = 4 \times 10^{-5}$), and 91% of HLA–DR+CD90+ synovial fibroblasts expressed STAT1. By re-analyzing raw AMP-RA bulk RNA-seq data, we confirmed that JAK1 mRNA expression dominated over JAK2 and JAK3 mRNA expression (Figure 5A). These data indicate that the signaling capacities of the IFNγ pathway in HLA–DR+CD90+ synovial fibroblasts are unaltered or increased in vivo, at least at the mRNA level.

JAK inhibition is a new and effective treatment strategy in RA. The approved JAK inhibitors tofacitinib, baricitinib, and upadacitinib are relatively specific to JAK1/3, JAK1/2, and JAK1, respectively. Upadacitinib had a significant, dose-dependent inhibitory effect on HLA–DR levels in synovial fibroblasts induced by both recombinant IFNγ and NK supernatant (Figures 5C–F). Similar to blocking anti-IFNγ antibody, treatment of synovial fibroblasts using upadacitinib prevented CD4+ T cell activation by SEB (after stimulation with NK supernatant) (Figures 5E and F). Tofacitinib and baricitinib also tended to inhibit NK supernatant–induced HLA–DR induction in synovial fibroblasts (Supplementary Figure 6, http://onlinelibrary.wiley.com/doi/10.1002/art.41958).

Because of the increased JAK2 mRNA levels in leukocyte-rich RA synovial samples in vivo (see above), we stimulated RASFs with NK supernatant and measured levels of JAK2 protein and its phosphorylation using Western blotting. We found that JAK2 protein levels were increased after stimulation over the course of 3 days. JAK2 was phosphorylated after 30 minutes of stimulation, but the intensity of phosphorylation of JAK2 attenuated after 3 days of stimulation with NK supernatant (Supplementary Figure 6, available on the *Arthritis & Rheumatology* website at http://onlinelibrary.wiley.com/doi/10.1002/art.41958).

Taken together, these findings indicate that NK cells can activate the JAK1/2 pathway in synovial fibroblasts. The induction of HLA–DR and the inflammatory characteristics of synovial fibroblasts induced by NK cell–derived IFNγ could be blocked using the JAK inhibitor upadacitinib.

Intrinsically enhanced capacity of HLA–DR+CD90+ RASFs induced by NK cell–derived IFNγ to activate CD4+ T cells, as compared to OASFs. Interestingly, we observed that synovial fibroblasts pretreated with NK supernatant could also induce CD69 in CD4+ T cells in the absence of SEB (Figure 6). This effect was ~4 times stronger in RASFs than in OASFs. While the allogenic experimental design may contribute to T cell activation, alloreactivity alone does not explain the differences between RASFs and OASFs. Induced HLA–DR levels were comparable in RASFs and OASFs (e.g., see Figure 5). SEB-independent CD69 up-regulation in CD4+ T cells was initiated by NK cell–derived IFNγ and could be blocked using anti-IFNγ and upadacitinib (Figures 6B and 5F). Taken together, these findings show that NK cell–derived IFNγ can increase cross-talk between RASFs and CD4+ T cells.

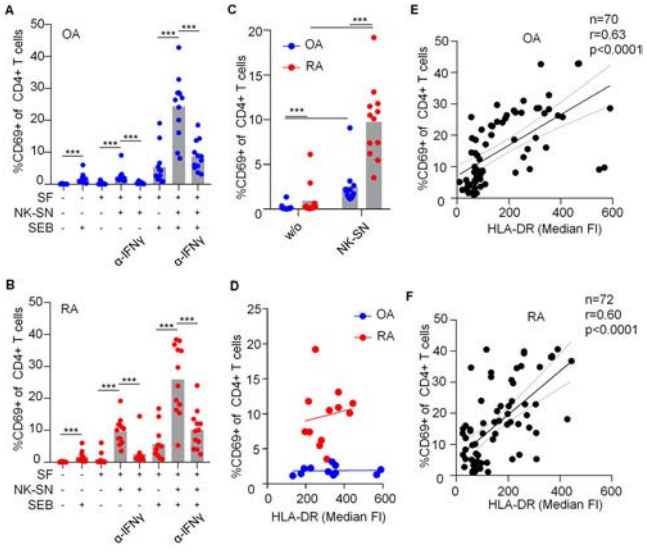

Figure 6. Intrinsically enhanced capacity of HLA–DR+CD90+ RASFs induced by NK cell–derived IFNγ to activate CD4+ T cells, as compared to OASFs. **A–D**, For a summarizing statistical analysis and direct comparison of the effect of OASFs and RASFs on CD4+ T cells, data derived from all experiments using *Staphylococcus aureus* enterotoxin B (SEB) under identical conditions were pooled (n = 12). **A** and **B**, Percentage of CD69+CD4+ T cells after coculture with OASFs (**A**) and RASFs (**B**) under the different culture conditions. **C**, Direct comparison of the effect of OASFs and RASFs on CD4+ T cell activation in the absence of SEB. **D**, Percentage of CD69+CD4+ T cells in relation to HLA–DR expression in OASFs and RASFs that were pretreated with pooled NK supernatant (n = 11 OA patients [exclusion of the outlier in **C** did not have a relevant effect on the statistical results; r = 0.160; $P = 0.6$]; n = 12 RA patients [r = 0.165; $P = 0.6$]). In **A**–**C**, *** = $P < 0.001$, by Wilcoxon's tests comparing groups of biological interest. **E** and **F**, Pooled data from all experiments and conditions in which the median FI of HLA–DR expression in synovial fibroblasts and the percentage of CD69+CD4+ T cells after coculture overnight were both assessed in parallel. Correlation analyses were performed using Spearman's correlation test; r = correlation coefficient. See Figure 1 for other definitions. Color figure can be viewed in the online issue, which is available at http://onlinelibrary.wiley.com/doi/10.1002/art.41958/abstract.

This proinflammatory RASF/CD4+ T cell cross-talk can be prevented with the use of JAK blockade on the side of RASFs.

DISCUSSION

Synovial fibroblasts are an attractive therapeutic target in RA. Findings from a recent resource study identified synovial fibroblast subsets in RA (5). HLA–DR+CD90+ synovial fibroblasts are expanded and are characterized by the presence of a proinflammatory phenotype and a strong IFNγ signature. These cells were suggested to be major producers of IL-6 and expressed genes that are involved in antigen processing and presentation. However, some of these findings have not yet been verified on the protein level. The signals relevant to the generation of HLA–DR+CD90+ synovial fibroblasts have not been validated in functional assays.

To address these open questions, we combined focused analyses of mass cytometry and transcriptomics patient data sets with a series of functional assays assessing human primary cells in vitro. Our findings confirm that on the protein level IFNγ induces an inflammatory HLA–DR+CD90+ phenotype in synovial fibroblasts. This includes the expression of HLA–DR and IFNγ-induced genes such as ICAM-1 and the secretion of IL-6. Importantly, we demonstrate that HLA–DR+CD90+ synovial fibroblasts possess a functional proinflammatory phenotype by physically interacting with cells from the adaptive immune system.

We hypothesized that NK cells may provide IFNγ to synovial fibroblasts. Findings from the mass cytometry analyses showed that CD16+ NK cells are physically present in synovial tissue and are activated in patients with active RA. Even though CD16+ NK cells include only 1 of 2 major NK cell subsets, these cells may be of importance in RA, given that the Fc-receptor CD16 can be triggered by local immune complexes and that CD16 is a potential risk gene for RA (20,30). CD16 triggers the secretion of IFNγ by NK cells, which may be enhanced by the proinflammatory environment (24). Evidence of synovial (CD16+) NK cells was also demonstrated in studies with smaller sample sizes by conducting bulk RNA-seq using CIBERSORTx (19) or by using clustering strategies for single-cell RNA-seq data to detect NK cells (18).

Indeed, NK cell–derived IFNγ induces HLA–DR in CD90+ synovial fibroblasts in vitro. Our findings indicate that activated NK cells induce a global proinflammatory fibroblast phenotype characterized by HLA–DR+CD90+IL-6+ICAM-1+HLA–ABC^{bright}JAK2^{bright} cells with inflammatory characteristics and (per its activation stimulus) an IFNγ signature that resembles the phenotype of HLA–DR+CD90+ synovial fibroblasts in vivo (5). Thus, the in vivo RNA expression profile of HLA–DR+CD90+ synovial fibroblasts is likely related to an inducible, functional phenotype with proinflammatory characteristics, consistent with findings in mouse models of arthritis (31).

Despite potential redundancy with CD8+ T cells, it is important to consider that NK cells provide IFNγ (5). Both cell types secrete IFNγ, but the stimuli for IFNγ secretion are different. Therefore, both cell types may be important depending on environmental conditions. The exact triggers of NK cell activation in vivo remain poorly characterized, but in our reporter model, we showed that soluble immune complexes within synovial fluid from seropositive RA patients can stimulate CD16 signaling. CD16 is a potential risk gene for RA (20,30). These data support the idea that immune complexes play a role in RA (32–34), and indicate immune complex–mediated activation of NK cells. Cytokines and direct cell–cell interaction involving innate NK cell receptor ligands may also contribute to the activation of synovial NK cells, and most likely a combination of these factors is found in vivo. We suggest that immune complex–activated NK cells may contribute to the more severe clinical disease course in seropositive RA compared to seronegative RA. Despite these functional considerations, the findings do not allow for a complete picture with regard to the quantitative contribution of NK cells to synovial IFNγ in RA.

Apart from being a suitable surface marker to distinguish HLA–DR+CD90+ synovial fibroblasts from other synovial fibroblast subsets (5), our findings show that surface MHC class II in synovial fibroblasts is stable, enabling superantigen presentation (11). Even though we did not investigate autoantigen presentation or antigen-specific T cell reactions, our findings regarding the presence of stable MHC class II following induction by NK supernatant in synovial fibroblasts are important, since results from other studies have demonstrated that synovial fibroblasts can present autoantigens/antigens via MHC class II (10–12). It is difficult to quantify antigen presentation by synovial fibroblasts in comparison to other antigen-presenting cells, like monocytes. However, synovial fibroblasts are the most numerous synovial cell type in OA synovium as well as in leukocyte-poor RA synovium, and they remain an important cell fraction upon leukocyte infiltration, with the subpopulation of HLA–DR+CD90+ synovial fibroblasts being increased 15-fold in active RA (5). We therefore suggest that antigen presentation by synovial fibroblasts may be relevant, especially since levels of the key MHC class II allele HLA–DRB1 were significantly increased only in synovial fibroblasts and were restricted to active RA.

Further studies sustain a role of local, i.e., synovial, antigen presentation to CD4+ T cells in RA (18). Synovial CD4+ peripheral helper T cells are expanded in seropositive RA and express activation markers such as CD69 (35). Peripheral helper T cells strongly express the IL-6 receptor and promote B cell differentiation and antibody production (18,35). Beyond this, not much is known about the impact of synovial fibroblasts on T cell activation, even though the release of chemokines and cytokines, as well as several membrane-bound molecules, such as CD54, were involved in the recruitment and activation of CD4+ T cells in RA, indicating complex reciprocal interactions (36–39). Taken together, evidence from several sources indicate that HLA–DR+CD90+ synovial fibroblasts may play a role in synovial antigen presentation and T cell support in RA. Our results add to these findings and indicate that this can be increased, or even initiated, by IFNγ, and, consequently, suppressed by JAK inhibition.

HLA–DR+CD90+ synovial fibroblasts from RA patients possess an intrinsically increased capability to activate CD4+ T cells in response to IFNγ. While it is well-described that synovial fibroblasts lose certain characteristics during culture in vitro (28), it is also broadly accepted that synovial fibroblasts possess an imprinted aggressive phenotype (40). Epigenetic factors may prime synovial fibroblasts for a phenotype of enhanced inflammation, probably paving the way for memory or recall inflammatory responses that may be initiated by IFNγ. Taken together with the findings from the study by Wei et al showing that the positional identity of synovial fibroblasts can be induced by Notch signaling (28), our data indicate that HLA–DR+CD90+ synovial fibroblasts represent an inducible phenotype in synovial fibroblasts, most likely equivalent to an activation state, and not a classic, unchangeable cell subset. Given that this phenotype may play a central role in RA pathogenesis, blocking induction of the HLA–DR+CD90+ synovial fibroblast phenotype may represent a promising, new fibroblast-centered therapeutic strategy. To date, it has not been investigated whether HLA–DR+CD90+ synovial fibroblasts can be specifically targeted.

Importantly, our data and findings from another study show that JAK inhibition suppresses the impact of IFNγ on synovial fibroblasts in vitro (41), including HLA–DR induction and the enhancing effect on fibroblast/CD4+ T cell interactions. The link between JAK inhibition and the pathogenic role IFNγ plays in RA has been mainly hypothetical to date (42). However, our data suggest that JAK1 inhibition using upadacitinib may block the development of HLA–DR+CD90+ synovial fibroblasts. Preventing synovial fibroblasts from acquiring this activation state may be an important, yet currently underappreciated, mechanism of action for upadacitinib in RA.

We conclude that the HLA–DR+CD90+ synovial fibroblast phenotype is an activation state that can be induced by IFNγ, potentially provided from infiltrating leukocytes such as CD16+ NK cells in inflamed synovial tissue. Generation of these proinflammatory, IL-6–producing, and likely antigen-presenting synovial fibroblasts can be targeted using the JAK1 inhibitor upadacitinib. Based on our findings and as depicted in Supplementary Figure 7 (http://onlinelibrary.wiley.com/doi/10.1002/art.41958), we propose that a proinflammatory vicious circle occurs within the complex proinflammatory environment in RA, involving self-reinforcing cross-talk between innate immune cells, stromal cells, and adaptive immune cells.

AUTHOR CONTRIBUTIONS

All authors were involved in drafting the article or revising it critically for important intellectual content, and all authors approved the final version to be published. Dr. Merkt had full access to all of the data in the study and takes responsibility for the integrity of the data and the accuracy of the data analysis.

Study conception and design. Tretter, Lorenz, Watzl, Wabnitz, Tykocinski, Merkt.

Acquisition of data. Zhao, Kolb, Chen, Andreeva, Tykocinski, Merkt.

Analysis and interpretation of data. Zhao, Grieshaber-Bouyer, Rao, Kolb, Chen, Andreeva, Tretter, Lorenz, Watzl, Wabnitz, Tykocinski, Merkt.

ACKNOWLEDGMENTS

We would like to thank the Accelerating Medicines Partnership for generating publicly accessible synovial tissue data. We also thank Peter Nigrovic for connecting people, Xin Guan for helping with the IL-6 enzyme-linked immunosorbent assays, Stefan Krienke and Sabine Wingert for technical support, and Doris Urlaub and Maren Claus for their valuable advice.

REFERENCES

1. McInnes IB, Schett G. The pathogenesis of rheumatoid arthritis. N Engl J Med 2011;365:2205–19.
2. Okada Y, Wu D, Trynka G, Raj T, Terao C, Ikari K, et al. Genetics of rheumatoid arthritis contributes to biology and drug discovery. Nature 2014;506:376–81.
3. Raychaudhuri S, Sandor C, Stahl EA, Freudenberg J, Lee HS, Jia X, et al. Five amino acids in three HLA proteins explain most of the association between MHC and seropositive rheumatoid arthritis. Nat Genet 2012;44:291–6.
4. Bartok B, Firestein GS. Fibroblast-like synoviocytes: key effector cells in rheumatoid arthritis. Immunol Rev 2010;233:233–55.
5. Zhang F, Wei K, Slowikowski K, Fonseka CY, Rao DA, Kelly S, et al. Defining inflammatory cell states in rheumatoid arthritis joint synovial tissues by integrating single-cell transcriptomics and mass cytometry. Nat Immunol 2019;20:928–42.
6. Chu CQ. Fibroblasts in rheumatoid arthritis. N Engl J Med 2020;383:1679–81.
7. Schett G. Physiological effects of modulating the interleukin-6 axis. Rheumatology (Oxford) 2018;57 Suppl 2:ii43–50.
8. Duraes FV, Thelemann C, Sarter K, Acha-Orbea H, Hugues S, Reith W. Role of major histocompatibility complex class II expression by non-hematopoietic cells in autoimmune and inflammatory disorders: facts and fiction. Tissue Antigens 2013;82:1–15.
9. Kambayashi T, Laufer TM. Atypical MHC class II-expressing antigen-presenting cells: can anything replace a dendritic cell? Nat Rev Immunol 2014;14:719–30.
10. Tran CN, Davis MJ, Tesmer LA, Endres JL, Motyl CD, Smuda C, et al. Presentation of arthritogenic peptide to antigen-specific T cells by fibroblast-like synoviocytes. Arthritis Rheum 2007;56:1497–506.
11. Carmona-Rivera C, Carlucci PM, Moore E, Lingampalli N, Uchtenhagen H, James E, et al. Synovial fibroblast-neutrophil interactions promote pathogenic adaptive immunity in rheumatoid arthritis. Sci Immunol 2017;2:eaag3358.
12. Sugawara E, Kato M, Kudo Y, Lee W, Hisada R, Fujieda Y, et al. Autophagy promotes citrullination of VIM (vimentin) and its interaction with major histocompatibility complex class II in synovial fibroblasts. Autophagy 2020;16:946–55.
13. Vivier E, Tomasello E, Baratin M, Walzer T, Ugolini S. Functions of natural killer cells. Nat Immunol 2008;9:503–10.
14. Yamin R, Berhani O, Peleg H, Aamar S, Stein N, Gamliel M, et al. High percentages and activity of synovial fluid NK cells present in patients with advanced stage active rheumatoid arthritis. Sci Rep 2019;9:1351.
15. Pridgeon C, Lennon GP, Pazmany L, Thompson RN, Christmas SE, Moots RJ. Natural killer cells in the synovial fluid of rheumatoid arthritis patients exhibit a $CD56^{bright}$,$CD94^{bright}$,$CD158^{negative}$ phenotype. Rheumatology (Oxford) 2003;42:870–8.
16. Dalbeth N, Gundle R, Davies RJ, Lee YC, McMichael AJ, Callan MF. $CD56^{bright}$ NK cells are enriched at inflammatory sites and can engage with monocytes in a reciprocal program of activation. J Immunol 2004;173:6418–26.

17. Dalbeth N, Callan MF. A subset of natural killer cells is greatly expanded within inflamed joints. Arthritis Rheum 2002;46:1763–72.
18. Stephenson W, Donlin LT, Butler A, Rozo C, Bracken B, Rashidfarrokhi A, et al. Single-cell RNA-seq of rheumatoid arthritis synovial tissue using low-cost microfluidic instrumentation. Nat Commun 2018;9:791.
19. Orange DE, Agius P, DiCarlo EF, Robine N, Geiger H, Szymonifka J, et al. Identification of three rheumatoid arthritis disease subtypes by machine learning integration of synovial histologic features and RNA sequencing data. Arthritis Rheumatol 2018;70:690–701.
20. Lee YH, Bae SC, Song GG. FCGR2A, FCGR3A, FCGR3B polymorphisms and susceptibility to rheumatoid arthritis: a meta-analysis. Clin Exp Rheumatol 2015;33:647–54.
21. Bryceson YT, March ME, Ljunggren HG, Long EO. Synergy among receptors on resting NK cells for the activation of natural cytotoxicity and cytokine secretion. Blood 2006;107:159–66.
22. Urlaub D, Zhao S, Blank N, Bergner R, Claus M, Tretter T, et al. Activation of natural killer cells by rituximab in granulomatosis with polyangiitis. Arthritis Res Ther 2019;21:277.
23. Corrales-Aguilar E, Trilling M, Reinhard H, Merce-Maldonado E, Widera M, Schaal H, et al. A novel assay for detecting virus-specific antibodies triggering activation of Fcγ receptors. J Immunol Methods 2013;387:21–35.
24. Campbell AR, Regan K, Bhave N, Pattanayak A, Parihar R, Stiff AR, et al. Gene expression profiling of the human natural killer cell response to Fc receptor activation: unique enhancement in the presence of interleukin-12. BMC Med Genomics 2015;8:66.
25. Chen H, Maul-Pavicic A, Holzer M, Huber M, Salzer U, Chevalier N, et al. Detection and functional resolution of soluble immune complexes by an FcγR reporter cell panel. EMBO Mol Med 2021:e14182.
26. Imai C, Iwamoto S, Campana D. Genetic modification of primary natural killer cells overcomes inhibitory signals and induces specific killing of leukemic cells. Blood 2005;106:376–83.
27. Prager I, Liesche C, van Ooijen H, Urlaub D, Verron Q, Sandstrom N, et al. NK cells switch from granzyme B to death receptor-mediated cytotoxicity during serial killing. J Exp Med 2019;216:2113–27.
28. Wei KV, Korsunsky I, Marshall JL, Gao AQ, Watts GF, Major T, et al. Notch signalling drives synovial fibroblast identity and arthritis pathology. Nature 2020;582:259–64.
29. Alspach E, Lussier DM, Schreiber RD. Interferon γ and its important roles in promoting and inhibiting spontaneous and therapeutic cancer immunity [review]. Cold Spring Harb Perspect Biol 2019;11:a028480.
30. Morgan AW, Barrett JH, Griffiths B, Subramanian D, Robinson JI, Keyte VH, et al. Analysis of Fcγ receptor haplotypes in rheumatoid arthritis: FCGR3A remains a major susceptibility gene at this locus, with an additional contribution from FCGR3B. Arthritis Res Ther 2006;8:R5.
31. Croft AP, Campos J, Jansen K, Turner JD, Marshall J, Attar M, et al. Distinct fibroblast subsets drive inflammation and damage in arthritis. Nature 2019;570:246–51.
32. Nielen MM, van Schaardenburg D, Reesink HW, van de Stadt RJ, van der Horst-Bruinsma IE, de Koning MH, et al. Specific autoantibodies precede the symptoms of rheumatoid arthritis: a study of serial measurements in blood donors. Arthritis Rheum 2004;50:380–6.
33. Arend WP, Firestein GS. Pre-rheumatoid arthritis: predisposition and transition to clinical synovitis [review]. Nat Rev Rheumatol 2012;8:573–86.
34. Pfeifle R, Rothe T, Ipseiz N, Scherer HU, Culemann S, Harre U, et al. Regulation of autoantibody activity by the IL-23-TH17 axis determines the onset of autoimmune disease. Nat Immunol 2017;18:104–13.
35. Rao DA, Gurish MF, Marshall JL, Slowikowski K, Fonseka CY, Liu Y, et al. Pathologically expanded peripheral T helper cell subset drives B cells in rheumatoid arthritis. Nature 2017;542:110–4.
36. Yoshitomi H. Regulation of immune responses and chronic inflammation by fibroblast-like synoviocytes. Front Immunol 2019;10:1395.
37. Bombara MP, Webb DL, Conrad P, Marlor CW, Sarr T, Ranges GE, et al. Cell contact between T cells and synovial fibroblasts causes induction of adhesion molecules and cytokines. J Leukoc Biol 1993;54:399–406.
38. Haynes BF, Grover BJ, Whichard LP, Hale LP, Nunley JA, McCollum DE, et al. Synovial microenvironment-T cell interactions: human T cells bind to fibroblast-like synovial cells in vitro. Arthritis Rheum 1988;31:947–55.
39. Tykocinski LO, Lauffer AM, Bohnen A, Kaul NC, Krienke S, Tretter T, et al. Synovial fibroblasts selectively suppress Th1 cell responses through IDO1-mediated tryptophan catabolism. J Immunol 2017;198:3109–17.
40. Bottini N, Firestein GS. Duality of fibroblast-like synoviocytes in RA: passive responders and imprinted aggressors [review]. Nat Rev Rheumatol 2013;9:24–33.
41. Karonitsch T, Beckmann D, Dalwigk K, Niederreiter B, Studenic P, Byrne RA, et al. Targeted inhibition of Janus kinases abates interfon γ-induced invasive behaviour of fibroblast-like synoviocytes. Rheumatology (Oxford) 2018;57:572–7.
42. Kato M. New insights into IFN-γ in rheumatoid arthritis: role in the era of JAK inhibitors. Immunol Med 2020;43:72–8.

Arthritis & Rheumatology
Vol. 74, No. 3, March 2022, pp 453–461
DOI 10.1002/art.41231

American College of Rheumatology
Empowering Rheumatology Professionals

Association Between Race and Radiographic, Symptomatic, and Clinical Hand Osteoarthritis: A Propensity Score–Matched Study Using Osteoarthritis Initiative Data

Farhad Pishgar,[1] Robert M. Kwee,[2] Arya Haj-Mirzaian,[3] Ali Guermazi,[4] Ida K. Haugen,[5] and Shadpour Demehri[3]

Objective. To determine the associations between Black race and the presence of radiographic, symptomatic, and clinical hand osteoarthritis (OA).

Methods. Using available hand radiographs from the Osteoarthritis Initiative cohort (total 4,699; n = 849 Black subjects [18.1%], n = 3,850 non-Black subjects [81.9%]), a propensity score–matching method was used to match Black subjects with non-Black subjects for known potential risk factors of hand OA (age, sex, body mass index, smoking status, cardiovascular disease, osteoporosis, excessive occupation- or recreation-related hand use, and knee OA). Posteroanterior radiographs of subjects' dominant hands were reviewed by a musculoskeletal radiologist in a blinded manner. To assess the severity of hand OA, the modified Kellgren/Lawrence (K/L) radiographic OA scoring scale (grades 0–4) was used, and the presence of erosive OA in the hand joints was recorded. Associations between race and the severity of hand OA (measured as the summed modified K/L grade), presence of radiographic hand OA (modified K/L grade ≥2), presence of erosive hand OA, presence of symptomatic hand OA (radiographic OA with hand pain), and presence of clinical hand OA (indicated by clinical findings of Heberden's nodes in the hands) were studied using regression models. In these models, beta coefficients or odds ratios (ORs) with 95% confidence intervals (95% CIs) were calculated for the associations between Black race and any of these radiographic and symptomatic hand OA phenotypes.

Results. Black subjects had less severe hand OA (β = –1.93 [95% CI –2.53, –1.34]), as well as a lower risk of developing radiographic hand OA (OR 0.79 [95% CI 0.66, 0.94]), erosive hand OA (OR 0.23 [95% CI 0.11, 0.47]), symptomatic hand OA (OR 0.63 [95% CI 0.49, 0.82]), and clinical hand OA (OR 0.49 [95% CI 0.41, 0.60]), as compared to non-Black subjects.

Conclusion. In contrast to the well-established association between Black race and knee or hip OA, the findings of this study suggest that the risk of hand OA is lower in Black subjects compared to non-Black subjects, which is not mediated by known hand OA risk factors. Future studies are warranted to determine the mediating protective factors for hand OA among Black subjects.

INTRODUCTION

Radiographic hand osteoarthritis (OA) is estimated to affect 55–67% of the general population (1), and when symptomatic, this disease is reported to have a clinical burden similar to that of rheumatoid arthritis (RA) in terms of the extent of pain and disability (2). However, there is limited evidence identifying the risk factors and clinical course of this condition. Older age, female sex,

This article was prepared using an Osteoarthritis Initiative (OAI) public-use data set, and its contents do not necessarily reflect the opinions or views of the OAI Study Investigators, the NIH, or the private funding partners of the OAI. The OAI is a public–private partnership between the NIH (contracts N01-AR-2-2258, N01-AR-2-2259, N01-AR-2-2260, N01-AR-2-2261, and N01-AR-2-2262) and private funding partners (Merck Research Laboratories, Novartis Pharmaceuticals, GlaxoSmithKline, and Pfizer, Inc.) and is conducted by the OAI Study Investigators.

[1]Farhad Pishgar, MD, MPH: Johns Hopkins University School of Medicine, Baltimore, Maryland, and Tehran University of Medical Sciences, Tehran, Iran; [2]Robert M. Kwee, MD, PhD: Johns Hopkins University School of Medicine, Baltimore, Maryland, and Zuyderland Medical Center, Heerlen, The Netherlands; [3]Arya Haj-Mirzaian, MD, MPH, Shadpour Demehri, MD: Johns Hopkins University School of Medicine, Baltimore, Maryland; [4]Ali Guermazi, MD, PhD: Boston University School of Medicine, Boston, Massachusetts; [5]Ida K. Haugen, MD, PhD: Diakonhjemmet Hospital, Oslo, Norway.

No potential conflicts of interest relevant to this article were reported.

Deidentified subject data regarding clinical and demographic characteristics are publicly available on the OAI project data repository at https://oai.nih.gov. The data set of hand radiograph readings and the R codes used in this study are available from the corresponding author upon reasonable request.

Address correspondence to Farhad Pishgar, MD, MPH, The Russell H. Morgan Department of Radiology and Radiological Science, Johns Hopkins University School of Medicine, 601 North Caroline Street, JHOC 3142, Baltimore, MD 21287. Email: Farhad.Pishgar@JHMI.edu or Farhad.Pishgar@gmail.com.

Submitted for publication October 24, 2019; accepted in revised form February 11, 2020.

and hereditary factors are associated with hand OA, though findings on other potential risk factors, e.g., body mass index (BMI), smoking status, and race, are still conflicting (3–6).

Previous studies demonstrated that Black subjects experience an increased prevalence and higher severity of radiographic and symptomatic knee and hip OA, and hereditary, environmental, and biomechanical factors have been suggested as possible explanations for this difference (7). However, there is little evidence supporting a potential association between race and hand OA; no difference in the prevalence of symptomatic hand OA was found between Black and non-Black subjects in cross-sectional surveys or between Russian and Buryat populations living in the same area (8,9).

Investigating the association between race and hand OA can lead to a better understanding of the pathogenesis of the disease and proper tailoring of preventive or therapeutic strategies according to race. The aim of the present study was to address this important knowledge gap. Using a propensity score (PS)–matching procedure, an optimal sample of subjects participating in the Osteoarthritis Initiative (OAI) was included in this analysis, their hand radiographs were reviewed by a musculoskeletal radiologist in a blinded manner, and the associations between race and hand OA phenotypes were investigated.

PATIENTS AND METHODS

Study design. Associations between race and hand OA phenotypes were assessed using post hoc analysis of data on radiographic hand OA severity in PS-matched subjects from the OAI cohort. The medical ethics review boards of the University of California, San Francisco (approval no. 10-00532) and the 4 OAI clinical centers recognized the project as Health Insurance Portability and Accountability Act–compliant.

Study population. The OAI project, a multicenter longitudinal study with the aim of assessing the natural history of knee OA development and progression, includes 45–79-year-old subjects with knee OA or who are at risk of knee OA. Subjects with physician-diagnosed inflammatory arthritis (e.g., RA, systemic lupus erythematosus, psoriatic arthritis, or other types of inflammatory arthritis), severe forms of knee OA, or subjects unwilling or unable to participate in the data collection procedures (due to comorbidities, pregnancy, or being unlikely to reside in the clinic area in the upcoming years) were excluded from the OAI (a detailed description of the project can be found at https://oai.nih.gov).

Of the 4,796 subjects who participated in the OAI, 97 subjects were excluded from our analysis due to a lack of available

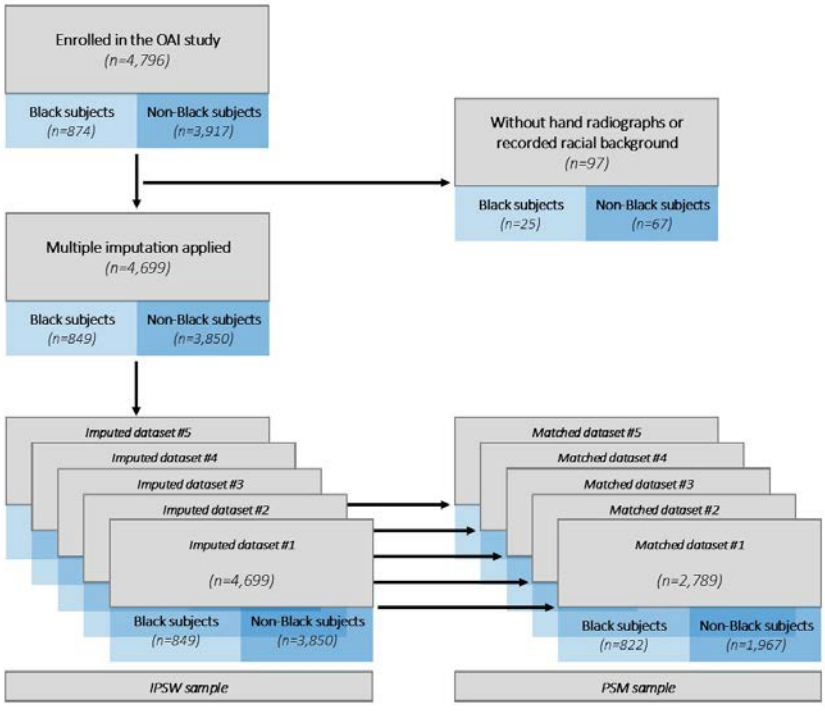

Figure 1. Study flow chart. After excluding subjects from the Osteoarthritis Initiative (OAI) who lacked available baseline hand radiographs (n = 92), as well as those lacking data regarding race (n = 5), 4,699 subjects were included in our analysis. A multiple imputation approach was used to account for missing data, and for each complete imputed data set, propensity score (PS) values were estimated and used in both the PS-matching procedure (for the PS-matched [PSM] sample) and for estimating the PS weights of subjects (for the inverse PS–weighted [IPSW] sample). Subsequently, the associations between race and hand osteoarthritis phenotypes were evaluated. Results were aggregated by pooling estimates obtained for all imputed data sets using Rubin's rules.

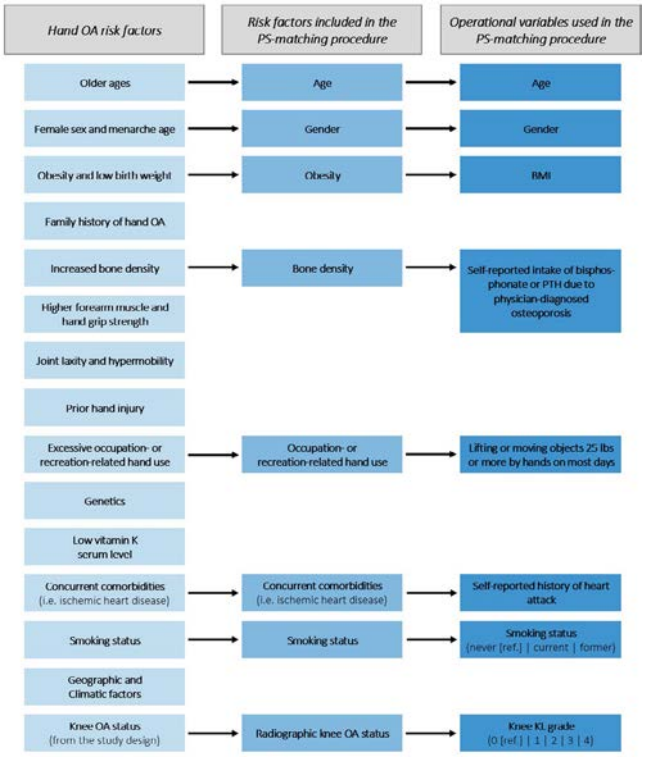

Figure 2. The PS-matching variables. Findings from 2 previously published systematic reviews were used to identify 14 groups of hand osteoarthritis (OA) risk factors. After review by a clinical expert and after limiting the list to the available data in the OAI, 8 operational variables were selected and used as PS-matching variables in the PS-matching procedure. PTH = parathyroid hormone; BMI = body mass index; K/L = Kellgren/Lawrence (see Figure 1 for other definitions).

baseline hand radiographs (n = 92) or lack of data regarding race (n = 5); thus, a total of 4,699 subjects were included (Figure 1).

Selecting PS-matching variables. Findings from the 2 previously published systematic reviews were used to identify 14 groups of hand OA risk factors (3,10). After review by a clinical expert (SD) and after limiting the list to the available data in the OAI, 7 operational variables (age, sex, BMI, smoking status, history of cardiovascular disease [CVD], history of osteoporosis, and excessive occupation- or recreation-related hand use) were selected and used as the matching variables in the model. Moreover, radiographic knee OA status was included in this model to address the potential role of knee OA in the associations between race and hand OA phenotypes (Figure 2).

Race and the PS-matching variable data collection. The online data repository of the OAI was used to obtain the subjects' recorded data regarding self-identified race, age, sex, BMI, smoking status (categorized as never, current, and former smokers), history of heart attack, history of osteoporosis (self-reported intake of bisphosphonate or parathyroid hormone [PTH] due to physician-diagnosed osteoporosis), and excessive occupation- or recreation-related hand use (defined as moving or lifting objects weighing ≥25 pounds on most days), as well as data on several other comorbidities.

Participating subjects underwent bilateral fixed knee flexion radiographic assessment at baseline, and these radiographs were centrally reviewed (11) by trained musculoskeletal radiologists to score OA-related changes using the Kellgren/Lawrence (K/L) scoring scale (ranging from grade 0 [no features of OA] to grade 4 [bone-on-bone appearance]) with acceptable levels of reliability (13).

Hand OA phenotype data collection. Participating subjects also underwent posteroanterior hand radiographic assessment at baseline. For this study, radiographs of the dominant hand or, in the case of ambidextrous subjects, either the dominant hand or the left hand were reviewed by a trained musculoskeletal radiologist (RMK, who has 7 years of experience in the practice) in a blinded manner. The severity of OA-related changes (using a modified K/L scoring scale; see below) and presence of erosive OA (a subtype of hand OA requiring the detection of radiographic central erosions [14]) were assessed in 16 joints of the hands (first interphalangeal [IP] joint, second through fifth distal IP [DIP] joints, second through fifth proximal IP [PIP] joints, first through fifth metacarpophalangeal [MCP] joints, first carpometacarpal [CMC] joint, and scaphotrapeziotrapezoidal [STT] joint). Moreover, the presence of chondrocalcinosis of the triangular fibrocartilage complex (TFCC) was evaluated.

The modified K/L grading system uses a 5-grade scoring scale to assess the severity of OA-related changes, with grade 0 indicating no presence of osteophytes or joint space narrowing (JSN), grade 1 indicating equivocal presence of osteophytes or JSN, grade 2 indicating presence of small osteophytes or mild JSN, grade 3 indicating presence of moderate osteophytes or moderate JSN, and grade 4 indicating presence of large osteophytes or severe JSN (15). Interreviewer reliability for scoring OA-related changes using the modified K/L scoring scale was evaluated by re-review of 61 randomly selected hand radiographs by a second trained reviewer (IKH). The interreviewer reliability was excellent with regard to the modified K/L sum scores, with an intraclass correlation coefficient of 0.88 (95% confidence interval [95% CI] 0.80, 0.93) (see Supplementary Appendix 1, available on the *Arthritis & Rheumatology* website at http://onlinelibrary.wiley.com/doi/10.1002/art.41231).

Erosive OA status of the hand joints and the modified K/L grades were used to define several hand OA summary variables (severity according to radiographic OA criteria, presence of radiographic OA, and presence of erosive OA) in the IP (PIP and DIP), MCP, base of the thumb (CMC and STT), and all hand joints (Table 1). Moreover, data regarding self-reported hand

symptoms (feeling pain, aching, or stiffness in the hands on most days) were obtained from the OAI data repository and used to define symptomatic OA in these hand joints groups (Table 1).

Furthermore, 2 ancillary sets of summary variables, i.e., clinical hand OA phenotype based on number or presence of Heberden's nodes as well as the presence of radiographic chondrocalcinosis of the TFCC, were defined and used in our analyses.

Statistical analysis. The PS-matching procedure was conducted using a logistic regression model with age, sex, BMI, smoking status, history of CVD, history of osteoporosis, excessive occupation- or recreation-related hand use, and radiographic knee OA as PS-matching variables. Black subjects were matched with non-Black subjects in a 1:3 ratio using the nearest neighbor–matching method and within a caliper value of 5% of the standard deviation of the logit PS values in the full sample distribution. The biases (standardized distance) of all PS-matching variables for all Black and non-Black subjects were calculated and reported after the matching procedure, which theoretically should be <5% for each variable (16).

A multiple imputation approach was adopted to account for missing data (BMI [n = 4 (0.1%)], smoking status [n = 59 (1.3%)], history of CVD [n = 109 (2.3%)], history of osteoporosis [n = 41 (0.9%)], and excessive occupation- or recreation-related hand use [n = 43 (0.9%)]). Given the nonignorable nature of the missing data in the OAI, a method previously suggested by Resseguier et al (17) was used to obtain 50 imputations after 10 iterations (5 imputed data sets) (see Supplementary Appendix 2, available on the *Arthritis & Rheumatology* website at http://onlinelibrary.wiley.com/doi/10.1002/art.41231). Then, for each complete imputed data set, PS values were estimated and used for the PS-matching procedure (from the PS-matched sample) and in calculating PS weights of subjects (from the inverse PS–weighted sample; see below). Associations between race and hand OA phenotypes were studied in each data set (for both PS-matched and inverse PS–weighted samples) and, finally, assuming normal distribution for the repeated parameter estimates, the pooled estimates and associated 95% CIs were obtained for all imputed data sets using Rubin's rules (the "match-then-pool" or the "within" matching approach) (18).

Linear or logistic regression models were used to assess the associations between race and the phenotypes of hand OA in the PS-matched sample (as well as in the inverse PS–weighted sample), and the estimated coefficient (beta coefficient) or odds ratio (OR) and 95% CI for Black subjects are reported.

The robustness of the PS-matching procedure was verified using 2 sensitivity analyses, which included the following: 1) the inverse PS–weighted method was used to include the entire (eligible) sample of subjects, weighted by the inverse PS values, in the regression analysis of the associations between race and hand OA phenotypes (the inverse PS–weighted sample) (19); and 2) subjects were stratified based on radiographic knee OA status (using baseline radiographic knee K/L grades or the presence of concurrent osteophytes and JSN), and the associations between race and hand OA phenotypes were assessed separately in these strata.

Data analyses were performed using the open-source R software version 3.6.0 (cobalt, MatchThem, mice, survey, and tableone packages).

Table 1. Defined summary variables for hand OA phenotypes*

Severity criteria	
IP joints	Modified K/L grade sum score of all DIP and PIP joints
MCP joints	Modified K/L grade sum score of all MCP joints
Thumb-base joints	Modified K/L grade sum score of the CMC and STT joints
All hand joints	Modified K/L grade sum score of all hand joints
Radiographic OA	
IP joints	Modified K/L grade >2 in at least 1 DIP and 1 PIP joint, concurrently
MCP joints	Modified K/L grade >2 in at least 1 MCP joint
Thumb-base joints	Modified K/L grade >2 in the CMC and STT joints, concurrently
All hand joints	Modified K/L grade >2 in at least 1 hand joint
Erosive OA	
IP joints	Erosive OA in at least 1 DIP or PIP joint
MCP joints	Erosive OA in at least 1 MCP joint
Thumb-base joints	Erosive OA in the CMC or STT joints
All hand joints	Erosive OA in at least 1 hand joint
Symptomatic OA	
IP joints	Radiographic OA in IP joints
MCP joints	Radiographic OA in MCP joints
Thumb-base joints	Radiographic OA in thumb-base joints
All hand joints	Radiographic OA in all hand joints

* In each joint category, symptomatic osteoarthritis (OA) includes concurrent symptoms of pain, aching, or stiffness in the same hand. IP = interphalangeal; K/L = Kellgren/Lawrence; DIP = distal interphalangeal; PIP = proximal interphalangeal; MCP = metacarpophalangeal; CMC = carpometacarpal; STT = scaphotrapeziotrapezoidal.

Table 2. Demographic and clinical characteristics of the patients, pre– and post–PS-matching*

	Pre–PS-matching (first inverse PS–weighted imputed data set)			Post–PS-matching (first PS-matched matched data set)		
	Black (n = 849)	Non-Black (n = 3,850)	Bias, %†‡	Black (n = 822)	Non-Black (n = 1,967)	Bias, %†§
Race			–			–
Black	849 (100.0)	0 (0.00)		822 (100.0)	0 (0.00)	
White	0 (0.00)	3,728 (96.8)		0 (0.00)	1,901 (96.6)	
Asian	0 (0.00)	44 (1.1)		0 (0.00)	17 (0.9)	
Other¶	0 (0.00)	78 (2.0)		0 (0.00)	49 (2.5)	
PS-matching variables						
Age, mean ± SD years	59.10 ± 8.41	61.66 ± 9.2	0.75	59.28 ± 8.40	59.93 ± 8.89	0.60
Sex			–0.28			–0.07
Female	578 (68.1)	2,160 (56.1)		556 (67.6)	1,253 (63.7)	
Male	271 (31.9)	1,690 (43.9)		266 (32.4)	714 (36.3)	
BMI, mean ± SD kg/m^2	31.12 ± 4.88	28.07 ± 4.64	–1.15	30.92 ± 4.75	30.02 ± 4.76	0.03
Smoking status						
Never	407 (47.9)	2,079 (54.0)	0.66	400 (48.7)	977 (49.7)	0.42
Current	126 (14.8)	194 (5.0)	–0.22	110 (13.4)	180 (9.2)	0.50
Former	316 (37.2)	1,577 (41.0)	–0.44	312 (38.0)	810 (41.2)	–0.92
History of OP#			0.14			–0.14
Negative	791 (93.2)	3,336 (86.6)		764 (92.9)	1,794 (91.2)	
Positive	58 (6.8)	514 (13.4)		58 (7.1)	173 (8.8)	
Excessive hand use**			–0.22			–0.21
Negative	572 (67.4)	2,417 (62.8)		552 (67.2)	1,299 (66.0)	
Positive	277 (32.6)	1,433 (37.2)		270 (32.8)	668 (34.0)	
History of heart attack			0.20			0.32
Negative	830 (97.8)	3,775 (98.1)		805 (97.9)	1,930 (98.1)	
Positive	19 (2.2)	75 (1.9)		17 (2.1)	37 (1.9)	
Knee K/L grade						
0	254 (29.9)	1,275 (33.1)	–0.20	244 (29.7)	628 (31.9)	–0.07
1	89 (10.5)	590 (15.3)	–0.08	89 (10.8)	215 (10.9)	0.05
2	290 (34.2)	1,036 (26.9)	0.47	279 (33.9)	617 (31.4)	0.20
3	177 (20.8)	702 (18.2)	0.00	171 (20.8)	396 (20.1)	–0.14
4	39 (4.6%)	247 (6.4)	–0.18	39 (4.7)	111 (5.6)	–0.04
Other comorbidities††						
History of diabetes			–			–
Negative	671 (83.6)	3,552 (94.0)		655 (84.2)	1,783 (92.6)	
Positive	132 (16.4)	226 (6.0)		123 (15.8)	143 (7.4)	
History of malignancy			–			–
Negative	789 (97.9)	3,642 (96.0)		764 (97.8)	1,868 (96.4)	
Positive	17 (2.1)	151 (4.0)		17 (2.2)	70 (3.6)	
History of stroke			–			–
Negative	795 (96.8)	3,679 (97.0)		769 (96.9)	1,877 (97.2)	
Positive	26 (3.2)	112 (3.0)		25 (3.1)	55 (2.8)	
Hypertension			–			–
Negative	269 (31.7)	2,027 (52.6)		259 (31.5)	1,007 (51.2)	
Positive	580 (68.3)	1,823 (47.4)		563 (68.5)	960 (48.8)	

* Except where indicated otherwise, values are the number (%) of patients. K/L = Kellgren/Lawrence; BMI = body mass index.
† Balance in the propensity score (PS)–matching variables was evaluated by assessing the bias (standardized distance) of the variables across Black and non-Black subjects after conducting PS-weighting and PS-matching procedures (reported frequencies are the mean of biases across the imputed data set after PS-weighting and PS-matching procedures).
‡ After PS-weighting.
§ After PS-matching.
¶ Other non-White race.
# Self-reported intake of bisphosphonate (e.g., alendronate, risedronate, etc. in the past 5 years) or parathyroid hormone (e.g., teriparatide, etc. in the past 6 months) due to physician-diagnosed osteoporosis (OP) was considered to be a positive history of OP.
** Excessive recreation- or occupation-related hand use was defined as self-reported lifting or moving objects weighing ≥25 pounds by hand on most days.
†† Frequencies of other comorbidities were evaluated by calculating the chi-square values for comparisons between Black and non-Black subjects. In the pre–PS-matching data set: for history of diabetes $P < 0.001$; for history of malignancy $P = 0.014$; for history of stroke $P = 0.833$; for hypertension $P < 0.001$. In the post–PS-matching data set: for history of diabetes $P < 0.001$; for history of malignancy $P = 0.071$; for history of stroke $P = 0.765$; and for hypertension $P < 0.001$.

RESULTS

In the current study, a total of 4,699 subjects (849 Black and 3,850 non-Black) with acceptable-quality hand radiographs and available data regarding race were included in our analysis (Figure 1).

PS-matching procedure. The PS-matching procedure was used to match Black and non-Black subjects in a 1:3 ratio in each of the 5 imputed data sets. In the first data set, 822 Black subjects were matched with 1,967 non-Black subjects; in the other 4 data sets, matching involved 828 Black subjects matched with 1,971 non-Black subjects, 822 Black subjects matched with 1,965 non-Black subjects, 822 Black subjects matched with 1,971 non-Black subjects, and 822 Black subjects matched with 1,968 non-Black subjects. All 5 PS-matched samples were reported to be well-balanced with regard to the PS-matching variables (Table 2).

Black race and radiographic or symptomatic hand OA phenotypes. Black subjects had less severe OA (modified K/L sum score) in all hand joints (β = –1.93 [95% CI –2.53, –1.34]) as well as IP joints (β = –1.81 [95% CI –2.26, –1.36]) and base-of-the-thumb joints (β = –0.40 [95% CI –0.52, –0.28]). Moreover, Black subjects had a lower risk of radiographic OA in all hand joints (OR 0.79 [95% CI 0.66, 0.94]), IP joints (OR 0.52 [95% CI 0.39, 0.68]), and base-of-the-thumb joints (OR 0.36 [95% CI 0.21, 0.64]) compared to non-Black subjects. Similar findings were obtained with regard to the risk of erosive hand OA in Black subjects compared to non-Black subjects, in all hand joints (OR 0.23 [95% CI 0.11, 0.47]) and in the IP joints (OR 0.21 [95% CI 0.10, 0.44]). Similarly, Black subjects had a lower prevalence of symptomatic OA in all hand joints (OR 0.63 [95% CI 0.49, 0.82]), IP joints (OR 0.39 [95% CI 0.24, 0.63]), and base-of-the-thumb joints (OR 0.29 [95% CI 0.10, 0.84]) compared to non-Black subjects (Table 3).

Moreover, Black subjects had a lower risk of chondrocalcinosis of the TFCC (OR 0.40 [95% CI 0.13–1.18]), though the association was not statistically significant (Supplementary Appendix 3, available on the *Arthritis & Rheumatology* website at http://onlinelibrary.wiley.com/doi/10.1002/art.41231).

Black race and clinical hand OA phenotypes. Black subjects had a lower risk of having at least 1 Heberden's node (OR 0.49 [95% CI 0.41, 0.60]) and a lower overall number of Heberden's nodes (β = –0.65 [95% CI –0.79, –0.52]) compared to non-Black PS-matched subjects (Supplementary Appendix 3, available on the *Arthritis & Rheumatology* website at http://onlinelibrary.wiley.com/doi/10.1002/art.41231).

Sensitivity analyses. The calculated PS values were used to estimate weights for each subject in the sample (using the inverse PS–weighting method), and the associations between race and hand OA phenotypes were determined in the inverse PS–weighted sample using weighted models (Table 3). Moreover, radiographic knee OA status (at-risk or with knee OA) was used to stratify the PS-matched sample, and the analyses were repeated separately in each stratum based on knee OA status (Supplementary Appendix 4, available on the *Arthritis & Rheumatology* website at http://onlinelibrary.wiley.com/doi/10.1002/art.41231). Both sensitivity analyses showed that the odds of radiographic, symptomatic, and clinical hand OA phenotypes, in several joints or joint groups of the hand, were lower in Black subjects than those observed in non-Black subjects.

DISCUSSION

Fewer studies have focused on the pathogenesis of hand OA when compared to the pathogenesis of other subtypes of OA (e.g., knee and hip OA), and the roles of risk factors in the clinical course of this debilitating condition are not well-understood. Older age, female sex, and excessive occupation- or recreation-related hand use have been identified as major risk factors for the development and progression of hand OA (3,10). Moreover, obesity, prior hand injury, lack of smoking history, and family history (among other factors) also possibly contribute to the development of hand OA (3,10). However, results regarding the association between race and hand OA are scarce.

Several studies have assessed the associations between race and the development of OA in the knee or hip and have shown that Black subjects have a higher risk of tricompartmental knee OA, in terms of both prevalence and severity (7,20). Moreover, studies have shown that Black subjects experience higher frequencies of hip OA–related changes (i.e., JSN, osteophytes, and subchondral cysts) (7,21). However, there are limited and conflicting pieces of evidence regarding the association between race and hand OA.

Previous studies have shown a lower prevalence of hand OA in women of Chinese descent (5) and lower lifetime risk of hand OA among Black subjects (4) compared to White subjects. However, the higher prevalence of other OA subtypes (knee and hip OA) in Black subjects and the descriptive methodology used in both of these studies (limiting the opportunity to adjust for the effects of other potential risk factors) made it unclear whether the reported associations were confounded by other variables. Moreover, the observation that there was similar prevalence and severity of hand OA between Russian and Buryat populations living in the same area (8) and no statistically significant difference in terms of the prevalence of symptomatic hand OA between Black and non-Black subjects in the Third National Health and Nutrition Examination Survey (9) suggests that environmental factors are most likely more important for the development of hand OA than racial differences.

Table 3. Associations between Black race and radiographic and symptomatic hand OA phenotypes*

	PS-matched sample				Inverse PS–weighted sample			
Phenotype	IP joints	MCP joints	Thumb-base joints	All joints	IP joints	MCP joints	Thumb-base joints	All joints
Severity criteria, mean ± SD score†								
Black	2.54 ± 4.00	0.66 ± 1.46	0.63 ± 1.11	4.47 ± 5.62	2.53 ± 3.99	0.65 ± 1.45	0.63 ± 1.11	4.45 ± 5.59
Non-Black	4.64 ± 6.25	0.37 ± 1.16	1.07 ± 1.65	6.77 ± 8.17	4.86 ± 6.41	0.43 ± 1.29	1.15 ± 1.68	7.13 ± 8.41
β (95% CI)	−1.81 (−2.26, −1.36)	0.31 (0.21, 0.41)	−0.40 (−0.52, −0.28)	−1.93 (−2.53, −1.34)	−1.71 (−2.00, −1.42)	0.32 (0.25, 0.39)	−0.38 (−0.46, −0.30)	−1.79 (−2.17, −1.40)
P	<0.001	<0.001	<0.001	<0.001	<0.001	<0.001	<0.001	<0.001
Radiographic OA‡								
Black	73 (8.9)	96 (11.7)	14 (1.7)	397 (48.3)	75 (8.8)	98 (11.5)	15 (1.8)	410 (48.3)
Non-Black	337 (17.1)	153 (7.8)	103 (5.3)	1,105 (56.2)	696 (18.1)	347 (9.0)	227 (5.9)	2,254 (58.5)
OR (95% CI)	0.52 (0.39, 0.68)	1.70 (1.28, 2.25)	0.36 (0.21, 0.64)	0.79 (0.66, 0.94)	0.54 (0.41, 0.70)	1.74 (1.34, 2.25)	0.38 (0.22–0.66)	0.80 (0.68, 0.94)
P	<0.001	<0.001	<0.001	0.007	<0.001	<0.001	0.001	0.008
Erosive OA								
Black	8 (1.0)	1 (0.1)	1 (0.1)	9 (1.1)	8 (0.9)	1 (0.1)	1 (0.1)	9 (1.1)
Non-Black	105 (5.3)	2 (0.1)	1 (0.1)	107 (5.4)	225 (5.8)	4 (0.1)	1 (0.0)	228 (5.9)
OR (95% CI)	0.21 (0.10, 0.44)	N/C	N/C	0.23 (0.11, 0.47)	0.19 (0.09, 0.40)	2.66 (0.28, 25.02)	7.27 (0.45, 116.55)	0.21 (0.11, 0.42)
P	<0.001	–	–	<0.001	<0.001	0.391	0.161	<0.001
Symptomatic OA								
Black	20 (2.4)	21 (2.6)	4 (0.5)	90 (10.9)	22 (2.6)	22 (2.6)	4 (0.5)	94 (11.1)
Non-Black	131 (6.7)	48 (2.4)	39 (2.0)	328 (16.7)	263 (6.8)	105 (2.7)	84 (2.2)	626 (16.3)
OR (95% CI)	0.39 (0.24, 0.63)	1.34 (0.77, 2.33)	0.29 (0.10, 0.84)	0.63 (0.49, 0.82)	0.42 (0.26, 0.66)	1.34 (0.82, 2.17)	0.32 (0.12, 0.88)	0.64 (0.50, 0.82)
P	<0.001	0.303	0.022	0.001	<0.001	0.243	0.028	<0.001

* Odds ratios (ORs) (or beta coefficients) for the associations between Black race and radiographic and symptomatic hand OA phenotypes are reported (reported frequencies of radiographic and symptomatic hand OA phenotypes are derived from the first imputed data set before the propensity score (PS)–matching procedure [inverse PS–weighted sample] and after the PS-matching procedure [PS-matched sample], while the reported ORs or beta coefficients are aggregated by pooling estimates obtained for all imputed data sets according to Rubin's rules). Except where indicated otherwise, values are the number (%) of patients. 95% CI = 95% confidence interval; N/C = not converged (see Table 1 for other definitions).
† Severity criteria refers to the modified K/L grade sum score.
‡ Radiographic OA denotes a modified K/L grade of ≥2.

The aim of this comparative analysis was to reassess this question and evaluate the effects of race on radiographic and symptomatic hand OA in a US population, since the effects of other hand OA risk factors are well-balanced. PS-matching was used to select a PS-matched sample of Black subjects and non-Black subjects who had available hand radiographs in order to compare radiographic, symptomatic, and clinical hand OA phenotypes between these 2 groups. We found consistent evidence that Black race was associated with a lower risk of radiographic, symptomatic, and clinical hand OA, as well as chondrocalcinosis of the TFCC.

The aim of the OAI is to study the associations between physical, imaging-derived, or laboratory-based biomarkers and knee OA development and progression in a longitudinal study. Hence, the inclusion and exclusion criteria for this study were designed to include an appropriate sample of subjects for that purpose. Post hoc analysis or reusing this sample to investigate new outcomes has the risk of selection biases, i.e., sampling and susceptibility biases. In our study, several steps were taken to address these biases: 1) to address the possible effects of nonrandomized selection of subjects for inclusion in the OAI (and its outcome) (sampling bias), PS-matching was performed to include a sample of Black and non-Black subjects matched for known (and available) risk factors for hand OA; and 2) since an association between knee and hand OA has been previously demonstrated (22,23) (susceptibility bias), and given the different prevalence of knee OA among Black and non-Black subjects in the pre–PS-matched sample, our results could have been affected by this variable. In the PS-matching procedure, to counteract the potential modifying role of knee OA, radiographic knee OA status was entered as an independent variable in the PS-matching model. After stratifying the data set by knee OA status, the association between Black race and experiencing a lower prevalence and severity of hand OA was still observed, demonstrating that these associations most likely exist in populations with knee OA prevalence different from that in this study.

PS-matching is a well-recognized statistical method used to select matched subjects from 2 groups with different baseline characteristics (24,25). In this study, we used findings from 2 systematic reviews to identify hand OA risk factors (3,10) and then matched Black subjects and non-Black subjects for those risk factors. However, one of the well-described limitations of PS-matching still applies here, i.e., there may still be degrees of residual confounding imposed by variables not entered in the model (risk factors not yet identified or risk factors with unavailable data) (26).

Well-balanced demographic and clinical characteristics among subjects of different races in this PS-matched comparative analysis ensured sufficient comparability between Black and non-Black subjects in the analyses of hand OA phenotypes (i.e., differences in OA prevalence and severity). Our findings showed that unlike the risk of knee and hip OA (7), the risk of radiographic, symptomatic, and clinical hand OA is lower among Black subjects. Future mechanistic studies are warranted to determine the mediating protective factors for hand OA among Black subjects.

AUTHOR CONTRIBUTIONS

All authors were involved in drafting the article or revising it critically for important intellectual content, and all authors approved the final version to be published. Dr. Pishgar had full access to all of the data in the study and takes responsibility for the integrity of the data and the accuracy of the data analysis.

Study conception and design. Pishgar, Kwee, Haj-Mirzaian, Demehri.
Acquisition of data. Pishgar, Kwee, Haj-Mirzaian, Guermazi, Haugen, Demehri.
Analysis and interpretation of data. Pishgar, Kwee, Haj-Mirzaian, Haugen, Demehri.

REFERENCES

1. Dahaghin S, Bierma-Zeinstra SM, Ginai AZ, Pols HA, Hazes JM, Koes BW. Prevalence and pattern of radiographic hand osteoarthritis and association with pain and disability (the Rotterdam study). Ann Rheum Dis 2005;64:682–7.
2. Michon M, Maheu E, Berenbaum F. Assessing health-related quality of life in hand osteoarthritis: a literature review. Ann Rheum Dis 2011; 70:921–8.
3. Zhang W, Doherty M, Leeb BF, Alekseeva L, Arden NK, Bijlsma JW, et al. EULAR evidence-based recommendations for the diagnosis of hand osteoarthritis: report of a task force of ESCISIT. Ann Rheum Dis 2009;68:8–17.
4. Qin J, Barbour KE, Murphy LB. Lifetime risk of symptomatic hand osteoarthritis: the Johnston County Osteoarthritis Project. Arthritis Rheumatol 2017;69:1204–12.
5. Zhang Y, Xu L, Nevitt MC, Niu J, Goggins JP, Aliabadi P, et al. Lower prevalence of hand osteoarthritis among Chinese subjects in Beijing compared with white subjects in the United States: the Beijing Osteoarthritis Study. Arthritis Rheum 2003;48:1034–40.
6. Haugen IK, Magnusson K, Turkiewicz A, Englund M. The prevalence, incidence, and progression of hand osteoarthritis in relation to body mass index, smoking, and alcohol consumption. J Rheumatol 2017; 44:1402–9.
7. Allen KD. Racial and ethnic disparities in osteoarthritis phenotypes. Curr Opin Rheumatol 2010;22:528–32.
8. Kalichman L, Malkin I, Batsevich V, Kobyliansky E. Radiographic hand osteoarthritis in two ethnic groups living in the same geographic area. Rheumatol Int 2010;30:1533–6.
9. Dillon CF, Hirsch R, Rasch EK, Gu Q. Symptomatic hand osteoarthritis in the United States: prevalence and functional impairment estimates from the third U.S. National Health and Nutrition Examination Survey, 1991-1994. Am J Phys Med Rehabil 2007;86:12–21.
10. Kalichman L, Hernandez-Molina G. Hand osteoarthritis: an epidemiological perspective [review]. Semin Arthritis Rheum 2010;39:465–76.
11. Eckstein F, Wirth W, Nevitt MC. Recent advances in osteoarthritis imaging—the osteoarthritis initiative [review]. Nat Rev Rheumatol 2012;8:622–30.
12. Kellgren JH, Lawrence JS. Radiological assessment of osteoarthrosis. Ann Rheum Dis 1957;16:494–501.
13. Kohn MD, Sassoon AA, Fernando ND. Classifications in brief: Kellgren-Lawrence classification of osteoarthritis [review]. Clin Orthop Relat Res 2016;474:1886–93.

14. Gelber AC. In the clinic. Osteoarthritis [review]. Ann Intern Med 2014; 161:ITC1–16.
15. Davis JE, Schaefer LF, McAlindon TE, Eaton CB, Roberts MB, Haugen IK, et al. Characteristics of accelerated hand osteoarthritis: data from the Osteoarthritis Initiative. J Rheumatol 2019;46:422–8.
16. Austin PC. An introduction to propensity score methods for reducing the effects of confounding in observational studies. Multivariate Behav Res 2011;46:399–424.
17. Resseguier N, Giorgi R, Paoletti X. Sensitivity analysis when data are missing not-at-random. Epidemiology 2011;22:282.
18. Mitra R, Reiter JP. A comparison of two methods of estimating propensity scores after multiple imputation. Stat Methods Med Res 2012;25:188–204.
19. Mansournia MA, Altman DG. Inverse probability weighting. BMJ 2016;352:i189.
20. Jordan JM, Helmick CG, Renner JB, Luta G, Dragomir AD, Woodard J, et al. Prevalence of knee symptoms and radiographic and symptomatic knee osteoarthritis in African Americans and Caucasians: the Johnston County Osteoarthritis Project. J Rheumatol 2007;34:172–80.
21. Nelson AE, Braga L, Renner JB, Atashili J, Woodard J, Hochberg MC, et al. Characterization of individual radiographic features of hip osteoarthritis in African American and White women and men: the Johnston County Osteoarthritis Project. Arthritis Care Res (Hoboken) 2010;62:190–7.
22. Dahaghin S, Bierma-Zeinstra SM, Reijman M, Pols HA, Hazes JM, Koes BW. Does hand osteoarthritis predict future hip or knee osteoarthritis? Arthritis Rheum 2005;52:3520–7.
23. Hirsch R, Lethbridge-Cejku M, Scott WW Jr, Reichle R, Plato CC, Tobin J, et al. Association of hand and knee osteoarthritis: evidence for a polyarticular disease subset. Ann Rheum Dis 1996; 55:25–9.
24. Urowitz MB, Ohsfeldt RL, Wielage RC, Kelton KA, Asukai Y, Ramachandran S. Organ damage in patients treated with belimumab versus standard of care: a propensity score-matched comparative analysis. Ann Rheum Dis 2019;78:372–9.
25. Graham GN, Jones PG, Chan PS, Arnold SV, Krumholz HM, Spertus JA. Racial disparities in patient characteristics and survival after acute myocardial infarction. JAMA Netw Open 2018;1:e184240.
26. D'Agostino RB Jr. Propensity score methods for bias reduction in the comparison of a treatment to a non–randomized control group. Stat Med 1998;17:2265–81.

American College of Rheumatology
Empowering Rheumatology Professionals

Arthritis & Rheumatology
Vol. 74, No. 3, March 2022, pp 462–474
DOI 10.1002/art.41988

SH2 Domain–Containing Phosphatase 2 Inhibition Attenuates Osteoarthritis by Maintaining Homeostasis of Cartilage Metabolism via the Docking Protein 1/ Uridine Phosphorylase 1/Uridine Cascade

Qianqian Liu,[1] Linhui Zhai,[2] Mingrui Han,[1] Dongquan Shi,[3] Ziying Sun,[3] Shuang Peng,[4] Meijing Wang,[1] Chenyang Zhang,[1] Jian Gao,[1] Wenjin Yan,[3] Qing Jiang,[3] Dijun Chen,[1] Qiang Xu,[1] Minjia Tan,[2] and Yang Sun[5]

Objective. Protein tyrosine kinases regulate osteoarthritis (OA) progression by activating a series of signal transduction pathways. However, the roles of protein tyrosine phosphatases (PTPs) in OA remain obscure. This study was undertaken to identify specific PTPs involved in OA and investigate their underlying mechanisms.

Methods. The expression of 107 PTP genes in human OA cartilage was analyzed based on a single-cell sequencing data set. The enzyme activity of the PTP SH2 domain–containing phosphatase 2 (SHP-2) was detected in primary chondrocytes after interleukin-1β (IL-1β) treatment and in human OA cartilage. Mice subjected to destabilization of the medial meniscus (DMM) and IL-1β–stimulated mouse primary chondrocytes were treated with an SHP-2 inhibitor or celecoxib (a drug used for the clinical treatment of OA). The function of SHP-2 in OA pathogenesis was further verified in *Aggrecan-Cre*^{ERT};*SHP2*$^{flox/flox}$ mice. The downstream protein expression profile and dephosphorylated substrate of SHP-2 were examined by tandem mass tag labeling–based global proteomic analysis and stable isotope labeling with amino acids in cell culture–labeled tyrosine phosphoproteomic analysis, respectively.

Results. SHP-2 enzyme activity significantly increased in human OA samples with serious articular cartilage injury and in IL-1β–stimulated mouse chondrocytes. Pharmacologic inhibition or genetic deletion of SHP-2 ameliorated OA progression. SHP-2 inhibitors dramatically reduced the expression of cartilage degradation–related genes and simultaneously promoted the expression of cartilage synthesis–related genes. Mechanistically, SHP-2 inhibition suppressed the dephosphorylation of docking protein 1 and subsequently reduced the expression of uridine phosphorylase 1 and increased the uridine level, thereby contributing to the homeostasis of cartilage metabolism.

Conclusion. SHP-2 is a novel accelerator of the imbalance in cartilage homeostasis. Specific inhibition of SHP-2 may ameliorate OA by maintaining the anabolic–catabolic balance.

INTRODUCTION

Osteoarthritis (OA) is one of the most common disabling joint disorders (1). OA is characterized by articular cartilage injury, accompanied by synovial inflammation and subchondral bone sclerosis (2,3). Maintenance of cartilage homeostasis through a balance between anabolism and catabolism of the cartilage matrix is imperative to improve joint function (4,5). Cartilage anabolism is stimulated by anabolic cytokines and growth factors, which induce the expression of chondrogenesis-related genes such as *Sox9*, *Col2a1*, and *Acan* (6). Catabolic regulators, including interleukin-1β (IL-1β), tumor necrosis factor, and IL-6, promote degradation of the extracellular matrix of the articular cartilage by up-regulating the expression of matrix metalloproteinases (MMPs)

Supported by the National Natural Science Foundation of China (grants 91853109, 81872877, 81730100, 81673436, and 32071432) and the Mountain-Climbing Talents Project of Nanjing University.

[1]Qianqian Liu, MS, Mingrui Han, BS, Meijing Wang, MS, Chenyang Zhang, BS, Jian Gao, PhD, Dijun Chen, PhD, Qiang Xu, PhD: Nanjing University, Nanjing, China; [2]Linhui Zhai, MS, Minjia Tan, PhD: Shanghai Institute of Materia Medica, Chinese Academy of Sciences, Shanghai, China; [3]Dongquan Shi, MD, PhD, Ziying Sun, MD, Wenjin Yan, PhD, Qing Jiang, MD, PhD: Nanjing Drum Tower Hospital, Nanjing, China; [4]Shuang Peng, MS: University of Berne, Berne, Switzerland; [5]Yang Sun, PhD: Nanjing University, Nanjing, China and Xuzhou Medical University, Xuzhou, China.

Drs. Liu, Zhai, Han, and Shi contributed equally to this work.

Author disclosures are available at https://onlinelibrary.wiley.com/action/downloadSupplement?doi=10.1002%2Fart.41988&file=art41988-sup-0001-Disclosureform.pdf.

Address correspondence to Qiang Xu, PhD, School of Life Sciences, Nanjing University, Nanjing 210023, China (email:qiangxu@nju.edu.cn); or to Minjia Tan, PhD, Shanghai Institute of Materia Medica, Chinese Academy of Sciences, Shanghai 201203, China (email: mjtan@simm.ac.cn); or to Yang Sun, PhD, School of Life Sciences, Nanjing University, Nanjing 210023, China (email: yangsun@nju.edu.cn).

Submitted for publication April 21, 2021; accepted in revised form September 23, 2021.

and aggrecanases of the ADAMTS family of proteases (7). Any disturbance in the balance between cartilage anabolism and catabolism causes degeneration of the cartilage (4,5,8). Although a variety of risk factors contributing to the imbalance between catabolic and anabolic activities in OA have been identified, the crucial molecular regulators and the underlying regulatory mechanisms remain unclear.

Protein tyrosine phosphatases (PTPs) belong to a large structurally diverse family of enzymes that work together with protein tyrosine kinases (PTKs) to regulate the reversible phosphorylation of proteins. PTKs have been implicated in OA pathogenesis where they activate a series of signal transduction pathways (9–11), whereas PTP functions have rarely been described in OA. In this study, we sought to identify specific PTPs that are involved in OA and to delineate the underlying mechanisms, with the aim of providing new targets and promising drug candidates for the clinical treatment of OA.

SH2 domain–containing phosphatase 2 (SHP-2) is a tyrosine phosphatase encoded by *PTPN11*. SHP-2 deficiency in chondrocytes leads to metachondromatosis in mice (12,13). Clinically, SHP-2 gain-of-function mutations are related to Noonan's syndrome (14), and SHP-2 loss-of-function mutations are associated with LEOPARD syndrome (15). Nevertheless, Noonan's syndrome and LEOPARD syndrome have similar skeletal characteristics, such as short stature, craniofacial deformities, and scoliosis (16). SHP-2 also regulates the osteogenic fate of growth plate hypertrophic chondrocytes in mice (17). Although the function of SHP-2 in regulating early development has been well elucidated, its role in OA progression after adulthood remains unknown.

In the present study, we investigated the essential roles of SHP-2 in articular cartilage homeostasis and identified the SHP-2/docking protein 1 (DOK1)/uridine axis as a novel pathway for the prevention and treatment of OA.

MATERIALS AND METHODS

Mice and experimental surgery. C57BL/6 mice were purchased from GemPharmatech. OA was induced in the right knee joints of 12-week-old mice by surgical destabilization of the medial meniscus (DMM) (18); sham-operated mice were used as controls. Animals were treated with 30 mg/kg SHP099 hydrochloride (purity >99%; synthesized by Professor Xiangbao Meng [School of Pharmaceutical Sciences, Peking University, Beijing, China]) or celecoxib (catalog no. S24587; Shanghai Yuanye Bio-Technology) on the second day after surgery. Mice were euthanized at 20 weeks of age.

SHP2$^{flox/flox}$ mice were generously provided by Professor Gen-Sheng Feng (University of California San Diego). *Aggrecan-Cre*^{ERT} mice were generously provided by Professor Ge Zhang (Hong Kong Baptist University). Chondrocyte-specific SHP-2–knockout mice (*Aggrecan-Cre*^{ERT}*;SHP2*$^{flox/flox}$) were generated by crossing *SHP2*$^{flox/flox}$ mice with *Aggrecan-Cre*^{ERT} mice. Male mice (*SHP2*$^{flox/flox}$ and *Aggrecan-Cre*^{ERT}*;SHP2*$^{flox/flox}$ mice) were injected with 6 μl of corn oil containing tamoxifen (20 mg/ml; MedChemExpress) into the articular cavity at 11 weeks of age 3 times a day every 2 days to induce specific knockout of SHP-2 in mouse chondrocytes and then subjected to DMM surgery at the age of 12 weeks. Uridine (catalog no. U6222; Macklin Pharmaceuticals) was injected into the joint cavity. Cartilage injury was scored according to the recommendations of the Osteoarthritis Research Society International (OARSI) (19).

Single-cell sequencing data processing. Single-cell count matrices were obtained from the GEO database (accession no. GSE104782) and converted to sparse matrices using the Seurat package (version 3.1.4) in R; cells expressing <200 genes or >6,000 genes, as well as cells with >20% mitochondrial reads, were excluded from the analysis. Filtered data were log-normalized and scaled, with cell–cell variation due to unique molecular identified counts and percent mitochondrial reads being regressed out.

Study approval. All animal experiments were carried out according to the Guide for the Care and Use of Laboratory Animals and approved by the Experimental Animal Care and Use Committee of Nanjing University (IACUC-2012012). All efforts were made to minimize the number of animals used and their suffering. All human studies were approved by the ethics committee of Nanjing Drum Tower Hospital, the Affiliated Hospital of Nanjing University Medical School (2020-156-01).

Clinical samples. Joint effusion and articular cartilage samples were obtained from OA patients undergoing total knee arthroplasty at Nanjing Drum Tower Hospital. Undamaged and damaged cartilage were obtained from each individual using the method of Snelling et al (20). Joint effusion was drawn from the joint cavity. OA patient information is shown in Supplementary Table 1, available on the *Arthritis & Rheumatology* website at https://onlinelibrary.wiley.com/doi/10.1002/art.41988.

Cell culture. Cartilage samples were obtained from the knee joints of wild-type C57BL/6 mice within 3 days of birth, cut into pieces, digested with 0.1% trypsin for 30 minutes at 37°C, and then digested with 0.2% type II collagenase for >2 hours at 37°C. Cells were then harvested in batches. Mouse chondrocytes were cultured with Dulbecco's modified Eagle's medium (DMEM)–Ham's F-12 (Corning) supplemented with 10% fetal bovine serum (FBS; Biological Industries) and 1% penicillin/streptomycin. ATDC5 cells (a generous gift from Professor Jian Luo [East China Normal University, Shanghai, China]) were cultured with DMEM (Gibco) supplemented with 5% FBS and 1% penicillin/streptomycin. All cells were maintained in a humidified incubator containing 5% CO_2 at 37°C until used for subsequent experiments. The drugs and reagents used to treat the assayed cells were SHP099 (catalog no. HY-100388; MedChemExpress), celecoxib (catalog no. HY-14398; MedChemExpress), uridine (catalog no.

HY-B1449; MedChemExpress), PHPS1 (Glpbio), SHP099 (catalog no. HY-100388; MedChemExpress), and IL-1β (catalog no. 401-ML-005; R&D Systems).

Chondrogenesis assay. The chondrogenesis assay method was adopted from that described by Feng et al (21). Briefly, cells were resuspended in DMEM–Ham's F-12 supplemented with 10% FBS and 1% penicillin/streptomycin. Droplets (15 μl) containing 2.5×10^5 cells were carefully placed in the middle of each well of a 24-well plate. Cells were then left to adhere at 37°C for 2 hours, and 500 ml of chondrogenic medium including 1% insulin–transferrin–selenium solution (Sigma), 10 ng/ml transforming growth factor β3 (PeproTech), 100 n*M* dexamethasone (Sigma), 1 m*M* sodium pyruvate (ThermoFisher Scientific), and 40 μg/ml proline (Sigma) were added. The medium was changed every 2 days. Micromass cultures were stained with Alcian blue on days 1 and 5.

Safranin O–fast green staining. Dewaxed paraffin sections were added to 0.1% Safranin O dye solution for 5 minutes and washed 3 times with triple distilled water; 0.05% fast green dye solution was then added for 5 minutes and washed 3 times with triple distilled water. Iced acetic acid (1%) was added for 10 seconds and washed 3 times with triple distilled water, 95% alcohol was added for 1–2 minutes, and 100% alcohol was added for 2 minutes. Sections were then mounted with xylene for 2 minutes.

Coimmunoprecipitation assay. Proteins from cells were incubated with 3 μg of the appropriate antibody and precipitated with Protein A/G Plus–Agarose beads (Santa Cruz Biotechnology). The immunoprecipitated proteins were separated by sodium dodecyl sulfate–polyacrylamide gel electrophoresis, and immunoblotting was performed with the indicated antibodies.

Statistical analysis. GraphPad Prism 8 was used for statistical analysis. One-way analysis of variance (ANOVA) with Tukey's multiple comparisons was used to compare the groups (parametric test). Nonparametric data (such as OARSI scores) were analyzed using the Kruskal-Wallis test with multiple comparisons. Student's paired or unpaired *t*-test (parametric or nonparametric test) was used to detect significant treatment effects when only 2 groups were compared. *P* values less than 0.05 were considered significant. All data are expressed as the mean ± SEM. Additional experimental procedures are described in the Supplementary Methods, available on the *Arthritis & Rheumatology* website at https://onlinelibrary.wiley.com/doi/10.1002/art.41988.

RESULTS

Involvement of SHP-2 in OA pathogenesis. To assess the potential involvement of PTPs in OA, we analyzed the expression abundance of 107 genes encoding PTPs (Supplementary Figures 1 and 2, available on the *Arthritis & Rheumatology* website at https://onlinelibrary.wiley.com/doi/10.1002/art.41988) in human OA cartilage, using a publicly accessible single-cell sequencing data set (22). This analysis revealed 9 PTP-encoding genes with high expression levels in different chondrocyte subtypes (Figures 1A and B). Next, we validated the expression of messenger RNA (mRNA) for these PTP genes in articular cartilage tissue samples from OA patients by real-time quantitative polymerase chain reaction (qPCR). The expression of mRNA for *PTPN11*, encoding tyrosine phosphatase SHP-2, was the highest among the 9 PTP genes (Figure 1C).

We next obtained the undamaged area and damaged area of the cartilage from the same OA patient, and performed verification analysis of OA-related marker genes (Supplementary Figures 3A and B, available on the *Arthritis & Rheumatology* website at https://onlinelibrary.wiley.com/doi/10.1002/art.41988). We correlated the expression of SHP-2 between undamaged OA cartilage and damaged OA cartilage. However, SHP-2 protein and mRNA levels did not change between undamaged areas and damaged areas of cartilage (Figures 1D and E). Similarly, SHP-2 expression did not vary between mouse chondrocytes stimulated with vehicle and mouse chondrocytes stimulated with IL-1β, consistent with the results observed in undamaged OA cartilage and damaged OA cartilage (Figure 1F). SHP-2 enzyme activity increased sharply in damaged OA cartilage compared to undamaged cartilage, and in IL-1β–stimulated mouse chondrocytes compared to vehicle-stimulated mouse chondrocytes (Figures 1G and H).

We speculated that the up-regulation of SHP-2 enzyme activity results from its phosphorylation. The level of pSHP-2 (Y542, Y580) was higher in damaged human OA cartilage and in mice with OA induced by DMM than in their respective controls, as assessed by immunofluorescence staining and Western blotting (Figures 1I and J). In addition, the pSHP-2 (Y542, Y580) level was significantly higher in the IL-1β–treated mouse chondrocytes than in the untreated mouse chondrocytes (Figure 1K). Taken together, these findings indicate that SHP-2 may be involved in the development of OA.

Amelioration of OA by pharmacologic inhibition or genetic deletion of SHP-2. OA is caused by a variety of etiologic factors, including biomechanical stress, genetic factors, senescence, and abnormalities in the articular cartilage or bone (23). To investigate the functional role of SHP-2 in OA progression, we applied SHP099, an allosteric inhibitor of SHP-2, in 2 widely used OA rodent models, namely, the DMM model and the aging model (Figure 2A and Supplementary Figure 4A, available on the *Arthritis & Rheumatology* website at https://onlinelibrary.wiley.com/doi/10.1002/art.41988). Celecoxib, a drug for the clinical treatment of OA, was used as a control medication.

Mice receiving SHP099 after DMM surgery demonstrated reduced cartilage damage compared with mice subjected to DMM and left untreated, as evident from Safranin O–fast green staining and OARSI scores (Figures 2B and C). In addition,

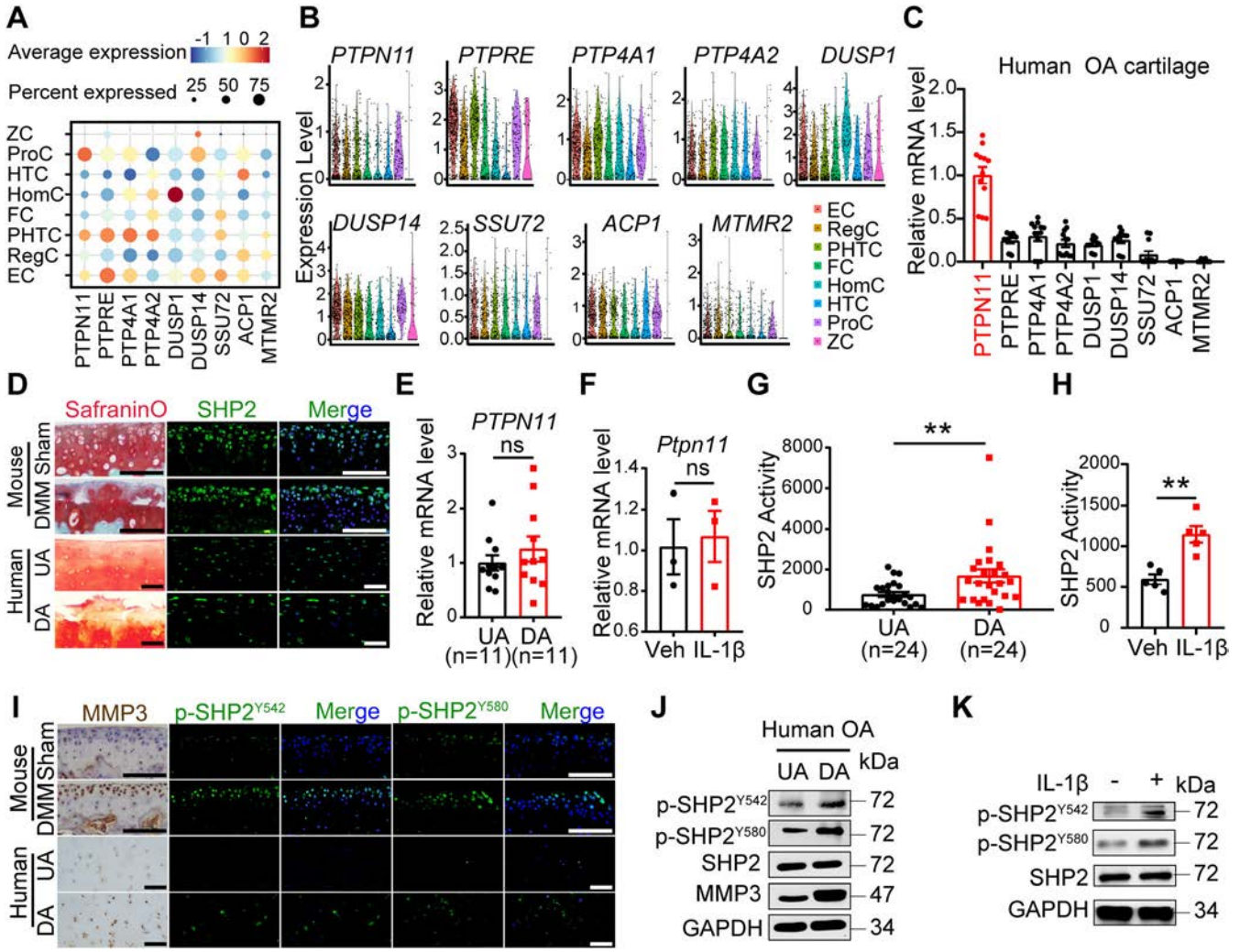

Figure 1. Role of SH2 domain–containing phosphatase 2 (SHP-2) in osteoarthritis (OA) pathogenesis. **A** and **B**, Bubble chart (**A**) and violin plots (**B**) showing levels of mRNA for 9 protein tyrosine phosphatase (PTP) genes in different chondrocyte subtypes. ZC = ZNF585B+ chondrocyte; ProC = proliferative chondrocyte; HTC = hypertrophic chondrocyte; HomC = homeostatic chondrocyte; FC = fibrocartilage chondrocyte; PHTC = prehypertrophic chondrocyte; RegC = regulatory chondrocyte; EC = effector chondrocyte. **C**, Relative levels of mRNA for the indicated genes in human OA cartilage (n = 11 per group), determined by real-time quantitative polymerase chain reaction (qPCR). Red indicates the gene with the highest mRNA level. **D**, Safranin O–fast green staining and SHP-2 immunostaining of cartilage from a sham-operated mouse, a mouse subjected to destabilization of the medial meniscus (DMM), and the undamaged area (UA) and damaged area (DA) of cartilage from a patient with OA. **E** and **F**, Relative levels of mRNA for *PTPN11* in the undamaged and damaged areas of OA cartilage (**E**) and mouse chondrocytes treated with vehicle (Veh) or 5 ng/ml interleukin-1β (IL-1β) for 12 hours (n = 3 per group) (**F**), determined by real-time qPCR. **G** and **H**, SHP-2 enzyme activity in undamaged and damaged human cartilage (**G**) and mouse chondrocytes treated with vehicle or 5 ng/ml IL-1β for 24 hours (n = 5 per group) (**H**). **I**, Immunostaining for the indicated proteins in cartilage from a sham-operated mouse, a mouse subjected to DMM, and the undamaged and damaged areas of cartilage from a patient with OA. Results are representative of 3 experiments. **J** and **K**, Immunoblotting of the indicated proteins in undamaged and damaged human OA cartilage (**J**) and mouse chondrocytes treated with vehicle or 5 ng/ml IL-1β for 2 hours (**K**). Results are representative of 3 experiments. In **C** and **E**–**H**, symbols represent individual samples; bars show the mean ± SEM. In **D** and **I**, bars = 100 μm. ** = $P < 0.01$ by Student's paired *t*-test. MMP-3 = matrix metalloproteinase 3; NS = not significant. Color figure can be viewed in the online issue, which is available at http://onlinelibrary.wiley.com/doi/10.1002/art.41988/abstract.

SHP099 treatment markedly decreased the expression of catabolism factors, such as MMP-13 and MMP-3 and the hypertrophic factor type X collagen, and increased the expression of the cartilage anabolism factor SOX9 (Figures 2B and C). Similar results were obtained in a mouse model of natural aging (Supplementary Figures 4A–C, available on the *Arthritis & Rheumatology* website at https://onlinelibrary.wiley.com/doi/10.1002/art.41988).

To exclude SHP099 off-target effects, we induced conditional *SHP2* gene deletion before performing DMM surgery (Figure 2D and Supplementary Figures 5A–C, available on the *Arthritis & Rheumatology* website at https://onlinelibrary.wiley.com/doi/10.1002/art.41988). Consistent with the results for SHP-2 inhibition, we observed reduced cartilage damage, suppressed cartilage catabolism, and enhanced cartilage anabolism

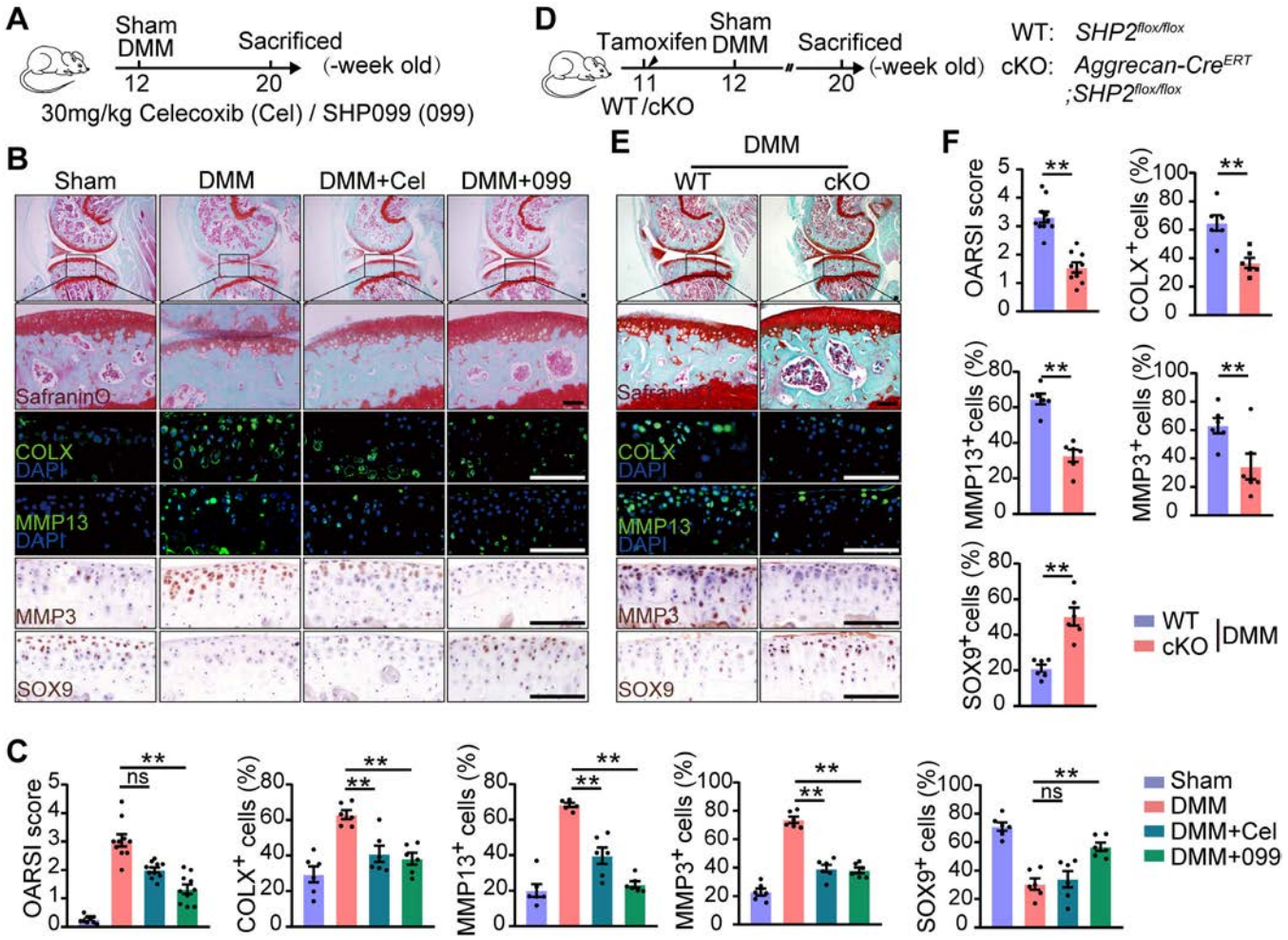

Figure 2. Decreased severity of OA after pharmacologic inhibition or genetic deletion of SHP-2 in a mouse model. **A**, Experimental design for the treatment of mice with an SHP-2 inhibitor. **B**, Representative images of Safranin O–fast green staining and immunostaining for the indicated proteins in sections from a sham-operated mouse, a mouse subjected to DMM and left untreated, a mouse subjected to DMM and treated with celecoxib (Cel), and a mouse subjected to DMM and treated with SHP099 (099). **C**, Osteoarthritis Research Society International (OARSI) scores and quantitation of the indicated proteins in mice treated as indicated (n = 10 per group for OARSI scores; n = 6 per group for protein quantitation). **D**, Experimental design for the genetic deletion of SHP-2 in mice. **E**, Safranin O–fast green staining and immunostaining for the indicated proteins in sections from wild-type (WT) mice and conditional knockout (cKO) littermates. **F**, OARSI scores and quantitation of the indicated proteins in WT and conditional knockout mice subjected to DMM (n = 9 or more per group for OARSI scores; n = 6 per group for protein quantitation). In **C** and **F**, symbols represent individual mice; bars show the mean ± SEM. In **B** and **E**, bottom panels for Safranin O–fast green staining show higher-magnification views of the boxed areas in the top panels. Results are representative of 9 or more experiments. Bars = 100 μm. ** = $P < 0.01$, by Kruskal-Wallis test for OARSI scores, by one-way analysis of variance for protein quantitation in **C**, and by Student's unpaired *t*-test for protein quantitation in **F**. See Figure 1 for other definitions. Color figure can be viewed in the online issue, which is available at http://onlinelibrary.wiley.com/doi/10.1002/art.41988/abstract.

in SHP-2–deficient mice (Figures 2E and F). As evident from the synovitis score (24), SHP-2 inhibition using SHP099 effectively suppressed synovial inflammation, as did celecoxib (Supplementary Figure 6A, available on the *Arthritis & Rheumatology* website at https://onlinelibrary.wiley.com/doi/10.1002/art.41988). SHP-2 loss in mouse chondrocytes also tended to inhibit synovitis, but no significant difference was observed compared with the control group (Supplementary Figure 6B).

Although celecoxib treatment had a tendency to decrease the cartilage damage caused by DMM surgery, the difference was not significant, and, compared to SHP099, celecoxib failed to reverse SOX9 expression (Figures 2B and C). Thus, SHP099 and celecoxib regulated the development of OA through different pathways. Taken together, our findings indicate that the pharmacologic inhibition or genetic deletion of SHP-2 results in the attenuation of cartilage damage. Enhancement of anabolism and/or inhibition of catabolism in the cartilage may contribute to protective effects.

Enhancement of anabolism and suppression of inflammatory responses by inhibition of SHP-2. To evaluate the effects of celecoxib and the SHP-2 inhibitor SHP099

in vitro, we cultured human OA cartilage explants in the presence or absence of celecoxib or SHP099 for 2 weeks. Considering the toxicity of the drugs on mouse chondrocytes, 0.1–3 μ*M* celecoxib or SHP099 was used in cell experiments (Supplementary Figure 7, available on the *Arthritis & Rheumatology* website at https://onlinelibrary.wiley.com/doi/10.1002/art.41988). SHP099 treatment dramatically increased the level of proteoglycan as compared with the vehicle group, while celecoxib treatment had no such effect (Figure 3A). Despite their similar inhibitory effects on MMP-3 expression, celecoxib failed to elevate SOX9 expression as SHP099 did (Figures 3B and C).

We also analyzed the efficiency of SHP099 and celecoxib in a chondrocyte differentiation culture system. Results of Alcian blue staining experiments showed that chondrocyte differentiation was promoted by the SHP-2 inhibitor SHP099 (0.1–3 μ*M*) (Figure 3D and Supplementary Figure 8A, available on the *Arthritis & Rheumatology* website at https://onlinelibrary.wiley.com/doi/10.1002/art.41988). The expression of the anabolic factors *Sox9*, *Col2a1*, and *Acan* was up-regulated upon SHP099 treatment but not after celecoxib treatment (Supplementary Figure 8C). Similar results were obtained in SHP-2–conditional knockout mouse chondrocytes (Figure 3E and Supplementary Figures 8B and 9, available on the *Arthritis & Rheumatology* website at https://onlinelibrary.wiley.com/doi/10.1002/art.41988). However, neither chondrocyte differentiation nor the expression of anabolic factors was altered by celecoxib (Figure 3D).

In IL-1β–stimulated mouse primary chondrocytes, the expression of the catabolic factors *Mmp3* and *Mmp13* decreased after SHP099 treatment (0.1–3 μ*M*) (Figure 3F and Supplementary Figure 10, available on the *Arthritis & Rheumatology* website at https://onlinelibrary.wiley.com/doi/10.1002/art.41988). Celecoxib did not alter *Sox9*, *Col2a1*, or

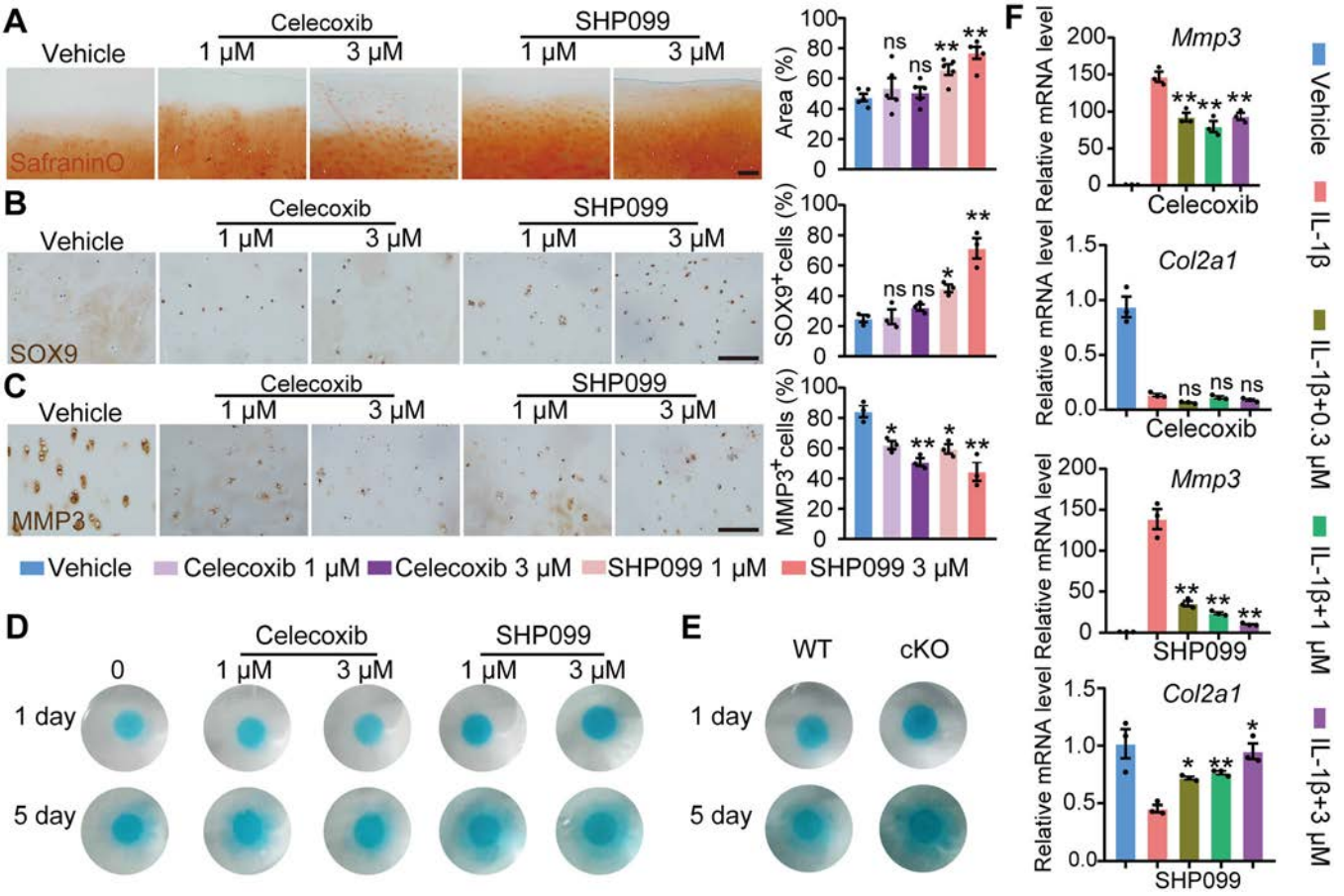

Figure 3. Increased anabolism and decreased inflammatory response upon inhibition of SHP-2. **A**–**C**, Safranin O–fast green staining for proteoglycan content (**A**), immunostaining for SOX9 (**B**), and immunostaining for MMP-3 (**C**) in human OA cartilage explants after 2 weeks of incubation with celecoxib or SHP099. Results are representative of 5 experiments in **A** and 3 experiments in **B** and **C**. Bars = 100 μm. Bar graphs show the proportion of proteoglycan area (**A**), SOX9+ cells (**B**), and MMP-3+ cells (**C**). **D**, Alcian blue staining showing chondrocyte differentiation in OA cartilage explants on days 1 and 5 after treatment with celecoxib or SHP099. **E**, Alcian blue staining showing chondrocyte differentiation in wild-type (WT) and conditional knockout (cKO) mice on days 1 and 5 after SHP-2 knockout. **F**, Relative levels of mRNA for the indicated marker genes in mouse primary chondrocytes treated with vehicle or 5 ng/ml IL-1β plus the indicated concentrations of celecoxib or SHP099 for 12 hours (n = 3 per group), determined by real-time qPCR analysis. In **A**–**C** and **F**, symbols represent individual samples; bars show the mean ± SEM. * = $P < 0.05$; ** = $P < 0.01$ versus vehicle in **A**–**C** and versus IL-1β alone in **F**, by one-way analysis of variance. See Figure 1 for other definitions. Color figure can be viewed in the online issue, which is available at http://onlinelibrary.wiley.com/doi/10.1002/art.41988/abstract.

Acan expression in IL-1β–stimulated mouse chondrocytes, but instead only inhibited *Mmp3* and *Mmp13* expression (Supplementary Figure 10, available on the *Arthritis & Rheumatology* website at https://onlinelibrary.wiley.com/doi/10.1002/art.41988). Moreover, PHPS1, an SHP-2 enzyme activity inhibitor, demonstrated effects similar to those of SHP099 (Supplementary Figures 7 and 11, available on the *Arthritis & Rheumatology* website at https://onlinelibrary.wiley.com/doi/10.1002/art.41988). The effect of celecoxib on anabolic activity was much weaker (at least at the gene expression level) than its effect on catabolic activity (Figure 3). However, in comparison with celecoxib, SHP-2 inhibitors exerted a dual effect by inhibiting cartilage degradation and promoting cartilage synthesis under inflammatory conditions. Thus, SHP099 offers the advantage of restoring the metabolic balance in cartilage tissue.

Reduction of uridine phosphorylase 1 (UPP1) expression by inhibition of SHP-2. To investigate the underlying changes after SHP-2 inhibition in mouse primary chondrocytes, we performed tandem mass tag (TMT) labeling–based quantitative proteomic analysis (Figure 4A). Compared with the untreated mouse chondrocytes, mouse chondrocytes treated with IL-1β showed 177 differentially expressed proteins (fold change >2 or fold change <0.5; $P < 0.05$ by one-way ANOVA) (Figure 4B). Among these proteins, 79 were up-regulated and 98 were down-regulated. Further analysis demonstrated that 7 proteins significantly up-regulated by IL-1β treatment were markedly down-regulated after SHP099 treatment, and 4 proteins significantly down-regulated by IL-1β treatment were markedly up-regulated after SHP099 treatment (Figure 4B).

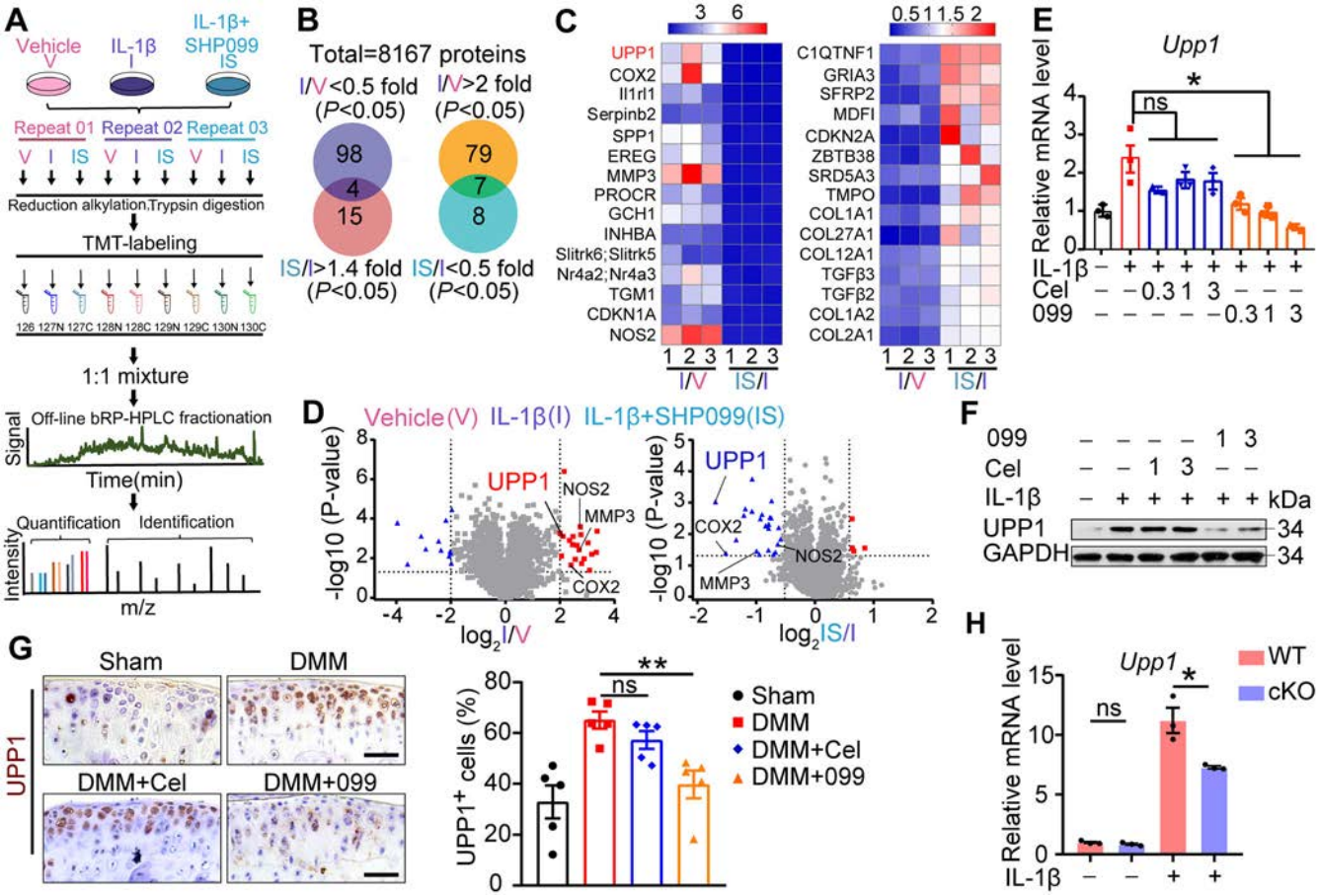

Figure 4. Reduced uridine phosphorylase 1 (UPP1) expression upon inhibition of SHP-2. **A**, Experimental design for tandem mass tag (TMT) labeling–based quantitative proteomic analysis in mouse primary chondrocytes treated with vehicle (V), IL-1β (I), or 1L-1β plus 3 μ*M* SHP099 (IS). **B**, Venn diagram showing the numbers of differentially expressed proteins in mouse primary chondrocytes treated as indicated. **C**, Heatmap of the proteins with significantly different levels in mouse primary chondrocytes treated as indicated (n = 3 samples per group). **D**, Volcano plot of protein expression in mouse primary chondrocytes treated as indicated. **E** and **F**, Relative levels of mRNA for *Upp1*, determined by real-time qPCR analysis (**E**), and levels of UPP1 protein, determined by immunoblotting (**F**), in mouse primary chondrocytes treated with 5 ng/ml IL-1β and the indicated concentrations of celecoxib (Cel) or SHP099. **G**, Immunostaining for UPP1 (left) and proportion of UPP1-positive cells (right) in sham-operated mice, mice subjected to DMM and left untreated, mice subjected to DMM and treated with celecoxib, and mice subjected to DMM and treated with SHP099. Bars = 50 μm. **H**, Relative levels of mRNA for *Upp1* in chondrocytes from wild-type (WT) mice and conditional knockout (cKO) mice, left untreated or treated with 5 ng/ml IL-1β for 12 hours (n = 3 per group). * = $P < 0.05$; ** = $P < 0.01$, by one-way analysis of variance. In **E**, **G**, and **H**, symbols represent individual mice; bars show the mean ± SEM. See Figure 1 for other definitions. Color figure can be viewed in the online issue, which is available at http://onlinelibrary.wiley.com/doi/10.1002/art.41988/abstract.

Interestingly, the level of cyclooxygenase 2 (COX-2), the target of celecoxib, was significantly decreased in the mouse chondrocytes treated with IL-1β plus SHP099 compared to the mouse chondrocytes treated with IL-1β alone. UPP1 expression was also significantly down-regulated in the mouse chondrocytes treated with IL-1β plus SHP099 compared to those treated with IL-1β alone (Figures 4C and D), and the decreased expression of UPP1 and COX-2 was further confirmed by qPCR and Western blotting (Figures 4E and F and Supplementary Figures 12A–D, available on the *Arthritis & Rheumatology* website at https://onlinelibrary.wiley.com/doi/10.1002/art.41988). In contrast, celecoxib had no obvious effect on the expression of UPP1 (Figures 4E, F, and G).

Consistent with the results in the cell model, the UPP1 level was significantly lower in the knee joint cartilage of mice subjected to DMM and treated with SHP099 than in the mice subjected to DMM and left untreated (Figure 4G). Similarly, the expression of *Upp1* was much lower in SHP-2–conditional knockout mouse chondrocytes than in wild-type mouse chondrocytes (Figure 4H). These findings indicate that the expression of UPP1 increases during the development of OA, and that inhibition of SHP-2 expression decreases the level of UPP1.

Involvement of the UPP1/uridine axis in the regulation of cartilage homeostasis. UPP1 is a key enzyme involved in uridine homeostasis (25,26). Cao et al reported that mice lacking UPP1 expression had increased concentrations of uridine in the intestine (27). We hypothesized that the decreased UPP1 expression upon SHP-2 inhibition and the consequent uridine accumulation was crucial for OA cartilage homeostasis. To test this hypothesis, we transfected ATDC5 cells with a small

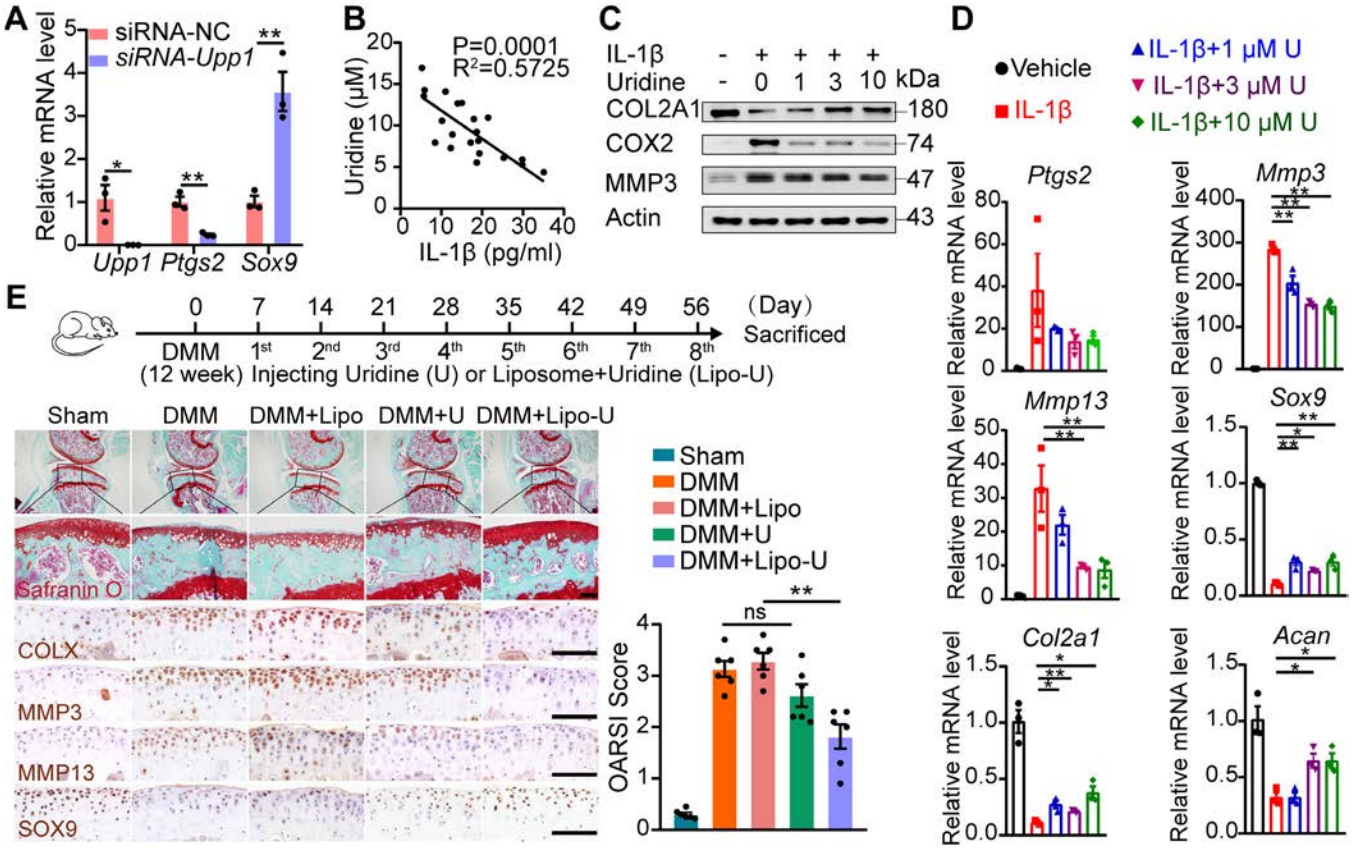

Figure 5. Role of the uridine phosphorylase 1 (UPP1)/uridine axis in cartilage homeostasis regulation. **A**, Relative levels of mRNA for the indicated genes in ATDC5 cells treated with 5 ng/ml IL-1β for 12 hours and transfected with negative control (NC) small interfering RNA (siRNA) or siRNA targeting UPP1, determined by real-time qPCR (n = 3 samples per group). **B**, Negative correlation of uridine levels with IL-1β levels in joint effusion from OA patients (n = 21). Uridine and IL-1β levels were determined by high-performance liquid chromatography and enzyme-linked immunosorbent assay, respectively. **C**, Immunoblotting of the indicated proteins in mouse chondrocytes pretreated with the indicated concentrations of uridine for 2 hours and then treated with 5 ng/ml IL-1β for 24 hours (n = 3 per group). **D**, Relative levels of mRNA for the indicated genes, determined by real-time qPCR, in mouse chondrocytes pretreated with the indicated concentrations of uridine for 2 hours and then treated with 5 ng/ml IL-1β for 12 hours (n = 3 per group). **E**, Top, Experimental design for uridine treatment in mice. Bottom left, Safranin O–fast green staining and immunostaining for the indicated proteins in mice subjected to sham surgery or DMM and treated with empty liposome (Lipo), uridine (U), or liposomal uridine (Lipo-U). Bottom panels for Safranin O–fast green staining show higher-magnification views of the boxed areas in the top panels. Bars = 100 μm. Bottom right, Osteoarthritis Research Society International (OARSI) scores in mice treated as indicated (n = 6 per group). In **A**, **D**, and **E**, symbols represent individual mice; bars show the mean ± SEM. * = $P < 0.05$; ** = $P < 0.01$, by two-way analysis of variance (ANOVA) in **A**, by one-way ANOVA in **D**, and by Kruskal-Wallis test in **E**. See Figure 1 for other definitions. Color figure can be viewed in the online issue, which is available at http://onlinelibrary.wiley.com/doi/10.1002/art.41988/abstract.

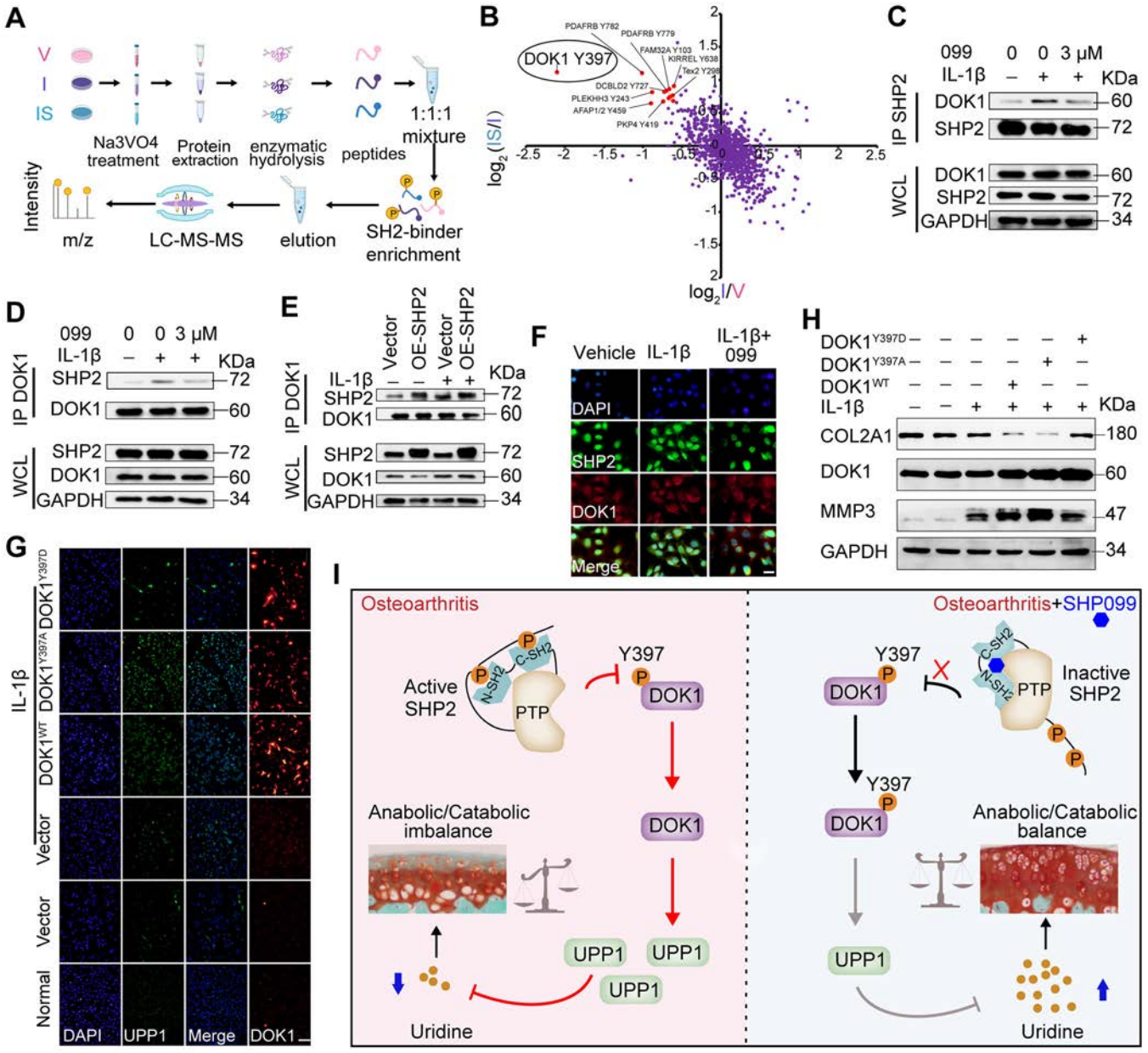

Figure 6. Reduction of uridine phosphorylase 1 (UPP1) levels upon inhibition of SHP-2. Inhibition of SHP-2 reduces UPP1 levels by suppressing the dephosphorylation of docking protein 1 (DOK1) at Tyr397. **A**, Experimental design for stable isotope labeling with amino acids in cell culture–based tyrosine phosphoproteomics in ATDC5 cells treated with vehicle (V), IL-1β (I), or 1L-1β plus 3 μ*M* SHP099 (IS). LC–MS/MS = liquid chromatography tandem mass spectrometry. **B**, Quadrant diagram for tyrosine phosphoproteomic analysis. **C** and **D**, Immunoprecipitation (IP) of ATDC5 cells pretreated with 3 μ*M* SHP099 (099) for 2 hours and then treated with 5 ng/ml IL-1β for 1 hour. Cell lysates were immunoprecipitated by SHP-2 (**C**) or DOK1 antibody (**D**). WCL = whole cell lysate. **E**, Immunoprecipitation of ATDC5 cells overexpressing SHP-2 (OE–SHP-2) and treated with 5 ng/ml IL-1β for 1 hour. Cell lysates were immunoprecipitated by DOK1 antibody. **F**, Immunofluorescence staining showing the colocalization of SHP-2 and DOK1 in ATDC5 cells pretreated with 3 μ*M* SHP099 for 2 hours and then treated with 5 ng/ml IL-1β for 1 hour. Bar = 20 μm. **G** and **H**, Immunofluorescence staining (**G**) and immunoblotting (**H**) of the indicated proteins in ATDC5 cells transfected with wild-type DOK1 (DOK1^{WT}), DOK1 mutant Y397A, or DOK1 mutant 397D plasmids, then treated with 5 ng/ml IL-1β for 24 hours. Bar = 100 μm. **I**, Graphic illustration of the role of SHP-2 and the UPP1/uridine axis in catabolic/anabolic imbalance in OA cartilage (left) and the mechanism of anabolic–catabolic balance in OA cartilage treated with the SHP-2 inhibitor SHP099 (right). P = phosphorylated (see Figure 1 for other definitions).

interfering RNA targeting *UPP1*. As shown in Figure 5A, knockdown of the *Upp1* gene led to the inhibition of *Ptgs2* expression and promoted *Sox9* expression in IL-1β–stimulated mouse chondrocytes.

Interestingly, the level of IL-1β in the joint effusion from OA patients was negatively correlated with the concentration of uridine, indicating the involvement of the UPP1/uridine axis in the development of OA (Figure 5B). As expected, UPP1 expression

was higher in undamaged than in damaged human OA cartilage (Supplementary Figure 13A, available on the *Arthritis & Rheumatology* website at https://onlinelibrary.wiley.com/doi/10.1002/art.41988). SHP099 significantly reduced the expression of UPP1 in the cartilage of aging mice (Supplementary Figure 13B). Uridine was nontoxic to mouse primary chondrocytes even at high concentrations (Supplementary Figure 7). Uridine treatment decreased *Mmp3*, *Mmp13*, and *Ptgs2* expression and partially increased *Sox9*, *Col2a1*, and *Acan* expression at both the mRNA and protein levels in IL-1β–stimulated mouse chondrocytes (Figures 5C and D and Supplementary Figure 14A, available on the *Arthritis & Rheumatology* website at https://onlinelibrary.wiley.com/doi/10.1002/art.41988).

If diminished uridine level contributes to the pathogenesis of OA, uridine repletion might serve as an approach for the treatment or prevention of OA. Considering its low oral bioavailability, extremely short half-life in the blood, degradation by enzymes from other bodily fluids, and cellular uptake (28), we formulated uridine in liposomes to prolong its half-life and evaluated the efficacy of liposomal uridine preparations in the mouse DMM model. Liposomal uridine, uridine, or empty liposomes were injected into the affected joint at the time of injury and supplemented every 7 days for a total of 8 injections (Figure 5E). Of note, liposomal uridine supplementation markedly reduced cartilage damage and synovial inflammation (Supplementary Figure 14B). Such supplementation also down-regulated the expression of MMP-3, MMP-13, and type X collagen and up-regulated SOX9 expression (Figure 5E). Taken together, these results indicate that the UPP1/uridine pathway is involved in the regulation of cartilage homeostasis. Thus, the intraarticular administration of liposomal uridine effectively prevented the development of OA in a mouse DMM model.

Inhibition of SHP-2 reduces UPP1 levels by suppressing the dephosphorylation of DOK1 at Tyr397. To clarify how SHP-2 is involved in the UPP1/uridine pathway, we performed quantitative tyrosine phosphoproteomic analysis using mass spectrometry–based stable isotope labeling with amino acids in cell culture (SILAC) and a superbinder–SH-2 domain affinity purification approach (Figure 6A). A total of 1,151 tyrosine phosphorylation sites, including 999 high-confidence sites (phosphosite localization probability >0.75) were identified (Supplementary Figure 15, available on the *Arthritis & Rheumatology* website at https://onlinelibrary.wiley.com/doi/10.1002/art.41988). Interestingly, the highest level of DOK1^{Y397} phosphorylation was observed after SHP099 treatment, as compared with that after IL-1β treatment (Figure 6B). Based on these results, we speculated that DOK1 was the substrate of SHP-2 in IL-1β–treated ATDC5 cells. Subsequent coimmunoprecipitation assays showed that the endogenous interaction between SHP-2 and DOK1 was augmented by IL-1β in ATDC5 cells, while SHP099 treatment significantly impaired the interaction between SHP-2 and DOK1 (Figures 6C and D). In contrast, overexpression of SHP-2 in ATDC5 cells markedly enhanced this interaction (Figure 6E). Reduced colocalization of SHP-2 and DOK1 after SHP099 treatment was also shown by immunofluorescence staining (Figure 6F).

Next, we constructed DOK1 mutants by replacing tyrosine at site 397 with aspartic acid (Y397D) to simulate permanent phosphorylation or with glycine (Y397A) to mimic permanent dephosphorylation, and then transfected ATDC5 cells with these constructs. In comparison with the wild-type DOK1, the DOK1^{Y397A} mutant showed significantly enhanced UPP1 expression and the DOK1^{Y397D} mutant had decreased UPP1 expression (Figure 6G). The phosphorylation or dephosphorylation of DOK1 at Tyr397 regulated catabolic and anabolic gene expression (Figure 6H and Supplementary Figure 16, available on the *Arthritis & Rheumatology* website at https://onlinelibrary.wiley.com/doi/10.1002/art.41988).

SHP-2 is in an inactive state in chondrocytes from normal cartilage but is phosphorylated and changed into active conformation in chondrocytes from OA cartilage. SHP-2 is recruited to dephosphorylate DOK1 at Tyr397, which subsequently promotes the expression of UPP1. Further, UPP1 degrades uridine to increase the expression of the cartilage degradation–related genes *Mmp3*, *Mmp13*, and *Ptgs2*, and simultaneously decreases the expression of the cartilage synthesis–related genes *Sox9*, *Col2a1*, and *Acan*, thereby accelerating the loss of cartilage homeostasis. Taken together, our data demonstrate that SHP-2 promotes UPP1-mediated uridine degradation by dephosphorylating DOK1 at Tyr397, thereby exacerbating an imbalance between anabolic and catabolic factors in the cartilage. Inhibition of SHP-2 activity is a potential new strategy for the treatment of OA (Figure 6I).

DISCUSSION

In recent years, an increasing number of novel chondroprotective strategies have been proposed and tested (5,29). However, none has been approved so far, and there are no new disease-modifying drugs available for the treatment of OA. The drug currently used for the treatment of OA, celecoxib, is used to relieve pain and inflammation but does not delay the progression of cartilage lesions (30). Other drugs considered to have cartilage synthesis ability, such as glucosamine, chondroitin sulfate, and hyaluronic acid, are subjects of controversy with respect to structural degradation or alleviation of symptoms in patients with OA (31). Surgery is the last treatment option for patients with advanced OA (32). Thus, there is an urgent need to develop drugs that can alleviate, halt, or even reverse the development of OA.

SHP099, a small-molecule inhibitor of SHP-2 that stabilizes SHP-2 in an autoinhibited conformation, is a valid therapeutic drug for the treatment of multiple types of cancers, including leukemia, lung cancer, breast cancer, and neuroblastoma (33). SHP-2 not only participates in oncogenic signaling by mediating the activation of Ras/MAPK signaling (34) but also mediates the programmed death 1/programmed death ligand 1 signaling pathway in T cells and promotes macrophage polarization (35). Our group has previously shown that SHP099 exerts antitumor effects by enhancing tumor immunity (36). In addition to its effect on immune and tumor cells, SHP-2 is thought to have an important function in bone-related cells (17,37,38). What draws our attention is that a young male patient with Noonan's syndrome carrying a *PTPN11*/SHP-2 gain-of-function mutation was reported to have a bone-related disease (39), strongly indicating some correlation between SHP-2 and OA progression. Whether and how SHP-2 is involved in the progression of OA is, however, unclear.

Herein, we report for the first time that SHP-2 is a key regulatory tyrosine phosphatase involved in OA. SHP-2 deficiency in chondrocytes or SHP-2 inhibition attenuated the progression of OA. In addition, we used the 10-plex TMT labeling–based global proteomic analysis and SILAC/SH-2 domain superbinder–based tyrosine phosphoproteomic analysis to systematically investigate the profile of differentially expressed proteins in IL-1β–treated chondrocytes. This quantitative approach provided the complete scenario of the expression patterns of 8,167 proteins, among which the expression level of UPP1 was dramatically increased in chondrocytes treated with IL-1β. UPP1 has recently been found to play an oncogenic role in glioma by suppressing tumor-related immune response (40). Uridine is a component of RNA and has been studied as a rescue agent to reduce the toxicities associated with 5-fluorouracil (41). In addition, uridine demonstrates benefits on brain function (42), depression relief (43), and nerve pain (44).

In this study, we identified UPP1 and uridine metabolism as the downstream mediator of SHP-2 action in regulating cartilage homeostasis. Mechanistically, SHP-2 promoted UPP1-mediated uridine degradation by dephosphorylating DOK1 at Tyr397; this observation is contradictory to the previously reported result that DOK1 is only a linker protein that mediates the SHP-2/β3 association (45). Notably, in addition to UPP1, the SHP-2 inhibitor SHP099 also exerted inhibitory effects on the expression of COX-2 enzyme, the target of celecoxib. However, celecoxib did not alter the expression of UPP1. This might partially explain why celecoxib appeared to be roughly as effective as SHP099 for cartilage injury and catabolic factors but did not promote cartilage anabolism in vitro and in vivo.

The present study has a few limitations. How SHP-2 is phosphorylated in the pathologic process of OA is still unclear. We did not conduct therapeutic administration experiments in the DMM model. We did not perform SHP099 treatment after 5 weeks of DMM modeling, before SHP-2–knockout experiments. In addition, how uridine regulates the synthesis and degradation of cartilage and whether there is a direct acting receptor for uridine need further investigation.

Although the precise mechanism by which uridine is chondroprotective is not elucidated in this study, our research reveals that SHP-2 inhibitors exert a dual effect of inhibiting cartilage degradation and promoting cartilage synthesis. Taken together, our findings reveal for the first time that SHP-2 inhibition exhibits chondroprotective effects through the DOK1/UPP1/uridine cascade, and that targeting SHP-2 may serve as a promising therapeutic approach in OA.

ACKNOWLEDGMENTS

We thank Professor Gen-Sheng Feng (University of California San Diego) for providing *SHP2*$^{flox/flox}$ mice. We thank Professor Ge Zhang (Hong Kong Baptist University) for providing *Aggrecan-Cre*^{ERT} mice. We thank Professor Xiangbao Meng (Peking University, Beijing, China) for providing SHP099 hydrochloride. We also thank Dr. Lifei Hou (Harvard Medical School, Boston, MA) for valuable advice on this project. The complementary DNA for Src SH-2 domain triple-mutant T183V/C188A/K206L was a gift provided by Precision Proteomics Inc. (Ontario, Canada).

AUTHOR CONTRIBUTIONS

All authors were involved in drafting the article or revising it critically for important intellectual content, and all authors approved the final version to be published. Drs. Liu and Y. Sun had full access to all of the data in the study and take responsibility for the integrity of the data and the accuracy of the data analysis.

Study conception and design. Xu, Tan, Y. Sun.

Acquisition of data. Liu, Zhai, Han, Shi, Z. Sun, Peng, Wang, Zhang, Gao, Yan.

Analysis and interpretation of data. Liu, Zhai, Jiang, Chen, Y. Sun.

REFERENCES

1. Mobasheri A, Batt M. An update on the pathophysiology of osteoarthritis. Ann Phys Rehabil Med 2016;59:333–9.
2. Martel-Pelletier J, Barr AJ, Cicuttini FM, Conaghan PG, Cooper C, Goldring MB, et al. Osteoarthritis. Nat Rev Dis Primers 2016;2:16072.
3. Kuyinu EL, Narayanan G, Nair LS, Laurencin CT. Animal models of osteoarthritis: classification, update, and measurement of outcomes. J Orthop Surg Res 2016;11:19.
4. Kim JH, Jeon J, Shin M, Won Y, Lee M, Kwak JS, et al. Regulation of the catabolic cascade in osteoarthritis by the zinc-ZIP8-MTF1 axis. Cell 2014;156:730–43.
5. Shi Y, Hu X, Cheng J, Zhang X, Zhao F, Shi W, et al. A small molecule promotes cartilage extracellular matrix generation and inhibits osteoarthritis development. Nat Commun 2019;10:1914.
6. Goldring MB, Otero M, Plumb DA, Dragomir C, Favero M, El Hachem K, et al. Roles of inflammatory and anabolic cytokines in cartilage metabolism: signals and multiple effectors converge upon MMP-13 regulation in osteoarthritis. Eur Cell Mater 2011;21:202–20.

7. Glasson SS, Askew R, Sheppard B, Carito B, Blanchet T, Ma HL, et al. Deletion of active ADAMTS5 prevents cartilage degradation in a murine model of osteoarthritis. Nature 2005;434:644–8.
8. Rabelink TJ, van den Berg BM, Garsen M, Wang G, Elkin M, van der Vlag J. Heparanase: roles in cell survival, extracellular matrix remodelling and the development of kidney disease. Nat Rev Nephrol 2017; 13:201–12.
9. Li K, Zhang Y, Zhang Y, Jiang W, Shen J, Xu S, et al. Tyrosine kinase Fyn promotes osteoarthritis by activating the β-catenin pathway. Ann Rheum Dis 2018;77:935–43.
10. Malemud CJ. Protein kinases in chondrocyte signaling and osteoarthritis. Clin Orthop Relat Res 2004;427 Suppl:S145–51.
11. Islam S, Kermode T, Sultana D, Moskowitz RW, Mukhtar H, Malemud CJ, et al. Expression profile of protein tyrosine kinase genes in human osteoarthritis chondrocytes. Osteoarthritis Cartilage 2001;9:684–93.
12. Kim HK, Aruwajoye O, Sucato D, Richards BS, Feng GS, Chen D, et al. Induction of SHP2 deficiency in chondrocytes causes severe scoliosis and kyphosis in mice. Spine 2013;38:E1307–12.
13. Yang W, Wang J, Moore DC, Liang H, Dooner M, Wu Q, et al. Ptpn11 deletion in a novel progenitor causes metachondromatosis by inducing hedgehog signalling. Nature 2013;499:491–5.
14. Tartaglia M, Mehler EL, Goldberg R, Zampino G, Brunner HG, Kremer H, et al. Mutations in PTPN11, encoding the protein tyrosine phosphatase SHP-2, cause Noonan syndrome. Nat Genet 2001;29: 465–8.
15. Kontaridis MI, Swanson KD, David FS, Barford D, Neel BG. PTPN11 (Shp2) mutations in LEOPARD syndrome have dominant negative, not activating, effects. J Biol Chem 2006;281:6785–92.
16. Kim HK, Feng GS, Chen D, King PD, Kamiya N. Targeted disruption of Shp2 in chondrocytes leads to metachondromatosis with multiple cartilaginous protrusions. J Bone Miner Res 2014;29:761–9.
17. Wang L, Huang J, Moore DC, Zuo C, Wu Q, Xie L, et al. SHP2 regulates the osteogenic fate of growth plate hypertrophic chondrocytes. Sci Rep 2017;7:12699.
18. Sophocleous A, Huesa C. Osteoarthritis mouse model of destabilization of the medial meniscus. Methods Mol Biol 2019;1914:281–93.
19. Glasson SS, Chambers MG, Van Den Berg WB, Little CB. The OARSI histopathology initiative: recommendations for histological assessments of osteoarthritis in the mouse. Osteoarthritis Cartilage 2010; 18 Suppl 3:S17–23.
20. Snelling S, Rout R, Davidson R, Clark I, Carr A, Hulley PA, et al. A gene expression study of normal and damaged cartilage in anteromedial gonarthrosis, a phenotype of osteoarthritis. Osteoarthritis Cartilage 2014;22:334–43.
21. Feng H, Xing W, Han Y, Sun J, Kong M, Gao B, et al. Tendon-derived cathepsin K-expressing progenitor cells activate Hedgehog signaling to drive heterotopic ossification. J Clin Invest 2020;130:6354–65.
22. Ji Q, Zheng Y, Zhang G, Hu Y, Fan X, Hou Y, et al. Single-cell RNA-seq analysis reveals the progression of human osteoarthritis. Ann Rheum Dis 2019;78:100–10.
23. Jimenez G, Cobo-Molinos J, Antich C, Lopez-Ruiz E. Osteoarthritis: trauma vs disease. Adv Exp Med Biol 2018;1059:63–83.
24. Krenn V, Morawietz L, Burmester GR, et al. Synovitis score: discrimination between chronic low-grade and high-grade synovitis. Histopathology 2006;49:358–34.
25. Cicko S, Grimm M, Ayata K, Beckert J, Meyer A, Hossfeld M, et al. Uridine supplementation exerts anti-inflammatory and anti-fibrotic effects in an animal model of pulmonary fibrosis. Respir Res 2015; 16:105.
26. Jeengar MK, Thummuri D, Magnusson M, Naidu VG, Uppugunduri S. Uridine ameliorates dextran sulfate sodium (DSS)-induced colitis in mice. Sci Rep 2017;7:3924.
27. Cao Z, Ma J, Chen XC, Zhou BP, Cai C, Huang D, et al. Uridine homeostatic disorder leads to DNA damage and tumorigenesis. Cancer Lett 2016;372:219–25.
28. Al Safarjalani ON, Zhou XJ, Rais RH, Shi J, Schinazi RF, Naguib FN, et al. 5-(Phenylthio)acyclouridine: a powerful enhancer of oral uridine bioavailability: relevance to chemotherapy with 5-fluorouracil and other uridine rescue regimens. Cancer Chemother Pharmacol 2005; 55:541–51.
29. Yahara Y, Takemori H, Okada M, Kosai A, Yamashita A, Kobayashi T, et al. Pterosin B prevents chondrocyte hypertrophy and osteoarthritis in mice by inhibiting Sik3. Nat Commun 2016;7:10959.
30. Apostu D, Lucaciu O, Mester A, Oltean-Dan D, Baciut M, Baciut G, et al. Systemic drugs with impact on osteoarthritis. Drug Metab Rev 2019;51:498–523.
31. Simental-Mendia M, Sanchez-Garcia A, Vilchez-Cavazos F, Acosta-Olivo CA, Pena-Martinez VM, Simental-Mendia LE. Effect of glucosamine and chondroitin sulfate in symptomatic knee osteoarthritis: a systematic review and meta-analysis of randomized placebo-controlled trials. Rheumatol Int 2018;38:1413–28.
32. Kloppenburg M, Berenbaum F. Osteoarthritis year in review 2019: epidemiology and therapy. Osteoarthritis Cartilage 2020;28:242–8.
33. Chen YN, LaMarche MJ, Chan HM, Fekkes P, Garcia-Fortanet J, Acker MG, et al. Allosteric inhibition of SHP2 phosphatase inhibits cancers driven by receptor tyrosine kinases. Nature 2016;535: 148–52.
34. Frankson R, Yu ZH, Bai Y, Li Q, Zhang RY, Zhang ZY. Therapeutic targeting of oncogenic tyrosine phosphatases [review]. Cancer Res 2017;77:5701–5.
35. Liu Q, Qu J, Zhao M, Xu Q, Sun Y. Targeting SHP2 as a promising strategy for cancer immunotherapy. Pharmacol Res 2020;152: 104595.
36. Zhao M, Guo W, Wu Y, Yang C, Zhong L, Deng G, et al. SHP2 inhibition triggers anti-tumor immunity and synergizes with PD-1 blockade. Acta Pharm Sin B 2019;9:304–15.
37. Bauler TJ, Kamiya N, Lapinski PE, Langewisch E, Mishina Y, Wilkinson JE, et al. Development of severe skeletal defects in induced SHP-2-deficient adult mice: a model of skeletal malformation in humans with SHP-2 mutations. Dis Model Mech 2011;4:228–39.
38. Wang L, Yang H, Huang J, Pei S, Wang L, Feng JQ, et al. Targeted Ptpn11 deletion in mice reveals the essential role of SHP2 in osteoblast differentiation and skeletal homeostasis. Bone Res 2021;9:6.
39. Rivera LM, Fernandes de Melo E, Araujo PD, Filho NA, Delgado Quiroz LA, Bica BE. Peripheral spondyloarthritis in a patient with Noonan's syndrome. Reumatol Clin 2015;11:112–5.
40. Wang J, Xu SH, Lv W, Shi F, Mei SS, Shan AJ, et al. Uridine phosphorylase 1 is a novel immune-related target and predicts worse survival in brain glioma. Cancer Med 2020;9:5940–7.
41. Saif MW, Diasio RB. Benefit of uridine triacetate (Vistogard) in rescuing severe 5-fluorouracil toxicity in patients with dihydropyrimidine dehydrogenase (DPYD) deficiency. Cancer Chemother Pharmacol 2016; 78:151–6.
42. Baumel BS, Doraiswamy PM, Sabbagh M, Wurtman R. Potential neuroregenerative and neuroprotective effects of uridine/choline-enriched multinutrient dietary intervention for mild cognitive impairment: a narrative review. Neurol Ther 2021;10:43–60.
43. Carlezon WA, Mague SD, Parow AM, Stoll AL, Cohen BM, Renshaw PF. Antidepressant-like effects of uridine and omega-3 fatty acids are potentiated by combined treatment in rats. Biol Psychiat 2005;57:343–50.
44. Goldberg H, Mibielli MA, Nunes CP, Goldberg SW, Buchman L, Mezitis SG, et al. A double-blind, randomized, comparative study of

the use of a combination of uridine triphosphate trisodium, cytidine monophosphate disodium, and hydroxocobalamin, versus isolated treatment with hydroxocobalamin, in patients presenting with compressive neuralgias. J Pain Res 2017;10:397–404.

45. Ling Y, Maile LA, Badley-Clarke J, Clemmons DR. DOK1 mediates SHP-2 binding to the alphaVβ3 integrin and thereby regulates insulin-like growth factor I signaling in cultured vascular smooth muscle cells. J Biol Chem 2005;280:3151–8.

DOI 10.1002/art.41956

Clinical Images: Extranodal Natural Killer/T Cell Lymphoma As a Rare Mimicker of Granulomatosis With Polyangiitis

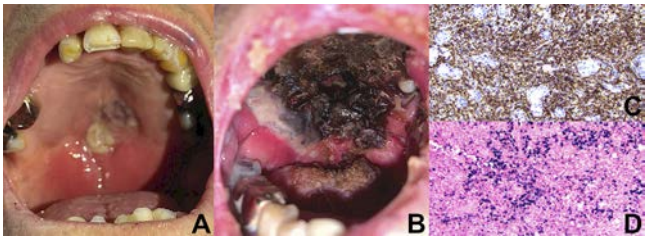

The patient, a 90-year-old man, presented with an ulcer of the hard palate (**A**) and unilateral orbital swelling following 3 months of nasal crusting. Findings of laboratory tests were as follows: white blood cell count 6,600/mm^3 (normal differential cell count with 1.7% eosinophils), hemoglobin 9.8 gm/dl, normal platelet count, erythrocyte sedimentation rate 98 mm/hour (normal <15), C-reactive protein 3.7 mg/dl (normal <0.5), negative test findings for antineutrophil cytoplasmic antibodies (ANCAs) and myeloperoxidase–proteinase 3 antibodies, elevated levels of IgG (2,170 mg/dl; normal <1,600) with normal levels of IgG4, and normal findings on urinalysis. Antibiotics were initiated for an *Actinomyces* infection. Biopsy of the ulcer revealed necrotizing vasculitis and 39 IgG4-positive plasma cells per high-power field, with an IgG4:IgG ratio of 0.68. Storiform fibrosis and obliterative phlebitis, which are expected in IgG4-related disease (IgG4-RD), were not seen. Both necrotizing vasculitis and necrosis, which should not be seen in IgG4-RD, were prominent. High-dose prednisone was started for a presumed diagnosis of granulomatosis with polyangiitis (GPA), as it was thought that the disease presentation in this patient represented a limited form of GPA. At least 10% of cases of GPA are ANCA-negative, and limited disease is associated more often with ANCA negativity (1). His condition worsened over the next 3 months, prompting initiation of intravenous immunoglobulin and rituximab. Ultimately, he developed palatal perforation (**B**) and necrosis extending into the sinuses with associated dacryocystitis. Subsequent staining of a lesion extracted from the palate revealed the presence of lymphocytes that were positive for CD3 (**C**) and CD56, as well as Epstein–Barr virus (EBV)–encoded RNA positivity (**D**), consistent with a diagnosis of extranodal natural killer/T cell lymphoma (NKTCL). Polymerase chain reaction analysis of the patient's peripheral blood revealed highly elevated levels of EBV (12,900 IU/ml; normal <48). Extranodal NKTCL is a rare cause of nasal obstruction, mass formation, and necrosis, most commonly seen in Latin America and Asia (2). Biopsy is critical for diagnosis. A diagnosis of extranodal NKTCL is supported by immunohistochemistry showing membranous CD56 and cytoplasmic CD3 positivity (3), and by in situ hybridization findings showing positivity for EBV. This condition has many histologic features in common with vasculitides such as GPA, including angiocentric distribution, necrosis (4), and increased numbers of IgG4-positive plasma cells. Thus, it is prudent to obtain adequate tissue for diagnosis and complete immunohistochemical stains to rule out the diagnosis of extranodal NKTCL.

Author disclosures are available at https://onlinelibrary.wiley.com/action/downloadSupplement?doi=10.1002%2Fart.41956&file=art41956-sup-0001-Disclosureform.pdf.

1. Rao JK, Weinberger M, Oddone EZ, Allen NB, Landsman P, Feussner JR. The role of antineutrophil cytoplasmic antibody (c-ANCA) testing in the diagnosis of Wegener granulomatosis: a literature review and meta-analysis. Ann Intern Med 1995;123:925–32.
2. Sánchez-Romero C, Paes de Almeida O, Henao JR, Carlos R. Extranodal NK/T-cell lymphoma, nasal type in Guatemala: an 86-case series emphasizing clinical presentation and microscopic characteristics. Head Neck Pathol 2019;13:624–34.
3. Schwartz EJ, Molina-Kirsch H, Zhao S, Marinelli RJ, Warnke RA, Natkunam Y. Immunohistochemical characterization of nasal-type extranodal NK/T-cell lymphoma using a tissue microarray: an analysis of 84 cases. Am J Clin Pathol 2008;130:343–51.
4. Lee YT, Chang YS, Lai CC, Chen WS, Yang AH, Tsai CY. Natural killer (NK)/T-cell lymphoma mimicking granulomatosis with polyangiitis (Wegener's) [letter]. Scand J Rheumatol 2012;41:407–8.

Jennifer Strouse, MD
Anand Rajan, KD, MD
University of Iowa Hospitals and Clinics
He B. Chang, MD
Mohamad D. Dimachkie, MD
Christopher Halbur, BS
University of Iowa
Brittany Bettendorf, MD
University of Iowa Hospitals and Clinics
Iowa City IA

Arthritis & Rheumatology
Vol. 74, No. 3, March 2022, pp 475–485
DOI 10.1002/art.42010

American College of Rheumatology
Empowering Rheumatology Professionals

Long-Term Efficacy and Safety of Guselkumab, a Monoclonal Antibody Specific to the p19 Subunit of Interleukin-23, Through Two Years: Results From a Phase III, Randomized, Double-Blind, Placebo-Controlled Study Conducted in Biologic-Naive Patients With Active Psoriatic Arthritis

Iain B. McInnes,[1] Proton Rahman,[2] Alice B. Gottlieb,[3] Elizabeth C. Hsia,[4] Alexa P. Kollmeier,[5] Xie L. Xu,[5] Yusang Jiang,[6] Shihong Sheng,[6] May Shawi,[7] Soumya D. Chakravarty,[8] Désirée van der Heijde,[9] and Philip J. Mease[10]

Objective. To assess long-term efficacy and safety of guselkumab, an interleukin-23 p19 subunit (IL-23p19) inhibitor, in patients with active psoriatic arthritis (PsA) from the phase III DISCOVER-2 trial.

Methods. In the DISCOVER-2 trial, patients with active PsA (≥5 swollen joints and ≥5 tender joints; C-reactive protein level ≥0.6 mg/dl) despite prior nonbiologic therapy were randomized to receive the following: guselkumab 100 mg every 4 weeks; guselkumab 100 mg at weeks 0 and 4 and then every 8 weeks; or placebo with crossover to guselkumab 100 mg every 4 weeks, beginning at week 24. Efficacy assessments included American College of Rheumatology ≥20%/50%/70% improvement criteria (ACR20/50/70), Investigator's Global Assessment (IGA) of psoriasis score of 0 (indicating complete skin clearance), resolution of enthesitis (Leeds Enthesitis Index) and dactylitis (Dactylitis Severity Score), and changes in the Sharp/van der Heijde modified radiographic scores for PsA. Clinical data (imputed as no response/no change from baseline if missing) and observed radiographic data were summarized through week 100; safety assessments continued through week 112.

Results. Of the 739 randomized and treated patients, 652 (88%) completed treatment through week 100. Across groups of guselkumab-treated patients (including those in the placebo–guselkumab crossover group), the following findings at week 100 indicated that amelioration of arthritis signs/symptoms and extraarticular manifestations was durable through 2 years: ACR20 response (68–76%), ACR50 response (48–56%), ACR70 response (30–36%), IGA score of 0 (55–67%), enthesitis resolution (62–70%), and dactylitis resolution (72–83%). Mean changes in the Sharp/van der Heijde modified score for PsA from weeks 52 to week 100 (range 0.13–0.75) indicated that the low rates of radiographic progression observed among guselkumab-treated patients at earlier time points extended through week 100. Through week 112, 8% (5.8 per 100 patient-years) and 3% (1.9 per 100 patient-years) of the 731 guselkumab-treated patients had a serious adverse event or serious infection, respectively; 1 death occurred (road traffic accident).

Conclusion. In biologic-naive PsA patients, guselkumab provided durable improvements in multiple disease domains with no unexpected safety findings through 2 years.

A video abstract of this article can be found at https://players.brightcove.net/3806881048001/default_default/index.html?videoId=6295462884001.

Supported by Janssen Research & Development.

[1]Iain B. McInnes, FRCP, PhD: University of Glasgow, Glasgow, UK; [2]Proton Rahman, MD: Memorial University of Newfoundland, St. Johns, Newfoundland, Canada; [3]Alice B. Gottlieb, MD, PhD: Icahn School of Medicine Mt. Sinai, New York, New York; [4]Elizabeth C. Hsia, MD: Janssen Research & Development, Spring House, Pennsylvania, and University of Pennsylvania, Philadelphia, Pennsylvania; [5]Alexa P. Kollmeier, MD, Xie L. Xu, PhD: Janssen Research & Development, LLC, San Diego, California; [6]Yusang Jiang, MA, Shihong Sheng, PhD: Janssen Research & Development, Spring House, Pennsylvania; [7]May Shawi, PhD: Janssen Pharmaceutical Companies of Johnson & Johnson, Horsham, Pennsylvania; [8]Soumya D. Chakravarty, MD, PhD: Janssen Scientific Affairs, Horsham, Pennsylvania, and Drexel University College of Medicine, Philadelphia, Pennsylvania; [9]Désirée van der Heijde, MD, PhD: Leiden University Medical Center, Leiden, The Netherlands; [10]Philip J. Mease, MD: Swedish Medical Center/Providence St. Joseph Health and University of Washington, Seattle, Washington.

Author disclosures are available at https://onlinelibrary.wiley.com/action/downloadSupplement?doi=10.1002%2Fart.42010&file=art42010-sup-0001-Disclosureform.pdf.

Address correspondence to Iain B. McInnes, PhD, University of Glasgow, Glasgow, UK. Email: iain.mcinnes@glasgow.ac.uk.

Submitted for publication May 26, 2021; accepted in revised form October 19, 2021.

INTRODUCTION

Psoriatic arthritis (PsA), an inflammatory disorder primarily affecting the skin and joints, can present with a variety of manifestations including skin and nail lesions, peripheral joint pain, spondylitis, dactylitis, and enthesitis. Symptoms typically begin in early to mid-adulthood, thus requiring long-term treatment. Current treatment guidelines advise choosing therapeutics directed at specific PsA disease domains affected in individual patients (1,2). Biologic therapies are often recommended for patients whose disease is not adequately controlled by conventional synthetic disease-modifying antirheumatic drugs (DMARDs). In addition, it is not uncommon for PsA patients to switch biologic treatments due to loss of efficacy over time or intolerance (3,4). Recent findings from an observational study of biologics in PsA patients show that treatment persistence and achieving low disease activity at 1 year was predictive of longer-term persistence and remission at 12 years (5), highlighting the current unmet need for treatments exhibiting durable efficacy and safety (6,7).

The Th17 cell line has been identified as a critical driver of skin inflammation in psoriasis (8,9) and may also drive articular disease pathogenesis, given that interleukin-17A (IL-17A) inhibitors have demonstrated therapeutic benefits in this compartment (10). IL-23 is known to promote differentiation and proliferation of Th17 cells in skin lesions from psoriasis patients (11,12), and this pathway has been implicated in PsA pathogenesis (13). Guselkumab, a monoclonal antibody targeting the IL-23p19 subunit, is approved both for adults with moderate-to-severe psoriasis and those with active PsA (14). In the phase III, randomized, placebo-controlled DISCOVER-1 (15) and DISCOVER-2 (16) studies, patients treated with guselkumab 100 mg, either every 4 weeks or every 8 weeks, achieved greater improvements and higher response rates in several measures of joint and skin disease at week 24 compared to those receiving placebo. Radiographic progression, assessed only in the DISCOVER-2 trial, was significantly lower in the guselkumab group treated every 4 weeks than in the placebo group at week 24. Improvements in the signs and symptoms of PsA and joint and skin response rates were maintained through 1 year, with safety findings consistent with the known profile of guselkumab (17,18). The DISCOVER-2 trial continued through 2 years, and the final clinical efficacy, radiographic progression, and safety results are reported herein.

PATIENTS AND METHODS

Patients. Patient eligibility criteria have been previously described (16). Briefly, the DISCOVER-2 trial enrolled adults with active PsA (≥5 tender joints and ≥5 swollen joints; C-reactive protein [CRP] level ≥0.6 mg/dl) despite standard nonbiologic treatment (DMARDs, apremilast, or nonsteroidal antiinflammatory drugs [NSAIDs]) who were naive to treatment with biologic agents and JAK inhibitors.

Study design. This phase III, randomized, double-blind study was conducted at 118 sites across 13 countries. The trial included a 6-week screening period, a 100-week treatment phase (placebo-controlled weeks 0–24, active treatment weeks 24–100), and 12 weeks of safety follow-up (weeks 100–112) (16). Eligible patients were randomized (1:1:1) to receive subcutaneous injections of guselkumab 100 mg every 4 weeks; guselkumab 100 mg at weeks 0 and 4 and then every 8 weeks; or placebo with crossover to guselkumab 100 mg every 4 weeks beginning at week 24. Patients had the option to self-administer guselkumab in weeks 56–96. Central randomization and study blinding details through week 24 have been previously reported (16). After crossover to guselkumab, patients and investigators remained blinded with regard to dosing regimen. Patients could continue stable baseline use of selected nonbiologic DMARDs, oral glucocorticoids (≤10 mg/day of prednisone or equivalent), and NSAIDs/other analgesics up to regionally approved doses.

The DISCOVER-2 trial (ClinicalTrials.gov identifier: NCT03158285) was conducted in accordance with Declaration of Helsinki and Good Clinical Practice guidelines. The protocol was approved by each site's governing ethical body, and all patients provided written informed consent.

Procedures. Efficacy was assessed through week 100. American College of Rheumatology (ACR) response components (tender joint count [0–68], swollen joint count [0–66], pain [0–10 cm visual analog scale (VAS)], physician global assessment [0–10 cm VAS], patient global assessment [0–10 cm VAS], physical function as assessed by the Health Assessment Questionnaire disability index [HAQ DI; 0–3], and CRP level [mg/dl]) were determined as previously described (16,17). Enthesitis (Leeds Enthesitis Index; total 0–6) (19) and dactylitis (Dactylitis Severity Score; total 0–60) (20) were also assessed.

Single radiographs of hands (posteroanterior) and feet (anteroposterior) were obtained at weeks 0, 24, 52, and 100 (or at discontinuation) and scored using the Sharp/van der Heijde modified scoring method for PsA (21). Findings previously described through week 24 and week 52 were derived from the first and second reading sessions, respectively (16,17). The third reading session included radiographs from all time points and were independently evaluated by 2 central primary readers, with a third reader for adjudication, blinded with regard to treatment group and time point. Assignment of readers to primary reader/adjudicator roles was the same for reading sessions 1 and 3, and scores of the 2 primary readers in each session were averaged together (16,17). Scores from a third adjudicator were utilized when the difference in change scores between the primary readers was >10 or if change scores from 1 primary reader were missing.

Skin symptoms were assessed using the Investigator's Global Assessment of psoriasis (IGA; 0 [cleared] to 4 [severe]) (22). The Psoriasis Area and Severity Index (PASI; 0–72) also

assessed the extent (percentage body surface area affected) and degree of associated redness, thickness, and scaling (each graded from 0 [none] to 4 [maximum]) (23). Health-related quality of life (HRQoL) was evaluated using Short Form 36 (SF-36) physical component summary (PCS) and mental component summary (MCS) scores (24).

Adverse events (AEs) and routine hematology and chemistry parameters were monitored. Serum samples collected through week 112 were assayed to measure guselkumab concentrations and detect antibodies to guselkumab (15,16).

Outcome measures. Outcome measures included the following: ACR ≥20%/50%/70% improvement criteria (ACR20/50/70) (25); IGA score 0/1 (score 0/1 and ≥2-grade improvement); skin responses (IGA 0 and ≥75%, 90%, or 100% improvement in PASI [PASI75/90/100]) in patients with ≥3% body surface area affected with psoriasis and IGA score ≥2 at baseline; changes in total Sharp/van der Heijde modified scores for PsA derived from images read in the third session; changes from baseline in HAQ DI and proportions of patients with HAQ DI response (reduction ≥0.35 among patients with a baseline score ≥0.35) or normalized HAQ DI (≤0.5 among patients with a baseline score >0.5); changes from baseline in SF-36 PCS and MCS scores and proportions of patients with a minimal clinically important difference (≥5) (26); resolution of enthesitis and dactylitis (score 0 among patients affected at baseline); and achievement of minimal disease activity (MDA) (27) or very low disease activity (VLDA) (28).

Safety outcomes included AEs, serious AEs (SAEs), AEs resulting in discontinuation of study drug, infections, serious infections, injection-site reactions, malignancies, major adverse cardiovascular events (MACE; predefined as cardiovascular death, nonfatal myocardial infarction, or nonfatal stroke), suicidal ideation or behavior (electronic Columbia-Suicide Severity Rating Scale questionnaire or reported AEs), and clinical laboratory abnormalities classified by the National Cancer Institute's Common Terminology Criteria for AEs.

Statistical analysis. DISCOVER-2 sample size estimates have been previously reported (16). All patients continuing treatment at week 24 received guselkumab going forward; no formal hypothesis testing was planned after week 24.

As previously reported (16), treatment failure rules were applied to all clinical efficacy analyses through week 24: patients who discontinued study treatment, terminated study participation, initiated/increased doses of DMARDs or oral glucocorticoids, or initiated protocol-prohibited PsA treatment were considered nonresponders for binary end points, or were considered to have no change from baseline for continuous end points. Missing data were imputed as nonresponse for categorical end points or using multiple imputation (assumed to be missing at random) for continuous end points. After week 24, the statistical analysis plan prespecified using observed data through week 100. Post hoc clinical efficacy (but not radiographic) analyses employed nonresponder imputation (NRI) in which patients with missing data were classified as nonresponders for categorical end points, and missing continuous end point data were imputed as having no change (for patients who discontinued study treatment), or were imputed using multiple imputation (assumed to be missing at random for patients with missing data for any other reason). Results of these post hoc analyses have been reported through week 52 (17) and are reported here through week 100. Additional post hoc analyses assessed the maintenance of ACR20/50/70 responses (NRI) at week 100 among patients with a response at week 52, the proportions of patients achieving ≥20% improvement in the individual ACR components (NRI) through week 100, and the median time to onset of treatment effect (for ACR20) using Kaplan–Meier curves. Least squares mean (LSM) changes in clinical efficacy and HRQoL measures were determined using analysis of covariance.

Observed changes in Sharp/van der Heijde scores from reading session 3 were summarized using descriptive statistics for patients who continued treatment at week 52. Cumulative probability plots show the observed cumulative distribution of these scores, ranked from lowest to highest, against the actual value according to study period (weeks 0–52 and weeks 52–100).

AEs were summarized by actual treatment received for patients who received ≥1 study agent administration. To account for the shorter placebo-controlled period compared to active treatment, incidences of AEs, SAEs, AEs leading to discontinuation, infections, and serious infections are also reported as the number of events per 100 patient-years of follow-up with 95% confidence intervals (95% CIs).

RESULTS

Patient disposition and characteristics. A total of 739 patients were randomized and treated (guselkumab 100 mg every 4 weeks [n = 245], guselkumab 100 mg every 8 weeks [n = 248], or placebo [n = 246]). Baseline demographic and disease characteristics were generally well balanced among treatment groups, and disease activity measures were consistent with active PsA (16); 60% of patients were receiving concomitant methotrexate (MTX) at baseline.

Patient dispositions through week 24 (16) and week 52 (17) have also been reported. The robust patient retention seen through 1 year (93%) was durable through week 100, when nearly 90% of randomized and treated patients completed study treatment (89% of the every-4-weeks group; 90% of the every-8-weeks group; 85% of the placebo–guselkumab crossover group) (Supplementary Figure 1, available on the *Arthritis & Rheumatology* website at https://onlinelibrary.wiley.com/doi/10.1002/art.42010). Among 687 patients who received ≥1 guselkumab administration at or after week 52, the most common reason for discontinuation was an AE (1.3% [3 of 227 patients], 2.2% [5 of

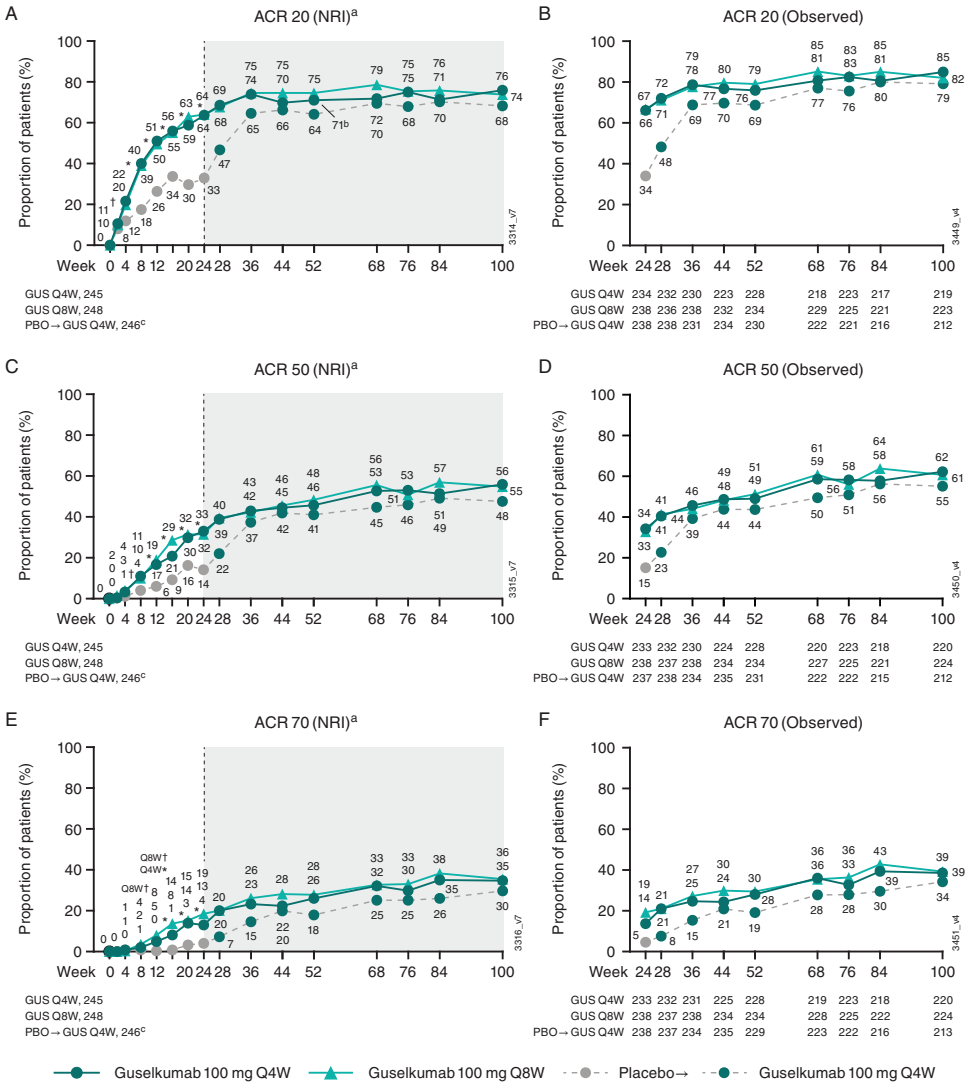

*p ≤ 0.001; †p < 0.05

a Includes patients randomized to Q4W & Q8W at Week 0 who received ≥1 dose of study agent.

b One patient's Week 52 visit, which was not captured in the interim data base lock, was included in the final data base lock.

c 238 crossed over to Q4W at Week 24 & 8 received placebo only before study agent discontinuation.

Figure 1. Proportions of patients achieving American College of Rheumatology ≥20% improvement criteria (ACR20) (**A** and **B**), ACR50 (**C** and **D**), and ACR70 (**E** and **F**) responses through week 100. Response rates derived using nonresponder imputation (NRI) for missing data (see Patients and Methods) are shown in panels **A**, **C**, and **E**; response rates from weeks 24–100 derived from observed data are shown in panels **B**, **D**, and **F**. The dashed vertical line at week 24 indicates placebo (PBO) crossover to guselkumab (GUS) administered every 4 weeks (Q4W); gray shading indicates post hoc NRI data. Q8W = every 8 weeks.

232 patients], and 3.1% [7 of 228 patients], respectively, in each of the aforementioned groups).

Efficacy. Clinical efficacy through week 24 and week 52 has been previously detailed (16,17). Briefly, the primary end point was achieved, with 64% of patients in both guselkumab dosing groups achieving an ACR20 response at week 24 versus 33% of patients in the placebo group (16). At week 100, 76% of patients in the guselkumab every-4-weeks group and 74% in the every-8-weeks group had an ACR20 response, 56% and 55%, respectively, had an ACR50 response, and 35% and 36%, respectively, had an ACR70 response (all NRI accounting for ~12% of patients with missing data) (Figure 1). Trends in ACR response rates over time using observed data were consistent with those determined using NRI (Figure 1). When evaluating the time to ACR20 response, separation from placebo was observed at week 4, with continued increases in response rate through week 24 for patients in the guselkumab groups (Supplementary Figure 2, https://onlinelibrary.wiley.com/doi/10.1002/art.42010). Among ACR components, 45–62% of guselkumab-treated patients achieved ≥20% improvement in tender and swollen joint counts, physician global assessment score, and CRP level by week 4

Table 1. Extraarticular and HRQoL assessments, composite indices, and radiographic progression through week 100 in the DISCOVER-2 study*

	Guselkumab Q4W			Guselkumab Q8W			Placebo–guselkumab crossover Q4W		
	Week 24	Week 52	Week 100	Week 24	Week 52	Week 100	Week 24	Week 52	Week 100
No. patients with enthesitis at week 0	170	170	170	158	158	158	178	178	178
Enthesitis resolution, %	44	57	62	54	61	70	30	64	65
LSM change (95% CI)	−1.5 (−1.8, −1.3)	−1.8 (−2.0, −1.6)	−1.9 (−2.1, −1.7)	−1.6 (−1.8, −1.4)	−1.9 (−2.1, −1.7)	−2.1 (−2.3, −1.8)	−1.0 (−1.3, −0.8)	−2.0 (−2.2, −1.8)	−2.1 (−2.3, −1.9)
No. patients with dactylitis at week 0	121	121	121	111	111	111	99	99	99
Dactylitis resolution, %	64	74	72	57	78	83	38	74	73
LSM change (95% CI)	−5.9 (−6.7, −5.0)	−6.5 (−7.2, −5.8)	−6.5 (−7.1, −5.8)	−6.0 (−6.8, −5.1)	−7.2 (−7.9, −6.5)	−7.5 (−8.1, −6.8)	−4.0 (−5.0, −3.1)	−6.9 (−7.6, −6.2)	−6.9 (−7.6, −6.2)
HAQ DI									
No. patients assessed	245	245	245	248	248	248	246	246	246
LSM change (95% CI)	−0.40 (−0.46, −0.34)	−0.49 (−0.56, −0.42)	−0.55 (−0.62, −0.48)	−0.37 (−0.43, 0.31)	−0.45 (−0.52, −0.38)	−0.53 (−0.59, −0.46)	−0.13 (−0.19, −0.07)	−0.35 (−0.42, −0.29)	−0.46 (−0.53, −0.40)
No. patients with HAQ DI ≥0.35 at week 0	228	228	228	228	228	228	236	236	236
Improvement ≥0.35, %	56	59	63	50	58	64	31	48	56
No. patients with HAQ DI >0.5 at week 0	214	214	214	211	211	211	218	218	218
HAQ DI score ≤0.5, %	29	36	40	23	28	35	14	31	33
SF-36									
No. patients assessed	245	245	245	248	248	248	246	246	246
LSM change in PCS (95% CI)	7.0 (6.1, 7.9)	8.6 (7.6, 9.6)	10.0 (8.9, 11.1)	7.4 (6.5, 8.3)	9.0 (7.9, 10.0)	10.4 (9.3, 11.5)	3.4 (2.5, 4.3)	7.5 (6.5, 8.6)	9.3 (8.2, 10.4)
Improvement ≥5, %	56	61	62	60	63	63	40	59	63
LSM change in MCS (95% CI)	4.2 (3.1, 5.3)	4.5 (3.4, 5.5)	4.9 (3.9, 6.0)	4.2 (3.1, 5.2)	4.3 (3.3, 5.4)	4.2 (3.2, 5.3)	2.1 (1.1, 3.2)	4.0 (3.0, 5.1)	3.9 (2.8, 4.9)
Improvement ≥5, %	34	36	39	38	42	42	31	39	37
Composite indices									
MDA, %	19	34	38	25	31	40	6	30	37
VLDA, %	5	11	14	4	16	17	1	7	13
Radiographic results†									
No. patients assessed	221	221	211	228	228	216	215	213	202
Changes in Sharp/van der Heijde modified score for PsA, mean ± SD	0.48 ± 2.70	0.57 ± 2.67	0.75 ± 4.02	0.68 ± 2.36	0.31 ± 1.57	0.46 ± 2.42	1.12 ± 3.80	0.34 ± 2.79	0.13 ± 3.74

* Data are summarized by treatment group with application of missing data handling rules, with the exception of radiographic results (see Patients and Methods). Clinical efficacy and health-related quality of life (HRQoL) results at week 24 (ref. 16) and week 52 (ref. 17) were previously published and are included here for reference. Q4W = every 4 weeks; Q8W = every 8 weeks; LSM = least squares mean; 95% CI = 95% confidence interval; HAQ DI = Health Assessment Questionnaire disability index; SF-36 = Short Form 36; PCS = physical component summary; MCS = mental component summary; PsA = psoriatic arthritis; MDA = minimal disease activity; VLDA = very low disease activity.
† Corresponding study periods for radiographic results are weeks 0–24, weeks 24–52, and weeks 52–100.

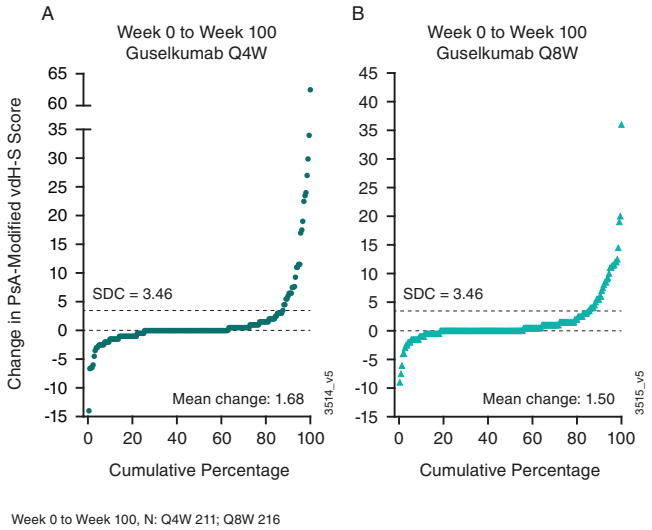

Figure 2. Cumulative probability plot of observed changes in Sharp/van der Heijde modified scores for psoriatic arthritis (PsA-modified vdH-S), from baseline to week 100, in patients randomized to receive guselkumab every 4 weeks (Q4W) (**A**) or every 8 weeks (Q8W) (**B**). SDC = smallest detectable change.

(Supplementary Figure 3, https://onlinelibrary.wiley.com/doi/10.1002/art.42010). In the guselkumab groups, the proportions of patients achieving ≥20% improvement were maintained or continued to increase through week 100 for all ACR components. In addition, at a group level, response rates for increasing levels of response (ACR50 and ACR70) increased over time through the second year of treatment. This suggests that individual patients may be improving over time and achieving higher levels of improvement with continued guselkumab treatment.

Among patients with available radiographs (reading session 3) in the guselkumab every-4-weeks and every-8-weeks groups, respectively, the observed mean changes in total Sharp/van der Heijde score were 0.48 and 0.68 from week 0 to week 24 (smallest detectable change [SDC] 2.18), 0.57 and 0.31 from week 24 to week 52 (SDC 2.25), and 0.75 and 0.46 from week 52 to week 100 (SDC 2.28) (Table 1). In the placebo crossover group, mean changes in Sharp/van der Heijde scores from week 24 to week 52 (0.34) and from week 52 to week 100 (0.13) indicated that, on average, patients in this group had less radiographic progression after initiating guselkumab compared to the 24-week placebo-controlled period (1.12). Low rates of radiographic progression were seen from week 0 to week 100 across both guselkumab dosing regimens (Figure 2). Mean changes in total Sharp/van der Heijde scores indicated less radiographic progression from week 52 to week 100 than from week 0 to week 52 in all 3 groups (Supplementary Figure 4, https://onlinelibrary.wiley.com/doi/10.1002/art.42010).

In prespecified pooled analyses of the DISCOVER-1 and DISCOVER-2 trials, guselkumab-treated patients had greater improvements in enthesitis and dactylitis scores and higher rates of resolution at week 24 compared to placebo-treated patients (16). In the DISCOVER-2 study, among patients affected at baseline, 62% in the every-4-weeks group and 70% in the every-8-weeks group achieved complete resolution of enthesitis and

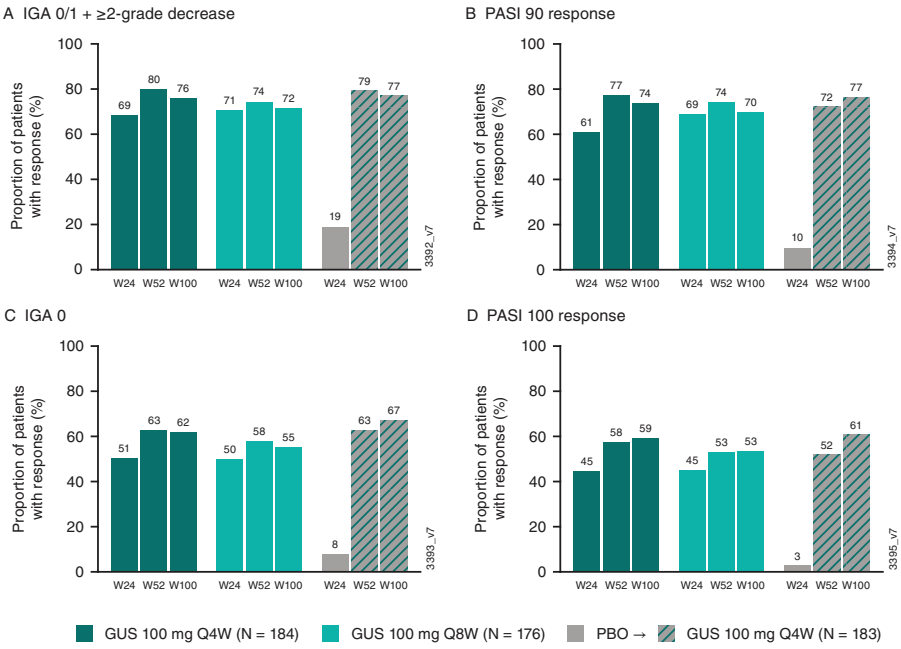

Figure 3. Proportions of patients achieving Investigator's Global Assessment (IGA) 0/1 response (**A**), ≥90% improvement in the Psoriasis Area and Severity Index (PASI90) response (**B**), IGA score 0 (**C**), and PASI100 response (**D**) through week 100 (W100). IGA and PASI scores were assessed in patients with ≥3% body surface area with psoriasis involvement and an IGA score of ≥2 at baseline. Response rates were derived using NRI for missing data. IGA response was defined as score of 0/1 and ≥2-grade improvement. See Figure 1 for other definitions.

72% and 83%, respectively, achieved complete resolution of dactylitis by week 100 (Table 1). Additionally, LSM changes from baseline in enthesitis and dactylitis scores at week 100 in the every-4-weeks group (−1.9 and −6.5, respectively) and in the every-8-weeks group (−2.1 and −7.5, respectively) were consistent with those reported at week 52 (17).

Improvements in physical function and HRQoL at week 24 were also significantly greater in the 2 guselkumab groups compared to placebo (16). At week 100, LSM changes from baseline in HAQ DI in the every-4-weeks (−0.55) and every-8-weeks (−0.53) groups were consistent with those at week 52, and 63–64% of patients had a clinically meaningful improvement in HAQ DI (≥0.35). Additionally, 35–40% of patients in the guselkumab groups achieved normalized physical function (HAQ DI ≤0.5) by week 100. In the guselkumab groups, improvements in HRQoL by week 100 were consistent with those observed at week 52, with LSM changes in SF-36 PCS and MCS scores ranging 10.0–10.4 and 4.2–4.9, respectively (Table 1).

At week 24, guselkumab-randomized patients had higher response rates for skin assessments (IGA and PASI) compared to placebo (16). Among patients receiving guselkumab from week 0, 62% of those in the every-4-weeks group and 55% in the every-8-weeks group had an IGA score of 0 at week 100, and 76% and 72% had an IGA 0/1 response, respectively (Figure 3). In addition, 82–83% of patients in the guselkumab groups achieved PASI75 at week 100, 70–74% achieved PASI90, and 53–59% achieved PASI100 (Figure 3).

Using composite measures of disease activity, 38% of those in the every-4-weeks group and 40% in the every-8-weeks group achieved MDA at week 100. Additionally, 14% and 17% of patients, respectively, achieved VLDA (Table 1).

For patients in the placebo–guselkumab crossover group, response rates for joint and skin manifestations and resolution of enthesitis and dactylitis, as well as improvements in these scores, at week 100 were similar to those at week 52. Low rates of radiographic progression and improvements in physical function and HRQoL also extended to week 100 in these patients. Also at week 100, 37% of placebo crossover patients achieved MDA and 13% achieved VLDA.

Among patients in the guselkumab groups who achieved an ACR20, ACR50, or ACR70 response at week 52, 91% in the every-4-weeks group and 87% in the every-8-weeks group maintained an ACR20 response, 83% and 79%, respectively, maintained an ACR50 response, and 72% and 80%, respectively, maintained an ACR70 response at week 100 (Figure 4). Among patients in these 2 groups who achieved the more stringent MDA criteria at week 52, 81% and 83%, respectively, maintained MDA at week 100.

AEs. Detailed safety results through week 24 and week 52 have been previously reported (16,17). Through week 112, a total of 731 patients received ≥1 administration of guselkumab,

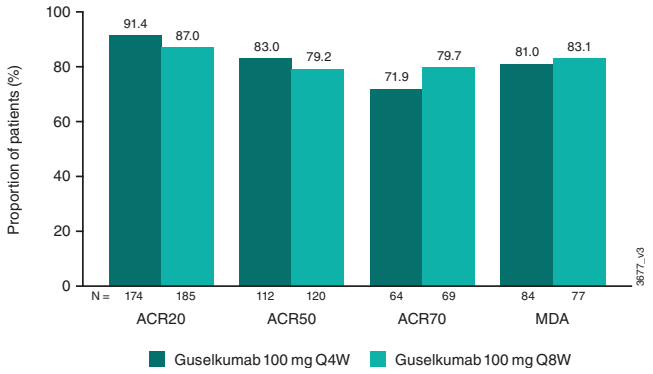

Figure 4. Proportions of patients maintaining ACR20, ACR50, or ACR70 responses or minimal disease activity (MDA) at week 100 among those who achieved these responses at week 52. Response rates were derived using NRI for missing data. See Figure 1 for other definitions.

including patients initially randomized to placebo who crossed over to guselkumab at week 24, for a total of 1,392 patient-years of follow-up.

Through week 112, as with earlier time points, infections were the most common type of AE reported in guselkumab-treated patients (Table 2). The most common infections were upper respiratory tract infection (8.5%) and nasopharyngitis (7.5%). Among all guselkumab-treated patients, 21 patients (every-4-weeks group [n = 5; 2%]; every-8-weeks group [n = 8; 3%]; placebo–guselkumab crossover group [n = 8; 3%]) reported a serious infection through week 112. Of these, 6 reported pneumonia (every-4-weeks group [n = 2]; every-8-weeks group [n = 3]; placebo crossover group [n = 1]), and 2 had diverticulitis (every-4-weeks group [n = 1, with perforation]; every-8-weeks group [n = 1]). Other serious infections that occurred included acute hepatitis B and oophoritis (in the every-4-weeks group); appendicitis, herpes zoster, cystitis, 1 patient with bacterial vaginosis and trichomoniasis, and 1 patient with pyrexia and urinary tract infection (in the every-8-weeks group); and acute hepatitis C, bacterial meningitis, costochondritis, dengue fever, infective periostitis, influenza, pericarditis, and tracheitis (in the placebo crossover group). The number of infections per 100 patient-years was 37.3 among guselkumab-treated patients compared to 50.5 among placebo-treated patients; the respective numbers of serious infections were 1.9 and 0.9 per 100 patient-years (Table 2).

One death occurred during the study (road traffic accident in the placebo crossover group post–week 52). Two malignancies occurred, both before week 24 (melanoma in situ in the every-8-weeks group and renal clear cell cancer in the placebo group) (16). Three patients experienced MACE (all nonfatal), including 2 patients in the every-4-weeks group who had an ischemic stroke: 1 had a history of hypertension, hyperlipidemia, and diabetes (16), and the second had a history of hypertension, stroke, and smoking. The third patient (also in the every-4-weeks group), who had a history of smoking, hypertension, and hyperlipidemia,

Table 2. AEs through week 112 of the DISCOVER-2 study*

	Placebo (weeks 0–24) (n = 246)	Placebo–guselkumab Q4W crossover (weeks 24–112) (n = 238)	Guselkumab Q4W (weeks 0–112) (n = 245)	Guselkumab Q8W (weeks 0–112) (n = 248)	All guselkumab (n = 731)†
Duration of follow-up, weeks	24.4	84.2	106.4	107.1	99.4
Patient-years of follow-up	115	384	499	509	1,392
AEs					
No. patient-years	85	240	225	224	690
Patients	101 (41)	126 (53)	172 (70)	178 (72)	476 (65)
No. events per 100 patient-years (95% CI)	188.9 (164.6, 215.8)	110.7 (100.5, 121.8)	121.2 (111.7, 131.2)	158.0 (147.3, 169.3)	131.7 (125.8, 137.9)
Serious AEs					
No. patient-years	113	368	476	487	1,330
Patients	7 (3)	16 (7)	22 (9)	22 (9)	60 (8)
No. events per 100 patient-years (95% CI)	6.1 (2.5, 12.6)	6.0 (3.8, 9.0)	5.2 (3.4, 7.6)	6.1 (4.1, 8.7)	5.8 (4.6, 7.2)
AEs leading to study discontinuation					
No. patient-years	114	381	496	507	1,383
Patients	4 (2)	10 (4)	13 (5)	8 (3)	31 (4)
No. events per 100 patient-years (95% CI)	3.5 (1.0, 8.9)	2.9 (1.4, 5.1)	3.2 (1.8, 5.2)	1.6 (0.7, 3.1)	2.5 (1.8, 3.5)
Infections					
No. patient-years	104	315	378	381	1,075
Patients	45 (18)	61 (26)	82 (34)	94 (38)	237 (32)
No. events per 100 patient years (95% CI)	50.5 (38.3, 65.3)	34.9 (29.3, 41.4)	35.8 (30.8, 41.5)	40.5 (35.1, 46.4)	37.3 (34.1, 40.6)
Serious infections					
No. patient-years	115	378	496	504	1,378
Patients	1 (0.4)	8 (3)	5 (2)	8 (3)	21 (3)
No. events per 100 patient-years (95% CI)	0.9 (0.02, 4.9)	2.6 (1.3, 4.8)	1.0 (0.3, 2.3)	2.2 (1.1, 3.9)	1.9 (1.2, 2.7)

* Except where indicated otherwise, values are the number (%) of patients. AEs = adverse events; 95% CI = 95% confidence interval; Q4W = every 4 weeks; Q8W = every 8 weeks.
† Includes all patients who received ≥1 administration of guselkumab, including patients who crossed over from placebo at week 24.

experienced a myocardial infarction. Opportunistic infections occurred in 3 guselkumab-treated patients (all post–week 52): fungal esophagitis (concomitant MTX, longstanding history of gastroesophageal reflux disease and recent course of antibiotics) and herpes zoster disseminated (no concomitant DMARDs, history of diabetes mellitus, and no zoster vaccination) in the every-8-weeks group, and meningitis listeria (concomitant MTX) in the placebo–guselkumab crossover group. No patients developed active tuberculosis. One patient in the every-8-weeks group reported unilateral iridocyclitis, which resolved following steroid and NSAID treatment. While no case of inflammatory bowel disease occurred in guselkumab-treated patients, 1 was suspected in a patient receiving placebo (16).

Four patients (1 receiving placebo and 3 receiving guselkumab) experienced suicidal ideation; 3 of these events occurred prior to week 52 (16,17). All 4 events were classified as level 1; no events of suicidal behavior or self-injurious behavior without suicidal intent were reported.

Among all patients who received ≥1 administration of guselkumab, 20 (2.7%) had an injection site reaction, with no apparent difference between the every-4-weeks regimen (12 of 483 patients [2.5%], including patients who crossed over from placebo) and the every-8-weeks regimen (8 of 248 patients [3.2%]). Most reactions were considered mild. Two patients discontinued treatment, prior to week 52, due to an injection site reaction (moderate injection site erythema/rash and erythema/swelling/warming) (17). No cases of anaphylaxis or serum sickness were reported.

A total of 727 patients received ≥1 administration of guselkumab and had available serum samples through week 112. Fifty-three guselkumab-treated patients (7.3%) tested positive for antibodies to guselkumab; of these, 3 (5.7%) were positive for

neutralizing antibodies. Among 22 guselkumab-randomized patients who tested positive for antibodies through week 100 and had ACR evaluations at week 100, 18 (81.8%) achieved ACR20 response and 12 (54.5%) achieved ACR50 response. Median steady-state trough guselkumab concentrations were maintained from week 52 to week 100, with both the every-4-weeks regimen (4.53 to 3.86 μg/ml) and every-8-weeks regimen (1.15 to 0.97 μg/ml).

Through week 112, grade 2 and grade 3 decreased neutrophil counts occurred in ~4% and 0.7%, respectively, of all guselkumab-treated patients, with no apparent differences between the 2 dosing regimens (Supplementary Table 1, https://onlinelibrary.wiley.com/doi/10.1002/art.42010). One patient (in the every-4-weeks group) had a grade 4 decreased neutrophil count (17). Generally, these decreased levels were transient and resolved spontaneously without discontinuation of study treatment. One infection (mild nasopharyngitis) was associated with a grade 2 decreased neutrophil count (17).

Among 725 patients who received guselkumab and had postbaseline samples available, grade 2 or 3 increased alanine aminotransferase (ALT) and aspartate aminotransferase (AST) levels were seen in ~5% of guselkumab-treated patients through week 112 (Supplementary Table 1, https://onlinelibrary.wiley.com/doi/10.1002/art.42010); no grade 4 ALT or AST elevation occurred. Grade 2 ALT elevations were reported in 7.0% of those in the every-4-weeks group and 2.4% in the every-8-weeks group; grade 3 ALT elevations were reported in 2.1% and 1.6% of these patients, respectively. Grade 2 increased AST levels occurred in 4.5% and 3.6%, of patients in these 2 groups, respectively, and grade 3 AST elevations occurred in 3.3% and 1.2% of patients. Most increased ALT and AST levels were transient and resolved without discontinuation of guselkumab, with few exceptions: 3 patients in the every-4-weeks group (1 each with acute hepatitis B, isoniazid-induced liver injury, and hepatic steatosis [this patient had a history of chronic liver disease]) discontinued the study, and another in the every-4-weeks group had an extended interruption in treatment primarily due to investigator concerns of alcohol use, hepatic steatosis, and chronic cholecystitis with persistently elevated transaminase levels (16,17), and discontinued due to investigator decision.

Three patients in the placebo–guselkumab crossover group discontinued guselkumab after week 52 (1 each with nonalcoholic fatty liver disease, acute hepatitis C, and grade 2 ALT/grade 3 AST elevations [AST-dominant in patient reporting alcohol use]) (16,17). Through week 112, ALT and AST elevations occurred in 48% and 34% of patients receiving concomitant MTX, respectively, and in 40% and 31% of patients without concomitant MTX. Increased bilirubin levels in guselkumab-treated patients were limited to grade 1 (6.3%) and grade 2 (1.8%) elevations (Supplementary Table 1, https://onlinelibrary.wiley.com/doi/10.1002/art.42010), which was consistent with results through week 52 (17). No elevation met the criteria for Hy's law (total bilirubin >2 × upper limit of normal [ULN] and either ALT or AST ≥3 × ULN).

DISCUSSION

Results through 2 years of the phase III DISCOVER-2 study demonstrated robust and sustained joint and skin response rates among biologic-naive patients with active PsA receiving guselkumab 100 mg every 4 weeks or every 8 weeks. At week 24, ACR, IGA, and PASI response rates and the proportions of patients achieving resolution of enthesitis and dactylitis and meaningful improvements in physical function and HRQoL were significantly greater in patients receiving guselkumab at either frequency compared to placebo. These response rates were sustained through week 52 (17) and through week 100 and were generally similar between the 2 dosing regimens. At week 24, patients in the every-4-weeks guselkumab group had significantly less radiographic progression compared to the placebo group (16). After week 24, when all patients were receiving guselkumab, further radiographic progression was limited across the 3 treatment groups through week 100.

The proportion of guselkumab-treated patients achieving MDA increased over time, with ~40% of patients meeting this treatment target at week 100, and ~80% of guselkumab-randomized patients who achieved MDA at week 52 maintained low levels of disease activity across disease domains at week 100. In an open-label study, a treat-to-target approach utilizing the MDA criteria was associated with greater improvements across joint and skin assessments, as well as patient-reported outcomes compared to a standard care approach (29). Because it assesses multiple disease domains, the MDA criteria can be used in all PsA patients regardless of their disease pattern, and the MDA criteria have been recommended by the Group for Research and Assessment of Psoriasis and Psoriatic Arthritis/Outcome Measures in Rheumatology Group to assess treatment target goals (30). With the growing number of treatment options for PsA, achieving and maintaining low disease activity in several disease domains should be an attainable goal for many patients.

Response rates for achieving PASI100 (53–59%) and achieving an IGA score of 0 (55–62%) at week 100 were similar to those observed at week 52. Guselkumab has consistently demonstrated a high level of efficacy in treating psoriatic skin lesions both in patients with PsA and those with plaque psoriasis. The PASI and IGA response rates observed in the DISCOVER-2 trial are consistent with those seen in phase III trials of psoriasis patients (31–33).

The IL-23/Th17 axis is thought to play a central role in the pathogenesis of both psoriasis and PsA (10). By specifically inhibiting IL-23 upstream in this pathway, guselkumab has demonstrated efficacy in a broad range of skin and articular symptoms, including enthesitis and dactylitis. Based on findings reported through 2 years of the DISCOVER-2 trial, this mechanism of

action appears to provide durable improvements across disease domains, an important feature for a therapy in the heterogeneous patient population with frequently treatment-resistant disease (1,2). In a pharmacodynamic analysis of patients from the DISCOVER-1 and 2 trials, guselkumab treatment was associated with marked decreases in acute phase proteins and IL-23/Th17 effector cytokines through week 24 (34). Although these decreases did not directly correlate with clinical response, this biomarker analysis was limited to the placebo-controlled period, and longer-term pharmacodynamic evaluations may provide additional insight into maintenance of response to guselkumab. In a separate analysis of whole-blood transcriptome profiling through week 24 in a subgroup of patients from the DISCOVER-1 and 2 studies, the majority of the disease-associated genes evaluated were modulated by guselkumab treatment, resulting in a transcriptome profile closer to that of healthy controls, with little change in the placebo group. Greater changes in the level of expression of disease-associated genes were observed in ACR20 responders than in nonresponders in both guselkumab groups (35).

In general, AEs in DISCOVER-2 patients were consistent with those reported in DISCOVER-1 (1-year study) and in the 5-year VOYAGE 1 and 2 studies in psoriasis patients (18,31, 32,36). Safety results reported in the present study, through 2 years in the DISCOVER-2 trial, represent the most comprehensive results for an IL-23p19 subunit inhibitor in PsA patients, who often receive concomitant therapy with MTX and oral glucocorticoids, in contrast with psoriasis patients. The majority of ALT and AST elevations were generally mild and transient, and patients receiving MTX had numerically higher rates of ALT and AST elevations than patients not receiving MTX. Among all patients, there were no cases of active tuberculosis, and in guselkumab-treated patients, there were no cases of inflammatory bowel disease.

Among treated patients in the DISCOVER-2 study, 89% randomized to receive guselkumab every 4 weeks and 90% randomized to receive guselkumab every 8 weeks completed treatment through 2 years; few guselkumab-treated patients discontinued due to inadequate efficacy. Given the chronic and progressive nature of PsA, maintaining long-term treatment persistence is critical to controlling disease activity and inhibiting radiographic progression to achieve optimal response. Achieving low disease activity at 1 year has been shown to be predictive of long-term treatment persistence, which, in turn, is predictive of achieving long-term remission (5).

Limitations of the DISCOVER-2 study include enrollment restricted to biologic-naive patients, thus potentially limiting the generalizability of the results. However, findings through 1 year were consistent with those in the DISCOVER-1 study, in which 31% of patients had previously received ≥1 tumor necrosis factor inhibitor (18). While no unexpected safety signals were identified through 2 years, this study was not powered to detect rare events. Patient retention was high through 2 years (88% completed study treatment) resulting in a relatively small number of patients with missing data. Furthermore, it should be noted that clinical efficacy analyses were conducted using a rigorous NRI approach for patients with missing data after week 24 to account for any effects of discontinuations over time.

Taken together, findings from the DISCOVER-2 trial demonstrate the robust and sustained efficacy of guselkumab in improving the signs and symptoms of PsA, including enthesitis and dactylitis, inhibiting radiographic progression, and decreasing the effects of PsA on physical function and HRQoL, with a safety profile through 2 years that is consistent with the known safety profile of guselkumab.

ACKNOWLEDGMENTS

The authors thank Rebecca Clemente, PhD and Mona Patel, PharmD of Janssen Scientific Affairs, for writing support, and Diane Harrison, MD, MPH, a consultant funded by Janssen Research & Development, LLC, for substantive review.

AUTHOR CONTRIBUTIONS

All authors were involved in drafting the article or revising it critically for important intellectual content, and all authors approved the final version to be published. Dr. McInnes had full access to all of the data in the study and takes responsibility for the integrity of the data and the accuracy of the data analysis.

Study conception and design. Hsia, Kollmeier, Xu.

Acquisition of data. Hsia, Kollmeier, Xu.

Analysis and interpretation of data. McInnes, Rahman, Gottlieb, Hsia, Kollmeier, Xu, Jiang, Sheng, Shawi, Chakravarty, van der Heijde, Mease.

ROLE OF THE STUDY SPONSOR

Janssen Research & Development, LLC facilitated the study design, provided writing assistance for the manuscript, and reviewed and approved the manuscript prior to submission. The authors independently collected the data, interpreted the results, and had the final decision to submit the manuscript for publication. Writing assistance was provided by Janssen Scientific Affairs, LLC. Publication of this article was not contingent upon approval by Janssen Research & Development, LLC.

REFERENCES

1. Coates LC, Kavanaugh A, Mease PJ, Soriano ER, Acosta-Felquer ML, Armstrong AW, et al. Group for Research and Assessment of Psoriasis and Psoriatic Arthritis 2015 treatment recommendations for psoriatic arthritis. Arthritis Rheumatol 2016;68:1060–71.
2. Gossec L, Baraliakos X, Kerschbaumer A, de Wit M, McInnes I, Dougados M, et al. EULAR recommendations for the management of psoriatic arthritis with pharmacological therapies: 2019 update. Ann Rheum Dis 2020;79:700–12.
3. Mateo Soria L, Prior-Espanol A, Grigorov MM, Holgado-Perez S, Aparicio-Espinar M, Martinez-Morillo M, et al. Long-term survival of biological therapy in psoriatic arthritis: 18-year analysis of a cohort in a tertiary hospital. Rheumatol Int 2021. doi: https://doi.org/10.1007/s00296-021-04928-x. E-pub ahead of print.
4. Merola JF, Lockshin B, Mody EA. Switching biologics in the treatment of psoriatic arthritis. Semin Arthritis Rheum 2017;47:29–37.

5. Murray K, Turk M, Alammari Y, Young F, Gallagher P, Saber T, et al. Long-term remission and biologic persistence rates: 12-year real-world data. Arthritis Res Ther 2021;23:25.
6. Harrold LR, Stolshek BS, Rebello S, Collier DH, Mutebi A, Wade SW, et al. Impact of prior biologic use on persistence of treatment in patients with psoriatic arthritis enrolled in the US Corrona registry. Clin Rheumatol 2017;36:895–901.
7. Mease PJ, Accortt NA, Rebello S, Etzel CJ, Harrison RW, Aras GA, et al. Persistence of tumor necrosis factor inhibitor or conventional synthetic disease-modifying antirheumatic drug monotherapy or combination therapy in psoriatic arthritis in a real-world setting. Rheumatol Int 2019;39:1547–58.
8. Harper EG, Guo C, Rizzo H, Lillis JV, Kurtz SE, Skorcheva I, et al. Th17 cytokines stimulate CCL20 expression in keratinocytes in vitro and in vivo: implications for psoriasis pathogenesis. J Invest Dermatol 2009;129:2175–83.
9. Liu Y, Lagowski JP, Gao S, Raymond JH, White CR, Kulesz-Martin MF. Regulation of the psoriatic chemokine CCL20 by E3 ligases Trim32 and Piasy in keratinocytes. J Invest Dermatol 2010; 130:1384–90.
10. Blauvelt A, Chiricozzi A. The immunologic role of IL-17 in psoriasis and psoriatic arthritis pathogenesis. Clin Rev Allergy Immunol 2018;55: 379–90.
11. Lee E, Trepicchio WL, Oestreicher JL, Pittman D, Wang F, Chamian F, et al. Increased expression of interleukin 23 p19 and p40 in lesional skin of patients with psoriasis vulgaris. J Exp Med 2004;199:125–30.
12. Yawalkar N, Tscharner GG, Hunger RE, Hassan AS. Increased expression of IL-12p70 and IL-23 by multiple dendritic cell and macrophage subsets in plaque psoriasis. J Dermatol Sci 2009;54: 99–105.
13. Veale DJ, Fearon U. The pathogenesis of psoriatic arthritis. Lancet 2018;391:2273–84.
14. Tremfya [package insert]. Horsham (PA): Janssen Biotech; 2020.
15. Deodhar A, Helliwell PS, Boehncke WH, Kollmeier AP, Hsia EC, Subramanian RA, et al. Guselkumab in patients with active psoriatic arthritis who were biologic-naive or had previously received TNFα inhibitor treatment (DISCOVER-1): a double-blind, randomised, placebo-controlled phase 3 trial. Lancet 2020;395:1115–25.
16. Mease PJ, Rahman P, Gottlieb AB, Kollmeier AP, Hsia EC, Xu XL, et al. Guselkumab in biologic-naive patients with active psoriatic arthritis (DISCOVER-2): a double-blind, randomised, placebo-controlled phase 3 trial. Lancet 2020;395:1126–36.
17. McInnes IB, Rahman P, Gottlieb AB, Hsia EC, Kollmeier AP, Chakravarty SD, et al. Efficacy and safety of guselkumab, an interleukin-23p19–specific monoclonal antibody, through one year in biologic-naive patients with psoriatic arthritis. Arthritis Rheumatol 2021;73:604–16.
18. Ritchlin CT, Helliwell PS, Boehncke WH, Soriano ER, Hsia EC, Kollmeier AP, et al. Guselkumab, an inhibitor of the IL-23p19 subunit, provides sustained improvement in signs and symptoms of active psoriatic arthritis: 1 year results of a phase III randomised study of patients who were biologic-naive or TNFα inhibitor-experienced. RMD Open 2021;7. https://doi.org/10.1136/rmdopen-2020-001457.
19. Healy PJ, Helliwell PS. Measuring clinical enthesitis in psoriatic arthritis: assessment of existing measures and development of an instrument specific to psoriatic arthritis. Arthritis Rheum 2008;59:686–91.
20. Antoni CE, Kavanaugh A, Kirkham B, Tutuncu Z, Burmester GR, Schneider U, et al. Sustained benefits of infliximab therapy for dermatologic and articular manifestations of psoriatic arthritis: results from the infliximab multinational psoriatic arthritis controlled trial (IMPACT). Arthritis Rheum 2005;52:1227–36.
21. Van der Heijde D, Sharp J, Wassenberg S, Gladman DD. Psoriatic arthritis imaging: a review of scoring methods. Ann Rheum Dis 2005; 64 Suppl:ii61–4.
22. Langley RG, Feldman SR, Nyirady J, van de Kerkhof P, Papavassilis C. The 5-point Investigator's Global Assessment (IGA) Scale: a modified tool for evaluating plaque psoriasis severity in clinical trials. J Dermatolog Treat 2015;26:23–31.
23. Fredriksson T, Pettersson U. Severe psoriasis: oral therapy with a new retinoid. Dermatologica 1978;157:238–44.
24. Ware JE Jr, Sherbourne CD. The MOS 36-item short-form health survey (SF-36). Conceptual framework and item selection. Med Care 1992;30:473–83.
25. Felson DT, Anderson JJ, Boers M, Bombardier C, Furst D, Goldsmith C, et al. American College of Rheumatology preliminary definition of improvement in rheumatoid arthritis. Arthritis Rheum 1995;38:727–35.
26. Lubeck DP. Patient-reported outcomes and their role in the assessment of rheumatoid arthritis. Pharmacoeconomics 2004;22:27–38.
27. Coates LC, Fransen J, Helliwell PS. Defining minimal disease activity in psoriatic arthritis: a proposed objective target for treatment. Ann Rheum Dis 2010;69:48–53.
28. Coates LC, Helliwell PS. Defining low disease activity states in psoriatic arthritis using novel composite disease instruments. J Rheumatol 2016;43:371–5.
29. Coates LC, Moverley AR, McParland L, Brown S, Navarro-Coy N, O'Dwyer JL, et al. Effect of tight control of inflammation in early psoriatic arthritis (TICOPA): a UK multicentre, open-label, randomised controlled trial. Lancet 2015;386:2489–98.
30. Coates LC, FitzGerald O, Merola JF, Smolen J, van Mens LJ, Bertheussen H, et al. Group for Research and Assessment of Psoriasis and Psoriatic Arthritis/Outcome Measures in Rheumatology consensus-based recommendations and research agenda for use of composite measures and treatment targets in psoriatic arthritis. Arthritis Rheumatol 2018;70:345–55.
31. Griffiths CE, Papp KA, Song M, Miller M, You Y, Shen YK, et al. Continuous treatment with guselkumab maintains clinical responses through 4 years in patients with moderate-to-severe psoriasis: results from VOYAGE 1. J Dermatolog Treat 2020. doi: https://doi.org/10.1080/09546634.2020.1782817. E-pub ahead of print.
32. Reich K, Armstrong AW, Foley P, Song M, Miller M, Shen YK, et al. Maintenance of response through up to 4 years of continuous guselkumab treatment of psoriasis in the VOYAGE 2 phase 3 study. Am J Clin Dermatol 2020;21:881–90.
33. Reich K, Armstrong AW, Langley RG, Flavin S, Randazzo B, Li S, et al. Guselkumab versus secukinumab for the treatment of moderate-to-severe psoriasis (ECLIPSE): results from a phase 3, randomised controlled trial. Lancet 2019;394:831–9.
34. Sweet K, Song Q, Loza MJ, McInnes IB, Ma K, Leander K, et al. Guselkumab induces robust reduction in acute phase proteins and type 17 effector cytokines in active psoriatic arthritis: results from phase 3 trials. RMD Open 2021;7:e001679.
35. Siebert S, Sweet K, Ritchlin CT, Hsia EC, Kollmeier A, Xu XL, et al. Guselkumab treatment modulates core psoriatic arthritis gene expression in two phase 3 clinical trials (DISCOVER-1 and -2) Ann Rheum Dis 2021;80:312.
36. Blauvelt A, Tsai TF, Langley RG, Miller M, Shen YK, You Y, et al. Consistent safety profile with up to 5 years of continuous treatment with guselkumab: pooled analyses from the phase 3 VOYAGE 1 and VOYAGE 2 trials of patients with moderate-to-severe psoriasis. J Am Acad Dermatol 2021. doi: https://doi.org/10.1016/j.jaad.2021.11.004. E-pub ahead of print.

Arthritis & Rheumatology
Vol. 74, No. 3, March 2022, pp 486–495
DOI 10.1002/art.41985

American College of Rheumatology
Empowering Rheumatology Professionals

Pregnancy Outcomes in Women With Psoriatic Arthritis in Relation to Presence and Timing of Antirheumatic Treatment

Katarina Remaeus,[1] Kari Johansson,[1] Fredrik Granath,[1] Olof Stephansson,[2] and Karin Hellgren[3]

Objective. To evaluate pregnancy outcomes in relation to antirheumatic treatment before and during pregnancy, as a proxy of disease severity in pregnant women with psoriatic arthritis (PsA), compared to those without PsA.

Methods. Our study focused on a Swedish nationwide registry–based cohort study that included 921 PsA pregnancies and 9,210 non-PsA pregnancies occurring between 2007 and 2017 (matched 1:10 based on maternal age, year of delivery, and parity). We estimated adjusted odds ratios (ORs) overall, with 95% confidence intervals (95% CIs), and stratified by presence, timing, and type of antirheumatic treatment. Adjustments were made for maternal body mass index, smoking, education level, and country of birth. The outcome of preterm birth was also stratified by parity.

Results. Pregnant women with PsA versus those without PsA were more obese, more often smokers, and more frequently had a diagnosis of pregestational hypertension and diabetes mellitus. Increased risks in PsA pregnancies versus non-PsA pregnancies were primarily preterm birth (adjusted OR 1.69 [95% CI 1.27–2.24]) and cesarean delivery (adjusted OR 1.77 [95% CI 1.43–2.20] for elective delivery, and adjusted OR 1.42 [95% CI 1.10–1.84] for emergency delivery). The risks differed according to the presence, timing, and type of antirheumatic treatment, with the most increased risk in PsA pregnancies (versus non-PsA) occurring with antirheumatic treatment during pregnancy (adjusted OR 2.30 [95% CI 1.49–3.56] for preterm birth). The corresponding adjusted OR for preterm birth in women with PsA who were exposed specifically to biologic treatment during pregnancy was 4.49 [95% CI 2.60–7.79]. Risk of preterm birth was primarily increased in first pregnancies.

Conclusion. Compared to non-PsA pregnancies, risks of preterm birth and cesarean delivery were mostly increased in those exposed to antirheumatic treatment during pregnancy, especially biologic treatments. As parity influences the risk of preterm birth in women with PsA, special attention to first pregnancies is warranted. Women with PsA should receive individualized monitoring during pregnancy.

INTRODUCTION

Psoriatic arthritis (PsA) is a chronic inflammatory arthritis disease that affects women of childbearing age and has a heterogeneous clinical presentation, with related extraarticular manifestations (1). Studies describing maternal and neonatal pregnancy outcomes in women with PsA are few (2–7), but some indicate an increased risk of preterm birth (4,8,9) and cesarean delivery (2,4). In a previous study of 541 pregnant women with PsA (8), we concluded that a diagnosis of PsA is associated with adverse pregnancy outcomes such as preterm birth and cesarean delivery, after taking into account comorbidities and confounders (e.g., smoking, body mass index [BMI], and maternal age). Studies on pregnancy outcomes in women with rheumatoid arthritis (RA) and systemic lupus erythematosus (SLE) indicate that disease activity/severity play a key role in the outcomes (10,11), underscoring the importance of keeping disease activity low in these women both before and during pregnancy. Corresponding data on disease activity/severity and its impact on maternal and neonatal outcomes in women with PsA are scarce,

[1]Katarina Remaeus, PhD, Kari Johansson, PhD, Fredrik Granath, PhD: Karolinska Institutet, Stockholm, Sweden; [2]Olof Stephansson, PhD: Karolinska Institutet and Karolinska Universitetssjukhuset, Stockholm, Sweden; [3]Karin Hellgren, PhD: Karolinska Institutet and Karolinska University Hospital, Stockholm, Sweden.

Author disclosures are available at https://onlinelibrary.wiley.com/action/downloadSupplement?doi=10.1002%2Fart.41985&file=art41985-sup-0001-Disclosureform.pdf.

Address correspondence to Katarina Remaeus, PhD, K2 Medicin, Solna, K2 Klinisk Epidemiologi, Karolinska Institutet, 171 77 Stockholm, Sweden. Email: katarina.remaeus@ki.se.

Submitted for publication October 18, 2020; accepted in revised form September 21, 2021.

although increased risk of moderately preterm birth was associated with a high score in the Health Assessment Questionnaire (HAQ) in gestational week 32 in one prospective cohort study (4,12).

As ongoing antirheumatic treatment around the time of pregnancy is often required to control PsA disease activity, it can be hypothesized that women treated with antirheumatic drugs before and/or during pregnancy have a more severe and active PsA disease compared to untreated women. On the other hand, antirheumatic treatment may improve clinical and inflammatory measures. It is thus important to consider the history of antirheumatic treatment before pregnancy when evaluating pregnancy outcomes.

The aim of this study was therefore to evaluate pregnancy outcomes in relation to antirheumatic treatment, which was used as a proxy for disease severity in PsA pregnancies compared to non-PsA pregnancies. Specifically, we wanted to assess this in relation to the timing and type of antirheumatic treatment.

PATIENTS AND METHODS

Study design, setting, and data sources. We performed a nationwide Swedish registry–based cohort study of births from July 1, 2007 to December 31, 2017, in which we compared pregnancy outcomes, with a focus on the presence and timing of antirheumatic treatment, between PsA and non-PsA pregnancies.

For this study, we used the Medical Birth Register (MBR) (13), the National Patient Register (NPR) (14), the Prescribed Drug Register (PDR) (15), the Total Population Register, the Educational Register (ER) (held by Statistics Sweden), and the Swedish Rheumatology Quality Register (SRQ) (16). Linkage of information between these registers was possible because of the use of the unique personal identification number assigned to each Swedish resident. In Sweden, pre- and postnatal care, as well as care during delivery, is tax-funded, and patients with PsA are typically cared for by hospital-based rheumatologists within public care.

Study population and definition of exposure. *PsA pregnancies.* We identified women with a diagnosis of PsA in the NPR according to International Classification of Diseases, Tenth Revision (ICD-10) codes L405, M070-1, and M073. We required ≥2 visits with a PsA diagnosis before the start of pregnancy, 1 of which had to be at a department of rheumatology or internal medicine. By linkage to the MBR, we identified first and subsequent singleton pregnancies of these women after their diagnosis of PsA (Supplementary Figure 1, available on the *Arthritis & Rheumatology* website at https://onlinelibrary.wiley.com/doi/10.1002/art.41985).

Non-PsA pregnancies. From the NPR and by linkage to the MBR, we identified first and subsequent singleton pregnancies in women without a diagnosis of inflammatory joint disease sampled from a preexisting linkage (17). Ten pregnancies in which the mothers did not have PsA were sampled and matched according to year of delivery, maternal age, and parity (Supplementary Figure 1). In total, we identified 921 PsA pregnancies and 9,210 non-PsA pregnancies.

Identification and definition of antirheumatic treatment. Information on dispensed prescriptions for antirheumatic treatment was retrieved from the PDR. The PDR holds information on all filled prescriptions at Swedish pharmacies since July 2005, including date dispensed and the Anatomical Therapeutic Chemical (ATC) code identifying the drugs. For the present study, we defined antirheumatic treatment as oral glucocorticoids, conventional synthetic disease-modifying antirheumatic drugs (csDMARDs), or biologic DMARDs (bDMARDs). ATC codes used to identify antirheumatic treatment are presented in Supplementary Table 1 (https://onlinelibrary.wiley.com/doi/10.1002/art.41985). A dispensed prescription within the prespecified time frame (one year before the start of pregnancy until delivery), according to the PDR, was considered as treatment. As the PDR does not include data on drugs administrated in specialist outpatient units in hospitals, we retrieved information on infusion of infliximab from the Swedish SRQ.

Stratification according to presence and timing of antirheumatic treatment. The 921 PsA pregnancies were stratified based on presence and timing of maternal antirheumatic treatment and compared to the matched 9,210 non-PsA pregnancies (Figure 1). First, the 921 pregnant women with PsA were divided into 2 groups: 1 group of 495 patients who had not received any treatment 1 year before pregnancy up until delivery, and 1 group of 426 PsA patients who had received any antirheumatic treatment during the same time frame (Figure 1). The group of 426 pregnant women included 19 women (not analyzed separately) with no previous treatment but who received treatment during pregnancy, and 407 women who received treatment in the year before pregnancy irrespective of treatment during pregnancy. This latter group was further stratified into 2 groups: 170 patients who received treatment only in the year before pregnancy (i.e., no treatment during pregnancy) and 237 patients who received treatment both in the year prior to and during pregnancy. Finally, the 19 patients who received treatment only during pregnancy were added to the group of 237 patients, resulting in 256 patients who received antirheumatic treatment during pregnancy.

Outcomes and covariates. We used ICD-10 codes in the MBR to identify prepregnancy comorbidities, such as hypertension and type 1 and type 2 diabetes mellitus (Supplementary Table 1, https://onlinelibrary.wiley.com/doi/10.1002/art.41985), as well as outcomes including preeclampsia (ICD-10 codes O14–O15), gestational diabetes (ICD-10 code O244), and gestational hypertension (ICD-10 code O13). Gestational age was estimated by ultrasonography or, if ultrasonography was unavailable, by the recorded date of the first day of the last menstrual period.

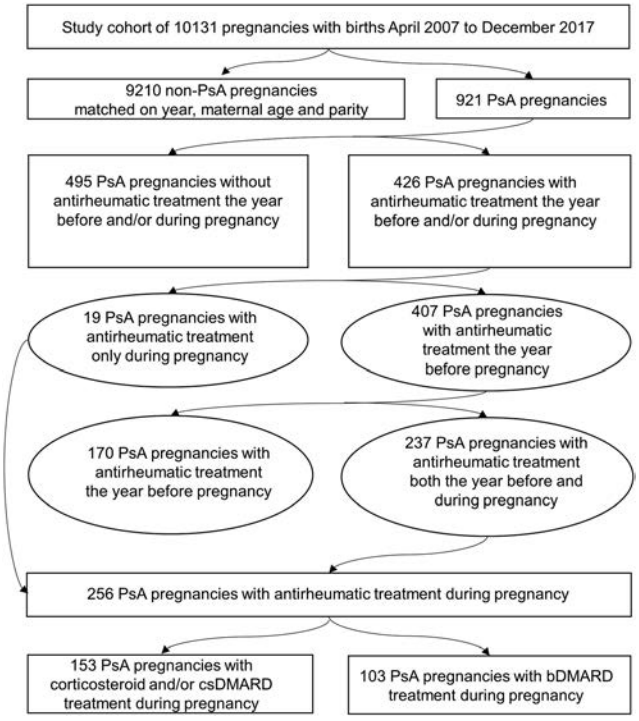

Figure 1. Flow chart of analyses stratified by presence, timing, and type of antirheumatic treatment. PsA = psoriatic arthritis; csDMARD = conventional synthetic disease-modifying antirheumatic drug; bDMARD = biologic disease-modifying antirheumatic drug.

Swedish women are routinely offered ultrasonography to estimate gestational age, generally early in the second trimester.

Preterm birth was defined as birth before 37 completed weeks of gestation and was further subcategorized into moderately preterm birth (32 weeks and 0 days to 36 weeks and 6 days) or very preterm birth (22 weeks and 0 days to 31 weeks and 6 days). We subcategorized preterm birth by onset (spontaneous or medically indicated). Further, we assessed the mode of delivery (vaginal birth or cesarean delivery). Cesarean deliveries were subcategorized as emergency or elective. For outcomes in the neonates, we assessed birth weight: small for gestational age was defined as a birth weight of >2 SD below the sex-specific mean weight for gestational age, and large for gestational age was defined as a birth weight of >2 SD above the sex-specific mean weight for gestational age.

Maternal age at delivery was categorized into groups of women/girls ages 13–24, 25–29, 30–34, or 35–55 years. The mother's country of birth was categorized as Nordic or non-Nordic. Parity was categorized as primiparous or parous. Measured weight and self-reported height at the first antenatal visit were used to calculate early pregnancy BMI, categorized as underweight or normal weight (11.0–24.9 kg/m^2), overweight (25.0–29.9 kg/m^2), or obese (≥30.0 kg/m^2). Self-reported information from the first antenatal visit regarding smoking status classified patients as nonsmoker or smoker. We collected data from the ER on the mother's highest level of education at the time of delivery and classified them as either ≤12 years or >12 years of education.

Statistical analysis. Baseline pregnancy characteristics are presented as numbers and percentages. Relative risks were estimated with a generalized model with logit link and assumption of binominal distribution as crude and adjusted odds ratios (ORs), hereafter named risk, with associated 95% confidence intervals (95% CIs). The analyses were performed on individual pregnancies, and since one woman could contribute more than one pregnancy, we used a generalized estimating equation method with the mother's identification as a cluster, assuming an exchangeable correlation structure. No risk estimates were calculated for outcomes with <5 events. Statistical interaction was assessed

Table 1. Maternal characteristics of PsA pregnancies and matched non-PSA pregnancies*

	Non-PsA pregnancies (n = 9,210)	PsA pregnancies (n = 921)
Maternal age at delivery, years		
13–24	720 (7.8)	72 (7.8)
25–29	2,030 (22.0)	203 (22.0)
30–34	3,420 (37.1)	342 (37.1)
35–55	3,040 (33.0)	304 (33.0)
Missing	0 (0.0)	0 (0.0)
Calendar year of delivery		
2007–2010	2,820 (30.6)	282 (30.6)
2011–2014	3,260 (35.4)	326 (35.4)
2015–2017	3,130 (34.0)	313 (34.0)
Missing	0 (0.0)	0 (0.0)
Mother's country of birth		
Nordic	7,629 (82.8)	845 (91.8)
Non-Nordic	1,580 (17.2)	76 (8.3)
Missing	1 (<0.1)	0 (0.0)
Parity		
Primiparous	3,390 (36.8)	339 (36.8)
Parous	5,820 (63.2)	582 (63.2)
Missing	0 (0.0)	0 (0.0)
BMI, kg/m^2		
11.0–24.99	5,219 (56.7)	421 (45.7)
25.0–29.99	2,228 (24.2)	245 (26.6)
30.0–60.0	1,158 (12.6)	183 (19.9)
Missing	605 (6.6)	72 (7.8)
Smoking habits in early pregnancy		
Nonsmoker	8,402 (91.2)	792 (86.0)
Smoker	486 (5.3)	85 (9.2)
Missing	322 (3.5)	44 (4.8)
Maternal education		
≤12 years	5,190 (56.4)	458 (49.7)
>12 years	3,984 (43.3)	461 (50.1)
Missing	36 (0.4)	2 (0.2)
Comorbidities before pregnancy		
Prepregnancy hypertension	70 (0.8)	13 (1.4)
Prepregnancy diabetes mellitus	47 (0.5)	12 (1.3)

* Pregnancies of women with psoriatic arthritis (PsA) and those of women without PsA were matched according to maternal age, year of delivery, and parity. Values are the number (%) of pregnancies. BMI = body mass index.

by inclusion of the interaction term exposure status (PsA) × parity. As the interaction term was significant for preterm birth, the analyses regarding this outcome were stratified according to parity (Supplementary Table 2, https://onlinelibrary.wiley.com/doi/10.1002/art.41985). Missing data on maternal characteristics are presented in Table 1 and Supplementary Table 3 (https://onlinelibrary.wiley.com/doi/10.1002/art.41985). All analyses were performed using complete data.

Confounders were chosen based on prior knowledge and literature (18–22). Adjustments in the main analysis were made for the highest level of education attained, smoking status, BMI, and country of birth. In the stratified analyses, the matching was broken, and thus, adjustment for maternal age, year of delivery, and parity was made.

Data were analyzed using SAS software, version 9.4. Ethical approval was obtained from the Ethics Review Board in Stockholm (no. 2015/1844-31/2).

RESULTS

Pregnant women with PsA compared to women without PsA were more often born in a Nordic country (91.8% versus 82.8%), had a higher rate of obesity (19.9% versus 12.6%), were more likely to be a smoker at the first antenatal visit (9.2% versus 5.3%), and were more likely to have attained a higher level of education (50.1% versus 43.3% with >12 years completed). It was also more common among pregnant women with PsA to have prepregnancy hypertension (1.4%) or type 1 or type 2 diabetes (1.3%) compared to pregnant women without PsA (0.8% and 0.5%, respectively). Maternal characteristics are presented in Table 1 and Supplementary Table 3 (https://onlinelibrary.wiley.com/doi/10.1002/art.41985).

With respect to treatment patterns before and during pregnancy, we observed that among pregnancies with antirheumatic treatment only before pregnancy (n = 170), the majority received monotherapy; 39.4% of women were treated with a csDMARD, either antimalarials, methotrexate, or sulfasalazine (Supplementary Table 4), whereas 24.1% were treated with oral glucocorticoids and 15.9% with tumor necrosis factor inhibitors (TNFi). Approximately 20% were treated with ≥2 types of antirheumatic drugs before pregnancy (Supplementary Table 4, https://onlinelibrary.wiley.com/doi/10.1002/art.41985).

When we stratified the group of 256 pregnant women who received treatment during pregnancy according to bDMARD use (yes/no), we observed that the majority of those not treated with bDMARDs (n = 153) received csDMARDs (41.8%) or glucocorticoids (41.8%) as monotherapy. Among those treated with bDMARDs (n = 103), the majority received TNFi as monotherapy (43.7%) or in combination with glucocorticoids (35.9%). In this same group, 9.7% of patients received a combination of TNFi and csDMARDs, and an equally large proportion, 9.7%, received TNFi, csDMARDs, and glucocorticoids (Supplementary Table 4).

Overall pregnancy outcomes. In the main analysis of 921 PsA pregnancies, we observed an increased risk of preterm birth (adjusted OR 1.69 [95% CI 1.27–2.24]) compared to the

Table 2. Outcomes in PsA pregnancies compared to non-PsA pregnancies*

	Non-PsA pregnancies (n = 9,210)	PsA pregnancies (n = 921)	Crude OR (95% CI)	Adjusted OR (95% CI)†
Outcomes among all births, total no.	9,210	921	–	–
Preeclampsia	264 (2.9)	42 (4.6)	1.58 (1.10–2.26)‡	1.35 (0.95–1.92)
Gestational diabetes mellitus	125 (1.4)	17 (1.9)	1.62 (0.95–2.77)	1.58 (0.91–2.74)
Gestational hypertension	147 (1.6)	18 (2.0)	1.38 (0.83–2.28)	1.10 (0.67–1.82)
Live births, total no.	9,172	918	–	–
Preterm birth (<37 GW)	417 (4.6)	73 (8.0)	1.77 (1.34–2.35)‡	1.69 (1.27–2.24)‡
Spontaneous preterm birth	277 (3.0)	43 (4.7)	1.49 (1.05–2.12)‡	1.45 (1.02–2.07)‡
Medically indicated preterm birth	140 (1.5)	30 (3.3)	2.19 (1.42–3.37)‡	2.04 (1.32–3.16)‡
Very preterm birth (<32 GW)	61 (0.7)	7 (0.8)	1.12 (0.45–2.84)	1.07 (0.46–2.49)
Moderately preterm birth (32–36 GW)	356 (3.9)	66 (7.2)	1.86 (1.38–2.50)‡	1.74 (1.29–2.34)‡
Elective cesarean delivery	902 (9.8)	142 (15.5)	1.76 (1.42–2.18)‡	1.77 (1.43–2.20)‡
Emergency cesarean delivery§	744 (9.0)	108 (13.9)	1.58 (1.24–2.03)‡	1.42 (1.10–1.84)‡
Small for gestational age¶	191 (2.1)	23 (2.5)	1.18 (0.74–1.88)	1.08 (0.66–1.76)
Large for gestational age#	360 (3.9)	54 (5.9)	1.55 (1.11–2.15)‡	1.30 (0.93–1.82)

* Pregnancies of women with psoriatic arthritis (PsA) and those of women without PsA were matched according to maternal age, year of delivery, and parity. Except where indicated otherwise, values are the number (%) of pregnancies. OR = odds ratio; 95% CI = 95% confidence interval; GW = gestational weeks.
† Adjusted for maternal country of birth, education level, smoking status, and body mass index.
‡ $P < 0.05$.
§ Analyses without elective cesarean deliveries in the denominator.
¶ Birth weight of >2 SD below the sex-specific mean weight per gestational age.
# Birth weight of >2 SD above the sex-specific mean weight per gestational age.

Table 3. Outcomes in PsA pregnancies with and those without any antirheumatic treatment in the year before and/or during pregnancy compared to non-PsA pregnancies*

	Non-PsA pregnancies	PsA pregnancies without treatment	Adjusted OR (95% CI)†	PsA pregnancies with treatment	Adjusted OR (95% CI)†
Outcomes among all births, total no.	9,210	495	–	426	–
Preeclampsia	264 (2.9)	22 (4.4)	1.38 (0.86–2.23)	20 (4.7)	1.22 (0.71–2.11)
Gestational diabetes mellitus	125 (1.4)	9 (1.8)	1.58 (0.77–3.23)	8 (1.9)	1.52 (0.69–3.36)
Gestational hypertension	147 (1.6)	7 (1.4)	0.74 (0.34–1.62)	11 (2.6)	1.54 (0.81–2.94)
Live births, total no.	9,172	493	–	425	–
Preterm birth (<37 GW)	417 (4.6)	35 (7.1)	1.43 (0.96–2.12)	38 (8.9)	1.98 (1.37–2.86)‡
Spontaneous preterm birth	277 (3.0)	18 (3.7)	0.98 (0.58–1.69)	25 (5.9)	1.98 (1.27–3.09)‡
Medically indicated preterm birth	140 (1.5)	17 (3.5)	2.23 (1.29–3.86)‡	13 (3.1)	1.86 (0.98–3.50)
Very preterm birth (<32 GW)	61 (0.7)	5 (1.0)	1.82 (0.66–5.00)	2 (0.5)	NA
Moderately preterm birth (32–36 GW)	356 (3.9)	30 (6.2)	1.38 (0.90–2.11)	36 (8.5)	2.15 (1.47–3.14)‡
Elective cesarean delivery	902 (9.8)	69 (14.0)	1.57 (1.17–2.10)‡	73 (17.2)	1.96 (1.47–2.63)‡
Emergency cesarean delivery§	744 (9.0)	56 (13.2)	1.22 (0.86–1.74)	52 (14.8)	1.67 (1.18–2.36)‡
Small for gestational age¶	191 (2.1)	12 (2.4)	1.14 (0.60–2.17)	11 (2.6)	1.01 (0.50–2.02)
Large for gestational age#	360 (3.9)	26 (5.3)	1.03 (0.64–1.65)	28 (6.6)	1.59 (1.02–2.48)‡

* Pregnancies of women without psoriatic arthritis (PsA) compared to those of women with PsA who received antirheumatic treatment before and/or during pregnancy and those with PsA who did not receive antirheumatic treatment. Except where indicated otherwise, values are the number (%) of pregnancies. 95% CI = 95% confidence interval; GW = gestational weeks; NA = not assessed.
† Odds ratios (ORs) are versus non-PsA pregnancies and were adjusted for maternal country of birth, education level, smoking status, body mass index, age, year of delivery, and parity.
‡ $P < 0.05$.
§ Analyses without elective cesarean deliveries in the denominator.
¶ Birth weight of >2 SD below the sex-specific mean weight per gestational age.
# Birth weight of >2 SD above the sex-specific mean weight per gestational age.

9,210 non-PsA pregnancies (Table 2). There were also statistically significant increased risks of spontaneous onset and medically indicated preterm birth, as well as for moderately, but not very, preterm birth. Furthermore, in pregnant women with PsA, there was an elevated risk of cesarean delivery, both elective (adjusted OR 1.77 [95% CI 1.43–2.20]) and emergency (adjusted OR 1.42 [95% CI 1.10–1.84]). There were no differences in the risk of preeclampsia, gestational diabetes, hypertension, neonatal small size for gestational age, or neonatal large size for gestational age in PsA pregnancies compared to non-PsA pregnancies (Table 2).

Pregnancy outcomes in relation to antirheumatic treatment before and during pregnancy. For the 495 PsA pregnancies without any antirheumatic treatment 1 year before or during pregnancy, we observed an increased risk of preterm birth compared to non-PsA pregnancies, but the association did not reach statistical significance (adjusted OR 1.43 [95% CI 0.96–2.12]) (Table 3). There was no increased risk of spontaneous preterm birth (adjusted OR 0.98 [95% CI 0.58–1.69]), while medically indicated preterm birth was more common among PsA pregnancies without treatment (adjusted OR 2.23 [95% CI 1.29–3.86]). The risk was statistically significantly increased for elective cesarean delivery (adjusted OR 1.57 [95% CI 1.17–2.10]), whereas risk of emergency cesarean delivery was not significantly increased (adjusted OR 1.22 [95% CI 0.86–1.74]). No other outcomes resulted in a statistically different risk between the groups.

For the 426 PsA pregnancies with antirheumatic treatment 1 year before and/or during pregnancy, compared to non-PsA pregnancies, the results were consistent with those of the main analysis, with an increased risk of preterm birth (adjusted OR 1.98 [95% CI 1.37–2.86]), spontaneous preterm birth (adjusted OR 1.98 [95% CI 1.27–3.09]), moderately preterm birth (adjusted OR 2.15 [95% CI 1.47–3.14]), and cesarean delivery, both elective (adjusted OR 1.96 [95% CI 1.47–2.63]) and emergency (adjusted OR 1.67 [95% CI 1.18–2.36]). There were no statistically significant differences in the risk of preeclampsia, gestational diabetes, or hypertension. We did not observe an increased risk of small size for gestational age at birth, but there was a slightly increased risk of large size at birth (Table 3).

Pregnancy outcomes in relation to timing of antirheumatic treatment. Among the 170 PsA pregnancies with antirheumatic treatment before (but not during) pregnancy compared to non-PsA pregnancies, we only observed a statistically significant increased risk for elective cesarean delivery (adjusted OR 1.72 [95% CI 1.09–2.71]) (Table 4). We abstained from assessing risk of gestational diabetes, gestational hypertension, very preterm birth, neonatal large size for gestational age, and neonatal small size for gestational age due to too few events.

Table 4. Outcomes in PsA pregnancies with antirheumatic treatment only before pregnancy and in PsA pregnancies with antirheumatic treatment during pregnancy compared to non-PsA pregnancies*

	Non-PsA pregnancies	PsA pregnancies with treatment only before pregnancy	Adjusted OR (95% CI)†	PsA pregnancies with treatment during pregnancy	Adjusted OR (95% CI)†
Outcomes among all births, total no.	9,210	170	–	256	–
Preeclampsia	264 (2.9)	5 (2.9)	0.80 (0.29–2.22)	15 (5.9)	1.44 (0.76–2.73)
Gestational diabetes mellitus	125 (1.4)	4 (2.4)	NA	4 (1.6)	NA
Gestational hypertension	147 (1.6)	4 (2.4)	NA	7 (2.7)	1.62 (0.74–3.55)
Live births, total no.	9,172	169	–	256	–
Preterm birth (<37 GW)	417 (4.6)	13 (7.7)	1.44 (0.75–2.77)	25 (9.8)	2.30 (1.49–3.56)‡
Spontaneous preterm birth	277 (3.0)	8 (4.7)	1.25 (0.55–2.86)	17 (6.6)	2.43 (1.45–4.06)‡
Medically indicated preterm birth	140 (1.5)	5 (3.0)	1.76 (0.63–4.91)	8 (3.1)	1.90 (0.88–4.13)
Very preterm birth (<32 GW)	61 (0.7)	2 (1.2)	NA	0 (0.0)	NA
Moderately preterm birth (32–36 GW)	356 (3.9)	11 (6.6)	1.44 (0.72–2.86)	25 (9.8)	2.58 (1.66–4.00)‡
Elective cesarean delivery	902 (9.8)	26 (15.4)	1.72 (1.09–2.71)‡	47 (18.4)	2.11 (1.47–3.03)‡
Emergency cesarean delivery§	744 (9.0)	19 (13.3)	1.50 (0.86–2.62)	33 (15.8)	1.74 (1.14–2.67)‡
Small for gestational age¶	191 (2.1)	2 (1.2)	NA	9 (3.5)	NA#
Large for gestational age**	360 (3.9)	13 (7.7)	1.76 (0.95–3.24)	15 (5.9)	1.48 (0.82–2.68)

* Pregnancies of women without PsA compared to those of women with PsA who received antirheumatic treatment only before pregnancy and those with PsA who received antirheumatic treatment during pregnancy. Except where indicated otherwise, values are the number (%) of pregnancies. See Table 3 for definitions.
† ORs are versus non-PsA pregnancies and were adjusted for maternal country of birth, education level, smoking status, body mass index, age, year of delivery, and parity.
‡ $P < 0.05$.
§ Analyses without elective cesarean deliveries in the denominator.
¶ Birth weight of >2 SD below the sex-specific mean weight per gestational age.
# The model did not converge.
** Birth weight of >2 SD above the sex-specific mean weight per gestational age.

Among the 256 PsA pregnancies with antirheumatic treatment during pregnancy (regardless of treatment before) compared to the 9,210 non-PsA pregnancies, we found somewhat stronger associations as compared to the main analysis, with an increased risk of preterm birth (adjusted OR 2.30 [95% CI 1.49–3.56]), spontaneous preterm birth (adjusted OR 2.43 [95% CI 1.45–4.06]), and moderately preterm birth (adjusted OR 2.58 [95% CI 1.66–4.00]), whereas there were no very preterm births among the PsA pregnancies with antirheumatic treatment during pregnancy. Furthermore, the risks of both elective cesarean delivery (adjusted OR 2.11 [95% CI 1.47–3.03]) and emergency cesarean delivery (adjusted OR 1.74 [95% CI 1.14–2.67]) were increased in the group of pregnant women with PsA who received antirheumatic treatment during pregnancy. For preeclampsia, gestational hypertension, and neonatal large size, there were no statistically significant differences. Adjusted ORs for gestational diabetes were not estimated due to too few events, and the model did not converge for calculation of adjusted ORs for neonatal small size for gestational age (Table 4).

Pregnancy outcomes in relation to type of antirheumatic treatment. Among the 256 pregnancies with antirheumatic treatment during pregnancy, we identified 153 PsA pregnancies with glucocorticoid and/or csDMARD treatment and 103 PsA pregnancies with bDMARD treatment. Compared to non-PsA pregnancies, the 153 pregnant women with PsA who received non-bDMARD treatment (e.g., glucocorticoids and/or csDMARDs) did not have a significantly increased risk of any of the outcomes, except for elective cesarean delivery (Table 5).

Conversely, among the 103 pregnant women with PsA who received bDMARD treatment, we observed increased risks of preterm birth (adjusted OR 4.49 [95% CI 2.60–7.79]), spontaneous preterm birth (adjusted OR 4.73 [95% CI 2.53–8.87]), moderately preterm birth (adjusted OR 5.06 [95% CI 2.91–8.79]), and cesarean delivery (both elective and emergency). Additionally, there was a significantly increased risk of preeclampsia (adjusted OR 2.88 [95% CI 1.35–6.17]) (Table 5).

Risk of preterm birth in relation to parity and antirheumatic treatment. In the analyses of preterm birth stratified by parity, there was a statistically significant increased risk in all analyses of preterm birth among first PsA pregnancies as compared to their matched first non-PsA pregnancies. On the contrary, no difference in risk of preterm birth was seen in the analysis of subsequent pregnancies comparing PsA to non-PsA pregnancies. The most elevated risk of preterm birth was seen in the 46 first PsA pregnancies with treatment only before

Table 5. Outcomes in PsA pregnancies with antirheumatic treatment during pregnancy according to treatment type compared to non-PsA pregnancies*

	Non-PsA pregnancies	PsA pregnancies with non-bDMARD treatment†	Adjusted OR (95% CI)‡	PsA pregnancies with bDMARD treatment	Adjusted OR (95% CI)‡
Outcomes among all births, total no.	9,210	153	–	103	–
Preeclampsia	264 (2.9)	6 (3.9)	0.77 (0.28–2.14)	9 (8.7)	2.88 (1.35–6.17)§
Gestational diabetes mellitus	125 (1.4)	2 (1.3)	NA	2 (1.9)	NA
Gestational hypertension	147 (1.6)	5 (3.3)	1.88 (0.74–4.77)	2 (1.9)	NA
Live births, total no.	9,172	153	–	103	–
Preterm birth (<37 GW)	417 (4.6)	7 (4.6)	1.08 (0.50–2.33)	18 (17.5)	4.49 (2.60–7.79)§
Spontaneous preterm birth	277 (3.0)	5 (3.3)	1.15 (0.46–2.85)	12 (11.7)	4.73 (2.53–8.87)§
Medically indicated preterm birth	140 (1.5)	2 (1.3)	NA	6 (5.8)	3.29 (1.28–8.46)§
Very preterm birth (<32 GW)	61 (0.7)	0 (0.0)	NA	0 (0.0)	NA
Moderately preterm birth (32–36 GW)	356 (3.9)	7 (4.6)	1.21 (0.56–2.62)	18 (17.5)	5.06 (2.91–8.79)§
Elective cesarean delivery	902 (9.8)	23 (15.0)	1.70 (1.05–2.76)§	24 (23.3)	2.72 (1.61–4.59)§
Emergency cesarean delivery¶	744 (9.0)	20 (15.4)	1.53 (0.89–2.63)	13 (16.5)	2.06 (1.04–4.07)§
Small for gestational age#	191 (2.1)	5 (3.3)	1.21 (0.43–3.35)	4 (3.9)	NA
Large for gestational age**	360 (3.9)	7 (4.6)	1.17 (0.54–2.55)	8 (7.8)	2.21 (0.97–5.05)

* Pregnancies of women without PsA compared to those of women with PsA who received treatment other than biologic disease-modifying antirheumatic drugs (non-bDMARDs) and those who received treatment with bDMARDs. Except where indicated otherwise, values are the number (%) of pregnancies. See Table 3 for other definitions.
† Non-bDMARD treatment is equivalent to treatment with glucocorticoids and/or conventional synthetic DMARDs.
‡ ORs are versus non-PsA pregnancies and were adjusted for maternal country of birth, education level, smoking status, body mass index, age, year of delivery, and parity.
§ $P < 0.05$.
¶ Analyses without elective cesarean deliveries in the denominator.
# Birth weight of >2 SD below the sex-specific mean weight per gestational age.
** Birth weight of >2 SD above the sex-specific mean weight per gestational age.

pregnancy (adjusted OR 3.95 [95% CI 1.43–10.95]) compared to the 460 matched non-PsA pregnancies (Supplementary Figure 2, https://onlinelibrary.wiley.com/doi/10.1002/art.41985).

DISCUSSION

In this nationwide cohort study of more than 900 PsA pregnancies, we demonstrated that pregnancy outcomes associated with increased risk in PsA compared to non-PsA pregnancies were primarily preterm birth and cesarean delivery. The risk estimates varied according to the presence, timing, and type of antirheumatic treatment, which was used as a proxy for disease severity and activity. The results may indicate that a more severe or active PsA disease that requires antirheumatic treatment during pregnancy, especially bDMARDs, is associated with increased risks of adverse pregnancy outcomes compared to non-PsA pregnancies. The risk of preterm birth in PSA pregnancies is further influenced by parity, with the most increased risks observed in first pregnancies.

The findings of increased risk of preterm birth and cesarean delivery in PsA pregnancies (versus non-PsA pregnancies) are consistent with previous, albeit few, available reports (4,8,9), including an earlier study from our group. This has also been described in other inflammatory diseases, even though the underlying cause is yet unknown (8,23–26). Preterm birth is important to study, since it is the leading cause of morbidity and mortality in the neonate (27,28). In the present study, we were able to stratify preterm births according to onset and gestational age. Spontaneous preterm birth, defined as spontaneous-onset labor with contractions or premature rupture of membranes and birth before 37 gestational weeks, is most likely to have a multifactorial underlying cause, even though maternal overweight and obesity (29) as well as gestational diabetes (30) have been linked to increased risks. An association of spontaneous preterm birth with RA and other autoimmune diseases has been reported (24,26). We found that risk of spontaneous preterm birth ranged from not being increased in pregnancies unexposed to antirheumatic treatment to ~4-fold increased risk in pregnancies with exposure to bDMARD treatment during pregnancy, thereby strengthening our hypothesis that disease severity has an impact, at least for spontaneous-onset preterm birth.

In contrast, medically indicated preterm birth reflects pregnancy complications but is also influenced by obstetric management. A recent publication addresses the mediation of adverse outcomes, including preterm birth and cesarean delivery, in autoimmune diseases. The strongest mediator for preterm birth in pregnancies in which the mother had RA, SLE, or psoriasis was preeclampsia/hypertensive disease, accounting for 20–33% of

excess risk (31). In the present study, a statistically significant increased risk of preeclampsia was seen only among PsA pregnancies with bDMARD treatment during pregnancy. This is difficult to explore further, however, as we lack information on indications for preterm delivery.

As previously mentioned, obesity, which was more common in women with PsA pregnancies than non-PsA pregnancies, is associated with unfavorable pregnancy outcomes, including preterm birth (29), preeclampsia, and cesarean delivery (32). These outcomes were also more common among PsA pregnancies compared to non-PsA pregnancies in our study. Our analyses included adjustment for BMI, but residual confounding may be present. However, the pregnancies with the most adverse outcomes compared to non-PsA pregnancies were those exposed to antirheumatic treatment during pregnancy, especially bDMARDs. The proportion of obesity among pregnant women with PsA who received bDMARD treatment during pregnancy, compared to pregnant women without PsA, was approximately the same (Supplementary Table 3, https://onlinelibrary.wiley.com/doi/10.1002/art.41985). This leads us to conclude that obesity is not the main contributor to the increased risks of preterm birth, preeclampsia, or cesarean delivery.

Regarding gestational age at preterm birth, there was no increased risk of very preterm birth (i.e., the majority were moderately preterm births). This is reassuring since there is a correlation between an earlier gestational age at birth and more severe morbidity in the neonate (33). When we stratified the analyses of preterm birth by parity, we found generally increased risks in first pregnancies but no statistically significant differences among subsequent pregnancies compared to matched non-PsA pregnancies. This observation is consistent with an earlier study by Wallenius et al (34) and also with what we reported in our recent study on PsA and pregnancy outcomes (8).

We also noted that the most pronounced preterm birth risk was among first pregnancies with treatment prior to (but not during) pregnancy, with a 4-fold increased risk compared to matched non-PsA pregnancies. The latter finding (i.e., that those without treatment during pregnancy had the most increased risk) was unexpected. This finding was not apparent when studying the group without stratifying for parity. The majority of pregnancies in which the mother discontinued antirheumatic treatment were subsequent pregnancies (73%) (Supplementary Table 3), so first pregnancies with discontinued antirheumatic treatment constituted a minority. A potential explanation from a clinical perspective could be that stopping antirheumatic treatment in the year before pregnancy in first pregnancies may lead to flares and/or increased disease activity. Since we do not have information about the reason for stopping treatment or measurements of disease activity, this remains speculation. Although data on the impact of disease activity on preterm birth in PsA are lacking, flares and increased disease activity during pregnancy have been associated with preterm birth in studies of other rheumatic diseases such as SLE (10), RA (25,35,36), axial spondyloarthritis (36), and juvenile idiopathic arthritis (25), suggesting that this scenario may be plausible.

In all of our analyses, the risk of elective cesarean delivery was increased in PsA pregnancies compared to non-PsA pregnancies, an expected result as increased rates of cesarean delivery have been described for chronic inflammatory arthritis diseases (2,11,24,34,37). The risk of emergency cesarean was, however, only significantly elevated in PsA pregnancies with antirheumatic treatment. Since our data do not provide information on the indications for cesarean deliveries, we cannot explore this further. However, it was apparent that PsA pregnancies with continued antirheumatic treatment during pregnancy had generally more adverse outcomes than PsA pregnancies with antirheumatic treatment confined to before the start of pregnancy.

Our interpretation is that PsA that requires continued antirheumatic treatment during pregnancy is more severe than PsA that does not require treatment. Thus, the increased risk of adverse outcomes in pregnancies with maternal antirheumatic treatment is probably attributed to disease severity rather than an effect of the medication itself. This is supported by a recent systematic review and meta-analysis by Tsao et al (38) regarding bDMARD exposure before and during pregnancy in women with chronic inflammatory arthritis and inflammatory bowel disease (IBD). They observed no association between the use of bDMARDs during pregnancy and risk of preterm birth compared to disease comparators exposed to non-bDMARDs. Furthermore, Bröms et al conducted a population-based study of pregnant women with IBD, RA, ankylosing spondylitis, PsA, and psoriatic skin disease (39). In that study, women treated with TNFi were at an increased risk for preterm birth, cesarean delivery, and neonatal small size for gestational age compared to women who received nonbiologic systemic treatment. The authors concluded that the diverse findings across disease groups may indicate an association related to the underlying disease activity rather than to agent-specific effects.

Interestingly, we observed that PsA pregnancies with exposure to glucocorticoid and/or csDMARD treatment during pregnancy had, in comparison to non-PsA pregnancies, just slightly and not statistically significant increased risks for most of the outcomes. A previous study showed that women with RA who had not received treatment with TNFi before pregnancy but who continued with other pregnancy-compatible antirheumatic drugs had mild and stable disease activity before and during pregnancy (40). Therefore, our results may indicate that glucocorticoid- and/or csDMARD-treated pregnant women have a better controlled maternal disease activity leading to more favorable outcomes compared to those needing treatment with bDMARDs.

We found no increased risk of neonatal small size for gestational age at birth. This is consistent with the results from Bröms et al (2) which assessed the risk of small size for gestational age at birth in PsA pregnancies, as well as a study by Mörk et al (7) which examined women with spondyloarthritis, including PsA.

Conversely, in studies focusing on RA in pregnant women, small size for gestational age at birth has commonly been reported (41–43).

This study has several strengths. The large study cohort of PsA pregnancies allowed for stratification according to timing and type of treatment, and we had the ability to adjust for important confounders such as maternal smoking status and BMI. We used independent sources for exposure and outcomes which minimize bias. Furthermore, the outcome variables are prospectively collected in the MBR. Registration of diagnoses in the NPR is mandatory, and in Sweden most rheumatologists work in specialist care, which allowed us to capture the majority of women with PsA. However, there remains a possibility that women with a diagnosis of PsA but with very few visits due to quiescent disease may be misclassified as not having PsA. This may skew the exposure to those with more severe disease.

There are also some limitations that need to be mentioned. Although we were able to stratify the PsA pregnancies by antirheumatic treatment as a proxy for disease severity, we did not have information on disease activity measurements such as the Disease Activity Score in 28 joints using C-reactive protein level (44) or the HAQ (12). As disease activity and antirheumatic treatment are closely linked, we acknowledge this as an important limitation. Further, we used information about dispensed prescriptions to assess antirheumatic treatment. There may be individuals who retrieve their medication from the pharmacy but do not use them. If so, we may have misclassified pregnancies as exposed to antirheumatic treatment when they were unexposed. Given our findings of worse outcomes in pregnancies with antirheumatic treatment, this misclassification of exposure may have biased the result toward the null by dilution. In spite of this large cohort size, we lacked statistical power to analyze rare outcomes. Finally, the lack of indication for medically indicated preterm births and cesarean delivery hampers the interpretation of the result.

In conclusion, we have demonstrated that pregnancy outcomes vary according to the presence, timing, and type of antirheumatic treatment. In comparison to non-PsA pregnancies, the risks of adverse outcomes were most increased in pregnancies exposed to antirheumatic treatment, especially bDMARDs, during pregnancy. As parity influences the risk of preterm birth, special attention to first PsA pregnancies is warranted to ensure optimal treatment strategies. From a clinical point of view, all women with PsA, regardless of antirheumatic treatment, should be counseled about pregnancy outcomes and receive individualized monitoring during pregnancy.

AUTHOR CONTRIBUTIONS

All authors were involved in drafting the article or revising it critically for important intellectual content, and all authors approved the final version to be published. Dr. Remaeus had full access to all of the data in the study and takes responsibility for the integrity of the data and the accuracy of the data analysis.

Study conception and design. Remaeus, Johansson, Granath, Stephansson, Hellgren.
Acquisition of data. Remaeus, Johansson, Granath, Hellgren.
Analysis and interpretation of data. Remaeus, Johansson, Granath, Stephansson, Hellgren.

REFERENCES

1. Van den Bosch F, Coates L. Clinical management of psoriatic arthritis. Lancet 2018;391:2285–94.
2. Broms G, Haerskjold A, Granath F, Kieler H, Pedersen L, Berglind IA. Effect of maternal psoriasis on pregnancy and birth outcomes: a population-based cohort study from Denmark and Sweden. Acta Derm Venereol 2018;98:728–34.
3. Mouyis MA, Thornton CC, Williams D, Giles IP. Pregnancy outcomes in patients with psoriatic arthritis. J Rheumatol 2017;44:128–9.
4. Smith CJ, Bandoli G, Kavanaugh A, Chambers CD. Birth outcomes and disease activity during pregnancy in a prospective cohort of women with psoriatic arthritis and ankylosing spondylitis. Arthritis Care Res (Hoboken) 2020;72:1029–37.
5. Ostensen M. Pregnancy in psoriatic arthritis. Scand J Rheumatol 1988;17:67–70.
6. Polachek A, Shlomi IP, Spitzer K, Pereira D, Ye JY, Chandran V, et al. Outcome of pregnancy in women with psoriatic arthritis compared to healthy controls. Clin Rheumatol 2019;38:895–902.
7. Mørk S, Voss A, Möller S, Bliddal M. Spondyloarthritis and outcomes in pregnancy and labor: a nationwide register-based cohort study. Arthritis Care Res (Hoboken) 2021;73:282–8.
8. Remaeus K, Stephansson O, Johansson K, Granath F, Hellgren K. Maternal and infant pregnancy outcomes in women with psoriatic arthritis: a Swedish nationwide cohort study. BJOG 2019;126:1213–22.
9. Strouse J, Donovan BM, Fatima M, Fernandez-Ruiz R, Baer RJ, Nidey N, et al. Impact of autoimmune rheumatic diseases on birth outcomes: a population-based study. RMD Open 2019;5:e000878.
10. Skorpen CG, Lydersen S, Gilboe IM, Skomsvoll JF, Salvesen K, Palm Ø, et al. Influence of disease activity and medications on offspring birth weight, pre-eclampsia and preterm birth in systemic lupus erythematosus: a population-based study. Ann Rheum Dis 2018;77:264–9.
11. Zbinden A, van den Brandt S, Ostensen M, Villiger PM, Forger F. Risk for adverse pregnancy outcome in axial spondyloarthritis and rheumatoid arthritis: disease activity matters. Rheumatology (Oxford) 2018;57:1235–42.
12. Fries JF, Spitz P, Kraines RG, Holman HR. Measurement of patient outcome in arthritis. Arthritis Rheum 1980;23:137–45.
13. Cnattingius S, Ericson A, Gunnarskog J, Kallen B. A quality study of a medical birth registry. Scand J Soc Med 1990;18:143–8.
14. Ludvigsson JF, Andersson E, Ekbom A, Feychting M, Kim JL, Reuterwall C, et al. External review and validation of the Swedish national inpatient register. BMC Public Health 2011;11:450.
15. Wettermark B, Hammar N, Fored CM, Leimanis A, Olausson PO, Bergman U, et al. The new Swedish Prescribed Drug Register: opportunities for pharmacoepidemiological research and experience from the first six months. Pharmacoepidemiol Drug Saf 2007;16:726–35.
16. Eriksson JK, Askling J, Arkema EV. The Swedish Rheumatology Quality Register: optimisation of rheumatic disease assessments using register-enriched data. Clin Exp Rheumatol 2014;32 Suppl:S147–9.
17. Askling J, Fored CM, Geborek P, Jacobsson LT, van Vollenhoven R, Feltelius N, et al. Swedish registers to examine drug safety and clinical issues in RA. Ann Rheum Dis 2006;65:707–12.
18. Urquia ML, Glazier RH, Gagnon AJ, Mortensen LH, Andersen AM, Janevic T, et al. Disparities in pre-eclampsia and eclampsia among

immigrant women giving birth in six industrialised countries. BJOG 2014;121:1492–500.
19. Cnattingius S. The epidemiology of smoking during pregnancy: smoking prevalence, maternal characteristics, and pregnancy outcomes [review]. Nicotine Tob Res 2004;6 Suppl:S125–40.
20. Hernandez-Diaz S, Toh S, Cnattingius S. Risk of pre-eclampsia in first and subsequent pregnancies: prospective cohort study. BMJ 2009; 338:b2255.
21. Waldenstrom U, Cnattingius S, Vixner L, Norman M. Advanced maternal age increases the risk of very preterm birth, irrespective of parity: a population-based register study. BJOG 2017;124:1235–44.
22. Catalano PM, Shankar K. Obesity and pregnancy: mechanisms of short term and long term adverse consequences for mother and child. BMJ 2017;356:j1.
23. Broms G, Granath F, Stephansson O, Kieler H. Preterm birth in women with inflammatory bowel disease: the association with disease activity and drug treatment. Scand J Gastroenterol 2016;51:1462–9.
24. Remaeus K, Johansson K, Askling J, Stephansson O. Juvenile onset arthritis and pregnancy outcome: a population-based cohort study. Ann Rheum Dis 2017;76:1809–14.
25. Smith CJ, Forger F, Bandoli G, Chambers CD. Factors associated with preterm delivery among women with rheumatoid arthritis and juvenile idiopathic arthritis. Arthritis Care Res (Hoboken) 2019;71: 1019–27.
26. Kolstad KD, Mayo JA, Chung L, Chaichian Y, Kelly VM, Druzin M, et al. Preterm birth phenotypes in women with autoimmune rheumatic diseases: a population-based cohort study. BJOG 2020;127:70–8.
27. Goldenberg RL, Culhane JF, Iams JD, Romero R. Epidemiology and causes of preterm birth. Lancet 2008;371:75–84.
28. Blencowe H, Cousens S, Chou D, Oestergaard M, Say L, Moller AB, et al. Born too soon: the global epidemiology of 15 million preterm births. Reprod Health 2013;10 Suppl:S2.
29. Cnattingius S, Villamor E, Johansson S, Bonamy AK, Persson M, Wikstrom AK, et al. Maternal obesity and risk of preterm delivery. JAMA 2013;309:2362–70.
30. Hedderson MM, Ferrara A, Sacks DA. Gestational diabetes mellitus and lesser degrees of pregnancy hyperglycemia: association with increased risk of spontaneous preterm birth. Obstet Gynecol 2003; 102:850–6.
31. Bandoli G, Singh N, Strouse J, Baer RJ, Donovan BM, Feuer SK, et al. Mediation of adverse pregnancy outcomes in autoimmune conditions by pregnancy complications: a mediation analysis of autoimmune conditions and adverse pregnancy outcomes. Arthritis Care Res (Hoboken) 2020;72:256–64.
32. Poston L, Caleyachetty R, Cnattingius S, Corvalan C, Uauy R, Herring S, et al. Preconceptional and maternal obesity: epidemiology and health consequences [review]. Lancet Diabetes Endocrinol 2016;4: 1025–36.
33. Bonamy AK, Zeitlin J, Piedvache A, Maier RF, van Heijst A, Varendi H, et al. Wide variation in severe neonatal morbidity among very preterm infants in European regions. Arch Dis Child Fetal Neonatal Ed 2019; 104:F36–45.
34. Wallenius M, Skomsvoll JF, Irgens LM, Salvesen KÅ, Nordvåg BY, Koldingsnes W, et al. Pregnancy and delivery in women with chronic inflammatory arthritides with a specific focus on first birth. Arthritis Rheum 2011;63:1534–42.
35. De Man YA, Hazes JM, van der Heide H, Willemsen SP, de Groot CJ, Steegers EA, et al. Association of higher rheumatoid arthritis disease activity during pregnancy with lower birth weight: results of a national prospective study. Arthritis Rheum 2009;60:3196–206.
36. Zbinden A, van den Brandt S, Ostensen M, Villiger PM, Forger F. Risk for adverse pregnancy outcome in axial spondyloarthritis and rheumatoid arthritis: disease activity matters. Rheumatology (Oxford) 2018; 57:1235–42.
37. Jakobsson GL, Stephansson O, Askling J, Jacobsson LT. Pregnancy outcomes in patients with ankylosing spondylitis: a nationwide register study. Ann Rheum Dis 2016;75:1838–42.
38. Tsao NW, Rebic N, Lynd LD, De Vera MA. Maternal and neonatal outcomes associated with biologic exposure before and during pregnancy in women with inflammatory systemic diseases: a systematic review and meta-analysis of observational studies. Rheumatology (Oxford) 2020;59:1808–17.
39. Broms G, Kieler H, Ekbom A, Gissler M, Hellgren K, Lahesmaa-Korpinen AM, et al. Anti-TNF treatment during pregnancy and birth outcomes: a population-based study from Denmark, Finland, and Sweden. Pharmacoepidemiol Drug Saf 2020;29:316–27.
40. Van den Brandt S, Zbinden A, Baeten D, Villiger PM, Ostensen M, Forger F. Risk factors for flare and treatment of disease flares during pregnancy in rheumatoid arthritis and axial spondyloarthritis patients. Arthritis Res Ther 2017;19:64.
41. Bharti B, Lee SJ, Lindsay SP, Wingard DL, Jones KL, Lemus H, et al. Disease severity and pregnancy outcomes in women with rheumatoid arthritis: results from the Organization of Teratology Information Specialists Autoimmune Diseases in Pregnancy Project. J Rheumatol 2015;42:1376–82.
42. Lin HC, Chen SF, Lin HC, Chen YH. Increased risk of adverse pregnancy outcomes in women with rheumatoid arthritis: a nationwide population-based study. Ann Rheum Dis 2010;69:715–7.
43. Norgaard M, Larsson H, Pedersen L, Granath F, Askling J, Kieler H, et al. Rheumatoid arthritis and birth outcomes: a Danish and Swedish nationwide prevalence study. J Intern Med 2010;268:329–37.
44. Prevoo ML, van't Hof MA, Kuper HH, van Leeuwen MA, van de Putte LB, van Riel PL. Modified disease activity scores that include twenty-eight–joint counts: development and validation in a prospective longitudinal study of patients with rheumatoid arthritis. Arthritis Rheum 1995;38:44–8.

American College of Rheumatology
Empowering Rheumatology Professionals

Arthritis & Rheumatology
Vol. 74, No. 3, March 2022, pp 496–507
DOI 10.1002/art.41987

Up-Regulated Interleukin-10 Induced by E2F Transcription Factor 2–MicroRNA-17-5p Circuitry in Extrafollicular Effector B Cells Contributes to Autoantibody Production in Systemic Lupus Erythematosus

Lingxiao Xu,[1] Lei Wang,[2] Yumeng Shi,[1] Yun Deng,[3] Jim C. Oates,[4] Diane L. Kamen,[3] Gary S. Gilkeson,[4] Fang Wang,[2] Miaojia Zhang,[2] Wenfeng Tan,[2] and Betty P. Tsao[3]

Objective. Elevated interleukin-10 (IL-10) levels in patients with systemic lupus erythematosus (SLE) have B cell–promoting effects, contributing to autoantibody production and tissue damage. We aimed to characterize up-regulated IL-10+ B cell subsets and dysregulated *IL10* expression in SLE B cells for new therapeutic options.

Methods. Proportions of Th10 and IL-10+ B cell subsets in peripheral blood mononuclear cells (PBMCs) were assessed using flow cytometry. The *IL10* 3′-untranslated region (3′-UTR) dual-luciferase vector was constructed and cotransfected with small interfering RNA (siRNA), microRNA (miRNA) mimics, or miRNA inhibitors into Raji cells. Transcript levels were quantified using TaqMan assays.

Results. Culture conditions that induced IL-10+ Breg cells in healthy controls resulted in expansion of IL-10+ double-negative 2 (DN2; IgD−CD27−CD21−CD11c+) B cells in SLE PBMCs. Proportions of IL-10+ DN2, but not those of IL-10− DN2, correlated with disease activity and levels of antibodies to double-stranded DNA (dsDNA) ($r = 0.60$, $P = 0.03$ for cohort 1; $r = 0.38$, $P = 0.03$ for cohort 2), and were associated with high levels or seropositivity of anti-Sm ($P = 0.03$ for cohort 1; $P = 0.01$ for cohort 2) and IgG anticardiolipin ($P < 0.01$ for cohort 1; $P = 0.02$ for cohort 2) in SLE patients from 2 cohorts, of mainly African American subjects (cohort 1) and of Asian subjects (cohort 2). Proportions of Th10 (CD45RA−CXCR5−CXCR3+PD-1^{high}CD4+) cells correlated with IL-10+ DN2 frequencies ($r = 0.60$, $P < 0.01$ for cohort 2), antinuclear antibody titers ($r = 0.52$, $P = 0.01$ for cohort 2), and proteinuria levels ($r = 0.72$, $P < 0.01$ for cohort 2) in SLE patients. Screening of predicted *IL10* 3′-UTR–targeting miRNAs in SLE B cells identified miRNA-17-5p (miR-17-5p) and miR-20a-5p, with their levels inversely correlated with *IL10* ($r = -0.47$, $P < 0.01$ for miR-17-5p; $r = -0.37$, $P = 0.03$ for miR-20-5p) and transcription factor *E2F2* ($r = -0.48$, $P = 0.04$ for miR-17-5p; $r = -0.45$, $P = 0.05$ for miR-20-5p). In Raji cells, knockdown of *E2F2* expression resulted in increased levels of miR-17-5p and miR-20a-5p and decreased *IL10* messenger RNA (mRNA) and protein levels, and overexpression and inhibition of miR-17-5p down-regulated and up-regulated, respectively, *IL10* mRNA levels, suggesting regulation of *IL10* expression by an *E2F2*-miR-17-5p loop.

Conclusion. IL-10 promotes extrafollicular autoimmune responses in patients with active SLE, which might be dampened by targeting the *E2F2*–miR-17-5p circuitry.

Supported by the National Institute of Arthritis and Musculoskeletal and Skin Diseases (grants P60-AR-062755 and P30-AR-072582) and by the Alliance for Lupus Research (Target Identification in Lupus grant to Dr. Tsao).

[1]Lingxiao Xu, MD, PhD, Yumeng Shi, PhD: Medical University of South Carolina, Charleston, and The First Affiliated Hospital of Nanjing Medical University, Nanjing, Jiangsu, China; [2]Lei Wang, PhD, Fang Wang, MD, PhD, Miaojia Zhang, MD, PhD, Wenfeng Tan, MD, PhD: The First Affiliated Hospital of Nanjing Medical University, Nanjing, Jiangsu, China; [3]Yun Deng, MD, PhD, Diane L. Kamen, MD, Betty P. Tsao, PhD: Medical University of South Carolina, Charleston; [4]Jim C. Oates, MD, Gary S. Gilkeson, MD: Medical University of South Carolina, Charleston, and Ralph H. Johnson VA Medical Center, Medical Service, Charleston, South Carolina.

Author disclosures are available at https://onlinelibrary.wiley.com/action/downloadSupplement?doi=10.1002%2Fart.41987&file=art41987-sup-0001-Disclosureform.pdf.

Address correspondence to Betty P. Tsao, PhD, Division of Rheumatology and Immunology, Department of Medicine, Medical University of South Carolina, 96 Jonathan Lucas Street, Clinical Science Building Suite 936C, Charleston, SC 29425. Email: tsaob@musc.edu.

Submitted for publication February 28, 2021; accepted in revised form September 23, 2021.

INTRODUCTION

Interleukin-10 (IL-10) is an antiinflammatory cytokine that also has B cell–promoting ability, contributing to autoantibody production and tissue damage in systemic lupus erythematosus (SLE) (1). It is well documented that elevated serum levels of IL-10 are associated with disease activity in patients with SLE (2). While SLE-associated risk variants contribute to transcript levels of *IL10*, a nongenetic disease state further augments IL-10 levels in SLE peripheral blood mononuclear cells (PBMCs), especially in B and T cells (3,4).

The identity of IL-10+ B cell subsets in SLE remains unclear. B cells producing IL-10, known as regulatory B (Breg) cells, contribute to the maintenance of immune tolerance (5,6). However, differentiation signals established in healthy controls to induce IL-10 production by $CD24^{high}CD38^{high}$ B cells are defective in SLE patients, and Breg cells from SLE patients are functionally impaired to restrain interferon-α (IFNα) production by plasmacytoid dendritic cells (pDCs) (7,8).

IL-10 is also produced by T helper cells in SLE, especially during active disease (4). A novel T cell subset, defined as Th10 ($CD4+CD45RA-CXCR5-CXCR3+PD\text{-}1^{high}$) cells, was expanded in the blood of SLE patients and enriched in kidneys, providing B cell help through secretion of IL-10 and succinate in extrafollicular autoimmune responses (9). The mitochondrial DNA (a Toll-like receptor 9 [TLR-9] ligand) released during the disease process of SLE is linked to the generation of this subset. Since TLR-9 ligands also play a critical role in the differentiation of IL-10–producing B cell subsets, IL-10 may promote T cell–B cell interaction in the extrafollicular humoral immune pathway.

IgD−CD27−CD21−CD11c+ (double-negative 2 [DN2]) B cells are expanded in PBMCs from SLE patients, especially in African American patients with active disease (10). DN2 cells, derived from autoreactive naive B cells, hyperactively respond to innate stimuli to become precursors of preplasma cells through extrafollicular reactions (11,12). DN2 B cells from SLE patients express IL-10 receptors, which make them a candidate to interact with Th10 in expanding extrafollicular autoimmune responses (10).

In this study we aimed to identify differentially up-regulated IL-10+ B cells in SLE patients, to understand the role of IL-10 in extrafollicular autoimmune responses, and to explore potential molecular targets that might dampen IL-10 expression in SLE B cells.

PATIENTS AND METHODS

Subjects. All SLE patients fulfilled at least 4 of the 11 American College of Rheumatology revised criteria for SLE (13). SLE patients and healthy controls in cohort 1 provided written consent forms for the study, which was approved by the Institutional Review Boards of the Medical University of South Carolina. The cohort 2 study was approved by the Ethical Committee of the First Affiliated Hospital of Nanjing Medical University, and all donors provided written informed consent. Disease activity was assessed using the Safety of Estrogens in Lupus Erythematosus National Assessment (SELENA) version of the Systemic Lupus Erythematosus Disease Activity Index (SLEDAI) score (14). The characteristics of the 2 cohorts are shown in Table 1.

Preparation of blood samples and flow cytometric analysis. PBMCs, isolated by Ficoll-Paque Plus (Amersham Biosciences) density-gradient centrifugation from participants' blood samples, pretreated with FC block (BD Bioscience) in phosphate buffered saline/0.5% bovine serum albumin/5m*M* EDTA for 10 minutes at 4°C, were incubated with specific monoclonal antibodies. Antigens for B cell subsets were CD19, IgD, CD27, CXCR5, CD21, CXCR3, IL-10 receptor antagonist (IL-10Ra), IL-21R, and CD95; antigens for T cell subsets were CD3, CD4, CD45RA, CXCR5, CXCR3, IL-21, IL-10, and programmed death 1 (PD-1), as described in Supplementary Table 1, available on the *Arthritis & Rheumatology* website at https://onlinelibrary.wiley.com/doi/10.1002/art.41987. For intracellular protein detection, PBMCs in 6-well plates were cultured with complete media (RPMI 1640, 10% fetal bovine serum [FBS], glutamine, and penicillin/streptomycin), 50 ng/ml phorbol myristate acetate (Sigma), 250 ng/ml ionomycin (Sigma), and GolgiPlug (BD Biosciences) for ≥5 hours, fixed and permeabilized, and stained with intracellular staining reagents for the detection of IL-10 and T-bet, according to the manufacturer's instructions (eBioscience). All samples were analyzed on a BD LSRFortessa X-20 system (cohort 1) or a BD Aria II system (cohort 2), and data were analyzed using FlowJo software (Tree Star).

B cell differentiation assay. Freshly isolated PBMCs (2×10^6 cells/ml) from SLE patients and healthy controls were cultured with medium alone or with class C CpG (1 μ*M*; InvivoGen) and IFNα (1,000 units/ml; PBL Biomedical Laboratories) in RPMI 1640 medium with 10% FBS for 24 hours. Subsequently, cells were washed, stained, and subjected to flow cytometry.

Cell isolation and cell sorting. B cells were isolated by positive selection from PBMCs using an EasySep Human CD19 Positive Selection Kit II (StemCell), according to the manufacturer's instructions. The purity of isolated B cells (>95%) was assessed by flow cytometric analysis. Enriched cells were then stained with BV650-conjugated anti-IgD, BV421-conjugated anti-CD27, and phycoerythrin (PE)–Cy5.5–conjugated anti-CD19 and sorted as IgD+CD27−CD19+ cells (naive), IgD−CD27+CD19+ cells (switched memory), IgD+CD27+CD19+ cells (unswitched memory), or IgD−CD27−CD19+ cells (double negative).

For blood CD4+ T cell subset sorting, frozen PBMCs from individuals with SLE were stained with BV711-conjugated anti-CD4, allophycocyanin-conjugated anti-CXCR5, PE–Cy7–conjugated anti-CD45RA, PE-conjugated anti–PD-1, BV650-conjugated anti-CD3,

Table 1. Demographic and clinical characteristics of the SLE patients and healthy controls in 2 cohorts*

	Cohort 1 (Charleston, SC)		Cohort 2 (Nanjing, China)	
	SLE patients (n = 51)	Controls (n = 25)	SLE patients (n = 61)	Controls (n = 40)
Sex, no. (%) female	49 (96.1)	25 (100)	56 (91.8)	34 (85.0)
Age, mean (range) years	46 (20–78)	41 (24–69)	33 (15–63)	36 (21–65)
Ancestry, no. (%)				
African American	40 (78.4)	19 (76.0)	–	–
Asian	1 (2.0)	3 (12.0)	61 (100)	40 (100)
European American	10 (19.6)	3 (12.0)	–	–
Disease manifestation, no. (%)				
Fever	5 (9.8)	–	25 (41.0)	–
Rash	10 (19.6)	–	32 (52.5)	–
Alopecia	11 (21.6)	–	21 (34.4)	–
Nonerosive arthritis	4 (7.8)	–	24 (39.3)	–
Oral ulcer	13 (25.5)	–	27 (44.3)	–
Cutaneous vasculitis	5 (9.8)	–	7 (11.5)	–
Serositis	6 (11.8)	–	17 (27.9)	–
NPSLE	2 (3.9)	–	5 (8.2)	–
LN	3 (5.9)	–	33 (54.1)	–
Leukopenia and/or thrombocytopenia	11 (21.6)	–	20 (32.8)	–
Laboratory features, mean ± SD				
IgG anti-dsDNA, IU/ml	28.9 ± 58.0	–	250 ± 257†	–
Anti-Sm, units/ml	28.1 ± 42.1	–	33 (54.1)‡	–
IgG anticardiolipin antibody, RU/ml	15.5 ± 8.3	–	15.0 ± 11.2	–
IgM anticardiolipin antibody, RU/ml	–	–	16.3 ± 11.9	–
IgG, gm/liter	–	–	16.0 ± 8.5	–
C3, gm/liter	1.25 ± 0.39	–	0.55 ± 0.22	–
C4, gm/liter	0.26 ± 0.10	–	0.11 ± 0.06	–
Proteinuria, mg/24 hours	–	–	1716.6 ± 2640.6	–
Proteinuria:creatinine ratio	176.3 ± 145.3	–	–	–
SLEDAI score, mean ± SD (range)	3.0 ± 3.7 (0–18)	–	10.9 ± 6.0 (2–29)	–
Medication, no. (%)				
Prednisone	18 (35.3)	–	58 (95.1)	–
Hydroxychloroquine	46 (90.2)	–	55 (90.2)	–
Cyclophosphamide	1 (2.0)	–	9 (14.8)	–
Azathioprine	24 (47.1)	–	8 (13.1)	–
Methotrexate	2 (3.9)	–	6 (9.8)	–
Mycophenolate mofetil	20 (39.2)	–	27 (44.3)	–
Cyclosporine	1 (2.0)	–	5 (8.2)	–
Tacrolimus	–	–	12 (19.7)	–

* SLE = systemic lupus erythematosus; NPSLE = neuropsychiatric SLE; LN = lupus nephritis; anti-dsDNA = anti–double-stranded DNA; SLEDAI = Systemic Lupus Erythematosus Disease Activity Index.
† Relative units [RU]/ml.
‡ Values are the number (%) of patients positive for anti-Sm.

Alexa Fluor 488–conjugated anti–IL-10, PerCP–Cyanine5.5–conjugated anti–IL-21, and BV421-conjugated anti-CXCR3. Then, the CXCR3+PD-1^{high}CD4+ T cell population was sorted from the CD3+CD4+CD45RA−CXCR5− cell fraction. Cell sorting was performed on a BD FACSAria II SORP using a 100-μm nozzle. Gating strategies were performed as described by Caielli et al (9). Cell purity was routinely >98%. For functional analyses, cells were sorted into cold RPMI/10% FBS.

B cell cultures. B cells were isolated as described above. For cocultures of B and T cells, CD19+ B cells (from healthy donors) were cocultured with CXCR3+PD-1^{high}CD4+ T cells (from SLE patients) (2×10^4 B cells and 2×10^4 Th10 cells) in RPMI supplemented with 10% heat-inactivated FBS. Anti–IL-10 (10 μg/ml) (clone JES3-9D7; BioLegend), anti-SUCNR1/GPR91 (20 μg/ml; Novus Biologicals), or anti–IL-21R (10 μg/ml) (clone 17A12; BioLegend) was added during the coculture. IgG concentrations in the supernatants were measured on day 7 using an IgG Human ELISA Kit (ThermoFisher).

Real-time quantitative reverse transcriptase–polymerase chain reaction (qRT-PCR) and enzyme-linked immunosorbent assay (ELISA). Total RNA was extracted from isolated B cells and cells of the Raji lymphoblastoid cell line (CCL-86; ATCC) using TRIzol reagent (Invitrogen), and reverse transcribed into complementary DNA using a Superscript II

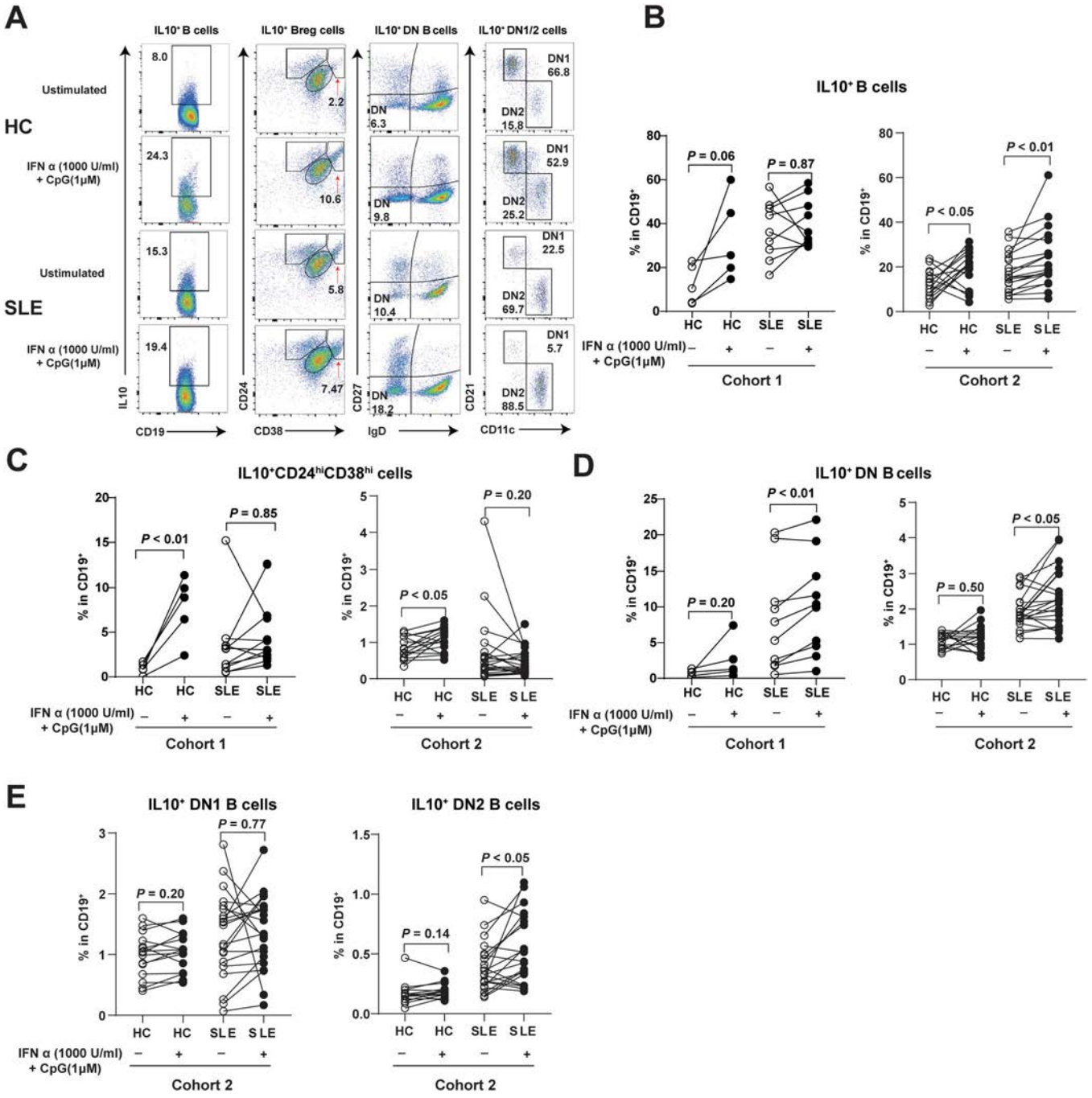

Figure 1. Up-regulation of Breg cells in healthy control (HC) peripheral blood mononuclear cells (PBMCs) and expansion of interleukin-10 (IL-10)+ double-negative (DN) and IL-10+ DN2 B cells in systemic lupus erythematosus (SLE) PBMCs under the same culture conditions. **A**, Representative flow cytometry plots for IL-10+ B cells, IL-10+ Breg cells, IL-10+ DN cells, and IL10+ DN1/2 cells in healthy control and SLE PBMCs left unstimulated or stimulated with class C CpG and interferon-α (IFNα). **B**–**D**, Changes in the frequency of IL-10+ B cells (**B**), IL-10+ Breg cells (IL-10+CD24^{high}CD38^{high}) (**C**), and IL-10+ DN B cells (IL-10+IgD−CD27−) (**D**) in healthy control and SLE PBMCs stimulated with class C CpG and IFNα (n = 5 healthy controls and 11 SLE patients in cohort 1; n = 16 healthy controls and 21 SLE patients in cohort 2). **E**, Changes in the frequency of IL-10+ DN1 B cells (IgD−CD27−CD21+CD11c−) and IL-10+ DN2 B cells (IgD−CD27−CD21−CD11c+) in healthy control and SLE PBMCs stimulated with class C CpG and IFNα (n = 16 healthy controls and 21 SLE patients in cohort 2). Open and solid symbols represent paired unstimulated and stimulated samples from individual subjects. *P* values were determined by paired *t*-test. Color figure can be viewed in the online issue, which is available at http://onlinelibrary.wiley.com/doi/10.1002/art.41987.

Reverse Transcription kit (Invitrogen) to measure levels of *IL10, E2F1, E2F2, E2F3*, and housekeeping gene (RPLP0 or GAPDH) using TaqMan assays (Life Technologies). The levels of 13 microRNAs (miRNAs) were quantified using TaqMan Advanced miRNA Assays (Life Technologies) normalized using levels of miR-361 (Life Technologies). All relative expression levels

were calculated by the $2^{-\Delta\Delta Ct}$ method and $\log_{10}$ transformed. The miRNA and mRNA primers used for real-time qRT-PCR are listed in Supplementary Table 2, available on the *Arthritis & Rheumatology* website at https://onlinelibrary.wiley.com/doi/10.1002/art.41987. IL-10 levels in supernatants were measured by ELISA kit (RayBiotech), according to the manufacturer's instructions.

Transfection of the miRNA mimics, antagomirs, and small interfering RNAs (siRNAs). Raji cells (CCL-86; ATCC) were cultured in RPMI 1640 medium with 10% FBS, seeded on a 24-well plate (1×10^6 cells/well), transfected with mimics/antagomirs of miR-17, miR-20a, miR-106a, or the negative control (200 n*M*, respectively; Ambion, Invitrogen) by electroporation using a Nucleofector system (Amaxa), and harvested after 24 hours for gene expression assay.

Accell siRNAs targeting E2F transcription factor 2 (E2F2; E-003260) and nontargeting sequences (as negative control; D-001910) were purchased from Dharmacon. Raji cells were cultured in Accell delivery media plus 1 μM siRNA, distributed to 24-well plates at 2×10^5 cells/well, and divided into silenced groups for *E2F2*, nontargeting, and medium-only mock controls. Cells were incubated at 37°C with 5% CO_2 for 72 hours, supernatants were collected, and cells were harvested to measure specific inhibition of *E2F2* by real-time qRT-PCR.

Plasmid construction and luciferase reporter assay. The amplification of 1,034-bp fragments of the 3′-UTR of *IL10* was achieved by PCR using genomic DNA from a healthy European American using the following primers: 5′-CCGC TCGAGCACAGCTCCAAGAGAAAGGC-3′ (forward) and 5′-AGAGCGGCCGCCTTGGGAGCTTTGAGAGAACA-3′ (reverse). PCR products were digested using restriction enzymes and subcloned into the psiCHECK-2 luciferase reporter vector (Promega). Raji cells were seeded on 24-well plates at 1×10^6 cells/well. The luciferase construct (1 μg) and empty psiCHECK-2 vector (1 μg) were electroporated either alone or together with oligonucleotides (antagomirs) using Nucleofector (Amaxa), and *Renilla* plasmid (10 ng) was used as the endogenous control. Luciferase activity in cell lysates was measured after 24 hours using a dual-luciferase reporter assay (Promega).

Statistical analysis. For comparisons between 2 groups, Student's *t*-test and paired *t*-test were used if the variance was normally distributed, whereas Mann-Whitney U test and Spearman's rank correlation were used if the variance was not normally distributed. *P* values less than 0.05 were considered significant. Data were analyzed using GraphPad Prism 8 software.

RESULTS

Expansion of IL-10+ DN B cells induced by IFNα and CpG in SLE PBMCs from 2 independent cohorts. To begin understanding the role of IL-10 expression in SLE B cells, we compared induced B cell subsets derived from healthy control or SLE PBMCs after culturing in the presence or absence of IFNα and a class C CpG (a TLR-9 ligand that could activate both pDCs and B cells present in PBMCs) for 24 hours, using flow cytometry (15) (Figures 1A and B). Intracellular staining for IL-10 demonstrated a trend toward a higher percentage of total IL-10+ B cells in IFNα-stimulated healthy control PBMCs but not IFNα-stimulated SLE PBMCs in cohort 1, which was mainly composed of African American subjects (Figure 1B and Table 1). The induced IL-10–expressing B cells were enriched among IL-10+ Breg cells in healthy controls (IL-10+CD24^{high}CD38^{high}) (Figure 1C), but among IL-10+ DN B cells in SLE patients (Figure 1D), confirming defective Breg cell induction in SLE patients (8). To independently verify that stimulation with CpG and IFNα resulted in the enlargement of the IL-10+ DN B cell subset in SLE PBMCs, we analyzed a second cohort, of Asian SLE patients (Table 1), which confirmed the findings in cohort 1 (Figures 1B–D) and showed up-regulation of IL-10+ DN2 B cells in SLE patients (Figure 1E).

Expansion of the IL-10+ DN2 B cell subset in ex vivo SLE PBMCs enriched in IL-10Ra. We next evaluated which B cell subset could account for the IL-10 overproduction in ex vivo SLE B cells from cohort 1, which consisted mainly of African American subjects, and cohort 2, which consisted of Asian subjects (Table 1). Flow cytometric analysis of intracellular IL-10 in peripheral B cells showed significantly higher frequencies of IL-10–expressing B cells in SLE patients than in healthy controls (Figure 2), but no significant up-regulation of IL-10+ B cells in patients with active disease, in both cohorts (Supplementary Figures 1B and C, available on the *Arthritis & Rheumatology* website at https://onlinelibrary.wiley.com/doi/10.1002/art.41987). These findings were consistent with the similar *IL10* mRNA levels observed in patients with different levels of disease activity in cohort 1 (Supplementary Figure 1A). The enlarged proportions of IL-10+ B cells in SLE in both cohorts were enriched in DN or DN2 B cell subsets (Figures 2B and C).

Compared to cohort 1, SLE patients in cohort 2 had higher disease activity (Table 1) with lower proportions of IL-10+ B cells (Figure 2A) and an expanded IL-10+ activated naive B cell subset, which was not significantly expanded in cohort 1 (Figure 2C). We confirmed previous findings that SLE patients had expanded DN2 B cells compared to healthy controls (Supplementary Figure 2, available on the *Arthritis & Rheumatology* website at https://onlinelibrary.wiley.com/doi/10.1002/art.41987). In both cohorts, differentially up-regulated IL-10+ B cells in SLE were observed in the DN2 rather than DN1 subset. The mean proportions of IL-10+ cells among DN2 B cells were 40% and 20% in SLE patients in cohort 1 and cohort 2, respectively (10) (Supplementary Figure 3B, available on the *Arthritis & Rheumatology* website at https://onlinelibrary.wiley.com/doi/10.1002/art.41987).

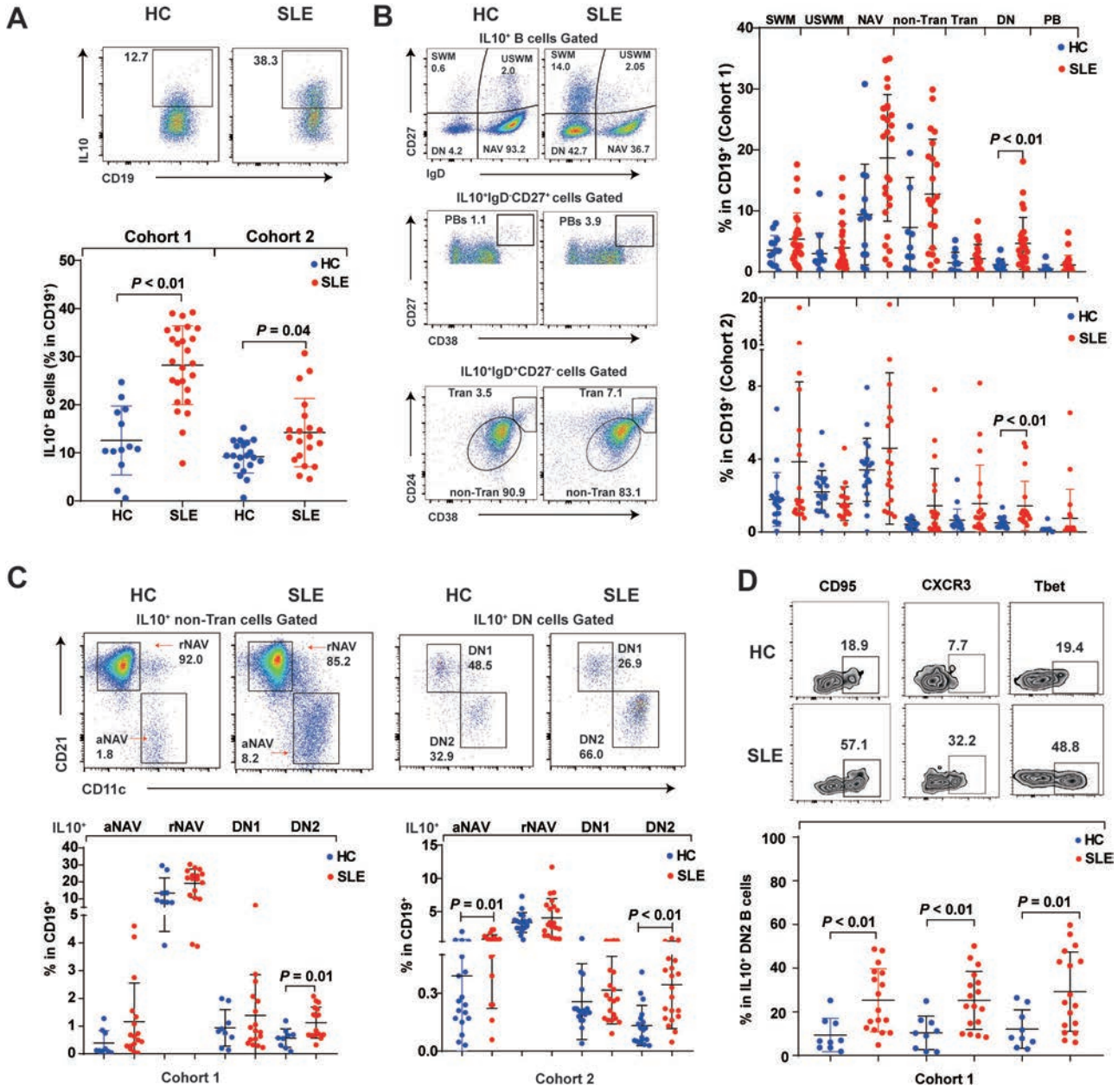

Figure 2. Enrichment of differentially up-regulated IL-10+ ex vivo SLE B cells in the DN2 subset in multiple cohorts. **A**, Flow cytometry plots (top) and quantification (bottom) of the frequency of IL-10+ B cells among CD19+ B cells in healthy controls (n = 13) and SLE patients (n = 26) in cohort 1 and healthy controls (n = 20) and SLE patients (n = 20) in cohort 2. **B**, Flow cytometry plots (left) and quantification (right) of the frequencies of IL-10+ B cell subsets in healthy controls and SLE patients in cohort 1 and cohort 2. IL-10+ B cell subsets were identified as switched memory (SWM; IgD−CD27+), unswitched memory (USWM; IgD+CD27+), double negative (DN; IgD−CD27−), naive (NAV; IgD+D27−), plasmablast (PB; IgD−CD27^{high}CD38^{high}), transitional (Tran; IgD+CD27−CD24+CD38^{high}), or nontransitional (non-Tran; IgD+CD27−CD24^{intermediate}CD38^{intermediate}). **C**, Flow cytometry plots (top) and quantification of results (bottom) showing further separation of nontransitional B cell and DN cell subsets, based on CD11c and CD21 levels, into IL-10+ activated naive (aNAV) B cells (IgD+CD27−CD21−CD11c+), IL-10+ resting naive (rNAV) B cells (IgD+CD27−CD21+CD11c−), IL-10+ DN1 cells, and IL-10+ DN2 cells in healthy controls (n = 9) and SLE patients (n = 17) in cohort 1 and in healthy controls (n = 18) and SLE patients (n = 20) in cohort 2. **D**, Flow cytometry plots (top) and quantification (bottom) of the expression of CD95, CXCR3, and T-bet by IL-10+ DN2 cells in healthy controls (n = 9) and SLE patients (n = 17) in cohort 1. Symbols represent individual subjects; horizontal lines and error bars show the mean ± SD. *P* values were determined by Mann–Whitney U test. See Figure 1 for other definitions.

The inducible subunit of IL-10Ra exhibited higher expression levels in DN2 and IL-10+ DN2 B cells from SLE patients in both cohorts (Supplementary Figure 3A). As previously reported by Jenks et al (10), we confirmed that the presence of IL-10Ra on SLE DN2 B cells in both cohort 1 and cohort 2, together with constitutively expressed IL-10Rb, provided IL-10+ DN2 B cells the possibility for autocrine signaling to become plasma cell precursors (16).

Further phenotype analysis confirmed that IL-10+ DN2 B cells from SLE patients in cohort 1 expressed higher levels of CD95, CXCR3, and T-bet than those from healthy controls (Figure 2D). These markers are also commonly found in 2 additional autoantibody-secreting B cell subsets in SLE: age-associated B cells and atypical memory B cells (17,18).

Correlation of proportions of IL-10+ DN2 B cells and Th10 cells with elevated disease activity and autoantibody production in SLE patients. The SLE DN2 B cell subset has previously been characterized as a precursor of autoantibody-producing plasma cells, and the proportions of DN2 cells among CD19+ cells from SLE patients correlate with

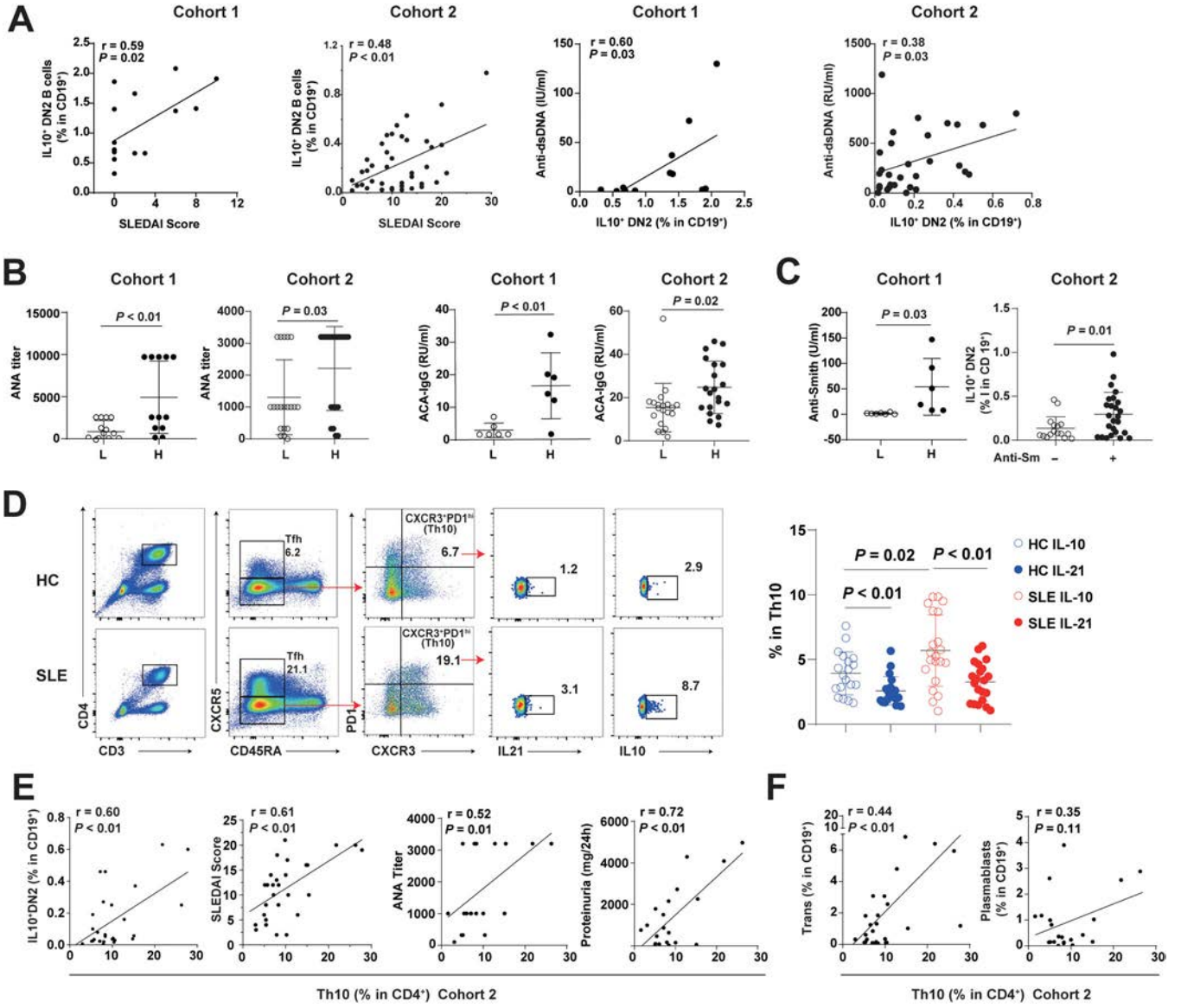

Figure 3. Correlation of the frequencies of IL-10+ DN2 cells and Th10 cells with disease activity and autoantibody production in SLE patients in multiple cohorts. **A**, Correlation of IL-10+ DN2 cell proportions with Systemic Lupus Erythematosus Disease Activity Index (SLEDAI) scores and serum levels of IgG anti–double-stranded DNA (anti-dsDNA) antibody in SLE patients in cohort 1 (n = 15) and cohort 2 (n = 41). **B**, Serum levels of antinuclear antibody (ANA) and IgG anticardiolipin antibody (ACA) in SLE patients in cohort 1 (n = 13) and cohort 2 (n = 30) with low (L) or high (H) frequencies of IL-10+ DN2 cells. **C**, Serum levels of anti-Sm antibody in SLE patients in cohort 1 (n = 25) with low or high frequencies of IL-10+ DN2 cells, and frequencies of IL-10+ DN2 cells in SLE patients in cohort 2 (n = 41) who were negative or positive for anti-Sm antibody. **D**, Gating strategy for Th10 cells (left) and frequencies of IL-10+ and IL-21+ cells among Th10 cells in healthy controls (n = 20) and SLE patients (n = 21) in cohort 2 (right). **E** and **F**, Correlations of Th10 cell frequencies with proportions of IL-10+ DN2 cells, SLEDAI scores, serum levels of ANA, and levels of 24-hour proteinuria (**E**) and with proportions of transitional B cells and plasmablast cells (**F**) in SLE patients in cohort 2. In **B**–**D**, symbols represent individual subjects; horizontal lines and error bars show the mean ± SEM. *P* values were determined by Mann–Whitney U test and Spearman's rank correlation. See Figure 1 for other definitions. Color figure can be viewed in the online issue, which is available at http://onlinelibrary.wiley.com/doi/10.1002/art.41987.

SLEDAI scores (10). To explore the potential role of the IL-10+ DN2 B cell subset in SLE, we assessed the relationship between the proportion of IL-10+ DN2 B cells and disease activity as well as levels of SLE-associated autoantibodies. The proportions of IL-10+ DN2 B cells in both cohort 1 and cohort 2 positively correlated with SLEDAI scores, levels of anti–double-stranded DNA (anti-dsDNA) (Figure 3A), antinuclear antibody (ANA) titers, levels of IgG anti-cardiolipin antibodies (Figure 3B), and levels of (or the presence of) anti-Sm autoantibody (Figure 3C), linking this cell subset with lupus autoantibody production.

Th10 has been reported to provide B cell help, independently of IL-21, through an IL-10– and succinate-dependent manner in the extrafollicular pathway contributing to SLE (9). Levels of IL-21R and IL-10Ra, which are critical for naive B cell differentiation and proliferation, were higher in IL-10+ DN2 and IL-10+ activated naive cells from SLE patients than those from healthy controls, suggesting that the expansion of IL-10+ DN2 in SLE patients was induced by elevated IL-10 and IL-21 levels (Supplementary Figure 4C). Similar to the results of a previous study (9), we confirmed that more Th10 cells in SLE PBMCs expressed IL-10 than produced IL-21 (Figure 3D). Our new data showed that the IgG content in the culture supernatant was significantly decreased by anti–IL-10 or anti-SUCRN1 blockade, but not by anti–IL-21 blockade, highlighting the importance of IL-10 and SUCRN1, independent of IL-21, in mediating Th10 cell–B cell interaction and antibody production (Supplementary Figure 4D).

We also found a correlation between the proportions of Th10 cells and the SLEDAI score in cohort 2 (9) (Figure 3E). The Th10 subset also showed a positive correlation with IL-10+ DN2 B cells (Figure 3E), suggesting that IL-10 receptors present on IL-10+ DN2 B cells could interact with IL-10–secreting Th10 cells during active disease. Furthermore, proportions of Th10 cells positively correlated with ANA titers and levels of 24-hour proteinuria (Figure 3E), highlighting the importance of IL-10–producing extrafollicular T helper cells in the pathogenesis of SLE and lupus nephritis. Of note, proportions of Th10 cells positively correlated with frequencies of transitional B cells, and showed a trend toward correlation with plasmablast frequencies, in cohort 2 (Figure 3F), which was consistent with the findings of a previous study (9).

Both DN2 and IL-10+ DN2 B cell subsets exhibited features linked to SLE manifestations. While the mean proportions of IL-10+ DN2 B cells represented a minor fraction of total DN2 B cells in either cohort (Supplementary Figure 3B), IL-10+ DN2 B cells captured most, if not all, features linked to SLE manifestations compared to the IL10− DN2 subset in both cohorts (Table 2). While most DN2 B cells were IL-10−, the IL-10+ DN2 subset was associated with major pathogenic features in SLE, contributing to extrafollicular responses of autoantibody production.

Regulation of *IL10* expression by interactions of *E2F2*, miR-17-5p, and miR-20a-5p. Dysregulated IL-10 expression in SLE B cells might be under posttranscriptional regulation, inducing miRNA to modulate transcript stability and translation activity. Using miRNA target prediction databases (19–21), we identified 13 potential miRNAs that could bind to the 3′-untranslated region (3′-UTR) of *IL10* mRNA (Supplementary Table 3) and assessed their relative expression levels in B cells isolated from 25 SLE patients and 12 controls in cohort 1 (Table 1). Consistent with flow cytometry data for cohort 1 and cohort 2, elevated *IL10* mRNA levels were observed in SLE B cells in cohort 1 (Figure 4A). Compared to healthy control B cells, SLE B cells showed differential expression levels for 6 of the 13 predicted miRNAs (Figure 4B).

Table 2. Correlations of the frequencies of the DN2, IL-10+ DN2, and IL-10− DN2 B cell subsets with SLE manifestations*

	Cohort 1 (n = 17)						Cohort 2 (n = 40)					
	DN2		IL-10+ DN2		IL-10− DN2		DN2		IL-10+ DN2		IL-10− DN2	
	r	*P*	r	*P*	r	*P*	r	*P*	r	*P*	r	*P*
SLEDAI	0.670	0.006	0.594	0.019	0.640	0.011	0.461	0.003	0.481	0.001	0.293	0.063
ANA titer	0.506	0.038	0.719	0.001	0.402	0.110	0.599	<0.001	0.353	0.027	0.296	0.068
IgG anti-dsDNA	0.625	0.022	0.722	0.005	0.546	0.053	0.548	0.002	0.379	0.038	0.422	0.018
IgG anticardiolipin antibody	0.466	0.291	0.669	0.100	0.544	0.279	0.424	0.007	0.353	0.025	0.190	0.241
Anti-Sm	0.370	0.240	0.617	0.032	0.259	0.416	ND	0.021†	ND	0.023†	ND	0.013†
C3	−0.745	0.001	−0.552	0.032	−0.738	0.002	−0.211	0.190	−0.102	0.526	0.059	0.714
C4	−0.571	0.026	−0.258	0.352	−0.616	0.015	−0.002	0.989	−0.130	0.480	0.231	0.219
IgM anticardiolipin antibody	ND	ND	ND	ND	ND	ND	0.081	0.621	0.061	0.702	0.013	0.936
Total IgG	ND	ND	ND	ND	ND	ND	0.080	0.621	0.206	0.196	0.013	0.935
24-hour proteinuria	ND	ND	ND	ND	ND	ND	0.090	0.586	0.342	0.111	−0.010	0.952
Th10 cell subset	ND	ND	ND	ND	ND	ND	0.347	0.048	0.438	0.011	0.328	0.062
Tfh-like cell subset	ND	ND	ND	ND	ND	ND	0.311	0.078	0.237	0.185	0.303	0.087

* DN2 = double-negative 2; IL-10 = interleukin-10; SLE = systemic lupus erythematosus; SLEDAI = Systemic Lupus Erythematosus Disease Activity Index; ANA = antinuclear antibody; anti-dsDNA = anti–double-stranded DNA; ND = not determined; Tfh = follicular helper T cell.
† *P* values for the presence or absence of anti-Sm antibody.

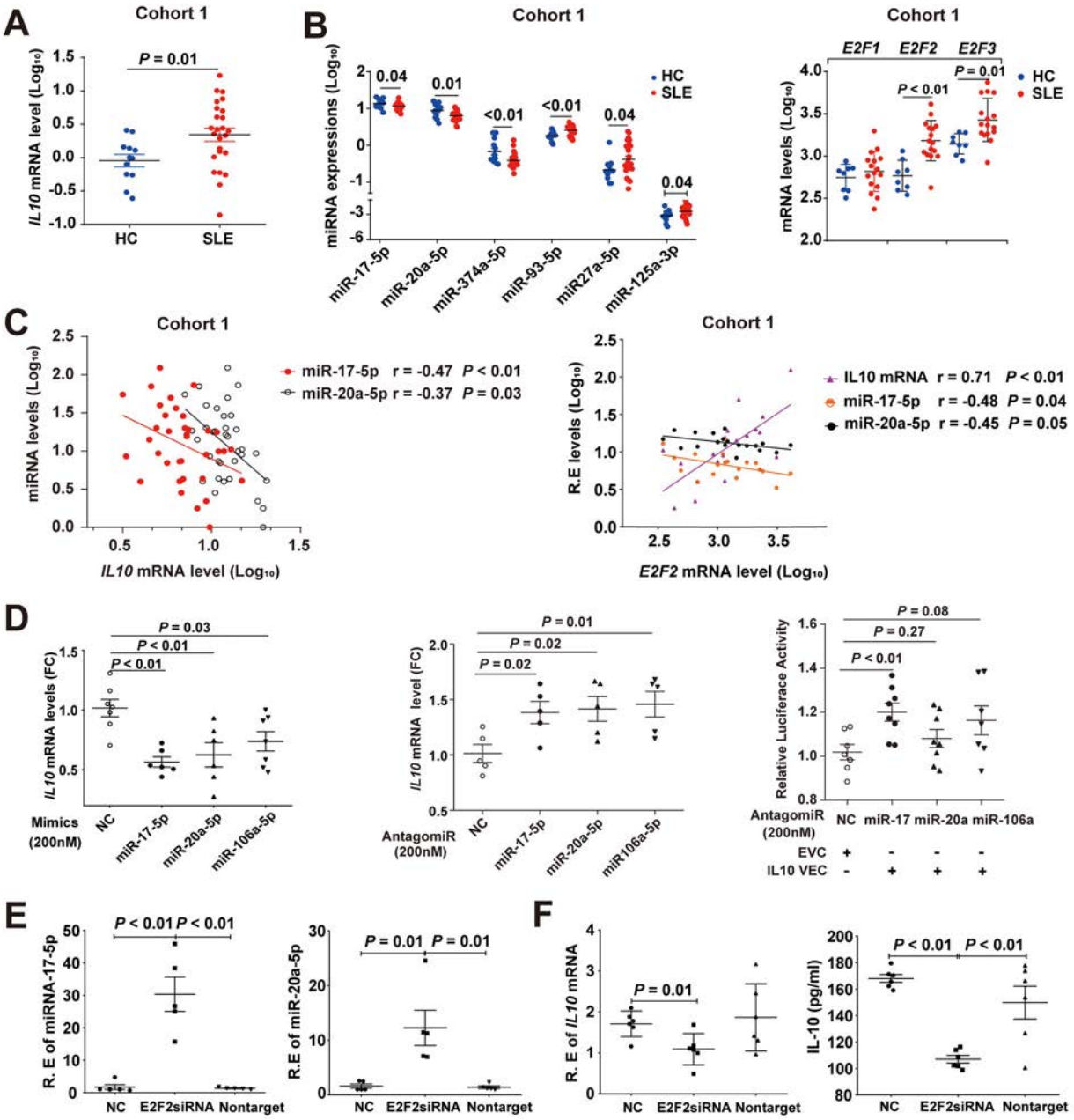

Figure 4. Dysregulated E2F transcription factor 2 (E2F2)–microRNA 17-5-p (miR-17-5p) autoregulatory loop contributes to overproduction of IL-10 in SLE B cells. **A**, Relative levels of *IL10* mRNA in healthy controls and SLE patients in cohort 1. **B**, Differential expression of candidate IL-10 3′-untranslated region (3′-UTR)–targeting miRNAs and E2F family members in SLE B cells compared to healthy control B cells in cohort 1. **C**, Correlations of *IL10* mRNA levels with miR-17-5p and miR-20a-5p levels, and correlations of *E2F2* mRNA levels with *IL10* mRNA, miR-17-5p, and miR-20a-5p levels in B cells from healthy controls and SLE patients in cohort 1. **D**, Modulation of endogenous *IL10* mRNA levels in the lymphoblastoid-like Raji cell line by transfection of microRNA mimics or antagomirs, and luciferase reporter gene activity driven by the 3′-UTR region of IL-10 in nontransfected Raji cells and Raji cells that were transfected with antagomirs. **E**, Up-regulation of miR-17-5p and miR-20a-5p by suppression of E2F2 transcription in Raji cells. **F**, Decreased mRNA and protein levels of *IL10* in Raji cells transfected with E2F2 small interfering RNA (siRNA). In **A**, **B**, and **D**–**F**, symbols represent individual subjects; horizontal lines and error bars show the mean ± SEM. *P* values were determined by Mann–Whitney U test. RE = relative expression; FC = fold change; NC = negative control; EVC = empty vector control; IL-10 VEC = psiCHECK-2 vector containing a 1-kb segment of the IL-10 3′-UTR region (see Figure 1 for other definitions). Color figure can be viewed in the online issue, which is available at http://onlinelibrary.wiley.com/doi/10.1002/art.41987.

Given that miRNAs usually negatively regulate the gene expression of their targeted mRNAs (22,23), we focused on 3 miRNAs (miR-17-5p, miR-20a-5p, and miR-374-5p) with significantly decreased levels in SLE B cells, and found that levels of miR-17-5p and miR-20a-5p inversely correlated with levels of *IL10* mRNA (Figures 4B and C). Both miR-17-5p and miR-20a-5p were

predicted to bind to the position 639–646 at the 3′-UTR of *IL10* mRNA. In addition, miR-106a-5p was previously reported to down-regulate *IL10* mRNA levels in the Raji cell line (Supplementary Figure 5) (24,25). We further transfected either mimics or antagomirs of miR-17-5p, miR-20a-5p, and miR-106a-5p into Raji cells to explore their effects on regulating *IL10* mRNA levels. Transfection with mimics of miR-17-5p, miR-20a-5p, or miR-106a-5p resulted in significant repression of endogenous *IL10* mRNA levels in Raji cells, while transfection with their respective antagomirs augmented *IL10* mRNA levels (Figure 4D). Next, we performed luciferase reporter assays to test if these 3 miRNAs could directly target the 3′-UTR region of *IL10*. Only transfection with the miR-17-5p antagomir showed significantly up-regulated luciferase activity (Figure 4D).

Both miR-17-5p and miR-20a-5p are members of the miR-17–92 cluster, the promoter of which contains binding sites of the E2F family of transcription factors to regulate its transcription, and miR-17 and miR-20 directly inhibit translation of *E2F1, E2F2*, and *E2F3*, forming an autoregulatory loop (26). To explore the role of the E2F family in regulating levels of miR-17-5p and miR-20a-5p that in turn indirectly modulate levels of *IL10* mRNA, we performed real-time qRT-PCR and showed elevated levels of *E2F2* and *E2F3* in B cells from SLE patients, compared with those from healthy controls, in cohort 1 (Figure 4B). Because *E2F2* levels were significantly higher in SLE B cells than in healthy control B cells, we explored the relationship of *E2F2* levels with levels of *IL10* and miRNAs of interest in B cells from cohort 1. We observed negative correlations between levels of *E2F2* and levels of either miR-17-5p or miR-20a-5p, and a positive correlation between levels of *E2F2* and levels of *IL10* transcripts (Figure 4C).

To assess if these correlations could have a cause-and-effect relationship in vivo, we used Raji cells as a model to study the effects of silencing *E2F2* expression by siRNA on levels of *IL10*, miR-17-5p, and miR-20a-5p. The expression of *E2F2* decreased by 43% in Raji cells treated with *E2F2* siRNA (Supplementary Figure 6). The administration of *E2F2* siRNA resulted in significantly increased levels of miR-17-5p and miR-20a-5p (Figure 4E) and decreased *IL10* at both the mRNA and protein levels (Figure 4F). These findings support the notion that the dysregulated *E2F2*-miR-17-5p autoregulatory loop could contribute to overproduction of IL-10 in SLE B cells.

DISCUSSION

The immunoregulatory IL-10 appears to paradoxically play a pathogenic role in SLE, presumably due to its effects on promoting the growth and differentiation of autoreactive B cells. However, the cellular source of pathogenic IL-10 and cellular targets in SLE are not entirely clear. Given that IL-10–producing Breg cells cannot be identified directly ex vivo, stimulation with IFNα and CpG, which induced IL-10+CD24^{high}CD38^{high} Breg cells in healthy controls, resulted in expansion of IL-10+IgD−CD27− DN B cells in SLE patients, especially in the IL-10+ DN2 B cell subset.

Compared to age-, sex-, and ancestry-matched controls, SLE patients exhibited increased proportions of IL-10+ DN2 cells, which correlated with disease activity and autoantibody levels. Intriguingly, an important feature of IL-10+ DN2 B cells was their strong correlation with the Th10 cell subset, which is distinct from follicular helper T (Tfh) cells and helps B cells by providing IL-10. We showed that proportions of the IL-10+ DN2 subset, which represents a minor fraction of SLE DN2 B cells, but not the IL-10− DN2 subset, strongly correlated with levels of autoantibodies and disease activity scores in SLE patients of mainly African American ancestry, and confirmed these findings independently in a cohort of Asian SLE patients. These findings support the notion of the involvement of IL-10 in the pathogenesis of lupus in patients from different genetic backgrounds and geographic locations.

A major characteristic of SLE is an autoreactive B cell compartment that is periodically reactivated, leading to the generation of new bursts of pathogenic antibody-secreting cells. While IgD−CD27− DN B cells have recently been shown to represent a small fraction of B cells in healthy individuals, this population is markedly expanded in patients with active SLE. The DN B cell subset, a TLR-7–induced B cell effector population derived from activated naive cells, is poised to differentiate into antibody-secreting cells in patients with active SLE. Most prominently, SLE DN2 cells display hyperresponsiveness to a number of stimuli known to contribute to SLE pathogenesis, including TLR-7, IL-21, and IL-10, and develop through extrafollicular reactions, leading to the generation of autoantibody-producing plasmablasts (10,27). It is generally considered that IL-10R signaling in B cells and/or plasmablasts is key to its pathogenic effects, which is consistent with the capacity of IL-10 to induce survival, proliferation, and differentiation of B cells in vitro. Elevated IL-10Ra expression was observed in both DN2 and IL-10+ DN2 B cells, supporting the notion that the autocrine function of these IL-10–producing B cells makes them well poised to become autoantibody-generating plasmablasts. Furthermore, the IL-10+ DN2 cell subset had elevated levels of CD95, CXCR3, and T-bet, consistent with previous findings in autoantibody-secreting B cell subsets in SLE (10,17,18).

While Tfh cells are the most potent B helper T cells, there is increasing evidence that autoreactive T cell–B cell interactions in SLE also occur outside of germinal centers of secondary lymphoid organs. Recently, extrafollicular B helper T cells have been identified, including PD-1^{high}CXCR5− peripheral helper T (Tph) cells and Th10 cells, and they are drivers of autoantibody production in a mouse model of lupus and in SLE patients (9,28). T cell–B cell interactions occur within the interstitium of kidneys in lupus nephritis patients, and these interactions may drive B cell differentiation into plasma cells within the kidney (29,30). While Tph cells provide help to B cells via IL-21 and *MAF*, Th10 cells promote B cell antibody responses in an IL-10– and succinate-dependent manner (9).

Through in vitro coculture studies, we observed a critical role for IL-10 in the function of Th10 cells from SLE patients. Th10 cells from SLE patients mainly express IL-10, as well as IL-21, and their ability to induce B cells to secrete IgG in vitro depends on IL-10 and succinate. Moreover, a large fraction of IL-10+CD3+ T cells appeared in close proximity to CD20+ B cells in class IV biopsy specimens from lupus nephritis patients, suggesting that B/T cells and IL-10 are prominent features of proliferative lupus nephritis infiltrates (9). In our study, the Th10 cell frequency in SLE PBMCs was strongly correlated with 24-hour proteinuria in cohort 2, implicating a role of Th10 in kidney damage. While proportions of IL-10+ DN2 B cells correlated with levels of antibodies to dsDNA and associated with levels of multiple autoantibodies, Th10 cell frequencies correlated with ANA titers and proteinuria levels in SLE patients, suggesting the pathogenic nature of these 2 cell subsets and the important role of IL-10 in extrafollicular autoimmune responses in SLE.

MicroRNAs are well-known to fine-tune cellular gene expression to control immune cell development and regulate adaptive and innate immune responses. We initiated a search for miRNAs that could down-regulate IL-10 levels in SLE B cells with the notion that specific miRNAs might be used as therapeutic agents. We observed that decreased levels of miR-17-5p and miR-20a correlated with levels of IL-10 overproduction in SLE B cells. These 2 miRNAs are in the polycistronic miR-17–92 family that regulates the cell cycle by inhibiting the E2F transcription factor for a cell to be committed to active cellular proliferation and has known immune functions to govern T helper cell differentiation, including to promote Tfh cell differentiation (31,32).

In addition to our observation that elevated levels of E2F2 upregulated IL-10 in B cells, *E2F2* was one of the top 10 highly expressed genes in IL-10+ enriched $CD24^{high}CD38^{high}$ transitional B cells compared to naive B cells (33). *E2F1* and *E2F2* were also the top differentially expressed genes in the Th10 cell subset, identified by gene ontology analysis (9). Another family member, *E2F7*, was prominently expressed in the SLE DN2 B cell subset (10). MicroRNAs associated with the miR-17–92 cluster are crucial regulators of the mammalian cell cycle, as they inhibit transcription factors related to the E2F family that tightly control decision-making events for a cell to be committed to active cellular proliferation.

Limitations of the present study include the following. First, given that the Th10 cell subset partly shares surface markers with the Tph cell subset, the Th10 cell subset in our study may have overlapped with Tph cells, which also play a pathogenic role in SLE through the extrafollicular pathway. Second, given that the IL-10+ DN2 and Th10 cell subsets each requires a number of fluorescent antibodies for their identification, we could not study their colocalization readily using biopsy specimens from lupus nephritis patients to obtain direct evidence of the interaction between them in the pathogenesis of lupus nephritis.

Our findings demonstrate a prominent role for IL-10+ DN2 B cells in the generation of SLE autoantibodies in 2 independent cohorts with different ethnic backgrounds and from 2 different continents, which also provides insight into the molecular underpinnings of abnormal IL-10 production in B cells, an E2F2–miR-17-5p/20a-5p autoregulatory feedback loop. These findings offer new insights into the mechanisms and regulatory networks of *IL10* expression, which could be a candidate pathway to develop strategies to modulate expansion of the extrafollicular pathway in active SLE.

ACKNOWLEDGMENTS

We thank the participants of this study and appreciate the help in subject recruitment provided by the National Institute of Arthritis and Musculoskeletal and Skin Diseases.

AUTHOR CONTRIBUTIONS

All authors were involved in drafting the article or revising it critically for important intellectual content, and all authors approved the final version to be published. Dr. Tsao had full access to all of the data in the study and takes responsibility for the integrity of the data and the accuracy of the data analysis.

Study conception and design. Xu, Deng, Tsao.
Acquisition of data. Oates, Kamen, Gilkeson, F. Wang, Zhang, Tan.
Analysis and interpretation of data. Xu, L. Wang, Shi, Deng.

REFERENCES

1. Diefenhardt P, Nosko A, Kluger MA, Richter JV, Wegscheid C, Kobayashi Y, et al. IL-10 receptor signaling empowers regulatory T cells to control Th17 responses and protect from GN. J Am Soc Nephrol 2018;29:1825–37.
2. Park Y, Lee S, Kim D, Lee J, Lee C, Song C. Elevated interleukin-10 levels correlated with disease activity in systemic lupus erythematosus. Clin Exp Rheumatol 1998;16:283–8.
3. Sakurai D, Zhao J, Deng Y, Kelly JA, Brown EE, Harley JB, et al. Preferential binding to Elk-1 by SLE-associated IL10 risk allele upregulates IL10 expression. PLoS Genet 2013;9:e1003870.
4. Hedrich CM, Rauen T, Apostolidis SA, Grammatikos AP, Rodriguez NR, Ioannidis C, et al. Stat3 promotes IL-10 expression in lupus T cells through trans-activation and chromatin remodeling. Proc Natl Acad Sci USA 2014;111:13457–62.
5. Mauri C, Blair PA. Regulatory B cells in autoimmunity: developments and controversies. Nat Rev Rheumatol 2010;6:636.
6. Tedder TF. B10 cells: a functionally defined regulatory B cell subset. J Immunol 2015;194:1395–401.
7. Menon M, Blair PA, Isenberg DA, Mauri C. A regulatory feedback between plasmacytoid dendritic cells and regulatory B cells is aberrant in systemic lupus erythematosus. Immunity 2016;44:683–97.
8. Blair PA, Noreña LY, Flores-Borja F, Rawlings DJ, Isenberg DA, Ehrenstein MR, et al. CD19+ CD24hiCD38hi B cells exhibit regulatory capacity in healthy individuals but are functionally impaired in systemic lupus erythematosus patients. immunity. 2010;32:129–40.
9. Caielli S, Veiga DT, Balasubramanian P, Athale S, Domic B, Murat E, et al. A CD4+ T cell population expanded in lupus blood provides B cell help through interleukin-10 and succinate. Nat Med 2019;25: 75–81.
10. Jenks SA, Cashman KS, Zumaquero E, Marigorta UM, Patel AV, Wang X, et al. Distinct effector B cells induced by unregulated Toll-like receptor 7 contribute to pathogenic responses in systemic lupus erythematosus. Immunity 2018;49:725–39. e6.

11. Jenks SA, Cashman KS, Woodruff MC, Lee FEH, Sanz I. Extrafollicular responses in humans and SLE. Immunol Rev 2019;288:136–48.
12. Scharer CD, Blalock EL, Mi T, Barwick BG, Jenks SA, Deguchi T, et al. Epigenetic programming underpins B cell dysfunction in human SLE. Nat Immunol 2019;20:1071–82.
13. Hochberg MC, for the Diagnostic and Therapeutic Criteria Committee of the American College of Rheumatology. Updating the American College of Rheumatology revised criteria for the classification of systemic lupus erythematosus [letter]. Arthritis Rheum 1997;40:1725.
14. Mikdashi J, Nived O. Measuring disease activity in adults with systemic lupus erythematosus: the challenges of administrative burden and responsiveness to patient concerns in clinical research. Arthritis Res Ther 2015;17:183.
15. Verthelyi D, Zeuner RA. Differential signaling by CpG DNA in DCs and B cells: not just TLR9. Trends Immunol 2003;24:519–22.
16. Heine G, Drozdenko G, Grün JR, Chang HD, Radbruch A, Worm M. Autocrine IL-10 promotes human B-cell differentiation into IgM-or IgG-secreting plasmablasts. Eur J Immunol 2014;44:1615–21.
17. Manni M, Gupta S, Ricker E, Chinenov Y, Park SH, Shi M, et al. Regulation of age-associated B cells by IRF5 in systemic autoimmunity. Nat Immunol 2018;19:407–19.
18. Wu C, Fu Q, Guo Q, Chen S, Goswami S, Sun S, et al. Lupus-associated atypical memory B cells are mTORC1-hyperactivated and functionally dysregulated. Ann Rheum Dis 2019;78:1090–100.
19. Maziere P, Enright AJ. Prediction of microRNA targets. Drug Discov Today 2007;12:452–8.
20. Sethupathy P, Megraw M, Hatzigeorgiou AG. A guide through present computational approaches for the identification of mammalian microRNA targets. Nat Methods 2006;3:881–6.
21. Watanabe Y, Tomita M, Kanai A. Computational methods for microRNA target prediction. Methods Enzymol 2007;427:65–86.
22. Carissimi C, Fulci V, Macino G. MicroRNAs: novel regulators of immunity. Autoimmun Rev 2009;8:520–4.
23. Bagga S, Bracht J, Hunter S, Massirer K, Holtz J, Eachus R, et al. Regulation by let-7 and lin-4 miRNAs results in target mRNA degradation. Cell 2005;122:553–63.
24. Sharma A, Kumar M, Aich J, Hariharan M, Brahmachari SK, Agrawal A, et al. Posttranscriptional regulation of interleukin-10 expression by hsa-miR-106a. Proc Natl Acad Sci U S A 2009;106:5761–6.
25. Sanctuary MR, Huang RH, Jones AA, Luck ME, Aherne CM, Jedlicka P, et al. miR-106a deficiency attenuates inflammation in murine IBD models. Mucosal Immunol 2019;12:200–11.
26. Concepcion CP, Bonetti C, Ventura A. The miR-17-92 family of microRNA clusters in development and disease. Cancer J 2012;18:262.
27. Wei C, Anolik J, Cappione A, Zheng B, Pugh-Bernard A, Brooks J, et al. A new population of cells lacking expression of CD27 represents a notable component of the B cell memory compartment in systemic lupus erythematosus. J Immunol 2007;178:6624–33.
28. Odegard JM, Marks BR, DiPlacido LD, Poholek AC, Kono DH, Dong C, et al. ICOS-dependent extrafollicular helper T cells elicit IgG production via IL-21 in systemic autoimmunity. J Exp Med 2008; 205:2873–86.
29. Chang A, Henderson SG, Brandt D, Liu N, Guttikonda R, Hsieh C, et al. In situ B cell-mediated immune responses and tubulointerstitial inflammation in human lupus nephritis. J Immunol 2011;186: 1849–60.
30. Liarski VM, Kaverina N, Chang A, Brandt D, Yanez D, Talasnik L, et al. Cell distance mapping identifies functional T follicular helper cells in inflamed human renal tissue. Sci Transl Med 2014;6:230ra46-ra46.
31. Baumjohann D, Kageyama R, Clingan JM, Morar MM, Patel S, De Kouchkovsky D, et al. The microRNA cluster miR-17∼ 92 promotes T FH cell differentiation and represses subset-inappropriate gene expression. Nat Immunol 2013;14:840.
32. Bai X, Hua S, Zhang J, Xu S. The MicroRNA family both in normal development and in different diseases: the miR-17-92 cluster. Biomed Res Int 2019;2019.
33. Bigot J, Pilon C, Matignon M, Grondin C, Leibler C, Aissat A, et al. Transcriptomic signature of the CD 24hi CD 38hi transitional B cells associated with an immunoregulatory phenotype in renal transplant recipients. Am J Transplant 2016;16:3430–42.

American College of Rheumatology
Empowering Rheumatology Professionals

Arthritis & Rheumatology
Vol. 74, No. 3, March 2022, pp 508–517
DOI 10.1002/art.41964

Performance of the 2017 European Alliance of Associations for Rheumatology/American College of Rheumatology Classification Criteria for Idiopathic Inflammatory Myopathies in Patients With Myositis-Specific Autoantibodies

Maria Casal-Dominguez,[1] Iago Pinal-Fernandez,[2] Katherine Pak,[3] Wilson Huang,[3] Albert Selva-O'Callaghan,[4] Jemima Albayda,[5] Livia Casciola-Rosen,[5] Julie J. Paik,[5] Eleni Tiniakou,[5] Christopher A. Mecoli,[5] Thomas E. Lloyd,[5] Sonye K. Danoff,[5] Lisa Christopher-Stine,[5] and Andrew L. Mammen[1]

Objective. We undertook this study to 1) determine the sensitivity of the European Alliance of Associations for Rheumatology (EULAR)/American College of Rheumatology (ACR) classification criteria for idiopathic inflammatory myopathies (IIMs) to properly classify myositis-specific autoantibody (MSA)–positive myositis patients, 2) describe the phenotype and muscle involvement over time in different MSA-positive patients, and 3) compare MSA subgroups to EULAR/ACR criteria–defined myositis subgroups for their capacity to predict clinical phenotypes in patients with IIMs.

Methods. The study included 524 MSA-positive myositis patients from the Johns Hopkins Myositis Center. Each patient was classified using the EULAR/ACR classification criteria. Patient phenotypes were summarized using factor analysis of mixed data (FAMD). We compared the ability of MSAs to that of the EULAR/ACR classification subgroups to predict the phenotype of patients by applying the Akaike information criterion (AIC) and the Bayesian information criteria (BIC) to the linear regression models.

Results. Overall, 91% of MSA-positive patients met the EULAR/ACR criteria to be classified as having myositis. However, 20% of patients with anti–hydroxymethylglutaryl-coenzyme A reductase (anti-HMGCR) and 50% of patients with anti–PL-7 were incorrectly classified as not having myositis. Furthermore, ~10% of patients with anti–signal recognition particle (anti-SRP) and patients with anti-HMGCR were misclassified as having inclusion body myositis. FAMD demonstrated that patients within each MSA-defined subgroup had similar phenotypes. Application of both the AIC and BIC to the linear regression models revealed that MSAs were better predictors of myositis phenotypes than the subgroups defined by the EULAR/ACR criteria.

Conclusion. Although the EULAR/ACR criteria successfully classified 91% of MSA-positive myositis patients, certain MSA-defined subgroups, including those with autoantibodies against HMGCR, SRP, and PL-7, are frequently misclassified. In myositis patients with MSAs, autoantibodies outperform the EULAR/ACR-defined myositis subgroups in predicting the clinical phenotypes of patients. These findings underscore the need to include MSAs in a revised myositis classification scheme.

Supported by the Intramural Research Program of the National Institute of Arthritis and Musculoskeletal and Skin Diseases, NIH (grant AR-041203), Dr. Peter Buck, and the Huayi and Siuling Zhang Discovery Fund. The Rheumatic Diseases Research Core Center, where some of the autoantibodies were assayed, is supported by the NIH (grant P30-AR-070254). Dr. Pinal-Fernandez' work was supported by the Myositis Association. Dr. Tiniakou's work was supported by the Jerome L. Greene Foundation.

[1]Maria Casal-Dominguez, MD, PhD, Andrew L. Mammen, MD, PhD: National Institute of Arthritis and Musculoskeletal and Skin Diseases, NIH, Bethesda, Maryland, and Johns Hopkins University School of Medicine, Baltimore, Maryland; [2]Iago Pinal-Fernandez, MD, PhD: National Institute of Arthritis and Musculoskeletal and Skin Diseases, NIH, Bethesda, Maryland, Johns Hopkins University School of Medicine, Baltimore, Maryland, and Universitat Oberta de Catalunya, Barcelona, Spain; [3]Katherine Pak, MD, Wilson Huang, MD: National Institute of Arthritis and Musculoskeletal and Skin Diseases, NIH, Bethesda, Maryland; [4]Albert Selva-O'Callaghan, MD, PhD: Vall d'Hebron Hospital and Autonomous University of Barcelona, Barcelona, Spain; [5]Jemima Albayda, MD, Livia Casciola-Rosen, PhD, Julie J. Paik, MD, Eleni Tiniakou, MD, Christopher A. Mecoli, MD, MHS, Thomas E. Lloyd, MD, PhD, Sonye K. Danoff, MD, PhD, Lisa Christopher-Stine, MD, MPH: Johns Hopkins University School of Medicine, Baltimore, Maryland.

Drs. Casal-Dominguez and Pinal-Fernandez contributed equally to this work. Drs. Danoff, Christopher-Stine, and Mammen contributed equally to this work.

Author disclosures are available at https://onlinelibrary.wiley.com/action/downloadSupplement?doi=10.1002%2Fart.41964&file=art41964-sup-0001-Disclosureform.pdf.

INTRODUCTION

The idiopathic inflammatory myopathies (IIMs) are a heterogeneous family of diseases affecting not only skeletal muscle, but often the skin, lungs, and/or joints (1). Given their marked heterogeneity, classification criteria are needed to create well-defined, relatively homogeneous cohorts for clinical research (2).

Importantly, myositis-specific autoantibodies (MSAs) are found in ~70% of IIM patients without inclusion body myositis (IBM), are not found in patients with other rheumatic or neuromuscular diseases, and are associated with different types of IIMs (3). Specifically, autoantibodies recognizing Mi-2, transcription intermediary factor 1γ (TIF1γ), NXP-2, and melanoma differentiation–associated protein 5 (MDA-5) are present in the group of IIM patients with the hallmark cutaneous features of dermatomyositis (DM); autoantibodies recognizing the transfer RNA synthetases including Jo-1, PL-7, and PL-12 are found in the group of IIM patients with myositis, interstitial lung disease (ILD), and/or arthritis (i.e., the antisynthetase syndrome); and autoantibodies recognizing signal recognition particle (SRP) or hydroxymethylglutaryl-coenzyme A reductase (HMGCR) are found in the group of patients with skeletal muscle–predominant IIM characterized by necrotizing muscle biopsy specimens (i.e., immune-mediated necrotizing myopathy [IMNM]). Furthermore, accumulating evidence suggests that individual MSAs define phenotypically distinct IIM subgroups.

The 2017 European Alliance of Associations for Rheumatology (EULAR)/American College of Rheumatology (ACR) criteria determine whether patients can be classified as having IIMs based on a set of epidemiologic, clinical, and laboratory variables (4). Adult patients meeting the criteria for IIM are subclassified as having polymyositis (PM)/IMNM, IBM, amyopathic dermatomyositis (ADM), or dermatomyositis (DM), based on additional clinical features. However, among all known MSAs, only anti–Jo-1 autoantibodies are included in the weighted score used to classify patients as having IIM. Furthermore, because serologic tests for MSAs other than anti–Jo-1 were not widely available when they were developed, the EULAR/ACR criteria do not utilize these for IIM subclassification (4).

To date, it remains unclear how accurately the EULAR/ACR criteria classify myositis patients with MSAs or how well MSAs compare to the EULAR/ACR criteria to predict patient phenotypes. Therefore, in this study, we determined the sensitivity of EULAR/ACR criteria to classify MSA-positive myositis patients, analyzed the phenotype and muscle involvement of different MSA-positive patients over time, and compared the ability of MSAs to that of the EULAR/ACR subgroups to predict the phenotype of the patients. Our findings suggest that MSAs should be included in a revised IIM classification scheme.

PATIENTS AND METHODS

Adult myositis patients and sera. Adult patients in whom myositis was suspected enrolled in the Johns Hopkins Myositis Center Longitudinal Cohort study between 2002 and 2018 were included in this study if they were positive for autoantibodies recognizing Mi-2, NXP-2, TIF1γ, MDA-5, Jo-1, PL-7, PL-12, SRP, or HMGCR, according to ≥2 immunologic techniques from among the following: enzyme-linked immunosorbent assay, immunoprecipitation of proteins generated by in vitro transcription and translation, line blotting (EuroLine myositis profile), or immunoprecipitation from ^{35}S-methionine–labeled HeLa cell lysates (5,6). Autoantibody groups with a prevalence of less than 2% (e.g., anti-OJ, anti-EJ) were excluded. Demographic data and clinical and laboratory features were collected prospectively at each visit as previously described (6) (see Supplementary Methods, available on the *Arthritis & Rheumatology* website at https://onlinelibrary.wiley.com/doi/10.1002/art.41964).

To validate the 2017 EULAR/ACR criteria in MSA-negative patients, we used an automated random drawing algorithm to select 500 patients who met the following conditions: 1) were classified as having ADM, DM, IBM, or PM based on the opinion of experts, and 2) were negative for the aforementioned MSAs.

The Muscle Diseases Unit (National Institutes of Health [NIH], Bethesda, MD) and the Vall d'Hebron Hospital (Barcelona, Spain) cohorts of patients were used to validate the proposed diagnostic/classification criteria for the different MSA groups.

According to the 2017 EULAR/ACR criteria, we used a minimum of 55% probability (score of 5.5 without biopsies; 6.7 with biopsies) to classify a patient as having an IIM.

Standard protocol approvals and patient consent. This study was approved by the institutional review boards of Johns Hopkins University, NIH, and Vall d'Hebron Hospital; written informed consent was obtained from each participant.

Statistical analysis. Factor analysis of mixed data (FAMD) (Supplementary Methods) was used to summarize the phenotype of the patients based on sex, race, age at onset, maximum creatine kinase (CK) level, presence of anti–Ro 52 autoantibodies, and the presence or absence during the disease course of muscle weakness, ILD, arthritis, heliotrope or Gottron's rash, calcinosis, Raynaud's phenomenon, mechanic's hands, dysphagia, and

Address correspondence to Iago Pinal-Fernandez, MD, PhD, Muscle Disease Unit, Laboratory of Muscle Stem Cells and Gene Regulation, National Institute of Arthritis and Musculoskeletal and Skin Diseases, NIH, 50 South Drive, Room 1141, Building 50, MSC 8024, Bethesda, MD 20892 (email: iago.pinalfernandez@nih.gov); or to Andrew L. Mammen, MD, PhD, Muscle Disease Unit, Laboratory of Muscle Stem Cells and Gene Regulation, National Institute of Arthritis and Musculoskeletal and Skin Diseases, NIH, 50 South Drive, Room 1141, Building 50, MSC 8024, Bethesda, MD 20892 (email: andrew.mammen@nih.gov).

Submitted for publication February 8, 2021; accepted in revised form August 31, 2021.

Table 1. Epidemiologic and clinical variables in the patients*

	Anti-SRP (n = 44)	Anti-HMGCR (n = 122)	Anti–Mi-2 (n = 59)	Anti–NXP-2 (n = 50)	Anti-TIF1γ (n = 62)	Anti–MDA-5 (n = 28)	Anti–Jo-1 (n = 127)	Anti–PL-7 (n = 12)	Anti–PL-12 (n = 20)	Total (n = 524)
Female sex	31 (70)	73 (60)†	37 (63)	35 (70)	54 (87)†	19 (68)	91 (72)	7 (58)	16 (80)	363 (69)
Race										
White	22 (50)†	91 (75)	38 (64)	38 (76)	55 (89)‡	18 (64)	84 (66)	3 (25)†	5 (25)‡	354 (68)
Black	19 (43)‡	21 (17)	9 (15)	7 (14)	4 (6)†	7 (25)	28 (22)	7 (58)†	15 (75)‡	117 (22)
Other	3 (7)	10 (8)	12 (20)†	5 (10)	3 (5)	3 (11)	15 (12)	2 (17)	0 (0)	53 (10)
Age at onset, mean ± SD years	42.4 ± 14.6†	54.2 ± 13.3‡	48.5 ± 15.1	47.3 ± 16.8	49.0 ± 14.5	44.5 ± 11.0	46.3 ± 12.9	48.8 ± 12.4	43.4 ± 12.5	48.3 ± 14.3
Cancer-associated myositis	2 (5)	5 (4)	6 (10)	5 (10)	7 (11)	1 (4)	1 (1)†	1 (8)	2 (10)	30 (6)
Death during follow-up	1 (2)	4 (3)	2 (3)	2 (4)	4 (6)	1 (4)	8 (6)	2 (17)	4 (20)§	28 (5)
Anti–Ro 52	18 (41)	18 (15)‡	10 (17)‡	8 (16)‡	13 (21)†	10 (36)	104 (82)‡	8 (67)	17 (85)‡	206 (39)
Duration of follow-up, mean ± SD years	4.0 ± 3.1	3.8 ± 3.9	4.2 ± 3.6	3.8 ± 3.4	4.7 ± 3.3	4.7 ± 4.3	4.6 ± 3.9	3.4 ± 3.3	5.8 ± 4.0	4.3 ± 3.7
No. of visits per participant, mean ± SD	11.4 ± 11.8	8.2 ± 7.5§	8.4 ± 6.7	9.2 ± 7.2	9.7 ± 6.4	12.4 ± 7.6§	9.1 ± 6.7	10.1 ± 7.5	13.6 ± 6.5§	9.5 ± 7.6
Treatment										
Glucocorticoids	36 (82)	87 (71)‡	52 (88)	43 (86)	46 (74)§	25 (89)	121 (95)‡	10 (83)	19 (95)	439 (84)
Azathioprine	15 (34)	28 (23)†	16 (27)	13 (26)	13 (21)§	14 (50)	64 (50)‡	5 (42)	14 (70)‡	182 (35)
Methotrexate	26 (59)	61 (50)	34 (58)	30 (60)	34 (55)	7 (25)†	60 (47)	1 (8)†	6 (30)	259 (49)
Mycophenolate	14 (32)	17 (14)‡	10 (32)	15 (30)	27 (44)§	11 (39)	50 (39)§	9 (75)†	5 (25)	167 (32)
IVIG	19 (43)	51 (42)	27 (46)	24 (48)	34 (55)§	9 (32)	47 (37)	3 (25)	7 (35)	221 (42)
Rituximab	22 (50)‡	18 (15)§	11 (19)	7 (14)	10 (16)	5 (18)	28 (22)	4 (33)	6 (30)	111 (21)
EULAR/ACR criteria										
Upper extremity proximal weakness	42 (95)§	116 (95)‡	54 (92)	46 (92)	45 (73)†	18 (64)†	102 (80)	9 (75)	15 (75)	447 (85)
Lower extremity proximal weakness	42 (95)	118 (97)§	58 (98)§	47 (94)	48 (77)‡	20 (71)†	116 (91)	11 (92)	17 (85)	477 (91)
Neck flexor greater than neck extensor weakness	27 (61)§	66 (54)†	24 (41)	32 (64)†	29 (47)	5 (18)†	41 (32)†	2 (17)	4 (20)§	230 (44)
Proximal greater than distal lower extremity weakness	40 (91)†	110 (90)‡	41 (69)	39 (78)	39 (63)§	14 (50)†	80 (63)†	6 (50)	15 (75)	384 (73)
Heliotrope rash	1 (2)‡	5 (4)‡	30 (51)§	28 (56)†	49 (79)‡	22 (79)‡	38 (30)	6 (50)	9 (45)	188 (36)
Gottron's papules	3 (7)‡	5 (4)‡	32 (54)†	22 (44)	48 (77)‡	23 (82)‡	42 (33)	2 (17)	9 (45)	186 (35)
Gottron's sign	2 (5)‡	5 (4)‡	30 (51)†	24 (48)§	43 (69)‡	18 (64)‡	39 (31)	2 (17)	8 (40)	171 (33)
Dysphagia or esophageal dysmotility	23 (52)	53 (43)	31 (53)	34 (68)†	31 (50)	10 (36)	47 (37)§	5 (42)	7 (35)	241 (46)
Elevated muscle enzymes	44 (100)†	122 (100)‡	58 (98)†	46 (92)	34 (55)‡	9 (32)‡	113 (89)	10 (8)	13 (65)§	449 (86)
Muscle biopsy available	26 (59)†	72 (59)‡	27 (46)	25 (50)	14 (23)†	4 (14)†	35 (28)†	2 (17)	3 (15)§	208 (40)
Endomysial infiltration surrounding myofibers¶	2 (8)	17 (24)	10 (37)	1 (4)§	1 (7)	0 (0)	16 (46)‡	0 (0)	0 (0)	47 (23)
Perifascicular atrophy¶	1 (4)‡	2 (3)‡	16 (59)†	15 (60)†	8 (57)	2 (50)	22 (63)‡	1 (50)	0 (0)	67 (32)
Perimysial and/or perivascular infiltration¶	8 (31)§	27 (38)‡	17 (63)	19 (72)§	11 (79)	1 (25)	27 (77)†	1 (50)	1 (33)	111 (53)
Rimmed vacuoles¶	3 (12)	11 (15)§	4 (15)	0 (0)	0 (0)	0 (0)	1 (3)	0 (0)	0 (0)	19 (9)

(Continued)

Table 1. (*Cont'd*)

	Anti-SRP (n = 44)	Anti-HMGCR (n = 122)	Anti–Mi-2 (n = 59)	Anti–NXP-2 (n = 50)	Anti-TIF1γ (n = 62)	Anti–MDA-5 (n = 28)	Anti–Jo-1 (n = 127)	Anti–PL-7 (n = 12)	Anti–PL-12 (n = 20)	Total (n = 524)
Other relevant clinical variables										
ILD	8 (18)§	2 (2)‡	3 (5)‡	3 (6)‡	0 (0)‡	20 (71)‡	99 (78)‡	12 (100)‡	17 (85)‡	164 (31)
Arthritis	3 (7)‡	7 (6)‡	12 (20)	7 (14)§	6 (10)‡	20 (71)‡	77 (61)‡	4 (33)	13 (65)‡	149 (28)
DM-specific skin involvement	4 (9)‡	10 (8)‡	54 (92)‡	43 (86)‡	62 (100)‡	28 (100)‡	71 (56)	6 (50)	14 (70)	292 (56)
Calcinosis	0 (0)†	1 (1)‡	5 (8)	18 (36)‡	8 (13)	13 (46)‡	12 (9)	0 (0)	0 (0)	57 (11)
Raynaud's phenomenon	17 (39)§	9 (7)‡	18 (31)	5 (10)†	12 (19)	15 (54)‡	46 (36)†	4 (33)	6 (30)	132 (25)
Mechanic's hands	2 (5)‡	5 (4)‡	13 (22)	6 (12)†	16 (26)	21 (75)‡	67 (53)‡	8 (67)†	15 (75)‡	153 (29)
Fever	4 (9)	8 (7)†	4 (7)	9 (18)	6 (10)	13 (46)‡	24 (19)	2 (17)	10 (50)‡	80 (15)

* Except where indicated otherwise, values are the number (%) of patients. Anti-SRP = anti–signal recognition particle; anti-HMGCR = anti–hydroxymethylglutaryl-coenzyme A reductase; anti-TIF1γ = anti–transcription intermediary factor 1γ; anti–MDA-5 = anti–melanoma differentiation–associated protein 5; IVIG = intravenous immunoglobulin; EULAR = European Alliance of Associations for Rheumatology; ACR = American College of Rheumatology; ILD = interstitial lung disease; DM = dermatomyositis.
† $P < 0.01$ versus the other subgroups, by chi-square or Fisher's exact test.
‡ $P < 0.001$ versus the other subgroups, by chi-square or Fisher's exact test.
§ $P < 0.05$ versus the other subgroups, by chi-square or Fisher's exact test.
¶ Percentage is based on the number of patients for whom muscle biopsy specimens were available in each subgroup.

fevers. All factors explaining >10% of the variance were retained for further analysis.

We compared the ability of MSA autoantibodies and EULAR/ACR subgroups to predict the resulting phenotypes using the Akaike information criterion (AIC) (7) and the Bayesian information criterion (BIC) of the linear regression (8) (Supplementary Methods, https://onlinelibrary.wiley.com/doi/10.1002/art.41964). Both the AIC and BIC are measures of the quality of a statistical model; the lower the AIC or the BIC, the better the variables predict the dependent variable (the factor analysis–derived phenotype in this case). As a guideline, a model with an AIC (9) or BIC (10) that is 10 points lower definitively fits the data better. Of note, both AIC and BIC penalize the number of parameters (it is harder to get low values with more parameters) and, in this analysis, there were more categories in the autoantibodies than in the EULAR/ACR subgroup classification.

Dichotomous variables are expressed as absolute frequencies and percentages, and continuous variables are reported as the mean ± SD. Lowess was used to study the evolution of the muscle strength and CK levels among autoantibody subgroups over time (Supplementary Methods). Comparisons between groups were made using chi-square test, Fisher's exact test, or Student's *t*-test. FactoMineR version 2.1 was used to compute the FAMD, and Stata 14 MP was used to perform the univariate, graphical, and regression analyses. A 2-sided *P* value less than 0.05 was considered significant with no correction for multiple comparisons.

RESULTS

Demographic data and clinical characteristics of MSA-positive IIM patients. Of the 2,475 patients consecutively evaluated at the Johns Hopkins Myositis Center, the present study included 524 myositis patients who were positive for a single MSA based on ≥2 separate techniques. Among these, 24% of patients had anti–Jo-1 autoantibodies (n = 127), 23% had anti-HMGCR autoantibodies (n = 122), 12% had anti-TIF1γ autoantibodies (n = 62), 11% had anti–Mi-2 autoantibodies (n = 59), 10% had anti–NXP-2 autoantibodies (n = 50), 8% had anti-SRP autoantibodies (n = 44), 5% had anti–MDA-5 autoantibodies (n = 28), 4% had anti–PL-12 autoantibodies (n = 20), and 2% had anti–PL-7 autoantibodies (n = 12).

The demographic and clinical features of these patients are provided in Table 1. Of note, the phenotypes associated with each MSA are consistent with prior reports. Thus, patients with autoantibodies against SRP and HMGCR uniformly experienced weakness and rarely had arthritis, skin involvement, or ILD (11,12). Among patients with autoantibodies against Mi-2, NXP-2, TIF1γ, and MDA-5, almost all had DM-specific skin rashes, most experienced weakness, and the presence of ILD and/or arthritis was uncommon except among those with anti–MDA-5 autoantibodies (13–16). Finally, the majority of patients with an antisynthetase autoantibody had weakness, ILD, skin involvement, and/or arthritis (6).

The 2017 EULAR/ACR criteria accurately classified 91% of MSA-positive myositis patients as having IIM but frequently misclassified those with autoantibodies recognizing HMGCR, SRP, and PL-7. First, we explored how accurately IIM patients with each MSA were classified by the 2017 EULAR/ACR criteria (Table 2 and Supplementary Tables 1–9, https://onlinelibrary.wiley.com/doi/10.1002/art.41964). Overall, among MSA-positive IIM patients, 91% were correctly classified by the 2017 EULAR/ACR criteria as having an IIM; 51%, 33%, and 4% were classified as having DM, PM/IMNM, and amyopathic DM, respectively. Surprisingly, 19 of 524 MSA-positive IIM patients (4%) were classified by the 2017 EULAR/ACR criteria as having IBM even though they all had MSAs, which are not found in IBM (Table 2). Patients misclassified as having IBM were severely affected patients with anti-HMGCR or anti-SRP autoantibodies who either had finger flexor weakness or whose disease was refractory to treatment (4 anti-HMGCR–positive and 1 anti-SRP–positive), and/or those who had muscle biopsy results with rimmed vacuoles (11 anti-HMGCR–positive and 3 anti-SRP–positive), which is characteristic of IBM but can also occur in other myopathic conditions (17). Anti-HMGCR–positive and anti-SRP–positive patients misclassified as having IBM did not have any other features suggesting the diagnosis of IBM, such as asymmetric muscle weakness, finger flexor weakness out of proportion to arm abductor weakness, or invasion of non-necrotic fibers by lymphocytes.

Overall, the 2017 EULAR/ACR criteria misclassified 9% of MSA-positive IIM patients as having "non-myositis." This included 20% of the anti-HMGCR–positive patients and 9% of the anti-SRP–positive patients, all of whom also had proximal muscle weakness and/or elevated CK levels that, along with the autoantibodies, define this disease (Table 2). Additionally, 11% of the anti–MDA-5–positive patients, 10% of the anti–PL-12–positive patients, and 50% of the anti–PL-7–positive patients failed to meet the 2017 EULAR/ACR classification criteria for IIM (Table 2). Patients positive for anti-HMGCR or anti-SRP who were classified as not having myositis had high levels of CK (100%), proximal muscle weakness (83%), and a necrotizing muscle biopsy (93%). Those positive for anti–PL-12 or anti–PL-7 who failed to be classified as having myositis had prominent ILD (100%) and frequent proximal weakness (75%). Finally, anti–MDA-5–positive patients not meeting the 2017 EULAR/ACR criteria all had either heliotrope, Gottron's sign, or papules, and they were predominantly amyopathic (66%).

Among anti–Jo-1–positive patients, the 2017 EULAR/ACR criteria classified 55% as having DM and 43% as having PM/IMNM. Notably, there were no significant differences in the proportion of patients with ILD, muscle weakness, arthritis, calcinosis, or Raynaud's phenomenon, or in the median proximal muscle strength or CK levels between those anti–Jo-1–positive patients classified as having DM and those classified as having PM. Also, anti-HMGCR patients who did not fulfill the 2017 EULAR/ACR criteria and those classified as having PM/IMNM had

Table 2. 2017 EULAR/ACR criteria for idiopathic inflammatory myopathies in autoantibody-positive adult myositis patients*

	Anti-SRP (n = 44)	Anti-HMGCR (n = 122)	Anti–Mi-2 (n = 59)	Anti–NXP-2 (n = 50)	Anti-TIF1γ (n = 62)	Anti–MDA-5 (n = 28)	Anti–Jo-1 (n = 127)	Anti–PL-7 (n = 12)	Anti–PL-12 (n = 20)	Total (n = 524)
Autoantibody negative	4 (9)	25 (20)†	3 (5)	2 (4)	1 (2)§	3 (11)	1 (1)†	6 (50)†	2 (10)	47 (9)
Disease subgroup										
PM/IMNM	32 (73)†	74 (61)†	2 (3)†	6 (12)†	0 (0)†	0 (0)†	54 (43)‡	0 (0)§	4 (20)	172 (33)
IBM	4 (9)	13 (11)†	1 (2)	0 (0)	0 (0)	0 (0)	1 (1)	0 (0)	0 (0)	19 (4)
ADM	0 (0)	0 (0)§	0 (0)	1 (2)	11 (18)†	4 (14)§	1 (1)	1 (8)	1 (5)	19 (4)
DM	4 (9)†	10 (8)†	53 (90)†	41 (82)†	50 (81)†	21 (75)‡	70 (55)	5 (42)	13 (65)	267 (51)
JM	0 (0)	0 (0)	0 (0)	0 (0)	0 (0)	0 (0)	0 (0)	0 (0)	0 (0)	0 (0)
JDM	0 (0)	0 (0)	0 (0)	0 (0)	0 (0)	0 (0)	0 (0)	0 (0)	0 (0)	0 (0)

* Values are the number (%) of patients. PM/IMNM = polymyositis/immune-mediated necrotizing myositis; IBM = inclusion body myositis; ADM = amyopathic DM; JM = juvenile myositis other than DM; JDM = juvenile DM (see Table 1 for other definitions).
† $P < 0.001$ versus the other subgroups, by chi-square or Fisher's exact test.
‡ $P < 0.01$ versus the other subgroups, by chi-square or Fisher's exact test.
§ $P < 0.05$ versus the other subgroups, by chi-square or Fisher's exact test.

equivalent strength and CK levels. Similarly, anti-TIF1γ–positive patients classified as having DM and those with ADM had a similar prevalence of arthritis or skin involvement (Supplementary Tables 1–9, https://onlinelibrary.wiley.com/doi/10.1002/art.41964).

Importantly, although the 2017 EULAR/ACR classification scheme requires a muscle biopsy for classification in patients with no skin rash, we applied the same criteria to all patients, regardless of the availability of muscle biopsy data. However, we also repeated the analysis excluding all the patients with no skin rash and no biopsy data available, and all conclusions of our analysis were still reproduced (Supplementary Tables 10–19 and Supplementary Figure 1, https://onlinelibrary.wiley.com/doi/10.1002/art.41964). The availability of muscle biopsy data was <60% in the MSA-positive patients. Patients with very myopathic forms of myositis had more muscle biopsy data available (e.g., anti-SRP, anti-HMGCR) than those with less myopathic forms of myositis (e.g., anti–MDA-5, anti-TIF1γ, anti–PL-7, anti–PL-12).

Distinct patterns of muscle involvement in patients with different MSAs. Overall, muscle weakness with or without CK elevations was present in >90% of the MSA-positive IIM patients and was the most common clinical feature shared between each of the MSA-defined subgroups. To determine whether the severity of weakness and serum CK elevations varied among patients with different MSAs, we analyzed these features over time in each MSA-defined subgroup using locally weighted polynomial regression. This revealed 5 distinct patterns of muscle involvement among patients with different MSAs (Figure 1).

First, patients with autoantibodies against Mi-2 or NXP-2 were initially moderately weak with moderately high CK levels; over time, they recovered strength and their CK levels were normalized. Second, those with autoantibodies against TIF1γ, MDA-5, or PL-12 generally had minimal weakness and normal CK levels throughout the course of the disease. Third, anti–Jo-1–positive patients and anti–PL-7–positive patients tended to present with mild weakness and elevated CK levels, both of which gradually normalized over time. Fourth, anti-HMGCR–positive patients presented with moderate weakness and severely elevated CK levels that improved but did not normalize over time. Fifth, anti-SRP–positive patients presented with the most severe weakness and severely elevated CK levels; even after 3 years of follow-up, these patients continued to experience moderately severe weakness and moderately elevated CK levels.

The same analysis performed on the subgroups defined by the 2017 EULAR/ACR classification criteria did not show apparent differences between patients classified as having PM/IMNM and those classified as having IBM. As expected, DM patients showed more severe muscle weakness and elevated CK levels than ADM patients but less than PM/IMNM and IBM patients (Supplementary Figure 2, https://onlinelibrary.wiley.com/doi/10.1002/art.41964). This graphical analysis suggests that a significant amount of information on relevant myositis subgroups may be lost by using only the 4 adult classification subgroups in the 2017 EULAR/ACR IIM criteria.

MSA-based clustering of IIM patients into phenotypically similar subgroups by FAMD. The above graphical analysis does not allow for a direct quantitative comparison between the autoantibodies and the 2017 EULAR/ACR classification subgroups. Moreover, although the graphical strength analysis suggests that different MSAs are associated with different patterns of muscle disease, it is not possible to compare the full phenotype associated with one MSA to that of another MSA by analyzing the strength, or any other single IIM disease manifestation, in isolation. Therefore, we used FAMD to mathematically summarize the clinical phenotype of each patient. Using this technique, we were able to include both quantitative features (i.e., age at onset, maximum CK level) and qualitative features (i.e., sex, race, and

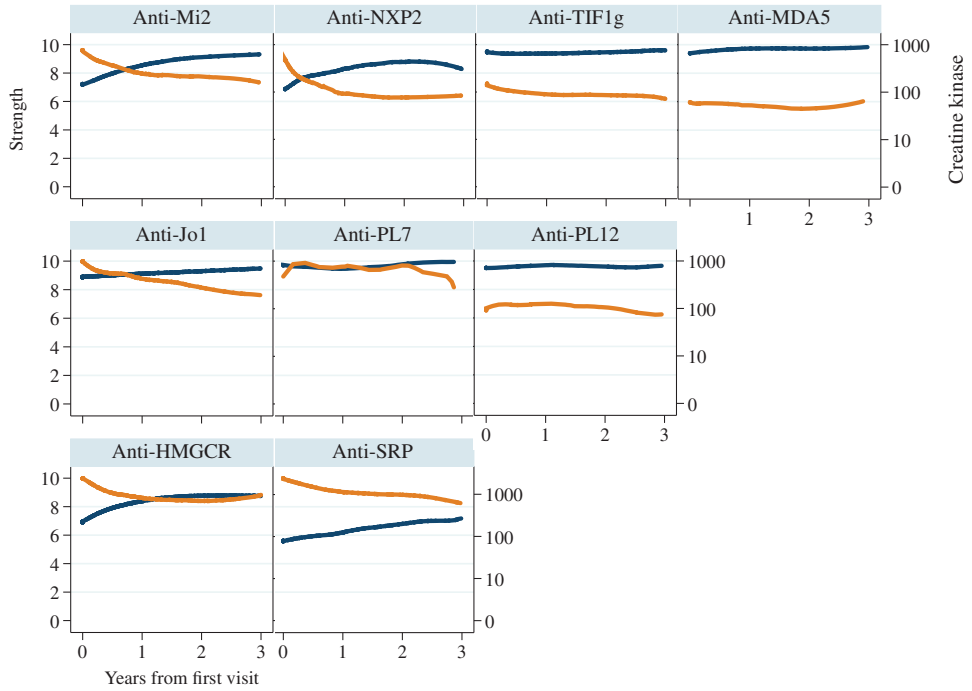

Figure 1. Evolution of muscle strength (blue line) and creatine kinase (orange line) levels over time, using lowess regression in patients with different myositis-specific autoantibodies. Anti-TIF1γ = anti–transcription intermediary factor 1γ; anti–MDA-5 = anti–melanoma differentiation–associated protein 5; anti-HMGCR = anti–hydroxymethylglutaryl-coenzyme A reductase; anti-SRP = anti–signal recognition particle.

presence or absence of weakness, ILD, arthritis, heliotrope or Gottron's rash, calcinosis, Raynaud's phenomenon, mechanic's hands, dysphagia, and fevers) to model the overall phenotype of each IIM patient included in this study.

Two principal component factors accounted for 18% (factor 1) and 11% (factor 2) of the clinical variability among all of the patients. The most heavily weighted factors in the first component (factor 1) were the presence of mechanic's hands, ILD, and arthritis. For factor 2, the most important parameters were maximum CK level, race, and the presence of either heliotrope or Gottron's rashes (Supplementary Figure 3, https://onlinelibrary.wiley.com/doi/10.1002/art.41964). Figure 2 depicts the value of both factors for each patient in 2 dimensions and demonstrates that those with the same MSA tended to cluster, indicating that they share a similar phenotype.

Although there was overlap between the different MSAs, there were unique locations occupied by the 9 different MSAs in the FAMD graphs (Figure 2). Patients with autoantibodies against HMGCR or SRP clustered together in the lower right part of the graph, whereas those with antisynthetase autoantibodies clustered in the upper-middle section of the graph. Patients with autoantibodies against Mi-2, NXP-2, or TIF1γ clustered lower than those with antisynthetase autoantibodies, with an increasing leftward shift observed in the progression of clusters in those with anti–Mi-2 to those with anti–NXP-2 to those with anti-TIF1γ autoantibodies. Anti–MDA-5–positive patients occupied the upper left portion of the graph.

When the factor analysis distribution was performed using the 2017 EULAR/ACR subgroup classifications of the patients, those classified as having PM/IMNM and those with IBM shared a similar region of the graph. Likewise, patients classified as having ADM overlapped with those classified as having DM (Supplementary Figure 4, https://onlinelibrary.wiley.com/doi/10.1002/art.41964). This graphical analysis also suggested that a significant amount of information on relevant myositis subgroups may be lost by using only the 4 adult classification subgroups in the 2017 EULAR/ACR IIM criteria.

MSAs outperformed the 2017 EULAR/ACR IIM classification criteria to predict clinical phenotypes. Both MSAs and the 2017 EULAR/ACR IIM classification subgroups were used to predict the factor analysis–derived phenotypes of the IIM patients using linear regression. In order to compare the relative quality of the models using the autoantibodies and the 2017 EULAR/ACR IIM classification subgroups, we first used the AIC to compare how well each model accounted for factor 1 and factor 2 from the FAMD. Both factor 1 and factor 2 were better modeled by MSAs than by the 2017 EULAR/ACR classification subgroups, with ΔAICs of 439 and 120, respectively. Similarly, using the BIC, MSAs outperformed the 2017 EULAR/ACR classification subgroups in modeling factor 1 and factor 2, with ΔBICs of 421 and 104, respectively (Supplementary Table 20, https://onlinelibrary.wiley.com/doi/10.1002/art.41964).

Taken together, these analyses provide quantitative evidence that MSAs outperform the 2017 EULAR/ACR classification subgroups in predicting the clinical phenotype of IIM patients.

MSAs can be used to build homogeneous autoantibody-based myositis subgroups. Based on our results, we developed a simple set of criteria to classify patients based on the presence of MSAs (Figure 3). In the Johns Hopkins Myositis Center Longitudinal Cohort, this set of criteria had perfect sensitivity (they were positive in all MSA-positive myositis patients in our cohort) and perfect specificity (they were negative in all other patients in the cohort) to identify the autoantibody subgroup (Supplementary Table 21, https://onlinelibrary.wiley.com/doi/10.1002/art.41964).

MSA plus one or more of the following:	1. Muscle weakness 2. Creatine kinase elevation 3. Interstitial lung disease 4. Arthritis 5. Gottron's sign or papules or heliotrope

Figure 3. Example of diagnostic/classification criteria for the different myositis-specific autoantibody (MSA) groups. All MSA-positive patients in this study fulfilled this set of criteria.

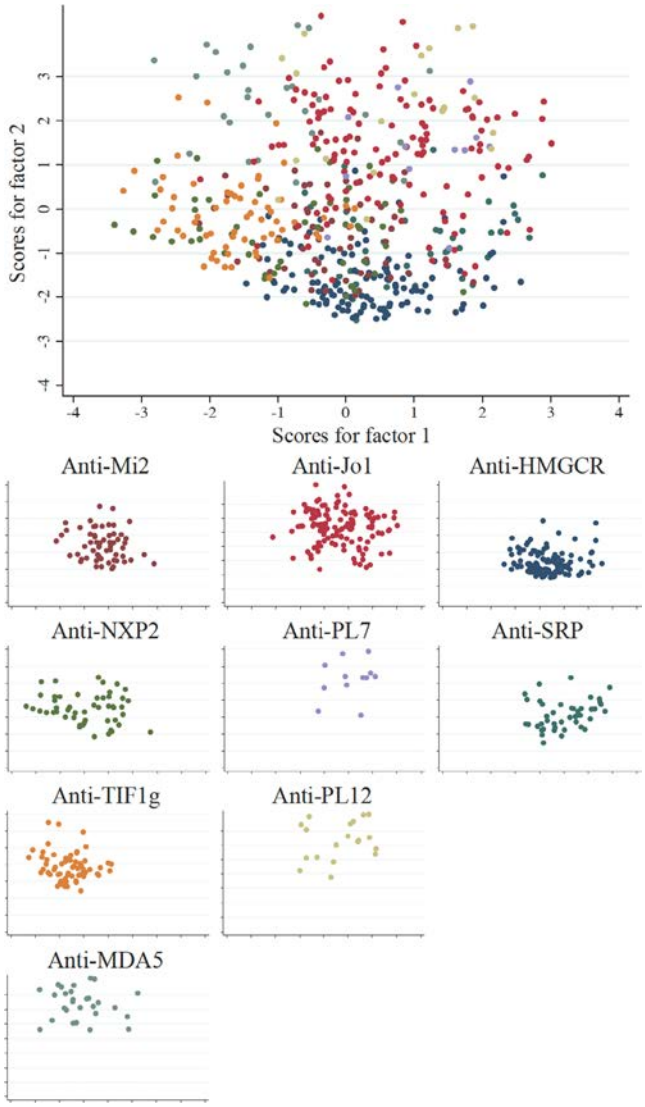

Figure 2. Factor analysis of mixed data summarizing the clinical phenotype of the autoantibody-positive adult myositis patients. The factor analysis of mixed data included the sex, race, age at onset, median and maximum creatine kinase levels, presence of anti–Ro 52 autoantibodies, and presence or absence during the course of the disease of the following: muscle weakness, interstitial lung disease, arthritis, heliotrope or Gottron's rash, calcinosis, Raynaud's phenomenon, mechanic's hands, dysphagia, and fevers. The only 2 factors explaining >10% of the variance (factor 1 and factor 2) were retained for further analysis. See Figure 1 for definitions.

To confirm our results, we externally validated the performance of this criteria in 2 cohorts of patients, 1 from the same demographic background (n = 109; NIH) and another with a different demographic background (n = 342; Vall d'Hebron Hospital). In both cohorts, the proposed criteria (Figure 3) showed perfect sensitivity and specificity to identify MSA-defined myositis subgroups (Supplementary Table 21). Of note, the NIH cohort included 28 patients who either had alternative diagnoses to myositis (e.g., neuropathy or muscle dystrophy) or could not be confidently identified as having myositis at the time of their evaluation according to the opinion of experts. All 28 of these patients were negative for the proposed criteria.

The 2017 EULAR/ACR criteria misclassified a significant proportion of autoantibody-negative patients as having "non-myositis." Among a random sample of 500 MSA-negative patients diagnosed as having myositis by experts, 23% (n = 116) failed to be classified as having myositis according to the 2017 EULAR/ACR criteria (Supplementary Table 22, https://onlinelibrary.wiley.com/doi/10.1002/art.41964). Most of the patients whose condition failed to meet the criteria were originally classified as having PM by the opinion of experts (n = 71). Also, 13% of the patients with IBM (n = 24), 11% of the patients with DM (n = 18), and 16% of the patients with ADM (n = 3) failed to be classified as having myositis (Supplementary Table 22). Of the 46% of PM patients classified as having myositis by the 2017 EULAR/ACR criteria, 48% were classified as having PM/IMNM and the remaining 52% as having IBM (Supplementary Table 22).

DISCUSSION

In this study that included more than 500 MSA-positive IIM patients, we have shown that the 2017 EULAR/ACR IIM classification scheme correctly identifies 91% of MSA-positive patients as having IIM. However, the accuracy of these criteria was not uniform across the different MSAs. Notably, patients with

autoantibodies recognizing HMGCR, SRP, or PL-7 were frequently misclassified as not having myositis. Furthermore, even among those anti-HMGCR–positive patients and anti-SRP–positive patients who were correctly identified as having IIM, ~10% were incorrectly subclassified as having IBM because their disease was refractory to treatment, they had distal weakness, and/or they had muscle biopsies showing vacuolar changes. These findings underscore significant limitations of the 2017 EULAR/ACR criteria for IIMs, which do not utilize MSAs other than anti–Jo-1. Additionally, by applying the 2017 EULAR/ACR criteria to 500 randomly selected MSA-negative myositis patients, we found that 54% of the MSA-negative PM patients failed to be classified as having myositis, and 52% of those who were classified as having myositis were categorized as having IBM.

The utility of autoantibodies to classify patients with myositis into homogeneous groups was first proposed by Love et al in 1991 (18). More recently, working groups at the European Neuromuscular Centre have proposed to classify patients as having IMNM (19) or DM (20) based on the presence of MSAs and clinical features compatible with muscle or skin involvement. To determine whether MSAs have the capacity to predict the phenotype of MSA-positive patients, we first provided graphical evidence that MSAs predict the course of muscle involvement over time. Second, we used FAMD to show that MSAs group individual IIM patients into relatively homogeneous groups. Finally, we sought to compare the use of MSA positivity with that of the 2017 EULAR/ACR criteria to predict the phenotype of MSA-positive myositis patients. Using the AIC and the BIC, 2 closely related analytic tools based on information theory, we demonstrated that the presence of MSAs outperform the 2017 EULAR/ACR criteria. Taken together, findings of these analyses strongly support using MSAs to help subclassify myositis patients into phenotypically homogeneous groups. As an example, we developed a simple set of criteria that had perfect diagnostic performance in our cohort to classify patients in MSA-defined groups (Figure 3). These criteria were externally validated in 2 cohorts of patients, one from the same demographic background and another from a different demographic background, supporting the diagnostic accuracy of this set of criteria to classify patients in autoantibody-defined groups. These criteria could be easily updated as new autoantibodies are discovered.

Although these analyses show only that MSAs predict distinct clinical manifestations (e.g., weakness, rash, arthritis, and ILD), prior studies support the underlying hypothesis that MSAs define unique pathologic states. For example, the concept that each DM-specific MSA defines a unique DM subtype is supported by the observations that patients with different DM-specific MSAs have distinct histologic features on muscle biopsy (21) and different gene expression profiles on transcriptomic analysis (22). Similarly, evidence that anti–Jo-1 autoantibodies define a single syndrome distinct from DM (i.e., antisynthetase syndrome) is supported by our observation that anti–Jo-1–positive patients with and those without rashes have otherwise indistinguishable clinical features including myositis, ILD, and arthritis. This is further supported by the observations that the histologic features of muscle biopsy tissue from anti–Jo-1–positive patients are the same whether they come from a patient with rash or one without a rash (21), and that gene expression profiles from antisynthetase syndrome patients are homogeneous and easily distinguishable from those with DM (22).

In summary, while the 2017 EULAR/ACR classification criteria for IIMs correctly identified and classified most MSA-positive myositis patients, we found that a significant number of patients with anti-SRP or anti-HMGCR autoantibodies were misclassified as either not having myositis or having IBM. We also showed that, when present, MSAs define more homogeneous subgroups than the categories of PM/IMNM, DM, ADM, and IBM defined by the 2017 EULAR/ACR criteria. Furthermore, along with prior studies, our findings here support the idea that antisynthetase syndrome should be considered a distinct entity and that patients with antisynthetase syndrome should not be subclassified into PM or DM subgroups based on the absence or presence of a rash, respectively. Although challenging, we propose that confirming these results in additional myositis cohorts and revising the IIM classification criteria to utilize MSAs should be priorities of the international myositis research community.

ACKNOWLEDGMENTS

This work is dedicated to the memory of Dr. Lori A. Love. The authors are grateful to Dr. Peter Buck, whose generous support made this work possible.

AUTHOR CONTRIBUTIONS

All authors were involved in drafting the article or revising it critically for important intellectual content, and all authors approved the final version to be published. Dr. Mammen had full access to all of the data in the study and takes responsibility for the integrity of the data and the accuracy of the data analysis.

Study conception and design. Casal-Dominguez, Pinal-Fernandez, Mammen.

Acquisition of data. Casal-Dominguez, Pinal-Fernandez, Pak, Huang, Selva-O'Callaghan, Albayda, Casciola-Rosen, Paik, Tiniakou, Mecoli, Lloyd, Danoff, Christopher-Stine, Mammen.

Analysis and interpretation of data. Casal-Dominguez, Pinal-Fernandez, Mammen.

REFERENCES

1. Selva-O'Callaghan A, Pinal-Fernandez I, Trallero-Araguas E, Milisenda JC, Grau-Junyent JM, Mammen AL. Classification and management of adult inflammatory myopathies [review]. Lancet Neurol 2018;17:816–28.
2. Aggarwal R, Ringold S, Khanna D, Neogi T, Johnson SR, Miller A, et al. Distinctions between diagnostic and classification criteria? [review]. Arthritis Care Res (Hoboken) 2015;67:891–7.
3. McHugh NJ, Tansley SL. Autoantibodies in myositis [review]. Nat Rev Rheumatol 2018;14:290–302.
4. Lundberg IE, Tjarnlund A, Bottai M, Werth VP, Pilkington C, de Visser M, et al. 2017 European League Against Rheumatism/American College of Rheumatology classification criteria for adult

and juvenile idiopathic inflammatory myopathies and their major subgroups. Arthritis Rheumatol 2017;69:2271–82.

5. Mammen AL, Chung T, Christopher-Stine L, Rosen P, Rosen A, Doering KR, et al. Autoantibodies against 3-hydroxy-3-methylglutaryl-coenzyme A reductase in patients with statin-associated autoimmune myopathy. Arthritis Rheum 2011;63:713–21.
6. Pinal-Fernandez I, Casal-Dominguez M, Huapaya JA, Albayda J, Paik JJ, Johnson C, et al. A longitudinal cohort study of the antisynthetase syndrome: increased severity of interstitial lung disease in black patients and patients with anti-PL7 and anti-PL12 autoantibodies. Rheumatology (Oxford) 2017;56:999–1007.
7. Akaike H. A new look at the statistical model identification. IEEE Trans Automat Contr 1974;19:716–23.
8. Schwarz G. Estimating the dimension of a model. Ann Statist 1978;6: 461–4.
9. Burnham KP, Anderson DR. Multimodel inference:understanding AIC and BIC in model selection. Sociol Methods Res 2004;33:261–304.
10. Raftery AE. Bayesian model selection in social research. Sociol Methodol 1995;25:111–63.
11. Tiniakou E, Pinal-Fernandez I, Lloyd TE, Albayda J, Paik J, Werner JL, et al. More severe disease and slower recovery in younger patients with anti-3-hydroxy-3-methylglutaryl-coenzyme A reductase-associated autoimmune myopathy. Rheumatology (Oxford) 2017;56:787–94.
12. Pinal-Fernandez I, Parks C, Werner JL, Albayda J, Paik JJ, Danoff SK, et al. Longitudinal course of disease in a large cohort of myositis patients with autoantibodies recognizing the signal recognition particle. Arthritis Care Res (Hoboken) 2017;69:263–70.
13. Pinal-Fernandez I, Mecoli CA, Casal-Dominguez M, Pak K, Hosono Y, Huapaya J, et al. More prominent muscle involvement in patients with dermatomyositis with anti-Mi2 autoantibodies. Neurology 2019;93: e1768–77.
14. Albayda J, Pinal-Fernandez I, Huang W, Parks C, Paik J, Casciola-Rosen L, et al. Antinuclear matrix protein 2 autoantibodies and edema, muscle disease, and malignancy risk in dermatomyositis patients. Arthritis Care Res (Hoboken) 2017;69:1771–6.
15. Fujimoto M, Hamaguchi Y, Kaji K, Matsushita T, Ichimura Y, Kodera M, et al. Myositis-specific anti-155/140 autoantibodies target transcription intermediary factor 1 family proteins. Arthritis Rheum 2012;64:513–22.
16. Sato S, Hoshino K, Satoh T, Fujita T, Kawakami Y, Fujita T, et al. RNA helicase encoded by melanoma differentiation–associated gene 5 is a major autoantigen in patients with clinically amyopathic dermatomyositis: association with rapidly progressive interstitial lung disease. Arthritis Rheum 2009;60:2193–200.
17. Murakami N, Takemitsu M, Kurashige T, Nonaka I. Significance of rimmed vacuoles in neuromuscular disorders–a comparative immunohistochemical study of inclusion body myositis and distal myopathy with rimmed vacuole formation. Rinsho Shinkeigaku 1994;34:782–7. In Japanese.
18. Love LA, Leff RL, Fraser DD, Targoff IN, Dalakas M, Plotz PH, et al. A new approach to the classification of idiopathic inflammatory myopathy: myositis-specific autoantibodies define useful homogeneous patient groups. Medicine (Baltimore) 1991;70:360–74.
19. Allenbach Y, Mammen AL, Benveniste O, Stenzel W, on behalf of the Immune-Mediated Necrotizing Myopathies Working Group. 224th ENMC international workshop: clinico-sero-pathological classification of immune-mediated necrotizing myopathies, Zandvoort, The Netherlands, 14–16 October 2016. Neuromuscul Disord 2018;28: 87–99.
20. Mammen AL, Allenbach Y, Stenzel W, Benveniste O, on behalf of the ENMC 239th Workshop Study Group. 239th ENMC international workshop: classification of dermatomyositis, Amsterdam, the Netherlands, 14–16 December 2018. Neuromuscul Disord 2019;30: 70–92.
21. Pinal-Fernandez I, Casciola-Rosen LA, Christopher-Stine L, Corse AM, Mammen AL. The prevalence of individual histopathologic features varies according to autoantibody status in muscle biopsies from patients with dermatomyositis. J Rheumatol 2015;42:1448–54.
22. Pinal-Fernandez I, Casal-Dominguez M, Derfoul A, Pak K, Plotz P, Miller, FW, et al. Identification of distinctive interferon gene signatures in different types of myositis. Neurology 2019;93:e1193–204.

Arthritis & Rheumatology
Vol. 74, No. 3, March 2022, pp 518–526
DOI 10.1002/art.41965

American College of Rheumatology
Empowering Rheumatology Professionals

Nintedanib in Patients With Systemic Sclerosis–Associated Interstitial Lung Disease: Subgroup Analyses by Autoantibody Status and Modified Rodnan Skin Thickness Score

Masataka Kuwana,[1] Yannick Allanore,[2] Christopher P. Denton,[3] Jörg H. W. Distler,[4] Virginia Steen,[5] Dinesh Khanna,[6] Marco Matucci-Cerinic,[7] Maureen D. Mayes,[8] Elizabeth R. Volkmann,[9] Corinna Miede,[10] Martina Gahlemann,[11] Manuel Quaresma,[12] Margarida Alves,[12] and Oliver Distler[13]

Objective. Using data from the SENSCIS trial, these analyses were undertaken to assess the effects of nintedanib versus placebo in subgroups of patients with systemic sclerosis–associated interstitial lung disease (SSc-ILD), based on characteristics previously identified as being associated with the progression of SSc-ILD.

Methods. Patients with SSc-ILD were randomized to receive either nintedanib or placebo, stratified by anti–topoisomerase I antibody (ATA) status. We assessed the rate of decline in forced vital capacity (FVC) (expressed in ml/year) over 52 weeks in subgroups based on baseline ATA status, modified Rodnan skin thickness score (MRSS) (<18 versus ≥18), and SSc subtype (limited cutaneous SSc [lcSSc] versus diffuse cutaneous SSc [dcSSc]).

Results. At baseline, 60.8% of 576 patients who received treatment with either nintedanib or placebo were positive for ATA, 51.9% had dcSSc, and 77.5% of 574 patients with MRSS data available had an MRSS of <18. The effect of nintedanib versus placebo on reducing the rate of decline in FVC (ml/year) was numerically more pronounced in ATA-negative patients compared to ATA-positive patients (adjusted difference in the rate of FVC decline, 57.2 ml/year [95% confidence interval (95% CI) –3.5, 118.0] versus 29.9 ml/year [95% CI –19.1, 78.8]), in patients with a baseline MRSS ≥18 compared to those with a baseline MRSS of <18 (adjusted difference in the rate of FVC decline, 88.7 ml/year [95% CI 7.7, 169.8] versus 26.4 ml/year [95% CI –16.8, 69.6]), and in patients with dcSSc compared to those with lcSSc (adjusted difference in the rate of FVC decline, 56.6 ml/year [95% CI 3.2, 110.0] versus 25.3 ml/year [95% CI –28.9, 79.6]). However, all exploratory interaction *P* values were nonsignificant (all $P > 0.05$), indicating that there was no heterogeneity in the effect of nintedanib versus placebo between these subgroups of patients.

Conclusion. In patients with SSc-ILD, reduction in the annual rate of decline in FVC among patients receiving nintedanib compared to those receiving placebo was not found to be heterogenous across subgroups based on ATA status, MRSS, or SSc subtype.

INTRODUCTION

Systemic sclerosis (SSc) is a complex autoimmune disease characterized by progressive fibrosis of the skin and internal organs (1). Interstitial lung disease (ILD) is a common manifestation of SSc and the leading cause of death in patients with SSc (2). Progressive SSc-ILD is associated with poor outcomes, and SSc patients who have progressive ILD need to be identified in

A video abstract of this article can be found at https://players.brightcove.net/3806881048001/default_default/index.html?videoId=6295470032001.

Supported by Boehringer Ingelheim.

[1]Masataka Kuwana, MD: Nippon Medical School Graduate School of Medicine, Tokyo, Japan; [2]Yannick Allanore, PhD: Descartes University, AP-HP, and Cochin Hospital, Paris, France; [3]Christopher P. Denton, PhD: University College London Division of Medicine, London, UK; [4]Jörg H. W. Distler, MD: University of Erlangen–Nuremberg, Erlangen, Germany; [5]Virginia Steen, MD: Georgetown University, Washington, DC; [6]Dinesh Khanna, MD: University of Michigan, Ann Arbor; [7]Marco Matucci-Cerinic, MD, PhD: University of Florence, Florence, Italy; [8]Maureen D. Mayes, MD: University of Texas McGovern Medical School, Houston; [9]Elizabeth R. Volkmann, MD: University of California, Los Angeles; [10]Corinna Miede, MSc: mainanalytics, Sulzbach, Germany; [11]Martina Gahlemann, MD: Boehringer Ingelheim, Basel, Switzerland; [12]Manuel Quaresma, Lic, Margarida Alves, MD: Boehringer Ingelheim International, Ingelheim, Germany; [13]Oliver Distler, MD: University Hospital Zurich and University of Zurich, Zurich, Switzerland.

Author disclosures are available at https://onlinelibrary.wiley.com/action/downloadSupplement?doi=10.1002%2Fart.41965&file=art41965-sup-0001-Disclosureform.pdf.

Address correspondence to Masataka Kuwana, MD, Department of Allergy and Rheumatology, Nippon Medical School, Sendagi 1-1-5, Bunkyo-ku, Tokyo, Japan. Email: kuwanam@nms.ac.jp.

Submitted for publication July 13, 2020; accepted in revised form August 31, 2021.

clinical practice so that the disease can be managed appropriately (3–5).

In clinical practice, patients with SSc are classified into 2 subtypes based on the extent of skin involvement: limited cutaneous SSc (lcSSc) and diffuse cutaneous SSc (dcSSc) (6). The dcSSc subtype is associated with earlier onset of non–Raynaud's phenomenon symptoms (7), higher mortality (8), and a greater risk of developing ILD (7), but ILD is also a common cause of death in patients with lcSSc (9). The course of skin fibrosis in patients with dcSSc typically involves worsening early in the course of the disease, followed by gradual improvement (10). Among patients with dcSSc in the European Scleroderma Trials and Research (EUSTAR) database, a high modified Rodnan skin thickness score (MRSS) at baseline was a predictor of improvement in the MRSS over the next 12 months, independent of disease duration, and an upper MRSS threshold of 18–25 was proposed to be an effective cutoff for identifying a cohort of SSc patients enriched for the phenotype of progressive skin fibrosis (11).

Specific autoantibody profiles have been associated with organ involvement and mortality in patients with SSc (8,12–15). Patients who are positive for anti–topoisomerase I antibody (ATA) have been reported to have a greater risk of developing clinically significant ILD (8,15). In the Genetics versus Environment in Scleroderma Outcome Study (GENISOS) cohort of 266 patients with early SSc, ATA positivity was associated with a greater rate of decline in forced vital capacity (FVC) over 3 years (16). In a single-center analysis, among 505 patients who developed SSc-ILD, ATA positivity was predictive of developing an FVC <70% predicted within 5 years of the onset of SSc (17).

Nintedanib is an intracellular inhibitor of tyrosine kinases that inhibits processes involved in the progression of pulmonary fibrosis (18). In patients with SSc-ILD in the SENSCIS trial, nintedanib was associated with a significant reduction in the rate of decline in FVC (expressed in ml/year) over 52 weeks compared to placebo, while there was no significant difference in the change from baseline in the MRSS (19). In addition, numerically lower proportions of patients treated with nintedanib showed a decline in FVC of >5% to ≤10% predicted or a decline in FVC of >10% over 52 weeks (20) compared to patients who received placebo. We used data from the SENSCIS trial to assess the progression of ILD, the progression of skin fibrosis, and the effects of nintedanib in subgroups based on baseline ATA status, MRSS, and SSc subtype.

PATIENTS AND METHODS

Trial design and patients. The SENSCIS trial (ClinicalTrials.gov identifier: NCT02597933) was a randomized, placebo-controlled trial conducted in 32 countries (19). The trial was conducted in accordance with the trial protocol, the principles of the Declaration of Helsinki, and the Harmonized Tripartite Guideline for Good Clinical Practice from the International Conference on Harmonisation and was approved by local authorities. Written informed consent was obtained from all patients before study entry.

The design of the SENSCIS trial has been published, together with the trial protocol and statistical analysis plan (19). In brief, patients enrolled in the study had SSc with onset of first non–Raynaud's phenomenon symptom ≤7 years before screening, had fibrotic ILD extending over ≥10% of the lung on a high-resolution computed tomography (HRCT) scan based on assessment of the whole lung, FVC ≥40% predicted, and diffusing capacity for carbon monoxide 30–89% predicted. Patients receiving prednisone ≤10 mg/day and/or stable therapy with mycophenolate or methotrexate for ≥6 months prior to randomization were allowed to participate. At screening, patients were classified as having lcSSc or dcSSc by the investigators. Patients were randomized 1:1 to receive nintedanib 150 mg twice a day or placebo, stratified by the presence of ATA. The participants' ATA status was determined based on review of historical information (local laboratory data recorded for each patient) or, if historical information was not available, based on detection of ATA in the patient's blood, using a BioPlex 2200 System bead assay (obtained at a central laboratory).

Patients received their randomized treatment in a blinded manner until the last patient had reached week 52 but for ≤100 weeks. Patients who discontinued trial medication were asked to attend all scheduled visits and undergo examinations as originally planned. Spirometry was performed in accordance with international guidelines (21) at baseline and at weeks 2, 4, 6, 12, 24, 36, and 52. The MRSS was measured at baseline and at weeks 12, 24, 36, and 52. The MRSS evaluates a patient's skin thickness through palpation of 17 areas using a scale of 0 to 3 to give a maximum score of 51 (22,23).

End points. Analyses conducted using the overall population of the SENSCIS trial have been described (19). Here we report the results of analyses in subgroups based on baseline ATA status (based on historical [local laboratory] information, as reported in the case report form, or on central laboratory data if historical information was not available), baseline MRSS (MRSS <18 versus MRSS ≥18 or MRSS ≤10 versus MRSS >10 to <22 versus MRSS ≥22), and SSc subtype (lcSSc versus dcSSc). In these subgroups, we assessed the annual rate of decline in FVC (expressed in ml/year) over 52 weeks. The following were assessed at week 52 in subgroups based on baseline ATA status, MRSS (<18 versus ≥18), and SSc subtype (lcSSc versus dcSSc): the proportions of patients who met proposed thresholds for minimum clinically important differences (MCIDs) for stable or improved FVC (increase in FVC or absolute decrease <3.3% predicted) and worsened FVC (absolute decrease ≥3.3% predicted), based on estimates derived from Scleroderma Lung Studies I and II, anchored to the health transition question from the Medical Outcomes Study Short Form 36 (24); and the change from baseline in the MRSS. In the overall population, we assessed the

Table 1. Annual rate of decline in FVC, proportions of patients with worsening of FVC and stable or improved FVC, and changes in the MRSS from baseline to week 52 in patients with systemic sclerosis–associated interstitial lung disease in each treatment group in the SENSCIS trial, according to baseline ATA status

Variable	ATA-positive		ATA-negative		*P* for interaction*
	Nintedanib (n = 173)	Placebo (n = 177)	Nintedanib (n = 115)	Placebo (n = 111)	
Annual rate of decline in FVC (ml/year)†					
Adjusted rate of decline in FVC over 52 weeks, ± SE, ml/year	−63.6 ± 18.0	−93.5 ± 17.3	−35.9 ± 21.8	−93.1 ± 21.9	
Adjusted difference (95% CI) vs. placebo, ml/year‡	29.9 (−19.1, 78.8)		57.2 (−3.5, 118.0)		0.49
Proportion of patients meeting proposed MCID thresholds for worsening of FVC and stable or improved FVC at week 52†§					
Decrease in FVC ≥3.3% predicted, no. (%)	62 (35.8)	81 (45.8)	37 (32.5)	45 (40.5)	
Odds ratio (95% CI) vs. placebo‡	0.66 (0.43, 1.02)		0.70 (0.41, 1.22)		0.86
Increase in FVC or decrease in FVC <3.3% predicted, no. (%)	111 (64.2)	96 (54.2)	77 (67.5)	66 (59.5)	
Odds ratio (95% CI) vs. placebo‡	1.51 (0.98, 2.32)		1.42 (0.82, 2.45)		0.86
Change from baseline in MRSS at week 52¶					
Adjusted change in MRSS at week 52, mean ± SE	−1.5 ± 0.3	−1.7 ± 0.3	−3.2 ± 0.4	−2.4 ± 0.4	
Adjusted difference (95% CI) vs. placebo‡	0.2 (−0.7, 1.2)		−0.8 (−2.0, 0.4)		0.18

* *P* values evaluated heterogeneity in the treatment effect of nintedanib versus placebo between the subgroups; annual rate of decline in forced vital capacity (FVC), *P* for treatment-by-time-by-subgroup interaction; proportions of patients meeting proposed minimum clinically important difference (MCID) thresholds for worsening of FVC and stable or improved FVC at week 52, *P* for treatment-by-subgroup interaction; change from baseline in the modified Rodnan skin thickness score (MRSS), *P* for treatment-by-visit-by-subgroup interaction.
† Post–baseline FVC data were not available for 1 anti–topoisomerase I antibody (ATA)–negative patient in the nintedanib group; this patient was excluded from the analysis.
‡ 95% CI = 95% confidence interval.
§ The proposed MCID thresholds for worsening of FVC and stable or improved FVC were based on estimates derived from the Scleroderma Lung Studies I and II, anchored to the health transition question from the Medical Outcomes Short Form 36 (24).
¶ Baseline MRSS data were not available for 2 ATA-positive patients in the placebo group; these patients were excluded from the analysis.

correlations between FVC (in ml) at baseline and change from baseline in MRSS at week 52, MRSS at baseline and change from baseline in FVC (in ml) at week 52, and changes from baseline in MRSS and FVC (in ml) at week 52. Finally, we assessed the rate of decline in FVC (expressed in ml/year) considering MRSS at baseline as a continuous variable.

Statistical analysis. All analyses were conducted in patients who received ≥1 dose of trial medication. A random coefficient regression model (with random slopes and intercepts) was used to analyze the annual rate of decline in FVC (expressed in ml/year) in the subgroups, with ATA status (ATA-positive, ATA-negative) and sex as fixed categorical effects, baseline FVC (in ml), age, and height as fixed continuous effects, and with baseline-by-time, treatment-by-subgroup, and treatment-by-subgroup-by-time interaction included as interaction terms. The analysis was based on all measurements obtained within the first 52 weeks, including those from patients who discontinued trial medication. The proportions of patients who met proposed thresholds for stable or improved FVC and worsened FVC at week 52 were compared between treatment groups using a logistic regression model, including treatment, ATA status, subgroup, and treatment-by-subgroup interaction as terms. Odds ratios were estimated for the independent effect of treatment within each subgroup. Missing values were imputed using a worst value carried forward approach. Subgroup analyses of change from baseline in the MRSS at week 52 were based on a mixed model for repeated measures (MMRM), using ATA status and treatment-by-subgroup-by-visit interaction as fixed categorical effects, and baseline MRSS-by-visit interaction as a fixed continuous covariate.

For every subgroup analysis, exploratory interaction *P* values were calculated (using an F test in random coefficient regression or MMRM analyses, or Wald's test in logistic regression analyses) to evaluate potential heterogeneity in the treatment effect of nintedanib versus placebo across the subgroups, with no adjustment for multiple testing. Spearman's correlation coefficients were calculated to analyze the correlations between FVC and MRSS described above. The rate of decline in FVC (expressed in ml/year) considering MRSS at baseline as a continuous variable was analyzed using a random coefficient regression model with treatment, ATA status, and sex as fixed categorical effects, baseline FVC (ml), age, and height as fixed continuous effects, and including baseline FVC-by-time, treatment-by-time, treatment-by-baseline MRSS, and treatment-by-baseline-MRSS-by-time as interaction terms.

RESULTS

Patients. The baseline characteristics of the patients in the SENSCIS trial have been described previously (19). At baseline, 173 patients (60.1%) in the nintedanib group and 177 patients (61.5%) in the placebo group were ATA-positive. ATA status based on historical information was generally consistent with that based on central laboratory data (see Supplementary Table 1, available on the *Arthritis & Rheumatology* website at https://onlinelibrary.wiley.com/doi/10.1002/art.41965). Compared to ATA-negative patients, the subgroup of ATA-positive patients had a lower proportion of male patients, a greater proportion of patients with dcSSc, and a higher mean MRSS at baseline (Supplementary Table 2, available on the *Arthritis & Rheumatology* website at https://onlinelibrary.wiley.com/doi/10.1002/art.41965). Similar proportions of ATA-positive and ATA-negative patients were receiving treatment with mycophenolate at baseline (49.1% and 47.3%, respectively).

Two patients in the placebo group did not have information on MRSS at baseline. Of the patients who had information on MRSS at baseline, 219 (76.0%) of 288 in the nintedanib group and 226 (79.0%) of 286 in the placebo group had an MRSS <18. All patients with an MRSS ≥18 and 37.8% of patients with an MRSS <18 were classified as having dcSSc. Compared to patients with an MRSS ≥18, patients with an MRSS <18 had a greater mean baseline FVC % predicted, and the MRSS <18 group had a higher proportion of male patients and a higher proportion of patients who were negative for ATA (Supplementary Table 3, available on the *Arthritis & Rheumatology* website at https://onlinelibrary.wiley.com/doi/10.1002/art.41965). A smaller proportion of patients with an MRSS <18 were receiving treatment with mycophenolate at baseline compared to patients who had an MRSS ≥18 (45.6% versus 58.1%, respectively). In the nintedanib and placebo groups, 153 (53.1%) of 288 patients and 146 (50.7%) of 288 patients, respectively, were classified as having dcSSc; their baseline characteristics are shown in Supplementary Table 4 (available on the *Arthritis & Rheumatology* website at https://onlinelibrary.wiley.com/doi/10.1002/art.41965).

Outcomes in subgroups by ATA status. In the placebo group, the adjusted annual rate of decline in FVC was consistent between patients who were ATA-positive and those who were ATA-negative at baseline (adjusted annual rate of decline in FVC, ± SE –93.5 ± 17.3 ml/year versus –93.1 ± 21.9 ml/year) (Table 1 and Figure 1A). In analyses of the adjusted annual rate of decline in FVC that also adjusted for use of mycophenolate at baseline, the rate of FVC decline among patients in the placebo group was similar between ATA-positive and ATA-negative patients (adjusted annual rate of decline in FVC ± SE –93.4 ± 17.3 ml/year versus –93.2 ± 21.9 ml/year). With regard to nintedanib, the effect of nintedanib on reducing the annual rate of decline in FVC compared with placebo was numerically more pronounced in ATA-negative patients compared to ATA-positive patients (adjusted difference in annual rate of decline in FVC, 57.2 ml/year [95% confidence interval (95% CI) –3.5, 118.0] versus 29.9 ml/year [95% CI –19.1, 78.8]), but the exploratory interaction *P* value did not indicate heterogeneity in the treatment effect of nintedanib versus placebo between the subgroups classified according to ATA status ($P = 0.49$) (Figure 1A).

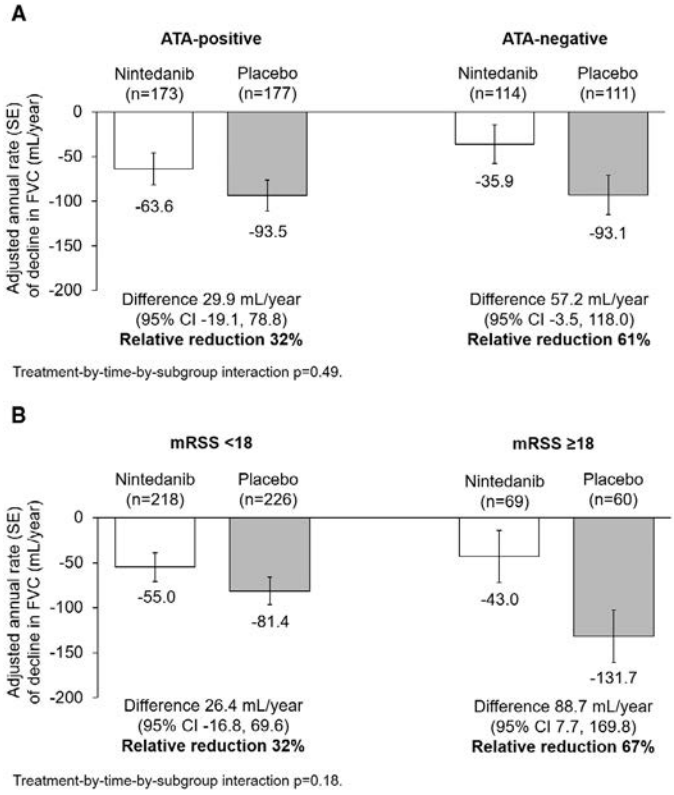

Figure 1. Adjusted annual rate of decline in forced vital capacity (FVC) (ml/year) in subgroups of patients with systemic sclerosis–associated interstitial lung disease based on anti–topoisomerase I antibody (ATA) status at baseline (**A**) and modified Rodnan skin thickness score (MRSS) at baseline (**B**) in the SENSCIS trial. The adjusted annual rate of decline in FVC ± SE is shown. The difference between treatment groups is shown with 95% confidence interval (95% CI) and relative reduction.

The proportion of patients with an absolute decrease in FVC of ≥3.3% predicted at week 52 was lower in the nintedanib group versus the placebo group among ATA-positive patients (35.8% versus 45.8%) as well as among ATA-negative patients (32.5% versus 40.5%); the exploratory interaction *P* value did not indicate heterogeneity in the treatment effect of nintedanib versus placebo between the subgroups based on ATA status ($P = 0.86$). The proportion of patients with an increase or absolute decrease in FVC of <3.3% predicted was higher in the nintedanib group versus the placebo group among ATA-positive patients (64.2% versus 54.2%) as well as among ATA-negative patients (67.5% versus 59.5%) (exploratory interaction $P = 0.86$) (Table 1).

Small reductions (improvements) in the MRSS were observed in patients who were ATA-positive and in patients who were ATA-negative. Reductions in the MRSS were similar between the nintedanib and placebo groups, with no heterogeneity in the treatment effect detected between subgroups classified by ATA status (Table 1).

Outcomes in subgroups by MRSS at baseline. In the placebo group, the adjusted annual rate of decline in FVC was greater in patients with an MRSS ≥18 compared to those with an MRSS <18 (adjusted annual rate of decline in FVC ± SE –131.7 ± 29.2 ml/year versus –81.4 ± 15.4 ml/year) (Table 2 and Figure 1B). The effect of nintedanib on reducing the annual rate of decline in FVC compared with placebo was numerically more pronounced in patients with a baseline MRSS ≥18 compared to those with a baseline MRSS <18 (adjusted difference in annual rate of decline in FVC, 88.7 ml/year [95% CI 7.7, 169.8] versus 26.4 ml/year [95% CI –16.8, 69.6]). However, the exploratory interaction *P* value did not indicate heterogeneity in the treatment effect of nintedanib versus placebo across the subgroups classified according to baseline MRSS ($P = 0.18$) (Figure 1B). Similarly, in analyses of subgroups based on different cutoffs for the baseline MRSS (MRSS ≤10 [n = 315] versus MRSS >10 to MRSS <22 [n = 182] versus MRSS ≥22 [n = 76]), the exploratory interaction *P* value did not indicate heterogeneity in the treatment effect of nintedanib compared to placebo across these MRSS subgroups ($P = 0.07$) (Supplementary Table 5, available on the *Arthritis & Rheumatology* website at https://onlinelibrary.wiley.com/doi/10.1002/art.41965).

The proportion of patients with an absolute decrease in FVC of ≥3.3% predicted was lower in the nintedanib group compared to the placebo group both among patients with a baseline MRSS ≥18 (42.0% versus 53.3%) and among those with a baseline MRSS <18 (32.1% versus 40.7%). The

Table 2. Annual rate of decline in FVC, proportions of patients with worsening of FVC and stable or improved FVC, and changes in the MRSS from baseline to week 52 in patients with systemic sclerosis–associated interstitial lung disease in each treatment group in the SENSCIS trial, according to baseline MRSS <18 and MRSS ≥18*

	MRSS <18		MRSS ≥18		
Variable	Nintedanib (n = 219)	Placebo (n = 226)	Nintedanib (n = 69)	Placebo (n = 60)	*P* for interaction†
Annual rate of decline in FVC, ml/year‡					
Adjusted rate of decline in FVC over 52 weeks, ± SE, ml/year	−55.0 ± 15.7	−81.4 ± 15.4	−43.0 ± 29.2	−131.7 ± 29.2	
Adjusted difference (95% CI) vs. placebo, ml/year§	26.4 (−16.8, 69.6)		88.7 (7.7, 169.8)		0.18
Proportions of patients meeting proposed MCID thresholds for worsening of FVC and stable or improved FVC at week 52‡¶					
Decrease in FVC ≥3.3% predicted, no. (%)	70 (32.1)	92 (40.7)	29 (42.0)	32 (53.3)	
Odds ratio (95% CI) vs. placebo§	0.69 (0.47, 1.02)		0.62 (0.31, 1.25)		0.79
Increase in FVC or decrease in FVC <3.3% predicted, no. (%)	148 (67.9)	134 (59.3)	40 (58.0)	28 (46.7)	
Odds ratio (95% CI) vs. placebo§	1.44 (0.98, 2.13)		1.61 (0.80, 3.24)		0.79
Change from baseline in MRSS at week 52					
Adjusted change in MRSS at week 52, mean ± SE	−2.2 ± 0.3	−2.1 ± 0.3	−2.1 ± 0.7	−1.6 ± 0.7	
Adjusted difference (95% CI) vs. placebo§	−0.1 (−1.0, 0.7)		−0.6 (−2.1, 1.0)		0.62

* Baseline modified Rodnan skin thickness score (MRSS) data were not available for 2 patients in the placebo group; these patients were excluded from all analyses shown.
† *P* values evaluated heterogeneity in the treatment effect of nintedanib versus placebo between the subgroups: annual rate of decline in forced vital capacity (FVC), *P* for treatment-by-time-by-subgroup interaction; proportions of patients meeting proposed minimum clinically important difference (MCID) thresholds for worsening of FVC and stable or improved FVC at week 52, *P* for treatment-by-subgroup interaction; change from baseline in the MRSS, *P* for treatment-by-visit-by-subgroup interaction.
‡ Post–baseline FVC data were not available for 1 patient with MRSS <18 at baseline in the nintedanib group; this patient was excluded from the analysis.
§ 95% CI = 95% confidence interval.
¶ The proposed MCID thresholds for worsening of FVC and stable or improved FVC were based on estimates derived from the Scleroderma Lung Studies I and II, anchored to the health transition question from the Medical Outcomes Short Form 36 (24).

proportion of patients with an increase or absolute decrease in FVC <3.3% predicted was higher in the nintedanib group than in the placebo group both among patients with a baseline MRSS ≥18 (58.0% versus 46.7%) and among those with a baseline MRSS <18 (67.9% versus 59.3%). Exploratory interaction *P* values did not indicate heterogeneity in the treatment effect of nintedanib versus placebo between the subgroups classified by baseline MRSS (Table 2).

Small reductions (improvements) in the MRSS were observed in patients with a baseline MRSS of ≥18 and in patients with a baseline MRSS of <18. Reductions in the MRSS were similar in the nintedanib and placebo groups, with no heterogeneity in treatment effect detected between the subgroups (Table 2). Similarly, there was no heterogeneity in the treatment effect of nintedanib across subgroups classified by a baseline MRSS ≤10 versus baseline MRSS >10 to <22 versus baseline MRSS ≥22 (Supplementary Table 5, available on the *Arthritis & Rheumatology* website at https://onlinelibrary.wiley.com/doi/10.1002/art.41965).

Relationships between FVC and MRSS. In the overall population, no meaningful correlations were observed between the FVC (in ml) at baseline and change in the MRSS from baseline to week 52, between the MRSS at baseline and change in the FVC (in ml) from baseline to week 52, or between change in the MRSS and change in the FVC (in ml) from baseline to week 52 (Supplementary Table 6, available on the *Arthritis & Rheumatology* website at https://onlinelibrary.wiley.com/doi/10.1002/art.41965). The analysis that considered MRSS at baseline as a continuous variable showed no significant interaction between baseline MRSS and the rate of decline in FVC (in ml/year) ($P = 0.12$).

Outcomes in subgroups with lcSSc or dcSSc. In the placebo group, the adjusted annual rate of decline in FVC was greater in patients with dcSSc compared to those with lcSSc (adjusted annual rate of decline ± SE −112.0 ± 19.1 ml/year versus −74.5 ± 19.2 ml/year). The effect of nintedanib on reducing the annual rate of decline in FVC compared with placebo was numerically more pronounced in patients with dcSSc compared to those with lcSSc (adjusted difference in annual rate of decline in FVC, 56.6 ml/year [95% CI 3.2, 110.0] versus 25.3 ml/year [95% CI −28.9, 79.6]). However, the exploratory interaction *P* value did not indicate heterogeneity in the treatment effect of nintedanib versus placebo between these subgroups of patients with lcSSc or dcSSc ($P = 0.42$). Small reductions (improvements) in the MRSS were observed in patients with lcSSc and in those with dcSSc. Reductions in the MRSS were similar in the nintedanib and placebo groups, with no heterogeneity in the between-group difference detected across subgroups based on SSc subtype (Supplementary Table 7, available on the *Arthritis & Rheumatology* website at https://onlinelibrary.wiley.com/doi/10.1002/art.41965).

DISCUSSION

We used data from the SENSCIS trial to assess the progression of ILD and skin fibrosis, and the effects of nintedanib versus placebo, in subgroups of patients with SSc-ILD based on baseline characteristics that have previously been associated with disease progression. In the placebo group, the rate of decline in FVC over 52 weeks was similar between ATA-positive patients and ATA-negative patients, greater in patients with a baseline MRSS ≥18 compared to those with a baseline MRSS <18, and greater in patients with dcSSc compared to those with lcSSc, as reported by the site investigator. Across these subgroups, a lower annual rate of decline in FVC was observed in patients who received nintedanib compared to those who received placebo, with no heterogeneity detected in the treatment effect of nintedanib versus placebo in any of the subgroups studied. These findings add to previous analyses of data from the SENSCIS trial showing that the effect of nintedanib on the annual rate of FVC decline was consistent across subgroups based on ATA status, SSc subtype, age, sex, race, and use of mycophenolate at baseline (19,25). MCIDs for improvement and worsening in FVC in patients with SSc-ILD have been proposed based on data from Scleroderma Lung Studies I and II, anchored to the health transition question from the Medical Outcomes Study Short Form 36 (24). Over 52 weeks, the proportion of patients who met the proposed threshold for MCID for improved or stable FVC was numerically greater, and the proportion of patients who met the proposed threshold for MCID for worsening of FVC was numerically lower, in patients who received nintedanib compared to those who received placebo across the subgroups based on ATA status, baseline MRSS, and SSc subtype, with no evidence of heterogeneity detected across the subgroups. These findings support a clinically meaningful benefit of nintedanib in reducing the rate of progression of ILD across a broad population of patients with SSc-ILD.

In the placebo group, we observed a numerically greater rate of decline in FVC over 52 weeks in patients with dcSSc compared to those with lcSSc. A single-center study of 105 patients with early SSc found that dcSSc was a predictor of decline in FVC of ≥10% predicted over a mean follow-up of 6 years (26). However, in the GENISOS cohort of 266 patients with early SSc, decline in FVC % predicted over a mean follow-up of 3.8 years was similar between patients with lcSSc and those with dcSSc (16). A recent analysis of data from >12,000 patients in the EUSTAR database also found that changes in FVC % predicted over 1, 2, and 3 years were similar between patients with lcSSc and those with dcSSc (27). In our analyses, 51% of patients classified as having lcSSc were ATA-positive at baseline. This is a much higher proportion than has been shown in data from large registries of patients with SSc (11–23%) (28–30). This may reflect either misclassification of some patients who had dcSSc and whose skin

fibrosis had regressed prior to screening, or selection bias in the SENSCIS trial for patients with lcSSc who had more progressive lung disease. These findings highlight the limitations of using the dcSSc versus lcSSc classification in large multicenter trials. While data from the GENISOS cohort suggested that ATA positivity was associated with an increased rate of decline in FVC in patients with early SSc (16), ATA status did not seem to affect the rate of progression of ILD in the SENSCIS trial. These different findings across studies may reflect patient populations at different stages of disease or confounders such as comedication.

Consistent with findings in the overall SENSCIS population (19), nintedanib was not found to have an effect on the change in MRSS in any of the subgroups analyzed. The MRSS improved in both the nintedanib group and the placebo group, reflecting the natural history of skin fibrosis in patients with SSc (10). In our analysis of subgroups based on baseline MRSS using a threshold of 18 (based on data suggesting an upper MRSS threshold of 18–25 to enrich a cohort of patients with dcSSc for patients with the phenotype of progressive skin fibrosis [11]), change in MRSS at week 52 was similar between patients with a baseline MRSS ≥18 and patients with a baseline MRSS <18.

Among all of the subgroups we analyzed, the rate of decline in FVC over 52 weeks was highest in patients in the placebo group who had a baseline MRSS ≥18; however, we found no meaningful correlation between MRSS at baseline and decline in FVC over 52 weeks. We observed no meaningful correlation between progression of skin fibrosis over 52 weeks and progression of SSc-ILD over the same period. The relationship between progression of skin fibrosis and later decline in FVC observed over several years of follow-up in patients with dcSSc in the EUSTAR database (31) could not be investigated using data from the SENSCIS trial due to the limited follow-up period.

A limitation of the subgroup analyses of data from the SENSCIS trial is that they were not powered for formal statistical testing of the individual subgroups, and the interaction *P* values should be regarded as exploratory. The results of these subgroup analyses should be interpreted with caution, particularly those in the relatively small subgroups. A further limitation was that progression of ILD was assessed solely by looking at changes in FVC and did not consider other metrics for ILD progression, such as changes in the extent of fibrosis on HRCT.

In conclusion, these analyses of data from the SENSCIS trial suggest that while the course of FVC decline in patients with SSc-ILD remains difficult to predict, nintedanib is effective at reducing the annual rate of progression of ILD across subgroups of patients based on ATA status, SSc subtype, and MRSS at baseline.

ACKNOWLEDGMENTS

We thank the patients who participated in the SENSCIS trial.

AUTHOR CONTRIBUTIONS

All authors were involved in drafting the article or revising it critically for important intellectual content, and all authors approved the final version to be submitted for publication. Dr. Kuwana had full access to all of the data in the study and takes responsibility for the integrity of the data and the accuracy of the data analysis.

Study conception and design. Kuwana, Mayes, Gahlemann, Alves, O. Distler.

Acquisition of data. Kuwana, Allanore, Denton, J. Distler, Steen, Khanna, Mayes, O. Distler.

Analysis and interpretation of data. Kuwana, Allanore, Denton, J. Distler, Steen, Khanna, Matucci-Cerinic, Mayes, Volkmann, Miede, Gahlemann, Quaresma, Alves, O. Distler.

ROLE OF THE STUDY SPONSOR

The SENSCIS trial was supported by Boehringer Ingelheim International GmbH. Boehringer Ingelheim participated in the study design, data collection, statistical analyses, data interpretation, and the writing of the report. Writing assistance was provided by Elizabeth Ng, BSc and Wendy Morris, MSc of FleishmanHillard, London, UK, which was contracted and funded by Boehringer Ingelheim. Boehringer Ingelheim was given the opportunity to review the manuscript for medical and scientific accuracy as well as intellectual property considerations. Dr. Kuwana had full access to all data and had final responsibility for the decision to submit for publication.

ADDITIONAL DISCLOSURES

Author Miede is an employee of mainanalytics.

REFERENCES

1. Van den Hoogen F, Khanna D, Fransen J, Johnson SR, Baron M, Tyndall A, et al. 2013 classification criteria for systemic sclerosis: an American College of Rheumatology/European League Against Rheumatism collaborative initiative. Arthritis Rheum 2013;65:2737–47.
2. Elhai M, Meune C, Boubaya M, Avouac J, Hachulla E, Balbir-Gurman A, et al. Mapping and predicting mortality from systemic sclerosis. Ann Rheum Dis 2017;76:1897–905.
3. Goh NS, Hoyles RK, Denton CP, Hansell DM, Renzoni EA, Maher TM, et al. Short-term pulmonary function trends are predictive of mortality in interstitial lung disease associated with systemic sclerosis. Arthritis Rheumatol 2017;69:1670–8.
4. Hoffmann-Vold AM, Fretheim H, Halse AK, Seip M, Bitter H, Wallenius M, et al. Tracking impact of interstitial lung disease in systemic sclerosis in a complete nationwide cohort. Am J Respir Crit Care Med 2019;200:1258–66.
5. Volkmann ER. Natural history of systemic sclerosis–related interstitial lung disease: how to identify a progressive fibrosing phenotype. J Scleroderma Relat Disord 2020;5 Suppl:31–40.
6. LeRoy EC, Black C, Fleischmajer R, Jablonska S, Krieg T, Medsger TA Jr, et al. Scleroderma (systemic sclerosis): classification, subsets and pathogenesis. J Rheumatol 1988;15:202–5.
7. Walker UA, Tyndall A, Czirják L, Denton C, Farge-Bancel D, Kowal-Bielecka O, et al. Clinical risk assessment of organ manifestations in systemic sclerosis: a report from the EULAR Scleroderma Trials and Research group database. Ann Rheum Dis 2007;66:754–63.
8. Nihtyanova SI, Schreiber BE, Ong VH, Rosenberg D, Moinzadeh P, Coghlan JG, et al. Prediction of pulmonary complications and long-term survival in systemic sclerosis. Arthritis Rheumatol 2014;66:1625–35.

9. Sánchez-Cano D, Ortego-Centeno N, Callejas JL, Fonollosa Plá V, Ríos-Fernández R, Tolosa-Vilella C, et al. Interstitial lung disease in systemic sclerosis: data from the Spanish scleroderma study group. Rheumatol Int 2018;38:363–74.
10. Wirz EG, Jaeger VK, Allanore Y, Riemekasten G, Hachulla E, Distler O, et al. Incidence and predictors of cutaneous manifestations during the early course of systemic sclerosis: a 10-year longitudinal study from the EUSTAR database. Ann Rheum Dis 2016;75:1285–92.
11. Dobrota R, Maurer B, Graf N, Jordan S, Mihai C, Kowal-Bielecka O, et al. Prediction of improvement in skin fibrosis in diffuse cutaneous systemic sclerosis: a EUSTAR analysis. Ann Rheum Dis 2016;75: 1743–8.
12. Steen VD. Autoantibodies in systemic sclerosis. Semin Arthritis Rheum 2005;35:35–42.
13. Fertig N, Domsic RT, Rodriguez-Reyna T, Kuwana M, Lucas M, Medsger TA Jr, et al. Anti-U11/U12 RNP antibodies in systemic sclerosis: a new serologic marker associated with pulmonary fibrosis. Arthritis Rheum 2009;61:958–65.
14. Kuwana M. Circulating anti-nuclear antibodies in systemic sclerosis: utility in diagnosis and disease subsetting [review]. J Nippon Med Sch 2017;84:56–63.
15. Nihtyanova SI, Sari A, Harvey JC, Leslie A, Derrett-Smith EC, Fonseca C, et al. Using autoantibodies and cutaneous subset to develop outcome-based disease classification in systemic sclerosis. Arthritis Rheumatol 2020;72:465–76.
16. Assassi S, Sharif R, Lasky RE, McNearney TA, Estrada-Y-Martin RM, Draeger H, et al. Predictors of interstitial lung disease in early systemic sclerosis: a prospective longitudinal study of the GENISOS cohort. Arthritis Res Ther 2010;12:R166.
17. Nihtyanova SI, Derrett-Smith E, Fonseca C, Ong V, Denton C. Frequency and predictors of meaningful decline in forced vital capacity during follow up of a large cohort of systemic sclerosis associated pulmonary fibrosis patients [abstract]. Arthritis Rheumatol 2019; 71 Suppl 10. URL:https://acrabstracts.org/abstract/frequency-and-predictors-of-meaningful-decline-in-forced-vital-capacity-during-follow-up-%d0%bef-a-large-cohort-of-systemic-sclerosis-associated-pulmonary-fibrosis-patients/.
18. Wollin L, Distler JH, Denton CP, Gahlemann M. Rationale for the evaluation of nintedanib as a treatment for systemic sclerosis-associated interstitial lung disease. J Scleroderma Relat Disord 2019;4:212–8.
19. Distler O, Highland KB, Gahlemann M, Azuma A, Fischer A, Mayes MD, et al. Nintedanib for systemic sclerosis-associated interstitial lung disease. N Engl J Med 2019;380:2518–28.
20. Maher TM, Mayes MD, Kreuter M, Volkmann ER, Aringer M, Castellvi I, et al. Effect of nintedanib on lung function in patients with systemic sclerosis–associated interstitial lung disease: further analyses of the SENSCIS trial. Arthritis Rheumatol 2021;73:671–6.
21. Miller MR, Hankinson J, Brusasco V, Burgos F, Casaburi R, Coates A, et al. Standardisation of spirometry. Eur Respir J 2005;26:319–38.
22. Clements PJ, Hurwitz EL, Wong WK, Seibold JR, Mayes M, White B, et al. Skin thickness score as a predictor and correlate of outcome in systemic sclerosis: high-dose versus low-dose penicillamine trial. Arthritis Rheum 2000;43:2445–54.
23. Khanna D, Furst DE, Clements PJ, Allanore Y, Baron M, Czirjak L, et al. Standardization of the modified Rodnan skin score for use in clinical trials of systemic sclerosis. J Scleroderma Relat Dis 2017;2: 11–8.
24. Kafaja S, Clements PJ, Wilhalme H, Tseng CH, Furst DE, Kim GH, et al. Reliability and minimal clinically important differences of forced vital capacity: results from the Scleroderma Lung Studies (SLS-I and SLS-II). Am J Respir Crit Care Med 2018;197:644–52.
25. Highland KB, Distler O, Kuwana M, Allanore Y, Assassi S, Azuma A, et al. Efficacy and safety of nintedanib in patients with systemic sclerosis-associated interstitial lung disease treated with mycophenolate: subgroup analysis of the SENSCIS trial. Lancet Respir Med 2021;9:96–106.
26. Gilson M, Zerkak D, Wipff J, Dusser D, Dinh-Xuan AT, Abitbol V, et al. Prognostic factors for lung function in systemic sclerosis: prospective study of 105 cases. Eur Respir J 2010;35:112–7.
27. Frantz C, Huscher D, Avouac J, Hachulla E, Balbir-Gurman A, Riemekasten G, et al. Outcomes of limited cutaneous systemic sclerosis patients: results on more than 12,000 patients from the EUSTAR database. Autoimmun Rev 2020;19:102452.
28. Meier FM, Frommer KW, Dinser R, Walker UA, Czirjak L, Denton CP, et al. Update on the profile of the EUSTAR cohort: an analysis of the EULAR Scleroderma Trials and Research group database. Ann Rheum Dis 2012;71:1355–60.
29. Srivastava N, Hudson M, Tatibouet S, Wang M, Baron M, Fritzler MJ, et al. Thinking outside the box: the associations with cutaneous involvement and autoantibody status in systemic sclerosis are not always what we expect. Semin Arthritis Rheum 2015;45:184–9.
30. Dougherty DH, Kwakkenbos L, Carrier ME, Salazar G, Assassi S, Baron M, et al. The Scleroderma Patient-Centered Intervention Network cohort: baseline clinical features and comparison with other large scleroderma cohorts. Rheumatology (Oxford) 2018;57: 1623–31.
31. Wu W, Jordan S, Graf N, de Oliveira Pena J, Curram J, Allanore Y, et al. Progressive skin fibrosis is associated with a decline in lung function and worse survival in patients with diffuse cutaneous systemic sclerosis in the European Scleroderma Trials and Research (EUSTAR) cohort. Ann Rheum Dis 2019;78:648–56.

Arthritis & Rheumatology
Vol. 74, No. 3, March 2022, pp 527–540
DOI 10.1002/art.41949

American College of Rheumatology
Empowering Rheumatology Professionals

Predictors of Rheumatic Immune-Related Adverse Events and De Novo Inflammatory Arthritis After Immune Checkpoint Inhibitor Treatment for Cancer

Amy Cunningham-Bussel,[1] Jiaqi Wang,[2] Lauren C. Prisco,[2] Lily W. Martin,[2] Kathleen M. M. Vanni,[2] Alessandra Zaccardelli,[2] Mazen Nasrallah,[3] Lydia Gedmintas,[1] Lindsey A. MacFarlane,[1] Nancy A. Shadick,[1] Mark M. Awad,[4] Osama Rahma,[4] Nicole R. LeBoeuf,[5] Ellen M. Gravallese,[1] and Jeffrey A. Sparks[1]

Objective. To identify predictors of rheumatic immune-related adverse events (irAEs) following immune checkpoint inhibitor (ICI) treatment for cancer.

Methods. We performed a case–control study to predict the occurrence of rheumatic irAEs in cancer patients who initiated ICI treatment at Mass General Brigham and the Dana-Farber Cancer Institute between 2011 and 2020. We screened for the presence of rheumatic irAEs by reviewing the medical records of patients evaluated by rheumatologists or those prescribed nonglucocorticoid immunomodulatory drugs after the time of ICI initiation (baseline). Review of medical records confirmed the presence of rheumatic irAEs and the indications necessitating immunomodulatory drug treatment. Controls were defined as patients who did not experience rheumatic irAEs, did not have preexisting rheumatic disease, did not have a clinical evaluation by a rheumatologist after ICI treatment, did not receive an immunomodulatory drug after ICI, did not receive systemic glucocorticoids after ICI, and survived at least 6 months after the initial ICI treatment. We used logistic regression to estimate the odds ratios (ORs) (with 95% confidence intervals [95% CIs]) for the risk of a rheumatic irAE in the presence of various baseline predictors.

Results. A total of 8,028 ICI recipients were identified (mean age 65.5 years, 43.1% female, 31.8% with lung cancer). After ICI initiation, 404 patients (5.0%) were evaluated by rheumatologists, and 475 patients (5.9%) received an immunomodulatory drug to treat any irAEs. There were 226 confirmed rheumatic irAE cases (2.8%) and 118 de novo inflammatory arthritis cases (1.5%). Rheumatic diseases (either preexisting rheumatic diseases or rheumatic irAEs) were a common indication for immunomodulatory drug use (27.9%). Baseline predictors of rheumatic irAEs included melanoma (multivariable OR 4.06 [95% CI 2.54–6.51]) and genitourinary (GU) cancer (OR 2.22 [95% CI 1.39–3.54]), both relative to patients with lung cancer; combination ICI treatment (OR 2.35 [95% CI 1.48–3.74]), relative to patients receiving programmed death 1 inhibitor monotherapy; autoimmune disease (OR 2.04 [95% CI 1.45–2.85]) and recent glucocorticoid use (OR 2.13 [95% CI 1.51–2.98]), relative to patients not receiving a glucocorticoid, compared to the 2,312 controls without rheumatic irAEs. Predictors of de novo inflammatory arthritis were similar to those of rheumatic irAEs.

Conclusion. We identified novel predictors of rheumatic irAE development in cancer patients, including baseline presence of melanoma, baseline presence of GU tract cancer, preexisting autoimmune disease, receiving or having received combination ICI treatment, and receiving or having received glucocorticoids. The proportion of cancer patients experiencing rheumatic irAEs may be even higher than was reported in the present study, since we used stringent criteria to identify cases of rheumatic irAEs. Our findings could be used to identify cancer patients at risk of developing rheumatic irAEs and de novo inflammatory arthritis and may help further elucidate the pathogenesis of rheumatic irAEs in patients with cancer who are receiving ICI treatment.

The funders had no role in the preparation of or the decision to publish this article. The content is solely the responsibility of the authors and does not necessarily represent the official views of Harvard University, its affiliated academic health care centers, or the NIH.

Dr. Sparks' work was supported by the National Institute of Arthritis and Musculoskeletal and Skin Diseases, NIH (grants K23-AR-069688, R03-AR-075886, L30-AR-066953, P30-AR-070253, and P30-AR-072577), the Rheumatology Research Foundation R Bridge award, and the R. Bruce and Joan M. Mickey Research Scholar Fund.

[1]Amy Cunningham-Bussel, MD, PhD, Lydia Gedmintas, MD, MPH, Lindsey A. MacFarlane, MD, MPH, Nancy A. Shadick, MD, MPH, Ellen M. Gravallese, MD, Jeffrey A. Sparks, MD, MMSc: Brigham and Women's Hospital and Harvard Medical School, Boston, Massachusetts; [2]Jiaqi Wang, MS, Lauren C. Prisco, BA, Lily W. Martin, BS, Kathleen M. M. Vanni, BA, Alessandra Zaccardelli, MS: Brigham and Women's Hospital, Boston, Massachusetts; [3]Mazen Nasrallah, MD: Massachusetts General Hospital and Harvard Medical School, Boston, Massachusetts; [4]Mark M. Awad, MD, PhD, Osama Rahma, MD: Harvard Medical School and Dana-Farber Cancer

INTRODUCTION

Up to 40% of all cancer patients in the US may soon be eligible to receive an immune checkpoint inhibitor (ICI) (1). Unrestrained immune activation by antagonizing the programmed death 1 (PD-1), programmed death ligand 1 (PD-L1), or CTLA-4 pathways in cancer treatment has caused the emergence of a collection of disparate iatrogenic immune diseases that can affect virtually any organ system, collectively referred to as immune-related adverse events (irAEs). Patients with severe irAEs and those with irAEs refractory to glucocorticoid treatment often require subspecialist evaluation and prescription of an immunomodulatory medication (2). The proportion of patients treated with ICIs that require evaluation by a rheumatologist has not been clearly defined (3–8). Relatively small observational studies of patients with diverse irAEs are currently available to advise clinicians on the selection of initial immunomodulatory therapy (no randomized clinical trials are currently available) (6,9–20).

De novo inflammatory arthritis is the most common type of rheumatic irAE, occurring in 2–7% of all ICI recipients, but baseline predictors at ICI initiation have not been identified (6,21–25). Prior studies often lacked a comparator group, and ICI clinical trials typically included patients with a single cancer type, powered for efficacy outcomes rather than predictors of uncommon irAEs. These limitations have precluded the identification of predictors of rheumatic irAEs (24,26–28).

Therefore, we aimed to 1) quantify the role of rheumatologists in the management of ICI recipients, 2) describe the initial immunomodulatory drug prescribed for treating severe/refractory irAEs, and 3) identify baseline predictors of rheumatic irAEs and de novo inflammatory arthritis in a large tertiary care center and cancer institute.

PATIENTS AND METHODS

Study design and population. We performed a retrospective study of all cancer patients from 2011–2020 who initiated an ICI at either Mass General Brigham, a tertiary health care system, or the Dana-Farber Cancer Institute, both located in Boston, Massachusetts. We examined the individual electronic data repositories for each institution, the Research Patient Data Registry at Mass General Brigham and the Oncology Data Retrieval System at the Dana-Farber Cancer Institute, to identify all individuals who had received an ICI up to May 1, 2020. In addition, we identified all patients who were evaluated by a rheumatologist during the study period or those who were or prescribed an immunomodulatory drug after the index date (with the index date being defined as the date of the initial ICI prescription), and we reviewed the electronic health records for cases of rheumatic and nonrheumatic irAEs. We then performed a case–control study to identify baseline predictors of outcomes after initiation of the ICI treatment. This study was approved by the institutional review boards of both Mass General Brigham and the Dana-Farber Cancer Institute.

Identification of initial ICI treatment and cancer diagnosis. We included patients who were >18 years of age and had received treatment with ≥1 ICI targeting PD-1 (pembrolizumab, nivolumab, cemiplimab), PD-L1 (atezolizumab, avelumab, durvalumab), and/or CTLA-4 pathway (ipilimumab, tremelimumab) as part of routine clinical care for cancer treatment. Cancer patients who received these medications in combination with traditional chemotherapy were also included. Combination therapy was defined as simultaneous administration of ICI drugs targeting both PD-1/PD-L1 and CTLA-4.

We used a hierarchical approach to identify the type of cancer for which an ICI was prescribed. We identified histologic tumor biopsy results if these data were available in the Oncology Data Retrieval System. If no histologic data were available, we searched for diagnosis codes in the electronic health records for the year prior to the index date. If a patient had a code for a single type of cancer, this defined the cancer type. For patients without a code or >1 code, we performed a medical record review to determine the cancer type. Cancer types were ultimately grouped by the site of origin, since the histologic subtype was not universally available. However, we reported the subtype of lung cancer (non–small cell, small cell, neuroendocrine, or other) for those who had histologic data available.

Rheumatology evaluation after ICI treatment. Among ICI recipients, we identified all patients who were evaluated by a rheumatologist after initiating ICI therapy, using codes to identify rheumatology clinic visits or inpatient consultation visits at each Mass General Brigham or Dana-Farber Cancer Institute location. We then reviewed the electronic health records to collect the following data: confirmation that the evaluation occurred after initial ICI treatment, reason for consultation, presence/type of preexisting rheumatic/autoimmune disease, rheumatologist's clinical impression, presence and type of any rheumatic or nonrheumatic irAEs throughout the follow-up. If patients with preexisting rheumatic disease experienced a flare after ICI treatment, these were not considered to be irAEs (e.g., a patient with rheumatoid arthritis [RA] who

Institute, Boston, Massachusetts; [5]Nicole R. LeBoeuf, MD, MPH: Harvard Medical School, Dana-Farber Cancer Institute, and Brigham and Women's Hospital, Boston, Massachusetts.

Author disclosures are available at https://onlinelibrary.wiley.com/action/downloadSupplement?doi=10.1002%2Fart.41949&file=art41949-sup-0001-Disclosureform.pdf.

Address correspondence to Jeffrey A. Sparks, MD, MMSc, or Amy Cunningham-Bussel MD, PhD, Division of Rheumatology, Inflammation, and Immunity, Brigham and Women's Hospital, 60 Fenwood Road, Boston, MA 02115. Email: jsparks@bwh.harvard.edu or acunningham-bussel@bwh.harvard.edu.

Submitted for publication May 8, 2021; accepted in revised form August 5, 2021.

presented with inflammatory arthritis after ICI was considered to have a flare, not a rheumatic irAE). If a patient with a preexisting rheumatic disease developed a new manifestation, this was considered a new rheumatic irAE (e.g., a patient with RA who presented with myositis after ICI treatment was considered to have a rheumatic irAE).

Immunomodulatory drug prescription after ICI treatment. To determine additional cases of rheumatic irAEs, we identified immunomodulatory drug prescriptions after initiation of the initial ICI treatment. The term "immunomodulatory" refers to any of 55 medications, excluding glucocorticoids and nonsteroidal antiinflammatory drugs, used to treat any irAE (for the immunomodulatory drug list, see Supplementary Table 1, available on the *Arthritis & Rheumatology* website at http://onlinelibrary.wiley.com/doi/10.1002/art.41949/abstract). The list of immunomodulatory drugs was created based on our review of published guidelines, expert advice, and clinical experience (9,14,29). A limited electronic health record screening was performed to exclude patients who received immunomodulatory drugs for indications other than irAEs (e.g., rituximab use for lymphoma treatment was excluded).

We then performed a detailed medical record review to collect the following data: presence/type of preexisting rheumatic/autoimmune disease, irAE type necessitating immunomodulatory therapy, type of subspecialist who prescribed the immunomodulatory drug, setting of the prescription (inpatient or outpatient), and all irAEs that occurred throughout follow-up. In order to avoid double counting, we reported only the immunomodulatory drug initially prescribed to the patient, and the date of first immunomodulatory drug prescription was used as a proxy for the date of irAE diagnosis. Only a subset of patients received many immunomodulatory drugs, but it was beyond the scope of this current study to present the clinical course and trajectory of these patients with refractory irAEs.

Rheumatic irAEs and de novo inflammatory arthritis. By reviewing all patients with clinical encounters with a rheumatologist and all immunomodulatory drug prescriptions after the initiation of ICI, we identified all patients with verifiable rheumatic irAEs and also enriched for cases of severe irAEs affecting a range of organ systems. We categorized rheumatic irAEs into clinical subtypes that included de novo inflammatory arthritis, arthralgia (without documented synovitis), polymyalgia rheumatica–like syndrome, myositis, myalgia (without objective evidence of myositis), vasculitis, sarcoidosis, sicca syndrome, dermatomyositis, and serositis based on symptoms, physical examination, imaging, and test results in clinical care. De novo inflammatory arthritis was defined as a new-onset inflammatory arthritis, classified as a rheumatic irAE that was diagnosed after initiation of the first ICI treatment in a patient who had no preexisting inflammatory arthritis. To be categorized as having de novo inflammatory arthritis, we required documentation of objective evidence of both joint tenderness and swelling on physical examination or imaging evidence compatible with synovitis (22,30). To confirm the presence of other types of rheumatic or nonrheumatic irAEs, we required documented evidence from a rheumatologist or treating physician supporting that diagnosis.

The medical records for all individuals with rheumatic irAEs included in this study were independently reviewed by at least 2 board-certified rheumatologists (ACB, LG, LAM, and JAS) to confirm the diagnoses (23,31). Disagreements were adjudicated by a third rheumatologist until there was complete agreement. It was possible for individual patients to have more than 1 rheumatic irAE. Evaluation by a rheumatologist or objective documentation of the rheumatic irAE was required to fulfill our strict case definition. However, those who never saw a rheumatologist or never received an immunomodulatory drug would not have been identified using our case-finding approach.

Controls without rheumatic irAEs. Controls were patients who did not experience rheumatic irAEs, did not have preexisting rheumatic disease, did not have a clinical evaluation by a rheumatologist after ICI treatment, did not receive an immunomodulatory drug after ICI treatment, did not receive systemic glucocorticoids after ICI treatment, and survived at least 6 months after the initial treatment with an ICI (to exclude patients with early death or insufficient follow-up time). Thus, the controls in this analysis were unlikely to have experienced a rheumatic irAE. We reviewed the medical records of 100 randomly selected patients fulfilling this definition, and none were found to have a rheumatic irAE (negative predictive value 100%). An alternative control group was defined using the same characteristics as above except that they were required to have received a glucocorticoid after ICI initiation, to examine whether findings were specific to rheumatic irAEs or could be explained by other types of irAEs. While our analysis focused on predictors at baseline (time of ICI initiation), we also considered post-baseline factors as mediators. Post-baseline mediating factors included the total number of infusions of ICI received and the duration of ICI, which were included in models as a secondary analysis to determine whether these mediators may explain the associations of baseline predictors with rheumatic irAE development.

Baseline predictors at the time of initial ICI treatment. To identify baseline predictors, we collected data from all patients through an electronic query form, which was completed by each patient as of, or prior to, the time of initial ICI treatment. These data included age, sex, race, cancer type, target of index ICI treatment, monotherapy or combination ICI therapy, comorbidities measured using the Charlson comorbidity index (over the preceding 365 days), preexisting rheumatic or nonrheumatic autoimmune disease identified using diagnosis codes noted in the electronic health records (Supplementary Table 2, available on the *Arthritis & Rheumatology* website at

http://onlinelibrary.wiley.com/doi/10.1002/art.41949/abstract), immunomodulatory drug use and timing (never use versus recent use [within 1 year of ICI initiation] versus distant use [more than 1 year prior to ICI initiation]), and systemic glucocorticoid use and timing (never use versus recent use [within 1 year of ICI initiation] versus distant use [more than 1 year prior to ICI initiation]) (32). We reviewed the medical records of 100 randomly selected patients who received a prescription for a glucocorticoid before ICI initiation to determine the indication for the prescription.

Statistical analysis. Descriptive statistics from the baseline time point are reported as the mean ± SD for normal continuous variables, median and interquartile range (IQR) for non-normal continuous variables, and frequency and proportions for categorical variables. We also reported descriptive statistics of type, count, and duration of ICI use according to each cancer type.

For those evaluated by a rheumatologist after ICI treatment, we reported descriptive statistics for predictor variables at baseline and after final evaluation, type of rheumatic irAE, disease type/organ involvement by other irAEs, and total number of irAEs experienced on a patient level. For those who initiated treatment with an immunomodulatory drug after initiation of the ICI treatment, we reported descriptive statistics for predictor variables at baseline and defined additional clinical outcomes surrounding the initiation

Table 1. Baseline demographic and clinical characteristics of the 8,028 cancer patients at initiation of ICI therapy*

Characteristic	Value	Characteristic	Value
Age		Target of ICI	
≤49 years	1,007 (12.5)	PD-1	6,118 (76.2)
50–≤59 years	1,650 (20.6)	CTLA-4	647 (8.1)
60–≤69 years	2,530 (31.5)	PD-L1	615 (7.7)
>70 years	2,841 (35.4)	Combination	648 (8.1)
Demographic characteristics		Preexisting autoimmune disease	
Age, mean ± SD years	65.5 ± 13.1	No autoimmune disease	5,704 (71.1)
White	7,268 (90.5)	Nonrheumatic autoimmune disease	1,935 (24.1)
Sex, female	3,463 (43.1)	Any rheumatic disease	389 (4.9)
Cancer type		RA	187 (2.3)
Lung	2,502 (31.2)	Unspecified vasculitis	63 (0.8)
Non–small cell	1,120 (14.0)	Polymyalgia rheumatica	62 (0.8)
Small cell	154 (1.9)	ANCA-associated vasculitis	56 (0.7)
Neuroendocrine	5 (0.1)	Inflammatory polyarthropathy	50 (0.6)
No histologic data available	1,223 (15.2)	Sarcoidosis	35 (0.4)
Melanoma	1,711 (21.3)	PsA	33 (0.4)
GU tract	1,204 (15.0)	SLE	25 (0.3)
GI tract	757 (9.4)	SSc	17 (0.2)
Head and neck	527 (6.6)	CREST syndrome	15 (0.2)
Hematologic	388 (4.8)	SS	10 (0.1)
Brain	302 (3.8)	AS	9 (0.1)
Breast	266 (3.3)	APS	9 (0.1)
More than 1 cancer type	17 (0.2)	MCTD	8 (0.1)
Other type	354 (4.4)	Inflammatory myositis	6 (0.1)
ICI therapy		Dermatomyositis	6 (0.1)
Monotherapy	7,380 (91.9)	Polyarteritis nodosa	3 (0.04)
Combination therapy	648 (8.1)	Charlson comorbidity index, mean ± SD	6 ± 1.5
Type of ICI		Immunomodulatory drug use	
Pembrolizumab	3,791 (47.2)	Never	7,627 (95.0)
Nivolumab	2,256 (28.1)	Distant only†	178 (2.2)
Ipilimumab	641 (8.0)	Recent‡	223 (2.8)
Ipilimumab and nivolumab	636 (7.9)	Glucocorticoid use	
Atezolizumab	587 (7.3)	Never	4,542 (56.6)
Durvalumab	49 (0.6)	Distant only†	501 (6.2)
Avelumab	28 (0.4)	Recent‡	2,985 (37.2)
Cemiplimab	22 (0.3)		
Ipilimumab and pembrolizumab	7 (0.1)		
Tremelimumab	6 (0.1)		
Durvalumab and tremelimumab	5 (0.1)		

* Except where indicated otherwise, values are the number (%) of patients. GU = genitourinary; GI = gastrointestinal; PD-1 = programmed death 1; PD-L1 = programmed death ligand 1; RA = rheumatoid arthritis; ANCA = antineutrophil cytoplasmic antibody; PsA = psoriatic arthritis; SLE = systemic lupus erythematosus; SSc = systemic sclerosis; CREST syndrome = calcinosis, Raynaud's phenomenon, esophageal dysmotility, sclerodactyly, telangiectasias; SS = Sjögren's syndrome; AS = ankylosing spondylitis; APS = antiphospholipid syndrome; MCTD = mixed connective tissue disease.
† Distant use indicates use >1 year after immune checkpoint inhibitor (ICI) initiation.
‡ Recent use indicates use ≤1 year after ICI initiation.

of an immunomodulatory drug as follows: the type and clinical indication for the immunomodulatory drug (e.g., irAE, flare of preexisting autoimmune disease), type of rheumatic irAE, number of irAEs, disease type/organ involvement in other irAEs, and finally, the clinical setting and prescriber of the immunomodulatory drug. We also reported the median number of days from baseline to either a rheumatology evaluation or immunomodulatory drug initiation, stratified according to the rheumatic irAE and preexisting rheumatic or autoimmune disease.

We then evaluated baseline predictors of the following outcomes in separate models. We used logistic regression to estimate the odds ratios (OR) and 95% confidence intervals (95% CIs) for the risk of occurrence of outcomes using the same set of baseline predictor variables as used in the main regression model. Base models were unadjusted. We then performed a multivariable model that included all potential predictors in a single model. We chose to include the target of ICI therapy in the multivariable models rather than individual ICIs. Lung cancer was chosen as

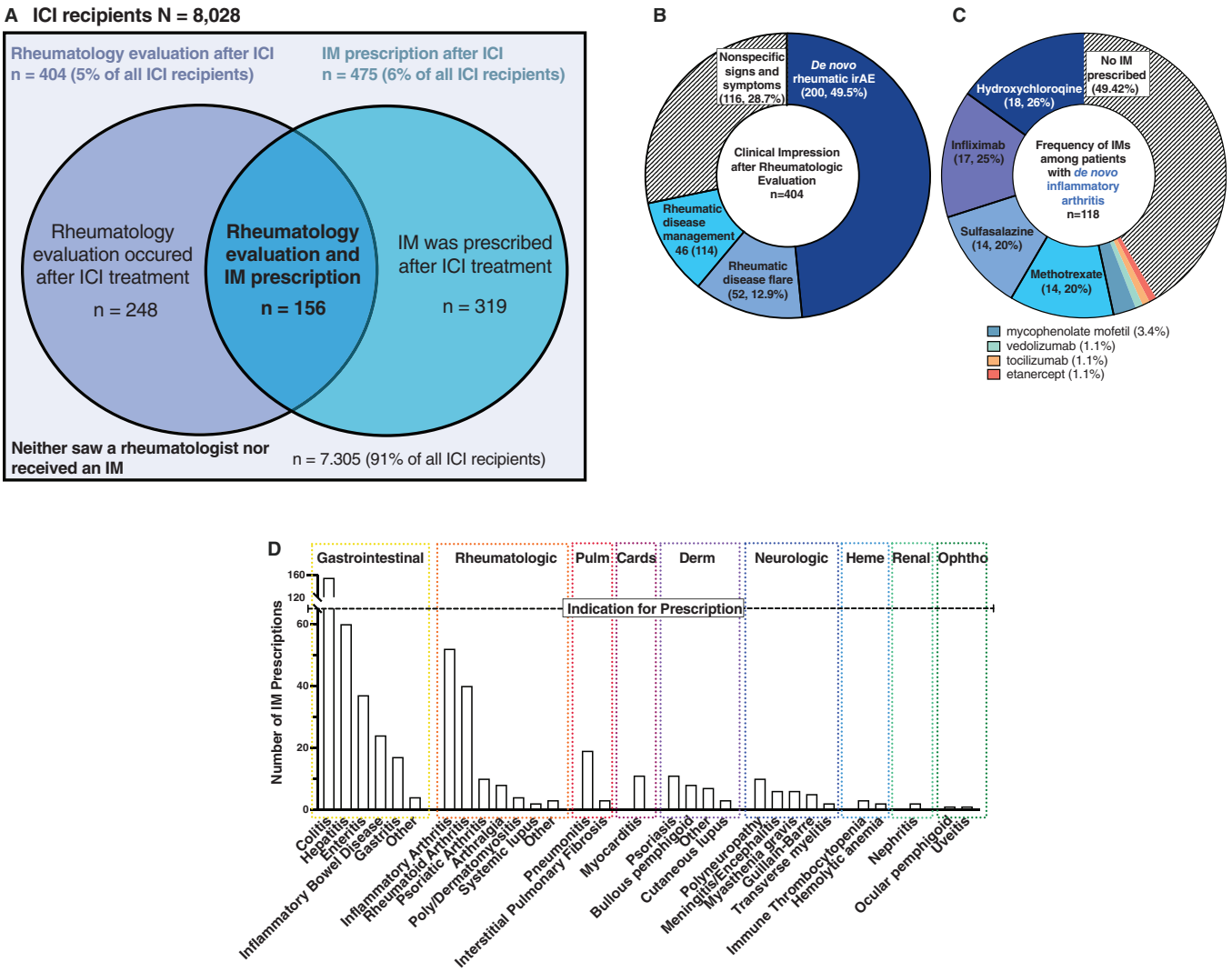

Figure 1. Rheumatology evaluation and immunomodulatory drug use after initial immune checkpoint inhibitor (ICI) treatment for cancer and the resulting occurrence of immune-related adverse events (irAEs). **A**, Venn diagram depicting the frequency and proportion of patients evaluated by a rheumatologist, patients who received a prescription for an immunomodulatory (IM) drug, and patients who received both a rheumatology evaluation and an immunomodulatory drug prescription. **B**, Clinical impressions following evaluation by a rheumatologist. **C**, The frequency and initial type of immunomodulatory drug prescribed among the 118 patients with de novo inflammatory arthritis. **D**, Frequency of specific irAEs, stratified according to the involved organ system (n = 475). Other indications necessitating treatment with immunomodulatory drugs were indications related to either the gastrointestinal (GI) tract, rheumatic diseases, or dermatologic (Derm) symptoms. GI indications included cholangitis (n = 1), pancreatitis (n = 1), and celiac disease (n = 2). Rheumatic disease–related indications included gout (n = 1), Sjögren's syndrome (n = 1), and tendonitis (n = 1). Dermatologic indications included dermatitis (n = 4), lichenoid eruption (n = 1), granuloma annulare (n = 1), and pemphigus vulgaris (n = 1). Pulm = pulmonary; Cards = cardiovascular; Heme = hematologic; Ophtho = ophthalmologic.

the reference group for all analyses considering cancer type, since it was the most common cancer.

Since it was possible that some rheumatic irAEs occurred that we did not detect, we performed a case–control study so that rheumatic irAE case or control status was known. Cases were defined as patients with rheumatic irAEs, while controls were defined as those unlikely to have a rheumatic irAE. We used the same modeling approach for the case–control analysis. We further performed a separate case–control analysis with de novo inflammatory arthritis cases as the outcome, since this was the most common rheumatic irAE and may be relatively homogeneous. Statistical significance was defined as a 2-sided *P* value less than 0.05. We did not adjust for multiple comparisons in this hypothesis-generating study. Analyses were performed using SAS software version 9.4 (SAS Institute).

RESULTS

Baseline demographic characteristics among all ICI recipients. We identified 8,028 patients who received treatment with an ICI (mean age 65.5 years, 43.1% female). Baseline characteristics are shown in Table 1. The most common cancer types were lung cancer (31.2%), melanoma (21.3%), and genitourinary (GU) tract cancer (15.0%). At baseline (the start of ICI treatment), for the initial ICI, 47.2% began treatment with pembrolizumab, 28.1% began treatment with nivolumab, and 8.0% began treatment with ipilimumab, while 7.9% were given combination treatment with ipilimumab and nivolumab. Additional descriptive statistics on type, count, and duration of ICI use after the baseline time point are included in Supplementary Tables 3 and 4 (available on the *Arthritis & Rheumatology* website at http://onlinelibrary.wiley.com/doi/10.1002/art.41949/abstract).

Among ICI recipients, 4.9% had preexisting rheumatic disease and 24.1% had preexisting nonrheumatic autoimmune disease. We identified 2,985 individuals (37.2%) who had received a systemic glucocorticoid within the year before the index date and 501 patients (6.2%) who had received a glucocorticoid >1 year before the index date. After reviewing 50 medical records from each of these groups, we determined that glucocorticoids were often administered along with traditional chemotherapy (see Supplementary Table 5, available on the *Arthritis & Rheumatology* website at http://onlinelibrary.wiley.com/doi/10.1002/art.41949/abstract). At baseline, 2.8% of patients had received an immunomodulatory drug within the year prior to the index date and 2.2% of patients had received an immunomodulatory drug >1 year before the index date.

Patients evaluated by a rheumatologist after initiation of an ICI. We identified 404 patients (5.0% of all ICI recipients) who were evaluated by a rheumatologist after initiating an ICI (Figure 1A and Table 2). The most common conclusion following the rheumatologist's clinical evaluation was the diagnosis of a rheumatic irAE, which was identified in 200 patients (49.5%), among whom 118 (29.2%) had de novo inflammatory arthritis, the most common rheumatic irAE. Of the remaining patients, rheumatologists diagnosed 98 patients (24.3%) as having a preexisting rheumatic disease, of whom 52 patients (12.9%) were determined to have experienced a flare following ICI initiation (Figure 1B and Table 3). The remaining 116 patients (28.7%) had nonspecific signs and symptoms not clearly attributable to ICI treatment. Of all irAEs that developed in the 404 patients, 234 unique rheumatic irAEs (57.9%) were identified. While 158 patients (39.1%) developed 1 irAE, 75 patients (18.6%) developed 2 irAEs, 34 patients (8.4%) developed 3 irAEs, and 26 patients (6.4%) developed ≥4 different irAEs.

Initial immunomodulatory drug treatment after initiation of an ICI. We identified 475 patients (5.9%) who received an immunomodulatory drug after initiating an ICI (Figure 1A and Table 3). Among patients who developed de novo inflammatory arthritis, the most frequently prescribed initial immunomodulatory drugs were hydroxychloroquine (18 [26%]), infliximab (17 [25%]), methotrexate (14 [20%]), and sulfasalazine (14 [20%]) (Figure 1C). The frequency of immunomodulatory drug treatment and the type of irAE, whether rheumatic or nonrheumatic, for which an immunomodulatory drug was prescribed are shown in Supplementary Figure 1 (http://onlinelibrary.wiley.com/doi/10.1002/art.41949/abstract) and Figure 1D, respectively.

The clinical indications for immunomodulatory drug treatment included nonrheumatic irAE (289 [60.8%]), rheumatic irAE (110 [23.2%]), flare of preexisting rheumatic disease (16 [3.4%]), and maintenance of quiescent rheumatic disease (6 [1.3%]). Overall, 117 immunomodulatory drugs (24.6%) were prescribed by rheumatologists in the outpatient setting (321 [67.6%]). Rheumatologists were the second most frequent immunomodulatory drug prescriber after inpatient physicians, and the most frequent outpatient subspecialist to prescribe any immunomodulatory drug to ICI recipients. Patients who were prescribed an immunomodulatory drug for a rheumatic irAE received this prescription a median of 228 days (IQR 87–476) after initiating an ICI, compared to a median of 132 days (IQR 58–274) after initiating an ICI for patients with a nonrheumatic indication.

Baseline predictors of rheumatic irAEs and de novo inflammatory arthritis. The case–control analysis to identify baseline predictors included 226 rheumatic irAE cases (the types of rheumatic irAE cases are listed in Supplementary Figure 2, available on the *Arthritis & Rheumatology* website at http://onlinelibrary.wiley.com/doi/10.1002/art.41949/abstract), of which 118 were de novo inflammatory arthritis cases, each compared to 2,312 controls (Table 4). The presence of melanoma (multivariable OR 4.06 [95% CI 2.54, 6.51]) and GU tract cancers (OR 2.22 [95% CI 1.39, 3.54]) was each associated with increased odds of developing a rheumatic irAE as compared

Table 2. Clinical characteristics of the patients who received ICI therapy and were evaluated by a rheumatologist or those who received ICI therapy and were treated with an immunomodulatory drug*

	ICI-treated patients evaluated by a rheumatologist (n = 404)	ICI-treated patients who received an immunomodulatory drug (n = 475)
Preexisting autoimmune disease	308 (76.2)	367 (77.3)
No autoimmune disease	91 (22.5)	74 (15.6)
Rheumatic disease		
RA	48 (11.9)	43 (9.1)
PsA	11 (2.7)	11 (2.3)
Polymyalgia rheumatica	9 (2.2)	4 (0.8)
Other inflammatory arthritis	7 (1.7)	4 (0.8)
SLE	5 (1.2)	4 (0.8)
PsO	0 (0)	3 (0.6)
DM/PM	3 (0.7)	2 (0.4)
Sarcoidosis	2 (0.5)	0 (0)
SS	2 (0.5)	2 (0.4)
SpA	2 (0.5)	1 (0.2)
AS	1 (0.2)	0 (0)
APS	1 (0.2)	1 (0.2)
GCA	1 (0.2)	0 (0)
MCTD	1 (0.2)	0 (0)
SSc	1 (0.2)	0 (0)
Vasculitis	1 (0.2)	0 (0)
Erythema nodosum	0 (0)	1 (0.2)
Other	5 (1.2)	34 (7.2)
Disease type or organ involved according to other irAE		
Rheumatic	234 (57.9)	126 (26.5)
GI	135 (33.4)	389 (81.9)
Endocrine	69 (17.1)	62 (13.1)
Pulmonary	33 (8.2)	49 (10.3)
Dermatologic	31 (7.7)	48 (10.1)
Ophthalmic	15 (3.7)	22 (4.6)
Cardiac	6 (1.5)	18 (3.8)
Renal	6 (1.5)	11 (2.3)
Neurologic	2 (0.5)	27 (5.7)
Hematologic	1 (0.2)	11 (2.3)
No. of irAEs		
0	111 (27.5)	61 (12.8)
1	158 (39.1)	209 (44.0)
2	75 (18.6)	113 (23.8)
3	34 (8.4)	59 (12.4)
≥4	26 (6.4)	33 (6.9)

* Values are the number (%) of patients. All immune-related adverse events (irAEs) were counted individually and were not grouped according to the patient. For example, sicca syndrome and inflammatory arthritis occurring in the same patient would be counted as 2 unique rheumatic irAEs. PsO = psoriasis; DM = dermatomyositis; PM = polymyositis; SpA = spondyloarthritis; GCA = giant cell arteritis (see Table 1 for other definitions).

to the presence of lung cancer, in models adjusted for age, sex, race, target of ICI therapy, preexisting autoimmune disease, comorbidities, and baseline immunomodulator/glucocorticoid use. Compared to PD-1 monotherapy, use of combination ICI therapy was associated with an OR of 2.35 (95% CI 1.48, 3.74) for developing a rheumatic irAE. Preexisting non-rheumatic autoimmune disease was associated with an OR of 2.04 (95% CI 1.45, 2.85) for developing a rheumatic irAE. Receipt of a glucocorticoid in the year prior to initiation of ICI treatment was associated with an OR of 2.13 (95% CI 1.51, 2.98) for developing a rheumatic irAE, as compared to no glucocorticoid use.

When restricting the case definition to only de novo inflammatory arthritis, the results were similar. For example, in the multivariable analysis, the presence of melanoma (OR 2.91 [95% CI 1.58, 5.35]) and GU tract cancer (OR 2.36 [95% CI 1.32, 4.19]) was each associated with increased odds of having de novo inflammatory arthritis as compared to the presence of lung cancer. The results were also similar in the sensitivity analysis, in which controls were defined as those who had received a glucocorticoid after initiating ICI therapy; of note, many of these control patients likely experienced other types of irAEs (see Supplementary Table 6, available on the *Arthritis & Rheumatology* website at http://onlinelibrary.wiley.com/doi/10.1002/art.41949/abstract).

Table 3. Features identified by rheumatologist's clinical evaluation, initiation of IM drug treatment based on features from the evaluation, duration of ICI treatment, type of rheumatic irAE diagnosed by a rheumatologist, setting of the initial IM drug initiation, and prescriber of the initial IM drug*

Rheumatologist's clinical evaluation	
Rheumatic irAE due to ICI	200 (49.5)
Rheumatic disease flare	52 (12.9)
Rheumatic disease management, no flare	46 (11.4)
Nonrheumatic irAE	–
Preexisting (nonrheumatic) autoimmune disease flare	–
Management of preexisting (nonrheumatic) autoimmune disease	–
Nonspecific signs and symptoms	116 (28.7)
Rheumatologist's diagnosis necessitating IM drug initiation	
Rheumatic irAE due to ICI	110 (23.2)
Rheumatic disease flare	16 (3.4)
Rheumatic disease management, no flare	6 (1.3)
Nonrheumatic irAE	289 (60.8)
Preexisting (nonrheumatic) autoimmune disease flare	13 (2.7)
Management of preexisting (nonrheumatic) autoimmune disease	22 (4.6)
Nonspecific signs and symptoms	–
Days from initial ICI treatment to rheumatology encounter, median (IQR)	
All patients seen by a rheumatologist or receiving an IM drug after ICI	166 (67,365) [missing n = 18]
Rheumatic irAE	182 (100,357) [missing n = 2]
Nonrheumatic irAE	
History of rheumatic disease	41 (21,115) [missing n = 16]
History of other autoimmune disease	290 (17,308)
No history of autoimmune disease	213 (111,444) [missing n = 2]
Days from initial ICI treatment to prescription of IM drug, median (IQR)	
All patients seen by a rheumatologist or receiving an IM drug after ICI	151 (63,308)
Rheumatic irAE	228 (87,476)
Nonrheumatic irAE	132 (58,274)
History of rheumatic disease	63 (25,201)
History of other autoimmune disease	62 (21,265)
No history of autoimmune disease	170 (80,343)
Type of rheumatic irAE diagnosed by a rheumatologist	
Inflammatory arthritis	118 (29.2)
Arthralgia	62 (15.3)
Polymyalgia rheumatica	23 (5.7)
Sicca syndrome	11 (2.7)
Vasculitis	11 (2.7)
Myositis	10 (2.5)
Myalgia	4 (1.0)
Dermatomyositis	2 (0.5)
Sarcoidosis	1 (0.2)
Serositis	1 (0.2)
Uveitis	1 (0.2)
Setting of the initial IM drug initiation	
Outpatient	321 (67.6)
Inpatient	151 (31.8)
Prescriber of the initial IM drug	
Inpatient physician	153 (32.2)
Rheumatologist	117 (24.6)
Gastroenterologist	97 (20.4)
Outpatient oncologist	64 (13.5)
Dermatologist	23 (4.8)
Pulmonologist	8 (1.7)
Neurologist	4 (0.8)
Cardiologist	3 (0.6)
Ophthalmologist	2 (0.4)

* Except where indicated otherwise, values are the number (%) of patients. IM = immunomodulatory; irAE = immune-related adverse event; IQR = interquartile range (see Table 1 for other definitions).

In the multivariable model with inclusion of total number of ICI infusions and duration of ICI infusions as potential mediators, the association of rheumatic irAE development with baseline presence of melanoma (OR 3.85 [95% CI 2.39, 6.19]) and baseline presence of GU tract cancers (OR 2.23 [95% CI 1.39, 3.57]) remained significant. The results of this analysis were also similar for associations with de novo inflammatory arthritis (Supplementary Table 7, available on the *Arthritis & Rheumatology*

Table 4. Odds of development of a rheumatic irAE (n = 226) or de novo inflammatory arthritis (n = 118) among cancer patients after ICI initiation, relative to controls (n = 2,312)*

	Any rheumatic irAE		De novo inflammatory arthritis	
	Unadjusted OR (95% CI)	Multivariable OR (95% CI)†	Unadjusted OR (95% CI)	Multivariable OR (95% CI)†
Age				
≤49 years	1.00 (Referent)	1.00 (Referent)	1.00 (Referent)	1.00 (Referent)
50–≤59 years	0.87 (0.54, 1.39)	0.99 (0.59, 1.65)	1.24 (0.63, 2.45)	1.14 (0.56, 2.34)
60–≤69 years	0.96 (0.63, 1.47)	1.00 (0.62, 1.61)	1.30 (0.69, 2.46)	1.08 (0.55, 2.13)
>70 years	0.70 (0.45, 1.08)	0.68 (0.41, 1.12)	0.95 (0.50, 1.83)	0.80 (0.40, 1.62)
Race				
White	1.00 (Referent)	1.00 (Referent)	1.00 (Referent)	1.00 (Referent)
Non-White	1.50 (0.87, 2.58)	1.19 (0.66, 2.14)	1.99 (0.87, 4.58)	1.65 (0.69, 3.95)
Sex				
Male	1.00 (Referent)	1.00 (Referent)	1.00 (Referent)	1.00 (Referent)
Female	1.03 (0.78, 1.35)	1.10 (0.81, 1.50)	1.23 (0.85, 1.78)	1.31 (0.87, 1.96)
Malignancy type				
Lung	1.00 (Referent)	1.00 (Referent)	1.00 (Referent)	1.00 (Referent)
Hematologic	1.04 (0.43, 2.51)	1.06 (0.42, 2.68)	0.87 (0.26, 2.95)	0.81 (0.23, 2.92)
GI tract	0.77 (0.38, 1.56)	0.84 (0.36, 1.81)	0.39 (0.12, 1.30)	0.45 (0.13, 1.55)
Melanoma‡	3.34 (2.28, 4.91)	4.06 (2.54, 6.51)	2.59 (1.59, 4.32)	2.91 (1.58, 5.35)
Head and neck	0.77 (0.34, 1.75)	0.66 (0.27, 1.63)	0.93 (0.35, 2.46)	0.70 (0.23, 2.14)
GU tract‡	2.02 (1.32, 3.09)	2.22 (1.39, 3.54)	2.09 (1.22, 3.58)	2.36 (1.32, 4.19)
Brain	0.69 (0.27, 1.77)	0.81 (0.30, 2.15)	0.23 (0.03, 1.72)	0.26 (0.03, 2.02)
Breast	0.48 (0.15, 1.59)	0.61 (0.18, 2.06)	0.27 (0.04, 2.02)	0.31 (0.04, 2.39)
Other	1.35 (0.66, 2.77)	1.39 (0.66, 2.96)	1.36 (0.55, 3.39)	1.31 (0.51, 3.40)
ICI therapy				
Monotherapy	1.00 (Referent)	1.00 (Referent)	1.00 (Referent)	1.00 (Referent)
Combination‡	2.91 (1.92, 4.41)	–	2.77 (1.59, 4.83)	–
Target of ICI				
PD-1	1.00 (Referent)	1.00 (Referent)	1.00 (Referent)	1.00 (Referent)
PD-L1	0.62 (0.34, 1.14)	0.67 (0.35, 1.28)	0.70 (0.32, 1.53)	0.71 (0.31, 1.60)
CTLA-4	1.75 (1.11, 2.75)‡	0.87 (0.51, 1.49)	1.74 (0.95, 3.20)	1.05 (0.51, 2.17)
Combination‡	2.96 (1.94, 4.52)	2.35 (1.48, 3.74)	2.84 (1.61, 5.00)	2.31 (1.26, 4.25)
Type of ICI				
Pembrolizumab	1.00 (Referent)	1.00 (Referent)	1.00 (Referent)	1.00 (Referent)
Nivolumab	1.46 (1.04, 2.04)	–	1.63 (1.04, 2.56)‡	–
Ipilimumab‡	2.08 (1.29, 3.34)	–	2.16 (1.14, 4.11)	–
Atezolizumab	0.56 (0.28, 1.14)	–	0.63 (0.25, 1.60)	–
Durvalumab	6.83 (1.68, 27.76)‡	–	4.55 (0.54, 38.63)	–
Avelumab‡	13.65 (2.71, 68.64)	–	18.20 (2.96, 111.76)	–
Tremelimumab	–	–	–	–
Cemiplimab	5.46 (1.04, 28.56)‡	–	5.46 (0.62, 47.75)	–
Combination‡	3.52 (2.26, 5.50)	–	3.52 (1.93, 6.44)	–
Autoimmune disease				
No history of autoimmune disease	1.00 (Referent)	1.00 (Referent)	1.00 (Referent)	1.00 (Referent)
Nonrheumatic‡	1.98 (1.46, 2.69)	2.04 (1.45, 2.85)	2.64 (1.79, 3.90)	2.74 (1.79, 4.19)
Charlson comorbidity index				
Score category				
6–7	1.00 (Referent)	–	1.00 (Referent)	–
7–8	1.17 (0.75, 1.84)	–	1.41 (0.80, 2.48)	–
≥9	1.02 (0.63, 1.63)	–	0.84 (0.42, 1.69)	–
Score in units	0.95 (0.86, 1.06)	0.97 (0.85, 1.09)	1.01 (0.87, 1.16)	0.90 (0.76, 1.07)
Immunomodulatory drug use§				
Never	1.00 (Referent)	1.00 (Referent)	1.00 (Referent)	1.00 (Referent)
Distant¶	3.91 (1.72, 8.89)‡	1.07 (0.24, 4.86)	1.87 (0.44, 8.07)	0.92 (0.11, 7.44)
Recent#	3.42 (1.44, 8.10)‡	1.46 (0.45, 4.79)	5.62 (2.23, 14.15)†	3.28 (1.00, 10.79)
Glucocorticoid use				
Never	1.00 (Referent)	1.00 (Referent)	1.00 (Referent)	1.00 (Referent)
Distant¶	1.42 (0.80, 2.54)	1.14 (0.58, 2.24)	0.97 (0.38, 2.44)	0.80 (0.31, 2.11)
Recent‡#	2.07 (1.54, 2.79)	2.13 (1.51, 2.98)	2.15 (1.45, 3.19)	1.96 (1.26, 3.05)

* Controls were defined as patients who did not have preexisting rheumatic disease, did not receive a steroid or immunomodulatory drug after ICI initiation, did not have a clinical evaluation by a rheumatologist after ICI treatment, and survived ≥6 months after the initial ICI treatment. Values are the odds ratio (OR) with 95% confidence interval (95% CI). irAE = immune-related adverse event (see Table 1 for other definitions).
† The multivariable models were mutually adjusted for all covariates listed.
‡ $P < 0.05$.
§ Value obtained at the time of ICI therapy initiation.
¶ Distant use indicates use >1 year after ICI initiation.
# Recent use indicates use ≤1 year after ICI initiation.

Table 5. Odds of receiving an evaluation by a rheumatologist (n = 404) or receiving an immunomodulatory drug (n = 475) after ICI therapy initiation according to baseline demographic and clinical characteristics (n = 8,028)*

	Rheumatology evaluation		Immunomodulatory drug prescribed	
	Unadjusted OR (95% CI)	Multivariable OR (95% CI)†	Unadjusted OR (95% CI)	Multivariable OR (95% CI)†
Age				
≤49 years	1.00 (Referent)	1.00 (Referent)	1.00 (Referent)	1.00 (Referent)
50–≤59 years	1.16 (0.81, 1.68)	1.17 (0.80, 1.72)	1.04 (0.76, 1.43)	1.23 (0.87, 1.72)
60–≤69 years	1.19 (0.84, 1.67)	1.18 (0.82, 1.69)	0.95 (0.70, 1.28)	1.15 (0.83, 1.59)
>70 years	1.04 (0.74, 1.47)	0.88 (0.61, 1.27)	0.82 (0.60, 1.10)	0.96 (0.69, 1.34)
Race				
Non-White	1.00 (Referent)	1.00 (Referent)	1.00 (Referent)	1.00 (Referent)
White	1.27 (0.87, 1.85)	0.96 (0.65, 1.42)	2.76 (1.72, 4.45)	1.98 (1.20, 3.26)
Sex				
Male	1.00 (Referent)	1.00 (Referent)	1.00 (Referent)	1.00 (Referent)
Female	1.04 (0.85, 1.27)	0.98 (0.79, 1.22)	1.13 (0.93, 1.36)	1.13 (0.92, 1.39)
Malignancy type				
Lung	1.00 (Referent)	1.00 (Referent)	1.00 (Referent)	1.00 (Referent)
Hematologic	0.66 (0.34, 1.28)	0.43 (0.21, 0.86)	1.05 (0.60, 1.84)	0.46 (0.25, 0.84)
GI tract	0.65 (0.39, 1.08)	0.72 (0.43, 1.21)	0.64 (0.38, 1.06)	0.70 (0.41, 1.19)
Melanoma	2.37 (1.82, 3.08)	2.75 (2.01, 3.77)	4.38 (3.42, 5.61)	4.21 (3.15, 5.53)
Head and neck	0.73 (0.42, 1.26)	0.78 (0.44, 1.38)	0.98 (0.59, 1.62)	1.00 (0.59, 1.68)
GU tract	1.84 (1.36, 2.48)	2.31 (1.67, 3.18)	1.09 (0.76, 1.55)	1.20 (0.83, 1.74)
Brain	0.67 (0.32, 1.40)	0.73 (0.34, 1.55)	1.27 (0.72, 2.26)	1.25 (0.68, 2.28)
Breast	0.57 (0.25, 1.32)	0.64 (0.27, 1.51)	1.35 (0.74, 2.44)	1.56 (0.84, 2.91)
Other	1.19 (0.70, 2.02)	1.31 (0.76, 2.28)	0.80 (0.42, 1.51)	0.68 (0.35, 1.32)
ICI therapy type				
Monotherapy	1.00 (Referent)	–	1.00 (Referent)	–
Combination	1.16 (0.82, 1.64)	–	2.53 (1.96, 3.27)	–
ICI target				
PD-1	1.00 (Referent)	1.00 (Referent)	1.00 (Referent)	1.00 (Referent)
PD-L1	0.91 (0.61, 1.36)	0.87 (0.56, 1.34)	0.38 (0.21, 0.67)	0.46 (0.25, 0.85)
CTLA-4	1.48 (1.07, 2.04)	0.91 (0.62, 1.34)	2.44 (1.86, 3.18)	1.13 (0.83, 1.56)
Combination	1.20 (0.84, 1.70)	1.03 (0.71, 1.50)	2.69 (2.08, 3.49)	2.17 (1.62, 2.90)
Type of ICI				
Pembrolizumab	1.00 (Referent)	–	1.00 (Referent)	–
Nivolumab	1.06 (0.83, 1.36)	–	1.08 (0.85, 1.36)	–
Ipilimumab	1.51 (1.08, 2.13)	–	2.51 (1.88, 3.33)	–
Atezolizumab	0.76 (0.48, 1.21)	–	0.37 (0.20, 0.69)	–
Durvalumab	2.33 (0.91, 5.96)	–	1.27 (0.39, 4.13)	–
Avelumab	5.60 (2.24, 13.99)	–	0.72 (0.10, 5.34)	-
Tremelimumab	3.24 (0.95, 11.06)	–	1.95 (0.45, 8.40)	–
Cemiplimab	4.11 (0.48, 35.35)	–	3.90 (0.45, 33.54)	–
Combination	1.24 (0.86, 1.79)	–	2.78 (2.11, 3.67)	–
Autoimmune disease				
None	1.00 (Referent)	1.00 (Referent)	1.00 (Referent)	1.00 (Referent)
Rheumatic disease	8.13 (6.22, 10.63)	6.02 (4.26, 8.50)	3.66 (2.73, 4.92)	1.78 (1.20, 2.62)
Other	1.24 (0.97, 1.59)	1.28 (0.98, 1.67)	1.32 (1.06, 1.64)	1.34 (1.05, 1.71)
Charlson comorbidity index				
Score category				
6–7	1.00 (Referent)	–	1.00 (Referent)	–
7–8	1.45 (1.09, 1.93)	–	1.21 (0.92, 1.60)	–
≥9	1.08 (0.80, 1.47)	–	0.83 (0.61, 1.12)	–
Score in units	1.03 (0.97, 1.10)	0.94 (0.87, 1.01)	0.98 (0.92, 1.05)	0.98 (0.91,1.06)
Immunomodulatory drug use‡				
Never	1.00 (Referent)	1.00 (Referent)	1.00 (Referent)	1.00 (Referent)
Distant§	5.23 (3.53, 7.76)	2.70 (1.70, 4.30)	3.46 (2.27, 5.28)	3.25 (2.00, 5.28)
Recent¶	7.17 (5.16, 9.95)	4.67 (3.15, 6.93)	9.41 (6.98, 12.68)	12.02 (8.22, 17.57)
Glucocorticoid use‡				
Never	1.00 (Referent)	1.00 (Referent)	1.00 (Referent)	1.00 (Referent)
Distant§	1.47 (1.00, 2.15)	1.11 (0.73, 1.69)	1.20 (0.83, 1.74)	1.30 (0.87, 1.96)
Recent¶	1.30 (1.05, 1.60)	1.12 (0.88, 1.42)	1.07 (0.88, 1.31)	1.12 (0.89, 1.40)

* Values are the odds ratio (OR) with 95% confidence interval (95% CI). See Table 1 for other definitions.
† The multivariable models were mutually adjusted for all covariates listed.
‡ Value obtained at the time of ICI therapy initiation.
§ Distant use indicates use >1 year after ICI initiation.
¶ Recent use indicates use ≤1 year after ICI initiation.

website at http://onlinelibrary.wiley.com/doi/10.1002/art.41949/abstract).

Baseline predictors associated with future evaluation by a rheumatologist after initiation of an ICI. Baseline variables that were significantly associated with future evaluation by a rheumatologist included baseline presence of melanoma (OR 2.75 [95% CI 2.01, 3.77]) or GU tract cancer (OR 2.31 [95% CI 1.67, 3.18]), both relative to patients with lung cancer; preexisting rheumatic disease (OR 6.02 [95% CI 4.26, 8.50]); and recently receiving or previously having received an immunomodulatory drug (OR 4.67 [95% CI 3.15, 6.93] and OR 2.70 [95% CI 1.70, 4.30], respectively), relative to patients with no baseline immunomodulatory drug use. Conversely, baseline presence of hematologic malignancy was inversely associated with future evaluation by a rheumatologist (OR 0.43 [95% CI 0.21, 0.86]), relative to patients with lung cancer (Table 5).

Baseline predictors of an immunomodulatory drug prescription after initiation of an ICI. Baseline factors positively associated with future receipt of any immunomodulatory drug included a diagnosis of melanoma (OR 4.21, [95% CI 3.15, 5.53]), relative to patients with lung cancer; receipt of combination ICI therapy (OR 2.17 [95% CI 1.62, 2.90]), relative to patients taking PD-1 monotherapy; preexisting rheumatic disease (OR 1.78 [95% CI 1.20, 2.62]); preexisting nonrheumatic autoimmune disease (OR 1.34 [95% CI 1.05, 1.71]); and receiving an immunomodulatory drug at baseline, either in the year prior to the initiation of ICI treatment (OR 12.02 [95% CI 8.22, 17.57]) or >1 year before initiating an ICI treatment (OR 3.25 [95% CI 2.00, 5.28]), both relative to patients with no baseline immunomodulatory drug use. Baseline presence of hematologic malignancy and receiving or having received PL-L1 antagonist treatment were each inversely associated with future receipt of an immunomodulatory drug (for hematologic malignancy, OR 0.46 [95% CI 0.25, 0.84]), relative to patients with lung cancer; for those receiving PL-L1 antagonist treatment (OR 0.46 [95% CI 0.25, 0.85]), relative to patients receiving PD-1 monotherapy (Table 5).

DISCUSSION

Among >8,000 ICI-treated cancer patients within a large, single-center hospital network and affiliated cancer institute, melanoma, GU tract cancers, preexisting nonrheumatic autoimmune disease, and receipt of combination therapy were identified as potential predictors for the development of rheumatic irAEs, as well as development of de novo inflammatory arthritis. In this large cohort, rheumatologists prescribed ~25% of all immunomodulatory drugs and were central to the care of patients who developed severe or refractory irAEs. These results build on prior research, contributing toward the identification of patients at risk of developing rheumatic irAEs.

A pervasive limitation to the study of rheumatic irAEs has been the challenge in assembling large cohorts with sufficient numbers of patients with systematically identified rheumatic irAEs. To date, only a limited set of clinical parameters have been identified as risk factors for the development of a rheumatic irAE, including a personal or family history of autoimmune disease, male sex, and age >65 years (33–36).

We identified melanoma and GU tract cancers as novel predictors of both rheumatic irAEs and de novo inflammatory arthritis. Melanoma was also associated with >4-fold increased odds of receiving or having received treatment with an immunomodulatory drug after ICI initiation. These associations were robust in both sensitivity analyses. In the first sensitivity analysis, the control group was defined as those control subjects who received treatment with glucocorticoids after ICI initiation. In the second sensitivity analysis, the post-baseline predictor variables included total number of ICI infusions and duration of ICI infusions. These results support the presence of an underlying biologic mechanism by which patients with melanoma and GU tract cancers may be uniquely susceptible to rheumatic irAEs. Importantly, these findings were consistent even after excluding patients from the control population who died soon after ICI treatment, to account for potential immortal time bias. Both melanoma and GU tract cancers are considered to be "inflammatory tumors," which may be what makes them highly responsive to ICI therapy (37). Inflammatory tumors have high numbers of somatic mutations within the tumor genome and express immunogenic, aberrant proteins referred to as tumor neoantigens (38). Thus, an intriguing hypothesis is that increased immune recognition of neoantigens within the tumor may culminate in a higher burden of inflammation at distant tissue, clinically recognized as irAEs (37,39). However, these findings may also be explained by nonbiologic factors.

The importance of rheumatologists in the evaluation and management of ICI-treated cancer is emphasized by the finding that rheumatologists were the most frequent prescribers of immunomodulatory drugs in the outpatient setting and that >60% of patients evaluated by a rheumatologist after ICI initiation were diagnosed as having a rheumatic irAE or had experienced a flare of a preexisting rheumatic disease. If the date of an immunomodulatory drug prescription is a proxy for the date of irAE diagnosis, patients with rheumatic irAEs were initially prescribed immunomodulatory drugs ~100 days later than those with nonrheumatic irAEs. This supports the possibility that there is a lack of recognition or delay in appropriate referral of rheumatic irAEs (40). However, it is also possible that the onset of rheumatic irAEs occurs relatively later in the immunomodulatory treatment course as compared to that of other types of irAEs, or that the development of a rheumatic irAE may be related to the increased survival of cancer patients who are receiving these treatments.

As it stands, relatively little data exist to guide the selection of appropriate immunomodulatory treatment for the diverse variety

of irAEs that can occur. There is a reliance on glucocorticoids as initial treatment for irAEs, as evidenced by our study of 8,028 patients, among whom only 475 (5.9%) received an immunomodulatory drug for an irAE, and clinicians generally hesitate to prescribe immunomodulatory treatment given the possibility that they might impede the anticancer response of ICIs. Case series of patients receiving immunomodulatory drugs after ICI initiation have been published, but these are typically small and do not include association analyses due to the undefined denominator from which these cases were identified (3,6–8,21,22,41). Similar to findings from previously published studies, we observed that hydroxychloroquine, infliximab, methotrexate, and sulfasalazine were the most commonly prescribed initial immunomodulatory drugs for patients with rheumatic irAEs (6,8,22,32,42,43). Notably, these results describe the most frequent immunomodulatory drugs prescribed to treat severe irAEs and may help to inform the selection of immunomodulatory treatments that will be studied in future randomized controlled trials.

Key strengths of these results include the systematic approach of case identification with a defined denominator in a large health system and cancer institute. The case definition of all rheumatic irAEs identified in this study was stringently reviewed, and the diagnosis was confirmed by at least 2 board-certified rheumatologists. In addition, detailed clinical data were collected from all patients. Furthermore, the total number of patients with rheumatic irAEs and patients with de novo inflammatory arthritis were sufficient to warrant a case–control analysis. In this analysis, we were able to incorporate multiple possible predictor variables, with the administrative data obtained from a large group of patients as of the date of initiation of the initial ICI treatment. While the type, count, and duration of ICI therapy after the baseline time point varied depending on the type of cancer, this was accounted for in the multivariable analyses, so it would not explain the associations that we report.

There were several limitations that are intrinsic to large, retrospective analyses. A full review of medical records was not able to be performed for all 8,028 patients. Detailed data were only collected for the subset of patients who were evaluated by a rheumatologist or those who received an immunomodulatory drug after ICI initiation. Therefore, while we were able to verify the cases of rheumatic irAEs, there may be rheumatic irAE cases that were not identified using this approach. For example, patients with a rheumatic irAE who only received treatment with glucocorticoids without referral to a rheumatologist would not have been identified. Thus, the prevalence of rheumatic irAEs may be even higher than was demonstrated in the present study, since we used stringent methods to identify cases.

It would have been infeasible to manually review the medical records for every patient who received glucocorticoids before ICI initiation, due to the high number of patients receiving these medications. However, we reviewed the medical records for a subset of patients and confirmed that the majority of glucocorticoids were prescribed as part of chemotherapy regimens and not as treatment for autoimmune diseases at baseline. Documentation in the electronic health records supporting rheumatic irAE case status in many patients would likely be incomplete for the purpose of objectively verifying rheumatic irAE presence. Also, if the patient was taking glucocorticoids or other immunomodulatory drugs for another type of irAE, this may have masked the emergence of a rheumatic irAE. To reduce this potential for misclassification, we chose, as control subjects, individuals who had no rheumatic disease at baseline, who had never received treatment with glucocorticoids after initiation of an ICI, who were never examined by a rheumatologist during the study period, and who had never received a prescription for an immunomodulatory drug after initiation of the ICI. We expect that any misclassification of a rheumatic irAE would bias the data toward the null, and therefore any misclassification of case status would likely not explain our results. In the sample of 100 controls in our case–control analysis, none were identified as having experienced rheumatic irAEs. Patients with rapidly fatal malignancies may not have had the chance to develop a rheumatic irAE, which can develop a median of 5 months after the initiation of ICI therapy (38). Therefore, for inclusion in the control group, we required that controls be individuals who survived at least 6 months after beginning the initial ICI treatment.

While a strength of this study is the large number of ICI recipients and the large number of rheumatic irAE cases, an important limitation was our inability to obtain detailed data for all desired variables, such as cancer subtypes. As a result, our study may be prone to residual confounding. While we were able to analyze many predictors of interest, we were unable to account for other potentially important variables, such as cancer severity, ICI dose, specific cancer therapy regimen, concurrent receipt of chemotherapy with ICI, indication for baseline glucocorticoid prescription across all recipients, prior cancer treatment regimens, body mass index, smoking status and pack-years, family history of autoimmune disease, performance status for activities of daily living, frailty, sarcopenia, and genetic factors that may affect these relationships. While all controls were required to have at least 6 months of follow-up, it is possible that some controls may have developed rheumatic irAEs later, after the electronic health records data had already been obtained for this study. Patients with aggressive cancer, particularly solid tumors, may have been monitored more vigilantly, which could have resulted in more opportunities for rheumatic irAEs to be detected. We were unable to completely account for these factors in our current analyses, and therefore such factors should be considered as additional potential contributors to the findings.

Furthermore, multicenter studies are needed to provide adequately sized patient populations which would allow for an analysis stratified by rheumatic irAE subtype and histologic cancer diagnosis. Moreover, future studies should be carried out with the aim of addressing additional outcomes in cancer patients

being treated with ICIs, such as the efficacy of selected immunomodulatory drugs in the treatment of irAEs, as well as the impact of immunomodulatory treatment on cancer progression and overall survival. Our study is one of the largest to focus on predictors of rheumatic irAEs within a definable large sample, though our findings may have limited generalizability.

In summary, among a large, single-center cohort of ICI-treated cancer patients, we were able to demonstrate that rheumatologists were the leading prescribers of immunomodulatory treatments in our outpatient setting, with ~25% of all cancer patients receiving treatment with an immunomodulatory drug. Furthermore, we identified melanoma and GU tract cancer as potential novel risk factors for the development of rheumatic irAEs and de novo inflammatory arthritis. In addition, our results suggest that the type of malignancy may be a central determinant of future irAE development. The potential biologic basis for this association should be the subject of future research.

ACKNOWLEDGMENT

We thank Weixing Huang, MSPH for assistance with the analysis.

AUTHOR CONTRIBUTIONS

All authors were involved in drafting the article or revising it critically for important intellectual contact, and all authors approved the final version to be published. Dr. Sparks had full access to all of the data in the study and takes responsibility for the integrity of the data and the accuracy of the data analysis.

Study conception and design. Cunningham-Bussel, Sparks.

Acquisition of data. Cunningham-Bussel, Wang, Prisco, Martin, Vanni, Zaccardelli, Sparks.

Analysis and interpretation of data. Cunningham-Bussel, Wang, Nasrallah, Gedmintas, MacFarlane, Shadick, Awad, Rahma, LeBoeuf, Gravallese, Sparks.

REFERENCES

1. Haslam A, Prasad V. Estimation of the percentage of US patients with cancer who are eligible for and respond to checkpoint inhibitor immunotherapy drugs. JAMA Netw Open 2019;2:e192535.
2. Postow MA, Sidlow R, Hellmann MD. Immune-related adverse events associated with immune checkpoint blockade [review]. N Engl J Med 2018;378:158–68.
3. Cappelli LC, Shah AA, Bingham CO. Immune-related adverse effects of cancer immunotherapy: implications for rheumatology [review]. Rheum Dis Clin North Am 2017;43:65–78.
4. Cappelli LC, Gutierrez AK, Baer AN, Albayda J, Manno RL, Haque U, et al. Inflammatory arthritis and sicca syndrome induced by nivolumab and ipilimumab. Ann Rheum Dis 2017;76:43–50.
5. Kostine M, Rouxel L, Barnetche T, Veillon R, Martin F, Dutriaux C, et al. Rheumatic disorders associated with immune checkpoint inhibitors in patients with cancer—clinical aspects and relationship with tumour response: a single-centre prospective cohort study. Ann Rheum Dis 2018;77:393–8.
6. Richter MD, Crowson C, Kottschade LA, Finnes HD, Markovic SN, Thanarajasingam U. Rheumatic syndromes associated with immune checkpoint inhibitors: a single-center cohort of sixty-one patients. Arthritis Rheumatol 2019;71:468–75.
7. Lidar M, Giat E, Garelick D, Horowitz Y, Amital H, Steinberg-Silman Y, et al. Rheumatic manifestations among cancer patients treated with immune checkpoint inhibitors. Autoimmun Rev 2018;17:284–9.
8. Roberts J, Ennis D, Hudson M, Ye C, Saltman A, Himmel M, et al. Rheumatic immune-related adverse events associated with cancer immunotherapy: a nationwide multi-center cohort [review]. Autoimmun Rev 2020;19:102595.
9. Haanen JB, Carbonnel F, Robert C, Kerr KM, Peters S, Larkin J, et al. Management of toxicities from immunotherapy: ESMO Clinical Practice Guidelines for diagnosis, treatment and follow-up. Ann Oncol 2017;28:iv119–42.
10. Wang Y, Abu-Sbeih H, Mao E, Ali N, Ali FS, Qiao W, et al. Immune-checkpoint inhibitor-induced diarrhea and colitis in patients with advanced malignancies: retrospective review at MD Anderson. J Immunother Cancer 2018;6:37.
11. Cappelli LC, Naidoo J, Bingham CO, Shah AA. Inflammatory arthritis due to immune checkpoint inhibitors: challenges in diagnosis and treatment [editorial]. Immunotherapy 2017;9:5–8.
12. Ghosh N, Tiongson MD, Stewart C, Chan KK, Jivanelli B, Cappelli L, et al. Checkpoint inhibitor-associated arthritis: a systematic review of case reports and case series. J Clin Rheumatol 2020. doi: 10.1097/RHU.0000000000001370. E-pub ahead of print.
13. Salem JE, Allenbach Y, Vozy A, Brechot N, Johnson DB, Moslehi JJ, et al. Abatacept for severe immune checkpoint inhibitor–associated myocarditis. N Engl J Med 2019;380:2377–9.
14. Brahmer JR, Lacchetti C, Schneider BJ, Atkins MB, Brassil KJ, Caterino JM, et al. Management of immune-related adverse events in patients treated with immune checkpoint inhibitor therapy: American Society of Clinical Oncology clinical practice guideline. J Clin Oncol 2018;36:1714–68.
15. Aldrich J, Pundole X, Tummala S, Palaskas N, Andersen CR, Shoukier M, et al. Inflammatory myositis in cancer patients receiving immune checkpoint inhibitors. Arthritis Rheumatol 2021;73:866–74.
16. Leonardi GC, Gainor JF, Altan M, Kravets S, Dahlberg SE, Gedmintas L, et al. Safety of programmed death–1 pathway inhibitors among patients with non–small-cell lung cancer and preexisting autoimmune disorders. J Clin Oncol 2018;36:1905–12.
17. Nabel CS, Severgnini M, Hung YP, Cunningham-Bussel A, Gjini E, Kleinsteuber K, et al. Anti-PD-1 immunotherapy-induced flare of a known underlying relapsing vasculitis mimicking recurrent cancer. Oncologist 2019;24:1013–21.
18. Singer S, Nelson CA, Lian CG, Dewan AK, LeBoeuf NR. Nonbullous pemphigoid secondary to PD-1 inhibition. JAAD Case Rep 2019;5:898–903.
19. Kostine M, Finckh A, Bingham CO, Visser K, Leipe J, Schulze-Koops H, et al. EULAR points to consider for the diagnosis and management of rheumatic immune-related adverse events due to cancer immunotherapy with checkpoint inhibitors. Ann Rheum Dis 2021;80:36–48.
20. Mooradian MJ, Nasrallah M, Gainor JF, Reynolds KL, Cohen JV, Lawrence DP, et al. Musculoskeletal rheumatic complications of immune checkpoint inhibitor therapy: a single center experience. Semin Arthritis Rheum 2019;48:1127–32.
21. Braaten TJ, Brahmer JR, Forde PM, Le D, Lipson EJ, Naidoo J, et al. Immune checkpoint inhibitor-induced inflammatory arthritis persists after immunotherapy cessation. Ann Rheum Dis 2020;79:332–8.
22. Cappelli LC, Gutierrez AK, Baer AN, Albayda J, Manno RL, Haque U, et al. Inflammatory arthritis and sicca syndrome induced by nivolumab and ipilimumab. Ann Rheum Dis 2016;76:43–50.
23. Cappelli LC, Gutierrez AK, Bingham CO III, Shah AA. Rheumatic and musculoskeletal immune-related adverse events due to immune checkpoint inhibitors: a systematic review of the literature. Arthritis Care Res (Hoboken) 2017;69:1751–63.
24. Allenbach Y, Anquetil C, Manouchehri A, Benveniste O, Lambotte O, Lebrun-Vignes B, et al. Immune checkpoint inhibitor-induced

myositis, the earliest and most lethal complication among rheumatic and musculoskeletal toxicities. Autoimmun Rev 2020;19:102586.

25. Anquetil C, Salem JE, Lebrun-Vignes B, Johnson DB, Mammen AL, Stenzel W, et al. Immune checkpoint inhibitor–associated myositis: expanding the spectrum of cardiac complications of the immunotherapy revolution. Circulation 2018;138:743–5.
26. Cappelli LC, Bingham CO. Spectrum and impact of checkpoint inhibitor-induced irAEs [review]. Nat Rev Rheumatol 2021;17:69–70.
27. Xu C, Chen YP, Du XJ, Liu JQ, Huang CL, Chen L, et al. Comparative safety of immune checkpoint inhibitors in cancer: systematic review and network meta-analysis. BMJ 2018;363:k4226.
28. Herbst RS, Baas P, Kim DW, Felip E, Pérez-Gracia JL, Han JY, et al. Pembrolizumab versus docetaxel for previously treated, PD-L1-positive, advanced non-small-cell lung cancer (KEYNOTE-010): a randomised controlled trial. Lancet 2016;387:1540–50.
29. Reid PD, Cifu AS, Bass AR. Management of immunotherapy-related toxicities in patients treated with immune checkpoint inhibitor therapy. JAMA 2021;325:482–3.
30. Smith MH, Bass AR. Arthritis after cancer immunotherapy: symptom duration and treatment response. Arthritis Care Res (Hoboken) 2019;71:362–6.
31. Calabrese LH, Calabrese C, Cappelli LC. Rheumatic immune-related adverse events from cancer immunotherapy [review]. Nat Rev Rheumatol 2018;14:569–79.
32. Quan H, Sundararajan V, Halfon P, Fong A, Burnand B, Luthi JC, et al. Coding algorithms for defining comorbidities in ICD-9-CM and ICD-10 administrative data. Med Care 2005;43:1130–9.
33. Pundole X, Sarangdhar M, Suarez-Almazor M. Rheumatic and musculoskeletal adverse events with immune checkpoint inhibitors: data from the United States Food and Drug Administration adverse event reporting system. J Immunother Precis Oncol 2019;2:65–73.
34. Ramos-Casals M, Brahmer JR, Callahan MK, Flores-Chávez A, Keegan N, Khamashta MA, et al. Immune-related adverse events of checkpoint inhibitors [review]. Nat Rev Dis Primers 2020;6:38.
35. Eun Y, Kim IY, Sun JM, Lee J, Cha HS, Koh EM, et al. Risk factors for immune-related adverse events associated with anti-PD-1 pembrolizumab. Sci Rep 2019;9:14039.
36. Hopkins AM, Rowland A, Kichenadasse G, Wiese MD, Gurney H, McKinnon RA, et al. Predicting response and toxicity to immune checkpoint inhibitors using routinely available blood and clinical markers [review]. Br J Cancer 2017;117:913–20.
37. Tran E, Ahmadzadeh M, Lu YC, Gros A, Turcotte S, Robbins PF, et al. Immunogenicity of somatic mutations in human gastrointestinal cancers. Science 2015;350:1387–90.
38. Yarchoan M, Hopkins A, Jaffee EM. Tumor mutational burden and response rate to PD-1 inhibition. N Engl J Med 2017;377:2500–1.
39. Bomze D, Ali OH, Bate A, Flatz L. Association between immune-related adverse events during anti-PD-1 therapy and tumor mutational burden. JAMA Oncol 2019;5:1633–5.
40. Cappelli LC, Brahmer JR, Forde PM, Le DT, Lipson EJ, Naidoo J, et al. Clinical presentation of immune checkpoint inhibitor-induced inflammatory arthritis differs by immunotherapy regimen. Semin Arthritis Rheum 2018;48:553–7.
41. Kim ST, Tayar J, Trinh VA, Suarez-Almazor M, Garcia S, Hwu P, et al. Successful treatment of arthritis induced by checkpoint inhibitors with tocilizumab: a case series. Ann Rheum Dis 2017;76:2061.
42. Calabrese C, Kirchner E, Kontzias A, Velcheti V, Calabrese LH. Rheumatic immune-related adverse events of checkpoint therapy for cancer: case series of a new nosological entity. RMD Open 2017;3:e000412.
43. Chan KK, Bass AR. Autoimmune complications of immunotherapy: pathophysiology and management. BMJ 2020;369:m736.

Arthritis & Rheumatology
Vol. 74, No. 3, March 2022, pp 541–548

AMERICAN COLLEGE of RHEUMATOLOGY
Empowering Rheumatology Professionals

LETTERS

DOI 10.1002/art.41978

Effective viral vector response to SARS–CoV-2 booster vaccination in a patient with rheumatoid arthritis after initial ineffective response to messenger RNA vaccine

To the Editor:

The COVID-19 pandemic has posed a unique challenge in the management of rheumatic diseases. Immunosuppressed patients are at an increased risk of developing severe COVID-19 and may not derive full protection from the vaccine (1–5). Thus, it is paramount that clinicians develop strategies to protect rheumatic disease patients from infection with SARS–CoV-2 and its variants.

In this letter, we describe the clinical response in a 74-year-old man with seropositive, erosive rheumatoid arthritis (RA) that was initially diagnosed in 1974. The patient is currently receiving 200 mg of hydroxychloroquine daily, 25 mg of etanercept weekly, and 20 mg of leflunomide daily. With this RA treatment regimen, low levels of disease activity have been maintained over the last 5 years.

The patient received 2 doses of the messenger RNA (mRNA) vaccine mRNA-1273 (Moderna) without interruption of his RA treatment, with the first dose administered January 18, 2021 and the second dose administered February 11, 2021. In mid-April, a semiquantitative analysis revealed a spike protein receptor-binding domain (RBD) antibody level of 53.9 units/ml (normal reference range 0–2,500), and the results of a SARS–CoV-2 anti-spike (S1/RBD) IgG test were negative. An assay designed to detect blocking of the interaction between the SARS–CoV-2 spike protein RBD and the human angiotensin-converting enzyme 2 (ACE-2) receptor demonstrated <10% blocking activity (6). The results of an interferon-γ–release assay detecting SARS–CoV-2–specific T cells were also negative (7). The patient and his care team presumed that his suboptimal response to the vaccine was due to the immunosuppressive medications he was taking at the time of vaccination.

Based on his test results, the patient obtained an additional vaccine dose on his own accord. On June 6, 2021, he received 1 dose of the viral vector SARS–CoV-2 vaccine Ad26.COV2.S (Johnson & Johnson). No side effects developed. In late June, a repeat semiquantitative analysis revealed a spike protein RBD antibody level of 2,455.0 units/ml, and the results of an S1/RBD IgG test were positive. The ACE-2 blocking assay demonstrated 90–100% blocking activity (Figure 1). The results of the interferon-γ release assay remained negative, suggesting that T cell–mediated immunity was not achieved. A blunted T cell response to the SARS–CoV-2 vaccine has been demonstrated in patients receiving medications such as methotrexate or tacrolimus, but, to our knowledge, it has not been evaluated in patients treated with leflunomide (8,9).

In summary, we describe an immunosuppressed patient who experienced an ineffective immune response after 2 doses of an mRNA SARS–CoV-2 vaccine. The patient subsequently achieved a robust antibody response after a booster vaccination with the Johnson & Johnson SARS–CoV-2 vaccine, all while continuing treatment with RA medications. Current guidance put forth by the American College of Rheumatology (ACR) does not recommend obtaining antibody testing after vaccination, in part due to a lack of clinically meaningful cutoff values for available antibody tests (10). The US Food and Drug Administration revised the emergency use authorization on August 12, 2021 for the 2 available mRNA SARS–CoV-2 vaccines to permit a third dose for certain immunocompromised patients, and the ACR does support

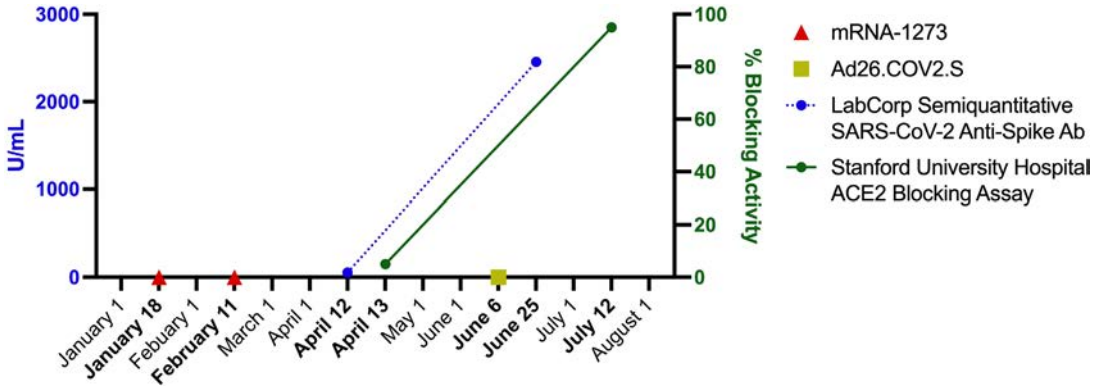

Figure 1. SARS–CoV-2 anti-spike IgG and human angiotensin-converting enzyme 2 (ACE-2) blocking activity before and after booster vaccination in an immunosuppressed patient with rheumatoid arthritis. Ab = antibody.

booster vaccination (11). Our report demonstrates the possibility of achieving humoral immunity against SARS–CoV-2 after initial failure through the use of a cross-platform booster vaccination strategy. Prior research has demonstrated that heterologous vaccination strategies may induce a more robust immune response in healthy adults (12–14). We believe future research is needed to establish relevant antibody reference values to identify patients without adequate protection against COVID-19 infection, and to understand the role of cross-platform booster vaccination when primary mRNA vaccination and/or booster vaccination fails to induce a sufficient immune response.

Author disclosures are available at https://onlinelibrary.wiley.com/action/downloadSupplement?doi=10.1002.2Fart.41978&file=art41978-sup-0001-Disclosureform.pdf.

Matthew C. Baker, MD, MS
Vamsee Mallajosyula, PhD
Mark M. Davis, PhD
Scott D. Boyd, MD, PhD
Kari C. Nadeau, MD, PhD
Stanford University
Stanford, CA
William H. Robinson, MD, PhD
Stanford University
Stanford, CA
and VA Palo Alto Health Care System
Palo Alto, CA

1. Pablos JL, Galindo M, Carmona L, Lledo A, Retuerto M, Blanco R, et al. Clinical outcomes of hospitalised patients with COVID-19 and chronic inflammatory and autoimmune rheumatic diseases: a multicentric matched cohort study. Ann Rheum Dis 2020;79:1544–9.
2. D'Silva KM, Serling-Boyd N, Wallwork R, Hsu T, Fu X, Gravallese EM, et al. Clinical characteristics and outcomes of patients with coronavirus disease 2019 (COVID-19) and rheumatic disease: a comparative cohort study from a US 'hot spot.' Ann Rheum Dis 2020;79:1156–62.
3. Deepak P, Kim W, Paley MA, Yang M, Carvidi AB, El-Qunni AA, et al. Glucocorticoids and B cell depleting agents substantially impair immunogenicity of mRNA vaccines to SARS-CoV-2 [preprint]. medRxiv 2021.
4. Mahil SK, Bechman K, Raharja A, Domingo-Vila C, Baudry D, Brown MA, et al. The effect of methotrexate and targeted immunosuppression on humoral and cellular immune responses to the COVID-19 vaccine BNT162b2: a cohort study. Lancet Rheumatol 2021;3:e627–37.
5. Simon D, Tascilar K, Schmidt K, Manger B, Weckwerth L, Sokolova M, et al. Humoral and cellular immune responses to SARS–CoV-2 infection and vaccination in autoimmune disease patients with B cell depletion. Arthritis Rheumatol 2022;74:33–7.
6. Roltgen K, Powell AE, Wirz OF, Stevens BA, Hogan CA, Najeeb J, et al. Defining the features and duration of antibody responses to SARS-CoV-2 infection associated with disease severity and outcome. Sci Immunol 2020;5:eabe0240.
7. Murugesan K, Jagannathan P, Pham TD, Pandey S, Bonilla HF, Jacobson K, et al. Interferon-γ release assay for accurate detection of SARS-CoV-2 T cell response. Clin Infect Dis 2021;73:e3130–2.
8. Hadjadj J, Planas D, Ouedrani A, Buffier S, Delage L, Nguyen Y, et al. Immunogenicity of BNT162b2 vaccine against the alpha and delta variants in immunocompromised patients [preprint]. medRxiv 2021.
9. Prendecki M, Clarke C, Edwards H, McIntyre S, Mortimer P, Gleeson S, et al. Humoral and T-cell responses to SARS-CoV-2 vaccination in patients receiving immunosuppression. Ann Rheum Dis 2021;80:1322–9.
10. Curtis JR, Johnson SR, Anthony DD, Arasaratnam RJ, Baden LR, Bass AR, et al. American College of Rheumatology guidance for COVID-19 vaccination in patients with rheumatic and musculoskeletal diseases: version 3. Arthritis Rheumatol 2021;73:e60–75.
11. American College of Rheumatology. COVID-19 vaccine clinical guidance summary for patients with rheumatic and musculoskeletal diseases: developed by the ACR COVID-19 Vaccine Clinical Guidance Task Force. October 2021. URL: https://www.rheumatology.org/Portals/0/Files/COVID-19-Vaccine-Clinical-Guidance-Rheumatic-Diseases-Summary.pdf.
12. Schmidt T, Klemis V, Schub D, Mihm J, Hielscher F, Marx S, et al. Immunogenicity and reactogenicity of heterologous ChAdOx1 nCoV-19/mRNA vaccination. Nat Med 2021;27:1530–5.
13. Barros-Martins J, Hammerschmidt SI, Cossmann A, Odak I, Stankov MV, Ramos GM, et al. Immune responses against SARS-CoV-2 variants after heterologous and homologous ChAdOx1 nCoV-19/BNT162b2 vaccination. Nat Med 2021;27:1525–9.
14. Tenbusch M, Schumacher S, Vogel E, Priller A, Held J, Steininger P, et al. Heterologous prime-boost vaccination with ChAdOx1 nCoV-19 and BNT162b2 [letter]. Lancet Infect Dis 2021;21:1212–3.

DOI 10.1002/art.41989

Potential residual confounders in an analysis of lifestyle factors and risk of incident systemic lupus erythematosus: comment on the article by Choi et al

To the Editor:

We read with great interest the article by Dr. Choi and colleagues on whether a combination of individual factors related to lifestyle are associated with lower risk of incident systemic lupus erythematosus (SLE) (1). However, it is unfortunate that the analyses were not adjusted for residual confounders.

We have found that endometriosis, infection, and comorbidities are correlated with SLE, and could act as residual confounders in this type of an association analysis. For example, in a recently published study it was demonstrated that the risk of developing SLE is higher in patients with endometriosis compared to the general population, which shows an association between endometriosis and SLE (2). Therefore, the occurrence of endometriosis needs to be discussed when the majority of the participants in a study are female.

Furthermore, with regard to infections as a potential confounder, an association between *Helicobacter pylori* infection and a higher risk of SLE has been observed (3), and these types of triggers should be taken into account. Moreover, patients with SLE may experience several medical comorbidities. A recent study by Hansen et al demonstrated that multiple comorbidities are highly prevalent in SLE patients and can be identified both at the time of SLE diagnosis and up to 10 years before SLE diagnosis (4). Hypertension, chronic pulmonary disease, and depression were the comorbidities most commonly identified

both at the time of SLE diagnosis and before the diagnosis of SLE (4). The fact that comorbidities could have an impact on morbidity and mortality rates, which could in turn decrease the accuracy of the findings, suggests that any comorbid conditions should be described in such association studies to avoid confounding bias.

Geographic regions should have been more thoroughly described in the article by Choi et al. Participants were from 11 US states in the Nurses' Health Study (NHS) cohort and 14 US states in the NHSII cohort. However, it has been reported that the incidence of SLE in North America varies widely, ranging between 3.7 cases per 100,000 person-years and 49 cases per 100,000 person-years (5). Therefore, the analysis by Choi et al should have adjusted for different geographic regions, in order to minimize selection bias.

Selection bias and recall bias are difficult to prevent in research using questionnaires to collect information from participants. Individuals with healthier lifestyles may have different attitudes toward questionnaires and medical care compared with individuals living an unhealthy lifestyle. Individuals experiencing illness may also be more likely to visit a doctor, and thus increase the number of opportunities for receiving a diagnosis of SLE.

In conclusion, we believe that the impact of the study by Choi et al would be enhanced by the consideration of confounders and regional differences to effectively address possible bias.

Drs. Kao and Ker contributed equally to this work. Author disclosures are available at https://onlinelibrary.wiley.com/action/downloadSupplement?doi=10.1002%2Fart.41989&file=art41989-sup-0001-Disclosureform.pdf.

Pei-En Kao, MD
Amy Ker, MD
Cheng-Ruei Yang, MD
Chung Shan Medical University
James Cheng-Chung Wei, MD, PhD
Chung Shan Medical University Hospital
Chung Shan Medical University and China Medical University
Taichung, Taiwan

1. Choi MY, Hahn J, Malspeis S, Stevens EF, Karlson EW, Sparks JA, et al. Association of a combination of healthy lifestyle behaviors with reduced risk of incident systemic lupus erythematosus. Arthritis Rheumatol 2022;74:274–83.
2. Fan YH, Leong PY, Chiou JY, Wang YH, Ku MH, Wei JC. Association between endometriosis and risk of systemic lupus erythematosus. Sci Rep 2021;11:532.
3. Wu MC, Leong PY, Chiou JY, Chen HH, Huang JY, Wei JC. Increased risk of systemic lupus erythematosus in patients with Helicobacter pylori infection: a nationwide population-based cohort study. Front Med (Lausanne) 2020;6:330.
4. Hansen RB, Simard JF, Faurschou M, Jacobsen S. Distinct patterns of comorbidity prior to diagnosis of incident systemic lupus erythematosus in the Danish population. J Autoimmun 2021;123:102692.
5. Barber MR, Drenkard C, Falasinnu T, Hoi A, Mak A, Kow NY, et al. Global epidemiology of systemic lupus erythematosus [review]. Nat Rev Rheumatol 2021;17:515–32.

DOI 10.1002/art.41990

Reply

To the Editor:

We thank Dr. Kao and colleagues for their comments on our article and appreciate the opportunity to address their concerns regarding bias and confounding. In doing so, we will highlight the strengths in the design of our study that make us confident in our findings on the association between lifestyle behaviors and the risk of developing SLE.

First, Kao et al discuss endometriosis, *Helicobacter pylori* infection, comorbidities, and geographic variation as potential confounders of the relationship between healthy lifestyle and SLE risk among women (Figure 1). We were careful and deliberate in the selection of potential confounders included in our models. By definition, a confounder is a prior common cause of both the exposure and the outcome, thereby inducing a spurious relationship between the two. We selected confounding variables, including reproductive and hormonal factors, that have previously been associated with the exposures under study and are well-established as risk factors for SLE (1); these comprise an important set of potential prior common causes. We considered including endometriosis or *H. pylori* infection as potential confounders, but decided not to include them as they could be mediators (on an explanatory pathway between healthy lifestyle factors and SLE) and are unlikely to be prior common causes of both healthy lifestyle behaviors and SLE (2–5). Other comorbidities would not be considered confounders either, as although they may be more common in women with established SLE and may alter lifestyle behaviors, they are unlikely prior causes of SLE. While we agree that certain comorbidities may influence mortality and morbidity in SLE, this is not the causal relationship that was being evaluated in our study, and for reasons stated above, we believe they are unlikely to be confounders of the relationship of interest.

As we have not found a significant relationship between residential regions of the US and SLE risk among the NHS cohort participants, we did not include region in our models. Moreover, it is more likely that a relationship between region and SLE would be explained by healthy lifestyle as a mediator, rather than the relationship between healthy lifestyle and SLE risk being mediated by (or confounded by) region. To respond to Kao et al, however, we ran our models again using 5 US residential regions and results were unchanged: the hazard ratio for the association of continuous Healthy Lifestyle Index Score with overall SLE risk was 0.79 (95% confidence interval 0.64–0.96).

Kao et al also raise the issues of selection and recall bias. Selection bias arises when the study population is not a random selection from the target population for which a statement is made. Prior work with the NHS cohorts suggests they provide reasonable representation of working White women in the US

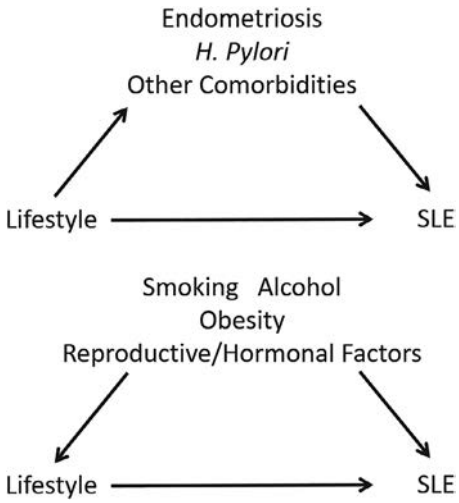

Figure 1. Directed acyclic graph (DAG) for potential relationships between lifestyle, mediators (such as endometriosis, *Helicobacter pylori* (*H. pylori*), and comorbidities), and systemic lupus erythematosus (SLE) suggested by Kao et al (top), and the DAG that was examined by our group (bottom) with lifestyle and SLE adjusted for confounders (potential prior common causes of both).

(1976–2017) and have been used to study a myriad of exposures and diseases, including SLE (6). Recall bias is an issue in retrospective studies in which participants may recall their exposures differentially based on their current diagnoses. One of the strengths of using the NHS cohorts to study exposures related to risk of disease development is that exposure data were prospectively collected well before the onset of disease, reducing any concerns regarding recall bias. Therefore, while the authors raise issues of bias and confounding, which are indeed fundamental threats to the validity of any epidemiologic study, by following the most rigorous epidemiologic methods available, potential bias and confounding were minimized in the design of our study and analysis.

May Y. Choi, MD, MPH, FRCPC
Brigham and Women's Hospital and Harvard Medical School Boston, MA and University of Calgary Calgary, Alberta, Canada
Jill Hahn, DSc
Susan Malspeis, MS
Emma F. Stevens, BA
Elizabeth W. Karlson, MD, MS
Jeffrey A. Sparks, MD, MMSc
Kazuki Yoshida, MD, MPH, ScD
Brigham and Women's Hospital and Harvard Medical School Boston, MA
Laura Kubzansky, PhD
Harvard University T. H. Chan School of Public Health Boston, MA

Karen H. Costenbader, MD, MPH
Brigham and Women's Hospital and Harvard Medical School Boston, MA

1. Barbhaiya M, Costenbader KH. Environmental exposures and the development of systemic lupus erythematosus. Curr Opin Rheumatol 2016;28:497–505.
2. Hediger ML, Hartnett HJ, Louis GM. Association of endometriosis with body size and figure. Fertil Steril 2005;84:1366–74.
3. Missmer SA, Chavarro JE, Malspeis S, Bertone-Johnson ER, Hornstein MD, Spiegelman D, et al. A prospective study of dietary fat consumption and endometriosis risk. Hum Reprod 2010;25:1528–35.
4. Cramer DW, Wilson E, Stillman RJ, Berger MJ, Belisle S, Schiff I, et al. The relation of endometriosis to menstrual characteristics, smoking, and exercise. JAMA 1986;255:1904–8.
5. Schubert TT, Schubert AB, Ma CK. Symptoms, gastritis, and Helicobacter pylori in patients referred for endoscopy. Gastrointest Endosc 1992;38:357–60.
6. Bao Y, Bertoia ML, Lenart EB, Stampfer MJ, Willett WC, Speizer FE, et al. Origin, methods, and evolution of the three Nurses' Health Studies. Am J Public Health 2016;106:1573–81.

DOI 10.1002/art.42002

Rituximab versus cyclophosphamide for remission induction in active, severe antineutrophil cytoplasmic antibody–associated vasculitis: comment on the article by Chung et al

To the Editor:

The American College of Rheumatology/Vasculitis Foundation recently released guidelines for the management of antineutrophil cytoplasmic antibody (ANCA)–associated vasculitis (AAV) (1). The first recommendation therein, which conditionally recommends rituximab (RTX) over cyclophosphamide (CYC) for remission induction in severe disease and considers intravenous and oral CYC to be equivalent, merits clarification.

Although RTX is the preferred maintenance therapy in AAV (due to survival benefit), the superiority of RTX over CYC for remission induction is questionable (with the exception of the subset of patients with proteinase 3 [PR3]–positive relapsing disease). In the guidelines, Dr. Chung and colleagues justify the recommendation for treatment with RTX over CYC by stating that a single course of CYC carries substantial risks of neutropenia, bladder injury, and infertility (1). While that may hold true for oral CYC (2 mg/kg/day for 3–6 months; cumulative dose of ~21.6 gm for a 6-month course) or for repeated treatment courses of CYC, a single course of intravenous CYC accounts for much lower cumulative doses (~5.4 gm for a 6-cycle course and 8.1 gm for a 9-cycle course).

The incidence of leukopenia was higher with CYC when compared to RTX in the Rituximab in ANCA-Associated Vasculitis (RAVE) trial (which used oral CYC) but not in the Rituximab versus Cyclophosphamide in ANCA-Associated Vasculitis (RITUXVAS) trial (which used intravenous CYC), and was higher with oral

CYC compared to intravenous CYC in the Pulse Versus Daily Oral Cyclophosphamide for Induction of Remission in ANCA-Associated Vasculitis (CYCLOPS) study, although this did not translate into an increased incidence of infections over longer follow-up in either the RAVE or the CYCLOPS trial (2–4). Hemorrhagic cystitis and bladder cancer are dose-dependent adverse effects typically seen at much higher cumulative doses of CYC (doses of >20–30 gm ranging up to, most commonly, a dose of >50 gm), which are not reached with a single course of intravenous CYC (5). In a previous study by our group in which we assessed 105 patients with granulomatosis with polyangiitis, of whom 90 received intravenous CYC, no toxic effects on the bladder were seen with this treatment during a median follow-up of 28 months (to date, a median of ~84 months of follow-up) (6). Infertility is another dose- (and age-) dependent adverse effect of CYC, and thus occurs more commonly with the use of oral CYC in older women. With cumulative doses of intravenous CYC of <5 gm, the incidence of sustained amenorrhea is much lower and can be further reduced with gonadotropin-releasing hormone agonists (7). Thus, the concern for toxicity resulting from a single course of intravenous CYC may be an overestimation.

However, the use of intravenous CYC for remission induction confers some benefits when compared to RTX. First, in rheumatic disease patients with COVID-19, CYC is considered to be a safer treatment option when compared to RTX, as RTX is associated with poorer outcomes (8). Second, in contrast to the COVID-19 management strategy in rheumatic disease patients receiving CYC, treatment with RTX interferes with the efficacy and timing of COVID-19 vaccine administration (9). Third, CYC is less expensive (notwithstanding the cost of consumables and monitoring adverse effects). Finally, remission induction therapy with CYC spares ~2 gm of RTX for subsequent maintenance therapy (500 mg for a 6-month course of RTX maintenance therapy versus 4 doses of 375 mg/m^2 each given 1 week apart or 2 doses of 1 gm each given 2 weeks apart for RTX induction therapy), which is important as we are transitioning toward longer durations of maintenance therapy in the treatment of severe AAV (10).

Thus, considering the ongoing COVID-19 pandemic, we believe that treatment with intravenous CYC should at least be considered equal to treatment with RTX, and superior to oral CYC, for remission induction in patients with AAV.

Author disclosures are available at https://onlinelibrary.wiley.com/action/downloadSupplement?doi=10.1002%2Fart.42002&file=art42002-sup-0001-Disclosureform.pdf.

Siddharth Jain, DM
G. S. R. S. N. K. Naidu, DM
Aman Sharma, MD, FRCP
Postgraduate Institute of Medical Education and Research
Chandigarh, India

1. Chung SA, Langford CA, Maz M, Abril A, Gorelik M, Guyatt G, et al. 2021 American College of Rheumatology/Vasculitis Foundation guideline for the management of antineutrophil cytoplasmic antibody–associated vasculitis. Arthritis Rheumatol 2021;73:1366–83.
2. Stone JH, Seo P, Hoffman GS, Clair EW, Webber L, Mieras K, et al. Rituximab versus cyclophosphamide for ANCA-associated vasculitis. N Engl J Med 2010;363:221–32.
3. Jones RB, Luqmani R, Savage CO, van Paassen P, Westman K. Rituximab versus cyclophosphamide in ANCA-associated renal vasculitis. N Engl J Med 2010;363:211–20.
4. De Groot K, Harper L, Jayne DR, Suarez LF, Gregorini G, Gross WL, et al. Pulse versus daily oral cyclophosphamide for induction of remission in antineutrophil cytoplasmic antibody–associated vasculitis: a randomized trial. Ann Intern Med 2009;150:670–80.
5. Monach PA, Arnold LM, Merkel PA. Incidence and prevention of bladder toxicity from cyclophosphamide in the treatment of rheumatic diseases: a data-driven review. Arthritis Rheum 2010;62:9–21.
6. Sharma A, Naidu GS, Rathi M, Verma R, Modi M, Pinto B, et al. Clinical features and long-term outcomes of 105 granulomatosis with polyangiitis patients: a single center experience from north India. Int J Rheum Dis 2018;21:278–84.
7. Luong SN, Isaacs A, Liu Z, Sin FE, Giles I. A systematic review and meta-analysis of the gonadotoxic effects of cyclophosphamide and benefits of gonadotropin releasing hormone agonists (GnRHa) in women of child-bearing age with autoimmune rheumatic disease [review]. Expert Rev Clin Immunol 2020;16:321–33.
8. Sparks JA, Wallace ZS, Seet AM, Gianfrancesco MA, Izadi Z, Hyrich KL, et al. Associations of baseline use of biologic or targeted synthetic DMARDs with COVID-19 severity in rheumatoid arthritis: results from the COVID-19 Global Rheumatology Alliance physician registry. Ann Rheum Dis 2021;80:1137–46.
9. Curtis JR, Johnson SR, Anthony DD, Arasaratnam RJ, Baden LR, Bass AR, et al. American College of Rheumatology Guidance for COVID-19 vaccination in patients with rheumatic and musculoskeletal diseases: version 2. Arthritis Rheumatol 2021;73:e30–45.
10. Charles P, Perrodeau É, Samson M, Bonnotte B, Néel A, Agard C, et al. Long-term rituximab use to maintain remission of antineutrophil cytoplasmic antibody–associated vasculitis: a randomized trial. Ann Intern Med 2020;173:179–87.

DOI 10.1002/art.41991

Reply

To the Editor:

We appreciate the insights and concerns shared by Dr. Jain and colleagues regarding the use of RTX and CYC for the treatment of granulomatosis with polyangiitis (GPA) and microscopic polyangiitis (MPA), as outlined in the American College of Rheumatology (ACR)/Vasculitis Foundation (VF) guideline for the treatment of AAV. These concerns are timely given the ongoing COVID-19 pandemic.

The first question raised by Jain et al is whether CYC is superior to RTX for remission induction in patients with severe GPA or MPA. The guideline describes the reasoning behind the conditional recommendation for the use of RTX over CYC for this patient population. Briefly, factors that influenced this recommendation included clinical considerations of efficacy, relapse, and toxicity, as well as patient preferences. In addition, GPA and MPA can be chronic diseases requiring repeated courses of remission induction therapy.

Jain et al acknowledge the increased efficacy of RTX for patients with PR3-ANCA–positive, relapsing disease. The ACR/VF Voting Panel considered all of these factors when developing the recommendation. As the recommendation is conditional, provider and patient-specific factors may influence the choice of therapy.

A second issue raised by Jain et al is that treatment with intravenous (IV) pulse CYC is preferable to daily oral CYC because IV pulse CYC has less toxicity. Whether IV pulse or daily oral CYC is a "better" treatment continues to be an area of debate. While the toxicity of a single course of IV pulse CYC is less than that of daily oral CYC (1), the benefit of this difference is unclear, because patients treated with IV pulse CYC have a significantly higher rate of relapse compared to those treated with daily oral CYC (2), and may need additional treatment. A single course of CYC can also have impactful, long-term consequences, such as affecting ovarian reserve (3). Because the toxicity of CYC can be dependent on the cumulative dose, duration of therapy with daily oral CYC is now usually much shorter than previously employed (e.g., 3 months versus 6 months). The toxicity of daily oral CYC may also be mitigated with proactive monitoring strategies (e.g., obtaining blood cell counts every 1–2 weeks during treatment). Based on these considerations, it is difficult to determine whether IV pulse or daily oral CYC should be preferred. Since both are valid options, physician experience and patient preferences should guide the choice of treatment.

The impact of treatment with RTX on COVID-19 infection and vaccine response is important to consider. Jain et al suggest that CYC is a "safer" medication than RTX during the COVID-19 pandemic. Currently, there are not sufficient data published to determine how outcomes of COVID-19 infection differ in patients treated with CYC compared to those treated with RTX. As a B cell–depleting agent, RTX is known to substantially affect antibody responses to COVID-19 vaccination. However, patients with GPA treated with CYC also develop substantial B cell lymphopenia, which can extend past discontinuation of CYC, and can also experience a reduction in B cell function (4,5). Thus, treatment with CYC may also impair vaccine responses. Because therapy with CYC or RTX to induce remission is typically given in conjunction with high-dose glucocorticoids, the relative safety of RTX or CYC use during the COVID-19 pandemic may not be easily determined.

Cost is also an appropriate factor to consider in making treatment decisions. These guidelines are based on practice in the United States, and thus the recommendations may need to be adjusted by physicians in other countries based on several factors, including costs and drug availability.

The comments of Jain et al highlight many of the unanswered questions that remain when considering treatment options for patients with AAV, as well as the challenges of treating these diseases during the COVID-19 pandemic. The published recommendations were developed for the "usual" settings, prior to the onset of the global pandemic. We are hopeful that as more data are gathered regarding the impact of immunosuppressive therapy on outcomes of COVID-19 infection, more informed and nuanced recommendations regarding treatment options can be developed.

Author disclosures are available at https://onlinelibrary.wiley.com/action/downloadSupplement?doi=10.1002%2Fart.41991&file=art41991-sup-0001-Disclosureform.pdf.

Sharon A. Chung, MD, MAS
University of California
San Francisco, CA
Philip Seo, MD, MHS
Johns Hopkins University School of Medicine
Baltimore, MD
Peter A. Merkel, MD, MPH
University of Pennsylvania
Philadelphia, PA
Carol A. Langford, MD, MHS
Cleveland Clinic
Cleveland, OH

1. De Groot K, Harper L, Jayne DR, Suarez LF, Gregorini G, Gross WL, et al. Pulse versus daily oral cyclophosphamide for induction of remission in antineutrophil cytoplasmic antibody-associated vasculitis: a randomized trial. Ann Intern Med 2009; 150:670–80.
2. Harper L, Morgan MD, Walsh M, Hoglund P, Westman K, Flossmann O, et al. Pulse versus daily oral cyclophosphamide for induction of remission in ANCA-associated vasculitis: long-term follow-up. Ann Rheum Dis 2012;71:955–60.
3. Clowse ME, Copland SC, Hsieh TC, Chow SC, Hoffman GS, Merkel PA, et al. Ovarian reserve diminished by oral cyclophosphamide therapy for granulomatosis with polyangiitis (Wegener's). Arthritis Care Res (Hoboken) 2011;63:1777–81.
4. Fauci AS, Dale DC, Wolff SM. Cyclophosphamide and lymphocyte subpopulations in Wegener's granulomatosis. Arthritis Rheum 1974; 17:355–61.
5. Cupps TR, Edgar LC, Fauci AS. Suppression of human B lymphocyte function by cyclophosphamide. J Immunol 1982;128: 2453–7.

DOI 10.1002/art.41960

Consideration of confounders, accuracy of diagnosis, and disease severity in assessing the risk of inflammatory bowel disease in patients with psoriasis and psoriatic arthritis/ankylosing spondylitis beginning interleukin-7 inhibitor treatment: comment on the article by Penso et al

To the Editor:

We read with great interest the article by Dr. Penso and colleagues, describing a study in which they investigated whether initiation of interleukin-17 inhibitor (IL-17i) therapy was related to an increased risk of inflammatory bowel disease (IBD) in patients with psoriasis and psoriatic arthritis/ankylosing spondylitis (1). We would like to discuss some points.

First, smoking is an important risk factor in IBD, as it can affect the composition of intestinal microbiota and alter the immune system (2). Although Crohn's disease (CD) and ulcerative

colitis (UC) are the 2 main forms of IBD and they share some clinical features, CD and UC differ in that smoking has been shown to exacerbate CD but has been shown to protect against the development of UC (3). In the study by Penso et al, 132 patients developed IBD, including 72 new users of IL-17i, 11 new users of apremilast, and 49 new users of etanercept. We suggest that this analysis should have been adjusted for smoking status, or at least had patients matched by smoking status, in order to avoid confounding.

Second, although the presence of fecal calprotectin is a useful marker for IBD, findings obtained by endoscopy are still the gold standard for diagnosis (4). In the study by Penso et al, a variety of methods were used to ascertain the IBD diagnosis. In order to reduce information bias, the algorithm used to diagnose IBD should be clearly defined.

Finally, Penso and colleagues found that new IL-17i users had a higher risk of IBD compared with new apremilast users but had a similar level of risk for IBD as that of new etanercept users. These results may be explained by a difference in disease severity. Furthermore, clinicians generally will avoid treating patients with a higher risk of IBD with an IL-17i, because IL-17i therapy is suspected to trigger the development of IBD (5), which can lead to confounding by indication. We believe that the severity of the underlying disease and comorbidities should be balanced or adjusted for in this study to minimize selection bias. In conclusion, we believe that considering confounders and the accuracy of IBD diagnoses will improve the validity of this study.

Drs. Yang and Ker contributed equally to this work. Author disclosures are available at https://onlinelibrary.wiley.com/action/downloadSupplement?doi=10.1002%2Fart.41960&file=art41960-sup-0001-Disclosureform.docx.

Cheng-Ruei Yang, MD
Amy Ker, MD
Pei-En Kao, MD
Chung Shan Medical UniversityTaichung, Taiwan
James Cheng-Chung Wei, MD, PhD
Chung Shan Medical University Hospital
Chung Shan Medical University
and China Medical University
Taichung, Taiwan

1. Penso L, Bergqvist C, Meyer A, Herlemont P, Weill A, Zureik M, et al. Risk of inflammatory bowel disease in patients with psoriasis and psoriatic arthritis/ankylosing spondylitis initiating interleukin-17 inhibitors: a nationwide population-based study using the French National Health Data System. Arthritis Rheumatol 2022;74:244–52.
2. Berkowitz L, Schultz BM, Salazar GA, Pardo-Roa C, Sebastián VP, Álvarez-Loboso MM, et al. Impact of cigarette smoking on the gastrointestinal tract inflammation: opposing effects in Crohn's disease and ulcerative colitis [review]. Front Immunol 2018;9:74.
3. Mahid SS, Minor KS, Soto RE, Hornung CA, Galandiuk S. Smoking and inflammatory bowel disease: a meta-analysis. Mayo Clin Proc 2006;81:1462–71.
4. Flynn S, Eisenstein S. Inflammatory bowel disease presentation and diagnosis [review]. Surg Clin North Am 2019;99:1051–62.
5. Targan SR, Feagan B, Vermeire S, Panaccione R, Melmed GY, Landers C, et al. A randomized, double-blind, placebo-controlled phase 2 study of brodalumab in patients with moderate-to-severe Crohn's disease. Am J Gastroenterol 2016;111:1599–607.

DOI 10.1002/art.41962

Reply

To the Editor:

We appreciate the comments from Dr. Yang and colleagues about our recent study. We demonstrated that treatment with IL-17i was not associated with a higher risk of IBD in patients with psoriasis (PsO) or psoriatic arthritis (PSA)/ankylosing spondylitis (AS) as compared to that in new etanercept users, as demonstrated in analyses in which the severity of the underlying disease was taken into account. The main strength of this study was the use of a large sample from a nationally representative database, the French National Health Data System (Système National des Données de Santé [SNDS]), which has contained comprehensive data on all reimbursements for health-related expenditures, on ambulatory care, and on hospitalizations since 2006 (1,2).

In response to the points made by Yang et al, we would first like to address the issue of smoking status. The SNDS does not include information on each patient's smoking status. Smoking is associated with IBD as a risk factor for CD and a protective factor against UC. Not considering tobacco use in the final model could only lead to a nondifferential bias. Indeed, there is no apparent reason that the proportion of smokers would have been different between the IL-17i, apremilast, and etanercept cohorts.

Second, as mentioned by Yang et al, limitations of this study included the lack of clinical information on newly diagnosed IBD cases. Our definition of IBD was based on 2 hospital discharge diagnoses of IBD (International Statistical Classification of Diseases and Related Health Problems, Tenth Revision [ICD-10] codes K50/K51), or 1 hospital discharge diagnosis code indicating IBD and a prescription filled for aminosalicylic acid, enteral budesonide, thiopurines, or vedolizumab, or by attribution of long-term IBD disease status. Indeed, the SNDS contains the patient's status for long-term diseases listed in the ICD-10, including CD and UC. Long-term disease is established by a national health insurance expert physician at the request of the patient's general practitioner, who certifies that the patient has IBD; 85% of IBD patients in our study had a status of long-term disease (3). Previous studies have used the same algorithm, allowing for estimated incidence rates of CD and UC in France that were within the range of those reported in the literature (3–5). We are confident that our definition of IBD is very specific. Moreover, any misclassification should have been similar regardless of the drug being administered and would have led to a nondifferential bias.

Finally, the SNDS does not contain all clinical data that would be pertinent to disease severity. We therefore used proxies to

estimate disease severity, including past use of biologic agents, nonbiologic systemic glucocorticoids, and systemic glucocorticoids in the 2 years preceding the index date. These variables, among others, were included in the propensity score and thus balanced between groups. The results were similar with multivariable models.

All data sources have strengths and limitations. Claims database studies, such as our study based on data from the SNDS, involve a large number of patients whose information is captured during routine medical care, and quality control is assured by using ICD-10 codes for diagnosis. This framework minimizes selection bias and allows for identification of a large number of outcome events. Strong methodology, including new-user design and the propensity score–matching method, helped to address confounding or selection bias. New evidence from registries of patients with PsO and/or PsA/AS (having lower statistical power but providing relevant clinical data) will reinforce our conclusions.

Emilie Sbidian, MD, PhD
EPI-PHARE
Université Paris Est Creteil
and Centre d'Investigation Clinique 1430
Henri Mondor Hôpital, AP-HP, INSERM
Laëtitia Penso, MSc
EPI-PHARE
and Université Paris Est Creteil

Antoine Meyer, MD, MSc
EPI-PHARE
Hôpital Bicetre, AP-HP
and Université Paris Sud
Paris, France

1. Tuppin P, Rudant J, Constantinou P, Gastaldi-Ménager C, Rachas A, de Roquefeuil L, et al. Value of a national administrative database to guide public decisions: from the Système National d'Information Interrégimes de l'Assurance Maladie (SNIIRAM) to the Système National des Données de Santé (SNDS) in France [review]. Rev Epidemiol Sante Publique 2017;65 Suppl 4:S149–67.
2. Vegas LP, Sbidian E, Penso L, Claudepierre P. Epidemiologic study of patients with psoriatic arthritis in a real-world analysis: a cohort study of the French health insurance database. Rheumatology (Oxford) 2021;60:1243–51.
3. Kirchgesner J, Lemaitre M, Rudnichi A, Racine A, Zureik M, Carbonnel F, et al. Therapeutic management of inflammatory bowel disease in real-life practice in the current era of anti-TNF agents: analysis of the French administrative health databases 2009-2014. Aliment Pharmacol Ther 2017;45:37–49.
4. Lemaitre M, Kirchgesner J, Rudnichi A, Carrat F, Zureik M, Carbonnel F, et al. Association between use of thiopurines or tumor necrosis factor antagonists alone or in combination and risk of lymphoma in patients with inflammatory bowel disease. JAMA 2017;318:1679–86.
5. Meyer A, Rudant J, Drouin J, Weill A, Carbonnel F, Coste J. Effectiveness and safety of reference infliximab and biosimilar in Crohn disease: a French equivalence study. Ann Intern Med 2019;170:99–107.